UNIVERSIDADE DE SANTIAGO DE COMPOSTELA

Spatial Propagation and Characterization of Quantum States of Light in Integrated Photonic Devices

Propagación Espacial y Caracterización de Estados Cuánticos de Luz en Dispositivos Fotónicos Integrados

Memoria para optar al grado de doctor presentada por

David Barral Raña

Directores de tesis

Prof. Dr. Jesús Liñares Beiras

Prof. Dr. Vicente Moreno de las Cuevas

Santiago de Compostela, Julio 2015

USC
UNIVERSIDADE
DE SANTIAGO
DE COMPOSTELA

D. Jesús Liñares Beiras, Catedrático de Universidad de la Facultad de Física, y D. Vicente Moreno de las Cuevas, Catedrático de Escuela Universitaria de la Facultad de Óptica y Optometría, hacen constar:

Que la memoria titulada **Propagación Espacial y Caracterización de Estados Cuánticos de Luz en Dispositivos Fotónicos Integrados**, ha sido realizada bajo su dirección en el Área de Óptica del Departamento de Física Aplicada de las Facultades de Física y Óptica y Optometría de la Universidad de Santiago de Compostela por D. David Barral Raña, constituyendo el trabajo de tesis del Programa de Doctorado de **Láser, Fotónica y Visión**, Facultad de Física, que presenta para optar al Grado de Doctor en Láser, Fotónica y Visión.

Santiago de Compostela, 28 de Julio de 2015.

Fdo. Director: Prof. Dr. D.
Jesús Liñares Beiras

Fdo. Director: Prof. Dr. D.
Vicente Moreno de las Cuevas

Fdo: Alumno D.
David Barral Raña

USC
UNIVERSIDADE
DE SANTIAGO
DE COMPOSTELA

AGRADECIMIENTOS

Aprovechando que, siendo optimista, nueve de cada diez lectores de esta tesis sólo van a leer esta sección, me permito la licencia de hacerles un resumen ligero, para que tengan una idea de qué ha estado haciendo éste tanto tiempo allí metido.

La física cuántica es una teoría que permite calcular la probabilidad de que en un experimento con partículas fundamentales obtengas un resultado dado. No te dice el valor que va a salir cada vez que repites el experimento, pero sí predice su valor medio y demás información estadística que obtendrías si lo repites muchas veces en las mismas condiciones. Las partículas fundamentales de la luz son los fotones y sus distintas combinaciones, los estados cuánticos de luz. Algunos de estos estados tienen características que son útiles para hacer medidas más precisas o ciertos cálculos más rápidamente, entre otras cosas. El objeto de esta tesis es aplicar la física cuántica a esos estados que recorren guías ópticas, primas hermanas de las fibras ópticas, gracias a las que internet llega a nuestras casas. Y su interés radica en que en el futuro quizás tengamos ordenadores más eficientes y comunicaciones más seguras usando estos estados y dispositivos ópticos, como los que aquí se estudian, que los generen y procesen. Tachán!. Trescientas páginas ahorradas... ¡Muchas gracias!

Y ahora toca pagar deudas. Los agradecimientos.

En primer lugar, me gustaría agradecer a mi director Suso Liñares la oportunidad de haber trabajado con él durante estos años. Es imposible cuantificar todo lo que he aprendido con él y de él, tanto a nivel científico como personal. Se nos acababan las tardes hablando de cuántica. Y gracias por animarme cuando todo se ha puesto en contra. Muchísimas gracias.

A mi codirector Vicente Moreno tengo que agredecerle sus consejos, disponibilidad y buen humor. He aprendido mucho con él en el laboratorio y su despacho siempre ha estado abierto para mi. Y gracias también por compartir conmigo su gran cultura, con algún que otro libro y disco.

Likewise, I would like to thank Professor Mark Thompson the opportunity to visit the *Center of Quantum Photonics* at the *University of Bristol*. I learned lots about theoretical and experimental quantum stuff and met

brilliant scientists and friends. Thanks.

En siguiente lugar me gustaría darle las gracias a mis compañeros de Óptica: los profesores Carlos Montero y Xesús Prieto, con los que *he tocado* la óptica integrada que aprendí en los libros, y Ana Alonso y Manuel Gómez, por su ayuda en el laboratorio y por hacer de esta área un lugar más ameno para trabajar.

Asimismo, tengo que agradecerle al profesor José Castillo (y a la profesora Isabel Lema) la oportunidad de trabajar durante tres años en el *laboratorio de investigación en neurociencias clínicas*, donde he aprendido cosas que nunca hubiera imaginado, desde hacer cultivos celulares a resonancias magnéticas, pasando por nanopartículas. Y donde sobre todo he hecho buenos amigos. Gracias a David, Jesús, Bárbara, Octavio, Raquel, Tomás, Pedro, Fran, Andrés, Esteban, Joserra y Alba. Y gracias por las clases de guitarra, Esteban.

Además, tengo que darle las gracias a toda la gente que conocí en Bristol durante esos tres maravillosos meses. En primer lugar, gracias a Martín, por acogerme cuando llegué y guiarme los primeros días. Siempre recordaré cuando, dos meses después de llegar a Bristol, me dijiste que no te acordabas de la semana que pasamos juntos en mi despacho en Santiago... ¡y me habías dejado pasar una semana en tu casa "sin conocerme"!. Muchísimas gracias. A mis compañeros de piso: Matt, Rado, Kim y, sobre todo, a Cris. El olor a café por las mañanas (todas las mañanas me acuerdo de ti), mis bizcochos nocturnos o la tortilla de esa cosa rara que tenéis en Valencia... recuerdos imborrables de días muy muy felices. A Quique, Jorge y el resto de *Booberos Villa*. Lo que no ganamos en el campo, lo bebimos en los pubs. Gracias Quique por esa paella típica de Salamanca y por ser mi amigo. Gracias a mi equipo mexicano por los *coffee-time* y en especial a Gerardo, por su ayuda y ganas de aprender. Y en especial, gracias a Laura. Gracias por hacerme participe de tu vida y darme tanto cariño.

I would also like to thank my fellows and friends Drs. Gary Sinclair and Damien Bonneau, from who I learned much more about quantum optics in two months than for years from books. Thanks for your attention and help. You guys, are two of the more brilliant scientists I ever met. It was a pleasure working with you.

A mis amigos de San Pedro. Porque hemos crecido y descubierto la vida juntos. Enri, Carlos, Lu, Balle, Berni, Andrés, Borja, Rober y sobre todo, Noe. Mil gracias por escucharme, en las victorias y en las derrotas. Te lo agradeceré siempre Amiga. Y no me olvido de los herederos, Estela y Marco. Y los que están por venir...

A mis compañeros de fútbol sala, donde liberamos el estrés pegándonos patadas. A Petado, Jesús y David por nuestras largas charlas sobre ellas. A Dani por aguantar mis desbarres desde el instituto hasta hoy y ayudarme en aquella mudanza... que significó mucho para mi, y a Javier por sus clases de física y filosofía de vida.

Gracias a Bárbara. Por ayudarme aquel día en *IBC* y por todo lo que vino después. Esta tesis también. Es un bonito recuerdo que me acompañará siempre. Y gracias a Lino, Nieves y Juan. Porque siempre me hicistéis sentir uno más. Gracias por todo lo vivido juntos.

"*Allí, en ese edificio feo y gris, en la Condesa, empezó todo*", dice mi buen amigo Davi. Mira si me gustó que aún hoy escribo estas líneas en él. Muchas gracias a mi *secta* por las horas de sofá, pinpón, grupo de cocina, fiestas y demás menesteres que allí, juntos, compartimos. Gracias Keki por ser mi compañero de batallas los últimos catorce años. Hemos pasado juntos muchos momentos felices y unos pocos tristes. Gracias por ser mi Amigo, con mayúsculas. Y gracias Ari, por estar siempre ahí si lo necesitaba. Tengo una deuda muy grande que gustoso pagaré en forma de apadrinamiento y llevando a vuestros hijos a parques de atracciones...(risas). Gracias al resto de la comuna de Santiago, los que se resisten a marcharse: Ele y Fran (cuya boda espero no coincida con la defensa de esta tesis... enhorabuena!), Davi, Javi y los habituales visitantes, Vero, Feli y Villa. Estos años han sido muy intensos y hemos pasado mucho juntos (algún Sella y San Fermín incluídos...). Gracias Javi por compartir el rosarieo conmigo. Mil gracias a todos por vuestro apoyo.

Gracias también a mi familia, en especial a Paula y Marta, con las que he pasado tardes muy alegres, alguna caída de culo incluída..., y a Nuria.

Grazas á Fraga, á chuvia, ó piorno, á Leria, a San Sadurniño e ós poliños. Grazas por facerme rir, gritar, soñar, sentir, rir, bailar, cantar, pensar, rir, escoitar, ler, buscar constelacións, ..., sentir afortunado. Grazas *Maga*. Esta tesis non sería posible sen os teus azos.

Y finalmente, gracias a los principales soportadores, consejeros, valedores... de todo esto. A mis padres David y Mari Carmen, que siempre han querido que tuvieramos lo que ellos no puediron tener. Gracias por educarme e inculcarme los valores que me han llevado hasta aquí, y que son vuestro mejor regalo. A mi abuela Julia, que tanto me quiere. "*¿Cando vén David?*". Y, por último, a mi hermana Alba. Gracias por ayudarme a progresar. Te echo de menos.

Gracias a todos los fuegos que alumbran este camino.

USC
UNIVERSIDADE
DE SANTIAGO
DE COMPOSTELA

A mis padres,
por llenar la casa de libros
y más libros... y por aquel
camión amarillo.
A mi abuela,
que reza todas las noches
por mi.
Y a mi hermana,
mi mejor amiga.

USC
UNIVERSIDADE
DE SANTIAGO
DE COMPOSTELA

Caminante, son tus huellas
el camino y nada más;
caminante, no hay camino,
se hace camino al andar.

Golpe a golpe, verso a verso...

Antonio Machado

Extracto de *Proverbios y cantares*

Un hombre del pueblo de Neguá, en la costa de Colombia, pudo subir al alto cielo. A la vuelta, contó. Dijo que había contemplado, desde allá arriba, la vida humana. Y dijo que somos un mar de fueguitos.
- El mundo es eso -reveló-. Un montón de gente, un mar de fueguitos.
Cada persona brilla con luz propia entre todas las demás. No hay dos fuegos iguales. Hay fuegos grandes y fuegos chicos y fuegos de todos los colores. Hay gente de fuego sereno, que ni se entera del viento, y gente de fuego loco, que llena el aire de chispas. Algunos fuegos, fuegos bobos, no alumbran ni queman; pero otros arden la vida con tantas ganas que no se puede mirarlos sin parpadear, y quien se acerca, se enciende.

Eduardo Galeano

El libro de los abrazos

USC
UNIVERSIDADE
DE SANTIAGO
DE COMPOSTELA

ABBREVIATIONS

BS	Beam Splitter
BHD	Balanced Homodyne Detector
DC	Directional Coupler
DPA	Degenerate Parametric Amplifier
EM	Electromagnetic
EO	Electro-Optic
ESCR	Equal Space Commutation Relations
FCA	Free Carrier Absorption
FWM	Four Wave Mixing
GRIPS	Generalized Rotations in Phase Space
IDC	Integrated Directional Coupler
IOW	Integrated Optical Waveguide
IPD	Integrated Photonic Device
IPW	Integrated Photonic Waveguide
IQP	Integrated Quantum Photonics
LE	Lewis-Ermakov
LIM	Longitudinally Inhomogeneous Media
LIW	Longitudinally Inhomogeneous Waveguide
LO	Local Oscillator
MSP	Multimode Single Photon

MUS	Minimum Uncertainty State
NWS	Nonlinear Waveguiding Device
OFS	Optical Field-Strength
OHT	Optical Homodyne Tomography
QIP	Quantum Information Processing
QST	Quantum State Tomography
QTE	Quasi Tranverse Electric
QTM	Quasi Transverse Magnetic
SHG	Second Harmonic Generation
SOI	Silicon On Insulator
SPDC	Spontaneous Parametric Down Conversion
SQL	Standard Quantum Limit
TE	Tranverse Electric
TM	Transverse Magnetic
TPA	Two Photon Absorption
WPD	Waveguiding Photonic Device

CONTENTS

LIST OF FIGURES

USC
UNIVERSIDADE
DE SANTIAGO
DE COMPOSTELA

CHAPTER

ONE

INTRODUCTION, AIMS AND METHODOLOGY

Context, motivation and aims

LIGHT surrounds us. Either in the form of radiation from natural sources like the sun or man-made devices, carrying large amount of data to and from our homes or even as a clean way of obtaining energy. The use of light for our benefit has been an active area of research for centuries. Fortuitously, this year coincides with the anniversaries of a series of important milestones in the history of the science of light [United Nations, 2013]: the pioneering works on optics by Ibn Al-Haytham in 1015, the notion of light as a wave proposed by Fresnel in 1815, the electromagnetic theory of light propagation established by Maxwell in 1865, Einstein's theory of the photoelectric effect in 1905 and the embedding of light in cosmology through general relativity in 1915, the discovery of the cosmic microwave background by Penzias and Wilson and Kao's achievements related with the transmission of light in fibres for optical communication, both in 1965. All these "little" works and many others revolutioned the way we understand either the universe or the tiny particles we are made up. Likewise, these insights have been the starting point to the develop of a myriad of technologies which improve our quality of life. United Nations proclaimed this year the International Year of Light and Light-based Technologies [Unesco, 2015]. In its resolution, it was stressed "*the importance of light and light-based technologies in the lives of the citizens of the world and for the future development of global society on many levels*", as well as considered that "*the applications of light science and technology are vital for existing and future advances in, inter alia, medicine, energy, information and communications, fibre optics, agriculture, mining, astronomy, architecture, archaeology, entertainment, art and culture, as well as many other industries and services, and that light-based technologies contribute to the fulfilment of internationally agreed development goals, including by providing access to information and increasing societal*

health and well-being" [United Nations, 2013]. These statements summarize the significance of light to mankind.

Between all the fields optics encompass, quantum optics is one of the largest-growing and more influential of the last century. Many of the discoveries and applications above introduced are directly or indirectly related to it. We have to go back to the begining of the previous century to find its birth. The pioneering works of Planck on the *black-body* radiation introduced the quantization of energy and the indistinguishability (bosonic nature) of these quanta of radiation [Planck, 1900a,b]. It was few years later when Einstein, based on Planck's ideas, using a particle-image of light explained the photoelectric effect with great success [Einstein, 1905]. These particles were later coined as *photons*. Furthermore, Bohr applied the quantization to atomic dynamics explaining the line spectra of gases [Bohr, 1913]. Likewise, few years later, Einstein explained the interaction of electromagnetic (EM) radiation with atoms leading to the idea of *stimulated emission* [Einstein, 1917], basis of the operation of lasers, and the introduction of non-local or *entangled quantum states* in [Einstein et al., 1935], a *sleepy beaty* of theoretical physics rediscovered almost 60 years later and now basis of *quantum information processing* (QIP). In the meantime, the foundations of quantum mechanics were established by Heisenberg, Jordan, Schrödinger and Dirac as well as conceptual leaps as De Broglie's wave-particle duality and Born's probabilistic nature of quantum mechanics [Born and Wolf, 1959] (and references therein). It was Dirac the first who extended the methods of quantum mechanics to the EM field [Dirac, 1927], starting which is known today as *quantum field theory* (QFT). But it was not till the 1950s, when the develop of masers by Townes and his group and, independently, by Basov and Prokhorov, and later the lasers by Townes and Shawlow[1] [Bertolotti, 2005], gave a boost to this research area and opened new fields like *nonlinear optics*, *fibre optics* and *quantum electronics*; being one of the most influential invention of all times. Remarkably, this discovery led Glauber, Sudarshan and Mandel to apply quantum theory to photodetection and the statistics of light, developing the quantum theory of coherence which represents the reawaken of quantum optics [Mandel and Wolf, 1995]. Glauber introduced the *coherent states* and the use of *quasiprobability distributions* for the study of quantum problems [Glauber, 1963a,b]. These works laid the foundation for new research areas like the study of *non-classical light* and its generation via *nonlinear optics* [Walls and Milburn, 1994], the *laser cooling* and *atom traps* [Schleich, 2001], or the use of the properties of these states for *quantum communications*, *metrology*, *computation* and so on [Gerry and Knight, 2005, Nielsen and Chuang, 2000]; research areas which are the basis of the technologies which nowadays are changing the way information is encoded, processed and transmitted [O'Brien et al.,

[1] Gould independently patented the laser but he never published his work.

2009].

On the other hand we have fiber and integrated optics, which have been paving the way for current optical communications and processing of light [Hunsperger, 2009]. These technologies are based on the confinement of light in material structures of the order of its wavelength [Kogelnik, 1988]. The main strengths of integrated optics are its scalability and sub-wavelength stability. The first one is customary when complex circuits are needed and the second when interference effects are involved, so outperforming bulk optics. These features have taken integrated optics to play a central role in the develop of quantum science through the so-called *integrated quantum photonics* (IQP). The first demonstration of an integrated quantum circuit was carried out in 2008 where quantum interference in a directional coupler (DC) and the operation of a CNOT gate on-chip was shown [Politi et al., 2008]. Since this breakthrough experiment, many highly successful new demonstrations have been carried out in this field: integrated quantum metrology by observing interference fringes with two- and four-photon entangled states [Matthews et al., 2009], reconfigurable photonic quantum chips for processing and measurement of qubits [Jin et al., 2014, Shadbolt et al., 2012], quantum walks and boson sampling in waveguides [Peruzzo et al., 2010, Spring et al., 2013], quantum interference between photons generated on-chip [Silverstone et al., 2014], quantum teleportation on a photonic circuit [Metcalf et al., 2014], generation of bright squeezing on-chip [Dutt et al., 2015], continuous-variable entanglement and homodyne detection on a quantum circuit [Masada et al., 2015] and so on.

What these *integrated photonic devices* (IPDs) have in common is that they use guided modes to encode quantum information and DCs to produce entanglement, the most striking feature of quantum mechanics [Einstein et al., 1935]. The operation of DCs is based on the coupling of these guided modes. Classical theory works finely in the analysis of linear and nonlinear usual IPDs which run with classical states of light [Kogelnik, 1988]. The problem appears when generation, manipulation and detection of quantum light in IPDs is carried out, and thus taking advantage of its unique features. Classical theory is unable to deal correctly with these problems, so it has to be left aside and give way to a quantum theory which describes correctly the operation of these photonic devices.

One of the main aims of this dissertation is to present a consistent theory of the propagation of quantum light encoded in guided modes in IPDs since the usual Hamiltonian approach presents several conceptual and formal inconsistencies when dealing with propagation in dielectric media. This was first shown for linear media by Abram in a seminal paper on quantum theory of light propagation [Abram, 1987] and later by Huttner *et al.* for nonlinear media [Huttner et al., 1990]. The standard theory of quantum propagation was based on an analogy between temporal evolu-

tion and spatial propagation. From the Hamiltonian, obtained by means of quantization of the energy density in a volume V and the use of spatial modes, a connection between space and time is established via an effective interaction time $t = -z/v$, with z the length of the medium and v the effective velocity of light within [Perinová et al., 1991, Shen, 1967]. However, this approach has two problems: firstly, the use of this identity implies the loss of one variable, such that this formalism only describes the propagation of stationary states and, secondly, this approach can not be applied rigorously to dispersive media, since each frequency propagates at a different velocity $v(\omega)$ and, therefore, $t(\omega) = -z/v(\omega) \equiv zn(\omega)/c$, with $n(\omega)$ the refractive index in the volume V, and we would need a temporal variable for each frequency ω [Huttner et al., 1990]. So, in this case, the use of the previous identity is no longer possible. Likewise, this argument can also be used to justify that the standard Hamiltonian formulation is unable to describe the counterpropagation because a negative time would be required [Ben-Aryeh et al., 1992, Toren and Ben-Aryeh, 1994]. Another example of this inconsistency can be easily seen in the interface between the free space and a homogeneous dielectric medium: the energy density is different inside and outside the homogeneous dielectric medium which would lead to a renormalization of the frequency (photon energy) which, however, is known to be invariant [Abram, 1987].

On the other hand, when dealing with nonlinear media these problems appear as well. For instance, in the case of propagation in a *degenerate parametric amplifier* (DPA), where $\omega_1 = \omega_2$, without fulfilling the *phase matching* condition or where a longitudinally inhomogeneity is present inside the considered volume, fact which can happen in linear media as well, the standard theory would lead to incorrect coupling coefficients, since the integration of the energy density in the volume would eliminate the z-dependence. In fact, the degenerate parametric amplifier without phase matching condition was the problem tackled in [Huttner et al., 1990], where both proper coupling coefficients for plane modes and correct solutions for the absorption and emission operators were obtained. Likewise, if we had considered the *non degenerate parametric amplifier* (NDPA) for frequencies $\omega_1 \neq \omega_2$, then the formal transition to spatial propagation by a simple change between t and z would not be longer possible and several non rigorous (and contradictory) depending-frequency changes (due to material or modal dispersion) would have to be made to derive the correct spatial equations and their solutions.

Hence, in order to avoid the mentioned inconsistencies, Huttner *et al.* [Huttner et al., 1990] presented a quantization procedure for linear and nonlinear homogeneous dielectric media based on both the temporal modes and the Momentum operator $\hat{M}$, which is the generator of translations [Landau and Lifshitz, 1973], and describes spatial propagation correctly. Following it, a series of studies polished the theory to get a fully consist-

ent one, taking the flux of momentum as the correct operator instead of the density of vectorial momentum and introducing proper *equal space commutation relations* (ESCR) [Ben-Aryeh and Serulnik, 1991, Ben-Aryeh et al., 1992, Serulnik and Ben-Aryeh, 1991].

The first theoretical works on quantum propagation in IPDs, such as a linear coupler, were made by Jansky *et al.* [Jansky et al., 1988] by means of a correspondence rule and therefore without a rigorous derivation of Heisenberg equations. Afterwards, studies of quantum light propagating in linear and nonlinear couplers were presented by Toren and Ben Aryeh [Toren and Ben-Aryeh, 1994] and Perina [Perina, 1995] [Perina Jr and Perina, 2000] (*and references therein*), respectively. However, the corresponding Momentum operators were either heuristically introduced or by transferring directly the results obtained with plane waves, whithout taking into account neither the vector structure nor the orthonormalization property of the guided modes. The first rigorous derivation of the quantum Momentum operator for planar integrated optical coupling devices operating under mode coupling was proposed in [Liñares and Nistal, 2003]. The most important difference regarding to homogeneous media is that the optical modes are guided, so they are confined and exhibit longitudinal components (optical vector modes) which can not be ignored. In fact, in integrated nano-optics these longitudinal components are still larger than in standard integrated optics. In this study, a quantization of 2D *transverse electric* (TE) modes is carried out based on the modal orthonormalization property on the cross section of the waveguide and the modal norms, deriving the right optical field operators and accordingly the correct Momentum operator.

In this dissertation we generalize this work to integrated devices with confinement in two dimensions, like rectangular waveguides but also photonic crystals, plasmonic waveguides and so on, by means of the use of 1D vectorial modes, showing an *ab initio* quantization of the fields [Liñares et al., 2008a] and deriving the Heisenberg equations of propagation the modes fulfill in integrated structures like DCs, gratings, junctions, interferometers and so on [Liñares et al., 2008b]; made of homogeneous and inhomogeneous, linear and nonlinear, lossless and lossy media (chapter 2). A remarkable feature these equations present is that they describe simultaneously both mode co-propagation and counter-propagation, that is, coupling between forward and backward modes, which in turn has no counterpart in temporal evolution. This is one of the most relevant results obtained by using a quantum optical propagation theory based on the Momentum operator, as above claimed. Likewise, z-dependent structures which made up IPDs like gratings or tapers, can be correctly designed with this approach unlike the Hamiltonian.

The canonical analysis of propagation above introduced is carried out in the Heisenberg picture. This approach is interesting when we deal with *discrete variables*, like path- or polarization-encoded Fock states in quantum

computation or communications, since the measurement is based on direct photoabsorption processes (*photocounting*). In this picture the absorption operator at any z is easily calculated and hence predictions of the performance of an IPD are quickly obained. However, there are other problems better suited to be dealt in the Schrödinger picture, for instance when dealing with *quantum polarization* or *quantum state tomography* (QST) or, in general, with *continuous variables*, where measurement is *phase-sensitive* (*homo- and heterodyne detection*). In this case the propagation of quantum states can be obtained by solving the *master equation* related with *quasiprobability distributions* in the coherent state basis [Mandel and Wolf, 1995] or, alternatively, by solving the *Schrödinger equation* or *Feynman path integrals* [Feynman and Hibbs, 1965] for probability distributions in the *optical-field strength (OFS)* representation [Vogel and Welsch, 1994]. This last approach keeps the physical intuition due to its great resemblance with propagation in classical optics. The use of path integrals is analogous to the classical geometrical optics where quadratic media act on quantum light in the same way as lenses on rays. Likewise, OFS probability distributions are well-behaved and they are directly measured by phase-sensitive techniques, unlike quasiprobability distributions where reconstruction methods have to be carried out [Lvovsky and Raymer, 2008]. Hence, we introduce a Lagrangian-type theory for spatial propagation problems and derive from it Feynman propagators used to calculate the propagation of quantum states in the OFS representation [Liñares et al., 2012]. Thus, applying the path integral approach in this space we obtain several interesting results (chapter 3).

In addition, we study via path integrals the remarkable case of separable longitudinally inhomogeneous media where the use of the standard theory would lead to squeezing of quantum light [Choi, 2004, Pedrosa and Rosas, 2009], [Fernández Guasti and Moya-Cessa, 2003, Yeon et al., 1994]. The discrete limit of this problem was studied by [Abram, 1987, Glauber and Lewenstein, 1991], where they showed that in the case of propagation through a discontinuity between two homogeneous media with different refractive index this squeezing is virtual and a scale transformation should be accomplished to sort it out. We solve the continuous limit of this problem by two methods involving unitary [Barral and Liñares, 2015a] and canonical [Barral and Liñares, 2015b] transformations, respectively. Besides, we show that the net effect this media produces is a quantum Gouy's phase not obtainable by classical methods and with direct application to QIP and quantum sensing.

Furthermore, it seems natural to analyze the features of the states processed in the IPDs. This is the second aim of this thesis: the characterization of these guided mode-encoded quantum states. It is usually carried out by means of *quasi-probability distributions* in the phase space or *density matrices* in the Fock representation [Schleich, 2001]. However, as above stated, it is either cumbersome and with a tedious processing of data after measur-

ing or it is only practical in the case of discrete variables (discrete Hilbert space), respectively. Once again we choose the OFS space to this purpose due to both the importance of the optical field and noise in quantum science and, likewise, its clear analogy with classical optics. In this case, we use the confinement of the probability distributions in particular regions of the N-dimensional OFS space, the so-called *generalized quantum polarization* due to its resemblance with classical polarization (chapter 4). Our definition includes both vectorial and spatial modes where, in the case of two-mode vectorial modes, it agrees with the common quantum polarization. On the other hand, in the case of spatial modes, like the propagation modes in integrated devices, the definition can be extended to N dimensions, where N is the number of propagating modes.

Polarization of quantum states is an active area of research. In the quantum domain, the standard concept of polarization fails for both *quasi*-classical states and states very apart from them, like number states, because the mean value of the optical field operator does not follow a definite curve of polarization on the two-mode OFS plane. Likewise, another problem arises in the transition from classical to quantum polarization, since the *semiclassical polarization degree* [Tanás and Kielich, 1990], defined in terms of the *Stokes operators* obtained by quantization of the classical *Stokes parameters*, shows several paradoxical results [Bjork et al., 2010, Luis, 2007]. Different approaches have been devised to avoid these inconsistencies. They are based on the concept of unpolarized light as that invariant under SU(2) transformations [Agarwal, 1971, Lehner et al., 1996, Prakash and Chandra, 1971, Söderholm et al., 2001]. One of them is based on the $SU(2)$ coherent states by introducing a suitable definition of the degree of quantum polarization as a distance measure to an unpolarized distribution and characterizing the quantum polarization states on the Poincarè sphere [Luis, 2003]. Another important perspective is based on the overlap between the wavefunction $|\psi\rangle$ and all its rotations in the Poincaré sphere, giving an idea of the sensitivity of the state to $SU(2)$ transformations [Björk et al., 2002].

Hence, following closely these ideas, we have developed a formalism to characterize quantum states by means of a *generalized polarization degree*. In our approach, the polarization degree gives us a measure of how different a quantum state is from a fully unpolarized state in the OFS space, an isotropic and gaussian state, so there is no priviledged confinement (polarization) in any Hilbert subspace, only dependent on the excitation manifold [Barral et al., 2013, Liñares et al., 2010, 2011]. Thus, we apply this theory to both N-dimensional stationary and non-stationary quantum states obtaining consistent results (chapter 4).

In addition, the characterization above introduced is based on measurements of quantum states in the OFS space which are carried out by means of phase-sensitive techniques, known as *optical homodyne tomography* (OHT) [Loudon and Knight, 1987]. These techniques are central in *quantum state*

tomography (QST). This is based on the relation between quasi-probability distributions and probability distributions of the rotated quadrature [Vogel and Risken, 1989]. A plethora of states has been characterized by these techniques in bulk optics: single and two-mode squeezed states, one and two photons Fock states, optical qubits, Schrödinger cats and *kittens*, photon added states and so on [Lvovsky and Raymer, 2008] (*and references therein*). Likewise, in the context of polarization, it has been shown recently the reconstruction of the Stokes fluctuations on the Poincaré sphere for a squeezed vacuum state [Klimov et al., 2010]. Besides, regarding to integrated photonics, the first demonstration of continuous-variable entanglement and measurement on-chip has been shown this year [Masada et al., 2015].

On the other hand, in the usual single-mode homodyne detection, QST is carried out by means of modulation of a *local oscillator* (LO) phase which turns out into a rotation in the phase space. When two modes are involved, three parameters are necessary. This can be carried out either by applying a set of transformations to a two-mode LO (*dual-mode-LO*) [Opatrny et al., 1997, Raymer et al., 1996] or to the two-mode signal before mixing in a *balanced homodyne detector* (BHD), so-called *generalized rotations in phase space* (GRIPS) [Raymer and Funk, 1999]. Multimode QST is also posible by means of nesting, but it is difficult to carry out with bulk optics due to the lack of scalability [Welsch et al., 1999]. Bearing all the above in mind, our third aim is to measure multimode quantum states of light in the OFS space and, particularly, to design a versatile and reliable integrated device to accomplish this goal.

In this context we propose an integrated device based on a electro-optic $\Delta\beta$ directional coupler [Kogelnik and Schmidt, 1976] which performs unitary transformations and, hence, allows fully integrated OHT of quantum states excited in two or N spatial modes following the GRIPS scheme proposed in [Raymer and Funk, 1999]. Other schemes based on Mach-Zehnder interferometers have been introduced to accomplish unitaries in quantum computation and communications [Metcalf et al., 2014, Shadbolt et al., 2012], however, our design outperforms them due to its ability to reduce the significance of fabrication errors of the couplers [Barral et al., 2015]. Likewise, this device can be used in any application in quantum technology where unitaries are needed and is suitable to be nested, opening new opportunities with N modes. In the end, we simulate the operation of this device in the measurement of generalized polarization (chapter 5).

Methodology

The previous section has established the general view of the problem we deal with in this dissertation. In this section we describe the resources and methods we have used and developed to face the questions we have

found. To this end, we summarize the problem and aims of this dissertation and introduce our methodology right after.

As above seen, in the context of IQP, there are conceptual and formal inconsistencies when the Hamiltonian theory is used. Quantum problems involving dispersive and longitudinally inhomogeneous waveguides, contrapropagating modes or even interfaces vacuum-waveguide, can not be tackled with this theory. Likewise, there are problems better suited to be studied either with discrete or continuous variables. Therefore, it is interesting to have tools to tackle both problems. On the other hand, the quantum states which are propagated in IPDs are measured and have to be characterized at their ouput. Some of the current methods used to obtain the information of these states are tedious and involve *ill behaved* statistical functions. Moreover, despite the huge growth of IQP in the last years, there are hardly proposals for carrying out these measurements with integrated devices. Bearing this in mind, the main aims of this dissertation are the following:

1. To present a consistent theory of the propagation of quantum light encoded in guided modes in IPDs since the usual Hamiltonian approach presents several conceptual and formal inconsistencies when dealing with propagation in dielectric media.

2. To solve the propagation in the Heisenberg and Schrödinger-Feynman pictures, better suited for discrete- and continuous-variable problems, respectively, and apply it to linear and nonlinear, homogeneous and inhomogeneous, losless and lossy integrated coupling devices.

4. To characterize these guided mode-encoded quantum states by means of a generalized quantum polarization.

5. To measure multimode quantum states of light and, particularly, to design a versatile and reliable integrated device to accomplish this goal.

The methodology we have used to accomplish the previous aims is the following:

A. Literature review of the problem related to spatial propagation of quantum light.

B. Look for the different drawbacks, limitations and gaps present in the field of quantum integrated photonics.

C. Use and development of physico-mathematics techniques: algebraic methods, temporal functional integration adapted and applied to space, analytical and numerical analysis.

D. Use of simulation techniques: application of Monte Carlo methods to the study of propagation, use of reconstruction methods to the simulated quantum states, testing the design of IPDs.

E. Use of symbolic and numerical sofware, and a graphics suite for sketching devices.

Finally, it is important to outline that we have selected for this report the most significant contributions, but others will be task of future research like perturbative techniques applied to path integrals to study higher order nonlinearities, a wider study of losses, other specific applications of IPDs to generation and manipulation of quantum states, applications of the quantum Gouy's phase and so on.

Thesis outline

The present report is organized in four chapters. Every chapter is divided in two parts, the first one with the conceptual ground, where the methods and principal results are shown, and the second with a selection of published and submitted papers or conference communications with the details and examples of the subject exposed in the first part. Thus, chapter 2 is devoted to present a consistent quantum theory of mode propagation. To this end, we will introduce classical concepts of integrated optics like the guided modes and linear and nonlinear mode coupling. Then, an overview of the quantum theory of propagation is carried out, where we accomplish a review of the previous works related to this area, highlighting the essential concepts, contrasting the different points of view they show and outlining the weaknesses to be sorted out. Right after we introduce our theory in the Heisenberg picture and demonstrate it produces consistent results. Next, we apply it to homogeneous and inhomogeneous, linear and nonlinear, lossless and lossy IPDs. Finally, we introduce the research work where our theory is shown in detail, and a conference communication with an example of the application of this theory to the generation of twin-photons in waveguides.

In chapter 3, a quantum theory for propagation in the Schrödinger picture by means of Feynman path integrals is derived. This is carried out from a spatial-type Lagrangian theory taking into account the concepts introduced in the previous chapter. This approach is useful when quantum noise is studied or in continuous-variable information encoding. We start the chapter introducing the quantum states of the field we will work with along the dissertation, showing their main features. Next, we will carry out a brief review of the descriptions available for quantum states of light, presenting right after the OFS representation and its strengths. Then, we

introduce the path integral formulation of the mode propagation and apply it to homogeneous and inhomogeneous, linear and nonlinear, lossless and lossy IPDs. Lastly, we present the research articles where this treatment along with examples is developed.

Chapter 4 is dedicated to the characterization of quantum states in the OFS space: *the generalized quantum polarization*. This is based on the analogy of this representation in the two-mode space with the classical polarization. Likewise, it allows us to characterize a quantum state with only one number, the *polarization degree*. We start the chapter presenting the classical concepts of polarization to, right after, introduce the quantum polarization, whit its main features and the problems to define a consistent quantum polarization degree, along with a review of the different degrees found in the literature. Next, we introduce the *generalized quantum polarization* and propose a polarization degree. We end with the research papers where this theory is analyzed in detail and applied to quantum states propagating in IPDs.

Finally, in chapter 5 we present the design of a measurement system of quantum states of light by means of integrated homodyne detection. This device is based on electro-optic DCs which perform SU(2) transformations allowing quantum state reconstruction and therefore its characterization. To clarify its operation we start the chapter with an introduction to phase-sensitive detection for 1 and N modes. Next, we review some of the main applications of this method in quantum optics. Right after, we present the main features of our detection scheme and its application to integrated two-mode homodyne detection. Lastly, we present the published research article where the design and application of this device to characterization of quantum states are detailed.

oOo

Papers by author

Published and submitted articles resulting from work in this thesis

1. J. Liñares, M.C. Nistal and D. Barral. QUANTIZATION OF COUPLED 1D VECTOR MODES IN INTEGRATED PHOTONIC WAVEGUIDES. New Journal of Physics. 10:063023, 2008.

2. J. Liñares, M.C. Nistal, D. Barral and V. Moreno. OPTICAL FIELD-STRENGTH POLARIZATION OF TWO-MODE SINGLE-PHOTON STATES. European Journal of Physics, 31, pp. 1-15, 2010.

3. J. Liñares, M.C. Nistal, D. Barral, V. Moreno, C. Montero and X. Prieto. QUANTUM INTEGRATED OPTICS: THEORY AND APPLICATIONS. Optica Pura y Aplicada – Special section: Quantum Optics, 44, 2, pp. 241-253, 2011.

4. J. Liñares, D. Barral, M.C. Nistal, and V. Moreno. OPTICAL FIELD - STRENGTH GENERALIZED POLARIZATION OF MULTIMODE SINGLE PHOTON STATES IN INTEGRATED DIRECTIONAL COUPLERS. Journal of Modern Optics, 58, 8, pp. 711-725, 2011.

5. J. Liñares, D. Barral and M.C. Nistal. SPATIAL PROPAGATION OF QUANTUM LIGHT IN NONLINEAR WAVEGUIDING DEVICES: THEORY AND APPLICATIONS. Journal of Nonlinear Optical Physics & Materials, 21, 3, 1250032, 2012.

6. D. Barral, J. Liñares and M.C. Nistal. OPTICAL FIELD - STRENGTH GENERALIZED POLARIZATION OF NON-STATIONARY QUANTUM STATES IN WAVEGUIDING PHOTONIC DEVICES. Journal of Modern Optics, 60, 12, pp. 941-955, 2013.

7. D. Barral, M. Thompson and J.Liñares. DETECTION OF TWO-MODE SPATIAL QUANTUM STATES OF LIGHT BY ELECTRO-OPTICAL INTEGRATED DIRECTIONAL COUPLERS. Journal of the Optical Society of America B, 32, 6, pp. 1165- 1173, 2015.

8. D. Barral, J. Liñares. SPATIAL PROPAGATION OF QUANTUM LIGHT IN LONGITUDINALLY INHOMOGENEOUS INTEGRATED WAVEGUIDING STRUCTURES. Submitted to the Journal of the Optical Society of America B.

9. D. Barral, J. Liñares. QUANTUM LIGHT PROPAGATION IN LONGITUDINALLY INHOMOGENEOUS MEDIA AS A SPATIAL LEWIS - ERMAKOV PHYSICAL INVARIANCE. Submitted to Optics Communications. ArXiv identifier: 1506.08523.

Conference communications resulting from work in this thesis

1. D. Barral, J. Liñares, M.C. Nistal, C.Montero and V. Moreno. CUANTIZACIÓN DE LA PROGRESIÓN DE MODOS ACOPLADOS EN GUÍAS FOTÓNICAS INTEGRADAS MEDIANTE EL OPERADOR MOMENTO. Libro de Actas Opoel'07: Quinta Reunión Española de Optoelectrónica, pp. 1-7, 2007.

2. J. Liñares, M.C. Nistal, D. Barral, V. Moreno and C. Montero. QUANTIZATION OF COUPLED WAVEGUIDED MODES PROGRESSION IN INTEGRATED PHOTONIC DEVICES. Proceedings of the SPIE Europe Photonics 2008, volumen 6996 de Silicon and Photonics and Photonic Integrated Circuits, 69961R-1, 2008.

3. J. Liñares, D. Barral, M.C. Nistal, V. Moreno, C.Montero and X. Prieto. QUANTUM ANALYSIS OF LINEAR AND NONLINEAR INTEGRATED DIRECTIONAL COUPLERS WITH SYNCHRONIC MONOMODE GUIDES. Reunión Nacional de Óptica 2009. PAN-79.

4. D. Barral, G. Sinclair, D. Bonneau, J. Silverstone, G. Villareal, J. Liñares, M. Thompson. GENERATION OF QUANTUM LIGHT IN SOI STRUCTURES. 23rd Congress of the International Comission for Optics, 2014. PI C4. ISBN 978-84-697-1027-2

5. D. Barral, V. Moreno, M.C. Nistal, X. Prieto, C. Montero, D. Mouriz, J. Crespo, E.F. Mateo, J. Liñares. SPATIAL PROPAGATION OF QUANTUM LIGHT IN LONGITUDINALLY INHOMOGENEOUS INTEGRATED WAVEGUIDE STRUCTURES. 23rd Congress of the International Comission for Optics, 2014. PI C3. ISBN 978-84-697-1027-2

Chapter 1 bibliography

I. Abram. Quantum theory of light propagation: Linear medium. *Physical Review A*, 35(11):4661–4672, 1987.

G.S. Agarwal. On the state of unpolarized radiation. *Lettere Al Nuovo Cimento*, 1(2):53, 1971.

D. Barral and J. Liñares. Spatial propagation of quantum light states in longitudinally inhomogeneous waveguides. *Submitted to the Journal of the Optical Society of America B*, 2015a.

D. Barral and J. Liñares. Quantum light propagation in longitudinally inhomogeneous media as a spatial lewis-ermakov physical invariance. *Submitted to Optics Communications*, ARXIV: 1506.08523, 2015b.

D. Barral, J. Liñares, and M.C. Nistal. Optical field-strength generalized polarization of non-stationary quantum states in waveguiding photonic devices. *Journal of Modern Optics*, 60(12):941, 2013.

D. Barral, M.G. Thompson, and J. Liñares. detection of two-mode spatial quantum states of light by electro-optic integrated directional couplers. *Journal of the Optical Society of America B*, 32(6):1165, 2015.

Y. Ben-Aryeh and S. Serulnik. The quantum treatment of propagation in non-linear optical media by the use of temporal modes. *Physics Letters A*, 155(8-9):473–479, 1991.

Y. Ben-Aryeh, A. Luks, and V. Perinová. The concept of equal space commutators in quantum optics. *Physics Letters A*, 165:19–27, 1992.

M. Bertolotti. *The history of the laser*. IOP Publishing, Bristol, 2005.

G. Björk, J. Söderholm, A. Trifonov, P. Usachev, L.L. Sánchez-Soto, and A. Klimov. Applications of entangled-state interference. In S.N. Bagayev, editor, *ICONO 2001: Quantum and Atomic Optics, High-Precision Measurements in Optics, and Optical Information Processing*, volume 4750, pages 1–12, 2002.

G. Bjork, J. Söderholm, L.L. Sánchez-Soto, A. Klimov, I. Ghiu, P. Marian, and Marian T.A. Quantum degrees of polarization. *Optics Communications*, 283:4440, 2010.

N. Bohr. On the constitution of atoms and molecules. *Philosophical Magazine*, 26(151):161, 1913.

M. Born and E. Wolf. *Principles of Optics*. Cambridge University Press, 7th edition, 1959.

J.-R. Choi. Coherent and squeezed states for light in homogeneous conducting linear media by an invariant operator method. *International Journal of Theoretical Physics*, 43(10):2113, 2004.

P.A.M. Dirac. The quantum theory of the emission and the absorption of radiation. *Proceedings of the Royal Society*, 114:243, 1927.

A. Dutt, K. Luke, S. Manipatruni, A.L. Gaeta, P. Nussenzveig, and M. Lipson. On-chip optical squeezing. *Physical Review Applied*, 3:044005, 2015.

A. Einstein. Über einen die erzeugung und verwandlung des lichtes betreffenden heuristischen gesichtspunkt. *Annalen der Physik*, 17(6):132, 1905.

A. Einstein. Quantentheorie der strahlung. *Physikalische Zeitschrift*, 18:121, 1917.

A. Einstein, B. Podolsky, and N. Rosen. Can quantum-mechanical description of physical reality be considered complete? *Physical Review*, 47(10): 777, 1935.

M. Fernández Guasti and H. Moya-Cessa. Solution of the schrödinger equation for time-dependent 1d harmonic oscillators using the orthogonal functions invariant. *Journal of Physics A: Mathematical and Theoretical*, 36:2069, 2003.

R.P. Feynman and A.R. Hibbs. *Quantum Mechanics and Path Integrals*. McGraw-Hill, 1965.

C.C. Gerry and P. L. Knight. *Introductory Quantum Optics*. Cambridge University Press, 2005.

R.J. Glauber. Photon correlations. *Physical Review Letters*, 10:84, 1963a.

R.J. Glauber. The quantum theory of optical coherence. *Physical Review*, 130:2529, 1963b.

R.J. Glauber and M. Lewenstein. Quantum optics of dielectric media. *Physical Review A*, 43(1):467, 1991.

R.G. Hunsperger. *Integrated Optics: Theory and Technology*, volume 33 of *Springer Series in Optical Sciences*. Springer Verlag, 6th edition, 2009.

B. Huttner, S. Serulnik, and Y. Ben-Aryeh. Quantum analysis of light propagation in a parametric amplifier. *Physical Review A*, 42(9):5594–5600, 1990.

J. Jansky, A. Sibilia, M. Bertolotti, and Y. Yushin. Non-classical light in a linear coupler. *Journal of Modern Optics*, 35:1757, 1988.

H. Jin, F.M. Liu, P. Xu, J.L. Xia, M.L. Zhong, Y. Yuan, J.W. Zhou, Y.X. Gong, W. Wang, and S.N. Zhu. On-chip generation and manipulation of entangled photons based on reconfigurable lithium-niobate waveguide circuits. *Physical Review Letters*, 113:103601, 2014.

A. Klimov, G. Björk, J. Söderholm, L.S. Madsen, M. Lassen, U.L. Andersen, J. Heersink, R. Dong, Ch. Marquardt, G. Leuchs, and L.L. Sánchez-Soto. Assesing the polarization of a quantum field from stokes fluctuations. *Physical Review Letters*, 105:153602, 2010.

H. Kogelnik. Theory of dielectric waveguides. In T. Tamir, editor, *Guided-wave optoelectronics*, chapter 2. Springer-Verlag, Berlin, 1988.

H. Kogelnik and R.V. Schmidt. Switched directional couplers with alternating $\delta\beta$. *IEEE journal of quantum electronics*, 12(7):396, 1976.

L.D. Landau and E.M. Lifshitz. *Curso de Física Teórica, vol. 2: Teoría Clásica de los Campos*. Editorial Reverté, 1973.

J. Lehner, U. Leonhardt, and H. Paul. Unpolarized light: Classical and quantum states. *Physical Review A*, 53(4):2727, 1996.

J. Liñares and M.C. Nistal. Quantization of coupled modes propagation in integrated optical waveguides. *Journal of Modern Optics*, 50(5):781–790, 2003.

J. Liñares, M.C. Nistal, and D. Barral. Quantization of coupled 1d vector modes in integrated photonic waveguides. *New Journal of Physics*, 10: 063023, 2008a.

J. Liñares, M.C. Nistal, D. Barral, V. Moreno, and C. Montero. Quantization of coupled waveguided modes progression in integrated photonic devices. In Giancarlo C. Righini, Seppo K. Honkanen, Lorenzo Pavesi, and Laurent Vivien, editors, *Proceedings of the SPIE Europe Photonics 2008*, volume 6996 of *Silicon Photonics and Photonic Integrated Circuits*, pages 69961R–69961R–12. S.P.I.E., 2008b.

J. Liñares, M.C. Nistal, D. Barral, and V. Moreno. Optical field-strength generalized polarization of two-mode single photon states. *European Journal of Physics*, 31:991, 2010.

J. Liñares, D. Barral, M.C. Nistal, and V. Moreno. Optical field-strength generalized polarization of multimode single photon states in integrated directional couplers. *Journal of Modern Optics*, 58(8):711, 2011.

J. Liñares, D. Barral, and M.C. Nistal. Spatial propagation of quantum light in nonlinear waveguiding devices: theory and applications. *Journal of Nonlinear Optical Physics and Materials*, 21(3):1250032, 2012.

R. Loudon and P.L. Knight. Squeezed light. *Journal of Modern Optics*, 34 (6-7):709, 1987.

A. Luis. Polarization correlations in quantum optics. *Optics Communications*, 216:165, 2003.

A. Luis. Polarization distributions and degree of polarization for quantum gaussian light fields. *Optics Communications*, 273:173, 2007.

A.I. Lvovsky and M.G. Raymer. Continuous-variable optical quantum state tomography. *Review of Modern Physics*, 81:299, 2008.

L. Mandel and E. Wolf. *Optical Coherence and Quantum Optics*. Cambridge University Press, 1995.

G. Masada, M. Kazunori, A. Politi, T. Hashimoto, J.L. O'Brien, and A. Furusawa. Continuous-variable entanglement on a chip. *Nature Photonics*, 9: 316–319, 2015.

J.C.F. Matthews, A. Politi, A. Stefanov, and J.L. O'Brien. Manipulation of multiphoton entanglement in waveguide quantum circuits. *Nature Photonics*, 3:346, 2009.

B.J. Metcalf, J.B. Spring, P.C. Humphreys, N. Thomas-Peter, M. Barbieri, W.S. Kolthammer, X.-M. Jin, N.K. Langford, D. Kundys, J.C. Gates, B.J. Smith, P.G.R. Smith, and I.A. Walmsley. Quantum teleportation on a photonic chip. *Nature Photonics*, 8(10):770, 2014.

M.A. Nielsen and I.L. Chuang. *Quantum Computation and quantum information*. Cambridge Series on Information and the Natural Sciences. Cambridge University Press, Cambridge, 2000.

J.L. O'Brien, A. Furusawa, and J. Vukovic. Photonic quantum technologies. *Nature Photonics*, 3:687, 2009.

T. Opatrny, D.-G. Welsh, and W. Vogel. Multi-mode density matrices of light via amplitude and phase control. *Optics Communications*, 134:112, 1997.

I.A. Pedrosa and A. Rosas. Electromagnetic field quantization in time-dependent linear media. *Physical Review Letters*, 103:010402, 2009.

J. Perina. Quantum-statistical properties of a nonlinear asymmetric directional coupler. *Journal of Modern Optics*, 42(7):1517–1522, 1995.

J. Perina Jr and J. Perina. Quantum statistics of nonlinear optical couplers. In E. Wolf, editor, *Progress in optics*, volume 41, pages 361–419. Elsevier Science B.V., 2000.

V. Perinová, A. Luks, J. Krepelka, C. Sibilia, and M. Bertolotti. Quantum statistics of light in a lossless linear coupler. *Journal of Modern Optics*, 38 (12):2429, 1991.

A. Peruzzo, M. Lobino, J.C.F. Matthews, N. Matsuda, A. Politi, K. Poulious, X.-Q. Zhou, Y. Lahini, N. Ismail, K. Wörhoff, Y. Bromberg, Y. Silberberg, M.G. Thompson, and J.L. O'Brien. Quantum walks for correlated photons. *Science*, 329:1500, September 2010.

M. Planck. Über eine verbesserung der wienschen spektralgleichung. *Verhandlungen der Deutschen Physikalischen Gesellschaft*, 2:202, 1900a.

M. Planck. Zur theorie des gesetzes der energieverteilung im normalspektrum. *Verhandlungen der Deutschen Physikalischen Gesellschaft*, 2:237, 1900b.

Alberto Politi, Martin J. Cryan, John G. Rarity, Siyuan Yu, and Jeremy L. O'Brien. Silica-on-silicon waveguide quantum circuits. *Science*, 2008.

H. Prakash and N. Chandra. Density operator of unpolarized radiation. *Physical Review A*, 4(2):796, 1971.

M.G. Raymer and A.C. Funk. Quantum-state tomography of two-mode light using generalized rotations in phase space. *Physical Review A*, 61: 015801, 1999.

M.G. Raymer, D.F. McAlister, and U. Leonhardt. Two-mode quantum-optical state measurement: sampling the joint density matrix. *Physical Review A*, 54(3):2397, 1996.

W.P. Schleich. *Quantum optics in phase space*. Wiley-VCH, Berlin, 2001.

S. Serulnik and Y. Ben-Aryeh. Space-time description of propagation in nonlinear dielectric media. *Quantum Optics*, 3:63–74, 1991.

P.J. Shadbolt, Verde M.R., A. Peruzzo, A. Politi, A. Laing, M. Lobino, J.C.F. Matthews, M.G. Thompson, and J.L. O'Brien. Generating, manipulating and measuring entanglement and mixture with a reconfigurable photonic circuit. *Nature Photonics*, 6(1):45, 2012.

Y.R. Shen. Quantum statistics of nonlinear optics. *Physical Review*, 155(3): 921–931, 1967.

J.W. Silverstone, D. Bonneau, K. Ohira, H. Yoshida, N. Iizuka, M. Ezaki, R.H. Hadfield, V. Zwiller, G.D. Marshall, J.G. Rarity, J.L. O'Brien, and M.G. Thompson. On-chip quantum interference between two silicon waveguide sources. *Nature Photonics*, 8(2):104, 2014.

J. Söderholm, G. Björk, and A. Trifonov. Unpolarized light in quantum optics. *Optics and Spectroscopy*, 91(4):532, 2001.

Justin B. Spring, Benjamin J. Metcalf, Peter C. Humphreys, W. Steven Kolthammer, Xian-Min Jin, Marco Barbieri, Animesh Datta, Nicholas Thomas-Peter, Nathan K. Langford, Dmytro Kundys, James C. Gates, Brian J. Smith, Peter G. R. Smith, and Ian A. Walmsley. Boson sampling on a photonic chip. *Science*, 339(6121):798, 2013.

R. Tanás and S. Kielich. Quantum fluctuations of the stokes parameters of light propagating in a kerr medium. *Journal of Modern Optics*, 37:1935, 1990.

M. Toren and Y. Ben-Aryeh. The problem of propagation in quantum optics, with applications to amplification, coupling of em modes and distributed feedback lasers. *Quantum Optics*, 6:425–444, 1994.

Unesco. International year of light and light-based technologies 2015, 2015. URL http://www.light2015.org/Home.html.

United Nations. International year of light and light-based technologies 2015. Resolution adopted by the General Assembly on 20 December 2013, December 2013.

W. Vogel and H. Risken. Determination of quasiprobability distributions in terms of probability distributions for the rotated quadrature phase. *Physical Review A*, 40(5):2847, 1989.

W. Vogel and D.-G. Welsch. *Lectures on Quantum Optics*. Akademie Verlag, Berlin, 1994.

D. F. Walls and G. J. Milburn. *Quantum Optics*. Springer Verlag, Berlin, 1994.

D.-G. Welsch, W. Vogel, and T. Opatrny. Homodyne detection and quantum state reconstruction. In E. Wolf, editor, *Progress in Optics*, volume XXXIX, page 63. Elsevier, 1999.

K.H. Yeon, H.J. Kim, Ch.I. Um, T.F. George, and L.N. Pandey. Wave function in the invariant representation and squeezed-state function of the time-dependent harmonic oscillator. *Physical Review A*, 50(2):1035, 1994.

USC
UNIVERSIDADE
DE SANTIAGO
DE COMPOSTELA

CHAPTER

TWO

QUANTUM THEORY OF THE MODE PROPAGATION IN INTEGRATED PHOTONIC DEVICES - CANONICAL APPROACH

THE present chapter is devoted to present a phenomenological theory about the propagation of quantum states of light in IPDs. This theory is based on the quantization of the classical EM flux of momentum using temporal modes and their orthogonality condition, turning out to be an useful and consistent tool in the study of propagation of quantum states of light. Likewise, this theory comprises all the different macroscopic features may present the optical media which make up the waveguide: it can deal with homogeneous and inhomogeneous media, lossless or lossy, as well as linear and nonlinear media. To this end, in section 1 we carry out a brief review of the classical theory of mode propagation in integrated waveguides, where we present concepts and relations we will use along this dissertation. In section 2 we accomplish a revision of the previous works our theory is based on, highlighting the essential concepts and contrasting the different points of view they show. In section 3 we introduce our quantum theory of mode propagation for the more general configuration, 1D vectorial modes. We quantize *ab initio* the Momentum operator and the vector fields and apply them to the calculation of Heisenberg propagation equations for linear and nonlinear coupling devices. Furthermore, we model lossy media by means of an effective coupling between the propagating modes and a reservoir. Finally, in section P1, we present a published research work where this theory is detailed and applied to linear and nonlinear mode coupling, with the specific example of a nonlinear 3-mode directional coupler, and a conference research work in section C1, where we show the specific application of this theory to the study of the generation of twin photon states in SOI waveguides.

2.1. Classical theory of mode propagation in IPDs

Integrated optical devices are the basic components of most of the devices which form the current optical communications, implemented in planar or channel waveguides processing the information that optical fibers route into them; the optical sensorization, which uses light to determine the variation of a certain magnitude in a medium via, for instance, a change in the refractive index or in the phase of an interferometric device; the optoelectronic signal processing, which transforms information carried by light into electrical signals by means of optical devices based on the electro-optic effect; and the optical processing of information, where an increasingly number of designs shows the ability to carry out computation with light [Hunsperger, 2009].

The science of integrated optics was born in the 1960s and is based on the transverse resonance of light in a higher refractive index area (core layer) than that corresponding to the surrounding substrate (top and bottom cladding layers), under certain boundary conditions the fields undergo in the discontinuities[1]. In this way optical waveguides are produced with $n_f > n_s, n_c$, where n_f, n_c and n_s are the core, the top cladding layer and the bottom cladding layer refractive indices, respectively (Figure 2.1.1a). Each one of these tranverse resonances is called optical propagation mode and it keeps its shape invariant along the waveguide. Every mode the waveguide structure allows propagates with a phase velocity under a limiting one (*cutoff*). This velocity is proportional to an effective refractive index with a value dependent on the fabrication parameters of the waveguide and the properties of light (frequency, polarization and so on). Depending on this value, either propagation of guided modes associated to a discrete spectrum is allowed, and the luminous energy is confined, or radiation modes appear, associated to a continuous spectrum and where the light is leaked to the surrounding. Guided modes show an oscillatory shape in the core and evanescent in the top and bottom cladding layers (Figure 2.1.1 b, c & d), and its transverse width is usually of the order of micro or nanometers. Likewise, the refractive index profile of the optical waveguide changes the mode structure as well. Depending on this profile the waveguides can be either step index (*STIN*), where the refractive index varies abruptly, or gradient index (*GRIN*), where the profile changes smoothly. In this last case the profiles can show various shapes: gaussian, parabolic, exponential and so on; which turn out into different spatial profiles for each optical mode.

[1] For sizes high enough ($>> \lambda$), this feature is analogous to the total internal reflection of plane waves under certain interference conditions, so-called *modal total internal reflection* (MTIR).

2.1.1. Optical modes

The propagation of light through any macroscopic medium is ruled in the classical regime by the Maxwell's equations. Under the usual premisses in integrated optics, that is, a region of space without EM sources and a field with an harmonic time dependence with frequency ω[2], the equations can be written as:

$$\nabla \wedge \mathbf{E} = i\omega\mu\mathbf{H}, \tag{2.1.1}$$
$$\nabla \wedge \mathbf{H} = -i\omega\epsilon\mathbf{E}, \tag{2.1.2}$$
$$\nabla \cdot \epsilon\mathbf{E} = 0, \tag{2.1.3}$$
$$\nabla \cdot \mu\mathbf{H} = 0, \tag{2.1.4}$$

with $\mathbf{E}$ and $\mathbf{H}$ the electric and magnetic fields, respectively; μ the permeability of the medium and ϵ the permittivity, which for non-dispersive media is given by $\epsilon(\omega, \mathbf{r}) = \epsilon(\mathbf{r})$, and which is related to the refractive index $n(\mathbf{r})$ via the Maxwell's relation $\epsilon(\mathbf{r}) = \epsilon_0 n^2(\mathbf{r})$, with ϵ_0 the vacuum permittivity and $\mathbf{r} = (x, y, z)$.

Let us consider monochromatic guided vector modes with frequency ω. Carrying out a rigorous analysis for waves propagating in the direction $\mathbf{z}$ through an 1D[3] waveguide, characterized by a refractive index profile with tranverse dependence $n(x, y)$, the vector field solutions for equations (2.1.1 - 2.1.4) will be given by [Kogelnik, 1988]:

$$\mathbf{E}_\nu(x, y, z, t) = \mathbf{E}_\nu(x, y) \exp\{i(\beta_\nu z - \omega t)\}, \tag{2.1.5}$$
$$\mathbf{H}_\nu(x, y, z, t) = \mathbf{H}_\nu(x, y) \exp\{i(\beta_\nu z - \omega t)\}, \tag{2.1.6}$$

solutions known as modal fields, where β_ν is the propagation constant of the ν-mode, with $\nu \in \mathbb{Z}^\star$, and $\{\mathbf{E}_\nu(x, y), \mathbf{H}_\nu(x, y)\}$ are the complex vector amplitudes of the guided modes. We should indicate that we need two subscripts ρ, σ for each mode. In fact, the propagation constant β would be a function of these ρ and σ, however, for the sake of expositional convenience, we use the contracted notation $\nu \equiv \rho\sigma$. Every solution, characterized by the subscript ν, is the so-called propagation mode and represents the wave propagating in the direction $\mathbf{z}$ with a phase velocity $v_\nu = \omega/\beta_\nu$. This enables to define the waveguide effective refractive index $N_\nu = \beta_\nu/k_0$, with $k_0 = \omega\sqrt{\epsilon_0\mu_0}$ the vacuum propagation constant, which can be interpreted as the index an homogeneous medium would show for a propagating wave given by (2.1.5, 2.1.6).

[2]The harmonic time dependence we assume can be written as $\mathbf{A}_R(t) = \frac{1}{2}(\mathbf{A}e^{-i\omega t} + \mathbf{A}^* e^{i\omega t})$, with $\mathbf{A}_R$ a real vectorial field and $\mathbf{A}$ a complex vectorial field.

[3]1D stands for propagation of light only in one direction, being localized in the other two. The propagation in 2D optical waveguides is a particular case of it.

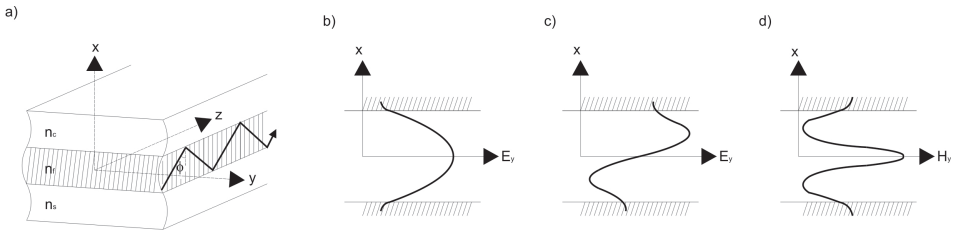

Figure 2.1.1: Sketch of : a) the geometry of the slab optical waveguide and modal total internal reflection (MTIR), b) the electric field cross-sectional distribution in a symmetric planar waveguide for a fundamental TE mode, c) the electric field cross-sectional distribution in a symmetric planar waveguide for the first TE mode, d) the magnetic field cross-sectional distribution in a symmetric planar waveguide for the second TM mode.

Substitution of solutions (2.1.5, 2.1.6) into Maxwell's equations (2.1.1 - 2.1.4), leads to:

$$\nabla_t \wedge \mathbf{E}_\nu + i\beta_\nu \mathbf{u}_z \wedge \mathbf{E}_\nu = i\omega\mu_0 \mathbf{H}_\nu, \tag{2.1.7}$$

$$\nabla_t \wedge \mathbf{H}_\nu + i\beta_\nu \mathbf{u}_z \wedge \mathbf{H}_\nu = -i\omega\epsilon_0 n^2 \mathbf{E}_\nu, \tag{2.1.8}$$

where $\nabla_t = (\partial/\partial x, \partial/\partial y, 0)$, $\mathbf{u}_z$ is an unitary vector in the $\mathbf{z}$ direction, that is, perpendicular to the transverse section of the waveguide, and where the guided mode amplitudes can be split into transverse field components $\{\mathbf{E}_{t\nu}(x,y),\ \mathbf{H}_{t\nu}(x,y)\}$ and longitudinal field components $\{\mathbf{E}_{z\nu}(x,y),\ \mathbf{H}_{z\nu}(x,y)\}$. These relations bring about a wave equation (or eingenvalue equation), formally similar to the time-independent Schrödinger equation from quantum mechanics, which provides solutions to the fields $\{\mathbf{E}_\nu, \mathbf{H}_\nu\}$ (eigenfunctions) along with the associated propagation constant β_ν (eigenvalue).

There are some fundamental relations in the modal theory of integrated optics which will be useful later on: the modal norm and the orthonormalization condition. From equations (2.1.7, 2.1.8), via standard procedures based on the Lorentz reciprocity theorem for optical waveguides, the following modal norms on a cross section z of the waveguide are obtained [Kogelnik, 1988]:

$$\|\mathbf{E}_\nu\| \equiv \|\mathbf{H}_\nu\| = \left\{2\,\mathrm{sgn}(\nu)\int\{\mathbf{E}_{t\nu} \wedge \mathbf{H}^*_{t\nu}\}\,\mathbf{u}_z\,dxdy\right\}^{1/2}, \tag{2.1.9}$$

where the function $\mathrm{sgn}(\nu)$ is defined to be +1 if $\nu > 0$, and -1 if $\nu < 0$. Likewise, denoting $\mathbf{e}_{t\nu}$ and $\mathbf{h}_{t\nu}$ as the transverse components of the normalized guided modes, the following quasi-complete orthonormalization condition on a cross section of the waveguide is derived:

$$2\,\mathrm{sgn}(\nu)\int\{\mathbf{e}_{t\nu} \wedge \mathbf{h}^*_{t\nu'}\}\,\mathbf{u}_z\,dxdy = \delta_{|\nu|,|\nu'|}, \tag{2.1.10}$$

where $\delta_{|\nu|,|\nu'|}$ is the Kronecker's delta function. This condition is called quasi-complete because for modes with $\nu = -\nu'$, (2.1.10) is not zero.

Another important expression is obtained carrying out scalar products of the modal equations (2.1.7, 2.1.8) with the appropriate modal field components and combining the results in an appropriate way, getting the following relations:

$$\nabla_t \left(\mathbf{E}_{z\nu} \wedge \mathbf{H}^{\star}_{t\nu}\right) + i\beta_\nu \mathbf{u}_z \left(\mathbf{E}_{t\nu} \wedge \mathbf{H}^{\star}_{t\nu}\right) = i\omega(\mu_o \mathbf{H}_{t\nu}\mathbf{H}^{\star}_{t\nu} - \epsilon \mathbf{E}_{z\nu}\mathbf{E}^{\star}_{z\nu}), \quad (2.1.11)$$

$$\nabla_t \left(\mathbf{E}_{t\nu} \wedge \mathbf{H}^{\star}_{z\nu}\right) + i\beta_\nu \mathbf{u}_z \left(\mathbf{E}_{t\nu} \wedge \mathbf{H}^{\star}_{t\nu}\right) = i\omega(\mu_o \mathbf{H}_{z\nu}\mathbf{H}^{\star}_{z\nu} - \epsilon \mathbf{E}_{t\nu}\mathbf{E}^{\star}_{t\nu}). \quad (2.1.12)$$

Integrating over the waveguide cross section and taking into account the 2D divergence theorem, we obtain the following relevant expression [Kogelnik, 1988]:

$$\mathrm{sgn}(\nu)\|\mathbf{E}_\nu\|^2 \beta_\nu \equiv \mathrm{sgn}(\nu)\|\mathbf{H}_\nu\|^2 \beta_\nu = \omega(W_{t\nu} - W_{z\nu}), \quad (2.1.13)$$

where $P_\nu = \mathrm{sgn}(\nu)\|\mathbf{E}_\nu\|^2$ is the modal power or energy flow (positive for forward modes and negative for backward modes) and where $W_{t\nu} = W^e_{t\nu} + W^m_{t\nu}$ and $W_{z\nu} = W^e_{z\nu} + W^m_{z\nu}$ are the total transverse and longitudinal energy densities per unit length under temporal averaging, respectively, defined as:

$$W^e_\nu = W^e_{t\nu} + W^e_{z\nu} = \int dxdy\, \epsilon_0 n^2\, \mathbf{E}_{t\nu}\mathbf{E}^*_{t\nu} + \int dxdy\, \epsilon_0 n^2\, \mathbf{E}_{z\nu}\mathbf{E}^*_{z\nu}, \quad (2.1.14)$$

$$W^m_\nu = W^m_{t\nu} + W^m_{z\nu} = \int dxdy\, \mu_o \mathbf{H}_{t\nu}\mathbf{H}^*_{t\nu} + \int dxdy\, \mu_o \mathbf{H}_{z\nu}\mathbf{H}^*_{z\nu}, \quad (2.1.15)$$

with W^e_ν and W^m_ν the corresponding electric and magnetic energy densities per unit length, respectively.

Finally, we make reference to the dimensions of light confinement, since this feature modifies the wave equation and the modal solutions. In this way we can classify the integrated structures as slab or planar waveguides (Figure 2.1.1a) with confinement in one spatial dimension (2D), and channel waveguides (Figure 2.1.2) with confinement in two spatial dimensions (1D). Slab waveguides show two kinds of modal solutions: the tranverse electric modes (TE) (Figure 2.1.1b & c), where there is no longitudinal electric field component ($E_z = 0$), and the transverse magnetic modes (TM) (Figure 2.1.1 d), with the longitudinal magnetic field component vanishing ($H_z = 0$). These modes lead to scalar wave equations for the components of every solution. On the other hand, 1D waveguides present fully vectorial modes, with the six components different from zero, fulfilling a vectorial wave equation. These modes can be regarded as *quasi*-TE (QTE) and *quasi*-TM (QTM) when the width of the core is higher than its thickness, a condition usually fulfilled to accomplish single mode regime. In Figure 2.1.2 we show the simulated E_x-field component of the fundamental quasi-TE mode propagated in a channel waveguide.

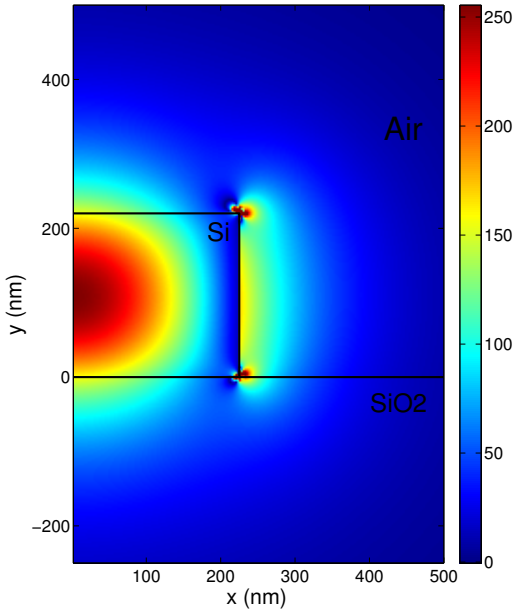

Figure 2.1.2: Normalized E_x-field component of the fundamental quasi-TE mode propagated in a 450×220 nm^2 *Silicon on insulator* channel waveguide. Simulation carried out with *Modesolver* for $\lambda = 1.55\mu$m, $n_{Si} = 3.5$ and $n_{SiO_2} = 1.56$.

2.1.2. Mode coupling in IPDs

The propagation modes of integrated optical waveguides show mode coupling, a feature many IPDs used in the current communication, metrology and computation technologies are based on. The mode-coupling theory is a very useful mathematical tool in the analysis of a great number of optical phenomena and devices based on mode propagation: waveguides as well as optical fibers, integrated gratings, directional couplers and so on. By this method, we obtain the relations between the modes propagating in the integrated system, characterizing the devices based on mode interaction. Right after, we present the derivation of the classical equations for mode coupling.

Maxwell's equations (2.1.1,2.1.2) in the presence of sources, represented by a polarization $\mathbf{P}(\mathbf{r})$, take the following form:

$$\nabla \wedge \mathbf{E} = i\omega\mu\mathbf{H}, \tag{2.1.16}$$

$$\nabla \wedge \mathbf{H} = -i\omega\epsilon\mathbf{E} - i\omega\mathbf{P}. \tag{2.1.17}$$

Taking two different solutions of these equations, each one with a polarization $\mathbf{P}$, we obtain the following expression [Kogelnik, 1988]:

$$\nabla \cdot (\mathbf{E}_1 \wedge \mathbf{H}_2^* + \mathbf{E}_2^* \wedge \mathbf{H}_1) = i\omega\mathbf{P}_1\mathbf{E}_2^* - i\omega\mathbf{P}_2^*\mathbf{E}_1 \tag{2.1.18}$$

Considering the solution 2 as a canonical mode of the unperturbed waveguide, that is $\mathbf{P}_2 = 0$, integrating over the cross section of the waveguide and applying the divergence theorem, we get:

$$\iint_{-\infty}^{+\infty} dxdy\, \partial_z(\mathbf{E}_1 \wedge \mathbf{H}_2^* + \mathbf{E}_2^* \wedge \mathbf{H}_1)|_z = i\omega \iint_{-\infty}^{+\infty} dxdy\, \mathbf{P}_1 \mathbf{E}_2^* \tag{2.1.19}$$

On the other hand, we apply the mode expansion of the field 1:

$$\mathbf{E}_1 = \sum_\nu (a_\nu + b_\nu)\mathbf{E}_{t\nu}, \quad \mathbf{H}_1 = \sum_\nu (a_\nu - b_\nu)\mathbf{H}_{t\nu}, \tag{2.1.20}$$

where $a_\nu(z)$ and $b_\nu(z)$ are the coefficients for the forward and backward ν modes, respectively, and $\{\mathbf{E}_{t\nu}, \mathbf{H}_{t\nu}\}$ the transverse part of the field vectors. Choosing the canonical optical field 2 exicted in a particular forward μ mode:

$$\mathbf{E}_2 = \mathbf{E}_{t\mu} e^{i\beta_\mu z}, \quad \mathbf{H}_2 = \mathbf{H}_{t\mu} e^{i\beta_\mu z}, \tag{2.1.21}$$

applying them to (2.1.19), and bearing in mind the modal orthogonality relation (2.1.10), the following coupled-mode equation is obtained:

$$\partial_z a_\mu = i\beta_\mu a_\mu + i\omega \int_{-\infty}^{+\infty} dxdy\, \mathbf{P}\, \mathbf{E}_{t\mu}^*. \tag{2.1.22}$$

This equation rules the classical interaction between the guided modes propagating in an optical integrated system via an arbitrary polarization $\mathbf{P}(\mathbf{r})$, which stands for anisotropy, nonlinearity and so on.

2.1.3. Nonlinear optics

The nonlinear response of a medium produced by the propagation of optical radiation, that is the nonlinear optics, is characterized by the effects caused by an intense optical field in the electric polarization of the medium in which is propagating. This optical field brings about an electric dipole moment which, likewise, reemits new waves which interact with the original one, leading to different nonlinear phenomena. Therefore, the electric polarization of the medium (macroscopic variable) is obtained adding up the induced dipole moments of the medium (microscopic variable).

In nonlinear optics, since the polarization of a medium depends on the induced electric field, it is described as a power series of the field, where each term of order n is dependent on the nth power in the electric field:

$$\mathbf{P}(\mathbf{r}, t) = \mathbf{P}^{(1)}(\mathbf{r}, t) + \mathbf{P}^{(2)}(\mathbf{r}, t) + \mathbf{P}^{(3)}(\mathbf{r}, t) + ... + \mathbf{P}^{(n)}(\mathbf{r}, t). \tag{2.1.23}$$

Each polarization order produces different optical phenomena: the first order term $\mathbf{P}^{(1)}$ describes the usual phenomena in linear optics like refraction, reflection, diffraction and so on; on the other hand, second order term

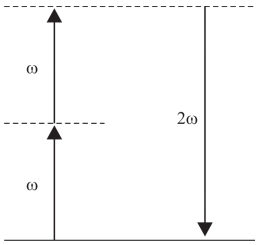

Figure 2.1.3: Sketch showing the mix of frequencies leading to generation of the second harmonic (SHG).

$\mathbf{P}^{(2)}$ brings about second harmonic generation (*SHG*), sum and difference frequency generation, parametric down-conversion (*PDC*) and so on; the third order $\mathbf{P}^{(3)}$ third harmonic generation (THG), self-phase modulation (SPM), four wave mixing (FWM) and so on; and even higher order processes are possible as well.

In this dissertation we will focus our attention on the second and thrid order polarization, since they are the cause of the main phenomena currently used in the generation of quantum states of light, namely the second harmonic generation, spontaneous parametric down conversion and four wave mixing, although higher order nonlinear processes can be studied via the theory here presented. In terms of exchange of photons, the SHG lies in the absorption of two photons with frequency ω by the medium, generating an excited state of energy, which returns to the fundamental state by means of releasing one photon of frequency 2ω (Figure 2.1.3). This is the degenerate case of the sum frequency generation. Likewise, PDC is the reverse process. One photon with higher energy generates two lower energy photons after propagation in the nonlinear medium. If the two photons have the same frequency the process is called *degenerate*. Likewise, in the case of FWM, a third order polarization effect, two photons with the same or different frequencies are absorbed generating two new photons with different frequencies.

Furthermore, it is important to outline that these phenomena are dependent on the symmetry properties of the induced polarization. On one hand, quadratic polarization only appears in noncentrosymmetric materials, due to the lack of inversion symmetry. However, in media which shows this feature, called centrosymmetric or isotropic materials, the even polarization orders are zero, because in these materials the polarization keeps invariant under change in the sign of the electric field [Boyd, 1992].

The general second order polarization which describes the mixing of two frequencies ω_i and ω_j, is given by the following tensor product:

$$\mathbf{P}^{(2)}(\mathbf{r},\omega) = \epsilon_0 \chi^{(2)}(\omega_i,\omega_j) : \mathbf{E}(\mathbf{r},\omega_i)\,\mathbf{E}(\mathbf{r},\omega_j), \tag{2.1.24}$$

where $\omega = \omega_i + \omega_j$ and $\chi^{(2)}$ is the second order electric susceptibility of

the medium. This polarization is responsible for the sum frequency wave generation, due to the mixing of frequencies of two monochromatic waves. For instance, in the case of SHG, we have $\omega_i = \omega_j \equiv \omega$, so a double frequency wave 2ω is produced. Likewise, $\chi^{(2)}$ is a third order tensor with 3×9 components, in consequence the nonlinear polarization (2.1.24) for each component in the SHG is given by:

$$\mathbf{P}_i^{(2)}(2\omega) = \epsilon_0 \sum_{jk} \chi_{ijk}^{(2)}(\omega,\omega)\,\mathbf{E}_j(\omega)\,\mathbf{E}_k(\omega), \tag{2.1.25}$$

with $i,j,k = x,y,z$. Due to the change between indices j and k has no physical significance, it is usual to replace both by a single index, which leads to the contracted tensor with 3×6 elements d_{ij} [Yariv, 1975]. The processes derived from quadratic interaction, like the electro-optic effect, parametric conversion, amplification and the SHG as well, are studied by applying this kind of relations into (2.1.22).

Finally, the third order polarization which represents the mix of 3 frequencies is given by the following tensor product:

$$\mathbf{P}^{(3)}(\mathbf{r},\omega) = \epsilon_0\,\chi^{(3)}(\omega_i,\omega_j,\omega_k) : \mathbf{E}(\mathbf{r},\omega_i)\,\mathbf{E}(\mathbf{r},\omega_j)\,\mathbf{E}(\mathbf{r},\omega_k), \tag{2.1.26}$$

where $\omega = \omega_i + \omega_j + \omega_k$ and $\chi^{(3)}$ is the third order electric susceptibility of the medium with 3×27 components. As an example, in the case of degenerate FWM, the ith component of (2.1.26) would be given by:

$$\mathbf{P}_i^{(3)}(\omega_{1,2}) = 3\epsilon_0 \sum_{jkl} \chi_{ijkl}^{(3)}(\omega,\omega,-\omega_{2,1})\,\mathbf{E}_j(\omega)\,\mathbf{E}_k(\omega)\,\mathbf{E}_l(-\omega_{2,1}), \tag{2.1.27}$$

with $i,j,k = x,y,z$ and $\omega_{1,2}$ are the frequencies of the new waves fulfilling $2\omega = \omega_1 + \omega_2$. The factor 3 in is consequence of the intrinsic permutation symmetry of $\chi^{(3)}$ [Boyd, 1992]. Other third and higher order nonlinear effects can be tackled in the same way.

2.2. Foundations of the quantum theory of propagation

The description of the mode coupling based on the Maxwell's equations above presented works finely in the analysis of linear and nonlinear common IPDs which show macroscopic sizes and run with classical light. The problem appears when we need to take into account quantum effects in the light-matter interaction within photonic materials, because of either extreme miniaturization of components (quantum dots and so on) or in the generation, manipulation and detection of quantum states of light in IPDs.

In these cases classical theory fails. For instance, research in ultra-sensitive photonic sensors with resolution below the diffraction limit is based on the use of squeezed states of light, or quantum cryptography and computing, two current technologies which are turning upside down communications and computation and which are based on the manipulation of entangled quantum states [O'Brien et al., 2009]. This is the reason because we need a quantum theory which describes in a precise way the operation these photonic devices carry out. Therefore, we introduce in the following sections our quantum theory of mode propagation. To begin, we present a brief review of the development of this theory in bulk optics, where we present its main concepts and the reasons why it is necessary, paving the way to our theory for guided modes we will present in the next section.

Around the first years of the 1990s a series of fundamental studies in the context of propagation of quantum light was carried out, induced by the inconsistencies resulting from the application of the conventional (or standard) Hamiltonian theory [Haken, 1981] to the study of spatial propagation of waves in dielectric media. This standard theory is based both on the quantization of the EM energy[4] in the vacuum enclosed in a volume V:

$$\hat{H} = \int_{\mathcal{V}} \hat{\mathcal{H}}\, dV, \tag{2.2.28}$$

where $\hat{\mathcal{H}}$ is the energy density in the volume, and also on the condition of spatial periodicity of the mode in the volume, given by:

$$k_\rho = \frac{2\pi\rho}{L}, \tag{2.2.29}$$

for the one dimensional case, with k_ρ the vacuum propagation constant in every possible mode ρ associated to the volume and L the quantization length. In this way the field is characterized in terms of spatial modes.

From classical field theory [Landau and Lifshitz, 1973] it is well known that the hamiltonian $\hat{H}$ is the generating function of temporal evolution for a given operator $\hat{\Omega}$ according to:

$$\frac{\partial \hat{\Omega}}{\partial t} = -\frac{i}{\hbar}[\hat{\Omega}, \hat{H}], \tag{2.2.30}$$

where $[\,,\,]$ stands for the commutator operator. By means of this approach the quantum optical field in vacuum is given as follows [Mandel and Wolf, 1995]:

$$\hat{\mathbf{e}} = \frac{i\sqrt{\hbar\omega}}{\sqrt{2\epsilon_0 V}} \sum_\rho \left\{ [\hat{a}(k_\rho, t)\mathbf{E}_\rho e^{ik_\rho z} - \hat{a}^\dagger(k_\rho, t)\mathbf{E}_\rho^* e^{-ik_\rho z}] \right\}, \tag{2.2.31}$$

[4] Or equally the function which represents it: the Hamiltonian $\hat{H}$.

with $\{\hat{a}, \hat{a}^\dagger\}$ the usual operators standing for absorption and emission of one photon in the quantization volume, respectively. This formulation has been shown successful describing the spontaneous emission effect and quantum effects of EM fields in cavities [Loudon, 1982].

On the other hand, when working with propagating fields, the standard method consists on an analogy between temporal evolution and spatial propagation:

$$\hat{G} = \mathbf{z}\,\hat{H}/v, \tag{2.2.32}$$

where $\hat{G}$ is the Momentum operator, the generator of spatial displacement along a given axis, in this case $\mathbf{z}$, and where the connection between space and time is established by using an effective interaction time $t = -z/v$, with z the length of the medium and v the effective velocity of light in the medium [Perinová et al., 1991, Shen, 1967]. This approach to the propagation problem has two fundamental limitations: on one hand, this identity implies the loss of one variable, so this formalism only describes the propagation of stationary states, that is those temporally invariant; on the other hand, this approach can not be applied rigorously to dispersive media, since in this media each frequency propagates at a different velocity $v(\omega)$. Therefore $t(\omega) = -z/v(\omega) \equiv zn(\omega)/c$, with $n(\omega)$ the refractive index in the volume V, and we would need a temporal variable for each frequency [Huttner et al., 1990]. So, in this case, the use of the previous identity is no longer possible. This argument can also be used to justify that the standard Hamiltonian formulation is unable to describe the counterpropagation because a negative time would be required [Ben-Aryeh et al., 1992, Toren and Ben-Aryeh, 1994].

Furthermore, applying this approach to linear dielectric media, the energy density would increase according to the inclusion of a polarization term, such that the total system energy would also rise [Abram, 1987]:

$$\hat{H}_{out} = \frac{1}{2}\int_{\mathcal{V}} (\epsilon_0 E^2 + \mu_0 H^2)\,dV, \qquad \hat{H}_{in} = \frac{1}{2}\int_{\mathcal{V}} (\epsilon_0 E^2 + \mu_0 H^2 + \mathbf{EP})\,dV, \tag{2.2.33}$$

where $\hat{H}_{out}$ and $\hat{H}_{in}$ stand for the vacuum and dielectric energies, respectively. Thus, for every non-zero polarization $\mathbf{P}$, the spatial integral would increase with respect to the vacuum one. This would lead to a frequency renormalization [Gerry and Knight, 2005]:

$$\hat{\Omega}(t) = e^{i\hat{H}t/\hbar}\hat{\Omega}(0)e^{-i\hat{H}t/\hbar}, \tag{2.2.34}$$

solution of (2.2.30), where $\hat{\Omega}$ is a given operator and $\hat{H}/\hbar \propto \omega$. This result leads to a inconsistence with experience, since there is no known experiment where propagation through a linear medium changes the frequency of the wave. Likewise, in the case of longitudinally inhomogeneous dielectric media[5], the standard theory is not valid either, since the integration

[5] That is z-dependent media.

in a volume V (2.2.28) eliminates the z-inhomogeneities by spatial averaging. Accordingly, modal phase mismatching, which can be regarded as a z-inhomogeneity to a certain extent, shows the same problem [Toren and Ben-Aryeh, 1994].

Another phenomenological approach widely used has been to take the classical Maxwell's equations in operational form and imposing commutation relations (C.R.) to the emission and absorption operators $\{\hat{a}^\dagger, \hat{a}\}$. Nevertheless, these C.R. have not been justified in a quantum canonical way and the physical interpretation of these operators has not been specified either [Caves and Crouch, 1987].

Due to these problems and the appearance of original experiments with non-classical states of light, it was necessary a new, rigorous and consistent theory able to describe the propagation of quantum states of light. From the classical field theory is known that the Momentum $\hat{G}$ produces the spatial equation of motion as follows [Landau and Lifshitz, 1973]:

$$\frac{\partial \hat{\Omega}}{\partial z} = \frac{i}{\hbar}[\hat{\Omega}, \hat{G}], \tag{2.2.35}$$

relation easily arguable in terms of the identity $z = -vt$ with (2.2.30) [Shen, 1967]. Considering this, Abram [Abram, 1987] proposes a quantum mechanical theory for the study of spatial propagation of light which solves the problem of energy increase in a dielectric medium (2.2.33). To this end, he takes a Hamiltonian $\hat{H}$ proportional to the energy flux $\hat{\mathbf{S}}$, conserved quantity for a vawe passing through dielectric media, and a Momentum operator $\hat{\mathbf{G}}$ proportional to the T^{33} element of the Maxwell energy-momentum tensor $\mathbf{T}$; both taken in a varying quantization volume such that $\hat{H}$ and $\hat{\mathbf{G}}$ continue invariant. This approach reproduces the results of classical optics, but it does not resolve the frequency dispersion problem above introduced, as in this case every mode should be quantized in a different volume because of energy conservation.

In spite of its limitations, this study shows original viewpoints which later Huttner, Serulnik and Ben-Aryeh will recover to draw up a new quantum theory of propagation [Huttner et al., 1990]. This is based on the use of a quantization period T with a time periodicity of the fields:

$$\omega_\rho = \frac{2\pi\rho}{T}, \tag{2.2.36}$$

instead of a volume V with spatial periodicity (2.2.29); and on the use of temporal modes and space-dependent operators instead on spatial modes and time-dependent operators:

$$\{\hat{a}(k_\rho, t), \hat{a}^\dagger(k_\rho, t)\} \to \{\hat{a}(z, \omega_\rho), \hat{a}^\dagger(z, \omega_\rho)\}, \tag{2.2.37}$$

with $\hat{a}$ and $\hat{a}^\dagger$ the annihilation and creation operators, respectively, associated to each mode ρ. This last hypothesis is a wise choice, since monochro-

matic temporal modes keep invariant inside and outside of the medium, as their frequency remains unchanged.

On the other hand, Huttner *et al.* follows Abram's idea about time evolution based on energy flux:

$$\hat{H} = \int_{t_0}^{t_0-T} \hat{S}(z,t)\,dt, \tag{2.2.38}$$

not medium-dependent unlike the energy density (2.2.33); while the spatial propagation is obtained from a Momentum operator:

$$\hat{G} = \int_{t_0}^{t_0+T} \hat{g}(z,t)\,dt, \tag{2.2.39}$$

where $\hat{g} = (\hat{\mathbf{D}} \wedge \hat{\mathbf{B}})_z \equiv T^{03}$ is the EM Momentum density operator in the **z** direction, with $\hat{\mathbf{D}}$ the electric displacement field given by $\hat{\mathbf{D}} = \epsilon_o \hat{\mathbf{E}} + \hat{\mathbf{P}}$. Huttner *et al.* choose a different element of the Maxwell's energy-momentum tensor **T** from Abram which, as it can be seen below, will produce theoretically inconsistent results.

Furthermore, another main concept arises from the use of temporal modes. That is the definition of apropriate C.R.: local or equal-space commutation relations (ESCR) instead of the canonical equal-time commutation relations (ETCR):

$$[\hat{a}(z,\omega_\rho), \hat{a}^\dagger(z,\omega_\sigma)] = \delta_{\rho,\sigma}, \tag{2.2.40}$$

where $\delta_{\rho,\sigma}$ is the Kronocker delta. Caves and Crouch showed in [Caves and Crouch, 1987] that the ESCR are compatible with a canonical quantization procedure.

On the surface, this theory leads to consistent results, but it carries on being a phenomenological one. It was necessary to give it solid foundations and derive it from first principles. With this in mind, Ben-Aryeh and Serulnik introduced two original studies, [Serulnik and Ben-Aryeh, 1991] and [Ben-Aryeh and Serulnik, 1991], where they tackle the propagation problem from a four-dimensional Lagrangian theory of the Maxwell's energy-momentum tensor **T** [Landau and Lifshitz, 1973]. These works introduce a reformulation of the Hillery and Modlinov's theory [Hillery and Modlinow, 1984] where they present a Lagrangian approach to the quantum electrodynamics in nonlinear media. This is based on the definition of new scalar and vector potentials which simplify the calculus of the tensor version of Maxwell equations. From these, and taking into account the polarization effects in nonlinear media, they get the Lagrangian and Hamiltonian densities which describe the EM fields and their interaction with polarization. Applying this result to the energy-momentum stress tensor and the

quantization principle[6], they obtain the quantum tensor which holds complete information about the EM field in the nonlinear medium (and linear as a particular case). Each element of this tensor represents a well-known variable in the following way:

$$\hat{T}^{\nu\mu} = \begin{bmatrix} \hat{\mathcal{H}} & \hat{g}_x & \hat{g}_y & \hat{g}_z \\ \hat{S}_x & \hat{\sigma}_{xx} & \hat{\sigma}_{xy} & \hat{\sigma}_{xz} \\ \hat{S}_y & \hat{\sigma}_{yx} & \hat{\sigma}_{yy} & \hat{\sigma}_{yz} \\ \hat{S}_z & \hat{\sigma}_{zx} & \hat{\sigma}_{zy} & \hat{\sigma}_{zz} \end{bmatrix} \tag{2.2.41}$$

with $\nu, \mu = 0, 1, 2, 3$, which stands for the time and each spatial dimension in the usual way. The tensor element $\hat{T}^{00}$ represents the energy density. The vector with elements $\hat{T}^{\nu 0}$ is the Poynting vector $\hat{\mathbf{S}}$ and accounts for the flux of energy density in the ν direction. Likewise, the vector with elements $\hat{T}^{0\mu}$ is the density of vectorial momentum $\hat{\mathbf{g}} \propto (\hat{\mathbf{D}} \wedge \hat{\mathbf{B}})$ in the μ direction. Finally, the $\hat{\sigma}$ 3×3 tensor represents the flux of the momentum density, where the columns μ describe the components of the momentum and the rows refer to a flux of the momentum in the propagation direction ν. Moreover, as was commented above, this tensor comprises information about the polarization of the medium, containing the linear and nonlinear features of the medium.

From $\hat{\mathbf{T}}$, equations (2.2.30) and (2.2.35) can be generalized to the four dimensional case as:

$$\frac{\partial \hat{\Omega}}{\partial \chi_\nu} = -\frac{i}{\hbar}[\hat{\Omega}(\chi), \hat{p}^\nu], \tag{2.2.42}$$

with χ a space-time point and where the displacement operator in the ν direction $\hat{p}^\nu$ is worked out via an integral over the corresponding hypersurface:

$$\hat{p}^\nu = \int_\sigma \hat{T}^{\nu\mu}(\chi) d\Sigma_\mu, \tag{2.2.43}$$

where $d\Sigma_\mu = (dxdydz, cdtdydz, cdtdxdz, cdtdxdy)$. With this formulation, the time evolution for a given operator $\hat{\Omega}$ is given by:

$$\frac{\partial \hat{\Omega}(\mathbf{r}, t)}{\partial t} = -\frac{i}{\hbar} \int d^3r' [\hat{\Omega}(\mathbf{r}', t), \hat{T}^{00}(\mathbf{r}', t)], \tag{2.2.44}$$

with $\hat{T}^{00} \equiv \hat{\mathcal{H}}$, so this expression is identical to (2.2.30). In geometrical terms, the right part of (2.2.44) represents the propagation perpendicular to an hyperplane where integration is performed and where, in the case of time, this propagation direction is ct. Likewise, in the case of spatial dependence, a Momentum operator is required. Serulnik and Ben-Aryeh use the previous relations to show which is the true Momentum operator related to propagation: following the steps of Huttner *et al.*, they apply

[6] Transforming classical variables into quantum operators which fulfill C.R.

the element of density of vectorial momentum $T^{0\mu}$ over an equitemporal surface $d\Sigma_0$. Looking for recovering the Maxwell equations, the electric field operator and the propagation direction **z** are chosen. Applying (2.2.42-2.2.43), the next expression is obtained:

$$\frac{\partial \hat{E}_i(\mathbf{r},t)}{\partial z} = -\frac{i}{\hbar}\int d^3r'[\hat{E}_i(\mathbf{r}',t),(\hat{\mathbf{D}}(\mathbf{r}',t)\wedge\hat{\mathbf{B}}(\mathbf{r}',t))_z], \tag{2.2.45}$$

which, after working out the right part of the equation, leads to:

$$= \frac{\partial \hat{E}_i(\mathbf{r},t)}{\partial z}. \tag{2.2.46}$$

This is an identity and therefore implies that (2.2.45) is not a true equation of motion (and to the same extent that in [Huttner et al., 1990]). As above commented, propagation along a direction implies integration on the perpendicular hyperplane. So, in our case, with propagation in the direction **z**, the chosen hyperplane should be $d\sigma_3 = cdtdxdy$, leading to the following equation of propagation:

$$\frac{\partial \hat{\Omega}}{\partial z} = \frac{i}{\hbar}[\hat{\Omega},\hat{p}^3], \tag{2.2.47}$$

where:

$$\hat{p}^3 \equiv \hat{M} = \iiint \hat{T}^{33} cdtdxdy \tag{2.2.48}$$

and with $\hat{M}$ the scalar quantum Momentum operator. Therefore, using (2.2.47), the spatial progression of any operator can be calculated in a consistent way[7].

Likewise, Ben-Aryeh and Serulnik use temporal modes (2.2.37) and the periodicity condition (2.2.36) in a volume of quantization AcT, where they reinterpret the number of photons in a volume V as the number of photons of a light beam passing through a cross section A during a time T. This is directly related with photodetection, where the flux of photons detected is that which is incident on the photodetector area A during a certain time T.

On the other hand, regarding to dielectric media, they use the following insight proposed by Abram [Abram, 1987], that is to take from classical optics the relations between the vacuum and the dielectric:

$$\hat{E}_{in} = \frac{\hat{E}_{out}}{\sqrt{n}}, \qquad \hat{B}_{in} = \hat{B}_{out}\sqrt{n}, \tag{2.2.49}$$

where the subscripts 'in' and 'out' stand for the fields within the dielectric and free space, respectively, and n is the refractive index of the medium. These relations come from the fact that the flux of energy is conserved

[7] The sign in (2.2.47) has been changed with respect to (2.2.42) to follow our prescription.

when an EM wave finds a dielectric medium in its propagation. With these premises, they propose the following heuristic quantum fields:

$$\hat{E}(z,t) = \sum_{\rho} \left(\frac{\hbar\omega_\rho}{Ac^2 T n(\omega_\rho)} \right)^{1/2} [\hat{a}(z,\omega_\rho) e^{-i\omega_\rho t} + h.c.], \tag{2.2.50}$$

$$\hat{B}(z,t) = \sum_{\rho} \left(\frac{\hbar\omega_\rho n(\omega_\rho)}{Ac^2 T} \right)^{1/2} [\hat{a}(z,\omega_\rho) e^{-i\omega_\rho t} + h.c.], \tag{2.2.51}$$

where h.c. stands for hermitian conjugate and the sum is extended to all modes propagating in the medium. To show the validity of this proposal, it is applied to the propagation of plane waves in a linear medium, leading to the trivial z dependence:

$$\hat{a}(z,\omega_\rho) = \hat{a}(0,\omega_\rho) e^{i\beta_\rho z}. \tag{2.2.52}$$

with ρ the index of the respective plane mode. Subsequent works have shown the consistency of the theory and it has been applied to different optical phenomena: co- and contradirectional coupling, spatial amplifiers, distributed feedback lasers (DFL) [Ben-Aryeh et al., 1992], [Toren and Ben-Aryeh, 1994], Raman scattering [Pospíchal, 1995] and so on.

It is important to outline that this theory is introduced in terms of plane modes in dielectric media. Pioneering works on canonical standard quantization using non-plane modes are introduced in [Dalton et al., 1996, 1999] [Dalton and Knight, 1999a,b]. These authors focus on the derivation of a quantum Hamiltonian operator via an orthonormalization condition obtained in the volume of the dielectric medium. These works describe successful applications to optical cavities and so on [Dalton and Knight, 1999a] [Dalton and Knight, 1999b]. Likewise, several illustrative studies on nonlinear coupling in integrated devices are presented in [Perina Jr and Perina, 2000] (*and references therein*). However, the corresponding Momentum operators are proposed by transferring directly the results obtained with plane waves, whithout taking into account neither the vector structure nor the orthonormalization property of the guided modes.

In order to extend the Momentum approach to integrated optics and use it in the quantum analysis of the coupled modes propagation in IPDs, Liñares y Nistal [Liñares and Nistal, 2003] carry out an study of propagation of 2D TE modes introducing heuristic quantum fields based on the modal orthonormalization property on the cross section of the waveguide (2.1.10) and the modal norms (2.1.9), and applying it to mode coupling successfully. Following this work, we carry out a generalization to 1D vectorial modes, showing an *ab initio* quantization of the field, unlike that introduced in (2.2.50, 2.2.51), and deriving the equations of propagation the modes fulfill in these structures for linear and nonlinear media [Liñares et al., 2008a]. In the next section we make a brief review emphasizing the main results of

this work and we add it at the end of the chapter for an in deep analysis of our theory (§ P1). Likewise, we also introduce as application of this theory the generation of twin-photon states for QIP in nonlinear waveguides in (§ C1).

2.3. Canonical quantization in 1D integrated optical waveguides

In the previous section we have reviewed the quantum theory of the spatial propagation. As we have seen, it is based on obtaining the Momentum operator of the system, which provides the equations which rule the propagation. In this section we present the main concepts and results of the phenomenological quantization approach for 1D modes in waveguides. A macroscopic quantization is good enough for this kind of structures ought to its size. This approach is mostly embodied in the research work [Liñares et al., 2008a], which makes the following section, but in [Liñares et al., 2008b, 2012] as well. However, we believe it is necessary to introduce the fundamental concepts here, due to they are repeatedly used all along the dissertation.

Following the previous section, a good canonical phenomenological quantization of propagation has to fulfill these criteria:

1. To be defined in terms of monochromatic temporal modes ($\exp\{\pm i\omega t\}$), as they do not change when pass through media with different refractive indices.

2. To choose the quantization volume for optical waves in vacuum as AcT, since it is the one associated to photodetection.

3. To define bosonic quantum operators $\{\hat{a}(z,\omega_\rho), \hat{a}^\dagger(z,\omega_\rho)\}$ instead of the standard $\{\hat{a}(\beta_\rho,t), \hat{a}^\dagger(\beta_\rho,t)\}$, which represents, respectively, the annihilation and creation of photons on the cross section A of a beam during a time T.

4. To take as starting point the flux of momentum density T^{33} associated to the problem.

5. To obtain quantum propagation equations and quantum fields consistent with experiments *ab initio*[8].

[8] In the revised literature the fields for dielectric media (2.2.50, 2.2.51) are heuristically introduced.

Taking advantage of point 2, we would like to outline here the importance of the modal structure of the fields in optical waveguides, since the majority of measurement methods in photonics are based on photoelectric detection, and this in the absorption of photons in an area A during a time T. This absorption is associated to the mean value of an intensity operator $\langle\hat{I}\rangle$, function of the modal structure of the field. That's why it is important to know the spatial shape of the field modes, since they contain the information about the transverse structure of the optical field.

2.3.1. Quantization of free propagation

Taking the previous points into account, we present a canonical quantization based on the analogy between both the free classical Momentum associated to vectorial modes ν and that related to a spatial harmonic oscillator (§ P1). As was shown in the previous section, the classical Momentum is obtained via integration of the element T^{33} of the energy-momentum stress tensor [Jackson, 1975] over the hyperplane $dxdycdt$ (2.2.48):

$$M_O = \iiint_0^T T^{33}\, dxdycdt = \\ = \iiint_0^T \frac{1}{2}\left[(\epsilon_o n^2 \mathbf{E}_t\mathbf{E}_t - \epsilon_o n^2 \mathbf{E}_z\mathbf{E}_z) + (\mu_o \mathbf{H}_t\mathbf{H}_t - \mu_o \mathbf{H}_z\mathbf{H}_z)\right] dxdycdt. \tag{2.3.53}$$

Applying the complex representation of the modal field with the norm given by equation (2.1.9) and the relation for modal power (2.1.13), the Momentum can be written as:

$$M_{O\nu} = \mathrm{sgn}(\nu)\frac{\beta_\nu}{\omega}\|\mathbf{E}_\nu\|^2 cT, \tag{2.3.54}$$

where $\|\mathbf{E}_\nu\|^2$ is given by (2.1.9). This equation is the starting point for our canonical cuantization of the Momentum and 1D vector modal fields. Rewriting the fields (2.1.5, 2.1.6) as follows:

$$\mathbf{F}_\nu(x,y,z,t) = A_{o\nu}(z)\,\mathbf{F}_{o\nu}(x,y,t) = A_{o\nu}(z)\,\mathbf{F}_{o\nu}(x,y)e^{-i\omega t}, \tag{2.3.55}$$

with $A_{o\nu}$ the complex modal amplitude to be quantized and where we have used $\mathbf{F} \equiv \mathbf{E}, \mathbf{H}$. Let us search for new canonical variables which relate (2.3.54) to a spatial harmonic oscillator. We define the following complex amplitudes:

$$A_{o\nu}(z) = \frac{1}{\sqrt{2cT\mathrm{sgn}(\nu)\|\mathbf{F}_{o\nu}\|^2\,\beta_\nu/\omega}}\,(\beta_\nu q_\nu + ip_\nu), \tag{2.3.56}$$

$$A^*_{o\nu}(z) = \frac{1}{\sqrt{2cT\mathrm{sgn}(\nu)\|\mathbf{F}_{o\nu}\|^2\,\beta_\nu/\omega}}\,(\beta_\nu q_\nu - ip_\nu), \tag{2.3.57}$$

with q and p the canonical position and momentum variables. Taking into account the modal orthonormalization (2.1.10), the classical Momentum can be written in the form of canonical equation for a spatial harmonic oscillator:

$$M_{O\nu} = \frac{1}{2}(p_\nu^2 + \beta_\nu^2 q_\nu^2). \tag{2.3.58}$$

Now, we apply the principle of quantization of quantum mechanics[9] on the canonical Momentum (2.3.58), that is to consider the classical complex amplitudes as operators fulfilling ESCR (2.2.40) in the following way:

$$\hat{a}_\nu = \frac{1}{\sqrt{2\hbar\,\mathrm{sgn}(\nu)\,\beta_\nu}}(\beta_\nu \hat{q}_\nu + i\hat{p}_\nu), \tag{2.3.59}$$

$$\hat{a}_\nu^\dagger = \frac{1}{\sqrt{2\hbar\,\mathrm{sgn}(\nu)\,\beta_\nu}}(\beta_\nu \hat{q}_\nu - i\hat{p}_\nu), \tag{2.3.60}$$

$$[\hat{a}_\nu, \hat{a}_{\nu'}^\dagger] = \mathrm{sgn}(\nu)\delta_{|\nu|,|\nu'|}. \tag{2.3.61}$$

These operators stand for the absorption and emission of photons on an area given by the modal norm (2.1.9) during a time T, as expected. Additionally, these ESCR are also adequate for backward modes by the use of the following identities [Liñares and Nistal, 2003]:

$$\hat{a}_{\nu<0} = -\hat{a}_{\nu>0}^\dagger, \quad \hat{a}_{\nu<0}^\dagger = -\hat{a}_{\nu>0}. \tag{2.3.62}$$

Applying this relations into (2.3.56, 2.3.57), and likewise into (2.3.55), the following quantum fields are obtained:

$$\hat{\mathbf{f}} = \sum_\nu \hat{\mathbf{f}}_\nu = \sum_\nu (\hat{\mathbf{f}}_\nu^{(+)} + \hat{\mathbf{f}}_\nu^{(-)}) = \sum_\nu \frac{\sqrt{\hbar\omega}}{\sqrt{cT}}\left\{\frac{1}{\|\mathbf{F}_\nu\|}[\hat{a}_\nu \mathbf{F}_\nu e^{-i\omega t} + \hat{a}_\nu^\dagger \mathbf{F}_\nu^* e^{i\omega t}]\right\}, \tag{2.3.63}$$

where $\mathbf{f} \equiv \mathbf{e}, \mathbf{h}$ are the normalized fields required for quantization [Liñares and Nistal, 2003]. These are the quantum field relations we propose to use to solve propagation problems in integrated optics. It should be stressed that the terms heuristically assumed in expressions (2.2.50, 2.2.51) to fulfill the continuity relations (2.2.49), that is the electric field divided by $n^{1/2}$ and the magnetic field multiplied by $n^{1/2}$, appear as a particular case of the modal norms for plane waves (§ P1).

On the other hand, coming back to the Momentum, applying equations (2.3.59, 2.3.60) into (2.3.58), we have:

$$\hat{M}_O = \hbar \sum_\nu \mathrm{sgn}(\nu)\beta_\nu(\hat{a}_\nu^\dagger \hat{a}_\nu + 1/2), \tag{2.3.64}$$

[9] Basically this consists on taking into account the noncommutivity when measuring canonical conjugate quantities. For instance, the mechanical position q and momentum p fulfill $(q_\nu, p_\nu) \to (\hat{q}_\nu, \hat{p}_\nu)$, where $[\hat{q}_\nu, \hat{p}_{\nu'}] = i\hbar\delta_{\nu,\nu'}$.

where we have used the ESCR (2.3.61). This result contains an important physical result: the function $\mathrm{sgn}(\nu)$ ensures the positivity of the Momentum, which was hypothesized in [Ben-Aryeh et al., 1992, Toren and Ben-Aryeh, 1994] and now appears naturally from the modal norms.

2.3.2. Quantization of lossless waveguiding coupling devices

Now, we extend our formalism to the analysis of modal coupling by introducing a dielectric perturbation to the original refractive index $n^2(x,y)$. This perturbation is introduced, as usual, by a material polarization which is represented by the operator $\hat{\mathbf{P}} = \Delta\epsilon\,\hat{\mathbf{e}}$, describing formally a perturbation of the electric permitivity that in turn can present isotropy, anisotropy, non-linearity and so on. It is assumed that the polarization operator can be expressed as a function of the non perturbed optical mode field operators $\hat{\mathbf{e}}_\nu$ and therefore as a function of the operators $\{\hat{a}_\nu, \hat{a}_\nu^\dagger\}$ in the waveguide, in a similar way to the mode expansion in the classical case [Kogelnik, 1988]. In short, there is an interaction term $\hat{\mathbf{P}}(\hat{\boldsymbol{e}})\,\hat{\mathbf{e}}$ and consequently a coupling between the guided vector modes described by the following perturbated Momentum operator:

$$\hat{M} = \hat{M}_O + \frac{1}{p+1}\iiint_0^T \hat{\mathbf{P}}\,\hat{\mathbf{e}}\;dxdydt = \hat{M}_O + \frac{1}{p+1}\iiint_0^T \hat{P}_i\,\hat{e}_i\;dxdydt, \tag{2.3.65}$$

with $p \geqslant 1$. The factor $(p+1)^{-1}$ accompanying the interaction term can be justified by the standard Lagrangian theory of the Maxwell equations in bulk media [Hillery and Modlinow, 1984]. Moreover, each component $i\,(=x,y,z)$ of the polarization operator can be written, in a formal way, as follows:

$$\hat{P}_i = \{\epsilon_o\,\chi_{ijklm\ldots}(z)\hat{e}_k\,\hat{e}_l\,\hat{e}_m\ldots\}\,\hat{e}_j, \qquad k,l,m,\ldots,j = (x,y,z), \tag{2.3.66}$$

where we assume that the nonlinear susceptibility can depend on z. It is usual to consider the linear and nonlinear polarization perturbations of the waveguiding device separately, that is, $\hat{\mathbf{P}} = \hat{\mathbf{P}}_L + \hat{\mathbf{P}}_{NL}$, therefore the total Momentum is written as:

$$\hat{M} = \hat{M}_O + \frac{1}{2}\iiint_0^T \hat{\mathbf{P}}_L\,\hat{\mathbf{e}}\;dxdydt + \frac{1}{p+1}\iiint_0^T \hat{\mathbf{P}}_{NL}\,\hat{\mathbf{e}}\;dxdydt, \tag{2.3.67}$$

where now $p \geqslant 2$ is the order of the non-linearity. For the sake of expositional convenience we analyze separately the linear and nonlinear interactions.

Linear waveguiding coupling

We start by quantizating the linear polarization corresponding to an isotropic and inhomogeneous perturbation given by $\hat{\mathbf{P}}_L = \Delta\epsilon\,\hat{\mathbf{e}} = \Delta\epsilon(x,y,z)$

$(\hat{\mathbf{e}}_t + \hat{\mathbf{e}}_l)$, where the subscripts t and l stand for transverse and longitudinal, respectively. Note that the Hamiltonian theory will fail for a z-inhomogeneity because of the integration in a volume V and therefore on z, as we anticipated in the previous section. The corresponding part of the Momentum operator will be:

$$\hat{M}_L = \frac{1}{2}\iiint_0^T \Delta\epsilon\, \hat{\mathbf{e}}\,\hat{\mathbf{e}}\; dxdydcdt = \frac{1}{2}\iiint_0^T \Delta\epsilon \sum_\nu \hat{\mathbf{e}}_\nu \sum_{\nu'} \hat{\mathbf{e}}_{\nu'}\; dxdydt. \tag{2.3.68}$$

Now, attention should be paid to the way longitudinal components are handled under a linear perturbation with longitudinal component $\mathbf{P}_l = \Delta\epsilon\,\mathbf{E}_l$, since only the transverse components fulfill the orthonormalization condition and therefore the mode expansion can only be carried out in terms of these components. This can be solved via the use of the quantized version of the complex Maxwell-Ampere law (§ P1). Applying both longitudinal components obtained in this way and transverse components given by (2.3.55), into equation (2.3.68), the Momentum operator takes the following form:

$$\hat{M}_L = \hbar \sum_\nu \mathrm{sgn}(\nu)\kappa_{\nu\nu}\,(\hat{a}_\nu^\dagger \hat{a}_\nu + 1/2) + \hbar \sum_{\nu<\nu'} \{\kappa_{\nu\nu'}\,\hat{a}_\nu \hat{a}_{\nu'}^\dagger + \mathrm{h.c.}\}. \tag{2.3.69}$$

The self-coupling coefficient $\kappa_{\nu\nu}$ and the cross-coupling coefficients $\kappa_{\nu\nu'}$ are given by the compact expression:

$$\kappa_{\nu\nu'} = \frac{\omega\iint(\Delta\epsilon\mathbf{E}_{t\nu}\mathbf{E}_{t\nu'}^* + F(\Delta\epsilon)\mathbf{E}_{l\nu}\mathbf{E}_{l\nu'}^*)dxdy}{\|\mathbf{E}_\nu\|\,\|\mathbf{E}_{\nu'}\|}, \tag{2.3.70}$$

where $F(\Delta\epsilon) = \epsilon/(\epsilon + \Delta\epsilon)$. It is important to outline that this approach incluces the longitudinally inhomogeneous case, since the coupling coefficients (2.3.70) can be z-dependent. In § 2.3.3 we will discuss this sort of media in detail.

Finally, it is easy to obtain, from both equations (2.3.64, 2.3.69) and the ESCR (2.3.61), the Heisenberg equations (2.2.47) for the forward and backward absorption operators $\hat{a}_{\nu>0}$ and $\hat{a}_{\nu<0}$, that is:

$$-i\hbar\partial_z\hat{a}_\nu = [\hat{a}_\nu, \hat{M}_{OL}] = \hbar\tilde{\beta}_\nu\hat{a}_\nu + \hbar\sum_{\nu'\neq\nu}\mathrm{sgn}(\nu')\,\kappa_{\nu\nu'}\,\hat{a}_{\nu'}. \tag{2.3.71}$$

where we have used the notation $\tilde{\beta}_\nu = \beta_\nu + \kappa_{\nu\nu}$ and $\hat{M}_{OL} = \hat{M}_O + \hat{M}_L$. These equations are the quantum analog of (2.1.22) and describe linear modal coupling of quantum fields in waveguiding devices such as directional couplers, integrated gratings, junctions and so on [Liñares et al., 2008b] (Figure 2.3.4). Likewise, equation systems like (2.3.71) are suited to be diagonalized via unitary transformations leading to quantum *supermode*

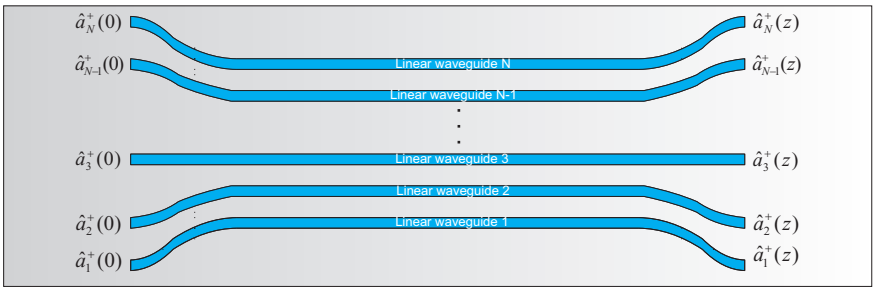

Figure 2.3.4: Sketch showing a N × N directional coupler composed by N linear waveguides.

operators which simplify the solution of the problem [Liñares et al., 2009]. This new set of operators are defined then to fulfill $\hat{a}_s(z) = \hat{a}_s(0)\, e^{i\beta_s z}$ and, likewise, they have to be linear combination of the canonical mode operators as follows:

$$\hat{a}_s = \sum_{\nu=1}^{N} c_{s\nu}\, \hat{a}_\nu, \qquad \hat{a}_\nu = \sum_{s=1}^{N} c_{\nu s}\, \hat{a}_s, \qquad \sum_{\nu} |c_{\nu s}|^2 = 1, \tag{2.3.72}$$

with $c_{s\nu} = c_{\nu s}^*$ complex coefficients and N the number of modes. By assuming both synchronic waveguides and coupling only between adjacent waveguides, the diagonalization of the matrix associated to the Heisenberg equations (2.3.71) leads to the following recurrent equation for $c_{\nu s}$:

$$\kappa\, c_{\nu s} + (\tilde{\beta} - \beta_s)\, c_{\nu+1\, s} + \kappa\, c_{\nu+2\, s} = 0, \tag{2.3.73}$$

where $\tilde{\beta} \equiv \tilde{\beta}_1 = \tilde{\beta}_2 = \cdots = \tilde{\beta}_N$, $\kappa \equiv \kappa_{12} = \kappa_{23} = \cdots = \kappa_{N-1\, N}$ and β_s stands for the eigenvalues of the system. Finally, by taking into account the constraints $c_{0s} = c_{N+1\, s} = 0$, the following values for the matrix eigenvectors and eigenvalues are obtained:

$$c_{s\nu} = \frac{\sin(\frac{s\nu\pi}{N+1})}{[\sum_\nu \sin^2(\frac{s\nu\pi}{N+1})]^{1/2}}, \qquad \beta_s = \tilde{\beta} + 2\kappa\cos\,(\frac{s\pi}{N+1}), \tag{2.3.74}$$

where $s = 1, \ldots, N$ is the supermode operator number and β_s is the propagation constant of the supermode operator. Therefore, the quantum propagation of an input quantum light state $|L_i\rangle$ excited in the canonical basis, may be carried out by taking the mentionated state in the basis of supermodes $|L_s\rangle$, and working out the action of the supermode operators on it to, finally, return to the canonical basis and thus obtaining the output state $|L_o\rangle$. This kind of approach can be interesting in the analysis of *quantum random walks* [Peruzzo et al., 2010]. Right after, we extend the present analysis to a nonlinear perturbation.

Nonlinear waveguiding coupling

For the sake of expositional convenience we only consider here nonlinearities of second order in a directional coupler, although results can be easily extended to nonlinearities of an arbitrary order (§ P2). Let us consider N coupled waveguides with operators $\hat{a}_\nu(\omega)$, $\hat{b}_\nu(2\omega)$, $\nu = 1, ..., N$. Then the total Momentum operator for forward propagation can be written as follows:

$$\hat{M} = \hat{M}_a + \hat{M}_b + \frac{1}{3}\iiint_0^T \hat{\mathbf{P}}^{(2)}_{NL}(x, y, z)\,\hat{\mathbf{e}}\;dxdydzdt, \tag{2.3.75}$$

where $\hat{M}_a$ and $\hat{M}_b$ are the linear Momentum operators for modes $\hat{a}_\nu(\omega)$ and $\hat{b}_\nu(2\omega)$, respectively, and the third term is the nonlinear mode coupling term, which after calculation is given by:

$$\hat{M}^{(2)}_{NL} = \hbar\sum_\nu\{\kappa^{(2)}_{\nu\nu}(z)\;\hat{b}^\dagger_\nu\hat{a}^2_\nu + h.c.\} + \hbar\sum_\nu\{\kappa^{(2)}_{\nu,\nu\pm1}(z)\;\hat{b}^\dagger_\nu\hat{a}^2_{\nu\pm1} + h.c.\}, \tag{2.3.76}$$

where only coupling between neighbour waveguides is supposed. Note that there is no linear coupling between modes of different frequency. The particular case of a $N \times N$ DC with $N-1$ linear waveguides and one nonlinear waveguide is sketched in Figure 2.3.5.

The expression of the coupling coefficients depends on the nonlinear coupling conditions, however by assuming that only one component of the field is relevant, for instance de y-component of a quasi-TE mode, then explicit expressions for the coupling coefficients could be obtained:

$$\kappa^{(2)}_{\nu\nu}(z) = \frac{2^{1/2}\omega^{3/2}\iint \epsilon_o\chi_{yyy}(z)\,\mathbf{E}^*_{yb\nu}\,\mathbf{E}^2_{ya\nu}dxdy}{8\,\|\mathbf{E}_{b\nu}\|\;\|\mathbf{E}_{a\nu}\|^2}. \tag{2.3.77}$$

Similar expressions can be obtained for the other coupling coefficients. Interestingly, it can be checked that factors equal to 2 are found in the Heisenberg equations, but they do not appear in the classical equations [Liñares et al., 2008a,b, Perina, 1995]. Likewise counterpropagation and longitudinal inhomogeneities $\kappa(z)$ (where mismatching is included) are included in the above equations. We also stress that starting from the Momentum operator (2.3.64) together with equations (2.3.69, 2.3.75), any of the Heisenberg equations heuristically introduced in the literature for nonlinear couplers with $p = 2$ (see for instance [Perina Jr and Perina, 2000] *and references therein*) can be easily derived and therefore justified. Even, for higher-order nonlinearities, terms neglected by the heuristic approach appear when the Momentum is considered. We will show further details of this analysis in sections P1 and P2.

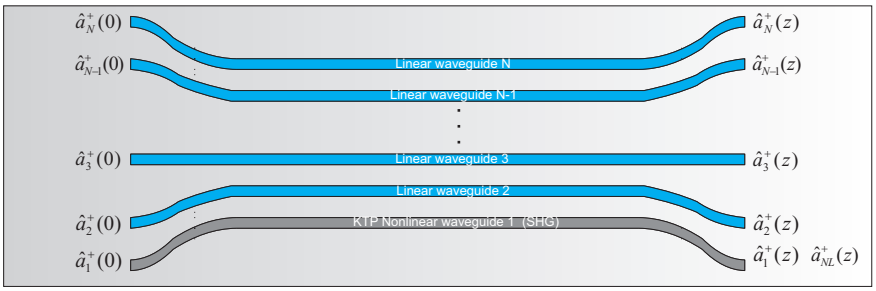

Figure 2.3.5: Sketch showing a $N \times N$ nonlinear directional coupler composed by $N-1$ linear waveguides and one nonlinear waveguide producing SHG.

2.3.3. Quantization of lossless waveguiding non-coupling devices: separable inhomogeneous media

In the case of longitudinally inhomogeneous media, we distinguish two cases that cover most of the practical configurations attending the spatial distribution of the refractive index: factorable and seprable. In the factorable case, the refractive index can be written as [Sodha and Ghatak, 1977]:

$$n^2(x,y,z) = n_0^2\, f^2(x,y)\, h^2(z), \tag{2.3.78}$$

with $f(0,0) = h(0) = 1$, where n_0 is the index at the origin, $h(z)$ is a general z-dependent function modulating the transverse part of the index $f(x,y)$ along the z axis, as for instance $f^2(x,y) = 1 + \Delta n^2\,(x^2+y^2)$ in the case of a transverse parabolic index. This case is dealt with in the same way as above shown for homogeneous media, that is by means of coupled modes like in § 2.3.2.

On the other hand we have the separable case, where there is no modal coupling and, accordingly, without losses due to radiation. Hence, the waveguiding elements made of these media like tapers, phase shifters, gradual transitions for anti-reflection, and so on; will present a good functionality. In this case the quantum propagation is studied in a different way from the homogeneous case: local propagating modes without coupling can be defined in such a way that a free Momentum is derived. The index in this case can be modelled by the following function [Sodha and Ghatak, 1977]:

$$n^2(x,y,z) = n_t^2(x,y) + n_l^2(z) \equiv n_0^2\, f^2(x,y) + \Delta n^2\, h^2(z), \tag{2.3.79}$$

where $f(x,y)$ and $h(z)$ are transverse and longitudinal functions, respectively, fulfilling $f(0,0) = 1$ and $h(0) = 0$, and n_0 and Δn are constants.

Starting from Maxwell equations (2.1.1 - 2.1.4), it is easy to show that the electric optical field $\mathbf{E}(x, y, z, t)$ obeys the following vectorial wave equation [Marcuse, 1974]

$$\nabla^2 \mathbf{E}_t + \nabla_t(\mathbf{E}\,\nabla \ln n^2) = \frac{n^2}{c^2}\frac{\partial^2 \mathbf{E}_t}{\partial t^2}, \tag{2.3.80}$$

with $\mathbf{E} = (E_x, E_y, E_z) \equiv (\mathbf{E}_t, E_z)$ and $\nabla = (\partial/\partial x, \partial/\partial y, \partial/\partial z) \equiv (\nabla_t, \partial/\partial z)$. Note the presence of a small coupling with the longitudinal component E_z if a longitudinal inhomogeneity is present. Taking monochromatic guided 1D vector modes with frequency ω (2.3.55), the normalized transverse complex amplitudes $\mathbf{F}_{o\nu}$ of the optical modes, obey the following mode equation:

$$\nabla_t^2 \mathbf{F}_{o\nu} + k_0^2 n_t^2 \mathbf{F}_{o\nu} + \nabla_t(\mathbf{F}_{o\nu}\nabla_t(\ln n_t^2)\,) = \beta_{t\nu}^2 \mathbf{F}_{o\nu}, \tag{2.3.81}$$

Likewise, bearing in mind the standard assumption for the electric components, $E_z \ll E_x,\ E_y$[10], we can apply equations (2.3.55) and (2.3.81) into (2.3.80) obtaining the following amplitude equation for each ν-mode :

$$\frac{d^2 A_{o\nu}}{dz^2} + \beta_\nu^2(z)\, A_{o\nu} = 0, \tag{2.3.82}$$

with $\beta_\nu^2(z) = \beta_{t\nu}^2 + k_0^2 \Delta n^2 h^2(z)$. This equation suggests a spatial harmonic oscillator with a z-dependent spatial frequency and therefore it can be directly derived from spatial type-Hamilton equations (see § 3.3.2) where the Hamiltonian is substituted by the Momentum:

$$M_\nu = \frac{1}{2}[p_\nu^2 + \beta_\nu^2(z)\, q_\nu^2], \tag{2.3.83}$$

where we have used $q_\nu = (A_{o\nu} + A_{o\nu}^*)/2$. The classical Momentum (2.3.83) is equivalent to the Hamiltonian of a time-dependent harmonic oscillator, with $\beta(z)$ playing the role of $\omega(t)$. Then, following the principle of quantization we obtain the following Momentum operator:

$$\hat{M}_\nu = \frac{1}{2}[\hat{p}_\nu^2 + \beta_\nu^2(z)\, \hat{q}_\nu^2]. \tag{2.3.84}$$

This is the generator of quantum spatial propagation in longitudinally inhomogeneous waveguides where $\hat{q}_\nu$ plays the role of the quantized electric field and fulfills equation (2.3.82). Other central figures in the propagation are the absorption $\hat{a}_\nu$ and emission $\hat{a}_\nu^\dagger$ operators. We define them in the following usual way [Kiss et al., 1994]:

$$\hat{a}_\nu(z) = \frac{1}{\sqrt{2\hbar\,\beta_\nu(z)}}[\beta_\nu(z)\hat{q}_\nu + i\hat{p}_\nu], \tag{2.3.85}$$

$$\hat{a}_\nu^\dagger(z) = \frac{1}{\sqrt{2\hbar\,\beta_\nu(z)}}[\beta_\nu(z)\hat{q}_\nu - i\hat{p}_\nu]. \tag{2.3.86}$$

[10] This assumption implies $\mathbf{E} \approx \mathbf{E}_t$.

If operators $\hat{a}_\nu$ and $\hat{a}_\nu^\dagger$ are substituted into equation (2.3.84), it leads to the well-known expression:

$$\hat{M}_\nu = \hbar \sum_\nu \beta_\nu(z)(\hat{n}_\nu + 1/2), \tag{2.3.87}$$

where $\hat{n}_\nu = \hat{a}_\nu^\dagger \hat{a}_\nu$ is the number operator whose eigenstates are the Fock states $|n_\nu\rangle$. Likewise, bearing in mind that the vector modal field operator $\mathbf{E}_t$ is proportional to $A_{o\nu}$, we can write its quantum counterpart applying equations (2.3.85) and (2.3.86) into (2.3.55) through $\hat{A}_{o\nu} = (2\hbar/\beta_\nu(z))^{1/2}\,\hat{a}_\nu$, as follows:

$$\hat{\mathbf{E}}_t(x,y,z,t) = \sum_\nu \sqrt{\frac{\hbar\omega}{T\beta_\nu(z)}}\mathbf{F}_{o\nu}(x,y)\,e^{-i\omega t}\hat{a}_\nu(z) + \text{h.c.}, \tag{2.3.88}$$

where T is the period of the temporal mode and normalization has been carried out to get appropriate units.

Likewise, the $\{\hat{a}, \hat{a}^\dagger\}$ operators fulfill Heisenberg equations. However, due to the z-dependence, these equations present partial derivatives which do not appear in the homogeneous case. To solve these equations, the relation between the local operators at any z and those at the beginning of the medium should be known, however that is a task not easy to carry out analytically [Kiss et al., 1994]. These difficulties can be overcome by solving (2.3.82) in terms of the quantized complex electric field $\hat{A}_{o\nu}$, in the following way:

$$\hat{A}_{o\nu}(z) = \rho_\nu\, e^{i\theta_\nu}\hat{A}_{o\nu}(0), \tag{2.3.89}$$

where ρ_ν and θ_ν are real functions obtained by solving:

$$\frac{d^2\rho_\nu}{dz^2} + \beta_\nu^2(z)\rho_\nu = \frac{\beta_{0\nu}}{\rho_\nu^3}, \tag{2.3.90}$$

$$\frac{d\theta_\nu}{dz} = \frac{\beta_{0\nu}}{\rho_\nu^2}, \tag{2.3.91}$$

with $\beta_{o\nu} \equiv \beta_\nu(0)$. Equation (2.3.90) is an Ermakov-Pinney equation with solutions given by [Pinney, 1950]:

$$\rho_\nu(z) = [(\beta_{o\nu}\,u_\nu(z))^2 + v_\nu^2(z)]^{1/2}, \tag{2.3.92}$$

$$\rho_\nu(0) = 1, \quad \rho_\nu'(0) = 0, \tag{2.3.93}$$

and where u_ν and v_ν are linearly independent functions that satisfy equation (2.3.82) and have the following initial conditions and Wronskian:

$$u_\nu(0) = v_\nu'(0) = 0, \tag{2.3.94}$$

$$u_\nu'(0) = v_\nu(0) = 1, \tag{2.3.95}$$

$$W_\nu = u_\nu'\,v_\nu - v_\nu' u_\nu = 1. \tag{2.3.96}$$

Since the quantum complex electric field $\hat{A}_{o\nu}$ and the absorption operator $\hat{a}_\nu$ are related by $\beta_\nu(z)^{1/2}$, then, by means of the use of the solution (2.3.89) and equation (2.3.91), the following solution to the Heiseberg equation is obtained:

$$\hat{a}_\nu(z) = \sqrt{\frac{\beta_\nu(z)}{\theta'_\nu(z)}}\, e^{i\theta_\nu}\, \hat{a}_\nu(0). \tag{2.3.97}$$

With this solution we can rewrite equation (2.3.88) in the following way:

$$\hat{E}_t(x,y,z,t) = \sum_\nu \sqrt{\frac{\hbar\omega}{T\theta'_\nu(z)}}\mathbf{F}_{o\nu}(x,y)\, e^{i(\theta_\nu(z)-\omega t)}\, \hat{a}_\nu(0) + h.c. \tag{2.3.98}$$

This equation shows that the real constant of propagation of the mode is $\tilde{\beta}_\nu = \theta'_\nu(z)$. Of course the expectation value of this operator for a coherent state recovers the values of the classical electric field.

2.3.4. Quantization of lossy waveguiding coupling devices

A problem not tackled till now is losses. A system in an optical waveguide is not isolated, because of the discontinuities that couple the guided modes with the environment (radiation modes) and the interaction with the waveguiding material leading to absorption[11]. This coupling is responsible for the leaking of energy from the waveguide and also for the introduction of environmental fluctuations in it, which can have a profound effect on quantum states propagating in it. This interaction is typically weak compared with couplings within the system of interest but, in general, it can not be neglected, so dissipative effects have to be included in a complete quantum model of propagation.

In the time domain, different approaches have been carried out. A common approach to model losses is that of an effective beam splitter (BS), where losses are ascribed to reflected light in the BS [Bachor and Ralph, 2004]. More rigorous approaches are either to take the dissipation as a damped or Caldirola-Kanai (CK) harmonic oscillator [Caldirola, 1941, Kanai, 1945] or, alternatively, the use of a reservoir in order to model the damping process, that is, a system coupled to an environment or thermal bath with many degrees of freedom[12] [Louisell, 1973, Yu and Sun, 1994]. Likewise, other more complicated models have been proposed, such as the Bateman-Feshbach-Tikochinsky oscillator, although its physical fundamentals are the same as those in the previous approaches [Kim et al., 2003]. Other approach is the use of complex-valued Hamiltonians [Rajeev, 2007], where a canonical formulation of dissipative mechanics is carried out via complex-valued Hamiltonians describing damping, in a similar way to the above

[11] We will not tackle here the losses associated to dispersion.
[12] This model contains in turn the CK model.

approaches. In addition, dissipation can be studied in terms of quasi-probability distributions, since the Fokker-Planck equation leads to stochastic equations which take into account losses [Risken, 1989], but this approach is far from the outline of this dissertation.

We must stress that all previous approaches have been developed for temporal evolution, however, in our case we are interested in spatial propagation. To include losses in our formalism based on the Momentum operator, we will show an approach based on the coupling between the system under study and a reservoir fulfilling the *random phase assumption* [Haken, 1981, Louisell, 1973]. Likewise, in Appendix A, we will show an alternative heuristic approach which follows closely Rajeev's work [Rajeev, 2007] using complex-valued Momentum operators and stochastic terms which account for the fluctuations (§ P2).

Quantum dissipation as a coupling to a reservoir

In this case we are going to consider the damping as a coupling between guided modes of the waveguide and the 'lossy modes' (scattering and absorption) by introducing a reservoir which represents the material system. To this end we will apply well-known ideas in the time domain to the propagation of quantum states [Louisell, 1973]. Considering free guided modes coupled to the reservoir, following section 2.3.2 we will have the Momentum of the total system:

$$\begin{aligned}\hat{M}_D = \hbar \sum_{\nu} \beta_\nu \left(\hat{a}_\nu^\dagger \hat{a}_\nu + 1/2\right) + \hbar \sum_{\nu'} \beta_{\nu'} \left(\hat{b}_\nu^\dagger \hat{b}_\nu + 1/2\right) \\ + \hbar \sum_{\nu<\nu'} \{g_{\nu\nu'}\, \hat{a}_\nu \hat{b}_{\nu'}^\dagger + \text{h.c.}\}.\end{aligned} \tag{2.3.99}$$

where $\hat{a}_\nu$ and $\hat{b}_\nu$ stand for the guided modes and reservoir (scattering and absorption) modes, respectively, and $g_{\nu\nu'}$ is the coupling coefficient between a pair of these modes ν and ν'. This reservoir is assumed to have a broad mode spectrum. Moreover, either $\hat{a}_\nu$ as $\hat{b}_\nu$ mode operators fulfill ESCR (2.3.61). From the Momentum (2.3.99), the reservoir modes obey the following equation (2.2.47):

$$\frac{\partial \hat{b}_{\nu'}}{\partial z} = i\beta_{\nu'} \hat{b}_{\nu'} + i \sum_{\nu'} g_{\nu\nu'} \hat{a}_\nu, \tag{2.3.100}$$

with the next formal solutions:

$$\hat{b}_{\nu'}(z) = \hat{b}_{\nu'}(0) e^{i\beta_{\nu'} z} + i g_{\nu\nu'} \int_0^z \hat{a}_\nu(z') e^{i\beta_{\nu'}(z-z')} dz', \tag{2.3.101}$$

and where the reservoir variables before coupling with the guided modes are excited in states such that they fulfill the following relations:

$$\langle \hat{b}_\nu(0) \rangle_R = \langle \hat{b}_\nu^\dagger(0) \rangle_R = 0,$$

$$\langle \hat{b}^{\dagger}_{\nu}(0)\, \hat{b}_{\nu'}(0)\rangle_R = \bar{n}_{\nu}\, \delta_{\nu\nu'}, \tag{2.3.102}$$

where the brackets stand for the average over the reservoir and $\bar{n}_{\nu}$ are the mean numbers of reservoir damping oscillators in the ν mode[13]. These relations form the so-called *random phase assumption* [Mandel and Wolf, 1995].

In the same way, the Heisenberg equations for the guided modes are:

$$\frac{\partial \hat{a}_{\nu}}{\partial z} = i\beta_{\nu}\hat{a}_{\nu} - \sum_{\nu'} |g_{\nu\nu'}|^2 \int_0^z \hat{a}(z')e^{i\beta_{\nu'}(z-z')}dz' + \hat{G}_{\nu}(z), \tag{2.3.103}$$

where we have used the solution for the reservoir modes (2.3.101) and defined the noise operators $\hat{G}_{\nu}(z) = i\sum_{\nu'} g^{*}_{\nu\nu'}\, \hat{b}_{\nu'}(0)\, e^{i\beta_{\nu'}z}$, which from equations (2.3.102) obey the following relations [Perina and Krepelka, 1992]:

$$\begin{aligned}
\langle \hat{G}_{\nu}(z)\rangle_R = \langle \hat{G}^{\dagger}_{\nu}(z)\rangle_R = 0,\\
\langle \hat{G}^{\dagger}_{\nu}(z)\hat{G}_{\nu'}(z')\rangle_R = \gamma_{\nu}\, \bar{n}_{\nu}\, \delta_{\nu\nu'}\, \delta(z-z'),\\
\langle \hat{G}_{\nu}(z)\hat{G}^{\dagger}_{\nu'}(z')\rangle_R = \gamma_{\nu}(\bar{n}_{\nu}+1)\, \delta_{\nu\nu'}\, \delta(z-z'),
\end{aligned} \tag{2.3.104}$$

with $\gamma_{\nu} = 2\pi D(\beta_{\nu})|g_{\nu\nu}|^2$ the system damping which encloses the linear losses like scattering or absorption, and $D(\beta_{\nu})$ the mode density evaluated at β_{ν}[14].

Interestingly, from the above cross correlations is derived the fluctuation-dissipation theorem which states that the system damping γ is determined by the reservoir noise operators which introduce fluctuations into the system:

$$\gamma_{\nu} = \frac{1}{\bar{n}_{\nu}} \int_0^{\infty} \langle \hat{G}^{\dagger}_{\nu}(z')\hat{G}_{\nu}(0)\rangle_R dz'. \tag{2.3.105}$$

The integrodifferential equation (2.3.103) can not be analytically solved. However, via Laplace transforms, we can apply the Wigner-Weisskopf approximation [Luks and Perinová, 2002], obtaining:

$$\hat{a}_{\nu}(z) = \hat{a}_{\nu}(0)e^{i\beta_{\nu}z}\, e^{-\gamma_{\nu}z/2} + \int_0^z e^{i\beta_{\nu}(z-z')}\, e^{-\gamma_{\nu}(z-z')/2}\, \hat{G}_{\nu}(z')dz', \tag{2.3.106}$$

where we have neglected small shifts in the propagation constants. This is the solution of a Langevin equation, so (2.3.103) can be considered as such. Finally, tracing out the bath variables and taking into account the relations (2.3.104), we obtain the following solution for the propagated field and the usual ESCR:

$$\langle \hat{a}_{\nu}(z)\rangle_R = \hat{a}_{\nu}(0)\, e^{i\beta_{\nu}z}\, e^{-\gamma_{\nu}z/2}, \tag{2.3.107}$$

[13] The average of the operator $\hat{O}$ is given by $\langle \hat{O}\rangle = \mathrm{Tr}\{\hat{\rho}\hat{O}\}$, where Tr stands for *trace* and $\hat{\rho}$ is the density operator defining a quantum ensemble [Gerry and Knight, 2005].

[14] This factor appears when the continuum aproximation in the reservoir is taken. As we hypothesize a broad mode spectrum, we can take $\sum_{\nu} \to \int D(\beta_{\nu})d\beta_{\nu}$, where $D(\beta_{\nu})d\beta_{\nu}$ is the number of modes between β_{ν} and $\beta_{\nu} + d\beta_{\nu}$.

$$\langle[\hat{a}_\nu(z), \hat{a}_{\nu'}(z)^\dagger]\rangle_R = \delta_{\nu\nu'}. \tag{2.3.108}$$

Therefore this theory recovers the usual expressions used in classical optics (2.3.107) and keeps the quantumness of the fields through (2.3.108). Likewise, this approach can be extended to any quadratic Momentum. So losses produced in nonlinear parametric processes can also be modelled by means of coupling to new reservoirs [Collet and Walls, 1985]. For example, for parametric cross two photon absorption (XTPA) we would have the following Momentum:

$$\hat{M}_{XTPA} = \hbar \sum_{\nu<\nu'} \{g_{\nu\nu'}\, \alpha\, \hat{a}_\nu \hat{b}^\dagger_{\nu'} + h.c.\}. \tag{2.3.109}$$

where α is the expectation value of a strong coherent field $|\alpha\rangle$, $\hat{a}_\nu$ the guided modes and $\hat{b}_{\nu'}$ the absorption modes. From this Momentum we derive Heisenberg-Langevin equations which describe this interaction. In section C1 we show an example of application of this theory.

oOo

In the above sections we have shown the main theoretical results on spatial propagation of quantum light in linear and nonlinear, homogeneous and inhomogeneous, lossless and lossy IPDs based on mode coupling. Next, the published research work § P1 is presented, where we go in deep with most of the concepts introduced along this chapter. Specifically, we start reviewing the classical treatment of propagation in integrated waveguides and, right after, we present a quantization scheme based on the use of temporal modes and the flux of momentum. Next, we generalize it to coupled guided modes in linear and nonlinear devices and show the example of a nonlinear symmetric 3×3 DC[15], stressing the difference with other approaches. On the other hand, we introduce the communication § C1 where we perform a detailed analysis of the generation of quantum light in *silicon-on-insulator* (SOI) waveguides taking into account the nonlinear and lossy nature of the material. We begin reviewing the interest and features this technology presents in QIP, and in particular in the generation of twin photon states via spontaneous four wave mixing (SFWM). Next, we propose a Momentum encompassing these features and derive Langevin equations. Finally, we study the conversion efficiency for two particular cases.

[15]For a detailed analysis of this device, see [Barral, 2008].

P1. QUANTIZATION OF COUPLED 1D VECTOR MODES IN INTEGRATED PHOTONIC WAVEGUIDES

NEW JOURNAL OF PHYSICS
VOL. 10 PAGES 063023
doi: 10.1088/1367-2630/10/6/063023

PUBLISHED 20 JUNE 2008

BY JESÚS LIÑARES, MARÍA C. NISTAL & DAVID BARRAL

UNIVERSIDADE DE SANTIAGO DE COMPOSTELA

Abstract: *A quantum mechanical analysis of the guided light in integrated photonics waveguides is presented. The analysis is made starting from one - dimensional (1D) guided vector modes by taking into account the modal orthonormalization property on a cross section of an optical waveguide, the vector structure of the guided optical modes and the reversal-time symmetry in order to quantize the 1D vector modes and to derive the quantum momentum operator and the Heisenberg equations. The results provide a quantum-consistent formulation of the linear and nonlinear quantum light propagations as a function of forward and backward creation and annihilation operators in integrated photonics. As an illustration, an application to an integrated nonlinear directional coupler is given, that is, both the nonlinear momentum and the Heisenberg equations of the nonlinear coupler are derived.*

P1.1. Introduction

In this work we present a quantum mechanical analysis of the optical propagation corresponding to coupled 1D vector modes in integrated waveguides [Yariv, 1973], that is, modes spatially confined in two dimensions and therefore propagating in one spatial dimension; obviously these modes contain the particular case of 2D modes, that is, modes spatially confined in one dimension and therefore with two free spacial dimensions for optical propagation. It is important to stress that the integrated photonic waveguides have as a common physical characteristic that the modes are confined in the order of the light wavelength. The optical 1D modes can be obtained in conventional integrated optical waveguides (which can be made in optical glasses, crystals, semiconductors, polymers, silicon, and so on) [Hunsperger, 2009], in photonic crystal waveguides [Johnson and Joannopoulos, 2002] and in nanophotonic waveguides (plasmonic modes) [Prasad, 2004]; all these possible waveguide structures are considered in this work as different kinds of integrated photonic waveguides for which a common quantum mechanical formulation will be presented.

Recently, a preliminar study about quantization of coupled 2D modes in integrated optical waveguides was presented [Liñares and Nistal, 2003]. In this work we generalize the above study to 1D vector modes in such a way that 1D modes are quantized in a macroscopic way and the quantum propagation is described by spatial coupling of operators creation and annihilation associated to the guided modes by a previous calculation of a general quantum Momentum operator with linear and non linear coupling terms. This analysis can be applied to different modal coupling problems between optical guides, which form the basis of many linear and non linear integrated photonic devices, such as: integrated couplers, integrated gratings, integrated junctions, integrated interferometers and so on; these coupled modes optical devices provide very interesting classical dynamic properties (see [Haus and Huang, 1991] and references therein) and geometric properties [Liñares and Nistal, 1992], therefore a proper quantization of the coupled modes propagation allows to increase the optical possibilities of these devices. It must be stressed that a proper quantization must be based on both the orthonormalization property of guided modes on the cross-section of optical guides and the complex vector structure of the guided modes; in fact, as it has been shown [Liñares and Nistal, 2003], the quantization results of propagation are only consistent when the longitudinal components of the guided modes are taken into account and when the orthonormalization property is used to construct the optical field operator. We will quantize the coupling of forward and backward guided modes propagating along an arbitrary η-direction (longitudinal direction), by calculating the quantum Momentum operator as a function of the operators $\hat{a}_{\rho\sigma}$ and $\hat{a}^{\dagger}_{\rho\sigma}$, where $\rho\sigma$ is a double positive or negative discrete in-

dex, different from zero, characterizing the guided $\rho\sigma$-modes; for forward modes (and forward operators): $\rho > 0$, $\sigma > 0$ (it will be denoted as $\rho\sigma > 0$) and for backward modes (and backward operators): $\rho < 0$, $\sigma < 0$ (it will be denoted as $\rho\sigma < 0$). In this context, it is important to point out the pioneering works on macroscopic canonical quantization [Dalton and Knight, 1999a,b, Dalton et al., 1996, 1999] based on mode functions; these works focussed the attention on the derivation of a quantum Hamiltonian operator and therefore on temporal interactions described by the dynamic of the operators $\hat{a}(t)$ and $\hat{a}^{\dagger}(t)$; consequently, the orthonormalization condition used in the quantization process was obtained in the volume of a dielectric medium; likewise, these works described successful applications to optical devices formed with material media with longitudinal dependence of the electrical permitivity, such as optical cavities [Dalton and Knight, 1999a,b]; in short, these works used, for first time, a formalism based on classical non plane modes. Nevertheless, in our case, we are interested on the derivation of the quantum Momentum operator $\hat{M}$ and therefore on spatial interactions described by the η-spatial evolution of the operators $\hat{a}_{\rho\sigma}(\eta)$ and $\hat{a}^{\dagger}_{\rho\sigma}(\eta)$; moreover, as it was commented above, a proper orthonormalization condition for guided modes must be defined and used on the cross-section of the optical guides; likewise, in our case, the arbitrary η-direction is the propagation direction and the $\xi\gamma$-plane is the plane where the guided modes are confined by a graded refractive index $n(\xi, \gamma)$, that is, 1D modes are considered, which contains as a particular case the 2D modes which are confined along one spatial dimension by means of a graded refractive index $n(\xi)$. The formalism developed in this work allows to describe in a fully consistent quantum way both linear and nonlinear integrated optical devices, in an analogous way to those 3D optical devices as beamsplitters, linear and nonlinear interferometers and so on, which, at present, have acquired a very relevant interest for their many and different quantum applications [Gerry and Knight, 2005, Loudon, 1982, Schleich, 2001].

Returning to the quantum propagation problem in space, we must also point out that several fundamental studies have been made [Abram, 1987, Ben-Aryeh and Serulnik, 1991, Ben-Aryeh et al., 1992, Huttner et al., 1990, Toren and Ben-Aryeh, 1994]; these studies have provided the background of the quantum theory of light propagation in space, that is, they have proven that the quantum operator which must be obtained, in order to describe quantum spatial propagation, is the Momentum operator which in turn must be calculated by integrating the energy tensor element T^{33} over the hyperplane $dxdydcdt$; nevertheless, and to our knowledge, this kind of studies were restricted to simple plane modes, and therefore they can be rigorously applied only to optical devices described by plane waves propagating along an arbitrary η-direction; the plane modes do not present longitudinal components like guided modes, and moreover, the corres-

ponding field operators have a particular expression [Ben-Aryeh and Serulnik, 1991]; in fact, in this work we will show that the above optical field operators are obtained as a limiting case of the optical field operators associated to guided modes.

On the other hand, several interesting and illustrative studies on nonclassical light in guided mode coupling devices were presented [Jansky et al., 1988, Korolkova and Perina, 1997, Perina, 1995, Perina and Perina Jr, 1995a,b], nevertheless, the corresponding Momentum operators were proposed by transferring, in a straightforward way, the results obtained with plane waves, and therefore without taking into account either vector structure or orthonormalization property of guided modes; likewise, analogies with optical quantum Hamiltonians, describing temporal interaction, were used to construct and propose Momentum operators for coupled mode devices. This work extends the pioneering results obtained in [Dalton and Knight, 1999a,b, Dalton et al., 1996, 1999] to the case of coupled mode quantum propagation in optical guides, justifies many of the considerations introduced in [Abram, 1987, Ben-Aryeh and Serulnik, 1991, Ben-Aryeh et al., 1992, Huttner et al., 1990, Toren and Ben-Aryeh, 1994] and generalizes the preliminar results presented in [Liñares and Nistal, 2003] to linear and nonlinear coupled 1D modes.

The primary aim of this work is to avoid methods based on heuristic arguments or mechanical analogies and thus to obtain *ab initio* the Momentum operators for the quantum mechanical analysis of the optical propagation corresponding to coupled 1D modes in waveguides and consequently the Heisenberg's equations governing the spatial coupling between the operators $\hat{a}_{\rho\sigma}(\eta)$ and $\hat{a}^{\dagger}_{\rho\sigma}(\eta)$. The plan of the work is as follows: first of all, we briefly review the orthonormalization property of guided 1D vector modes on a cross-section of an optical guide (these modes are supported in channel guides, optical fibers and so on) which contains as limiting case the guided 2D vector modes (which are supported in planar guides). Next, we calculate, in an explicit and detailed way, the corresponding quantum Momentum operators when there is not coupling between guided modes, that is, the free field part of the Momentum operator. Next, we will derive the Momentum operator for modal coupling by the quantization of a classical (linear and nonlinear) polarization $\mathbf{P}(\xi, \gamma)$ perturbing the free Momentum operator, and, by using the time-reversal symmetry, the Momentum operator for a general linear contradirectional coupling will be obtained as a function of the operators $\hat{a}_{\rho\sigma}(\eta)$ and $\hat{a}^{\dagger}_{\rho\sigma}(\eta)$. Finally, and as an illustration, an application to a wellknown integrated nonlinear directional coupler is given, that is, both its Momentum operator and its quantum Heisenberg's equations are derived *ab initio*.

P1.2. Classical analysis of guided 1D vector modes

Let us consider monochromatic guided 1D vector modes, that is, with only one temporal mode of frequency ω in an optical waveguide characterized by a refractive index profile $n^2(\xi,\gamma)$ and represented by a vector field solution with the following complex amplitude:

$$\mathbf{E}_{\rho\sigma}(\xi,\gamma,\eta,t) = \mathcal{E}_{\rho\sigma}(\xi,\gamma,\eta)\, e^{-i\omega t} = \mathbf{E}_{\rho\sigma}(\xi,\gamma)\, e^{\{i[\beta_{\rho\sigma}\eta-\omega t]\}} \quad \text{(P1.1)}$$

$$\mathbf{H}_{\rho\sigma}(\xi,\gamma,\eta,t) = \mathcal{H}_{\rho\sigma}(\xi,\gamma,\eta)\, e^{-i\omega t} = \mathbf{H}_{\rho\sigma}(\xi,\gamma)\, e^{\{i[\beta_{\rho\sigma}\eta-\omega t]\}} \quad \text{(P1.2)}$$

where $\beta_{\rho\sigma}$ is the propagation constant of the $\rho\sigma$-mode, with $\rho\sigma = \pm m \pm n$ $(m, n > 0)$ and $\{\mathbf{E}_{\rho\sigma}(\xi,\gamma), \mathbf{H}_{\rho\sigma}(\xi,\gamma)\}$ is the complex vector amplitude of the guided 1D modes. By taking into account the expressions (P1.1, P1.2) it is easy to derive from the Maxwell's equations the following modal equations for the complex amplitudes of guided 1D vector modes:

$$\boldsymbol{\nabla}_t \wedge \mathbf{E}_{\rho\sigma} + i\beta_{\rho\sigma}\mathbf{u}_\eta \wedge \mathbf{E}_{\rho\sigma} = i\omega\mu\mathbf{H}_{\rho\sigma} \quad \text{(P1.3)}$$

$$\boldsymbol{\nabla}_t \wedge \mathbf{H}_{\rho\sigma} + i\beta_{\rho\sigma}\mathbf{u}_\eta \wedge \mathbf{H}_{\rho\sigma} = -i\omega\epsilon\mathbf{E}_{\rho\sigma} \quad \text{(P1.4)}$$

where $\boldsymbol{\nabla}_t = (\partial_\xi, \partial_\gamma, 0)$ and $\mathbf{u}_\eta$ is a unit vector pointing in the η-direction, that is, perpendicular to a cross-section of the optical waveguide. The amplitudes of the guided modes can be separated into the transverse field components $\{\mathbf{E}_{t\rho\sigma}(\xi,\gamma), \mathbf{H}_{t\rho\sigma}(\xi,\gamma)\}$ and the longitudinal field components $\{\mathbf{E}_{l\rho\sigma}(\xi,\gamma), \mathbf{H}_{l\rho\sigma}(\xi,\gamma)\}$, in such a way that from equations (P1.3, P1.4), and by using standard procedures based on the Lorentz reciprocity theorem for optical waveguides [Kogelnik, 1988], it is found that the norm of a guided $\rho\sigma$-mode, on a cross-section η of the waveguide, is given by the expression [Kogelnik, 1988, Liñares and Nistal, 1996, 2003]:

$$\|\mathbf{E}_{\rho\sigma}\| \equiv \|\mathbf{H}_{\rho\sigma}\| = \left\{2\,\mathrm{sgn}(\rho\sigma)\int\{\mathbf{E}_{t\rho\sigma} \wedge \mathbf{H}^{\star}_{t\rho\sigma}\}\mathbf{u}_\eta\, d\xi d\gamma\right\}^{1/2} \quad \text{(P1.5)}$$

where the function $\mathrm{sgn}(\rho\sigma)$ is defined to be +1 if $\rho\sigma > 0$, and -1 if $\rho\sigma < 0$; as it will be shown, this function will justify one of the more important results used in quantum light propagation problems, i.e., the positivity of the Momentum [Ben-Aryeh and Serulnik, 1991, Toren and Ben-Aryeh, 1994]. Next, by denoting the transverse componentes of the normalized guided 1D vector mode as: $\mathbf{e}_{t\rho\sigma}, \mathbf{h}_{t\rho\sigma}$, the following quasi-complete orthonormalization condition, on a cross-section of an optical guide, is obtained [Kogelnik, 1988, Liñares and Nistal, 1996]:

$$2\,\mathrm{sgn}(\rho\sigma)\int\{\mathbf{e}_{t\rho\sigma} \wedge \mathbf{h}^{\star}_{t\rho'\sigma'}\}\mathbf{u}_\eta\, d\xi d\gamma = \delta_{|\rho\sigma|,|\rho'\sigma'|} \quad \text{(P1.6)}$$

where $\delta_{|\rho\sigma|,|\rho'\sigma'|}$ is the Kronecker delta; note that the orthonormalization condition is determined only by the transverse field components of the

guided modes and it is a quasi-complete orthonormalization condition since for the cases $\rho\sigma = -\rho' - \sigma'$, equation (P1.5) is not equal to zero; however, in spite of that, it will be a very useful relationship for obtaining the quantum Momentum operator.

On the other hand, we will assume dispersion-free and non-magnetic media and distinguish between modal electrical and magnetic energy stored per unite guide length and under temporal averaging by means of the following standard expressions:

$$W^{e}_{\rho\sigma} = W^{e}_{t\rho\sigma} + W^{e}_{l\rho\sigma} = \int d\xi d\gamma\, \epsilon \mathbf{E}_{t\rho\sigma}\mathbf{E}^{\star}_{t\rho\sigma} + \int d\xi d\gamma\, \epsilon \mathbf{E}_{l\rho\sigma}\mathbf{E}^{\star}_{l\rho\sigma} \quad \text{(P1.7)}$$

$$W^{m}_{\rho\sigma} = W^{m}_{t\rho\sigma} + W^{m}_{l\rho\sigma} = \int d\xi d\gamma\, \mu_o \mathbf{H}_{t\rho\sigma}\mathbf{H}^{\star}_{t\rho\sigma} + \int d\xi d\gamma\, \mu_o \mathbf{H}_{l\rho\sigma}\mathbf{H}^{\star}_{l\rho\sigma} \quad \text{(P1.8)}$$

where it has been also distinguished between the energy fractions stored by the tranverse ($t \equiv \xi\gamma$) and longitudinal ($l \equiv \eta$) modal field componentes; next, by forming scalar products of the modal equations (P1.3, P1.4) with the appropriate modal field components and also combining the results in an appropriate way we obtain the following relations:

$$\boldsymbol{\nabla}_t \left(\mathbf{E}_{l\rho\sigma} \wedge \mathbf{H}^{\star}_{t\rho\sigma}\right) + i\beta_{\rho\sigma}\mathbf{u}_\eta \left(\mathbf{E}_{t\rho\sigma} \wedge \mathbf{H}^{\star}_{t\rho\sigma}\right) = i\omega\mu_o \mathbf{H}_{t\rho\sigma}\mathbf{H}^{\star}_{t\rho\sigma} - i\omega\epsilon \mathbf{E}_{l\rho\sigma}\mathbf{E}^{\star}_{l\rho\sigma} \quad \text{(P1.9)}$$

$$\boldsymbol{\nabla}_t \left(\mathbf{E}_{t\rho\sigma} \wedge \mathbf{H}^{\star}_{l\rho\sigma}\right) + i\beta_{\rho\sigma}\mathbf{u}_\eta \left(\mathbf{E}_{t\rho\sigma} \wedge \mathbf{H}^{\star}_{t\rho\sigma}\right) = i\omega\mu_o \mathbf{H}_{l\rho\sigma}\mathbf{H}^{\star}_{l\rho\sigma} - i\omega\epsilon \mathbf{E}_{t\rho\sigma}\mathbf{E}^{\star}_{t\rho\sigma} \quad \text{(P1.10)}$$

Now by integrating over the guide cross-section and taking into account the two-dimensional divergence theorem we obtain the following relevant expression:

$$\mathrm{sgn}(\rho\sigma)\|\mathbf{E}_{\rho\sigma}\|^2 \beta_{\rho\sigma} \equiv \mathrm{sgn}(\rho\sigma)\|\mathbf{H}_{\rho\sigma}\|^2 \beta_{\rho\sigma} = \omega(W_{t\rho\sigma} - W_{l\rho\sigma}) \quad \text{(P1.11)}$$

with $P_{\rho\sigma} = \mathrm{sgn}(\rho\sigma)\|\mathbf{E}_{\rho\sigma}\|^2$ the modal power or energy flow (positive for forward modes and negative for backward modes), and with $W_{t\rho\sigma} = W^{e}_{t\rho\sigma} + W^{m}_{t\rho\sigma}$ and $W_{l\rho\sigma} = W^{e}_{l\rho\sigma} + W^{m}_{l\rho\sigma}$, that is, the total transverse and total longitudinal energies, respectively.

P1.3. Quantization of the free Momentum of guided 1D vector modes

In this section we will quantize the free Momentum operator, that is the Momentum operator associated to the 1D vector modes without interaction among them, in order to clarify the consistency of the method; afterwards, the operator Momentum for coupled modes will be derived. First of all, we present the optical 1D vector mode field operator by using the normalized monochromatic modes, where the temporal mode fulfils a periodic condition in time such as it was established in [Ben-Aryeh and

Serulnik, 1991], that is, $\mathbf{E}_{\rho\sigma}(\xi,\gamma,\eta,0) = \mathbf{E}_{\rho\sigma}(\xi,\gamma,\eta,T)$, where T defines the mentioned periodic condition; next, the quantum free Momentum operator is derived, and finally a simple canonical quantization of the Momentum operator is presented.

Optical 1D vector mode field operator

Although later we will justify the expression of the modal field operator associated to a spatial multimode regime, one can write, by taking into account the usual field operator in quantum optics [Gerry and Knight, 2005, Loudon, 1982, Schleich, 2001, Walls and Milburn, 1994], the modal field operator $\{\hat{\mathbf{e}}, \hat{\mathbf{h}}\}$ as a superposition of normalized guided vector mode operators [Liñares and Nistal, 2003], that is:

$$\hat{\mathbf{e}} = \sum_{\rho\sigma} \hat{\mathbf{e}}_{\rho\sigma} = \\ = \sum_{\rho\sigma} (\hat{\mathbf{e}}^{(+)}_{\rho\sigma} + \hat{\mathbf{e}}^{(-)}_{\rho\sigma}) = \sum_{\rho\sigma} \frac{\sqrt{\hbar\omega}}{\sqrt{cT}} \left\{ \frac{1}{\|\mathbf{E}_{\rho\sigma}\|} [\hat{a}_{\rho\sigma}\mathbf{E}_{\rho\sigma}e^{-i\omega t} + \hat{a}^{\dagger}_{\rho\sigma}\mathbf{E}^{\star}_{\rho\sigma}e^{i\omega t}] \right\} \tag{P1.12}$$

$$\hat{\mathbf{h}} = \sum_{\rho\sigma} \hat{\mathbf{h}}_{\rho\sigma} = \\ = \sum_{\rho\sigma} (\hat{\mathbf{h}}^{(+)}_{\rho\sigma} + \hat{\mathbf{h}}^{(-)}_{\rho\sigma}) = \sum_{\rho\sigma} \frac{\sqrt{\hbar\omega}}{\sqrt{cT}} \left\{ \frac{1}{\|\mathbf{H}_{\rho\sigma}\|} [\hat{a}_{\rho\sigma}\mathbf{H}_{\rho\sigma}e^{-i\omega t} + \hat{a}^{\dagger}_{\rho\sigma}\mathbf{H}^{\star}_{\rho\sigma}e^{i\omega t}] \right\} \tag{P1.13}$$

where the superscripts $(+)$ and $(-)$ denote the wellknown field operators with positive and negative frequency, respectively [Gerry and Knight, 2005, Schleich, 2001]; the factor $(cT)^{1/2}$, introduced in [Ben-Aryeh and Serulnik, 1991], can be regarded as a normalization condition of the temporal mode; moreover, note that the creation $\hat{a}$ and annihilation $\hat{a}^{\dagger}$ operators are dimensionless as usual. On other hand, we must note that the norm, given by equation (P1.5), represents a generalization of the transmission conditions claimed in [Abram, 1987, Ben-Aryeh and Serulnik, 1991, Huttner et al., 1990]; in these works it was assumed that the electrical field must be divided by $n^{1/2}$ and the magnetic field multiplied by $n^{1/2}$; however, we can prove that these factors are obtained as a particular case of the modal norms for plane modes in an homogeneous medium with a constant index n and therefore with a propagation constant equal to $\beta = \omega n/c$. If we assume, for sake of simplicity, that the plane waves have amplitude equal to one on a cross-section A then the modal norms, obtained from equation (P1.5), for both TE and TM plane modes are as follows [Liñares and Nistal, 2003]: $\|\mathbf{E}_{\rho\sigma}\|_{TE} = \{2(\epsilon_o/\mu_o)^{1/2}An\}^{1/2}$ and $\|\mathbf{E}_{\rho\sigma}\|_{TM} = \{2(\mu_o/\epsilon_o)^{1/2}A/n\}^{1/2}$; these expressions are, excepting constants related to the system of units, identical

to those ones assumed in [Abram, 1987, Ben-Aryeh and Serulnik, 1991, Huttner et al., 1990] by using arguments of continuity of the field; however, as it has been just shown, they can be obtained in a natural way from the modal norms. Likewise, with the above results, $\|\mathbf{E}_{\rho\sigma}\|_{TE}$ and $\|\mathbf{E}_{\rho\sigma}\|_{TM}$, it is easy to prove that the operators $\{\hat{\mathbf{e}}_{\rho\sigma}, \hat{\mathbf{h}}_{\rho\sigma}\}$ contain, as a particular case, the usual expression of the operator associated to a mode plane $\rho\sigma$ with amplitude unity, propagating in the free space along η-direction and considered in a volume $V = AcT$, that is, if we consider the case of a TE mode, then by taking into account that in the vacuum the density of energy is related to the density of the energy flow [Born and Wolf, 1959] by the constant c, then the norm $\|\mathbf{E}_{\rho\sigma}\|_V$ in the volume V must be related to the propagating mode norm as follows: $(cT)^{1/2}\|\mathbf{E}_{\rho\sigma}\|_{TE} = c^{1/2}\|\mathbf{E}_{\rho\sigma}\|_V$, therefore, $\|\mathbf{E}_{\rho\sigma}\|_V = (2\epsilon_o AcT)^{1/2} = (2\epsilon_o V)^{1/2}$, which allow us to obtain the usual operator field for a plane mode in a volume V [Gerry and Knight, 2005, Loudon, 1982, Schleich, 2001].

Quantum free Momentum operator

Next, we will evaluate the quantum Momentum operator by integrating, over the hyperplane $d\xi d\gamma c dt$, the energy tensor element T^{33} [Ben-Aryeh and Serulnik, 1991, Jackson, 1975, Kogelnik, 1988, Landau and Lifshitz, 1975], whose classical expression, by using the normalized 1D vector modes, can be written as follows:

$$T^{33} = \frac{1}{2}[(\epsilon_o n^2 \mathbf{e}_t \mathbf{e}_t - \epsilon_o n^2 \mathbf{e}_l \mathbf{e}_l) + (\mu_o \mathbf{h}_t \mathbf{h}_t - \mu_o \mathbf{h}_l \mathbf{h}_l)] \tag{P1.14}$$

Therefore, the free quantum Momentum operator for the 1D vector modes takes the form [Ben-Aryeh and Serulnik, 1991, Liñares and Nistal, 2003]:

$$\hat{M}_O = \frac{1}{2}\iiint_0^T [\epsilon_o n^2(\hat{\mathbf{e}}_t\hat{\mathbf{e}}_t - \hat{\mathbf{e}}_l\hat{\mathbf{e}}_l) + \mu_o(\hat{\mathbf{h}}_t\hat{\mathbf{h}}_t - \hat{\mathbf{h}}_l\hat{\mathbf{h}}_l)]\, d\xi d\gamma c dt = \hat{M}_O^e + \hat{M}_O^m \tag{P1.15}$$

where the operator $\hat{M}_O$ can be separated into the electric and magnetic contributions $\hat{M}_O^e, \hat{M}_O^m$; likewise, it is important to note the presence of the longitudinal components, which are essential to derive the quantum Momentum operator, as it was previously made clear for 2D vector modes TE and TM [Liñares and Nistal, 2003], which are a limiting case of the 1D modes analyzed in this work. Now, by inserting equations (P1.12, P1.13) into the equation (P1.15), we can distinguish between terms (crossing terms) which rapidly oscillate over time as follows: $exp\{\pm 2i\omega t\}$, therefore the temporal integration (which is equivalent to a temporal averaging) of all these terms is equal to zero, and on the other hand, there are terms (non-crossing terms) whose temporal dependende has been cancelled, that is, temporal integration over the period T is equal to one, therefore the electric and magnetic contributions to the quantum Momentum operator can be rewritten

as follows:

$$\hat{M}^{e}_{O} = \frac{\hbar\omega}{2\|\mathbf{E}_{\rho\sigma}\|^2} \sum_{\rho\sigma} \iint [\epsilon_o n^2 (\mathbf{E}_{t\rho\sigma}\mathbf{E}^{\star}_{t\rho\sigma} - \mathbf{E}_{l\rho\sigma}\mathbf{E}^{\star}_{l\rho\sigma})(\hat{a}_{\rho\sigma}\hat{a}^{\dagger}_{\rho\sigma} + \hat{a}^{\dagger}_{\rho\sigma}\hat{a}_{\rho\sigma})]\, d\xi d\gamma \tag{P1.16}$$

$$\hat{M}^{m}_{O} = \frac{\hbar\omega}{2\|\mathbf{H}_{\rho\sigma}\|^2} \sum_{\rho\sigma} \iint [\mu_o (\mathbf{H}_{t\rho\sigma}\mathbf{H}^{\star}_{t\rho\sigma} - \mathbf{H}_{l\rho\sigma}\mathbf{H}^{\star}_{l\rho\sigma})(\hat{a}_{\rho\sigma}\hat{a}^{\dagger}_{\rho\sigma} + \hat{a}^{\dagger}_{\rho\sigma}\hat{a}_{\rho\sigma})]\, d\xi d\gamma \tag{P1.17}$$

Taking into account equation (P1.11) the above integrals can be identified with the $\rho\sigma$-modal electric and magnetic energy flows and therefore the sum of the equations (P1.16) and (P1.17) gives the following free Momentum operator:

$$\hat{M}_O = \hat{M}^{e}_{O} + \hat{M}^{m}_{O} = \sum_{\rho\sigma} \frac{\hbar}{2} \operatorname{sgn}(\rho\sigma)\beta_{\rho\sigma}(\hat{a}_{\rho\sigma}\hat{a}^{\dagger}_{\rho\sigma} + \hat{a}^{\dagger}_{\rho\sigma}\hat{a}_{\rho\sigma}) \tag{P1.18}$$

Quantum relations and Commutation Rules for forward and backward modes were derived in reference [Liñares and Nistal, 2003] by using the reversal-time symmetry of the Maxwell's equations and the η-reversal symmetry of modes, that is,

$$\hat{a}_{\rho\sigma<0} = -\hat{a}^{\dagger}_{\rho\sigma>0} \qquad \hat{a}^{\dagger}_{\rho\sigma<0} = -\hat{a}_{\rho\sigma>0} \tag{P1.19}$$

$$[\hat{a}_{\rho\sigma}, \hat{a}^{\dagger}_{\rho'\sigma'}] = \operatorname{sgn}(\rho\sigma)\, \delta_{|\rho\sigma||\rho'\sigma'|} \tag{P1.20}$$

Now, by taking into account equation (P1.20) and choosing a positive contribution of the vacuum fluctuations, the free Momentum operator can be rewritten in a normal order as follows:

$$\hat{M}_O = \sum_{\rho\sigma} \hbar \operatorname{sgn}(\rho\sigma)\beta_{\rho\sigma}\hat{a}^{\dagger}_{\rho\sigma}\hat{a}_{\rho\sigma} \tag{P1.21}$$

where the fluctuations of the vacuum have been cancelled; moreover this result contains important physical content: the function $\operatorname{sgn}(\rho\sigma)$ ensures the positivity of Momentum, which was assumed in [Ben-Aryeh et al., 1992, Toren and Ben-Aryeh, 1994], and now it is a natural consequence of the modal norms.

A simple canonical quantization

As a complementary view of the Momentum quantization we present a simple macroscopic canonical quantization analogous to that one used for the Hamiltonian quantization. We start obtaining the classical Momentum of a 1D vector mode $\rho\sigma$ by using the complex representation of the modal field, compatible with the modal norm given by equation (P1.5), that is,

$$\mathbf{E}_{\rho\sigma}(\xi,\gamma,t) = \{\mathbf{E}_{\rho\sigma}(\xi,\gamma,t) + \mathbf{E}^{\star}_{\rho\sigma}(\xi,\gamma,t)\} \tag{P1.22}$$

$$\mathbf{H}_{\rho\sigma}(\xi,\gamma,t) = \{\mathbf{H}_{\rho\sigma}(\xi,\gamma,t) + \mathbf{H}^{\star}_{\rho\sigma}(\xi,\gamma,t)\} \tag{P1.23}$$

which must be inserted into the energy tensor element T^{33} (now without using normalized modes) and integrated over the hypercross-section of the guide $d\xi d\gamma c dt$; therefore by making the temporal integration in the interval $[0, T]$ the following free classical Momentum is obtained:

$$M_{O\rho\sigma} = cT \int d\xi d\gamma \, [\epsilon_o n^2 (\mathbf{E}_{t\rho\sigma}\mathbf{E}^{\star}_{t\rho\sigma} - \mathbf{E}_{l\rho\sigma}\mathbf{E}^{\star}_{l\rho\sigma}) + \mu_o (\mathbf{H}_{t\rho\sigma}\mathbf{H}^{\star}_{t\rho\sigma} - \mathbf{H}_{l\rho\sigma}\mathbf{H}^{\star}_{l\rho\sigma})] \tag{P1.24}$$

Now, by taking into account the equation (P1.11) the following expression is obtained for the classical Momentum:

$$M_{O\rho\sigma} = \mathrm{sgn}(\rho\sigma) \frac{\beta_{\rho\sigma}}{\omega} \|\mathbf{E}_{\rho\sigma}\|^2 cT \tag{P1.25}$$

where $\|\mathbf{E}_{\rho\sigma}\|^2$ is given by equation (P1.5); the above expression is the starting point for obtaining a simple canonical quantization of the Momentum and the 1D vector modal fields simultaneously; that is, we rewrite the 1D vector mode fields as follows:

$$\mathbf{E}_{\rho\sigma}(\xi, \gamma, \eta, t) = E_{o\rho\sigma}(\eta)\mathbf{e}_{\rho\sigma}(\xi, \gamma, t) = E_{o\rho\sigma}(\eta)\mathbf{e}_{\rho\sigma}(\xi, \gamma)e^{-i\omega t} \tag{P1.26}$$

$$\mathbf{H}_{\rho\sigma}(\xi, \gamma, \eta, t) = E_{o\rho\sigma}(\eta)\mathbf{h}_{\rho\sigma}(\xi, \gamma, t) = E_{o\rho\sigma}(\eta)\mathbf{h}_{\rho\sigma}(\xi, \gamma)e^{-i\omega t} \tag{P1.27}$$

where $E_{o\rho\gamma}$ is a constant complex amplitude and $\mathbf{e}_{\rho\sigma}, \mathbf{h}_{\rho\sigma}$ are the normalized modes; now, by inserting these expressions into equation (P1.25), and taking into account the modal normalization, we obtain:

$$M_{O\rho\sigma} = \mathrm{sgn}(\rho\sigma) \frac{\beta_{\rho\sigma}}{\omega} cT \, E_{o\rho\sigma}(\eta) \, E^{\star}_{o\rho\sigma}(\eta) \tag{P1.28}$$

Let us choose new canonical variables in order to obtain a classical Momentum which can be identified with a wellknown mechanical problem, that is, an harmonic oscillator, but now the role of time will be played by the longitudinal variable η and the role of frequency will be played by the propagation constant $\beta_{\rho\sigma}$, therefore, let us consider:

$$E_{o\rho\sigma}(\eta) = \frac{1}{\sqrt{2cT\mathrm{sgn}(\rho\sigma)\,\beta_{\rho\sigma}/\omega}} (\beta_{\rho\sigma} q_{\rho\sigma} + i p_{\rho\sigma}) \tag{P1.29}$$

$$E^{\star}_{o\rho\sigma}(\eta) = \frac{1}{\sqrt{2cT\mathrm{sgn}(\rho\sigma)\,\beta_{\rho\sigma}/\omega}} (\beta_{\rho\sigma} q_{\rho\sigma} - i p_{\rho\sigma}) \tag{P1.30}$$

accordingly the classical Momentum fulfils the equation of a (spatial) harmonic oscillator, that is,

$$M_{O\rho\sigma} = \frac{1}{2} (p^2_{\rho\sigma} + \beta^2_{\rho\sigma} q^2_{\rho\sigma}) \tag{P1.31}$$

which can be also easily obtained by starting from the modal wave equation for 1D vector modes propagating along the η-direction, that is:

$$\frac{\partial^2 E_{\rho\sigma}}{\partial \eta^2} + \beta_{\rho\sigma}^2 E_{\rho\sigma} = 0 \tag{P1.32}$$

which clearly suggests a spatial harmonic oscillator, that is, with η substituting the time t and $\beta_{\rho\sigma}$ substituting the frecuency ω of an temporal harmonic oscillator. It must be stressed that spatial harmonic and anharmonic oscillators appears in a natural way in linear and nonlinear classical optical propagation problems [Liñares, 1989, Mateo and Liñares, 2005], which can be described by means of a functional variational formulation based on spatial density functionals (spatial Lagrangians) [Mateo and Liñares, 2005] which is fully compatible with the canonical results used in this subsection.

Next, by using the principle of quantization in the classical Momentum operator given by equation (P1.31) and the following change of operators:

$$\hat{a}_{\rho\sigma} = \frac{1}{\sqrt{2\hbar\, \mathrm{sgn}(\rho\sigma)\, \beta_{\rho\sigma}}} (\beta_{\rho\sigma}\hat{q}_{\rho\sigma} + i\hat{p}_{\rho\sigma}) \tag{P1.33}$$

$$\hat{a}^{\dagger}_{\rho\sigma} = \frac{1}{\sqrt{2\hbar\, \mathrm{sgn}(\rho\sigma)\, \beta_{\rho\sigma}}} (\beta_{\rho\sigma}\hat{q}_{\rho\sigma} - i\hat{p}_{\rho\sigma}) \tag{P1.34}$$

the complex amplitude $E_{o\rho\sigma}$ can be quantized and accordingly the 1D vector modal field too, that is, from equations (P1.29, P1.33), we obtain :

$$\hat{\mathbf{e}}^{(+)}_{\rho\sigma}(\xi,\gamma,\eta,t) = \hat{E}_{o\rho\gamma}(\eta)\mathbf{e}_{\rho\sigma}(\xi,\gamma)e^{-i\omega t} = (\hbar\omega)^{1/2}\frac{\mathbf{E}_{\rho\sigma}e^{-i\omega t}}{(cT)^{1/2}\|\mathbf{E}_{\rho\sigma}\|}\hat{a}_{\rho\sigma} \tag{P1.35}$$

$$\hat{\mathbf{e}}^{(-)}_{\rho\sigma}(\xi,\gamma,\eta,t) = \hat{E}^{\dagger}_{o\rho\gamma}(\eta)\mathbf{e}_{\rho\sigma}(\xi,\gamma)e^{+i\omega t} = (\hbar\omega)^{1/2}\frac{\mathbf{E}_{\rho\sigma}e^{+i\omega t}}{(cT)^{1/2}\|\mathbf{E}_{\rho\sigma}\|}\hat{a}^{\dagger}_{\rho\sigma} \tag{P1.36}$$

It is obvious that the sum of the above equations gives the optical 1D vector mode field $\hat{\mathbf{e}}_{\rho\sigma}$ defined in equation (P1.12) such as we have proven. This ends the simple canonical quantization, where spatial harmonic oscillators $\rho\sigma$ have been quantized, that is, when we consider the spatial propagation of a 1D vector mode then the optical field fulfils the equation of a classical η-spatial harmonic oscillator with spatial "frequency" $\beta_{\rho\sigma}$, which can be quantized by means of the standard methods.

P1.4. Quantization of the Momentum of coupled guided 1D vector modes

We will analyze the modal coupling by introducing a dielectric perturbation of the original refractive index $n^2(\xi,\gamma)$; this perturbation is described, as usual, by a material polarization which is a new operator $\hat{\mathbf{P}} = (\Delta\hat{\epsilon})\,\hat{\mathbf{e}}$, where $(\Delta\hat{\epsilon})$ denotes a perturbation of the electrical permitivity which can present isotropy, anisotropy, non-linearity and so on, and $\hat{\mathbf{e}}$ denotes the

total optical field operator in the guide; moreover it is assumed that the polarization operator can be expressed as a function of the non perturbed field operators, in a similar way to the classical case [Kogelnik, 1988], therefore, the Momentum operator for guided 1D vector modes coupled by means of a polarization $\hat{\mathbf{P}}$ can be written as:

$$\hat{M} = \hat{M}_O + \frac{1}{2}\iiint_0^T \hat{\mathbf{P}}\,\hat{\mathbf{e}}\;d\xi d\gamma c dt = \hat{M}_O + \frac{1}{2}\iiint_0^T \hat{P}_i\,\hat{e}_i\;d\xi d\gamma c dt \qquad \text{(P1.37)}$$

where each component $i\,(=\xi,\gamma,\eta)$ of the polarization operator can be written, in a formal way, as follows:

$$\hat{P}_i = \{\epsilon_o\,\chi_{ijklm\ldots}\hat{e}_k\,\hat{e}_l\,\hat{e}_m\ldots\}\,\hat{e}_j, \qquad k,l,m,\ldots,j = (\xi,\gamma,\eta) \qquad \text{(P1.38)}$$

However, it is usual that the device present several kinds of perturbation simultaneously, in particular, let us consider that the integrated optical device is perturbed by both a linear and a nonlinear polarization, that is, $\hat{\mathbf{P}} = \hat{\mathbf{P}}_L + \hat{\mathbf{P}}_{NL}$, therefore de total Momentum is written as:

$$\hat{M} = \hat{M}_O + \frac{1}{2}\iiint_0^T \hat{\mathbf{P}}_L\,\hat{\mathbf{e}}\;d\xi d\gamma c dt + \frac{1}{2}\iiint_0^T \hat{\mathbf{P}}_{NL}\,\hat{\mathbf{e}}\;d\xi d\gamma c dt \qquad \text{(P1.39)}$$

We will analyze these two perturbations in a separated way: the linear perturbation was analyzed for 2D vector modes and now it will be generalized to 1D vector modes, and next, for expositional convencience, a particular nonlinear perturbation will be considered.

Quantization of the linear Momentum of coupled guided 1D vector modes

We start with the quantization of the linear polarization corresponding to an isotropic and inhomogeneous perturbation, that is, $\hat{\mathbf{P}}_L = \Delta\epsilon\,\hat{\mathbf{e}} = \Delta\epsilon\,(\hat{\mathbf{e}}_t + \hat{\mathbf{e}}_l)$, therefore the corresponding contribution to the Momentum operator will be

$$\hat{M}_L = \frac{1}{2}\iiint_0^T \Delta\epsilon\,\hat{\mathbf{e}}\,\hat{\mathbf{e}}\;d\xi d\gamma c dt = \frac{1}{2}\iiint_0^T \Delta\epsilon \sum_{\rho\sigma}\hat{\mathbf{e}}_{\rho\sigma}\sum_{\rho'\sigma'}\hat{\mathbf{e}}_{\rho'\sigma'}\;d\xi d\gamma c dt \qquad \text{(P1.40)}$$

Now it should be paid attention to the particular way in which longitudinal components are handled under a linear perturbation with longitudinal component $\mathbf{P}_l = \Delta\epsilon\,\boldsymbol{e}_l$; it is necessary because only the transverse components are orthogonal and the mode expansion can be only applied to these components; therefore, by taking into account the quantized complex Maxwell-Ampere Law for the perturbated problem with field operators with positive frequency, the mentioned mode expansion with the transverse components of the 1D vector mode operators with positive frequency

such as given by equation (P1.13), and again the complex Maxwell-Ampere Law for each mode operator, then we obtain the following expression for the longitudinal component of the optical field operator with positive frequency, $\hat{\mathbf{e}}_l^{(+)}$:

$$(\epsilon + \Delta\epsilon)\hat{\mathbf{e}}_l^{(+)} = \frac{i}{\omega}\boldsymbol{\nabla}_t \wedge \hat{\mathbf{h}}_t^{(+)} = \epsilon \frac{\sqrt{\hbar\omega}}{\sqrt{cT}} \sum_{\rho\sigma} \left\{ \frac{1}{\|\mathbf{E}_{\rho\sigma}\|} \hat{a}_{\rho\sigma} \mathbf{E}_{l\rho\sigma} e^{-i\omega t} \right\} \tag{P1.41}$$

therefore for the perturbated problem the longitudinal component of the optical field operator must be rewritten as follows:

$$\hat{\mathbf{e}}_l = \frac{\epsilon}{\epsilon + \Delta\epsilon} \frac{\sqrt{\hbar\omega}}{\sqrt{cT}} \sum_{\rho\sigma} \left\{ \frac{1}{\|\mathbf{E}_{\rho\sigma}\|} [\hat{a}_{\rho\sigma} \mathbf{E}_{l\rho\sigma} e^{-i\omega t} + \hat{a}_{\rho\sigma}^{\dagger} \mathbf{E}_{l\rho\sigma}^{\star} e^{i\omega t}] \right\} \tag{P1.42}$$

Now, by inserting both the transverse components of the field operators given by equation (P1.12) and the longitudinal component given by equation (P1.42) into equation (P1.40), by performing temporal integration and by taking into account that the creation and annihilation operators commute for different modes, we obtain non-crossing terms ($\rho\sigma = \rho'\sigma'$) and crossing terms ($\rho\sigma \neq \rho'\sigma'$) different from zero, therefore the linear operator Momentum of coupled modes is given by the following expression:

$$\hat{M}_L = \sum_{\rho\sigma} \hbar\, \mathrm{sgn}(\rho\sigma) \kappa_{\rho\sigma,\rho\sigma}\, \hat{a}_{\rho\sigma}^{\dagger} \hat{a}_{\rho\sigma} + \sum_{\rho\sigma<\rho'\sigma'} \{\hbar\, \kappa_{\rho\sigma,\rho'\sigma'}\; \hat{a}_{\rho\sigma} \hat{a}_{\rho'\sigma'}^{\dagger} + \mathrm{h.c.}\} \tag{P1.43}$$

where, as in the free case, commutation rules given by equation (P1.20) have been used in the calculation of non-crossing terms, in such a way that positive contribution of the vacuum fluctuations were chosen; moreover, the self - coupling coefficient $\kappa_{\rho\sigma,\,\rho\sigma}$ and the cross - coupling coefficients $\kappa_{\rho\sigma,\,\rho'\sigma'}$ are given by the expressions:

$$\kappa_{\rho\sigma,\,\rho\sigma} = \frac{\omega \iint \Delta\epsilon\, \mathbf{E}_{t\rho\sigma} \mathbf{E}_{t\rho\sigma}^{\star} d\xi d\gamma}{2 \iint \{\mathbf{E}_{t\rho\sigma} \wedge \mathbf{H}_{t\rho\sigma}^{\star}\} \mathbf{u}_\eta\, d\xi d\gamma} + \frac{\omega \iint\, \Delta\epsilon\, F(\Delta\epsilon)\, \mathbf{E}_{l\rho\sigma} \mathbf{E}_{l\rho\sigma}^{\star} d\xi d\gamma}{2 \iint \{\mathbf{E}_{\rho\sigma} \wedge \mathbf{H}_{t\rho\sigma}^{\star}\} \mathbf{u}_\eta\, d\xi d\gamma} \tag{P1.44}$$

$$\kappa_{\rho\sigma,\rho'\sigma'} = \frac{\omega \iint \Delta\epsilon\, \mathbf{E}_{t\rho\sigma} \mathbf{E}_{t\rho'\sigma'}^{\star} d\xi d\gamma}{\|\mathbf{E}_{\rho\sigma}\|\;\|\mathbf{E}_{\rho'\sigma'}\|} + \frac{\omega \iint \Delta\epsilon\, F(\Delta\epsilon)\, \mathbf{E}_{l\rho\sigma} \mathbf{E}_{l\rho'\sigma'}^{\star} d\xi d\gamma}{\|\mathbf{E}_{\rho\sigma}\|\;\|\mathbf{E}_{\rho'\sigma'}\|} \tag{P1.45}$$

where $F(\Delta\epsilon) = \epsilon/(\epsilon + \Delta\epsilon)$; note that for modes weakly coupled, that is, $\Delta\epsilon/\epsilon \ll$, the following approximation can be used $F(\Delta\epsilon) \approx 1$, which simplifies equations (P1.44, P1.45); moreover, by denoting $\tilde{\beta}_{\rho\sigma} = \beta_{\rho\sigma} + \kappa_{\rho\sigma,\,\rho\sigma}$, the sum of free and linear Momentums given by equations (P1.21) and

(P1.43) can be written as follows:

$$\hat{M}_{OL} = \hat{M}_O + \hat{M}_L = \sum_{\rho\sigma} \hbar\, sgn(\rho\sigma)\tilde{\beta}_{\rho\sigma}\, \hat{a}^{\dagger}_{\rho\sigma}\hat{a}_{\rho\sigma} + \sum_{\rho\sigma<\rho'\sigma'} \{\hbar\, \kappa_{\rho\sigma,\rho'\sigma'}\ \hat{a}_{\rho\sigma}\hat{a}^{\dagger}_{\rho'\sigma'} + h.c.\} \tag{P1.46}$$

which is the quantum Momentum operator for coupled guided 1D vector modes under a linear coupling polarization; modes can be forward or backward. Interesting quantum analysis has been recently made for counterpropagating modes [Perinová et al., 2006], whose linear coupling has been analyzed by quantization by means of the standard correspondence principle. It is easy to obtain, from both the equation (P1.46) and the commutation rules (P1.20), the Heisenberg's equations for the forward and backward annihilation operators $\hat{a}_{\rho\sigma>0}$ and $\hat{a}_{\rho\sigma<0}$, that is:

$$-i\hbar\partial_\eta \hat{a}_{\rho\sigma} = [\hat{a}_{\rho\sigma}, M_{oL}] = \hbar\tilde{\beta}_{\rho\sigma}\hat{a}_{\rho\sigma} + sgn(\rho'\sigma') \sum_{\rho'\sigma'\neq\rho\sigma} \hbar\, \kappa_{\rho\sigma,\rho'\sigma'}\ \hat{a}_{\rho'\sigma'} \tag{P1.47}$$

Note that the function $sgn(\rho'\sigma')$ in the coupling terms appears in a natural way by starting from: the Momentum operator, commutation rules and Heisenberg's equations. This Momentum operator can describe quantum modal linear coupling in directional couplers, in integrated gratings, integrated junctions and so on. Obviously, for the free case the spatial evolution of the annihilation operator is that one corresponding to a classical mode, that is, $\hat{a}_{\rho\sigma}(\eta) = \hat{a}_{\rho\sigma}(0) exp\{i\beta_{\rho\sigma}\eta\}$, therefore: $\hat{a}^{\dagger}_{\rho\sigma}(\eta) = \hat{a}^{\dagger}_{\rho\sigma}(0)$ $exp\{-i\beta_{\rho\sigma}\eta\}$; this suggests to use the well-known interaction picture, that is, by substituting the change: $\hat{a}_{\rho\sigma}(\eta) = \hat{A}_{\rho\sigma}(\eta)\, exp\{i\beta_{\rho\sigma}\eta\}$ into equation (P1.46), or into equation (P1.47), thus the first term in the Momentum operator is a constant, which can be not considered, and therefore the Momentum can be rewritten in the interaction picture (I) as follows:

$$\hat{M}^{I}_{OL} = \sum_{\rho\sigma<\rho'\sigma'} \{\hbar\, \kappa_{\rho\sigma,\rho'\sigma'}\ \hat{A}_{\rho\sigma}\hat{A}^{\dagger}_{\rho'\sigma'}\, e^{i(\beta_{\rho\sigma}-\beta_{\rho'\sigma'})\eta} + h.c.\} \tag{P1.48}$$

This ends the derivation of the linear Momentum operator for weakly or strongly coupled modes in a photonic waveguide structure or integrated photonic device.

Quantization of the nonlinear Momentum of coupled guided 1D vector modes

In this section we will extend the present analysis to a nonlinear perturbation. Obviously, a great deal of nonlinear problems can be presented and their general treatment would be very complex, therefore by expositional convenience we will center our attention on a particular problem, for

example, a directional coupler formed by $N = 3$ guides weakly-coupled of which one of them is nonlinear with a χ^2 nonlinearity generating a second-harmonic mode in a KTP material (Figure P1.1)[16]; this problem was proposed and solved in a classical way by Assanto et.al. in reference [Assanto et al., 1994] for the case of $N = 2$ (a linear waveguide and other nonlinear one); the quantum treatment was made later by Peřina [Perina Jr and Perina, 2000] starting from a Momentum operator proposed in an heuristic way; our aim will be to obtain *ab initio* the above nonlinear Momentum operator by using the theoretical formulation given in this work; for that, let us consider, for expositional convenience, N=3 (that is, a 3x3 coupler) where there are two linear waveguides and one nonlinear central waveguide, in such a way that it illustrates the general procedure to derive any other nonlinear Momentum operator in a waveguide structure.

First of all it is important to remember the nonlinear suceptibility tensor of the KTP crystal and to connect it with the waveguide structure; for that, let us consider the following relationship between the subindices $\{123\}$ to characterize the nonlinear susceptibility of the KTP crystal and the subindices $\{\xi\gamma\eta\}$ characterizing the waveguide structure: $1 \equiv \eta$, $2 \equiv \xi$, $3 \equiv \gamma$; we also remember that KTP is a crystal belonging to the $mm2$ crystal class, with coefficients of the nonlinear susceptibility tensor, in contracted notation, fullfilling the following order relationship: $d_{33} > d_{24} > d_{31} > d_{15} > d_{32}$.

On the other hand, we assume that guides 1, 2 and 3 of the coupler are monomode, therefore the quasi-TE fundamental modes ($\rho\sigma = 11$) are allowed in the guides, and accordingly the photons are excited in modes with a dominant γ-component for the associated field operator, that is: $\mathbf{e}_{\gamma 11(1,2,3)}$ ($\gg \mathbf{e}_{\eta 11(1,2,3)} \gg \mathbf{e}_{\xi 11(1,2,3)}$); moreover, we assume that linear guide 1(or linear guides 1 and 3) is (are coherentely) excited in the mode $\mathbf{e}_{\gamma 11(1)}$ (in the modes $\mathbf{e}_{\gamma 11(1,3)}$) and by means of directional coupling the energy is transferred to the central guide 2 (nonlinear guide) in the mode $\mathbf{e}_{\gamma 11(2)}$ and SHG is produced in this guide in the mode $\mathbf{e}_{\gamma 11(4)}$; we also assume that linear coupling between $\mathbf{e}_{\gamma 11(4)}$ and $\mathbf{e}_{\gamma 11(1,3)}$ is negligible because of the different frequencies of these modes. In short, since any general optical field in the coupler will be a quasi-TE field, that is $\mathbf{e}_\gamma$, it is clear that only the term d_{33} gives an important contribution to the SHG because it provides a dominant nonlinear polarization component, that is: $\mathbf{P}_{NL} \approx 2d_{\gamma\gamma}e_\gamma^2\mathbf{u}_\gamma$, therefore the nonlinear Momentun operator is given by the expression:

$$\hat{M}_{NL} = \frac{1}{2}\iiint_0^T \hat{\mathbf{P}}_{NL}\,\hat{\mathbf{e}}\;d\xi d\gamma c dt \approx \frac{1}{2}\iiint_0^T 2d_{\gamma\gamma}\hat{e}_\gamma^2\,\hat{e}_\gamma\;d\xi d\gamma c dt \qquad \text{(P1.49)}$$

The rest of terms, by taking into account the commutativity of the components of the modal field operator [Mandel and Wolf, 1995], are of the

[16]This figure does not appear in the original paper. We have added it here for the sake of clarity in the discussion.

type: $\hat{e}_\xi^2\,\hat{e}_\gamma$, $\hat{e}_\eta^2\,\hat{e}_\gamma$, however, according to the previous analysis they can be regarded as negligible terms. Now we can calculate the nonlinear Momentum operator taking into account the four modes, that is, $\rho\sigma m = 11m$ with $m = 1,2,3,4$, therefore by substituting into equation (P1.49) the following operator field:

$$\hat{e}_\gamma = \sum_{11(m)} \frac{\sqrt{\hbar\omega_m}}{\sqrt{c\overline{T}}}\Big\{\frac{1}{\|\mathbf{E}_{11m}\|}[\hat{a}_{11m}E_{\gamma 11m}e^{-i\omega_m t} + \hat{a}_{11m}^\dagger E_{\gamma 11m}^\star e^{i\omega_m t}]\Big\} \tag{P1.50}$$

where $\omega_4 = 2\omega_1 = 2\omega_2 = 2\omega_3$, by performing integration, and by taking into account that $2d_{\gamma\gamma}$ is localized in the guide (2) (that is, there is a negligible nonlinear coupling between modes $m = 1,4$ and $m = 3,4$), we easily obtain:

$$\hat{M}_{NL} = \hbar\{\kappa_{112,114}\,\hat{a}_{112}^2\,\hat{a}_{114}^\dagger + h.c.\} \tag{P1.51}$$

where $\kappa_{112,114}$ is the nonlinear coupling coefficient between modes 112 and 114, propagating in the guide (2), obtained after performing the integration indicated in equation (P1.49). Now, remaking equation (P1.46) for the free and linear coupling of this coupler (with copropagating modes) we obtain:

$$\hat{M}_{OL} = \sum_{11m=111}^{114} \hbar\,\tilde{\beta}_{11m}\,\hat{a}_{11m}^\dagger\hat{a}_{11m} + \sum_{11m\neq 11n} \{\hbar\,\kappa_{11m,11n}\;\hat{a}_{11m}\hat{a}_{11n}^\dagger + h.c.\} \tag{P1.52}$$

however, as we assume, the linear coupling between modes $m = 1,4$ and $m = 3,4$ is negligible because of the different frequencies; likewise, the linear coupling between $m = 2,4$ is also negligible because there is no linear perturbation $\Delta\epsilon$ between them, and finally the linear coupling between modes $m = 1,3$ is negligible because of the large separation between them, therefore there is only linear coupling between guides 1 and 2, and between guides 2 and 3; now, by using a contracted notation ($11m \equiv m$) and taking into account equations (P1.51, P1.52) the following total Momentum operator is obtained:

$$\hat{M} = \sum_{m=1}^{4} \hbar\,\tilde{\beta}_m\,\hat{a}_m^\dagger\hat{a}_m + \sum_{n=1}^{2} \hbar\{\kappa_{2,2n-1}\,\hat{a}_{2n-1}\hat{a}_2^\dagger + h.c.\} + \hbar\{\kappa_{2,4}\,\hat{a}_2^2\,\hat{a}_4^\dagger + h.c.\} \tag{P1.53}$$

The corresponding Heisenberg's equations are calculated as it was made in (P2.32), therefore, by considering that the three guides are equals, that is: $\tilde{\beta}_1 = \tilde{\beta}_2 = \tilde{\beta}_3 = \tilde{\beta}_L \neq \beta_4 = \tilde{\beta}_{NL}$, $\kappa_{2,1} = \kappa_{2,3} = \kappa_L$ and writting $\kappa_{2,4} = \kappa_{NL}$, we obtain, after a simple calculation, the following equations:

$$-i\partial_\eta\hat{a}_1 = \tilde{\beta}_L\hat{a}_1 + \kappa_L^\star\hat{a}_2 \tag{P1.54}$$

$$-i\partial_\eta\hat{a}_2 = \tilde{\beta}_L\hat{a}_2 + \kappa_L\hat{a}_1 + \kappa_L\hat{a}_3 + 2\kappa_{NL}^\star\hat{a}_2^\dagger\hat{a}_4 \tag{P1.55}$$

$$-i\partial_\eta\hat{a}_3 = \tilde{\beta}_L\hat{a}_3 + \kappa_L^\star\hat{a}_2 \tag{P1.56}$$

$$-i\partial_\eta\hat{a}_4 = \tilde{\beta}_{NL}\hat{a}_4 + \kappa_{NL}\hat{a}_2^2 \tag{P1.57}$$

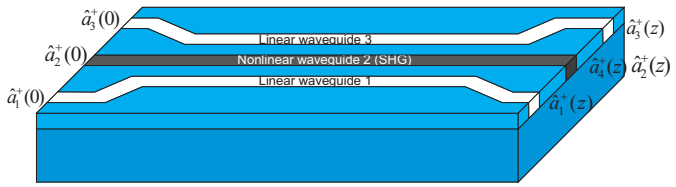

Figure P1.1: Sketch showing a nonlinear symmetric 3×3 directional coupler.

This result is clearly identical to that one proposed in [Perina, 1995, Perina Jr and Perina, 2000] if the interaction picture is used and guide 3 is removed; accordingly, equation (P1.56) for $\hat{a}_3$ has to be removed and it must be taken $\hat{a}_3 = 0$ in equation (P1.55). As it was also pointed out in [Perina, 1995] the main novelty of this Momentum operator is that the Heisenberg's equations are different to those ones obtained directly from the classical coupling equations by applying the correspondence principle, in particular the factor 2 in the term $2\kappa_{NL}^{\star}\hat{a}_2^{\dagger}\hat{a}_4$ of equation (P1.55); therefore, the theoretical formulation presented in this work allow to obtain many others Momentum operators in such a way that the corresponding Heisenberg's equations can not be obtained by direct quantization of classical equations, which justifies the interest of this formulation about the quantization of the Momentun operator. Analogous results will arise with the Spin operator in integrated photonics, which will be presented in a next work.

P1.5. Summary

We have derived the linear and nonlinear quantum Momentum operators for integrated photonic waveguide devices described by coupled mode propagation. Quantization has been obtained by taking into account the modal orthonormalization on a cross - section of an integrated photonic waveguide, the modal vector structure and the modal reversal - time symmetry; likewise, a simple canonical quantization for the free Momentun operator based on the flow of energy in a photonic integrated waveguide has been presented. Finally, by calculating the Heisenberg's equations for a general linear modal coupling problem and a particular nonlinear directional coupling problem it has been proven that the quantum results are fully consistent with both the classical descriptions and the usual prescriptions used in quantum optical propagation, specially in counterporpagation problems and nonlinear copropagation problems.

USC
UNIVERSIDADE
DE SANTIAGO
DE COMPOSTELA

C1. GENERATION OF QUANTUM LIGHT IN SOI STRUCTURES

PROCEEDINGS OF THE 23rd INTERNATIONAL COMISSION FOR OPTICS (ICO) CONFERENCE
QUANTUMOPT - 216 - 355
ISBN: 978 - 84 - 697 - 1027 - 2

CELEBRATED 26-29 AUGUST 2014

BY DAVID BARRAL[1], GARY SINCLAIR[2], DAMIEN BONNEAU[2], JOSH SILVERSTONE[2], GERARDO VILLAREAL[2], JESÚS LIÑARES[1] & MARK G. THOMPSON[2]

[1]UNIVERSIDADE DE SANTIAGO DE COMPOSTELA
[2]UNIVERSITY OF BRISTOL

Abstract: *In this communication we present a quantum theory of the propagation of light in silicon on insulator waveguides: from a quantum Momentum operator $\hat{\mathrm{M}}$ which takes into account dissipation, we derive and solve Heisenberg-Langevin's equations in the parametric approximation and briefly analyze some cases of practical interest.*

C1.1. Introduction

Integrated quantum photonics circuits are a promising technology for quantum information processing as it has been shown last years [Thompson et al., 2011]. However, the sources of these circuits, quantum states of light, are generated conventionally by spontaneous parametric down conversion (SPDC) in bulk crystals. Future quantum photonic circuits will require on-chip single photon sources to carry out applications in quantum communication, sensing and computation. One potential candidate for making them is the silicon-on-insulator (SOI) material, because of its compatibility with the existing silicon-based microelectronics technology, its high refractive index contrast and the large Kerr nonlinearity it presents. These last features enable an enhanced spontaneous four wave mixing (SFWM) and therefore an efficient single photon source. However it is not all story because near the telecommunication wavelength of 1.55 μm, silicon exhibits two-photon absorption (TPA) and, as a consequence, free carrier absorption (FCA) and dispersion (FCD), imposing an intrinsic limit on single photon generation. Moreover, resonant interaction with optical phonons introduces spontaneous Raman scattering (SpRS). This effect is polarization-dependent, being absent for TM modes, but appearing 15.6 THz away from the pump for TE modes. For all this we consider of interest a theoretical study on the propagation of light in this kind of media. In this communication we present a quantum theory of the propagation of light in SOI waveguides: from a quantum Momentum operator $\hat{M}$ which takes into account dissipation, we derive and solve Heisenberg-Langevin's equations in the parametric approximation and briefly analyze some cases of practical interest.

C1.2. Langevin's equations & conversion efficiency in SOI

It is well-known that the operator that describes correctly the quantum spatial propagation along an arbitrary direction z is the Momentum operator $\hat{M}$. Recently it has been applied to the study of nonlinear dissipative waveguides [Liñares et al., 2012]. We apply this approach to a Kerr $\chi^{(3)}$ waveguide (Fig. 1)[17], with the pump $|\zeta\rangle$ treated classically, that is $\langle \hat{a}_p \rangle \equiv \zeta = |\zeta(z)|\, e^{i\beta_p z + i\phi(z)}$ with $\phi(z)$ the nonlinear phase shift, and assuming it as a cw TE mode which remains undepleted because it is much more intense than the signal and idler waves. This pump will couple to signal and idler waves fulfilling energy conservation, $2\omega_p = \omega_s + \omega_i$, where we assume that the frequency detuning $|\omega_{s,i} - \omega_p|$ is far away from 15.6 THz, which allow us to ignore SpRS. Besides we consider the nonlinear interaction instantaneous, as this frequency detuning is much smaller than

[17] These figures were presented in the poster session dedicated to Quantum Optics at the conference. We have added them here to improve the clarity of the text.

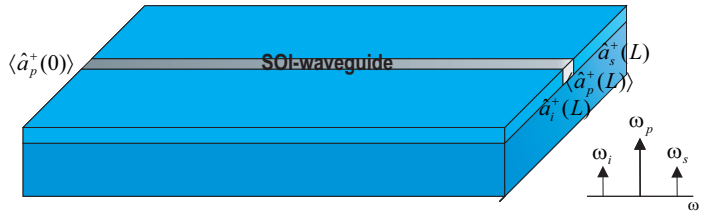

Figure C1.1: Sketch of an integrated SOI waveguide performing FWM.

the inverse of the medium's nonlinear response time τ_M. Taking all this into account we can write the Momentum operator as $\hat{M} = \hat{M}_0 + \hat{M}_{NL} + \hat{M}_F$:

$$\hat{M}_0 = \hbar \sum_\rho \beta_\rho (\hat{a}_\rho^\dagger \, \hat{a}_\rho + 1/2), \tag{C1.1}$$

$$\begin{aligned} \hat{M}_{NL} = \hbar \kappa_{FWM} (\hat{a}_s^\dagger \, \hat{a}_i^\dagger \, \zeta^2 + h.c.) - \hbar \sum_\rho \kappa_{FCD} (\hat{a}_\rho^\dagger \, \hat{a}_\rho + 1/2) \\ + \hbar \sum_\rho \kappa_{XPM} |\zeta|^2 \hat{a}_\rho^\dagger \, \hat{a}_\rho, \end{aligned} \tag{C1.2}$$

$$\begin{aligned} \hat{M}_F = \hbar \sum_\sigma \beta_\sigma (\hat{b}_\sigma^\dagger \, \hat{b}_\sigma + 1/2) + \hbar \sum_{\sigma,\rho} ((g_{\sigma\rho}^L + g_{\sigma\rho}^{FCA}) \, \hat{b}_\sigma \hat{a}_\rho^\dagger + h.c.) \\ + \hbar \sum_{\sigma,\rho} (g_{\sigma\rho}^{XTPA} \, \zeta^* \, \hat{b}_\sigma \hat{a}_\rho^\dagger + h.c.), \end{aligned} \tag{C1.3}$$

where $\rho = s, i$ and σ are the infinite modes of the reservoir which represents the material system. $\hat{M}_0$ stands for the free Momentum with β_ρ the propagation constant. $\hat{M}_{NL}$ stands for the nonlinear part, where κ_{FWM}, κ_{FCD} and κ_{XPM} are the FWM, the FCD and cross-phase modulation (XPM) coupling constants, respectively. Considering lowest order modes, the overlapping integrals for signal and idler are similar, and therefore we can consider the coupling constants the same. It is important to outline that the strength of the XPM term is the double of the FWM and self-phase modulation (SPM) terms. Finally, $\hat{M}_F$ stands for the dissipative and fluctuating part, where $\hat{b}_\sigma$ represent the modes of a reservoir and $g_{\sigma\rho}$ the linear and nonlinear coupling strengths between the medium and the idler and signal modes. The linear part represents linear scattering and FCA loss, and the nonlinear part the cross-TPA (XTPA) loss. We neglect the TPA loss in the signal and idler waves, because it is very small compared to other terms, as well as thermo-optic effects (TOE). Moreover, we stress the different origin of the TPA and FCA terms. Meanwhile TPA terms appear as consequence of the complex nature of the electronic Kerr nonlinearity,

the FCA term origin is a TPA-induced free electrons/holes density $N_c(z,t)$, which not only absorb light, but also change the refractive index (FCD). For cw pumps this density is stationary and it is given by $N_c(z) = \tau_c\, p\, |\zeta(z)|^4$ where τ_c is the effective carrier lifetime and $p = \gamma_{XTPA}/(2\hbar\omega)$, and it leads to a loss term $\gamma_{FCA}(z) = \sigma_\rho\, N_c(z) \equiv \tilde{\gamma}_{FCA}\, |\zeta(z)|^4$, and a dispersive term $\kappa_{FCD}(z) = 2\,u_\rho \gamma_{FCA}(z)$, where σ_ρ and u_ρ are parameters controlling the different behaviour of FCA and FCD at different wavelengths.

From this Momentum we calculate the Langevin's equations. Applying the Wigner-Weisskopff approximation we obtain the following equation for the signal wave:

$$\begin{aligned}\partial_z \hat{a}_s = i\,[\,(\beta_s + i\gamma/2) + (\kappa_{XPM} + i\gamma_{XTPA}/2)|\zeta(z)|^2 \\ -(\kappa_{FCD}(z) - i\gamma_{FCA}(z)/2)\,]\,\hat{a}_s + i\,\kappa_{FWM}\,\zeta^2(z)\,\hat{a}_i^\dagger + \hat{G}_s(z),\end{aligned} \tag{C1.4}$$

where γ and γ_{XTPA} are the linear and nonlinear losses, respectively, which we consider the same for both modes, and $\hat{G}_s(z) = \hat{m}_s + \hat{m}_{FCA} + \zeta\,\hat{m}_{XTPA}$ is a linear combination of the usual Langevin noise source operators coming from $\hat{M}_F$ [Louisell, 1973], fulfilling:

$$[\hat{m}_j(z,\omega_\rho), \hat{m}_j^\dagger(z',\omega_\sigma)] = \gamma_j \delta_{\rho\sigma}\delta(z-z'), \tag{C1.5}$$

where $j = s, i, FCA, XTPA$ and $\rho, \sigma = s, i$. In a similar way, modified equation for $\hat{a}_i^\dagger$ can be obtained. Performing a change of variable $\hat{a} = \tilde{a}\, e^{i\,\theta(z) - \int^z \gamma_T(z')dz'/2}$ with $\theta(z) = (\beta_s + \Delta\beta/2)z + \phi(z)$, after long but straightforward calculations we obtain:

$$\begin{aligned}\partial_z \begin{pmatrix}\tilde{a}_s \\ \tilde{a}_i^\dagger\end{pmatrix} = \begin{pmatrix} i\delta_z\Delta\Xi(z)/2 & i\,\kappa_{FWM}\,|\zeta(z)|^2 \\ -i\,\kappa_{FWM}\,|\zeta(z)|^2 & -i\delta_z\Delta\Xi(z)/2\end{pmatrix}\begin{pmatrix}\tilde{a}_s \\ \tilde{a}_i^\dagger\end{pmatrix} \\ + \begin{pmatrix}\hat{G}_s\, e^{i\,\theta(z) - \int^z \gamma_T(z')dz'/2} \\ \hat{G}_i^\dagger\, e^{-i\,\theta(z) - \int^z \gamma_T(z')dz'/2}\end{pmatrix},\end{aligned} \tag{C1.6}$$

where $\Delta\beta \approx \beta_2(\omega_p)\Delta\Omega^2 + (1/12)\beta_4(\omega_p)\Delta\Omega^4$, with β_2 and β_4 the group velocity dispersion (GVD) and fourth-order dispersion (FOD) terms, respectively, and $\Delta\Omega = |\omega_p - \omega_s|$ the detuning between pump and signal; $\gamma_T(z) = \gamma + \gamma_{FCA}(z) + \gamma_{XTPA}|\zeta(z)|^2$ the total loss and $\Delta\Xi(z) = \Delta\beta z - 2\phi(z) + 2\kappa_{XPM}\int^z |\zeta(z')|^2 dz' - 2\int^z \kappa_{FCD}(z')dz'$ the total mismatch. Equation (C1.6) can be solved by standard linear algebra. Coming back to the original quantum operators, we have at $z = l$:

$$\hat{a}_s(l) = [\mu(l)\,\hat{a}_s(0) + \nu(l)\,\hat{a}_i^\dagger(0) + \hat{\Gamma}_s(l)]\, e^{i\,\theta(l) - \int_0^l \gamma_T(z')dz'/2}, \tag{C1.7}$$

$$\hat{a}_i^\dagger(l) = [\nu^*(l)\,\hat{a}_s(0) + \mu^*(l)\,\hat{a}_i^\dagger(0) + \hat{\Gamma}_i^\dagger(l)]\, e^{-i\,\theta(l) - \int_0^l \gamma_T(z')dz'/2}, \tag{C1.8}$$

where:

$$\mu(l) = (1/2)[(e^{\lambda(l)} + e^{-\lambda(l)}) + \frac{i\,\Delta\Xi(l)}{2\,\lambda(l)}(e^{\lambda(l)} - e^{-\lambda(l)})], \tag{C1.9}$$

$$\nu(l) = \frac{i\,\kappa_{FWM}\int_0^l |\zeta(z')|^2\,dz'}{2\,\lambda(l)}(e^{\lambda(l)} - e^{-\lambda(l)}), \tag{C1.10}$$

$$\lambda(l) = [\,(\kappa_{FWM}\int_0^l |\zeta(z')|^2 dz')^2 - \Delta\Xi(l)^2/4\,]^{1/2}, \tag{C1.11}$$

$$\hat{\Gamma}_s(l) = \int_0^l dz'\, e^{\int^{z'}\gamma_T(z'')dz''/2}[\,\mu(l-z')\,\hat{G}_s(z')\,e^{-i\theta(z')} + \nu(l-z')\,\hat{G}_i(z')^\dagger\,e^{i\theta(z')}], \tag{C1.12}$$

$$\hat{\Gamma}_i^\dagger(l) = \int_0^l dz'\, e^{\int^{z'}\gamma_T(z'')dz''/2}[\,\nu^*(l-z')\,\hat{G}_s(z')\,e^{-i\theta(z')} + \mu^*(l-z')\,\hat{G}_i(z')^\dagger\,e^{i\theta(z')}]. \tag{C1.13}$$

Equations (C1.7, C1.8) are Bogoliubov transformations (plus noise terms) where $|\mu|^2 - |\nu|^2 = 1$, therefore the propagation in the Kerr medium performs squeezing on the fields.

Now we can calculate the number of photons generated by the SFWM. Considering the photon reservoir as a thermal one, working at the communication wavelength, the reservoir mean population is zero, so we can treat it as vacuum [Lin and Agrawal, 2006]. Therefore, averaging over vacuum for signal, idler and the Langevin noise sources, we have the conversion efficiency of the SFWM process:

$$\langle \hat{n}_{s,i}(l)\rangle = |\nu(l)|^2\, e^{-\int_0^l \gamma_T(z')dz'} + \int_0^l dz' e^{-\int_{z'}^l \gamma_T(z'')dz''} |\nu(l-z')|^2\,\gamma_T(z'). \tag{C1.14}$$

We can distinguish two sources of single photons in equation (C1.14): the first one is the proper SFWM, source of correlated single photons which we are interested in (Fig. 2), meanwhile the second one is made up of noise photons generated through SFWM seeded by loss induced noise, named usually accidentals [Lin and Agrawal, 2006]. We outline that in the lab it is possible to discriminate between correlated and accidental counts by means of a time interval analyzer (TIA). Besides, it is important to say that the gain of the correlated photons is reduced with the $\Delta\Xi(l)$ mismatch which takes into account all the linear and nonlinear dispersive effects present.

C1.3. Examples

As we have seen in the above section, the efficiency of the single photon generation is highly dependent on the behaviour of the pump. In this sec-

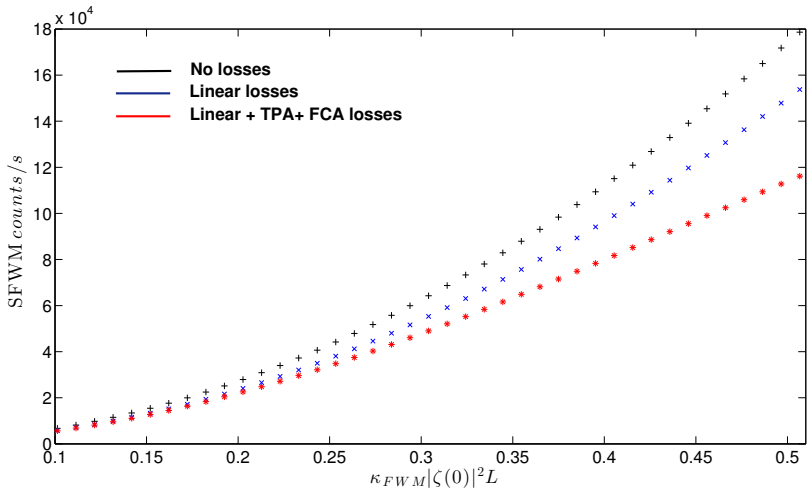

Figure C1.2: Sketch showing the influence of nonlinear losses on the generation of correlated photon pairs for a SOI-waveguide with L = 1.5 cm and input powers in the order of mW.

tion we are going to study two particular cases from the point of view of the evolution of the pump through the nonlinear waveguide:

TPA dominant

In the case of ultrashort pulses with modest energies, we can neglect both FCA and FCD. In this case the pump fulfills [Yin and Agrawal, 2007]:

$$|\zeta(z)|^2 = \frac{|\zeta(0)|^2\, e^{-\gamma z}}{1+\gamma_{TPA}\,|\zeta(0)|^2\, L_{eff}(z)},$$

$$\phi(z) = \frac{\kappa_{SPM}}{\gamma_{TPA}}\, \ln(1+\gamma_{TPA}\,|\zeta(0)|^2\, L_{eff}(z)), \tag{C1.15}$$

where $L_{eff}(z) = (1-e^{-\gamma z})/\gamma$. Applying (C1.15) in equations (C1.9-C1.14), we obtain $\lambda(l) \equiv \tilde{\lambda}(l)l = [(\phi(l)/l)^2 - ((\Delta\beta) + (\phi(l)/l))^2]^{1/2} l$ and $\Delta\Xi(l) = \Delta\beta\, l + 2\phi(l)$. Then, assuming that $\kappa_{FWM} \approx \kappa_{SPM}$, the correlated-counts conversion efficiency (C1.14) is given by:

$$\langle \hat{n}_{cc}(l)\rangle \approx \eta\, e^{-\gamma l}[\,\phi(l)\,\frac{\sinh(\tilde{\lambda}l)}{\tilde{\lambda}l}\,]^2, \tag{C1.16}$$

where cc stands for correlated counts and $\eta = (1+\gamma_{TPA}\,|\zeta(0)|^2\, L_{eff}(l))^{-\frac{\gamma_{XTPA}}{\gamma_{TPA}}}$ for the absorption due to XTPA. Therefore the gain scales with the square

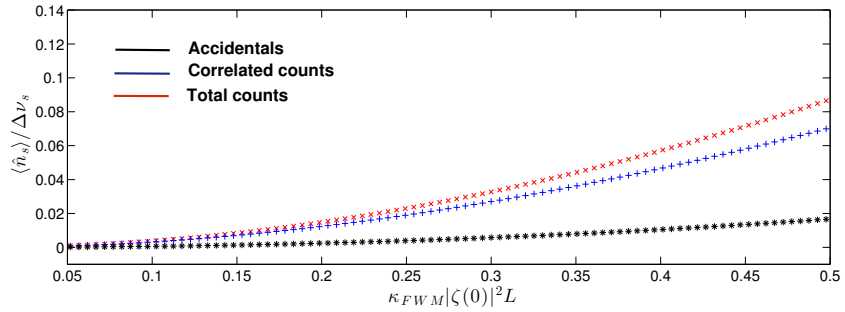

Figure C1.3: Sketch showing the normalized photon flux of correlated and accidental signal photons for a TPA-dominant approach.

of the nonlinear phase shift and it is highly dependent on the total phase mismatch, with a XTPA-loss factor being more important as more powerful is the input pulse.

FCA dominant

In the case of cw pulses the impact of TPA attenuation on the optical waves propagating in the waveguide is small compared with FCA. In this case the pump field is [Rukhlenko et al., 2010]:

$$|\zeta(z)|^2 = \frac{|\zeta(0)|^2\, e^{-\gamma z}}{[\,1 + 2\,\tilde{\gamma}_{FCA}\,|\zeta(0)|^4\, L_{eff}(z)\,]^{1/2}},$$

$$\phi(z) = \kappa_{SPM}\,|\zeta(0)|^2\,\tilde{L}_{eff}(z) - \frac{\kappa_{FCD}}{\tilde{\gamma}_{FCA}}\,[\ln(\frac{|\zeta(0)|^2}{|\zeta(z)|^2}) - \gamma\, z], \tag{C1.17}$$

where $L_{eff}(z) = (1 - e^{-2\gamma z})/2\gamma$ and:

$$\tilde{L}_{eff}(z) = \frac{1}{\sqrt{\gamma\,\tilde{\gamma}_{FCA}}\,|\zeta(0)|^2}\,\tan^{-1}(\sqrt{\tilde{\gamma}_{FCA}/\gamma}\,|\zeta(z')|^2)|_0^z. \tag{C1.18}$$

So the total mismatch is $\Delta\Xi(l) = \Delta\beta\, l + 2\,\tilde{\phi}(l)$, with $\tilde{\phi}(l) = \kappa_{SPM}\,|\zeta(0)|^2\,\tilde{L}_{eff}(l)$ and $\lambda(l) \equiv \tilde{\lambda}(l)l = [(\tilde{\phi}(l)/l)^2 - ((\Delta\beta) + (\tilde{\phi}(l)/l))^2]^{1/2} l$. Again, assuming that $\kappa_{FWM} \approx \kappa_{SPM}$, the correlated conversion efficiency (C1.14) is:

$$\langle \hat{n}_{cc}(l) \rangle \approx \eta\, e^{-\gamma l}\,[\,\tilde{\phi}(l)\,\frac{\sinh(\tilde{\lambda} l)}{\tilde{\lambda} l}\,]^2, \tag{C1.19}$$

where $\eta = (1 + 2\,\tilde{\gamma}_{FCA}\,|\zeta(0)|^2\,L_{eff}(l)\,)^{-1/2}$. The form of equation (C1.19) is analogous as (C1.16), but the physical outcome is quite different, as either the efficiency as the loss are FCA-dependent.

C1.4. Conclusions and perspectives

We have presented a theoretical study of quantum propagation and generation of light in SOI devices. From a nonlinear dissipative Momentum operator we have derived the Langevin's equations and solved them. We have calculated the conversion efficiency of the system taking into account the fluctuating terms. Finally we have applied them to two limit cases.

In a future work we will apply this approach in a basis of continuum fields, better suited for the study of pulsed waves, and apply it to a ring resonator, as it is one of the more promising candidates for implementing integrated single-photon sources. Moreover, we will fit our theory to experimental results.

Chapter 2 bibliography

I. Abram. Quantum theory of light propagation: Linear medium. *Physical Review A*, 35(11):4661–4672, 1987.

G. Assanto, A. Laureti-Palma, C. Sibilia, and M. Bertolotti. All-optical switching via second harmonic generation in a nonlinearly asymmetric directional coupler. *Optics Communications*, 110:599, 1994.

H.A. Bachor and T.C. Ralph. *A Guide to Experiments in Quantum Optics*. Wiley-VCH, 2004.

D. Barral. Propagación cuántica de luz en materiales fotónicos guiantes. Master's thesis, Facultad de Física. Departamento de Física Aplicada, Santiago de Compostela, 2008.

Y. Ben-Aryeh and S. Serulnik. The quantum treatment of propagation in non-linear optical media by the use of temporal modes. *Physics Letters A*, 155(8-9):473–479, 1991.

Y. Ben-Aryeh, A. Luks, and V. Perinová. The concept of equal space commutators in quantum optics. *Physics Letters A*, 165:19–27, 1992.

M. Born and E. Wolf. *Principles of Optics*. Cambridge University Press, 7th edition, 1959.

R.W. Boyd. *Nonlinear optics*. Academic Press Inc, San Diego, 1992.

P. Caldirola. Forze non conservative nella meccanica quantistica. *Nuovo Cimento*, 18:393, 1941.

C.M. Caves and D.C. Crouch. Quantum wideband traveling-wave anlysis of a degenerate parametric amplifier. *Journal of the Optical Society of America B*, 4(10):1535–1545, 1987.

M.J. Collet and D. F. Walls. Squeezing spectra for nonlinear optical systems. *Physical Review A*, 32(5):2887, 1985.

B.J. Dalton and P. L. Knight. The standard model in cavity quantum electrodynamics. i. general features of mode functions for a fabry-perot cavity. *Journal of Modern Optics*, 46:1817, 1999a.

B.J. Dalton and P. L. Knight. The standard model in cavity quantum electrodynamics. ii. coupling constants and atom field interaction. *Journal of Modern Optics*, 46:1839, 1999b.

B.J. Dalton, E.S. Guerra, and P. L. Knight. Field quantization in dielectric media and the generalized multipolar hamiltonian. *Physical Review A*, 54: 2292, 1996.

B.J. Dalton, S.M. Barnett, and P. L. Knight. Quasi-mode theory of macroscopic canonical quantization in quantum optics and cavity quantum electrodynamics. *Journal of Modern Optics*, 46:1315, 1999.

C.C. Gerry and P. L. Knight. *Introductory Quantum Optics*. Cambridge University Press, 2005.

H. Haken. *Light*. North-Holland, Amsterdam, 1981.

H. Haus and W.P. Huang. Coupled-mode theory. *Proceedings of the IEEE*, 79:1505, 1991.

M. Hillery and L.D. Modlinow. Quantization of electrodynamics in nonlinear dielectric media. *Physical Review A*, 30(4):1860–1865, 1984.

R.G. Hunsperger. *Integrated Optics: Theory and Technology*, volume 33 of *Springer Series in Optical Sciences*. Springer Verlag, 6th edition, 2009.

B. Huttner, S. Serulnik, and Y. Ben-Aryeh. Quantum analysis of light propagation in a parametric amplifier. *Physical Review A*, 42(9):5594–5600, 1990.

J.D. Jackson. *Classical Electrodynamics*. John Wiley and sons, 1975.

J. Jansky, A. Sibilia, M. Bertolotti, and Y. Yushin. Non-classical light in a linear coupler. *Journal of Modern Optics*, 35:1757, 1988.

S.G. Johnson and J.D. Joannopoulos. *Photonic Crystals: The Road from Theory to Practice*. Kluwer Academic Publishers, 2002.

E. Kanai. On the quantization of the dissipative systems. *Progress of Theoretical Physics*, 3:440, 1945.

S.P. Kim, A.E. Santana, and F.C. Khana. Decoherence of quantum damped oscillators. *Journal of the Korean Physical Society*, 43(4):452, 2003.

T. Kiss, J. Janszky, and P. Adam. Time evolution of harmonic oscillators with time-dependent parameters: a step-function approximation. *Physical Review A*, 49(6):4935, 1994.

H. Kogelnik. Theory of dielectric waveguides. In T. Tamir, editor, *Guided-wave optoelectronics*, chapter 2. Springer-Verlag, Berlin, 1988.

N. Korolkova and J. Perina. Kerr nonlinear coupler with varying linear coupling coefficient. *Journal of Modern Optics*, 44:1525, 1997.

L.D. Landau and E.M. Lifshitz. *Curso de Física Teórica, vol. 2: Teoría Clásica de los Campos*. Editorial Reverté, 1973.

L.D. Landau and E.M. Lifshitz. *The classical theroy of fields*. Pergamon, Oxford, 1975.

Q. Lin and G.P. Agrawal. Silicon waveguides for creating quantum-correlated photon pairs. *Optics Letters*, 31(21):3140, 2006.

J. Liñares. Maxwell paraxial wave optics in inhomogeneous media by path integral formalism. *Physics Letters A*, 141:207, 1989.

J. Liñares and M.C. Nistal. Geometric phases in multidirectional electromagnetic coupling theory. *Physics Letters A*, 162:7, 1992.

J. Liñares and M.C. Nistal. Single local mode propagation through ion-exchanged waveguide elements with quasi-abrupt transitions. *Japanesse Journal of Applied Physics*, 35:L1596, 1996.

J. Liñares and M.C. Nistal. Quantization of coupled modes propagation in integrated optical waveguides. *Journal of Modern Optics*, 50(5):781–790, 2003.

J. Liñares, M.C. Nistal, and D. Barral. Quantization of coupled 1d vector modes in integrated photonic waveguides. *New Journal of Physics*, 10: 063023, 2008a.

J. Liñares, M.C. Nistal, D. Barral, V. Moreno, and C. Montero. Quantization of coupled waveguided modes progression in integrated photonic devices. In Giancarlo C. Righini, Seppo K. Honkanen, Lorenzo Pavesi, and Laurent Vivien, editors, *Proceedings of the SPIE Europe Photonics 2008*, volume 6996 of *Silicon Photonics and Photonic Integrated Circuits*, pages 69961R–69961R–12. S.P.I.E., 2008b.

J. Liñares, D. Barral, M.C. Nistal, V. Moreno, C. Montero, and X. Prieto. Quantum analysis of linear and nonlinear integrated directional couplers with synchronic monomode guides. In *Libro de Actas Reunión Nacional de Optica*, pages PAN–79. Sociedad Española de Optica, September 2009.

J. Liñares, D. Barral, and M.C. Nistal. Spatial propagation of quantum light in nonlinear waveguiding devices: theory and applications. *Journal of Nonlinear Optical Physics and Materials*, 21(3):1250032, 2012.

R. Loudon. *The Quantum Theory of Light*. Clarendon Press, Oxford, 1982.

W.H. Louisell. *Quantum Statistical Properties of Radiation*. Wiley, New York, 1973.

A. Luks and V. Perinová. Canonical quantum description of light propagation in dielectric media. In E. Wolf, editor, *Progress in optics*, volume 43, page 295. North-Holland, 2002.

L. Mandel and E. Wolf. *Optical Coherence and Quantum Optics*. Cambridge University Press, 1995.

D. Marcuse. *Theory of dielectric optical waveguides*. Academic Press Inc, London, 1974.

E. F. Mateo and J. Liñares. Analysis of dissipative effects on intrinsic optical bistability in a kerr integrated device. *Optics Communications*, 246:173, 2005.

J.L. O'Brien, A. Furusawa, and J. Vukovic. Photonic quantum technologies. *Nature Photonics*, 3:687, 2009.

J. Perina. Quantum-statistical properties of a nonlinear asymmetric directional coupler. *Journal of Modern Optics*, 42(7):1517–1522, 1995.

J. Perina and J. Krepelka. Forward and backward four wave mixing of nonclassical light with pump depletion. *Journal of Modern Optics*, 39(12):2405, 1992.

J. Perina and J. Perina Jr. Photon statistics of a contradirectional nonlinear coupler. *Quantum Semiclassical Optics*, 7:849, 1995a.

J. Perina and J. Perina Jr. Quantum statistical properties of codirectional and contradirectional nonlinear couplers with phase mismatch. *Quantum Semiclassical Optics*, 7:863, 1995b.

J. Perina Jr and J. Perina. Quantum statistics of nonlinear optical couplers. In E. Wolf, editor, *Progress in optics*, volume 41, pages 361–419. Elsevier Science B.V., 2000.

V. Perinová, A. Luks, J. Krepelka, C. Sibilia, and M. Bertolotti. Quantum statistics of light in a lossless linear coupler. *Journal of Modern Optics*, 38 (12):2429, 1991.

V. Perinová, A. Luks, and J. Krepelka. Linear coupling, loss and gain of counterpropagating beams. *Journal of Physics B: Atomic, Molecular and Optical Physics*, 39:2267, 2006.

A. Peruzzo, M. Lobino, J.C.F. Matthews, N. Matsuda, A. Politi, K. Poulious, X.-Q. Zhou, Y. Lahini, N. Ismail, K. Wörhoff, Y. Bromberg, Y. Silberberg, M.G. Thompson, and J.L. O'Brien. Quantum walks for correlated photons. *Science*, 329:1500, September 2010.

E. Pinney. The nonlinear equation $y'' + p(x)y + cy^{-3} = 0$. *Proceedings of the American Mathematical Society*, 1(5):681, 1950.

M. Pospíchal. Quantum theory of light propagation i. general theory. *Czechoslovak Journal of Physics*, 45(10):821–830, 1995.

P.N. Prasad. *Nanophotonics*. Wiley, Hoboken, 2004.

S.G. Rajeev. A canonical formulation of dissipative mechanics using complex-valued hamiltonians. *Annals of Physics*, 322:1541, 2007.

H. Risken. *The Fokker-Planck equation: methods of solution and applications*. Springer-Verlag, 1989.

I.D. Rukhlenko, M. Premaratne, and G.P. Agrawal. Analyitical study of optical bistability in silicon ring resonators. *Optics Letters*, 35(1):55, 2010.

W.P. Schleich. *Quantum optics in phase space*. Wiley-VCH, Berlin, 2001.

S. Serulnik and Y. Ben-Aryeh. Space-time description of propagation in nonlinear dielectric media. *Quantum Optics*, 3:63–74, 1991.

Y.R. Shen. Quantum statistics of nonlinear optics. *Physical Review*, 155(3): 921–931, 1967.

M.S. Sodha and A.K. Ghatak. *Inhomogeneous optical waveguides*. Plenum Press, New York, 1977.

M.G. Thompson, A. Politi, J.C.F. Matthews, and J.L. O'Brien. Integrated waveguide circuits for optical quantum computing. *Circuits, Devices & Systems, IET*, 5:94, 2011.

M. Toren and Y. Ben-Aryeh. The problem of propagation in quantum optics, with applications to amplification, coupling of em modes and distributed feedback lasers. *Quantum Optics*, 6:425–444, 1994.

D. F. Walls and G. J. Milburn. *Quantum Optics*. Springer Verlag, Berlin, 1994.

A. Yariv. Coupled-mode theory for guided-wave optics. *IEEE Journal of Quantum Electronics*, 9:919, 1973.

A. Yariv. *Quantum Electronics*. John Wiley and sons, New York, 2nd edition, 1975.

L. Yin and G.P. Agrawal. Impact of two-photon absorption on self-phase modulation in silicon waveguides. *Optics Letters*, 32(14):2031, 2007.

L.H. Yu and C. Sun. Evolution of the wave function in a dissipative system. *Physical Review A*, 49:592, 1994.

USC
UNIVERSIDADE
DE SANTIAGO
DE COMPOSTELA

CHAPTER

THREE

QUANTUM PROPAGATION IN THE OPTICAL FIELD-STRENGTH SPACE - PATH INTEGRAL FORMULATION

AFTER introducing the canonical approach to mode propagation we show a different perspective to the problem. This is the Feynman or *space-time* formulation of quantum mechanics and we will apply it to propagation in IPDs. When information about the quantum noise of the radiation field is important, the optical field-strength (OFS) representation of quantum states is appropriate and the Feynman propagator provides the information of the spatial evolution of the quantum system. This approach is elegant and highly flexible since it can be applied to media with different optical features like inhomogeneities, nonlinearities or losses; obtaining analytical or approximated solutions. To this end, in section 1 we begin introducing some of the more important quantum states of light. In section 2, we review the statistical functions which describe these states and symbolize what we know about the system, focusing our attention on the optical field-strength space and the wavefunction in this representation. Then, in section 3 we present the main features of path integrals in the OFS representation and apply it to different problems in IPDs: homogeneous and longitudinally inhomogeneous, linear and nonlinear, lossless and lossy media. Finally we introduce the research works where these concepts are detailed and applied to different media (§ P2, § P3 & § P4).

3.1. Quantum states of light

In this section we review the most important features of the different classes of states the optical field may present. Specifically, we will deal

with optical field-strength states, number states, coherent states, squeezed and entangled states of light.

3.1.1. Optical field-strength states

It is always an interesting goal to describe a system in terms on quantities we are able to measure. In the previous chapter we have introduced the quantum field (2.3.63) in terms of absorption and emission operators (2.3.59, 2.3.60), given in terms of dimensionless canonical position $\hat{q}$ and momentum $\hat{p}$ operators. Taking into account the following quantum-optical units $cT\|\mathbf{E}_{0\nu}\|^2/\hbar\omega = 1$ [Loudon, 1982], we define the following rescaled operators, so-called canonical optical field-strength and optical momentum operators for each mode ν of the field:

$$\hat{\mathcal{E}}_\nu = \sqrt{\frac{\beta_\nu}{2\hbar}}\,\hat{q}_\nu = \frac{\hat{a}_\nu + \hat{a}_\nu^\dagger}{2}, \tag{3.1.1}$$

$$\hat{\mathcal{P}}_\nu \equiv -i\hbar\frac{\partial}{\partial\mathcal{E}_\nu} = \sqrt{\frac{2\hbar}{\beta_\nu}}\,\hat{p}_\nu = i\hbar(\hat{a}_\nu^\dagger - \hat{a}_\nu), \tag{3.1.2}$$

fulfilling the following ESCR:

$$[\hat{\mathcal{E}}_\nu, \hat{\mathcal{P}}_{\nu'}] = i\hbar\delta_{\nu,\nu'}. \tag{3.1.3}$$

The OFS operator fulfills the following eigenvalue equation [Vogel and Welsch, 1994]:

$$\hat{\mathcal{E}}_\nu|\mathcal{E}_\nu\rangle = \mathcal{E}_\nu|\mathcal{E}_\nu\rangle, \tag{3.1.4}$$

with $\mathcal{E}_\nu$ and $|\mathcal{E}_\nu\rangle$ the optical field-strength eigenvalues and eigenstates, respectively. Hence an electric field in such a state has a well defined amplitude. This space can be used to represent any quantum state by means of the following orthogonality and closure relations:

$$\langle\mathcal{E}|\mathcal{E}'\rangle = \delta(\mathcal{E} - \mathcal{E}'), \qquad \int\{|\mathcal{E}\rangle\}\{\langle\mathcal{E}|\}\,d\{\mathcal{E}\} = \hat{1}, \tag{3.1.5}$$

where $\{|\mathcal{E}\rangle\} \equiv |\mathcal{E}_1, \ldots, \mathcal{E}_N\rangle$ and $d\{\mathcal{E}\} \equiv d\mathcal{E}_1 \ldots d\mathcal{E}_N$. Likewise, it is important to outline that both OFS canonical operators are equivalent to the field quadratures for $\hbar = 1/2$[1]. Following this prescription, we can define the rotated OFS operator for the ν mode [Schleich, 2001]:

$$\hat{\mathcal{E}}_\theta = \hat{\mathcal{E}}\cos\theta + \hat{\mathcal{P}}\sin\theta, \tag{3.1.6}$$

with $0 \leqslant \theta < \pi$ and where $\hat{\mathcal{E}}_0 \equiv \hat{\mathcal{E}}$ and $\hat{\mathcal{E}}_{\pi/2} \equiv \hat{\mathcal{P}}$ are the field quadratures. This operator fulfills as well relations (3.1.4) and (3.1.5) for a given

[1] It is very common to redefine $\hbar$ to obtain simpler expressions.

θ. In terms of the above-mentioned quantum-optical units, this operator is equivalent to the quantum field opertaror (2.3.63) for $\theta = \omega t + \delta(z)$, with $\delta(z)$ the phase gained after propagation. This relation is very important as the difference photocurrent obtained in homodyne measurements is proportional to the rotated OFS values [Schleich, 2001]. Chapter 4 is devoted to this issue.

Finally, it is interesting to introduce the Heisenberg uncertainty relation in the OFS space:

$$\langle(\Delta\hat{\mathcal{E}})^2\rangle\langle(\Delta\hat{\mathcal{P}})^2\rangle \geqslant 1/16^2, \tag{3.1.7}$$

where $\langle(\Delta\hat{A})^2\rangle = \langle\hat{A}^2\rangle - \langle\hat{A}\rangle^2$ is the variance[3] of the observable $\hat{A} \equiv \hat{\mathcal{E}}, \hat{\mathcal{P}}$. Quantum states fulfilling the equality are called minimum uncertainty states (MUS). If the uncertainties are equally distributed, their value is 1/4 being the so-called standard quantum limit (SQL).

3.1.2. Number states

As we have seen in the previous chapter, from the canonical spatial quantization we have a free Momentum (2.3.64):

$$\hat{M}_O = \hbar \sum_\nu sgn(\nu)\beta_\nu(\hat{a}_\nu^\dagger \hat{a}_\nu + 1/2) = \hbar \sum_\nu \beta_\nu \, \hat{a}_\nu^\dagger \hat{a}_\nu,$$

where we have used the relation between forward and backward propagation constants $\beta_{-\nu} = -\beta_\nu$ in the last equality. The operator $\hat{a}_\nu^\dagger \hat{a}_\nu$ appearing in this expression has an special meaning in quantum optics. It is known as number or Fock operator and is written as $\hat{n}_\nu$, since its eigenstates have a well defined number of photons. It fulfills the following eigenvalue equation:

$$\hat{n}_\nu|n_\nu\rangle = n_\nu|n_\nu\rangle, \tag{3.1.8}$$

with n_ν and $|n_\nu\rangle$ the number eigenvalues and eigenstates, respectively. This implies that the number states are also eigenstates of the Momentum (2.3.64). The action of the absorption and emission operators on a number state is:

$$\hat{a}_\nu|n_\nu\rangle = \sqrt{n_\nu}\,|n_\nu - 1\rangle, \tag{3.1.9}$$

$$\hat{a}_\nu^\dagger|n_\nu\rangle = \sqrt{n_\nu + 1}\,|n_\nu + 1\rangle. \tag{3.1.10}$$

Likewise, any N-dimensional number state $\{|n\rangle\} \equiv |n_1, \ldots, n_N\rangle$ is generated via repeated application of the emission operator on the vacuum

[2] We have used the prescription $\hbar = 1/2$. From now on we will use this prescription when talking about variances.

[3] Also called uncertainty, dispersion or noise.

$\{|0\rangle\} \equiv |0_1, \ldots, 0_N\rangle$ [Mandel and Wolf, 1995]:

$$\{|n\rangle\} = \prod_{\nu} \frac{(\hat{a}_\nu^\dagger)^{n_\nu}}{\sqrt{n_\nu!}} \{|0\rangle\}. \tag{3.1.11}$$

Moreover, the number states are orthogonal and form a complete set, features which enable representing arbitrary states in this space:

$$\langle n'|n\rangle = \delta_{nn'}, \quad \sum_{\{n\}} \{|n\rangle\}\{\langle n|\} = \hat{1}. \tag{3.1.12}$$

Finally, in order to obtain the uncertainty relations (3.1.7) corresponding to these states, we evaluate the variance of the rotated field quadrature (3.1.6) in the number representation for the ν mode:

$$\langle (\Delta\hat{\mathcal{E}}_\theta)^2\rangle = \frac{2n+1}{4}. \tag{3.1.13}$$

Hence, this variance is independent on the phase θ and the Heisenberg uncertainty relation is given by:

$$\langle (\Delta\hat{\mathcal{E}})^2\rangle\langle (\Delta\hat{\mathcal{P}})^2\rangle = (\frac{2n+1}{4})^2. \tag{3.1.14}$$

Therefore, the number states are not MUS except the vacuum.

3.1.3. Coherent states

The most classical quantum states are the so-called coherent states [Gerry and Knight, 2005]. This class of quantum states shows the feature of recovering the classical value of the electric field in the regime of high photonic excitation, unlike the field number states, from which we have $\langle n|\hat{\mathbf{e}}|n\rangle = 0$. From here the so-called name of classical states.

The coherent states, written as $|\alpha\rangle$, are eigenstates of the non-hermitian absorption operator $\hat{a}$ with complex eigenvalues α. For a single mode state [4], we have:

$$\hat{a}\,|\alpha\rangle = \alpha\,|\alpha\rangle \tag{3.1.15}$$

$$\langle\alpha|\,\hat{a}^\dagger = \alpha^*\langle\alpha| \tag{3.1.16}$$

The relation (3.1.15) represents how the repetitive absorption of EM photons from a coherent state does not change the state of the field.

On the other hand, since the number states form a complete set, we can expand the state $|\alpha\rangle$ in the basis of Fock states in the following way:

$$|\alpha\rangle = e^{-|\alpha|^2/2} \sum_{n=0}^{\infty} \frac{\alpha^n}{\sqrt{n!}} |n\rangle. \tag{3.1.17}$$

[4] This is easily extended to multimode states as in the previous sections.

The probability of measuring n photons in a coherent state is then given by:

$$P(n) = |\langle n|\alpha\rangle|^2 = \frac{\langle\hat{n}\rangle^n}{n!}e^{-\langle\hat{n}\rangle}. \tag{3.1.18}$$

where $\langle\hat{n}\rangle = |\alpha|^2$ is the average photon number in a coherent state. This is a Poisson distribution in n with parameter $\langle\hat{n}\rangle$. Furthermore, applying the relation (3.1.11) into (3.1.17), we obtain the following expression:

$$|\alpha\rangle = e^{-|\alpha|^2/2}e^{\alpha\,\hat{a}^\dagger}|0\rangle, \tag{3.1.19}$$

which shows how a coherent state $|\alpha\rangle$ can be considered as a displaced vacuum state. Thus, a displacement operator can be defined as $\hat{D}(\alpha) = e^{-|\alpha|^2/2}\,e^{\alpha\hat{a}^\dagger} = e^{(\alpha\hat{a}^\dagger - \alpha^*\hat{a})}$, which generates a field coherent state from the vacuum:

$$|\alpha\rangle = \hat{D}(\alpha)|0\rangle. \tag{3.1.20}$$

Moreover, it should be outlined that the coherent states are not orthogonal, since for two different states we have: $|\langle\alpha'\,|\,\alpha\rangle|^2 = e^{-|\alpha'-\alpha|^2} \neq 0$. This relation resembles a Dirac delta function. The lack of orthogonality is only significant for two close coherent states. The coherent-states set is called overcomplete, in the sense of lack of uniqueness in the representation of any quantum state in terms of coherent states. This is given by the following closure relation:

$$\frac{1}{\pi}\int |\alpha\rangle\langle\alpha|\,d^2\alpha = \hat{1}, \tag{3.1.21}$$

where $d^2\alpha = dRe(\alpha)\,dIm(\alpha)$. By means of this relation we can write any quantum state in terms of the coherent-states basis.

Lastly, the variance of the rotated quadrature in this case is given by:

$$\langle(\Delta\hat{\mathcal{E}}_\theta)^2\rangle = \frac{1}{4}. \tag{3.1.22}$$

This value does not depend either on θ nor the complex amplitude α, so the uncertainty relation (3.1.7) is given by:

$$\langle(\Delta\hat{\mathcal{E}})^2\rangle\langle(\Delta\hat{\mathcal{P}})^2\rangle = \frac{1}{16}. \tag{3.1.23}$$

Therefore, any coherent state is a MUS[5].

[5]This was expected from the definition of a coherent state as a displaced vacuum (3.1.20) and the result (3.1.14).

3.1.4. Squeezed states

The Heisenbeg uncertainty relation (3.1.7) imposses a constraint on the simultaneous knowledge of two conjugate quantum variables. Nevertheless, it allows to increase the information of one of the variables at the expense of the other. When the uncertainty of one of the two quadratures is less than the SQL:

$$\langle \Delta\hat{\mathcal{E}})^2\rangle < \frac{1}{4}, \qquad \langle (\Delta\hat{\mathcal{P}})^2\rangle < \frac{1}{4}, \tag{3.1.24}$$

the state is said to be squeezed. Mathematically, the squeezing is generated by means of the following operator [Walls and Milburn, 1994]:

$$\hat{S}(\zeta) = exp[\frac{1}{2}(\zeta^* \hat{a}^2 - \zeta \hat{a}^{\dagger 2})], \tag{3.1.25}$$

where $\zeta = re^{i\phi}$ is the complex squeezing parameter and $\hat{S}$ is an unitary operator so-called squeezing operator[6]. This operator is a kind of two-photon generalization of the displacement operator $\hat{D}$ used to define single-mode coherent states introduced in the previous section 3.1.3. Acting on the vacuum, this operator would produce a two-photon coherent state, since photons would be absorbed and emitted in pairs by the action of this operator [Gerry and Knight, 2005].

For a clearer view of the operation of this operator we use the quadrature space. A $\phi/2$ rotation in the quadrature space is given by:

$$\hat{\mathcal{E}}' + i\hat{\mathcal{P}}' = (\hat{\mathcal{E}} + i\hat{\mathcal{P}})e^{-i\phi/2}, \tag{3.1.26}$$

The action of the squeezing operator is better seen in this rotated quadrature:

$$\hat{S}^\dagger(\zeta)(\hat{\mathcal{E}}' + i\hat{\mathcal{P}}')\hat{S}(\zeta) = e^{-r}\hat{\mathcal{E}}' + ie^{r}\hat{\mathcal{P}}'. \tag{3.1.27}$$

Therefore, the squeezing operator carries out a scale transformation in a rotated frame. The uncertainty in $\hat{\mathcal{E}}'$ is decreased by a factor e^{-r} meanwhile that corresponding to $\hat{\mathcal{P}}'$ is increased by e^{r}.

Likewise, squeezed coherent states are defined as follows[7]:

$$|\alpha, \zeta\rangle = \hat{D}(\alpha)\hat{S}(\zeta)|\alpha\rangle. \tag{3.1.28}$$

These states show an appealing feature which can be seen calculating the variance of the rotated field quadrature (3.1.6) [Loudon and Knight, 1987]:

$$\langle (\Delta\hat{\mathcal{E}}_\theta)^2\rangle = \frac{1}{4}[\cosh 2r - \sinh 2r \sin(2\theta - \phi)]^{8}. \tag{3.1.29}$$

[6] This approach is easily extended to multimode squeezing. See, for instance, [Walls and Milburn, 1994].

[7] This is the definition presented by Caves. An alternative definition produces the so-called *two-photon coherent states* and was introduced by Yuen [Loudon and Knight, 1987].

[8] Some authors use a *cosine* function instead of a *sine*. The prescription depends on the arbitrary election of the phase ϕ.

So, for $r > 0$, the quadratures will show minimum (lower than the SQL) and maximum uncertainty (higher than the SQL) for $\theta = \phi/2 + \pi/4$ and $\theta = \phi/2 + 3\pi/4$, respectively:

$$\langle(\Delta\hat{\mathcal{E}}_{\phi/2+\pi/4})^2\rangle = \frac{e^{-2r}}{4}, \tag{3.1.30}$$

$$\langle(\Delta\hat{\mathcal{E}}_{\phi/2+3\pi/4})^2\rangle \equiv \langle(\Delta\hat{\mathcal{P}}_{\phi/2+\pi/4})^2\rangle = \frac{e^{2r}}{4}. \tag{3.1.31}$$

3.1.5. Entangled states

The entangled states are purely quantum states, without a classical analog, formed by linear combinations of substates of any class: Fock, coherent, squeezed and so on; associated to the different subspaces of Hilbert space, like energetic excitations of atoms, spin momentum of particles, polarization modes, spatial propagation modes and so on; not factorables in these subspaces and where strong non-classical correlations between the substates appear, turning out in violations of the classical Bell's inequalities [Mandel and Wolf, 1995]. The correlation degree is such that measurements made on one of the parts of the system, goberns the state of its entangled counterpart. This feature is independent on the space-time between the parts, fact which constitutes the characteristic non-local character of these states, *the spooky action at a distance* [Einstein et al., 1935].

Let $|\Psi\rangle_{12}$ be the state vector of a two-subspace system. Then $|\Psi\rangle_{12}$ can be written as [Suhara, 2009]:

$$|\Psi\rangle_{12} = \sum_{\psi,\phi} c(\psi,\phi)|\psi\rangle_1|\phi\rangle_2, \tag{3.1.32}$$

using a set of orthogonal state vectors for subspace 1, $|\psi\rangle_1$, and that for subspace 2, $|\phi\rangle_2$. If the coefficient $c(\psi,\phi)$ does not factor into $c_1(\psi)c_2(\phi)$, the system is entangled. For instance, the entangled states can be realized with one photon enconded in two orthogonal polarization states such as horizontally and vertically polarized single photons $|H\rangle$ and $|V\rangle$, or right-handed and left-handed circular polarization states $|R\rangle$ and $|L\rangle$, or two orthogonal propagating modes $|1\rangle$ and $|2\rangle$, as these propagating in two-mode waveguides. Quantum information can be coded in quantum bits (qubits) consisting of a linear superposition of the two basis states such as $|\Psi\rangle = c_1|1\rangle + c_2|2\rangle$ (or $c_H|H\rangle + c_V|V\rangle$, $c_R|R\rangle + c_L|L\rangle$ and so on) with arbitrary complex coefficients c_1 and c_2 satisfying the normalization condition $|c_1|^2 + |c_2|^2 = 1$. Likewise, this feature can even be accomplished with coherent (*quasi*-classical) states, leading to the well-known *Schrödinger's cat states* $|\Psi\rangle = c_\alpha|\alpha\rangle + c_{-\alpha}|-\alpha\rangle$ [Gerry and Knight, 2005].

3.2. General descriptions of quantum states

Given an arbitrary quantum system, a representation is necessary in order to characterize completely it. This is commonly carried out by assigning it a state vector $|\Psi\rangle$. This state vector is a vector in the Hilbert space of the system, such that it can be written in any of the bases shown in the previous section and where complex coefficients define the state. For instance, in some experimental situations number states $\{|n\rangle\}$ can be the best-suited basis. In this case, we can write:

$$|\Psi\rangle = \sum_{n_1=0}^{\infty} \cdots \sum_{n_N=0}^{\infty} c_{n_1,\ldots,n_N} |n_1,\ldots,n_N\rangle, \tag{3.2.33}$$

which is constrained to the normalization condition $|\langle\Psi|\Psi\rangle|^2 = 1$ and where $c_{n_1,\ldots,n_N}$ are the complex numbers which characterize the state of the system.

Likewise, the state vector enables to predict the average value $\bar{A}$ of a set of measurements on the system via:

$$\bar{A} = \langle\Psi|\hat{A}|\Psi\rangle, \tag{3.2.34}$$

where $\hat{A}$ is a given operator describing the measurement. Likewise, higher order moments of the quantum probability distribution can be obtained. But in the case of a system made up of an ensemble of subsystems, this representation is no longer valid, as it does not take into account statistical information of the ensemble. In this section we present a brief review of the different representations of quantum states of light. Specifically, the density operator, the quasi-probability distributions and the probability distributions in the optical field-strength space.

3.2.1. Density operator

A quantum system made up of an ensemble of smaller N subsystems can not in general be characterized by a single state $|\Psi\rangle$. Every fraction P_i ($i = 1 \ldots N$) of this ensemble is represented by a state $|\Psi_i\rangle$. If all the subsystems are characterized by the same state, the state of the total system is $|\Psi\rangle = |\Psi_i\rangle$ and the state is called *pure*. In the opposite case, where each subsystem has its own state, it is called *completely random*. In between we have the so-called *mixed states*, which can be thought as a combination of a pure and a random state. Because of this, a quantum mechanical variable containing both statistical and quantum mechanical information is necessary. This variable is the density operator of an ensemble given by [Gerry and Knight, 2005]:

$$\hat{\rho} = \sum_{i}^{N} P_i |\Psi_i\rangle\langle\Psi_i|, \tag{3.2.35}$$

where the fractions P_i are the probability densities in each subsystem i. In this case, the average $\bar{A}$ is given by:

$$\bar{A} = \sum_i P_i \langle \Psi_i | \hat{A} | \Psi_i \rangle \equiv Tr\{\hat{\rho}\hat{A}\}, \tag{3.2.36}$$

where Tr stands for *trace* and both statistical and quantum average are performed. Likewise, the parameter which characterizes the amount of "statistical noise" in the system is the *purity* $p = Tr\hat{\rho}^2$, a quantity equals to one in the case of pure states, where only quantum fluctuations are present, and where $p < 1$ in the case of mixed states.

Furthermore, this operator can be represented in any other state basis. In some state basis $\{|\phi\rangle\}$, we have:

$$\hat{\rho} = \sum_i \sum_j \rho_{ij} |\phi_i\rangle\langle\phi_j|, \tag{3.2.37}$$

where $\rho_{ij} = \langle\phi_i|\hat{\rho}|\phi_j\rangle$ is the ij element of the *density matrix*. For instance, in terms of the number state basis as:

$$\hat{\rho} = \sum_m \sum_n \rho_{mn} |m\rangle\langle n|. \tag{3.2.38}$$

It is important to outline that the diagonal elements of this matrix are the probabilities of finding n photons in the quantum system.

3.2.2. Quasi-probability distributions

The operator density is a very useful mathematical tool which provides complete quantum information, but it lacks of clarity identifying the quantum system it represents. This task is better suited for *s-parametrized or generalized quasi-probability distributions* in the phase space [Cahill and Glauber, 1969]. These functions are not proper classical probability distributions, as they can have negative regions or may also be ill-behaved, but they are useful for calculating expectation values for operators of different orderings in $\{\hat{a}, \hat{a}^\dagger\}$ determined by the parameter s. The generalized quasi-distribution is defined as:

$$\mathcal{W}(\xi, s) = \frac{1}{\pi^2} \int e^{\xi\eta^* - \xi^*\eta}\, \mathcal{C}(\eta, s)\, d^2\eta,$$

$$\mathcal{C}(\eta, s) = Tr[\hat{\rho}\, e^{\eta\hat{a}^\dagger - \eta^*\hat{a}}]\, e^{s|\eta|^2/2}, \tag{3.2.39}$$

where s is the ordering parameter and $\mathcal{C}(\eta, s)$ is called the *charasteristic function*. For $s = 0$ (symmetrical order) we have the W or *Wigner function*, while for $s = 1$ (normal ordering) we have the $\mathcal{P}$ or *Glauber-Sudarshan distribution* and for $s = -1$ (anti-normal ordering) the $\mathcal{Q}$ or *Husimi-Kano distribution*.

The most used quasi-probability distribution in quantum optics problems is the Wigner function, as it is a phase space quasiprobability density defined as [Lvovsky and Raymer, 2008]:

$$W(\mathcal{E},\mathcal{P}) = \frac{1}{2\pi}\int_{-\infty}^{\infty} \langle \mathcal{E} + \frac{1}{2}\mathcal{E}'|\hat{\rho}|\mathcal{E} - \frac{1}{2}\mathcal{E}'\rangle\, e^{-i\mathcal{P}\mathcal{E}'}\, d\mathcal{E}', \tag{3.2.40}$$

which has the appealing property of yielding the correct marginal distribution of any rotated quadrature [Vogel and Risken, 1989]:

$$P(\mathcal{E}_\theta) = \int_{-\infty}^{\infty} W(\mathcal{E}_\theta \cos\theta - \mathcal{P}_\theta \sin\theta, \mathcal{E}_\theta \sin\theta + \mathcal{P}_\theta \cos\theta) d\mathcal{P}_\theta. \tag{3.2.41}$$

So the histogram $P(\mathcal{E}_\theta)$ is the integral projection of the Wigner function onto a vertical plane oriented at angle θ to the $\mathcal{E}$ axis. This probability is that measured in homodyne detection experiments $P(\mathcal{E}_\theta)$. This means that measuring marginal distributions in a number of different directions till get enough statistical material, it is possible to obtain the Wigner function by direct inversion of (3.2.41), called *inverse Radon transformation*, or other reconstruction algorithms, as those reviewed in [Lvovsky and Raymer, 2008].

3.2.3. OFS probability distribution

Along this dissertation we will focus mainly on pure states defined in terms of state vectors (3.2.33). As shown above § 3.1.1, any pure multimode quantum state of light $|L\rangle$ can be written as a superposition of eigenstates $\{|\mathcal{E}\rangle\}$ of the optical field-strength operators $\{\hat{\mathcal{E}}\}$:

$$|L\rangle = \int \langle \mathcal{E}_1,\ldots,\mathcal{E}_N|L\rangle |\mathcal{E}_1,\ldots,\mathcal{E}_N\rangle\, d\mathcal{E}_1 \ldots d\mathcal{E}_N, \tag{3.2.42}$$

where:

$$\langle \mathcal{E}_1,\ldots,\mathcal{E}_N|L\rangle \equiv \Psi(\boldsymbol{\mathcal{E}}) = |\Psi(\boldsymbol{\mathcal{E}})|\, e^{i\,\varphi(\mathcal{E})}, \tag{3.2.43}$$

is the complex probability amplitude or wavefunction in the optical field-strength domain $\boldsymbol{\mathcal{E}} \equiv (\mathcal{E}_1,\ldots,\mathcal{E}_N)$. In this way, the other states previously reviewed in § 3.1, can be written in terms of this space as follows:

- Number states:

$$\Psi_{|n\rangle}(\mathcal{E}_\nu) = \left(\frac{\sqrt{2}}{2^n\sqrt{\pi}\,n!}\right)^{1/2} H_n(\sqrt{2}\mathcal{E}_\nu)\, e^{-\mathcal{E}_\nu^2}. \tag{3.2.44}$$

- Coherent states:

$$\Psi_{|\alpha\rangle}(\mathcal{E}_\nu) = \left(\frac{2}{\pi}\right)^{1/4} \exp\{-[\mathcal{E}_\nu - |\alpha|\cos\phi_\alpha]^2\}\, e^{i\delta}, \tag{3.2.45}$$

  where $\delta = \sin\phi_\alpha\,[|\alpha|^2\cos\phi_\alpha - 2|\alpha|\mathcal{E}_\nu]$ and ϕ_α is the phase associated to the coherent state.

- Squeezed states:

$$\Psi_{|\alpha,\zeta\rangle}(\mathcal{E}_\nu) = (\frac{2}{\pi\Delta\mathcal{E}_\nu^2})^{1/4} exp\{\frac{-[\mathcal{E}_\nu - |\alpha|\cos\phi_\alpha]^2}{\Delta\mathcal{E}_\nu^2}\} e^{-i\delta}, \quad (3.2.46)$$

where δ and ϕ_α are the same as above and $\Delta\mathcal{E}_\nu^2$ is the quantum noise (3.1.29).

Likewise, the probability distribution in the N-dimensional optical field-strength space, is given by:

$$P(\boldsymbol{\mathcal{E}}) = |\langle\mathcal{E}_1,\ldots,\mathcal{E}_N|L\rangle|^2 \equiv |\Psi(\boldsymbol{\mathcal{E}})|^2. \quad (3.2.47)$$

In the case of a mixed state defined in terms of a density operator $\hat{\rho}$, the probability distribution is given by:

$$P(\boldsymbol{\mathcal{E}}) = Tr[\hat{\rho}\,|\mathcal{E}_1,\ldots,\mathcal{E}_N\rangle\langle\mathcal{E}_1,\ldots,\mathcal{E}_N|]. \quad (3.2.48)$$

The main advanges of this distribution are two: it is a well-behaved probability distribution for the field strength $\mathcal{E}$ and it can be directly measured by homodyne detection [Vogel, 1990]. Other distributions like the previously generalized quasi-probability distributions (3.2.39) are not distributions of measured quantities, but they can be obtained from a set of OFS distributions [Vogel and Risken, 1989]. Likewise, the density matrices can be as well obtained as two-fold Fourier transforms of OFS distributions [Kühn et al., 1994]. We will focus on this representation of quantum states of light because of these properties and, as we will see in the next chapter, due to it is a natural space for the study of polarization of quantum light. Furthermore, the propagation of the wavefunctions defined in this space is easily tacked by means of propagators, as we will show in the next secion.

3.3. Path integral formulation of quantum propagation

The most common approachs to quantum mechanics are based on the Schrödinger and Heisenberg equations which are directly related with the Hamiltonian formulation of classical mechanics. The nonvanishing classical Poisson brackets between position and momentum lead us to introduce noncommuting operators in quantum mechanics, the so-called *quantization principle*. The Hamilton function turns into the Hamilton operator, the central object in the Schrödinger and Heisenberg formulations.

However, there exists an alternative formulation of quantum mechanics based on the Lagrange formalism of classical mechanics. This approach,

developed by Feynman in the 1940's [Feynman and Hibbs, 1965], avoids the use of operators and instead of finding eigenfunctions of a Hamiltonian (or Momentum), a functional integral which yields the propagator required to determine the temporal (or spatial) evolution of the quantum system is evaluated. Moreover, since Feynman's formulation and classical mechanics are very close, the path integral formalism has the advantage of providing a much more intuitive approach [Ingold, 2002].

Therefore, the aim of this section is to introduce the main features of the Feynman formulation of path integration in the OFS representation. This formulation is suitable to analyze spatial quantum propagation in the Schrödinger picture and can be regarded as complementary to others such as those ones based on number states, coherent states, and so on.

3.3.1. Path integrals in the OFS space

To derive the general form of the spatial propagator we start with the total quantized Momentum, a sum of abstract spatial quantum harmonic oscillators with spatial frequencies β_ν[9], given by (2.3.58):

$$\hat{\mathcal{M}}_O = \frac{1}{2}\sum_{\nu=1}^{N}(\hat{p}_\nu^2 + \beta_\nu^2\hat{q}_\nu^2). \tag{3.3.49}$$

Bearing in mind that $\hat{\mathcal{M}}$ is the generator of displacements [Luks and Perinová, 2002], that is $\hat{\mathcal{M}} \to -i\hbar\partial/\partial z$, and the definition of OFS conjugate operators (3.1.1), applying (3.3.49) on a given quantum state $|\Psi\rangle$, we obtain the following Schrödinger-type equation for spatial propagation of quantum states on a N-dimensional OFS space (3.2.43):

$$-i\frac{\partial}{\partial z}\Psi(\mathcal{E}_1,\ldots,\mathcal{E}_N;z) = \sum_{\nu=1}^{N}\beta_\nu\Big\{-\frac{1}{4}\frac{\partial^2}{\partial\mathcal{E}_\nu^2} + \mathcal{E}_\nu^2\Big\}\Psi(\mathcal{E}_1,\ldots,\mathcal{E}_N;z), \tag{3.3.50}$$

In order to solve the above Schrödinger equation by a path integral approach we present a Lagrangian formulation with generalized coordinates $\mathcal{E}_\nu$ and velocities $d\mathcal{E}_\nu/dz = \mathcal{E}'_\nu$. From the classical spatial harmonic oscillator given in (2.3.58) in terms the classical counterpart of the OFS variables given by (3.1.1), that is commuting variables $\mathcal{E} = \beta^{1/2}q$ and $\mathcal{P} = \beta^{-1/2}p$, we have the following Momentum:

$$\mathcal{M}(\boldsymbol{\mathcal{E}},\boldsymbol{\mathcal{P}}) = \frac{1}{2}\sum_{\nu}\beta_\nu[\mathcal{P}_\nu^2 + \mathcal{E}_\nu^2]. \tag{3.3.51}$$

[9]The propagation constant β for z-propagation is analogous to the frequency ω for time evolution.

Likewise, Hamilton-type equations and the associated spatial Lagrangian can be obtained as follows:

$$\mathcal{E}'_\nu = \partial\mathcal{M}/\partial\mathcal{P}_\nu, \qquad \mathcal{P}'_\nu = -\partial\mathcal{M}/\partial\mathcal{E}_\nu, \tag{3.3.52}$$

$$\mathcal{L}(\boldsymbol{\mathcal{E}}, \boldsymbol{\mathcal{E}}') = \boldsymbol{\mathcal{P}}_\nu \boldsymbol{\mathcal{E}}'_\nu - \mathcal{M}(\boldsymbol{\mathcal{E}}, \boldsymbol{\mathcal{P}}), \tag{3.3.53}$$

where $\boldsymbol{\mathcal{E}}, \boldsymbol{\mathcal{E}}', \boldsymbol{\mathcal{P}}$ are N-dimensional variables, $\mathcal{M}$ plays the role of a Hamiltonian-type function and $\mathcal{L}$ is the corresponding Lagrangian-type function obtained via Legendre transformation of the classical Momentum (3.3.51)[10]. Therefore, according to the Feynman approach [Feynman and Hibbs, 1965], the propagator in the $\boldsymbol{\mathcal{E}}$ space is given by the following functional integral:

$$K(\boldsymbol{\mathcal{E}}_f, \boldsymbol{\mathcal{E}}_0; z_f) = b^{-1/2} \int_{\boldsymbol{\mathcal{E}}_0}^{\boldsymbol{\mathcal{E}}_f} \mathcal{D}\boldsymbol{\mathcal{E}}(z) e^{-\frac{i}{\hbar} \mathcal{S}(\boldsymbol{\mathcal{E}}_f, \boldsymbol{\mathcal{E}}_0; z_f)}, \tag{3.3.54}$$

with $b = \beta_1 \dots \beta_N$ and $\mathcal{S}$ the action functional. The optical propagator K is the sum over all paths $\boldsymbol{\mathcal{E}}(z) = (\mathcal{E}_1(z), \dots, \mathcal{E}_N(z))$ of the quantity $\exp\{(-i/\hbar)\ \mathcal{S}(\boldsymbol{\mathcal{E}}_f, \boldsymbol{\mathcal{E}}_0; z_f)\}$ evaluated on the path connecting the points $\boldsymbol{\mathcal{E}}_0 \equiv \boldsymbol{\mathcal{E}}(0)$ and $\boldsymbol{\mathcal{E}}_f \equiv \boldsymbol{\mathcal{E}}(z_f)$. The action functional is given by $\mathcal{S} = \int_0^{z_f} \mathcal{L}\, dz$, with $\mathcal{L}$ the spatial Lagrangian associated to the problem (3.3.53).

It is well known that the path integration can be performed in an exact way or by means of approximations such as the semiclassical limit, the approximated quadratic Lagrangians, perturbative techniques, and so on. It is interesting to note, as shown later, that in a semiclassical limit the classical paths $\boldsymbol{\mathcal{E}}(z)$ could also be derived from Heisenberg's equations through the trajectories followed by the operators $\hat{\mathbf{a}}(z)$ associated to the absorption operators, since their eigenvalues are the coherent states via (3.1.15). These trajectories can be also obtained in an exact way or by approximate techniques such as the adiabatic, WKB, perturbative, and so on.

Hence, if we know the N-modal quantum state of light $|L\rangle$ at the start of the medium, $\Psi(\boldsymbol{\mathcal{E}}_0; z = 0) = \langle \mathcal{E}_{01}, \dots, \mathcal{E}_{0N} | L \rangle$ in the OFS representation, the wavefunction at some plane $z_f > 0$ can be obtained by the following N-dimensional integral [Feynman and Hibbs, 1965]:

$$\Psi(\boldsymbol{\mathcal{E}}_f; z_f) = b^{-1/2} \int_{-\infty}^{+\infty} K(\boldsymbol{\mathcal{E}}_f, \boldsymbol{\mathcal{E}}_0; z_f)\, \Psi(\boldsymbol{\mathcal{E}}_0) d\boldsymbol{\mathcal{E}}_0. \tag{3.3.55}$$

where the integration is performed over all the possible values of $\boldsymbol{\mathcal{E}}_0$.

[10] Note that there is a change of sign with respect to the classical Hamiltonian theory in time.

3.3.2. Propagation in linear lossless homogeneous media

To calculate the optical propagator (3.3.54) corresponding to this kind of media, from (3.3.51) we obtain the following classical Lagrangian[11]:

$$\mathcal{L} = \sum_{\nu} \mathcal{P}_{\nu} \frac{\partial \mathcal{M}}{\partial \mathcal{P}_{\nu}} - \mathcal{M} = \sum_{\nu} \frac{1}{2\beta_{\nu}} [\mathcal{E}_{\nu}'^{2} - \beta_{\nu}^{2} \mathcal{E}_{\nu}^{2}], \tag{3.3.56}$$

In general, performing the integral (3.3.54) to calculate the propagator is a tough problem [Feynman and Hibbs, 1965]. However, the above Lagrangian is a quadratic one and the integral has a remarkably simple solution. The exact optical propagator related to linear homogeneous waveguides is given by [Liñares, 1989]:

$$K(\boldsymbol{\mathcal{E}}_f, \boldsymbol{\mathcal{E}}_0; z_f) = F(z_f)\, e^{-2i\mathcal{S}(\boldsymbol{\mathcal{E}}_f, \boldsymbol{\mathcal{E}}_0; z_f)}, \tag{3.3.57}$$

where $F(z_f)$ is worked out by means of the Van Vleck determinant:

$$F(z_f) = \left(\frac{-i}{\pi}\right)^{N/2} b^{1/2} \left(\det \frac{\partial^2 \mathcal{S}}{\partial \boldsymbol{\mathcal{E}}_f\, \partial \boldsymbol{\mathcal{E}}_0}\right)^{1/2}. \tag{3.3.58}$$

From (3.3.56), it can be easily proved that the general form of the action functional $\mathcal{S}$ in the field-strength space is given by [Gómez-Reino and Liñares, 1987]:

$$\mathcal{S}(\boldsymbol{\mathcal{E}}_f, \boldsymbol{\mathcal{E}}_0) = \sum_{\nu} \frac{1}{2\beta_{\nu}} [\mathcal{E}_{\nu}'(z)\, \mathcal{E}_{\nu}(z)]\Big|_0^{z_f}. \tag{3.3.59}$$

Likewise, the condition for the action $\mathcal{S}$ to assume an extreme value leads to the Euler's equation:

$$\mathcal{E}_{\nu}'' + \beta_{\nu}^{2} \mathcal{E}_{\nu} = 0. \tag{3.3.60}$$

The general solution of (3.3.60) is given by:

$$\mathcal{E}_{\nu}(z) = v_{\nu}(z) \mathcal{E}_{0\nu} + u_{\nu}(z) \mathcal{E}_{0\nu}', \tag{3.3.61}$$

where $v_{\nu}(z)$ and $u_{\nu}(z)$ are N-modal linearly independent functions that satisfy equation (3.3.60) and initial conditions:

$$\mathbf{u}(0) = \boldsymbol{\nu}'(0) = 0, \tag{3.3.62}$$

$$\mathbf{u}'(0) = \boldsymbol{\nu}(0) = 1, \tag{3.3.63}$$

$$\mathcal{W} = \mathbf{u}'\boldsymbol{\nu} - \boldsymbol{\nu}'\mathbf{u} = 1. \tag{3.3.64}$$

where $\mathcal{W}$ is the wronskian of the solutions.

[11] We will use the prescription $\hbar = 1/2$ all along this section for the sake of clarity and without loss of generality, since it does not appears in the final form of the propagators.

Likewise, applying equation (3.3.61) into (3.3.59), with initial conditons $\mathcal{E}_\nu(0) = \mathcal{E}_{0\nu}$ and $\mathcal{E}_\nu(z_f) = \mathcal{E}_{f\nu}$, we obtain the following action functional, or optical propagator phase,

$$\mathcal{S}(\boldsymbol{\mathcal{E}_f}, \boldsymbol{\mathcal{E}_0}) = \sum_\nu \frac{1}{2\beta_\nu u_\nu}[u'_\nu \mathcal{E}^2_{f\nu} + v_\nu \mathcal{E}^2_{0\nu} - 2\mathcal{E}_{f\nu}\mathcal{E}_{0\nu}], \tag{3.3.65}$$

with $v_\nu \equiv v_\nu(z_f)$ and $u_\nu \equiv u_\nu(z_f)$. Applying equation (3.3.65) into (3.3.58), the optical propagator amplitude is obtained. Finally, we can write the propagator (3.3.57) as follows:

$$K(\boldsymbol{\mathcal{E}_f}, \boldsymbol{\mathcal{E}_0}; z_f) = (\frac{i}{\pi})^{N/2} \prod_\nu u_\nu^{-1/2} \exp\{\frac{-i}{\beta_\nu u_\nu}[u'_\nu \mathcal{E}^2_{f\nu} + v_\nu \mathcal{E}^2_{0\nu} - 2\mathcal{E}_{f\nu}\mathcal{E}_{0\nu}]\}. \tag{3.3.66}$$

Now, in order to gain insight into the quantum light propagation with this approach we present the next two examples:

- A coherent state $|\alpha\rangle$ propagating in a single-mode linear homogeneous waveguide with propagation constant β at a certain frequency ω. The propagation of this state in the OFS space is obtained by inserting the OFS representation of the coherent state (3.2.45) and equation (3.3.66) into equation (3.3.55), and taking into account the solutions of the Euler equation (3.3.60):

$$u(z) = \sin \beta z/\beta, \quad v(z) = \cos \beta z. \tag{3.3.67}$$

  Therefore, after a straightforward calculation it is obtained:

$$\begin{aligned}\Psi_{|\alpha\rangle}(\mathcal{E}_f; z) = (\frac{2}{\pi})^{1/4} &\exp\{-[\mathcal{E}_f - |\alpha| \cos(\phi_\alpha + \beta z)]^2\} \\ &\exp\{-i(\delta_z - \beta z/2)),\end{aligned} \tag{3.3.68}$$

  with $\delta_z = \sin(\phi_\alpha + \beta z)\,[|\alpha|^2 \cos(\phi_\alpha + \beta z) - 2|\alpha|\,\mathcal{E}_f]$. So the action of the linear homogeneous waveguide on the coherent state is to add a phase. In Figure 3.3.1 we show the spatial propagation of an input coherent state in a linear waveguide. We have simulated the measurements a balanced homodyne detector would take via a Monte Carlo method.

- A Twin photon state $|1_1\, 1_2\rangle$ propagating in a synchronous DC. In the case of linear coupling between the propagating modes, more general propagators will be obtained, as we will see in the section dedicated to nonlinear coupling (§ 3.3.4). But for some problems the free propagator is still useful. The Momentum operator for a two-mode synchronous DC is given by (2.3.69):

$$\hat{M}_{DC} = \hbar \sum_{\nu=1}^{2} \beta\,(\hat{a}^\dagger_\nu \hat{a}_\nu + 1/2) + \hbar\kappa(\hat{a}_1 \hat{a}^\dagger_2 + h.c.). \tag{3.3.69}$$

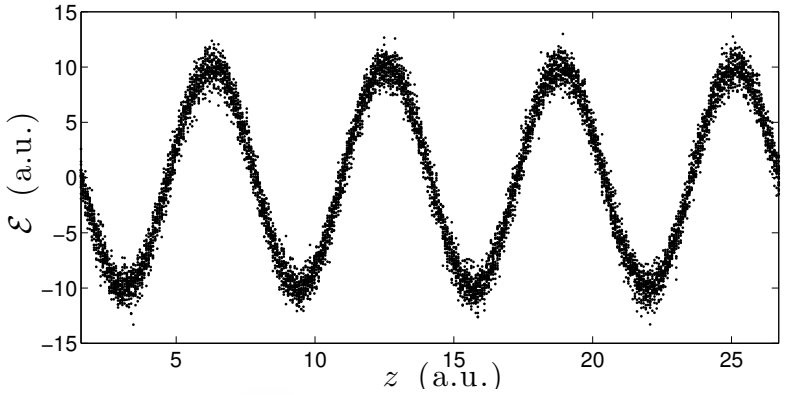

Figure 3.3.1: Optical-field strength probability distribution of a coherent state propagating in a linear homogeneous waveguide. Points simulate the values an homodyne detector would get at each plane of propagation.

We can diagonalize this Momentum to a supermode basis applying the following transformation:

$$\begin{pmatrix} \hat{a}_1 \\ \hat{a}_2 \end{pmatrix} = \begin{pmatrix} 1/\sqrt{2} & 1/\sqrt{2} \\ -1/\sqrt{2} & 1/\sqrt{2} \end{pmatrix} \begin{pmatrix} \hat{b}_1 \\ \hat{b}_2 \end{pmatrix}, \tag{3.3.70}$$

the following diagonal Momentum is obtained:

$$\hat{M}_{DC} = \hbar \sum_{\nu=\tilde{1}}^{\tilde{2}} \tilde{\beta}_\nu \, (\hat{b}_\nu^\dagger \hat{b}_\nu + 1/2), \tag{3.3.71}$$

where $\tilde{\beta}_\nu = \beta + (-1)^\nu \kappa$ and $\{\hat{b}_{\tilde{1}}, \hat{b}_{\tilde{2}}\}$ are the new supermode operators. Now, we can use the propagator (3.3.66) and apply the inverse of (3.3.70) to get back to the original mode basis. In the case of a twin photon state $|1_1\, 1_2\rangle$, in the supermode basis we obtain the following entangled state $(-|2_{\tilde{1}}\, 0_{\tilde{2}}\rangle + |0_{\tilde{1}}\, 2_{\tilde{2}}\rangle)/\sqrt{2}$. Applying the OFS representation for Fock states (3.2.44) and (3.3.66) into (3.3.55), and taking into account the following integral:

$$\int_{-\infty}^{\infty} e^{-ax^2+bx} \, \mathcal{H}_n(cx) dx = \sqrt{\frac{\pi}{a}} \, e^{b^2/4a} \, (1 - \frac{c^2}{a})^{n/2} \, \mathcal{H}_n(\frac{bc}{2a\sqrt{1-\frac{c^2}{a}}}), \tag{3.3.72}$$

we obtain the following supermode state after propagating a distance z:

$$\begin{aligned} \Psi(\mathcal{E}_{f\tilde{1}}, \mathcal{E}_{f\tilde{2}}; z) =& (\frac{1}{8\pi})^{1/2} \, e^{-\mathcal{E}_{f\tilde{1}}^2 - \mathcal{E}_{f\tilde{2}}^2} \\ & \{\mathcal{H}_2(\sqrt{2}\mathcal{E}_{f\tilde{2}}) e^{2i\tilde{\beta}_{\tilde{2}} z} - \mathcal{H}_2(\sqrt{2}\mathcal{E}_{f\tilde{1}}) e^{2i\tilde{\beta}_{\tilde{1}} z}\}. \end{aligned} \tag{3.3.73}$$

Now, due to the linear relation between OFS and $\{\hat{a}, \hat{a}^\dagger\}$ operators given by (3.1.1), it is easy to prove that the transformation (3.3.70) is also fulfilled by the OFS variables. Therefore, applying the inverse of (3.3.70) to (3.3.73), we obtain the following output state:

$$\Psi(\mathcal{E}_{f1}, \mathcal{E}_{f2}; z) = (\frac{1}{\pi})^{1/2}\, e^{-\mathcal{E}_{f1}^2-\mathcal{E}_{f2}^2}\, e^{2i\beta z}$$
$$\{\cos 2\kappa z \mathcal{H}_1(\sqrt{2}\mathcal{E}_{f1})\, \mathcal{H}_1(\sqrt{2}\mathcal{E}_{f2}) + i\frac{\sin 2\kappa z}{2}[\mathcal{H}_2(\sqrt{2}\mathcal{E}_{f1}) + \mathcal{H}_2(\sqrt{2}\mathcal{E}_{f2})]\,\}. \tag{3.3.74}$$

This is the well-known entangled state used in quantum interference experiments to test the indistinguishability of two photons [Politi et al., 2009] and leading to the Hong-Ou-Mandel interference pattern measured in the coincidence basis [Mandel and Wolf, 1995].

3.3.3. Propagation in linear lossless inhomogeneous media

As was advanced in § 2.3.3, inhomogeneous refractive index media can be divided in two big groups: factorable and separable media. The factorable case shows coupling and can be tackled in the same way as the homogeneous case. Nevertheless, the separable case is different as there is no coupling between modes. In this section we analyze the effects this sort of media has on quantum states of light.

Thus, following the the steps carried out above for homogeneous media (§ 3.3.2), we can work out the propagation in the OFS representation after taking into account (3.3.60), but substituting the constant β_ν^2 by:

$$\beta_\nu^2(z) = \beta_{t\nu}^2 + k_0^2 \Delta n^2 h^2(z), \tag{3.3.75}$$

as introduced in § 2.3.3. In order to clarify the propagation, we take once more the coherent state $|\alpha\rangle$ propagating in a single-mode linear inhomogeneous waveguide with propagation constant $\beta(z)$ fulfilling $\beta(0) = \beta_0$. The propagation of this state in the OFS space is obtained by inserting the OFS representation of the coherent state (3.2.45) and equation (3.3.66) into equation (3.3.55) for general $u(z)$ and $\nu(z)$ functions, obtaining:

$$\Psi(\mathcal{E}_f; z_f) = (\frac{2}{\pi})^{1/4}\, \rho^{-1/2}\, \exp\{-[\frac{\mathcal{E}_f}{\rho} - |\alpha|\,\cos(\phi+\theta)\,]^2\}$$
$$\exp\{-i(\frac{\rho'}{\beta_0\rho}\mathcal{E}_f^2 + \delta)\}\, e^{i\theta/2}, \tag{3.3.76}$$

with $\delta = \sin(\phi+\theta)\,[|\alpha|^2\cos(\phi+\theta) - 2|\alpha|\,\mathcal{E}_f/\rho]$ and ρ, θ where defined in (2.3.89), and are related with the solutions u, ν by:

$$\nu(z) = \rho\,\cos\,\theta, \qquad \beta_0\, u(z) = \rho\,\sin\,\theta, \tag{3.3.77}$$

Hence, the wavefunction (3.3.76) shows squeezing given by $\rho(z)$ and acquires a global quantum phase $\theta/2$ and a phase delay θ. However this squeezing is not measured experimentally. As was pointed out by Abram in his seminal paper about quantization of light in dielectric media [Abram, 1987], when quantum states propagating in a dielectric are represented in the basis of free-space photons, they seem to be squeezed, but inside a dielectric there is no experiment that can detect free-space photons. This happens because if we wish to detect photons inside the medium the fields would experiment an effective refractive index equivalent to the squeezing parameter and, therefore, a scale change is necessary. Likewise, Glauber and Lewestein in [Glauber and Lewenstein, 1991] carried out a similar analysis. In this study is stressed that the measurement of quantum states of light is based on photoabsorption processes carried out in the basis which diagonalizes the Hamiltonian in every medium. This is so because the photocount distribution is given by a normal ordered correlation product in the local basis, result of the physical property of the photoabsorption process that the energy of the field decreases when a photon is absorbed. But in any other basis this is not true, because of the mixing of absorption and emission operators, and therefore of frequencies, lacking the normal ordering in the correlation product. Thereby the state in these bases can not be measured and the photons are so-called virtual and, accordingly, the squeezing is virtual as well. Since the inhomogeneous medium can be regarded as a continuous succession of effective discontinuities, we can interpret that the coherent state has undergone virtual squeezing accumulated under spatial propagation and left its effect by producing different phase changes.

In the following sections we present two approaches to solve this problem. The first one is based on propagating and right after performing unitary transformations on the wavefunction. The second one is based on taking into account canonical transformations on the Momentum before quantization. Both perspectives are equivalent.

Method 1: the Infeld-Prebanski unitary transformation approach

The method here shown is detailed in § P3. We start focusing on equation (3.3.76). It is easy to realize that noise squeezing disappears if a scale change is made in the variable $\mathcal{E}$. Let us justify this transformation considering the simple example of an interface between two dielectric homogeneous media with refractive indices n_1 and n_2 when, for the sake of simplicity and without loss of generality, reflection is neglected (§ P3.9). From photon flux conservation we have:

$$\sqrt{n_1}\,\hat{q}_1 = \sqrt{n_2}\,\hat{q}_2, \tag{3.3.78}$$

where $\hat{q}_1$ and $\hat{q}_2$ are the optical fields quantized in every medium up to constants. Moreover, since we use a wavefunction in the OFS space, the

above relationship is also fulfilled by their eigenvalues, so $\sqrt{n_1}q_1 = \sqrt{n_2}q_2$. This scale transformation should be accomplished at every discontinuity the wavefunction finds during propagation. As we are dealing with optical modes, we will have a continuous longitudinal change of an effective refractive index. Therefore we can rewrite the above equations by using effective refractive indices and, hence, modal propagation constants as well, that is:

$$\sqrt{\beta_1}q_1 = \sqrt{\beta_2}q_2, \tag{3.3.79}$$

where $\beta = k_o N$ is the modal propagation constant of the propagating mode and N the its effective refractive index. Of course, performing this scale change differentially in the propagator we would eliminate the squeezing at each plane z and none signature of it would be obtained. Taking into account our definition of the optical field-strength operator (3.1.1) and the invariant (2.3.91), we can write for the eigenvalues $\mathcal{E}$:

$$\frac{\mathcal{E}_f}{\rho} = \sqrt{\frac{\beta_0}{2\hbar\rho^2}}\, q\,(z_f) = \sqrt{\frac{\theta'}{2\hbar}}\, q_f \tag{3.3.80}$$

Let us recall that $\tilde{\beta} \equiv \theta'$ is the real propagation constant of the optical mode. Therefore, at the end of the z-inhomogeneous medium there is an effective (or real) discontinuity at $z = z_f$, such that from this plane the medium has a transverse propagation constant β_e, then equation (3.3.80) can be written as:

$$\frac{\mathcal{E}_f}{\rho} = \frac{\sqrt{\tilde{\beta}}}{2\hbar}\, q_f = \frac{\sqrt{\beta_e}}{2\hbar}\, q_e \equiv \mathcal{E}_e \tag{3.3.81}$$

Thus, by taking into account this relationship, that is $\mathcal{E}_f = \rho\,\mathcal{E}_e$, the wavefunction given by equation (3.3.76) can be rewritten as

$$\begin{aligned}\Psi(\mathcal{E}_e; z_f) = (\frac{2}{\pi})^{1/4}\, &\exp\{-[\mathcal{E}_e - |\alpha|\,\cos(\phi+\theta)\,]^2\} \\ &\exp\{-i(\frac{\rho\rho'}{\beta_0}\mathcal{E}_e^2 + \delta_e\}\, e^{i\theta/2},\end{aligned} \tag{3.3.82}$$

with $\delta_e = \sin(\phi+\theta)\,[|\alpha|^2\cos(\phi+\theta) - 2|\alpha|\,\mathcal{E}_e]$. Thus the quantum fluctuations are again equal to one, that is, there is no squeezing. Note that the prefactor $\rho^{-1/2}$ in equation (3.3.76), has also been cancelled because of normalization. However, the wavefunction (3.3.82) still presents a quadratic phase term in the field-strength which would produce squeezing under temporal evolution of the state. This phase is an artifact resulting from the use of a propagator which does not rescale the variables at each z. Hence, for the sake of consistency, this phase is not compatible with no squeezing or, in other words, is not compatible with relationship (3.3.78), and consequently should be eliminated. By means of a gauge transformation

$\exp\{i(\frac{\rho'}{\beta_0\rho})\hat{\mathcal{E}}_e^2\}$ on the wavefunction (3.3.82), we obtain:

$$\Psi(\mathcal{E}_e; z_f) = (\frac{2}{\pi})^{1/4} \exp\{-[\mathcal{E}_e - |\alpha| \cos(\phi + \theta)]^2\} \exp\{-i\delta_e\} e^{i\theta/2}. \quad (3.3.83)$$

Therefore we can say that the state has undergone virtual squeezing, as it recovers the coherent shape. Moreover, the quantum state given by equation (3.3.83) is the one we would measure by means of photodetectors placed just at the end of the medium, that is, a coherent one with an OFS mean value shifted by an amount θ, and also a global z-dependent phase whose effect could be observed in quantum interference experiments. This example clearly reflects how time-dependent Hamiltonians and z-dependent Momentum operators present different behaviours, which underlines the importance of a quantum theory of light propagation.

In the case of a squeezed state of light propagating in a z-inhomogeneous medium more interesting results are obtained. Let us consider a single-mode squeezed state given in the OFS representation by (3.2.46), with quantum noise in the input face of the waveguide $\Delta\mathcal{E}_o^2 \neq 1$. Once more, by inserting equations (3.3.66) and (3.2.46) into (3.3.55), after a long but straightforward calculation and by carrying out both the scale change and the quadratic phase cancellation, we obtain the following normalized wavefunction at the end of the waveguide:

$$\begin{aligned} \Psi(\mathcal{E}_e; z_f) = (\frac{2}{\pi})^{1/4} (\frac{\rho}{\Delta\mathcal{E}_o \rho_s})^{1/2} e^{i\theta_s/2} e^{-i\delta_s} \\ \exp\{-\frac{1}{\Delta\mathcal{E}_o^2 (\rho_s/\rho)^2} [\mathcal{E}_e - |\alpha| \cos(\phi + \theta)]^2\}, \end{aligned} \quad (3.3.84)$$

where

$$\frac{\rho_s}{\rho} = [\cos^2\theta + \text{sen}^2\theta / \Delta\mathcal{E}_o^4]^{1/2}, \quad (3.3.85)$$

$$\theta_s = \arctan(\tan\theta / \Delta\mathcal{E}_o^2). \quad (3.3.86)$$

Note that no new squeezing appears. However, like in the coherent case, the oscillation period has changed due to the function $\theta(z)$ (phase delay) as expected, and therefore the squeezing oscillation, the distance where quantum noise value is repeated, has changed as well. Likewise, equation (3.3.86) indicates that the quantum phase θ_s obtained in (3.3.84) is different from the modal phase θ. Due to its analogy to Gouy's phase in classical optics [Boyd, 1980], we call it quantum Gouy's phase. This phase has not classical counterpart because it depends on the characteristics of the quantum light state, in this case on the optical noise parameter $\Delta\mathcal{E}_o^2$. Examples of its emergence in particular LIM are shown in sections § P3 & § P4.

Likewise, both the scale change and phase cancellation above introduced can be formulated in terms of unitary transformations in the following way:

$$\hat{U}_\rho = \hat{S}(\ln\rho)\hat{P}(\rho). \quad (3.3.87)$$

where:

$$\hat{S}(\ln\rho) = \exp\{\frac{\ln\rho}{2}(\hat{a}^2 - \hat{a}^{\dagger 2}\} = \exp\{i\frac{\ln\rho}{2}(\hat{\mathcal{E}}_f\hat{\mathcal{P}}_f + \hat{\mathcal{P}}_f\hat{\mathcal{E}}_f\}, \tag{3.3.88}$$

$$\hat{P}(\rho) = \exp\{i(\frac{\rho'}{\beta_0\rho})\hat{\mathcal{E}}_f^2\}. \tag{3.3.89}$$

The first one is a Bogolyubov or squeezing transformation (3.1.25) with a real squeezing parameter $\zeta = \ln\rho$ and the second one is a gauge transformation. Interestingly, the total transformation is just an unitary Infeld-Plebanski transformation [Infeld and Plebanski, 1955] used studying optical squeezing as a way to simplify calculations [Fernández Guasti and Moya-Cessa, 2003]. However, in this case, it is a real transformation implemented by the longitudinally inhomogeneous medium. Therefore, by employing directly this transformation over state given by equation (3.3.76), equation (3.3.83) is obtained. In short, by applying equations (3.3.55) and (3.3.66) to any input quantum state expressed in the OFS space, and performing the unitary transformation (3.3.87) to the corresponding result, a real expression for spatial propagation in longitudinally inhomogeneous media is obtained.

On the other hand, equation (3.3.83) enables us to justify, in a heuristic way, the optical propagator in a longitudinally inhomogeneous medium. That is, the wavefunction (3.3.83), analogous to (3.3.68), is obtained if we rewrite the optical propagator given by equation (3.3.66) for a single-mode guide, as follows:

$$K(\mathcal{E}_f, \mathcal{E}_0; z_f) = (\frac{i}{\pi})^{1/2}(\sin\theta)^{-1/2}\exp\{\frac{-i}{\sin\theta}[\cos\theta(\mathcal{E}_f^2 + \mathcal{E}_0^2) - 2\mathcal{E}_f\mathcal{E}_0]\}. \tag{3.3.90}$$

Method 2: the generalized canonical transformations approach

The method here presented is detailed in § P4. In this case we look for some transformation which takes the classical Momentum (2.3.83) to be a constant of motion suitable to be quantized and simultaneously get rid of the virtual squeezing in a continuous way. Taking into account what we have seen in the previous section, we propose the following generalized canonical transformations from a generating function $G_2(q, \tilde{P}) = \tilde{P}q/\rho$ and z transformation [Chetouani et al., 1989]:

$$\tilde{Q}_\nu = \frac{q_\nu}{\rho_\nu}, \quad \tilde{P}_\nu = \rho_\nu p_\nu, \quad s_\nu = (\int_0^z \rho_\nu^2(z)\,dz)^{-1}; \tag{3.3.91}$$

and the next gauge transformations related to the new s-frame:

$$Q_\nu = \tilde{Q}_\nu, \qquad P_\nu = \tilde{P}_\nu - \frac{\dot{\rho}_\nu}{\rho_\nu}\tilde{Q}_\nu, \tag{3.3.92}$$

with the dot standing for an s-derivative. Applying these relations into (2.3.83), we directly obtain the following Momentum:

$$\mathcal{M}_\nu(Q,P,s)=\frac{1}{2}[P_\nu^2(s)+\beta_{0\nu}^2\,Q_\nu^2(s)], \tag{3.3.93}$$

where we have used the auxiliar equation (2.3.90). It is remarkable that these new phase space and longitudinal coordinates (Q,P,s) are analogous to the comoving coordinates and the conformal (or arc-parameter) time used in cosmology and, likewise, the canonical momentum transformation (3.3.92) is related to the Hubble's law [Misner et al., 1973]. After these transformations, the continuous change in the value of the harmonic potential appears as constant in the new comoving frame of reference [Takagi, 1990]. So, in this frame, there are not scale changes differentially and the medium seems to be homogeneous. The generalized canonical transformations eliminate the squeezing at each plane z and none signature of it is obtained. These insights lead us to consider the comoving frame as the physical one and therefore the proper one for quantization. Furthermore, interestingly, if we rewrite this Momentum in the original phase space, we obtain:

$$\mathcal{M}_\nu(q,p,z)=\frac{1}{2}[(\rho_\nu\,p_\nu-q_\nu\,\rho_\nu')^2+\beta_{0\nu}^2(q_\nu/\rho_\nu)^2]. \tag{3.3.94}$$

This is the space-analog of an Ermakov-Lewis invariant [Lewis, 1967]. So, it can be said that the Momentum (3.3.93) is a spatial Ermakov-Lewis invariant in a comoving frame and that this invariant is the generator of spatial propagation in this kind of media.

Now, following the principle of quantization of quantum mechanics $(Q_\nu,P_\nu)\to(\hat{Q}_\nu,\hat{P}_\nu)$, where $[\hat{Q}_\nu,\hat{P}_{\nu'}]=i\hbar\delta_{\nu,\nu'}$, we obtain the Momentum operator:

$$\hat{\mathcal{M}}_\nu=\frac{1}{2}[\hat{P}_\nu^2(s)+\beta_{0\nu}^2\,\hat{Q}_\nu^2(s)]. \tag{3.3.95}$$

In order to obtain the eigenvalues and eigenfunctions of this operator, we define the following annihilation and creation operators:

$$\hat{A}_\nu(s)=\frac{1}{\sqrt{2\hbar\beta_{0\nu}}}[\beta_{0\nu}\hat{Q}_\nu+i\hat{P}_\nu], \tag{3.3.96}$$

$$\hat{A}_\nu^\dagger(s)=\frac{1}{\sqrt{2\hbar\beta_{0\nu}}}[\beta_{0\nu}\hat{Q}_\nu-i\hat{P}_\nu]. \tag{3.3.97}$$

Therefore, equation (3.3.95) in terms of (3.3.97) can be rewritten as:

$$\hat{\mathcal{M}}_\nu=\hbar\beta_{0\nu}[\hat{A}_\nu^\dagger\hat{A}_\nu+1/2]. \tag{3.3.98}$$

The eigenstates of this Momentum are the same as those of the Number operator $\hat{N}_\nu=\hat{A}_\nu^\dagger\hat{A}_\nu$, which fulfills the next eigenvalue equation:

$$\hat{N}_\nu|N_\nu\rangle=N_\nu|N_\nu\rangle, \tag{3.3.99}$$

where N_ν and $|N_\nu\rangle$ are eigenvalues and eigenstates for the Number operator, respectively. In terms of quantum-optical units [Loudon, 1982], we can redefine the quantum comoving scaled position $\hat{Q}_\nu$ as the OFS operator $\hat{\mathcal{E}}_\nu = \sqrt{\beta_{0\nu}/2\hbar}\,\hat{Q}_\nu$. The eigenstates $|N_\nu\rangle$ in the optical field-strength $\mathcal{E}$ basis are given in terms of Hermite-Gauss functions (3.2.44) and their quantum propagation is given by a spatial Schrödinger equation:

$$\hat{\mathcal{M}}_\nu\,\Psi_N \equiv \hbar\beta_{0\nu}\,[-\frac{1}{4}\frac{\partial^2}{\partial{\mathcal{E}_\nu}^2} + \mathcal{E}_\nu^2]\,\Psi_N = \hbar\beta_{0\nu}\,\Psi_N. \tag{3.3.100}$$

The solution of this equation yields the following propagated eigenstates $|N_\nu\rangle$:

$$\Psi_N(\mathcal{E}_\nu; s) = \frac{2^{1/4}\,e^{i(N+1/2)\theta_\nu}}{\sqrt{2^N\pi^{1/2}\,N!}}\,H_N(\sqrt{2}\mathcal{E}_\nu)\,e^{-\mathcal{E}_\nu^2}, \tag{3.3.101}$$

with $\theta_\nu = \beta_{0\nu}s_\nu$ the total accumulated phase, in the same way as a quantum state propagating in a homogeneous medium, but in this case in a comoving frame, which is the physical one for this kind of problems as shown above. As in the previous section, the quantum Gouy's phase is the net effect of the propagation.

From the wavefunction (3.3.101) and Mehler's formula [Yeon et al., 1994], the propagator of the system is easily obtained:

$$K(\mathcal{E}, \mathcal{E}_0; z, 0) = (\frac{i}{\pi})^{N/2}\prod_\nu (\sin\theta_\nu)^{-1/2}\,e^{-\frac{i}{\sin\theta_\nu}[\cos\theta_\nu\,(\mathcal{E}_\nu^2+\mathcal{E}_{0\nu}^2)-2\mathcal{E}_\nu\mathcal{E}_{0\nu}]}, \tag{3.3.102}$$

This propagator is exactly the same as that heuristically inferred in the above section (3.3.90). Indeed, taking into account the OFS representation of the coherent and squeezed states of light, (3.3.83) and (3.3.84) are easily obtained.

Details and examples of the application of both approaches to particular longitudinally inhomogeneous refractive indices can be found in sections § P3 & § P4.

3.3.4. Propagation in nonlinear lossless media

Any nonlinear Momentum is suitable to be treated with this formalism. As shown above, in the case of quadratic Momenta, the semiclassical approximation is exact, so the propagation in nonlinear waveguides in a parametric regime can be directly tackled in this way. The general case has to be dealt with approximate techniques as adiabatic, perturbative or WKB. In the nonlinear regime, each case has to be treated particularly. As an example, we show the results for a spatially *degenerate parametric amplifier* (DPA), based on a *degenerate parametric down-conversion* (DPDC) process, formed by two modes with propagation constants $\beta = \beta(\omega)$ and

$\beta_p = \beta(2\omega)$. These modes are nonlinearly coupled, where the first mode is the amplified mode and the second is assumed to be a non-depleting classical pump mode. A nonlinear z-coupling coefficient $\kappa_{NL}(z)/2$, with $\kappa_{NL}(z) = \kappa_0 f_{NL}(z)$, and a pump phase δ_p, are considered. Therefore, following section 2.3.2, the Momentum operator associated to this problem is written as:

$$\hat{M} = \hbar\beta(\hat{a}^\dagger\hat{a} + 1/2) + \hbar\frac{\kappa_{NL}(z)}{2}(\hat{a}^2 e^{-i(\beta_p z+\delta_p)} + \text{h.c.}). \tag{3.3.103}$$

The classical Momentum in terms of OFS variables, $\mathcal{M}(\mathcal{E},\mathcal{P})$, corresponding to this problem will be:

$$\mathcal{M} = \frac{\beta}{2}(c_+\mathcal{E}^2 + c_-\mathcal{P}^2) + \kappa_{NL}(z)\, s\, \mathcal{E}\mathcal{P}, \tag{3.3.104}$$

with $c_\pm = 1 \pm [\kappa_{NL}(z)\cos(\beta_p z + \delta_p)/\beta]$ and $s = \sin(\beta_p z + \delta_p)$. Following the steps of section (3.3.2) the propagator is obtained as follows:

$$K(\mathcal{E}_f, \mathcal{E}_o, z) = (\frac{i\beta c(z)}{\pi u(z)})^{1/2} \exp\{\frac{-i}{u(z)}[a(z)\mathcal{E}_f^2 + b(z)\mathcal{E}_o^2 - 2c(z)\mathcal{E}_f\mathcal{E}_o]\}, \tag{3.3.105}$$

where:

$$a(z) = \frac{u'(z) - \kappa_{NL}(z)\, s\, u(z)}{\beta\, c_-}, \quad b(z) = \frac{v(z)}{\beta - \kappa_0}, \tag{3.3.106}$$

$$c(z) = \frac{1}{2}\Big[\frac{W}{\beta\, c_-} + \frac{1}{\beta - \kappa_0}\Big], \tag{3.3.107}$$

$$W = \frac{\beta}{\beta - \kappa_0}\Big[1 - \frac{\kappa_0}{\beta}\cos(\beta_p z + \delta_p)\Big], \tag{3.3.108}$$

with $\kappa_0 \equiv \kappa_{NL}(0)$ and W is the wronskian. Note that for $\kappa_{NL} = 0$ (no mode coupling), $a = u'/\beta$, $b = v/\beta$ and $c = 1/\beta$, the free propagator (3.3.66) obtained in § 3.3.2 is recovered.

The next step is to calculate the functions u and v. In this case, unlike the linear homogeneous case, the Euler equation (3.3.60) is not obtained. Instead, an Ince-type equation is derived, which is not easy to solve in general [Cordero-Soto and Suslov, 2011]. To circumvent this, we write the Heisenberg equations for the operators $\hat{a}$ and $\hat{a}^\dagger$ related to the Momentum (3.3.103) as follows:

$$\frac{\partial\hat{a}}{\partial z} = i\beta\hat{a} + i\kappa_{NL}(z)\hat{a}^\dagger e^{i(\beta_p z+\delta_p)}, \tag{3.3.109}$$

$$\frac{\partial\hat{a}^\dagger}{\partial z} = -i\beta\hat{a}^\dagger - i\kappa_{NL}(z)\hat{a} e^{-i(\beta_p z+\delta_p)}, \tag{3.3.110}$$

with solutions:

$$\hat{a}(\tau) = \hat{a}(0)\cosh[\kappa_0\,\tau(z)] + ie^{i\delta_p}\hat{a}^\dagger(0)\sinh[\kappa_0\,\tau(z)]\}\, e^{i\beta z}, \tag{3.3.111}$$

where $\tau = \int_0^z f_{NL}(z')dz'$ and we have considered for the sake of clarity phase matching $\beta_p = 2\beta$[12]. So, writing $\mathcal{E}(z)$ in terms of the mean values of $\{\hat{a}(z), \hat{a}^\dagger(z)\}$ for a coherent state, and comparing the result with equation (3.3.61), the functions $u(z)$ and $v(z)$ are given by:

$$u(z) = \frac{1}{\beta - \kappa_0}\,[\cosh(\kappa_0\tau)\mathrm{sen}(\beta z) - \sinh(\kappa_0\tau)\cos(\beta z + \delta_p)], \quad (3.3.112)$$

$$v(z) = \cosh(\kappa_0\tau)\cos(\beta z) - \sinh(\kappa_0\tau)\sin(\beta z + \delta_p). \quad (3.3.113)$$

With all these tools, the propagator (3.3.105) allows to evaluate the quantum light propagation in any DPDC device with a z-inhomogeneity $\kappa_{NL}(z)$. Interestingly, at the planes z_m, where $b(z_m) = v(z_m) = 0$, we obtain the Fourier transform of the probability amplitude distribution of an input quantum state $\Psi(\mathcal{E}, 0)$, with a scale factor depending on κ_{NL}; for the particular case of $\kappa_{NL}(z) = \kappa_0$, $\beta z_m = m\pi + \arctan\{\mathrm{cotanh}(\kappa_o z_m)\}$ is obtained. On the other hand, at planes z_n fulfilling $u(z_n)$=0, a scale transform (like an "image" condition) of the probability amplitude distribution of an input quantum state $\Psi(\mathcal{E}_0, 0)$ is obtained. The corresponding scale factor measures the amplification level reached; for the particular case $\kappa_{NL}(z) = \kappa_0$, $\beta z_n = n\pi + \arctan\{\tanh(\kappa_o z_n)\}$ is obtained. Likewise, there are z's where the quantum noise is maximum or minimum, so we have a squeezing transform; for instance, for vacuum states and media with $\kappa_{NL}(z) = \kappa_0$ and pump phase $\delta_p = 2\pi$, squeezing is obtained at the planes fulfilling $2\beta z_p = (p + 1/2)\pi$, with quantum noise $e^{\pm\kappa_0 z_p}$.

Next, in order to get further insight in the behaviour of a DPA device, we study the generation of squeezed light and pairs of photons through *spontaneous parametric down-conversion* (SPDC). This process is analogous to that above shown, but in this case the quantum state to be amplified is the vacuum[13]. Then, inserting the OFS representation of the vacuum (3.2.44) and the DPA propagator (3.3.105) into equation (3.3.55), the probability amplitude $\Psi(\mathcal{E}_f; z)$ of measuring the optical-field strength with value $\mathcal{E}_f$ at a distance z can be expressed as:

$$\Psi(\mathcal{E}_f; z) = \left(\frac{2}{\pi\,\Delta\mathcal{E}^2(z)}\right)^{1/4} \exp\left\{-\frac{\mathcal{E}_f^2}{\Delta\mathcal{E}^2(z)}\right\} e^{i\beta z/2}, \quad (3.3.114)$$

where $\Delta\mathcal{E}^2(z)$ is the quantum noise at each plane z, and whose expression is given by:

$$\Delta\mathcal{E}^2(z) = [\cosh(2\kappa_0\,\tau) - \sinh(2\kappa_0\,\tau)\,\sin(2\beta z + \delta_p)]. \quad (3.3.115)$$

[12] This condition is highly desirable as the efficiency in the amplification process scales with $\beta_p - 2\beta$. Normally this condition is attained with integrated gratings via *quasi-phase matching*, with ring resonators via filtering and so on.

[13] Hence the term *spontaneous*.

This is a single-mode squeezed vacuum state. In Figure 3.3.2 we show the spatial generation of this squeezed light in a waveguiding DPA. We have simulated the measurements a balanced homodyne detector would take placed at each plane z via a Monte Carlo method. It is shown the spatial z-squeezing, leading to planes with quantum noise under the SQL. Note the transition from the initial vacuum state to the squeezed vacuum. Likewise, it is important to outline that once the state arrives the detector, the quantum noise will oscillate harmonically in time without amplification, but depending on $\Delta\mathcal{E}^2(z_f)$.

On the other hand, it is important to outline that this state has photons. Indeed, its expected value is $\langle\hat{n}\rangle = \sinh^2(r)$, with $r = \ln(\Delta\mathcal{E}^2)^{-1/2}$. Re-writing this state in the Fock basis, we see that this state contains only even photon numbers [Lvovsky, 2015]:

$$\Psi(\mathcal{E}_f; z) = \frac{1}{\cosh r}\sum_{m=0}^{\infty}(-\tanh r)^m \frac{\sqrt{2m!}}{2^m m!}\Psi_{|2m\rangle}(\mathcal{E}_f; z), \tag{3.3.116}$$

with $\Psi(\mathcal{E}_f; z) = \langle\mathcal{E}|0; r\rangle$ the squeezed vacuum in the OFS representation. Interestingly, if $r << 1$, we have:

$$\Psi(\mathcal{E}_f; z) = \Psi_{|0\rangle}(\mathcal{E}_f; z) - \frac{r}{\sqrt{2}}\Psi_{|2\rangle}(\mathcal{E}_f; z) + O(r^2), \tag{3.3.117}$$

Therefore, quantum states corresponding to pairs of photons $|2\rangle$ are produced. This is due to energy conservation: a pump photon can only split into two photons with half its energy. Likewise, when the process is non-degenerate, twin photon states $|1_1\, 1_2\rangle$ as those above used as an example in § 3.3.2, are obtained. This phenomenon is the same as that shown in § C1 but in that case pairs of photons are produced via a third order nonlinear process, specifically SFWM.

3.3.5. Propagation in lossy media

Another feature to take into account in the propagation problem are the losses. In the previous chapter we tackled them from a Heisenberg point of view. Now we will show some results for the Feyman approach. As it was shown in appendix A, losses can be modelled by means of coupling to stochastic forces. The semiclassical optical propagator in the OFS space for a single-mode quantum state coupled to a Langevin force is given by the following formal expression:

$$K(\mathcal{E}_f, \mathcal{E}_0; z) = \left\{\frac{\tilde{\beta}}{4i\pi\hbar^2}\frac{\partial^2 S}{\partial\mathcal{E}_f\partial\mathcal{E}_0}\right\}^{1/2} e^{-(i/\hbar)\int_0^z \mathcal{L}(\mathcal{E}_F, \mathcal{E}_F')dz}, \tag{3.3.118}$$

with $\tilde{\beta} = \beta + i\gamma/2$ and the subscript F indicates that now the solutions should be corrected by fluctuations. Quantum fluctuations are a source

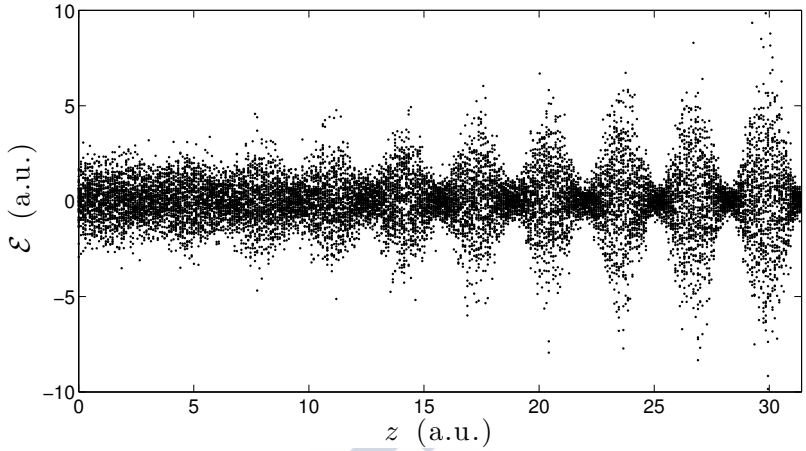

Figure 3.3.2: Optical-field strength probability distribution of the squeezed vacuum state generated by propagation of an input pump mode in a waveguiding PDA. Points simulate the values an homodyne detector would get at each plane of propagation.

of noise. Therefore, for a small noise source (or quadratic Lagrangians as shown in the free case) the paths can be formally written as:

$$\mathcal{E}_F(\mathcal{E}_0, \mathcal{E}_f, z) = \mathcal{E}(\mathcal{E}_0, \mathcal{E}_f, z) + \delta\mathcal{E}(z), \tag{3.3.119}$$

where $\delta\mathcal{E}(z)$ represents the deviation from the classical paths due to fluctuations and $\langle\mathcal{E}_F\rangle = \mathcal{E}$. So, by taking into account that from a statistical point of view a function $f(x_F)$, with x_F a stochastic variable not strongly fluctuating, fulfills, in a good approximation, $\langle f(x_F)\rangle \approx f(\langle x_F\rangle)$, the propagator (3.3.118) can be approximated to second order as follows:

$$\langle K(\mathcal{E}_f, \mathcal{E}_o; z)\rangle \approx \left\{\frac{\tilde{\beta}}{4i\pi\hbar^2}\frac{\partial^2 S}{\partial\mathcal{E}_f\partial\mathcal{E}_o}\right\}^{1/2} e^{-(i/\hbar)\int_0^z \mathcal{L}(\mathcal{E},\mathcal{E}')dz}\,[1 + O(g^2) + ...]. \tag{3.3.120}$$

The terms of first-order $O(g)$ are zero because of the statistical properties of the noise. The terms of order equal to, or greater than, $O(g^2)$ introduce small corrections to the optical propagator, but the main contribution comes from the classical paths without noise. This approach can be seen as an approximation to the more general method of the influence functional introduced by Feynman and Vernon [Feynman and Vernon, 1963].

Now, as an illustrative example, it is interesting to calculate the propagation of a *quasi*-classical state of the electric field. To this end, let us retake the first example we show in § 3.3.2, that is a coherent state $|\alpha\rangle$ propagating in a linear medium, but in this case, taking into account losses. The $O(g^0)$ contribution to (3.3.120) can be formally written changing β by $\tilde{\beta}$ in equation (3.3.66) and using the free propagation solutions to the Euler equation

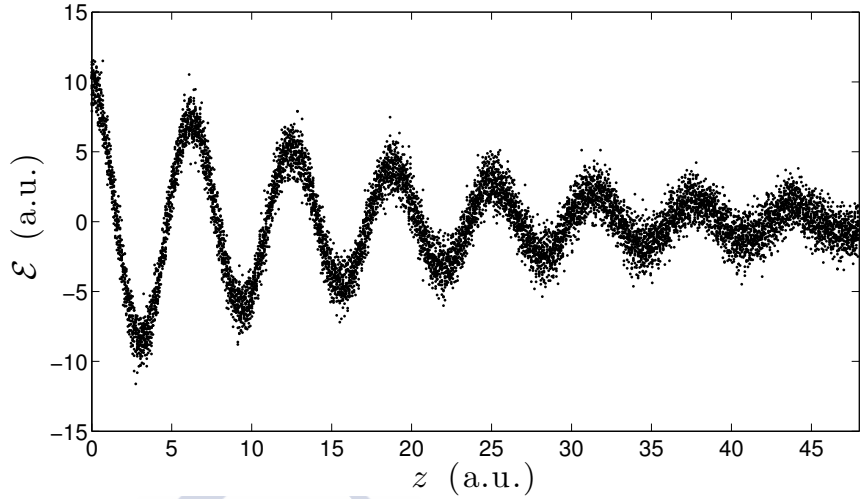

Figure 3.3.3: Optical-field strength probability distribution of a coherent state propagating in a lossy medium. Points simulate the values an homodyne detector would get at each plane of propagation.

(3.3.67), leading to:

$$\langle K(\mathcal{E}_f, \mathcal{E}_o, z)\rangle = \left\{\frac{i\tilde{\beta}}{2\pi\hbar \sin\tilde{\beta}z}\right\}^{1/2} e^{-\frac{i}{\sin(\tilde{\beta}z)}\{(\mathcal{E}_f^2+\mathcal{E}_o^2)\cos(\tilde{\beta}z)-2\mathcal{E}_f\mathcal{E}_o\}}. \tag{3.3.121}$$

By using the OFS representation of this state (3.2.45), and applying it and the propagator equation (3.3.121) into (3.3.55), we obtain:

$$\begin{aligned}\Psi_{|\alpha\rangle}(\mathcal{E}_f; z) = (\frac{2}{\pi})^{1/4}\ &\exp\{-[\mathcal{E}_f - |\alpha|\, e^{-\gamma z/2}\cos(\phi_\alpha+\beta z)\,]^2\}\\ &\exp\{-i(\delta_z - \beta z/2)),\end{aligned} \tag{3.3.122}$$

with $\delta_z = \sin(\phi_\alpha+\beta z)e^{-\gamma z/2}\,[|\alpha|^2 e^{-\gamma z/2}\cos(\phi_\alpha+\beta z) - 2|\alpha|\,\mathcal{E}_f]$. So the mean number of photons will be $\langle\hat{n}\rangle = |\alpha\, e^{-\gamma z}|^2$, as expected. Likewise, if the distance of propagation is long enough, $z >>$, the above probability amplitude will be given approximately by:

$$\Psi_{|\alpha\rangle}(\mathcal{E}_f; z >>) \to (\frac{2}{\pi})^{1/4} e^{-\mathcal{E}_f^2}\, e^{i\beta z/2}, \tag{3.3.123}$$

that is, the coherent field state will become the vacuum state due to the losses in the medium as shown in Figure 3.3.3. It is important to outline that this is the result expected by the classical theory and that is obtained by taking into account only the $O(g^0)$ contribution to the propagator (3.3.120). In the case of states where quantum correlations are important, it is expected that higher order contributions will show the degradation this statistical noise produces on quantum correlations.

oOo

In the following sections we present the published and submitted research works on propagation in the OFS space where we go in depth with the concepts above introduced and their application to IPDs. Specifically, in (§ P2) we review the quantization scheme seen in chapter 2 and extend it to higher order nonlinearities, showing additional terms neglected in other approaches which naturally appear with the Momentum approach. Next, we introduce the path integral formulation in the OFS space, derive the propagator and apply it to the particular case of a *degenerate parametric amplifier* (DPA) with a z-dependent nonlinear coefficient as well as to coupling in DCs. Right after, we present an heuristic formulation of the dissipation in the context of propagation of quantum states in IPDs and apply it to the DPA. On the other hand, in § P3 and § P4 we study the propagation of quantum states of light in longitudinally inhomogeneous waveguides by means of the path integral formulation in the OFS representation. In particular, in § P3 we start presenting a quantization approach for this kind of media as well as the path integral formalism associated. By means of propagation of a coherent state we find the problem of virtual squeezing associated with propagation through media with change in the refractive index. We review the literature concerning this problem, find a physical argument to withdraw virtual squeezing and propose Infeld-Plebanski transformations which neglect this effect. Finally we find that the net effect of propagation is a quantum Gouy's phase and show the specific example of propagation of a Bessel-Gauss quantum state in a parametric family of longitudinally inhomogeneous media. Likewise, in § P5, we study the same problem by a different point of view. In this case we derive the classical Momentum and ask ourselves which frame of reference makes virtual squeezing dissapear. By means of generalized canonical transformations we find this frame and realize this new Momentum is a Lewis-Ermakov invariant. Next, we quantize this Momentum and derive the propagator. Finally we analyze the effect a cosine-type inhomogeneous medium produces on quantum gaussian states of light.

USC
UNIVERSIDADE
DE SANTIAGO
DE COMPOSTELA

P2. SPATIAL PROPAGATION OF QUANTUM LIGHT IN NONLINEAR WAVEGUIDING DEVICES: THEORY & APPLICATIONS

JOURNAL OF NONLINEAR OPTICAL PHYSICS & MATERIALS
VOL. 21 NO. 3 PAGES 1250032
doi: 10.1142/S0218863512500324

PUBLISHED 5 AUGUST 2012

BY JESÚS LIÑARES, DAVID BARRAL & MARÍA C. NISTAL

UNIVERSIDADE DE SANTIAGO DE COMPOSTELA

Abstract: *We present the main theoretical results on spatial propagation of quantum light in nonlinear waveguiding devices together with a few applications. We show that the quantization of the classical Momentum provides a consistent quantum mechanical formulation of both the linear and the nonlinear quantum light propagation in waveguiding devices. The Momentum operator allows us to derive the correct spatial Heisenberg's equations for the forward and backward absorption and emission operators and consequently to analyze the spatial propagation in the multimode optical-field strength space. For that purpose we use the Feynman's path integral method in order to derive the quantum spatial optical propagators of different nonlinear waveguiding devices and accordingly to calculate the spatial propagation of the optical-field strength probability amplitude of quantum states in these nonlinear devices. Likewise, we present a preliminary and heuristic formulation of quantum dissipation in order to take into account the losses under spatial quantum propagation in lossy nonlinear waveguiding devices. It must be stressed that these optical-field strength probabilities have the advantage of being measured by homodyne techniques and therefore their theoretical analysis is of a remarkable interest in the optical characterization of quantum states obtained under linear and nonlinear propagation in waveguiding devices.*

P2.1. Introduction

Fundamental studies on both a phenomenological quantization and the quantum propagation problem in free space and in dielectric homogeneous media without losses appeared about twenty years ago. In Ref. [Luks and Perinová, 2002] is presented a wide and detailed review about spatial quantum propagation in dielectric media and references can be found therein. All these studies have provided the background of the quantum theory of light propagation, that is, they have proven that the quantum operator which must be used, in order to describe quantum spatial propagation along an arbitrary direction z, is the Momentum operator which, in turn, must be calculated by using temporal modes and integrating the energy - momentum tensor element T^{zz} over the hyperplane $dxdycdt$. It is important to remember that the calculation of the momentum flux along with its integration on time can be physically interpreted as follows: the variation in a volume V of the total momentum have to be equal to the momentum flux through a surface enclosing the referred volume during a time T, which is fully consistent with light propagation and with its detection on a surface during a certain time. Thus the time T must be greater than the cycle period but much less than the coherence time because of both experimental (photodetection) and theoretical reasons [Loudon, 1982]. In many studies of spatial propagation the connection space-time was established by using an effective interaction time $t = z/v$, with z the the length of the medium. However if we have several modes propagating at different speeds (dispersion) then the standard $\hat{H}$ operator is not valid because we would need several temporal variables, which is a contradiction by itself. We must underline that the same argument can be used to justify that standard Hamiltonian formulation is unable to describe counterpropagation because a negative time would be required. Likewise, $\hat{H}$ operator is not valid either for z-variant media because the Hamiltonian formulation performs a spatial integration, in particular, in a volume V, and therefore the z-inhomogeneities are eliminated by a spatial averaging. Accordingly, the $\hat{H}$ operator is not valid either for modal phase mismatching, which, to a certain extent, can be regarded as a z-inhomogeneity. Only in the vacuum the spatial propagation can be exchanged for the temporal evolution, or even it can be made in a non dispersive homogeneous medium, although in this case the physical constants of the Hamiltonian would be wrong.

In waveguiding devices, and in particular in integrated optics (or photonics), the first works on quantum propagation in waveguiding devices, such as a linear coupler, were made by Jansky et.al.[Jansky et al., 1988], although a detailed and justified use of the Momentum operator in problems of copropagation and/or counterpropagation of coupled modes in integrated photonics was started with the seminal works of Toren et.al [Toren and Ben-Aryeh, 1994] (linear couplers) and Peřina[Perina, 1995] (lin-

ear and nonlinear couplers) followed by other works such as those ones of Refs. [Korolkova and Perina, 1997, Perina and Perina Jr, 1995a,b, Perina Jr and Perina, 2000, Perinová et al., 2006]. Likewise, both the development and the particular application of the phenomenological quantization to integrated photonic waveguides have been recently presented, that is, the Momentum operator $\hat{M}$ has been derived *ab initio* for both copropagation and counterpropagation of coupled modes in integrated photonic devices [Liñares and Nistal, 2003, Liñares et al., 2008]. It must be stressed that such a quantization approach was based on both the vector orthonormalization property of forward and backward guided vector modes and the complex vector structure of the guided modes. In fact, the vector structure of guided modes $\mathbf{E}_\nu$ is incompatible with a Hamiltonian operator, for instance, the longitudinal components of guided modes give rise to incorrect expressions for the operator $\hat{H}$. In this regard, we have proven that the quantization results of spatial propagation in integrated guides are only consistent when the imaginary longitudinal components of the guided modes are taken into account [Liñares and Nistal, 2003]. We must also indicate that only vector plane modes have no longitudinal components but they would provide wrong nonlinear coupling coefficients if we used a Hamiltonian formulation. Likewise, the modal norm of guided modes is incompatible with a Hamiltonian formulation because normalization must be made in a spatio-temporal volume, that is, on the cross-section of the guides during a time of detection T.

In this work we present the main theoretical results on spatial propagation of quantum light in nonlinear waveguiding devices on the optical-field strength space, including also a preliminary study of dissipation. As commented above the quantization of the classical Momentum provides a consistent quantum mechanical formulation of both the linear and nonlinear quantum light propagation in waveguiding devices, that is, a Momentum operator which allows us to derive the correct spatial Heisenberg's equations for the forward and backward absorption and emission operators, $\hat{a}(z)$ and $\hat{a}^\dagger(z)$, and accordingly to analyze the spatial quantum propagation on a multimode optical-field strength space. Therefore the plan of this work is as follows: in section 2, we present the main results on quantization in nonlinear waveguiding devices, in order to obtain the correct Momentum operators. In section 3, we use the Feynman's path integral formulation to derive the quantum spatial optical propagators of different nonlinear waveguiding devices and accordingly to calculate the spatial propagation of the optical-field strength probability amplitude of quantum states in these nonlinear devices. It must be stressed that these optical-field strength probabilities have the advantage of being measured by homodyne techniques so that their theoretical analysis can become of a remarkable interest in the optical characterization of quantum states obtained under linear and/or nonlinear propagation in waveguiding devices. We must

also indicate that our study of the propagation of quantum light on the optical-field strength space can be considered as a complementary study to those ones made with other quantum representations of quantum states. In section 4, we present a preliminary and heuristic formulation of quantum dissipation in order to analyze the effect of the losses on quantum states under saptial propagation in lossy nonlinear waveguiding devices. It is based on the use of both the damped classical paths on the optical-field strength space and a fluctuating force due to the environment coupled to the waveguiding device. Finally, in section 5, a summary is presented.

P2.2. Momentum operator and Heisenberg equations

In this section we derive the main results of quantization in waveguiding nonlinear devices. We start with a brief classical analysis of optical modes in order to both justify the orthonormalization condition and present an important relationship between energy flow and energy stored at the cross-section of a waveguide. Next, by taking into account these classical results we obtain the expression of the Momentum operator by using a phenomenological quantization approach. Finally, we apply the results to nonlinear waveguiding devices, that is, we derive the corresponding Momentum operators and Heisenberg's equations, which present some interesting differences with respect to both the classical coupled-modes equations and nonlinear optical problems described by the standard Hamiltonian operator.

Classical analysis of guided vector modes

Let us consider monochromatic guided vector modes, that is, with only one temporal mode of frequency ω in an optical waveguide characterized by a refractive index profile $n^2(x,y)$. Theses modes are represented by a vector field solution with the following complex amplitude:

$$\mathbf{E}_\nu(x,y,z,t) = \mathcal{E}_\nu(x,y,z)\, e^{-i\omega t} = \mathbf{E}_\nu(x,y)\, e^{\{i[\beta_\nu z - \omega t]\}}, \qquad \text{(P2.1)}$$

$$\mathbf{H}_\nu(x,y,z,t) = \mathcal{H}_\nu(x,y,z)\, e^{-i\omega t} = \mathbf{H}_\nu(x,y)\, e^{\{i[\beta_\nu z - \omega t]\}}, \qquad \text{(P2.2)}$$

where β_ν is the propagation constant of the ν-mode, with $\nu \in \mathbb{Z}^\star$, and $\{\mathbf{E}_\nu(x,y), \mathbf{H}_\nu(x,y)\}$ are the complex vector amplitude of the guided modes. We must indicate that we need two subindices $\rho\sigma$ for each mode, in fact the propagation constant β would be a function of ρ and σ, however for the sake of expositional convenience, we use the contracted notation $\nu \equiv \rho\sigma$. By taking into account the expressions (P2.1, P2.2) it is easy to derive from the Maxwell's equations the following equations for the complex amp-

litudes of guided vector modes [Kogelnik, 1988]:

$$\boldsymbol{\nabla}_t \wedge \mathbf{E}_\nu + i\beta_\nu \mathbf{u}_z \wedge \mathbf{E}_\nu = i\omega\mu_o \mathbf{H}_\nu, \tag{P2.3}$$

$$\boldsymbol{\nabla}_t \wedge \mathbf{H}_\nu + i\beta_\nu \mathbf{u}_z \wedge \mathbf{H}_\nu = -i\omega\epsilon \mathbf{E}_\nu, \tag{P2.4}$$

with $\boldsymbol{\nabla}_t=(\partial_x, \partial_y, 0)$ and $\mathbf{u}_z$ is a unit vector pointing in the z-direction, that is, perpendicular to a cross-section of the optical waveguide. The amplitudes of the guided modes can be separated into the transverse field components $\{\mathbf{E}_{t\nu}(x,y), \mathbf{H}_{t\nu}(x,y)\}$ and the longitudinal field components $\{\mathbf{E}_{z\nu}(x,y), \mathbf{H}_{z\nu}(x,y)\}$, in such a way that from Eqs. (P2.3, P2.4), and by using standard procedures based on the Lorentz reciprocity theorem for optical waveguides [Kogelnik, 1988], it is found that the norm of a guided ν-mode, on a cross-section z of the waveguide, is given by the expression [Kogelnik, 1988, Liñares and Nistal, 2003, Liñares et al., 2008]:

$$\|\mathbf{E}_\nu\| \equiv \|\mathbf{H}_\nu\| = \Big\{\frac{1}{2}\,\mathrm{sgn}(\nu)\int\{\mathbf{E}_{t\nu} \wedge \mathbf{H}^\star_{t\nu}\}\mathbf{u}_z\, dxdy\Big\}^{1/2}, \tag{P2.5}$$

where the function $\mathrm{sgn}(\nu)$ is defined to be +1 if $\nu > 0$, and -1 if $\nu < 0$. As shown further along, this function will justify one of the more important results used in quantum light propagation problems, i.e., the positivity of the Momentum [Toren and Ben-Aryeh, 1994]. Next, by taking into account Eq. (P2.5) and by denoting the transverse components of a normalized guided vector mode as $\mathbf{e}_{t\nu}, \mathbf{h}_{t\nu}$, the following quasi-complete orthonormalization condition on a cross-section of an optical guide is obtained:

$$\frac{1}{2}\,\mathrm{sgn}(\nu)\int\{\mathbf{e}_{t\nu} \wedge \mathbf{h}^\star_{t\nu'}\}\mathbf{u}_\eta\, d\xi d\gamma = \delta_{|\nu|,|\nu'|}, \tag{P2.6}$$

where $\delta_{|\nu|,|\nu'|}$ is the Kronecker delta. Note that the orthonormalization condition is determined only by the transverse field components of the guided modes and it is a quasi-complete orthonormalization condition since for the counterpropagating case $\nu > 0, \nu' < 0$, Eq. (P2.6) is not equal to zero. However, in spite of that, it is a very useful relationship for obtaining the quantum Momentum operator. On the other hand, by taking into account the transverse and longitudinal modal electrical and magnetic energies stored per unite guide length under temporal averaging, that is, $2W^e_{d\nu}=\iint \epsilon\, \mathbf{E}_{d\nu}\mathbf{E}^\star_{d\nu}\, dxdy$ and $2W^m_{d\nu}=\iint \mu_o\, \mathbf{H}_{d\nu}\mathbf{H}^\star_{d\nu}\, dxdy$, with $d = t, z$, and by using again Eqs. (P2.3, P2.4) we obtain the following remarkable expression[Liñares et al., 2008]:

$$2\beta_\nu P_\nu = 2\mathrm{sgn}(\nu)\beta_\nu\|\mathbf{E}_\nu\|^2 \equiv 2\mathrm{sgn}(\nu)\|\mathbf{H}_\nu\|^2\,\beta_\nu = \omega(W_{t\nu} - W_{z\nu}), \tag{P2.7}$$

where P_ν is the average modal power or energy flow and $W_{t\nu} = W^e_{t\nu}+W^m_{t\nu}$ and $W_{z\nu} = W^e_{z\nu} + W^m_{z\nu}$ are the total transverse and longitudinal energies, respectively.

A phenomenological quantization

For the sake of simplicity we present a phenomenological canonical quantization of a waveguiding device. We follow, for our purposes, a quantization procedure analogous to that one used for the Hamiltonian quantization. We start from the ν-mode and its classical Momentum $M_{o\nu}$ which is defined as the energy tensor element T^{33} (without using normalized modes) integrated over the hypercross-section $dxdydt$ of the guide [Jackson, 1975, Liñares and Nistal, 2009], that is,

$$M_{o\nu} = \frac{1}{2}\int [(\epsilon_o n^2 \mathbf{E}_t \mathbf{E}_t - \epsilon_o n^2 \mathbf{E}_z \mathbf{E}_z) + (\mu_o \mathbf{H}_t \mathbf{H}_t - \mu_o \mathbf{H}_z \mathbf{H}_z)]dxdydt. \quad \text{(P2.8)}$$

Therefore, by making the temporal integration in the interval $[0, T]$, and by taking into account Eq. (P2.7), the following notable expression is obtained

$$M_{o\nu} = \text{sgn}(\nu)\frac{\beta_\nu}{\omega}\|\mathbf{E}_\nu\|^2 T, \quad \text{(P2.9)}$$

where $\|\mathbf{E}_\nu\|^2$ is given by Eq. (P2.5). The above expression is the starting point for obtaining both a simple canonical quantization of the Momentum and the vector modal field operators. To that end, we rewrite the vector mode fields as follows:

$$\mathbf{E}_\nu(x,y,z,t) = A_{o\nu}(z)\mathbf{E}_{o\nu}(x,y,t) = A_{o\nu}(z)\mathbf{E}_{o\nu}(x,y)e^{-i\omega t}, \quad \text{(P2.10)}$$
$$\mathbf{H}_\nu(x,y,z,t) = A_{o\nu}(z)\mathbf{H}_{o\nu}(x,y,t) = A_{o\nu}(z)\mathbf{H}_{o\nu}(x,y)e^{-i\omega t}, \quad \text{(P2.11)}$$

where $A_{o\nu}$ is a complex modal amplitude. Now, by inserting these expressions into Eq. (P2.9), and by taking into account the definition of the modal normalization, we obtain:

$$M_{o\nu} = \text{sgn}(\nu)\frac{\beta_\nu}{\omega} T \|\mathbf{E}_{o\nu}\|^2 A_{o\nu}(z)\, A^\star_{o\nu}(z). \quad \text{(P2.12)}$$

Now, let us search for a canonical variables to obtain an expression of the classical Momentum that can be identified with a well-known mechanical problem, that is, an harmonic oscillator, but now the role of time will be played by the longitudinal variable z, and the role of frequency will be played by the propagation constant β_ν. Therefore, let us consider the following transformations:

$$A_{o\nu}(\eta) = \frac{1}{\|\mathbf{E}_{o\nu}\|\sqrt{2T\text{sgn}(\nu)\,\beta_\nu/\omega}}(\beta_\nu q_\nu + ip_\nu), \quad \text{(P2.13)}$$
$$A^\star_{o\nu}(\eta) = \frac{1}{\|\mathbf{E}_{o\nu}\|\sqrt{2T\text{sgn}(\nu)\,\beta_\nu/\omega}}(\beta_\nu q_\nu - ip_\nu), \quad \text{(P2.14)}$$

accordingly, the classical Momentum is equivalent to the equation of a (spatial) harmonic oscillator, that is, from Eqs. (P2.12 -P2.14), we obtain

$$M_{o\nu} = \frac{1}{2}(p_\nu^2 + \beta_\nu^2 q_\nu^2). \quad \text{(P2.15)}$$

It is worth noting that this result can also be easily obtained by starting from the modal wave equation for vector modes propagating along the z-direction, that is, $\partial^2 \mathbf{E}_\nu/\partial z^2 + \beta_\nu^2 \mathbf{E}_\nu = 0$. This equation clearly suggests a spatial harmonic oscillator, that is, with z substituting the time t and β_ν substituting the frequency ω of a temporal harmonic oscillator.

Next, by using both the principle of quantization in the classical Momentum operator given by Eq. (P2.15) and the following change of operators

$$\hat{a}_\nu = \frac{1}{\sqrt{2\hbar\,\mathrm{sgn}(\nu)\,\beta_\nu}}\,(\beta_\nu \hat{q}_\nu + i\hat{p}_\nu), \tag{P2.16}$$

$$\hat{a}_\nu^\dagger = \frac{1}{\sqrt{2\hbar\,\mathrm{sgn}(\nu)\,\beta_\nu}}\,(\beta_\nu \hat{q}_\nu - i\hat{p}_\nu), \tag{P2.17}$$

the Momentum operator for each mode ν and therefore the total Momentum for all the modes is obtained, that is,

$$\hat{M}_o = \sum_\nu \hat{M}_{o\nu} = \frac{1}{2}\sum_\nu \hbar\,\mathrm{sgn}(\nu)\beta_\nu\,(\hat{a}_\nu^\dagger \hat{a}_\nu + \hat{a}_\nu \hat{a}_\nu^\dagger). \tag{P2.18}$$

Now, the complex amplitude $A_{o\nu}$ can be quantized as $\hat{A}_{o\nu}$ and accordingly the vector mode field can also be quantized, that is, from Eqs. (P2.13, P2.16), we obtain:

$$\hat{\mathbf{e}}_\nu^{(+)}(x,y,z,t) = \hat{A}_{o\nu}(z)\,\mathbf{e}_{o\nu}(x,y)e^{-i\omega t} = (\hbar\omega)^{1/2}\frac{\mathbf{E}_\nu(x,y)e^{-i\omega t}}{T^{1/2}\|\mathbf{E}_\nu\|}\hat{a}_\nu(z), \tag{P2.19}$$

$$\hat{\mathbf{e}}_\nu^{(-)}(x,y,z,t) = \hat{A}_{o\rho\nu}^\dagger(z)\,\mathbf{e}_{o\nu}(x,y)e^{i\omega t} = (\hbar\omega)^{1/2}\frac{\mathbf{E}_\nu(x,y)e^{i\omega t}}{T^{1/2}\|\mathbf{E}_\nu\|}\hat{a}_\nu^\dagger(z), \tag{P2.20}$$

$$\hat{\mathbf{e}}_\nu(x,y,z,t) = \frac{1}{2}\{\hat{\mathbf{e}}_\nu^{(+)}(x,y,z,t) + \hat{\mathbf{e}}_\nu^{(-)}(x,y,z,t)\}. \tag{P2.21}$$

Note that quantization requires a normalized mode $\mathbf{e}_{o\nu}(x,y)$ [Liñares and Nistal, 2003]. Alternatively, we could have started from the the standard optical mode field operators but by using both temporal modes and taking into account the modal norm given by Eq. (P2.5). That is, by using Eqs. (P2.19 - P2.21) into Eq. (P2.8) we would obtain the same results for the Momentum operator [Liñares et al., 2008]. Finally, quantum relationships and commutation rules for forward and backward modes can be derived [Liñares and Nistal, 2003] by using the reversal-time symmetry on the Maxwell's equations, that is,

$$\hat{a}_{\nu<0} = \hat{a}_{\nu>0}^\dagger \qquad \hat{a}_{\nu<0}^\dagger = \hat{a}_{\nu>0}, \tag{P2.22}$$

$$[\hat{a}_\nu, \hat{a}_{\nu'}^\dagger] = \mathrm{sgn}(\nu)\,\delta_{\nu\nu'}. \tag{P2.23}$$

This last calculation ends the phenomenological quantization without modal coupling, which is the basis for the analysis of spatial quantum propagation of linear and nonlinear modal coupling.

Quantization of waveguiding coupling devices

We analyze the modal coupling by introducing a dielectric perturbation of the original refractive index $n^2(x,y)$. This perturbation is introduced, as usual, by a material polarization which is represented by the operator $\hat{\mathbf{P}} = \Delta\hat{\epsilon}\,\hat{\mathbf{e}}$ describing formally a perturbation of the electrical permitivity that in turn can present isotropy, anisotropy, non-linearity and so on. It is assumed that the polarization operator can be expressed as a function of the non perturbed optical mode field operators $\hat{\mathbf{e}}_\nu$ and therefore as a function of the operators $(\hat{a}_\nu, \hat{a}_\nu^\dagger)$ in the waveguide, in a manner similar to the mode expansion in the classical case [Kogelnik, 1988]. In short, there is an interaction term $\hat{\mathbf{P}}(\hat{\mathbf{e}})\,\hat{\mathbf{e}}$ and consequently a coupling among the guided vector modes described by the following perturbated Momentum operator:

$$\hat{M} = \hat{M}_o + \frac{1}{p+1}\iiint_0^T \hat{\mathbf{P}}\,\hat{\mathbf{e}}\;dxdydt = \hat{M}_o + \frac{1}{p+1}\iiint_0^T \hat{P}_i\,\hat{e}_i\;dxdydt, \quad \text{(P2.24)}$$

where $p \geqslant 1$. The factor $(p+1)^{-1}$ accompanying the interaction term can be justified by the standard Lagrangian theory of the Maxwell equations in bulk media [Hillery and Modlinow, 1984]. Moreover, each component $i\,(= x,y,z)$ of the polarization operator can be written, in a formal way, as follows:

$$\hat{P}_i = \{\epsilon_o\,\chi_{ijklm\ldots}(z)\hat{e}_k\,\hat{e}_l\,\hat{e}_m\ldots\}\,\hat{e}_j, \qquad k,l,m,\ldots,j = (x,y,z), \quad \text{(P2.25)}$$

where we assume that the nonlinear susceptibility can depend on z. It is usual to consider the linear and a nonlinear polarization perturbation of the waveguiding device separately, that is, $\hat{\mathbf{P}} = \hat{\mathbf{P}}_L + \hat{\mathbf{P}}_{NL}$, therefore de total Momentum is written as:

$$\hat{M} = \hat{M}_o + \iiint_0^T \frac{1}{2}\,\hat{\mathbf{P}}_L\,\hat{\mathbf{e}}\;dxdydt + \frac{1}{p+1}\,\hat{\mathbf{P}}_{NL}\,\hat{\mathbf{e}}\;dxdydt, \quad \text{(P2.26)}$$

where now $p \geqslant 2$ is the order of the non-linearity. For the sake of expositional convenience we analyze separately the linear and nonlinear interactions.

Linear Waveguiding Coupling

We start by quantizating the linear polarization corresponding to an isotropic and inhomogeneous perturbation, that is, $\hat{\mathbf{P}}_L = \Delta\epsilon\,\hat{\mathbf{e}} = \Delta\epsilon(x,y,z)\,(\hat{\mathbf{e}}_t + \hat{\mathbf{e}}_z)$. Note that the Hamiltonian theory will fail for a z-inhomogeneity because of the integration in a volume V and therefore on z. The corresponding contribution to the Momentum operator will be

$$\hat{M}_L = \frac{1}{2}\iiint_0^T \Delta\epsilon\,\hat{\mathbf{e}}\,\hat{\mathbf{e}}\;dxdycdt = \frac{1}{2}\iiint_0^T \Delta\epsilon\sum_\nu \hat{\mathbf{e}}_\nu \sum_{\nu'} \hat{\mathbf{e}}_{\nu'}\;dxdydt. \quad \text{(P2.27)}$$

It is worth paying attention to the particular way in which longitudinal components are handled under a linear perturbation with longitudinal component $\mathbf{P}_z = \Delta\epsilon\,\mathbf{E}_z$. It is wellknown that only the transverse components fulfil the orthogonality relationship and therefore the mode expansion can only be made by means of these components [Kogelnik, 1988]. However, if the perturbation is not very large the longitudinal component can also be obtained by mode expansion [Kogelnik, 1988, Liñares et al., 2008], that is, in a good approximation we can use:

$$\hat{\mathbf{P}}_L \approx \frac{1}{2}\sum_\nu [\Delta\epsilon\,\hat{\mathbf{e}}_\nu^{(+)}(x,y,t) + \Delta\epsilon^\star\,\hat{\mathbf{e}}_\nu^{(-)}(x,y,t)] = \sum_\nu \Delta\epsilon_r\,\hat{\mathbf{e}}_\nu(x,y,t), \tag{P2.28}$$

where, for the moment and for the sake of simplicity, we have assumed that the electrical permitivity is a real function $\Delta\epsilon_r$. Now, by inserting both the transverse and the longitudinal components of the field operators given by Eqs. (P2.19 -P2.21) into Eq. (P2.27), performing temporal integration and taking into account that the absorption and emission operators commute for different modes, we obtain several non-crossing terms ($\nu = \nu'$) and crossing terms ($\nu \neq \nu'$) different from zero, in such a way that the linear operator Momentum of coupled modes takes the form

$$\hat{M}_L = \frac{1}{2}\sum_\nu \hbar\,\mathrm{sgn}(\nu)\kappa_{\nu\nu}\,(\hat{a}_\nu^\dagger\hat{a}_\nu + \hat{a}_\nu\hat{a}_\nu^\dagger) + \sum_{\nu<\nu'}\{\hbar\,\kappa_{\nu\nu'}\,\hat{a}_\nu\hat{a}_{\nu'}^\dagger + \mathrm{h.c.}\}. \tag{P2.29}$$

The self-coupling coefficient $\kappa_{\nu\nu}$ and the cross-coupling coefficients $\kappa_{\nu\nu'}$ are given by the compact expression:

$$\kappa_{\nu\nu'} = \frac{\omega\iint\Delta\epsilon_r\,(\mathbf{E}_{t\nu}\mathbf{E}_{t\nu'}^\star + \mathbf{E}_{z\nu}\mathbf{E}_{z\nu'}^\star)dxdy}{4\,\|\mathbf{E}_\nu\|\,\|\mathbf{E}_{\nu'}\|}. \tag{P2.30}$$

Likewise, by denoting $\bar{\beta}_\nu = \beta_\nu + \kappa_{\nu\nu}$, the sum of free and linear coupling Momentums $\hat{M}_o$ and $\hat{M}_L$ is written as follows:

$$\hat{M}_{oL} = \frac{1}{2}\sum_\nu \hbar\,\mathrm{sgn}(\nu)\bar{\beta}_\nu(\hat{a}_\nu^\dagger\hat{a}_\nu + \hat{a}_\nu\hat{a}_\nu^\dagger) + \sum_{\nu<\nu'}\{\hbar\,\kappa_{\nu,\nu'}\,\hat{a}_\nu\hat{a}_{\nu'}^\dagger + \mathrm{h.c.}\}. \tag{P2.31}$$

Finally, it is easy to obtain, from both the Eq. (P2.31) and the commutation rules (P2.23), the Heisenberg's equations for the forward and backward absorption (annihilation) operators $\hat{a}_{\nu>0}$ and $\hat{a}_{\nu<0}$, that is:

$$-i\hbar\partial_z\hat{a}_\nu = [\hat{a}_\nu, M_{oL}] = \hbar\bar{\beta}_\nu\hat{a}_\nu + \mathrm{sgn}(\nu')\sum_{\nu'\neq\nu}\hbar\,\kappa_{\nu\nu'}\,\hat{a}_{\nu'}. \tag{P2.32}$$

Note that the function $\mathrm{sgn}(\nu')$ appears in a natural way by starting from the Momentum operator, commutation rules and Heisenberg's equations.

Moreover this result contains an important physical content: the function $\mathrm{sgn}(\nu)$ ensures the positivity of Momentum, which was assumed in other approaches [Toren and Ben-Aryeh, 1994] but now it is a natural consequence of the modal norms. In short, this linear Momentum operator can describe quantum linear modal coupling in waveguiding devices such as directional couplers, integrated gratings, integrated junctions and so on. Now we extend the present analysis to a nonlinear perturbation.

Nonlinear waveguiding coupling

For the sake of expositional convenience we consider non-linearities of second, third and fifth order in a directional coupler, although results can be easily extended to non-linearities of an arbitrary order. Let us consider N coupled waveguides with operators $\hat{a}_\nu(\omega)$, $\hat{b}_\nu(2\omega)$, $\nu = 1, ..., N$. Then the total Momentum operator for copropagation can be written as follows:

$$\hat{M} = \hat{M}_a + \hat{M}_b + \frac{1}{3}\iiint_0^T \hat{\mathbf{P}}^{(2)}_{NL}(x, y, z)\,\hat{\mathbf{e}}\; dxdydcdt, \tag{P2.33}$$

where $\hat{M}_a$ and $\hat{M}_b$ are the linear Momentum operators for modes $\hat{a}_\nu(\omega)$ and $\hat{b}_\nu(2\omega)$, respectively, that is,

$$\hat{M}_a = \frac{1}{2}\sum_{\nu=1}^{N} \hbar\,\mathrm{sgn}_\nu \bar{\beta}_{a\nu}(z)\,(\hat{a}^\dagger_\nu \hat{a}_\nu + \hat{a}_\nu \hat{a}^\dagger_\nu) + \sum_{\nu<\nu'} \{\hbar\,\kappa_{\nu\nu'}(z)\;\hat{a}_\nu \hat{a}^\dagger_{\nu'} + h.c.\}, \tag{P2.34}$$

$$\hat{M}_b = \frac{1}{2}\sum_{\nu} \hbar\,\mathrm{sgn}_\nu \bar{\beta}_{b\nu}(z)\,(\hat{b}^\dagger_\nu \hat{b}_\nu + \hat{b}_\nu \hat{b}^\dagger_\nu) + \sum_{\nu<\nu'} \{\hbar\,\kappa_{\nu\nu'}(z)\;\hat{b}_\nu(z)\hat{b}^\dagger_{\nu'} + h.c.\}, \tag{P2.35}$$

and the third term in Eq. (P6.4) is the nonlinear modal coupling term, which can be calculated by performing the temporal integration, that is,

$$\hat{M}^{(2)}_{NL} = \sum_{\nu}\{\hbar\,\kappa^{(2)}_{\nu\nu}(z)\;\hat{b}^\dagger_\nu \hat{a}^2_\nu + h.c.\} + \sum_{\nu}\{\hbar\,\kappa^{(2)}_{\nu,\nu\pm1}(z)\;\hat{b}^\dagger_\nu \hat{a}^2_{\nu\pm1} + h.c.\}. \tag{P2.36}$$

We have only considered the values ($\nu' = \nu + 1$), that is, only neighbour waveguides undergo modal coupling. Note that there is no linear coupling between modes of different frequency. The expression of the coupling coefficients depends on the nonlinear coupling conditions, however by assuming that only one component of the field is relevant, for instance de y-component of a quasi-TE mode, then explicit expressions for the coupling coefficients can be obtained. For instance, the coupling coefficients $\kappa^{(2)}_{\nu\nu}(z)$ in the above equation (P2.36) are given by:

$$\kappa^{(2)}_{\nu\nu}(z) = \frac{2^{1/2}\omega^{3/2}\iint \epsilon_o \chi_{yyy}(z)\,\mathbf{E}^\star_{yb\nu}\,\mathbf{E}^2_{ya\nu}\,dxdy}{8\,\|\mathbf{E}_{b\nu}\|\;\|\mathbf{E}_{a\nu}\|^2}. \tag{P2.37}$$

Similar expressions can be obtained for the other coupling coefficients. On the other hand, it can be checked that factors equal to 2 are found in the Heisenberg's equations, but they do not appear in classical equations [Perina, 1995] [Liñares et al., 2008]. Likewise counterpropagation is included in the above equations in a natural way. Moreover, with notation $\kappa(z)$ we emphasize that longitudinal inhomogeneities can be present in the device, where mismatching is included. Likewise, in a good approximation, a z-dependence can be also considered for the propagation constants β (tapered waveguides), for instance under an adiabatic approximation [Liñares and Nistal, 1996]. We must stress that starting from Momentum operator (P6.4) together with Eqs. (P2.34 -P2.36) any of the Heisenberg's equations obtained in the literature for nonlinear couplers with $p = 2$ can be easily derived and therefore justified.

Now, let us consider third and fifth non-linearities in a directional coupler with N coupled guides. In this case, we assume that the contribution of the harmonics is negligible, that there is mismatching in the coupler and moreover that there is only coupling between neighbour guides. For third-order nonlinear coupling we obtain:

$$\hat{M} = \sum_{\nu} \hbar\, \mathrm{sgn}_{\nu} \bar{\beta}_{a\nu}(z)\, \hat{a}_{\nu}^{\dagger}\hat{a}_{\nu} + \sum_{\nu<\nu'} \{\hbar\, \kappa_{\nu\nu'}(z)\ \hat{a}_{\nu}\hat{a}_{\nu'}^{\dagger} + \mathrm{h.c.}\} + M_{\mathrm{NL}}^{(3)}, \quad \text{(P2.38)}$$

where

$$M_{\mathrm{NL}}^{(3)} = \sum_{\nu} \{\hbar\, \kappa_{\nu}^{(3)}(z)\ \hat{a}_{\nu}^{\dagger 2}\hat{a}_{\nu}^{2} + \mathrm{h.c.}\} + \sum_{\nu} \{\hbar\, \kappa_{\nu}^{\prime(3)}(z)\ \hat{a}_{\nu}^{\dagger}\hat{a}_{\nu}\hat{a}_{\nu+1}^{\dagger}\hat{a}_{\nu+1} + \mathrm{h.c.}\} +$$
$$\sum_{\nu} \{\hbar\, \kappa_{\nu}^{\prime\prime(3)}(z)\ \hat{a}_{\nu}^{\dagger 2}\hat{a}_{\nu+1}^{2} + \mathrm{h.c.}\} + \sum_{\nu} \{\hbar\, \kappa_{\nu}^{\prime\prime\prime(3)}(z)\ \hat{a}_{\nu+1}^{\dagger}\hat{a}_{\nu}^{\dagger}\hat{a}_{\nu}^{2} + \mathrm{h.c.}\}. \quad \text{(P2.39)}$$

We must stress that new terms appear with respect to a Hamiltonian formulation, in particular terms presenting mismatching, that is, the third and fourth sums on the right hand side of above equation. Now, for fifth-order nonlinear coupling, under the same conditions as the third-order case, we obtain:

$$M_{\mathrm{NL}}^{(5)} = \sum_{\nu} \{\hbar\, \kappa_{\nu}^{\prime(5)}(z)\ \hat{a}_{\nu}^{\dagger 3}\hat{a}_{\nu}^{3} + \mathrm{h.c.}\} + \sum_{\nu} \{\hbar\, \kappa_{\nu}^{\prime\prime(5)}(z)\ \hat{a}_{\nu}^{\dagger 3}\hat{a}_{\nu+1}^{3} + \mathrm{h.c.}\} +$$
$$\sum_{\nu} \{\hbar\, \kappa_{\nu}^{\prime\prime\prime(5)}(z)\ \hat{a}_{\nu}^{\dagger 3}\hat{a}_{\nu}^{2}\hat{a}_{\nu+1} + \mathrm{h.c.}\} + \ldots \quad \text{(P2.40)}$$

Again, additional terms appear which are not present in a Hamiltonian approach, in particular, the second and third sums on the right hand side of above equation. Likewise, as in the two-order nonlinear coupling case, additional factors appear as a correction to the classical coupling coefficients in the Heisenberg's Equations. Once again, many heuristic nonlinear quantum Momentum operators used in the literature are justified and even

improved. In short, exact Heisenberg's equations for nonlinear copropagation and counterpropagation can be obtained (commutation rule for backward and forward modes must be used), and moreover, and much more important, the Momentum formulation allows to achieve a Schrödinger-type equation for studying quantum spatial propagation on the optical-field strength space, as shown in next section.

P2.3. Path integral formulation

Up to now we have described how to derive the Momentum operator, and therefore the Heisenberg's equations, for nonlinear waveguiding coupling. Now, we are interested in proposing an useful approach to describe the spatial propagation of quantum states on the optical-field strength (OFS) space [Vogel, 1990]. In particular, we choose the Feynman approach, that is, we present a path integral formulation on the OFS space. This formulation is suitable to analyze spatial quantum propagation and it can be regarded as complementary to others such as those ones based on number states, coherent states, and so on. First of all we have to obtain an optical Lagrangian in the OFS space starting from the Momentum operator [Liñares et al., 2011b]. Next, the path integrals can be performed, however, we make directly use of the complex paths followed by the emission and absorption operators (semiclassical approximation of path integrals), which simplifies notably the calculations and in some cases gives exact solutions. We must also stress that the quantum states represented in the OFS space can be detected by the well-known homodyne and heterodyne techniques, that is, their optical-field strength probability distributions can be measured.

Path integrals in the OFS space

Let us start by considering the operators $\hat{A}_{o\nu}$, $\hat{A}^{\dagger}_{o\nu}$ obtained by applying the principle of correspondence to Eqs. (P2.13, P2.14). Accordingly, we obtain the physical expression of the "position" variable, that is:

$$\hat{q}_\nu = \sqrt{T\|\mathbf{E}_{o\nu}\|^2 \operatorname{sgn}_{\nu\sigma}/(2\beta_\nu\omega)}\,(\hat{A}_{o\nu}+\hat{A}^{\dagger}_{o\nu}) = \sqrt{T\|\mathbf{E}_{o\nu}\|^2 \operatorname{sgn}_{\nu}/(\beta_\nu\omega)}\;\hat{\mathcal{E}}_\nu, \tag{P2.41}$$

where $\hat{\mathcal{E}}_\nu=(\hat{A}_{o\nu}+\hat{A}^{\dagger}_{o\nu})/2^{1/2}$ is the optical-field strength operator which is proportional to the first quadrature $\hat{X}=(\hat{a}_\nu+\hat{a}^{\dagger}_\nu)/2^{1/2}$. Moreover, by using the quantum-optical units: $T\|\mathbf{E}_{o\nu}\|^2/\hbar\omega=1$, we obtain $\hat{q}_\nu=(\hbar/\beta_\nu)^{1/2}\hat{\mathcal{E}}_\nu$. Therefore by taking into account the abstract quantum harmonic oscillator of "frequency" β_ν (z-propagation) given by Eq. (P2.15), and by using the fact that $\hat{M}$ is the generator of displacements [Luks and Perinová, 2002], that is, $\hat{M}\rightarrow -i\hbar\partial/\partial z$, we obtain the following Schrödinger-type equation

for spatial propagation of quantum states on a N-dimensional OFS space $\mathcal{E}_1...\mathcal{E}_N$ (that is, with N modes):

$$-i\hbar\frac{\partial}{\partial z}\Psi(\mathcal{E}_1,...,\mathcal{E}_N;z)=\{\sum_{\nu=1}^{N}-\hbar\beta_\nu\frac{\partial^2}{\partial\mathcal{E}_\nu^2}+\hbar\beta_\nu\mathcal{E}_\nu^2\}\,\Psi(\mathcal{E}_1,...,\mathcal{E}_N;z), \tag{P2.42}$$

where $\hat{\mathcal{E}}_\nu|\mathcal{E}_\nu\rangle=\mathcal{E}_\nu|\mathcal{E}_\nu\rangle$. Note that we use a formulation equivalent to a Hamiltonian one, that is, with canonical variables $\mathcal{P}_\nu=-i\hbar\partial/\partial\mathcal{E}_\nu=\sqrt{\frac{\hbar}{\beta_\nu}}\hat{p}$ and $\mathcal{E}_\nu=\sqrt{\frac{\beta_\nu}{\hbar}}\hat{q}$, however, in order to solve the above Schrödinger equation by path integrals we need a Lagrangian formulation with generalized coordinates $\mathcal{E}_\nu$ and generalized velocities $d\mathcal{E}_\nu/dz=\mathcal{E}'_\nu$. Likewise, from the Momentum operator $\hat{\mathcal{M}}$ we can define a "classical" Momentum $\mathcal{M}(\mathcal{E}_1,...,\mathcal{E}_N,\mathcal{P}_1,...,\mathcal{P}_N,z)$, in such a way that the following "classical" variables and expressions can be introduced:

$$\mathcal{E}'_\nu=\partial\mathcal{M}/\partial\mathcal{P}_\nu;\;\;\mathcal{P}'_\nu=-\partial\mathcal{M}/\partial\mathcal{E}_\nu, \tag{P2.43}$$

$$\mathcal{L}(\boldsymbol{\mathcal{E}},\boldsymbol{\mathcal{E}}')=\boldsymbol{\mathcal{P}}_\nu\boldsymbol{\mathcal{E}}'_\nu-\mathcal{M}(\boldsymbol{\mathcal{E}},\boldsymbol{\mathcal{P}}), \tag{P2.44}$$

with $\boldsymbol{\mathcal{E}}=(\mathcal{E}_1,...,\mathcal{E}_N)$, $\boldsymbol{\mathcal{E}}'=(\mathcal{E}'_1,...,\mathcal{E}'_N)$, $\boldsymbol{\mathcal{P}}=(\mathcal{P}_1,...,\mathcal{P}_N)$ and where $\mathcal{M}$ plays the role of a Hamiltonian-type function and $\mathcal{L}$ is the corresponding Lagrangian-type function. The procedure starts with the Momentum operator for N modes, $\hat{\mathcal{M}}(\hat{a}_1,\hat{a}_2,...,\hat{a}_N,\hat{a}_1^\dagger,\hat{a}_1^\dagger,...,\hat{a}_N^\dagger)$, and then by using the canonical variables $\mathcal{P},\mathcal{E}$, a "classical" Momentum: $\mathcal{M}(\mathcal{E}_1,...,\mathcal{E}_N,\mathcal{P}_1,...,\mathcal{P}_N)$ is obtained. Next, by using a Legendre Transformation we obtain a "classical" Lagrangian: $\mathcal{L}(\boldsymbol{\mathcal{E}},\boldsymbol{\mathcal{E}}')$. Therefore, according to the Feynman approach [Feynman and Hibbs, 1965] the propagator in the $\mathcal{E}_1...\mathcal{E}_N$ space is given by:

$$K(\boldsymbol{\mathcal{E}}_f,\boldsymbol{\mathcal{E}}_o;z_f)=\frac{\hbar^{N/2}}{\beta_1^{1/2}...\beta_N^{1/2}}\int...\int\mathcal{D}\,\boldsymbol{\mathcal{E}}(z)e^{-(i/\hbar)\int_0^{z_f}\mathcal{L}(\boldsymbol{\mathcal{E}},\boldsymbol{\mathcal{E}}')dz}, \tag{P2.45}$$

with $\boldsymbol{\mathcal{E}}(z_f)\equiv\boldsymbol{\mathcal{E}}_f=(\mathcal{E}_{f1},...,\mathcal{E}_{fN})$ and $\boldsymbol{\mathcal{E}}(0)\equiv\boldsymbol{\mathcal{E}}_o=(\mathcal{E}_{o1},...,\mathcal{E}_{oN})$ and where the integral is performed all over the paths $\boldsymbol{\mathcal{E}}(z)=(\mathcal{E}_1(z),...,\mathcal{E}_N(z))$ connecting the points $\boldsymbol{\mathcal{E}}_f$ and $\boldsymbol{\mathcal{E}}_o$. Note that there is a change of sign with respect to the classical Hamiltonian theory in time. It is wellknown that the path integration can be performed in an exact way or by using approximations such as the semiclassical limit, the approximated quadratic Lagrangians, perturbative techniques, and so on. It is interesting to note, as shown later, that in a semiclassical limit the classical paths $\boldsymbol{\mathcal{E}}(z)$ can be derived from Heisenberg's equations through the trajectories followed by the operators $\hat{\boldsymbol{a}}(z)$ and $\hat{\boldsymbol{a}}^\dagger(z)$ associated to the absorption and emission operators. These trajectories can be also obtained in an exact way or by approximate techniques such as the adiabatic, WKB, perturbative, and so on. Finally, the

spatial quantum propagation is given by the following simple equation:

$$\Psi(\mathcal{E}_f;z_f) = \frac{\hbar^{N/2}}{\beta_1^{1/2}...\beta_N^{1/2}} \int ... \int K(\mathcal{E}_f,\mathcal{E}_o;z)\Psi(\mathcal{E}_o;z)\, d\mathcal{E}_o. \tag{P2.46}$$

We must stress that homodyne and heterodyne techniques can be used to measure the probability distribution $P(\mathcal{E}_f) = |\Psi(\mathcal{E}_f)|^2$. In fact, we will show further on a few examples of these probabilities by simulating a homodyne detection.

Spatial optical propagators in the OFS space

In order to make clear the procedure we present a canonical example of calculation of a spatial optical propagator, in particular, a spatially degenerated parametric amplifier formed by two modes with propagation constants $\beta = \beta(\omega)$ and $\beta_p = \beta(2\omega)$. These modes are nonlinearly coupled, where the first mode is an amplified mode and the second one is assumed to be a non-depleting and classical pump mode. A nonlinear z-coupling coefficient, such as that one by Eq. (P2.37) and denoted as $\kappa_{NL}(z)/2$, is considered. Therefore, the Momentum operator (P6.4) is written as:

$$\hat{M} = \hbar\frac{\beta}{2}(\hat{a}^\dagger\hat{a} + \hat{a}\hat{a}^\dagger) + \hbar\frac{\kappa_{NL}(z)}{2}(\hat{a}^2 e^{-i\beta_p z} + c.h.). \tag{P2.47}$$

By using Eqs. (P2.16) and (P2.17) into the above equation the "classical" Momentum $\mathcal{M}(\mathcal{E},\mathcal{P})$ is obtained after a long but straightforward calculation, that is,

$$\mathcal{M} = \{\frac{\beta c_-}{2\hbar}\mathcal{P}^2 + \frac{\hbar\beta c_+}{2}\mathcal{E}^2 + s\,\kappa_{NL}\mathcal{P}\mathcal{E}\}, \tag{P2.48}$$

where: $c_\pm = 1 \pm \frac{\kappa_{NL}(z)}{\beta}\cos\beta_p z$, $s = \sin\beta_p z$. Next, by using Eqs. (P2.43) and (P2.44), expressions for the Lagrangian $\mathcal{L}(\mathcal{E}',\mathcal{E},z)$ and the momentum $\mathcal{P}(\mathcal{E}',\mathcal{E},z)$ are derived:

$$\mathcal{L} = \frac{\hbar}{\beta}\{\frac{\mathcal{E}'^2}{2c_-} + \frac{\kappa_{NL}(z)\,s\,\mathcal{E}\mathcal{E}'}{c_-} - [\beta^2 c_+ - \frac{\kappa_{NL}^2(z)\,s^2}{c_-}]\frac{\mathcal{E}^2}{2}\}, \tag{P2.49}$$

$$\mathcal{P} = \frac{\hbar}{\beta}\frac{\mathcal{E}' - \kappa_{NL}s\mathcal{E}}{c_-}. \tag{P2.50}$$

Note that if κ_{NL}=0 the "free" Lagrangian is recovered. With these results we can already obtain the optical propagator in the OFS space. First of all, we see that the Lagrangian is quadratic therefore the semiclassical propagator is exact [Feynman and Hibbs, 1965], that is,

$$K(\mathcal{E}_f,\mathcal{E}_o;z_f) = F(z_f)\, e^{-(i/\hbar)\int_0^{z_f}\mathcal{L}(\mathcal{E},\mathcal{E}')dz} = F(z_f)\, e^{-(i/\hbar)S(\mathcal{E}_f,\mathcal{E}_o;z_f)}, \tag{P2.51}$$

where $S(\mathcal{E}_f, \mathcal{E}_o; z_f)$ plays the role of an action and $F(z_f)$ is obtained by means of the well-known Van Vleck determinant, which in our unidimensional case is given by the expression:

$$F(z_f) = \left\{ \frac{i\beta}{2\pi\hbar^2} \frac{\partial^2 S}{\partial \mathcal{E}_f \partial \mathcal{E}_o} \right\}^{1/2}. \tag{P2.52}$$

The action S can be formally integrated by using the Euler-Lagrange equations obtained from the Lagrangian $\mathcal{L}$ [Gómez-Reino and Liñares, 1987, Liñares, 1991]. After a certain calculation it is obtained:

$$S(\mathcal{E}_f, \mathcal{E}_o; z_f) = \frac{\hbar}{2\beta} \left\{ \frac{\mathcal{E}'(z_f) + \kappa_{NL}(z_f) s(z_f) \mathcal{E}_f}{c_-(z_f)} \mathcal{E}_f - \frac{\mathcal{E}'(0)}{c_-(0)} \mathcal{E}_0 \right\}. \tag{P2.53}$$

We must stress that in this case we only need classical trajectories, therefore, by calculating them we can obtain the action $S(\mathcal{E}_f, \mathcal{E}_o; z_f)$. At that end, we start by taking into account Eq. (P2.50), together the initial conditions $\mathcal{E}(0) = \mathcal{E}_o$ and $\mathcal{E}'(0) = \mathcal{E}'_o$, in such a way that we can write the general expression for the classical paths as

$$\mathcal{E}(z) = \mathcal{E}_o \, v(z) + \mathcal{E}'_o \, u(z), \tag{P2.54}$$

where $u(z)$ and $v(z)$ are functions fulfilling the initial conditions: $u(0) = v'(0) = 0$, $v(0) = u'(0) = 1$ and they can be obtained from $\hat{a}(z)$ and $\hat{a}^\dagger(z)$ fulfilling (in most cases) simpler equations (Heisenberg's equations) than $\mathcal{E}(z)$. Likewise, by using boundary conditions: $\mathcal{E}(0) = \mathcal{E}_o$ and $\mathcal{E}(z) = \mathcal{E}_f$ we can rewrite the classical paths as [Gómez-Reino and Liñares, 1987, Liñares, 1991]:

$$\mathcal{E}(z) = \mathcal{E}_o \, v(z) + \frac{\mathcal{E}_f - \mathcal{E}_o \, v(z_f)}{u(z_f)} u(z). \tag{P2.55}$$

Therefore by inserting Eq. (P2.55) into Eq. (P2.53), by using the Van Vleck determinant and by substituting all these results into Eq. (P2.51), we obtain the following optical propagator:

$$K(\mathcal{E}_f, \mathcal{E}_o, z) = \left\{ \frac{ic(z)}{2\pi\hbar u(z)} \right\}^{1/2} e^{-\frac{i}{2u(z)}\{a(z)\mathcal{E}_f^2 + b(z)\mathcal{E}_o^2 - 2c(z)\mathcal{E}_f\mathcal{E}_o\}}, \tag{P2.56}$$

where

$$a(z) = \frac{u'(z) - \kappa_{NL}(z) s(z) u(z)}{\beta \, c_-}, \quad b(z) = \frac{v(z)}{\beta - \kappa_o}, \tag{P2.57}$$

$$c(z) = \frac{1}{2}\left[\frac{W(u,v)}{\beta \, c_-} + \frac{1}{\beta - \kappa_o} \right], \tag{P2.58}$$

with $W = u'v - uv'$ the Wronskian of the functions u, v, which, after a certain calculation, is given by the expression:

$$W = \frac{\beta}{\beta - k_o} \left[1 - \frac{\kappa}{\beta} \cos(\beta_p z) \right]. \tag{P2.59}$$

Therefore we only need to calculate the functions u and v. For that purpose, we start by using the Heisenberg's equations for the operators $\hat{a}$ and $\hat{a}^\dagger$, next we make the changes: $\hat{a} = \hat{A}e^{i\beta z}$, $\kappa_{NL}(0) = \kappa_o$, $\kappa_{NL}(z) = \kappa_o f_{NL}(z)$, $\tau = \int_0^z f_{NL}(z')dz'$ and $\beta_p = 2\beta$ (phase matching), and then we obtain the following Heisenberg's equations for the operators $\hat{A}$ and $\hat{A}^\dagger$:

$$\frac{\partial \hat{A}}{\partial \tau} = i\kappa_o \hat{A}^\dagger, \quad \frac{\partial \hat{A}^\dagger}{\partial \tau} = -i\kappa_o \hat{A}. \tag{P2.60}$$

A phase matching has been assumed for sake of expositional convenience and without loss of generality, however mismatching could be included in a straightforward way as shown further on. The solution of the above equation is easily calculated, that is, $\hat{a}(\tau)$ is given by

$$\hat{a}(\tau) = \{i\hat{a}^\dagger(0)\text{sinh}[\kappa_o\tau(z)] + \hat{a}(0)\text{cosh}[\kappa_o\tau(z)]\}e^{i\beta z}. \tag{P2.61}$$

Next, by taking into account that in quantum-optical units the variable $\mathcal{E}$ is the first quadrature we use the above equation to evaluate $\mathcal{E}(z)$, and after a straightforward calculation the result is compared with Eq. (P2.54) and then the expressions of the functions $u(z)$ and $v(z)$ are obtained, that is,

$$u(z) = \frac{1}{\beta - \kappa_o}[\text{cosh}(\kappa_o\tau)\text{sen}(\beta z) - \text{sinh}(\kappa_o\tau)\text{cos}(\beta z)], \tag{P2.62}$$

$$v(z) = \text{cosh}(\kappa_o\tau)\text{cos}(\beta z) - \text{sinh}(\kappa_o\tau)\text{sin}(\beta z). \tag{P2.63}$$

In short, the quantum optical propagator given by (P2.56) allows to evaluate the quantum light propagation in a nonlinear waveguide with a z-inhomogeneity $\kappa_{NL}(z)$. Thus for distances of propagation z_m, where $b(z_m) = v(z_m) = 0$, we obtain the Fourier Transform (with a scale factor depending on κ_{NL}) of the probability amplitude distribution of an input quantum state $\Psi(\mathcal{E}, 0)$; for the particular case $\kappa_{NL}(z) = \kappa_o$ it is obtained $\beta z_m = m\pi + \text{atn}\{\text{cotanh}(\kappa_o z_m)\}$. On the other hand, at distances of propagation z_n, where $u(z_n)$=0, a Scale Transform (like an "image" condition) of the probability amplitude distribution of an input quantum state $\Psi(\mathcal{E}, 0)$ is obtained. The corresponding scale factor measures the level of amplification reached; for the particular case $\kappa_{NL}(z) = \kappa_o$ we obtain $\beta z_n = n\pi + \text{atn}\{\text{tanh}(\kappa_o z_n)\}$. Likewise, there are planes where maximum or minimum extension of the probability of the quantum state is obtained, that is, we obtain a Squeezing Transform; for instance for vacuum states, with $\kappa_{NL}(z) = \kappa_o$, squeezing is obtained at $2\beta z_p = (p + 1/2)\pi$, with the standard noise $e^{\pm\kappa_o z}$. In the general case of coherent states such planes fulfil the equation $\{b(ab - c^2) + \beta(\beta - \kappa_o)^2u^2a = 0\}$. Note that for $\kappa_{NL} = 0$ it is obtained $a = b = c = 1$, that is, the limit of "free propagation" (non modal coupling) in the waveguide (analogous to temporal evolution) is obtained. Next, in order to get further insight in the behaviour of the waveguiding

degenerate parametric amplifier, we calculate the spatial propagation of a coherent state. A coherent state $|\alpha\rangle = |\alpha|e^{i\phi}$ is represented in the OFS space as:

$$\Psi(\mathcal{E}_o;0) = \frac{1}{\pi^{1/4}} \exp\{-\frac{1}{2}(\mathcal{E}_o - |\alpha|\cos\phi)^2\}e^{-i\varphi}, \tag{P2.64}$$

$$\varphi = \frac{1}{2}\sin\phi\,(|\alpha|^2\cos\phi - 2|\alpha|\mathcal{E}_o), \tag{P2.65}$$

where $\phi = -\omega t$ gives the temporal evolution at each plane z. Now the spatial propagation of this quantum state of light can be carried out by inserting equations (P2.56) and P2.64) into equation (P2.46), and after a long but straightforward calculation, the probability $\mathcal{P}(\mathcal{E}_f)$ of measuring the optical-field strength with value $\mathcal{E}_f$ at a distance z_f can be expressed as:

$$\mathcal{P}(\mathcal{E}_f;z_f) = \frac{1}{\pi^{1/4}\,\Delta\mathcal{E}(z_f)} \exp\left\{-\frac{\{\mathcal{E}_f - |\alpha'|\,[\cos(\phi+\delta(z_f))]\}^2}{\Delta\mathcal{E}^2(z_f)}\right\}, \tag{P2.66}$$

where $\Delta\mathcal{E}(z_f)$ is the quantum noise at each plane z_f, and whose expression is given by

$$\Delta\mathcal{E}^2(z_f) = [\cosh(2\kappa_o\,\tau_f) - \sinh(2\kappa_o\,\tau_f)\sin(2\beta z_f)], \tag{P2.67}$$

and where $|\alpha'|$ is the mean optical-field strength and δ is a z-dependent phase; their values at each plane z_f are given by the following expressions:

$$|\alpha'| = |\alpha|\sqrt{\mathcal{V}_-^2(z_f) + \mathcal{W}_-^2(z_f)},\ \ \tan\delta = \frac{\mathcal{V}_-(z_f)}{\mathcal{W}_-(z_f)}, \tag{P2.68}$$

with

$$\mathcal{V}_-(z_f) = \cosh(\kappa_o\,\tau_f)\cos(\beta z_f) - \sinh(\kappa_o\,\tau_f)\sin(\beta z_f), \tag{P2.69}$$

$$\mathcal{W}_-(z_f) = \cosh(\kappa_o\,\tau_f)\sin(\beta z_f) - \sinh(\kappa_o\,\tau_f)\cos(\beta z_f), \tag{P2.70}$$

with $\tau_f = \tau(z_f)$. In Fig. P2.1 we show the spatial propagation of an initial coherent state in a nonlinear waveguide where a spatially degenerated parametric amplifier has been implemented. It is shown the well-known amplification effect and, from a quantum point of view, the spatial z-squeezing. Note that we have simulated measurements of the quantum state as a homodyne detection technique is used. In Fig. P2.2 we present again the spatial propagation of an initial coherent state but with a nonlinear z-inhomogeneity $\kappa_{NL}(z) = \kappa_o e^{-h_o z}$. Note that the particular value h_o chosen is such that, from a certain distance, a squeezed state with a constant quantum noise is obtained under spatial propagation. Obviously for greater values than h_o there will be no longer amplification and z-squeezing.

Finally, we must stress that if mismatch is considered we would obtain other functions $\tilde{u}(z)$ and $\tilde{v}(z)$ but no new relevant concepts or calculations

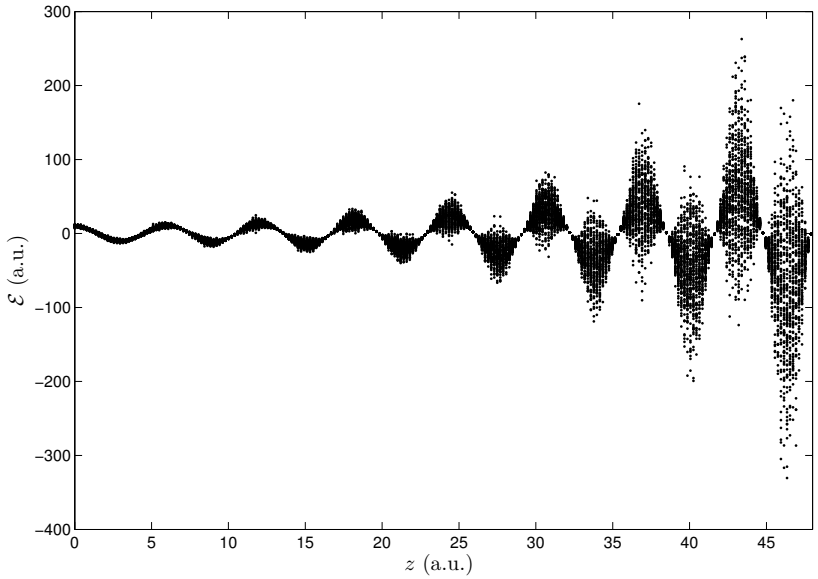

Figure P2.1: Optical-field strength probability distribution of the spatial propagation of an initial coherent state in a waveguiding parametric amplifier. Points correspond to a simulation of measurements under homodyne detection.

are required. For sake of completitude we give the expressions of these functions with $\kappa_{NL}(z) = \kappa_o$, that is,

$$\tilde{u}(z) = \frac{1}{\beta - \kappa_o}\left[\cosh(\tilde{\kappa}_o z)\mathrm{sen}(\tilde{\beta}_p z) - \frac{2\kappa_o + \Delta\beta}{2\tilde{\kappa}}\sinh(\tilde{\kappa_o} z)\cos(\tilde{\beta}_p z)\right], \tag{P2.71}$$

$$\tilde{v}(z) = \cosh(\tilde{\kappa}_o z)\cos(\tilde{\beta}_p z) - \frac{2\kappa_o - \Delta\beta}{2\tilde{\kappa}}\sinh(\tilde{\kappa}_o z)\mathrm{sen}(\tilde{\beta}_p z), \tag{P2.72}$$

where the following constants have been used: $\Delta\beta = \beta_p - 2\beta$, $\tilde{\kappa}_o = [\kappa_o^2 - (\Delta\beta/2)^2]^{1/2}$ and $\tilde{\beta}_p = \beta_p/2$. Once again, by taking into account Eqs. (P2.71), (P2.72), (P2.55) and (P2.53), by using the Van Vleck determinant, and by substituing the results into Eq. (P2.51) the corresponding optical propagator K_m for the mismatching case is easily obtained.

Application to directional couplers

Leu us consider an asynchronous nonlinear coupler 2x2 with two pumping modes in phase, that is, mutually coherent, then by taking into account

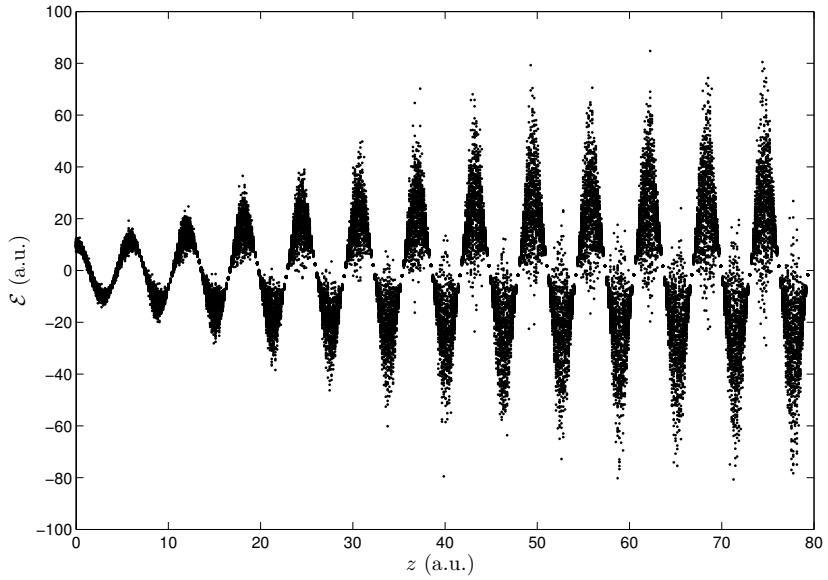

Figure P2.2: Optical-field strength probability distribution of the spatial propagation of an initial coherent state in a waveguiding parametric amplifier with a nonlinear z-inhomogeneity. A decreasing exponential nonlinear coupling has been considered.

the results of section 2, the Momentum operator for two modes ($\nu = 2$) is:

$$\begin{aligned}\hat{M} = &\frac{\hbar\beta_1}{2}(\hat{a}_1^\dagger\hat{a}_1 + \hat{a}_1\hat{a}_2^\dagger) + \frac{\hbar\beta_2}{2}(\hat{a}_2^\dagger\hat{a}_2 + \hat{a}_2\hat{a}_2^\dagger)\\ &+\hbar\kappa(z)(\hat{a}_1^\dagger\hat{a}_2 + \hat{a}_2^\dagger\hat{a}_1) + \frac{\hbar\kappa_{NL}(z)}{2}[\hat{a}_1^{\dagger 2}e^{i\beta_p z} + \hat{a}_2^{\dagger 2}e^{i\beta_p z} + h.c.].\end{aligned} \tag{P2.73}$$

Now, by using supermode operators, that is, by making a rotation of the original operators a separate Momentum operator can be obtained, that is,

$$\hat{b}_1 = (\cos\theta\hat{a}_1 + \sin\hat{a}_2), \qquad \hat{b}_2 = (-\sin\theta\hat{a}_1 + \cos\theta\hat{a}_2), \tag{P2.74}$$

and accordingly

$$\begin{aligned}\hat{M} = &\frac{\hbar\tilde{\beta}_1(z)}{2}(\hat{b}_1^\dagger\hat{b}_1 + \hat{b}_1\hat{b}_2^\dagger) + \frac{\hbar\tilde{\beta}_2(z)}{2}(\hat{b}_2^\dagger\hat{b}_2 + \hat{b}_2\hat{b}_2^\dagger) +\\ &+ \frac{\hbar\kappa_{NL}(z)}{2}[\hat{b}_1^{\dagger 2}e^{i\beta_p z} + \hat{b}_2^{\dagger 2}e^{i\beta_p z} + h.c.].\end{aligned} \tag{P2.75}$$

Therefore two "effective" spatial degenerate parametric amplifiers decoupled with mismatching have been obtained, and thus by using the results

of the propagator with mismatching K_m we can solve the propagation of quantum light in this nonlinear coupler but in a new OFS space, that is,

$$K_m(\mathcal{F}_{f1}, \mathcal{F}_{o1}, \mathcal{F}_{f2}, \mathcal{F}_{o2}, z) = K_m(\mathcal{F}_{f1}, \mathcal{F}_{o1}, z)\, K_m(\mathcal{F}_{f2}, \mathcal{F}_{o2}, z). \tag{P2.76}$$

with

$$\mathcal{F}_1 = (\cos\theta\mathcal{E}_1 + \sin\theta\mathcal{E}_2), \quad \mathcal{F}_2 = (\sin\theta\mathcal{E}_1 - \cos\theta\mathcal{E}_2). \tag{P2.77}$$

Next, we can make calculations with states $\Psi(\mathcal{F}_{o1}, \mathcal{F}_{o2})$ and at the end, we return to the more accessible (experimentally) space $\mathcal{E}_1\mathcal{E}_2$, that is, $\Psi(\mathcal{F}_{f1}, \mathcal{F}_{f2})$ $\rightarrow \Psi(\mathcal{E}_{f1}, \mathcal{E}_{f2})$.

P2.4. Heuristic formulation of quantum dissipation

In most problems of nonlinear propagation the losses (dissipation) can not be completely neglected, therefore we are interested in presenting an approach to this problem in the context of the nonlinear waveguiding coupling but from a quantum point of view. It is wellknown that a rigourous approach to this problem is a very hard task, for that reason we make use of a heuristic formulation, which in turn could be justified in a more rigourous way. Examples of rigourous approachs to the quantum dissipation are based on the Caldirola-Kanai (CK) quantum oscillator, or, alternatively, the use of a reservoir in order to model the damping process, that is, a system coupled to an environment or thermal bath with many degrees of freedom, which contains in turn the CK model [Yu and Sun, 1994]. Likewise, other more complicated models have been proposed, such as the Bateman-Feshbach-Tikochinsky oscillator, although its physical fundamentals are the same than in the previous approaches. However, recently Rajeev [Rajeev, 2007] has proposed a canonical formulation of dissipative mechanics by using complex-valued Hamiltonians, that is, the use of complex Hamiltonians describe damping in a similar way as above approaches do. We must stress that all previous approaches have been developed for temporal evolution, however, in our case we are interested in spatial propagation. In our heuristic approach we will follow a way close to that one proposed by Rajeev, that is, we will make use of complex-valued Momentum operators. Likewise, it is wellknown the presence of fluctuations when damping is present, therefore stochastic terms must be included in the Momentum, which in turn provides a consistent quantum formulation [Haken, 1981]. We start by presenting a heuristic derivation of a complex-valued Momentum operator for describing damping (losses) in a waveguiding device. Next, we will evaluate the optical propagator by taking into account the quantum fluctuations, and finally, an application to a parametric amplifier with losses is presented.

Quantum dissipation in waveguiding devices

Let us consider that losses, or equivalently damping, can be considered as a perturbation, therefore we must obtain an expression for the linear polarization, thus, by taking into account Eq. (P2.28) but with an imaginary electrical permitivity $i\Delta\tilde{\epsilon}_\nu$ for the ν-mode, we can write the following hermitian Polarization operator,

$$\hat{\mathbf{P}}_{oi} \approx -i\Delta\tilde{\epsilon}_\nu \, [\hat{\mathbf{e}}_\nu^{(-)}(x,y,t) - \hat{\mathbf{e}}_\nu^{(+)}(x,y,t)]. \tag{P2.78}$$

We can consider several types of damping, for example, by means of ohmic losses where the medium has a conductivity σ. Thus, by making the change $\epsilon \to \epsilon + i\sigma/\omega$ into Eq. (P2.4) we introduce the ohmic losses and accordingly for a ν-mode the perturbation can be written as follows: $\Delta\tilde{\epsilon}_\nu = \epsilon_o\beta_\nu\gamma_\nu/k_o^2$, with $\gamma_\nu = \omega\sigma\mu_o/\beta_\nu$. A similar expression is obtained for absorption losses, where now $\Delta\tilde{\epsilon}_\nu = \epsilon_o\chi_i = \epsilon_o\beta_\nu\gamma'_\nu/k_o^2$, with $\gamma'_\nu = \chi_i k_o^2/\beta_\nu$. Note, on the other hand, that the material polarization given by Eq. (P2.78) is proportional to the operator $\hat{\mathbf{e}}_{\nu\_}(x,y,t) = \hat{\mathbf{e}}_\nu^{(-)}(x,y,t) - \hat{\mathbf{e}}_\nu^{(+)}(x,y,t)$, unlike a lossless medium where it is proportional to the operator $\hat{\mathbf{e}}_\nu(x,y,t) = \hat{\mathbf{e}}_\nu^{(+)}(x,y,t) + \hat{\mathbf{e}}_\nu^{(-)}(x,y,t)$, therefore, in a heuristic way and in agreement with Eq. (P2.26), we establish that the quantum correction to the Momentum operator is given by the operator

$$\hat{M}_{oi} = \iiint_0^T \frac{1}{2}\,\hat{\mathbf{P}}_{oi}\,\hat{\mathbf{e}}_{\nu\_}\,dxdydt = \iiint_0^T -i\frac{\Delta\tilde{\epsilon}_\nu}{2}\,\hat{\mathbf{e}}_{\nu\_}\hat{\mathbf{e}}_{\nu\_}\,dxdydt. \tag{P2.79}$$

We must stress that $\hat{\mathbf{e}}_{\nu\_}(x,y,t)$, and not $-\hat{\mathbf{e}}_{\nu\_}(x,y,t)$, has been chosen for sake of physical consistency, that is, the results for the classic limit case are correctly recovered. Likewise, this heuristic derivation could be also applied to a medium with gain, that is, with $-i\Delta\tilde{\epsilon}_\nu$ and then we would obtain the same result but with a positive sign in Eq. (P2.79), and again it would be consistent with the derivation of the classic limit. Note that operator $\hat{M}_{oi}$ is not hermitian, therefore the momentum is not conserved, that is, an amount of the optical momentum is transferred to the medium. Now, by taking into account the expressions for the optical field operators given by Eqs. (P2.19, P2.20) we can derive an explicit expression for $\hat{M}_{oi}$. In order to illustrate it in an explicit form we focus on the particular case of TE modes [Liñares and Nistal, 2003] in a planar guide, therefore from Eq. (P2.79), and after a straightforward calculation, we obtain:

$$\hat{M}_{oi} = i\hbar\frac{\gamma_\nu}{4}\,(\hat{a}_\nu^\dagger\hat{a}_\nu + \hat{a}_\nu\hat{a}_\nu^\dagger), \tag{P2.80}$$

where we have used the particular expression for the norm of TE modes, that is, $\|\mathbf{E}_\nu\| = (\beta_\nu/2\omega\mu_o)\iint E_y^2\,dxdy$. We will follow this heuristic procedure for the calculation of linear and nonlinear modal coupling with

losses, that is, we consider that there is a complex electrical permitivity $\Delta\epsilon = \Delta\epsilon_r + i\Delta\epsilon_i$ which couples the optical modes. The real part of the electrical permitivity has been discussed previously and now we are interested in the imaginary part $\Delta\epsilon_i$. By following a procedure similar to that developed for the real case, but by using the new field operator related to losses (damping), that is, $\hat{\mathbf{e}}_{\nu\_}(x, y, t)$ and by taking into account all the ν-modes, we get that the following integral has to be evaluated:

$$\hat{M}_{Li} = -\frac{i}{2} \iiint_0^T \Delta\epsilon_i \sum_{\nu} \hat{\mathbf{e}}_{\nu\_} \sum_{\nu'_-} \hat{\mathbf{e}}_{\nu'} \, dxdydt. \tag{P2.81}$$

After a straightforward calculation, we obtain the following non hermitian Momentum operator describing the losses in a linear modal coupling device:

$$\hat{M}_{Li} = \sum_{\nu} i\hbar\gamma_{\nu\nu}\frac{1}{2}(\hat{a}^\dagger_\nu\hat{a}_\nu + \hat{a}_\nu\hat{a}^\dagger_\nu) + \sum_{\nu<\nu'} i\hbar\gamma_{\nu\nu'}(\hat{a}^\dagger_\nu\hat{a}_{\nu'} + h.c.), \tag{P2.82}$$

where

$$\gamma_{\nu\nu'} = \frac{\omega \iint \Delta\epsilon_i \, (\mathbf{E}_{t\nu}\mathbf{E}^\star_{t\nu'} + \mathbf{E}_{z\nu}\mathbf{E}^\star_{z\nu'})dxdy}{4\,\|\mathbf{E}_\nu\|\,\|\mathbf{E}_{\nu'}\|}. \tag{P2.83}$$

In short, losses have included complex coupling coefficients, as expected. In the same way we can assume that nonlinear coupling will be described by complex coefficientes: $\kappa_{NL} + i\gamma_{NL}$. Therefore the Momentum operator will be modified by all these imaginary terms. However it is not all story because it is wellknown that these imaginary terms violate the commutation rules and therefore the quantum mechanical consistency is destroyed. In order to avoid this inconsistency we will introduce fluctuating operators $\hat{B}$ (quantum noise operators) along z-direction in the Momentum operator in a manner similar to that followed in the Hamiltonian formulation. These fluctuating operators have a well-defined statistical properties in such a way that commutation rules are preserved. The physical origin of these operators is the incoherent properties of the medium with losses, that is, the damping mechanism is a statistical process described by stochastic terms modelling the coupling between the light and the medium. Thus the following heuristic additional term in the Momentum operator must be introduced:

$$\hat{M}_F = \sum_{\nu} \hbar g_\nu \, (\hat{a}^\dagger_\nu\hat{B} + \hat{a}_\nu\hat{B}^\dagger), \tag{P2.84}$$

where g_ν is the coupling strength between the medium and the ν-mode. For the sake of making clear this point we analyse firstly the free case with losses, that is, a single mode in a lossy medium. In this case the Momentum operator in the ν-mode and the corresponding Heisenberg's equation are:

$$\hat{M}_\nu = \frac{\hbar}{2}(\beta + i\frac{\gamma_\nu}{2}) \, (\hat{a}^\dagger_\nu\hat{a}_\nu + \hat{a}_\nu\hat{a}^\dagger_\nu) + \hbar g_\nu(\hat{a}^\dagger_\nu\hat{B} + \hat{a}_\nu\hat{B}^\dagger), \tag{P2.85}$$

$$\frac{\partial\hat{a}_\nu}{\partial z} = (i\beta_\nu - \frac{\gamma_\nu}{2})\hat{a}_\nu + ig_\nu\hat{B}. \tag{P2.86}$$

Note that Eq. (P2.86) is analogous to the Heisenberg-Langevin equation in the temporal domain. Likewise, note that if $g_\nu = 0$ then $\hat{a}_\nu(z) = \hat{a}_\nu(0)\, e^{i\beta_\nu z}\, e^{-\frac{\gamma_\nu}{2}z}$. This solution is exactly equal to the classical solution with a damping factor γ_ν, but from a quantum point of view it is obtained $[\hat{a}_\nu(z), \hat{a}_\nu^\dagger(z)] = e^{-\gamma_\nu z} \to 0$, and therefore the quantum nature is lost. However by considering the fluctuating term we obtain the following formal solution:

$$\hat{a}_\nu(z) = \hat{a}_\nu(0) e^{i\beta_\nu z}\, e^{-\frac{\gamma_\nu}{2}z} + i e^{i\beta_\nu z}\, e^{-\frac{\gamma_\nu}{2}z} \int_0^z e^{-i\beta_\nu z'}\, e^{\frac{\gamma_\nu}{2}z'} g_\nu \hat{B}(z')\mathrm{d}z'. \tag{P2.87}$$

Now, we must take into account the statistical properties of the operators $\hat{B}, \hat{B}^\dagger$, that is, it is assumed that under the z-spatial averaging these operators fulfil [Haken, 1981]:

$$\langle \hat{B}(z) \rangle_z = \langle \hat{B}(z)^\dagger \rangle_z = 0, \tag{P2.88}$$

$$\langle \hat{B}(z)\hat{B}(z')^\dagger \rangle_z = \frac{\gamma_\nu}{g_\nu^2}(a_o + 1)\delta(z - z'), \tag{P2.89}$$

$$\langle \hat{B}(z)^\dagger \hat{B}(z') \rangle_z = \frac{\gamma_\nu}{g_\nu^2} a_o\, \delta(z - z'), \tag{P2.90}$$

where a_o is a constant depending on the type of reservoir. For a thermal reservoir [Haken, 1981] it is obtained $a_o = \bar{n}$, that is, the mean photon number in the spatio-temporal volume of quantization. With the above properties together with Eq. (P2.87) it is obtained that the spatial propagation of the averaging of operators $\hat{a}_\nu(z)$ and $\hat{a}_\nu(z)^\dagger$ provides the same solution as that one of the complex classical fields, that is,

$$\langle \hat{a}_\nu(z) \rangle_z \approx \hat{a}_\nu(0) e^{i\beta_\nu z}\, e^{-\frac{\gamma_\nu}{2}z}. \tag{P2.91}$$

But moreover, after a few calculations, it can be shown that the commutation rules are preserved, at least in a spatial averaging, that is,

$$\langle [\hat{a}_\nu(z), \hat{a}_\nu(z)^\dagger] \rangle_z = 1. \tag{P2.92}$$

In short, the more general Momentum operator for nonlinear waveguiding coupling with losses would be:

$$\hat{M} = \hat{M}_{oi} + \hat{M}_{Li} + \hat{M}_F + \hat{M}_{(\kappa_{NL} + i\gamma_{NL})}, \tag{P2.93}$$

where $\hat{M}_{oL}$, $\hat{M}_{oi}$, $\hat{M}_{Li}$ and $\hat{M}_F$ are given by Eqs. (P2.31), (P2.80), (P2.82) and (P2.84), and moreover $\hat{M}_{(\kappa_{NL} + i\gamma_{NL})}$ is the nonlinear Momentum operator, as those ones presented in section 2, but, such as subindex $(\kappa_{NL} + i\gamma_{NL})$ is indicating, each one of the nonlinear coupling coefficients is transformed into a complex amount.

Dissipative spatial optical propagator

We apply the above results to recalculate the spatial optical propagator in order to see how losses influence on the quantum propagation. For a dissipative monomode case with a coupling strength factor g between the medium and an arbitrary mode, the semiclassical optical propagator in the OFS space is given by the formal expression:

$$K(\mathcal{E}_f, \mathcal{E}_o; z_f) = \left\{ \frac{i\tilde{\beta}}{2\pi\hbar^2} \frac{\partial^2 S}{\partial \mathcal{E}_f \partial \mathcal{E}_o} \right\}^{1/2} e^{-(i/\hbar)\int_0^{z_f} \mathcal{L}(\mathcal{E}_F, \mathcal{E}_F')dz}, \tag{P2.94}$$

where we have defined $\tilde{\beta} = \beta + i\gamma/2$ and where subindex F indicates that now the solutions must be corrected by fluctuations. Quantum fluctuations is a source of noise, therefore for a small noise source (or quadratic Lagrangians as shown in the free case) the paths can be formally written as:

$$\mathcal{E}_F(\mathcal{E}_o, \mathcal{E}_f, z) = \mathcal{E}(\mathcal{E}_o, \mathcal{E}_f, z) + \delta\mathcal{E}(z), \tag{P2.95}$$

where $\langle \mathcal{E}_F \rangle = \mathcal{E}$. By taking into account that from a statistical point of view a function $f(x_F)$, with a stochastic variable x_F not strongly fluctuating, fulfils, in a good approximation, $\langle f(x_F) \rangle \approx f(\langle x_F \rangle)$, then in our case, that is, $x_F \equiv \mathcal{E}_F$, we obtain at first order:

$$\langle K(\mathcal{E}_f, \mathcal{E}_o; z_f) \rangle \approx \left\{ \frac{i\tilde{\beta}}{2\pi\hbar^2} \frac{\partial^2 S}{\partial \mathcal{E}_f \partial \mathcal{E}_o} \right\}^{1/2} e^{-(i/\hbar)\int_0^{z_f} \mathcal{L}(\mathcal{E}, \mathcal{E}')dz} [1 + O(g^2) + ...]. \tag{P2.96}$$

The terms of first-order $O(g)$ are zero because of the statistical properties of the noise. The terms of order equal to, or greater than, $O(g^2)$ introduce small corrections to the optical propagator, but the main contribution comes from the classical paths without noise. The study of these terms will be made in a future work. Therefore, for our purpose it is enough to consider a zero-order contribution, which gives a suffice information about the damping undergone by the quantum state under spatial propagation. Likewise, the zero-order contribution would give the classical results when quasi-classical states are used. As an illustrative example we present the case of free propagation in a guided mode and afterwards we will analyze a parametric amplifier. In the free case we have the following independent solutions:

$$u(v) = \frac{\sin(\tilde{\beta}z)}{\tilde{\beta}}, \quad v(z) = \cos(\tilde{\beta}z). \tag{P2.97}$$

By inserting these functions into Eq. (P2.56) for $\kappa_o = 0$ and by taking into account Eq. (P2.96) we obtain the optical propagator:

$$\langle K(\mathcal{E}_f, \mathcal{E}_o, z) \rangle = \left\{ \frac{i}{\pi \sin(\tilde{\beta}z)\hbar} \right\}^{1/2} e^{-\frac{i}{\sin(\tilde{\beta}z)}\{(\mathcal{E}_f^2 + \mathcal{E}_o^2)\cos(\tilde{\beta}z) - 2\mathcal{E}_f\mathcal{E}_o\}}. \tag{P2.98}$$

Now it is interesting to calculate the propagation of a quantum state. Let us consider, for the sake of simplicity, an optical-field state, that is, $\Psi(\mathcal{E}_o;0) = \delta(\mathcal{E}_o - \mathcal{E}_i)$, which can be ideally interpreted as a highly squeezed coherent state. Then, by using Eq. (P2.46) we obtain:

$$\Psi(\mathcal{E}_f;z_f) = \frac{i}{\pi \sin(\tilde{\beta}z)\hbar}\, e^{-\frac{i}{\sin(\tilde{\beta}z)}\{(\mathcal{E}_f^2+\mathcal{E}_i^2)\cos(\tilde{\beta}z) - 2\mathcal{E}_f\mathcal{E}_i\}}. \tag{P2.99}$$

For a large distance of propagation $z_f >>$, and in a good approximation, we can rewrite the above probability amplitude, in a normalized form as usual, as follows:

$$\Psi(\mathcal{E}_f;z_f >>) \approx (\frac{\pi}{2})^{1/4}\, e^{i\frac{\beta z}{2}}\ \ e^{-\mathcal{E}_f^2}. \tag{P2.100}$$

that is, the optical-field state become the vacuum state due to the losses in the medium. Now we will present the effect of the losses on a parametric amplifier.

Application to a parametric amplifier

In this subsection we apply the previous results to a waveguiding parametric amplifier with losses and therefore with quantum fluctuations. Let us consider a strong pump mode although with a small depleting caused by losses, that is, it is assumed that the depleting produced by losses is much greater than the depleting produced by nonlinear coupling. Likewise, linear losses are considered, that is, both the amplified mode and the pump mode have a complex propagation constant. Moreover, we consider nonlinear losses (complex nonlinear coupling coefficient). In short, there will be a stochastic momentum modelling the coupling between the environment and the amplifier, and accordingly we can rewrite Eq. (P2.47) as follows:

$$\hat{M} = \hbar\frac{\tilde{\beta}}{2}(\hat{a}^\dagger\hat{a}+\hat{a}\hat{a}^\dagger)+\hbar\frac{\tilde{\kappa}_{NL}(z)}{2}(\hat{a}^2e^{-i\beta_p z}+h.c.)+\hbar g(\hat{a}\hat{B}^\dagger+\hat{a}^\dagger\hat{B}), \tag{P2.101}$$

with $\tilde{\kappa}_{NL}(z) = \tilde{\kappa}_0 e^{-\gamma_p z/2}$ and $\tilde{\kappa}_0 = \kappa_{NL} + i\gamma_{NL}/2$, where $\tilde{\kappa}_0$ depends on both the nonlinear coupling coefficient and the strength of the pump mode at $z = 0$. By following the steps presented in subsection 3.2, and after a straightforward calculation, the following expression for the action, analogous to Eq. (P2.53) but with complex constants and fluctuating factors, is obtained:

$$S(\mathcal{E}_f,\mathcal{E}_o;z_f) = \frac{\hbar}{2\tilde{\beta}}\left\{\frac{\mathcal{E}'(z)+\tilde{\kappa}_{NL}(z)s(z)\mathcal{E}(z)}{c_-(z)}\mathcal{E}(z) - ig\frac{\hat{B}(z)-\hat{B}^\dagger(z)}{(2^{1/2})\,c_-(z)}\mathcal{E}(z)\right\}_0^{z_f}$$

$$-\frac{\hbar g}{2^{3/2}\tilde{\beta}}\int_0^z\Big\{\tilde{\beta}(\hat{B}(z')+\hat{B}^\dagger(z'))\mathcal{E}(z')+i(\hat{B}(z')-$$

$$-\hat{B}^{\dagger}(z'))\frac{(\mathcal{E}'+\tilde{\kappa}_{NL}(z')\,s(z')\mathcal{E}(z'))}{c_{-}(z')}\Big\}dz'+\frac{\hbar\gamma}{2\tilde{\beta}}(a+\frac{1}{2})\int_0^z c_{-}^{-1}(z')dz', \quad \text{(P2.102)}$$

where in the last term the z-spatial averaging properties of the fluctuating operators $\hat{B}(z)$, $\hat{B}^{\dagger}(z)$ given by Eqs. (P2.88-P2.90) have been taken into account. It is important to outline that the fluctuating terms are dependent of the field strength, so that all of them will influence on the optical-field strength probability, except the last term which provides a global phase factor. Moreover, as commented above, we consider that the fluctuating terms contribute as a small correction to the propagator, therefore we use the optical propagator given by equation (P2.98) as a good first approximation to describe the quantum spatial propagation in a lossy medium.

Again to evaluate the propagator we need the corresponding functions $u(z)$ and $v(z)$ associated to the problem with losses. If we consider, for the sake of simplicity, the case of phase matching, that is, the real part of the propagation constants fulfils $\beta_p = 2\beta$, then from the Heisenberg's equations, with $\tau = \int_0^z e^{-\gamma_p z'/2}dz'$ and complex values for $\tilde{\kappa}_0$ and $\tilde{\beta}$, we obtain the following solution for $\hat{a}(\tau)$:

$$\hat{a}(\tau) = \{i\hat{a}^{\dagger}(0)\sinh[\tilde{\kappa}_o\tau(z)] + \hat{a}(0)\cosh[\tilde{\kappa}_o\tau(z)]\}e^{i\tilde{\beta}z} + \hat{F}(\tau), \quad \text{(P2.103)}$$

where

$$\hat{F}(\tau) = ige^{i\tilde{\beta}z(\tau)}\int_0^{\tau}\{C(\tau')\hat{B}e^{-i\beta z'(\tau')}+i\,S(\tau')\hat{B}^{\dagger}e^{i\beta z'(\tau')}\}e^{-(\gamma+\gamma_p)z'(\tau')/2}d\tau', \quad \text{(P2.104)}$$

with $C(\tau') = \cosh[\tilde{\kappa}_0(\tau-\tau')]$, $S(\tau') = \sinh[\tilde{\kappa}_0(\tau-\tau')]$. As in the case without losses, from $\hat{a}(\tau)$ and $\hat{a}^{\dagger}(\tau)$ the optical-field strength operator $\hat{\mathcal{E}}$ is derived, and therefore the following expressions for $u(z)$ and $v(z)$ are obtained:

$$u(z) = \frac{1}{\tilde{\beta}-\tilde{\kappa}_o}\,[\cosh(\tilde{\kappa}_o\tau(z))\mathrm{sen}(\tilde{\beta}z) - \sinh(\tilde{\kappa}_o\tau(z))\cos(\tilde{\beta}z)], \quad \text{(P2.105)}$$

$$v(z) = \cosh(\tilde{\kappa}_o\tau(z))\cos(\tilde{\beta}z) - \sinh(\tilde{\kappa}_o\tau(z))\mathrm{sen}(\tilde{\beta}z). \quad \text{(P2.106)}$$

Now, we can get further insight in the behaviour of the lossy waveguiding degenerate parametric amplifier by calculating again the spatial propagation of a coherent state in the waveguiding device. The expression of the coherent state on the OFS space at $z = 0$ is given by Eq. (P2.64). The spatial propagation of this quantum state of light, disregarding the small fluctuating terms for the sake of clarity, can be carried out by means of the propagator given by Eq. (P2.56) with the functions $u(z)$ and $v(z)$ given by Eqs. (P2.105) and (P2.106). After a long but straightforward calculation, the probability $\mathcal{P}(\mathcal{E}_f)$ of measuring the optical-field strength with value $\mathcal{E}_f$ at a distance z_f can be expressed as follows:

$$\mathcal{P}(\mathcal{E}_f; z_f) = \frac{1}{\pi^{1/4}\,\Delta\mathcal{E}(z_f)}\exp\Big\{-\frac{\{\mathcal{E}_f - |\alpha|\,[f_1(z_f)\cos(\phi) - f_2(z_f)\sin(\phi)]\}^2}{\Delta\mathcal{E}^2(z_f)}\Big\} \quad \text{(P2.107)}$$

with:

$$\Delta\mathcal{E}^2(z_f) = \cos(\gamma_{NL}\,\tau_f)\cosh(\gamma z_f)\,[\cosh(2\kappa_{NL}\,\tau_f) - \sinh(2\kappa_{NL}\,\tau_f)\sin(2\beta z_f)] + \cos(\gamma_{NL}\,\tau_f)\,\sinh(\gamma z) - \sinh(\gamma_{NL}\,\tau_f)\cos(2\beta z_f), \quad \text{(P2.108)}$$

and

$$f_1(z_f) = \sinh(\gamma z_f/2)\,[\cos(\gamma_{NL}\tau_f/2) + \sin(\gamma_{NL}\tau_f/2)]\,\mathcal{V}_+(z_f) + + \cosh(\gamma z_f/2)\,[\cos(\gamma_{NL}\tau_f/2) - \sin(\gamma_{NL}\tau_f/2)]\,\mathcal{V}_-(z_f), \quad \text{(P2.109)}$$

$$f_2(z_f) = \cosh(\gamma z_f/2)\,[\cos(\gamma_{NL}\tau_f/2) + \sin(\gamma_{NL}\tau_f/2)]\,\mathcal{W}_-(z_f) + + \sinh(\gamma z_f/2)\,[\cos(\gamma_{NL}\tau_f/2) - \sin(\gamma_{NL}\tau_f/2)]\,\mathcal{W}_+(z_f), \quad \text{(P2.110)}$$

where we have defined the following auxiliary functions $\mathcal{V}_\pm(z_f)$ and $\mathcal{W}_\pm(z_f)$:

$$\mathcal{V}_\pm(z_f) = \cosh(\kappa_{NL}\,\tau_f)\cos(\beta z_f) \pm \sinh(\kappa_{NL}\,\tau_f)\sin(\beta z_f),$$
$$\mathcal{W}_\pm(z_f) = \cosh(\kappa_{NL}\,\tau_f)\sin(\beta z_f) \pm \sinh(\kappa_{NL}\,\tau_f)\cos(\beta z_f). \quad \text{(P2.111)}$$

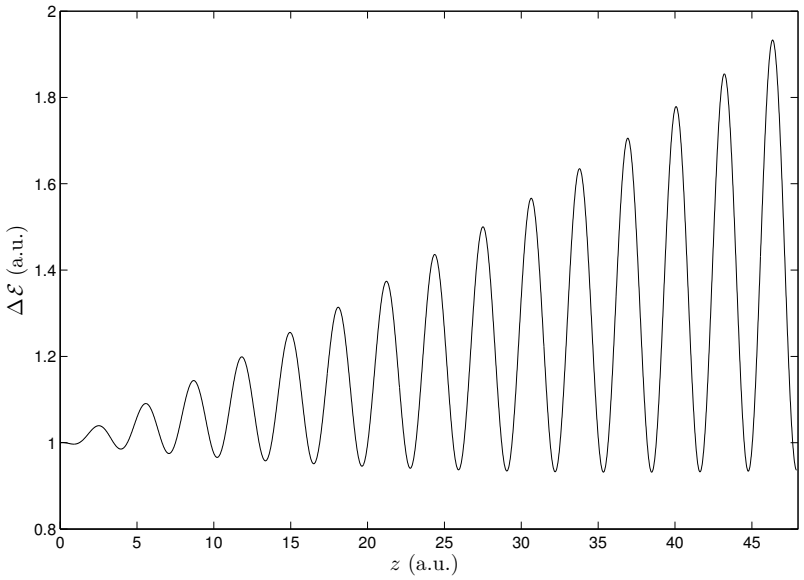

Figure P2.3: z-propagation of the optical-field strength quantum noise of an input coherent state under linear losses of the amplified mode ($\gamma \neq 0$).

Again $\Delta\mathcal{E}$ is the quantum noise at each plane z_f, and functions $f_1(z_f)$ and $f_2(z_f)$ provide the main value of the optical-field strength at each plane z_f, that is,

$$|\alpha'| = |\alpha|\sqrt{f_1^2(z_f) + f_2^2(z_f)}. \quad \text{(P2.112)}$$

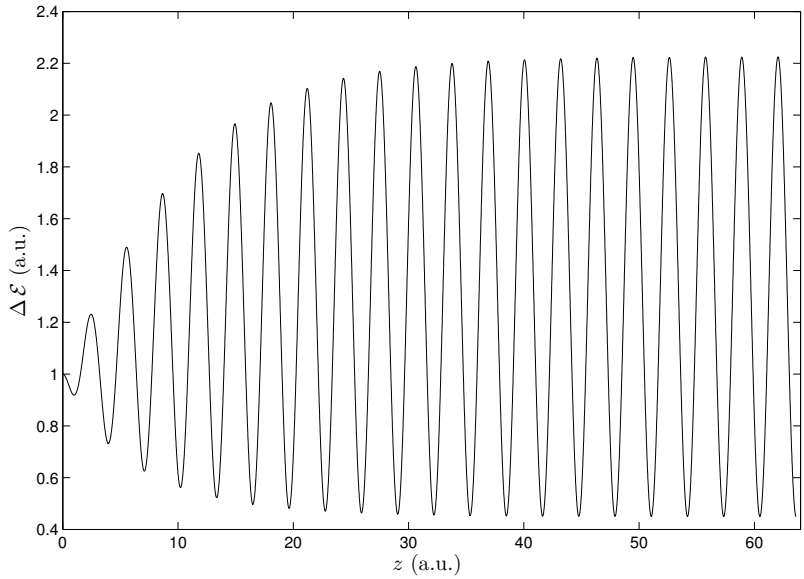

Figure P2.4: Spatial z-propagation of the optical-field strength quantum noise of an input coherent state under linear losses of the pump mode ($\gamma_{\rm p} \neq 0$).

Note that if the losses are neglected, that is, $\gamma = \gamma_{\rm p} = \gamma_{\rm NL} = 0$ then the results for a lossless nonlinear guide given in Eqs. (P2.66), (P2.67) and (P2.68) are recovered.

Now we show some relevant results in a graphical way. In Fig. P2.3 we show the z-propagation of the quantum noise under linear losses in the amplified mode, that is, $\gamma \neq 0$. The value of γ has been chosen in such a way that the squeezing reaches a stable minimum value although amplification continues. In Fig. P2.4 we consider a complex propagation constant for the pump mode, that is, $\gamma_{\rm p} \neq 0$. The value of $\gamma_{\rm p}$ is such that both amplification and squeezing reach a constant value. Finally, in Fig. P2.5 we show the effect of losses in the nonlinear coupling, that is, $\gamma_{\rm NL} \neq 0$. Note that a periodic modulation of amplification is obtained (enveloping). To some extent a behaviour analogous to revivals is obtained. In this case the more remarkable quantum outcome is that there are planes where an enveloping squeezing effect is also obtained.

P2.5. Summary

We have presented the main theoretical results on spatial propagation of quantum light in nonlinear waveguiding devices. We have shown that

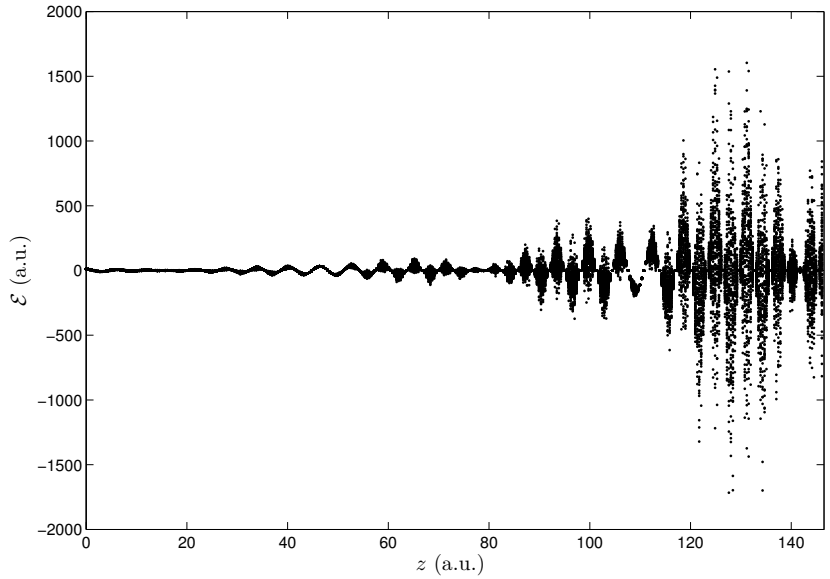

Figure P2.5: Optical-field strength probability distribution of the spatial propagation of an initial coherent state in a waveguiding parametric amplifier with nonlinear losses ($\gamma_{\mathrm{NL}} \neq 0$).

the quantization of the classical Momentum provides a consistent quantum mechanical formulation of the both linear and nonlinear quantum light spatial propagation in waveguiding devices, and consequently it allows to analyze the spatial propagation in the multimode optical-field strength space. For that purpose we have used the Feynman's path integral method in order to derive the quantum spatial optical propagators of different nonlinear waveguiding devices and thus to analyze the spatial propagation of quantum states. We have calculated the spatial propagation of the optical-field strength probability amplitude for the case of a z-dependent nonlinearity. In particular, we have analyzed the spatial propagation of a coherent state in a waveguiding degenerate parametric amplifier with a z-inhomogeneity. The above results of propagation can be applied to directional couplers that can be reduced to degenerate parametric amplifiers decoupled under coordinate transformations in the OFS space. It must be stressed that these optical-field strength probabilities have the advantage of being measured by homodyne techniques, therefore the results have been plotted by simulating the measurements obtained by such a homodyne technique of detection. Likewise, we present a preliminary and heuristic formulation of dissipation in order to take into account the losses un-

der spatial quantum propagation in lossy nonlinear waveguiding devices. Again we have analysed the spatial propagation of the optical-field strength probability amplitude of a coherent state in different cases: linear losses, pumping losses and nonlinear absorption. In a first approximation we have neglected the effects due to the quantum fluctuations by dissipation, that is, small non-linearities have been taken into account, which is consistent with non high losses in the medium. In fact, for non high non-linearities the average Kernel can be used, which is formally equal to the propagator without fluctuations, and therefore an interesting and useful first approximation to the quantum optical propagation in lossy nonlinear waveguides is obtained. Effects such as compensation of amplification, stable squeezing and enveloping squeezing have been shown. Obviously, all classical results can be recovered as a limiting case. The study of the small effects introduced by quantum fluctuating terms will be studied in a future work.

P3. SPATIAL PROPAGATION OF QUANTUM LIGHT STATES IN LONGITUDINALLY INHOMOGENEOUS WAVEGUIDES

Submitted to the JOURNAL OF THE OPTICAL SOCIETY OF AMERICA B

BY DAVID BARRAL & JESÚS LIÑARES

UNIVERSIDADE DE SANTIAGO DE COMPOSTELA

Abstract: *We study the propagation of quantum states of light in separable longitudinally inhomogeneous waveguides based on the Momentum operator. This is carried out in the optical field-strength space & by means of the optical propagator obtained by the path integral formalism. We analyze virtual squeezing appearing in these media and its effect on quantum states of light, that is, Gouy's quantum phases depending on both the longitudinal inhomogeneity and the quantum state. It is justified as well that these media perform unitary Infeld-Plebanski transformations avoiding thus real squeezing. Likewise, WKB and exact results are presented for the propagation of coherent and squeezed states of light and, additionally, Bessel-Gauss quantum states of light propagating in a power-law parametric family of longitudinally inhomogeneous waveguides are studied in detail.*

P3.1. Introduction

Longitudinally inhomogeneous media are widely used in optics, and in particular longitudinally inhomogeneous waveguides are present in fiber and integrated optical devices as modal converters, phase shifters, gradual transitions, and so on [Burns and Milton, 1994, Sodha and Ghatak, 1977, Tabib-Azar, 1995]. Classical problems involving these media have been extensively studied either directly [Gómez-Reino and Liñares, 1987, Gómez-Reino et al., 1986, Khalaj-Amirhosseini, 2006, Tovar and Casperson, 1994] or by means of quantum theoretical approaches [Krivoshlykov and Sauter, 1992, Liñares, 1989, Moya-Cessa et al., 2009]. Increasing synergies between quantum mechanics and fiber and integrated optics technology are being currently exploited in quantum computation, sensing, metrology and communications [O'Brien et al., 2009]. Hence, the quantum study of waveguiding elements can contribute to the advance of quantum technology based on optical fibers and integrated photonics. Several theoretical studies have been carried out, in particular for longitudinally homogeneous media, however, to our knowledgment, longitudinally inhomogeneous waveguiding media have not been considered, with the exception of the seminal studies accomplished by Abram [Abram, 1987] about single optical discontinuities between homogeneous media, and by Glauber and Lewenstein [Glauber and Lewenstein, 1991], about inhomogeneous media but with a Hamiltonian approach which does not provides the spatial propagation of quantum states inside the medium.

Therefore, the primary aim of this work is to carry out a phenomenological quantum mechanical analysis of the propagation of light in longitudinally inhomogeneous waveguiding elements, corresponding to both integrated or fiber optic elements, with a separable index profile, that is, the refractive index profile can be represented by the addition of a transverse inhomogeneity, represented by a transverse index profile function $n_t(x, y)$, and a longitudinal inhomogeneity along the z-direction, represented by a index profile function $n_l(z)$. We should stress that non-separable longitudinal inhomogeneities, that is, a product of transverse and longitudinal inhomogeneities, are not considered, because these media present modal coupling, including coupling to radiation modes (losses), and they have to be studied by taking into account a quantum multimodal coupling [Liñares et al., 2008]. In the separable case there is no modal coupling and, accordingly, there are not radiation losses. Hence, the waveguiding elements made of these media (phase shifters, gradual transitions for antireflection, and so on) will present a good functionality. We will center our attention on single-mode and two-mode waveguiding elements, although results can be extended to elements involving several modes in an straightforward way.

As it was commented above, the fundamental works [Abram, 1987,

Glauber and Lewenstein, 1991] predicted virtual squeezing of quantum states of light propagating through a single optical discontinuity. We extend this result to longitudinally inhomogeneous waveguiding elements and analyze their effect on quantum states of light. To this end, a relationship between the optical-field strength $\mathcal{E}$ in two waveguiding homogeneous media with different effective refractive index is obtained from photon number conservation. This result makes possible to interpret the quantum propagation in these media by means of a virtual squeezing and to show that its effect on the light is the generation of a quantum phase, which takes a classical value for coherent states. This phase can be regarded as an spatial Gouy's phase [Boyd, 1980] but in the quantum domain. Likewise, this virtual squeezing enables us to justify that these media perform an Infeld-Plebanski transformation [Infeld and Plebanski, 1955] in such a way that light emerges from the media without real squeezing. Obviously, the study contains the limit case of a longitudinally inhomogenous layer whose optical mode is a plane-type wave.

On the other hand, quantum propagation problems are usually analyzed by means of a Hamiltonian approach, where the connection between space and time is established by using an effective interaction time $t = z/v$, with z the length of the medium and v the effective velocity of light in the medium. However, in dispersive media, where optical modes propagate with different speeds, the standard Hamiltonian operator is not valid anymore because of the need of several temporal variables. The same problem appears with counter-propagation, where a negative time would be required. Likewise, this connection is not valid either for the longitudinally inhomogeneous media studied in this work because the Hamiltonian formulation performs a spatial integration in a volume V, and therefore the z-dependence is eliminated by spatial averaging [Liñares et al., 2012]. This approach is still being used even although the first fundamental studies on both phenomenological quantization and the quantum propagation problem in free space and dielectric homogeneous media were carried out more than twenty years ago. A wide and detailed review about spatial quantum propagation in dielectric media is presented in [Luks and Perinová, 2002] and references therein. These studies provided the background of the quantum theory of light propagation showing that the quantum operator that describes correctly the quantum spatial propagation along an arbitrary direction z is the Momentum operator $\hat{M}$. Thus, quantization of the classical Momentum is the starting point to calculate the propagation of quantum states in waveguiding elements. We must stress that in this case spatial-temporal modes are used, unlike the Hamiltonian approach where only spatial modes are taken into account. In this way, spatial propagation of quantum states is obtained together with information about its quantum noise.

Likewise, depending on our aims, every quantum propagation problem

is better suited to be dealt with a particular representation. It can be, for instance, the Fock or number space $|n\rangle$, the coherent-state representation $|\alpha\rangle$ and so on. Specifically, we will use the N-dimensional optical field-strength space (OFS) $\mathcal{E}$, that is, the set of eigenvalues of the optical field-strength operator $\hat{\mathcal{E}}$. The complex probability amplitude in the OFS space $\Psi(\mathcal{E})$ gives us complete information about the optical field of quantum states of light [Vogel, 1990]. Such an information can be used, for instance, to assess the generalized quantum polarization of the quantum state of light [Barral et al., 2013, Liñares et al., 2011a]. Moreover, propagation in this space can be carried out by means of the quantum spatial optical propagator calculated by the path integral formalism [Liñares et al., 2012]. The main advantage of this approach is the flexibility it offers in dealing with complex quantum states which are difficult to cope with in other bases. In fact, as it will be shown, both the determination of virtual squeezing and the calculation of Gouy's quantum phases are quite direct with this procedure. Additionally, another important attribute this space shows is that it is the natural one in quantum measurement detection schemes based on homodyne techniques.

The plan of the paper is as follows: in Section 2 we obtain the Momentum operator that describes the propagation of quantum states of light in separable longitudinally inhomogeneous waveguides and calculate the quantum evolution of the spatial mode. In Section 3 we figure out the propagation of quantum states of light in these media by using spatial optical propagators, derived from path integrals in the OFS space. Likewise, we study the propagation of a single-mode coherent state and introduce the WKB approximation. In Section 4 we discuss the results obtained in the above section, in particular, the virtual squeezing undergone by a single-mode coherent state and reason out the virtual character of such a squeezing by means of photon flux conservation. In Section 5 we analyze the effect of virtual squeezing on quantum light leading to Gouy's quantum phases depending on both the longitudinal inhomogeneity and the input quantum state. Likewise, we justify the vanishing of the squeezing via an unitary Infeld-Plebanski transformation accomplished by the medium. In Section 6 we show the propagation of a two-mode Bessel-Gauss state in a family of longitudinally inhomogeneous refractive index profiles depending on several parameters. Finally, a summary is presented.

P3.2. Quantization in longitudinally inhomogeneous waveguides

In this section we will study the light quantization in dispersion-free and non-magnetic optical media with separable inhomogeneous refractive index, like longitudinally inhomogeneous waveguides [Sodha and Ghatak, 1977], whose index can be written as

$$n^2(x,y,z) = n_t^2(x,y) + n_l^2(z) \equiv n_0^2\, f^2(x,y) + \Delta n^2\, h^2(z), \tag{P3.1}$$

where $f(x,y)$ and $h(z)$ are transverse and longitudinal functions, respectively, and n_0 and Δn are constants. Our quantization procedure resembles that carried out in the time domain via a Hamiltonian approach in [Pedrosa and Rosas, 2009].

Starting from Maxwell equations, it is easy to show that the electric (optical) field $\mathbf{E}(x,y,z,t)$ obeys the following vectorial wave equation [Marcuse, 1974]

$$\nabla^2\mathbf{E}_t + \nabla_t(\mathbf{E}\,\nabla \ln n^2) = \frac{n^2}{c^2}\frac{\partial^2\mathbf{E}_t}{\partial t^2}, \tag{P3.2}$$

with $\mathbf{E} = (E_x, E_y, E_z) \equiv (E_t, E_z)$ and $\nabla = (\partial/\partial x, \partial/\partial y, \partial/\partial z) \equiv (\nabla_t, \partial/\partial z)$. Note the presence of a small coupling with the longitudinal component E_z if a longitudinal inhomogeneity is present. But let us focus first on the homogeneous refractive index $n_t(x,y)$. Considering monochromatic guided 1D vector modes with frequency ω, the transverse part of the optical field can be represented by a superposition of vector optical modes of the homogeneous index $n_t(x,y)$, which in complex notation is given by

$$\mathbf{E}_t(x,y,z,t) = \sum_\sigma q_{\sigma c}(z)\boldsymbol{\xi}_{t\sigma}(x,y)\,e^{-i\omega t}, \tag{P3.3}$$

where, for the sake of simplicity we have used σ standing for the modal numbers ν, μ in each transverse direction. Likewise, the z-dependent complex coefficients $q_{\sigma c}(z)$ fulfill $\sum_\sigma |q_{\sigma c}(z)|^2 = 1$, with $\sigma = 1, ..., N$ denoting N modes. Taking into account quasi-TE or quasi-TM modes [Burns and Milton, 1994, Liñares et al., 2008], the normalized transverse complex amplitudes $\boldsymbol{\xi}_{t\sigma}(x,y)$ of the optical modes, obey the following modal equation [Kogelnik, 1988]

$$\nabla_t^2\,\boldsymbol{\xi}_{t\sigma} + k_0^2 n_t^2\,\boldsymbol{\xi}_{t\sigma} + \nabla_t(\boldsymbol{\xi}_{t\sigma}\,\nabla_t(\ln n_t^2)\,) = \beta_{t\sigma}^2\,\boldsymbol{\xi}_{t\sigma}, \tag{P3.4}$$

with $k_0 = \omega/c$ and $\beta_{t\sigma}$ the propagation constant. We stress that $\boldsymbol{\xi}_{t\sigma}$ are vectorial functions fulfilling a *quasi*-complete orthonormalization condition [Liñares et al., 2008].

Let us consider now the refractive index profile given by equation (P3.1), that is, with a longitudinal inhomogeneity. Then, by using the standard assumption for the electric components, $E_z \ll E_x, E_y$, we can apply equations (P3.3) and (P3.4) into (P3.2) and accordingly we obtain for each σ-mode the following amplitude equation

$$\frac{d^2 q_\sigma}{dz^2} + \beta_\sigma^2(z)\,q_\sigma = 0, \tag{P3.5}$$

where $q_\sigma = (q_{\sigma c} + q_{\sigma c}^*)/2$ are the real coefficients of the electric field and we have defined the local propagation constant $\beta_\sigma(z)$ as

$$\beta_\sigma^2(z) = \beta_{t\sigma}^2 + k_0^2\Delta n^2 h^2(z). \tag{P3.6}$$

It is important to outline that equation (P3.5) is exact in the case of TE modes. This equation suggests an spatial harmonic oscillator with a z-dependent spatial frequency and therefore it can be directly derived from spatial type-Hamilton equations where the Hamiltonian is substituted by the Momentum [Liñares et al., 2012], as it is the generator of spatial translations, that is

$$M_\sigma = \frac{1}{2}[p_\sigma^2 + \beta_\sigma^2(z)\, q_\sigma^2], \tag{P3.7}$$

where $p_\sigma = dq_\sigma/dz \equiv q'_\sigma$. This result is analogous to that obtained in [Pedrosa and Rosas, 2009] where time-dependent linear media was studied. The classical Momentum (P3.7) is equivalent to the Hamiltonian of a time-dependent harmonic oscillator, with $\beta(z)$ playing the role of $\omega(t)$. Then, following the principle of quantization of quantum mechanics $(q_\sigma, p_\sigma) \rightarrow (\hat{q}_\sigma, \hat{p}_\sigma)$, where $[\hat{q}_\sigma, \hat{p}_{\sigma'}] = i\hbar\delta_{\sigma\sigma'}$, we obtain the following Momentum operator

$$\hat{M}_\sigma = \frac{1}{2}[\hat{p}_\sigma^2 + \beta_\sigma^2(z)\, \hat{q}_\sigma^2]. \tag{P3.8}$$

This is the generator of quantum spatial propagation in longitudinally inhomogeneous waveguides. Of course, $\hat{q}_\sigma$ plays the role of the quantized electric field and fulfills equation (P3.5). Other central figures in the propagation are the absorption $\hat{a}_\sigma$ and emission $\hat{a}_\sigma^\dagger$ operators. We define them in the following usual way [Kiss et al., 1994]

$$\hat{a}_\sigma(z) = \frac{1}{\sqrt{2\hbar\,\beta_\sigma(z)}}[\beta_\sigma(z)\hat{q}_\sigma + i\hat{p}_\sigma], \tag{P3.9}$$

$$\hat{a}_\sigma^\dagger(z) = \frac{1}{\sqrt{2\hbar\,\beta_\sigma(z)}}[\beta_\sigma(z)\hat{q}_\sigma - i\hat{p}_\sigma]. \tag{P3.10}$$

If operators $\hat{a}_\sigma$ and $\hat{a}_\sigma^\dagger$ are substituted into equation (P3.8), it leads to the well-known expression

$$\hat{M}_\sigma = \hbar \sum_\sigma \beta_\sigma(z)(\hat{n}_\sigma + 1/2), \tag{P3.11}$$

where $\hat{n}_\sigma = \hat{a}_\sigma^\dagger \hat{a}_\sigma$ is the number operator whose eigenstates are the Fock states $|n_\sigma\rangle$. This equation is formally equivalent to that obtained for longitudinally homogeneous waveguides [Liñares et al., 2008].

On the other hand, by taking into account that the vector modal field operator $\mathbf{E}_t$ is proportional to $q_{\sigma c}$, we can write its quantum counterpart applying equations (P3.9) and (P3.10) into (P3.3) through $\hat{q}_{\sigma c} = \sqrt{2\hbar/\beta_\sigma(z)}\ \hat{a}_\sigma$, as follows [Liñares et al., 2008]

$$\hat{\mathbf{E}}_t(x, y, z, t) = \sum_\sigma \sqrt{\frac{\hbar\omega}{T\beta_\sigma(z)}}\boldsymbol{\xi}_{t\sigma}(x, y)\, e^{-i\omega t}\hat{a}_\sigma(z) + \text{h.c.}, \tag{P3.12}$$

where T is the period of the temporal mode, h.c. stands for hermitian conjugate and normalization has been carried out to get appropriate units.

All the above operators are z-dependent, so we have to use the complete Heisenberg equations. Thus, the spatial evolution of the absorption operator $\hat{a}_\sigma$ is given by

$$\frac{d\hat{a}_\sigma}{dz} = \frac{\partial \hat{a}_\sigma}{\partial z} + \frac{i}{\hbar}[\hat{a}_\sigma, \hat{M}_\sigma]. \tag{P3.13}$$

These equations present partial derivatives which do not appear in the homogeneous case. To solve this kind of equations we need to know the relation between the local operators at any z and those at the beginning of the medium, and that is in general a task not easy to carry out analytically [Kiss et al., 1994]. These difficulties can be overcome in the following way. Considering equation (P3.12) together with the definition of $\hat{q}$, via equations (P3.9,P3.10), the quantum version of equation (P3.5) is obtained. Therefore, for a given mode σ, we can write $\hat{q}_\sigma = (\hat{q}_{\sigma c} + \hat{q}^\dagger_{\sigma c})/2$, where $\hat{q}_{\sigma c}$ is the quantized complex electric field. Solution of equation (P3.5) in terms of $\hat{q}_{\sigma c}$ is given by

$$\hat{q}_{\sigma c}(z) = \rho_\sigma \, e^{i\theta_\sigma} \hat{q}_{\sigma c}(0), \tag{P3.14}$$

where ρ_σ and θ_σ are real functions obtained by solving

$$\frac{d^2\rho_\sigma}{dz^2} + \beta_\sigma^2(z)\rho_\sigma = \frac{\beta_{0\sigma}}{\rho_\sigma^3}, \tag{P3.15}$$

$$\frac{d\theta_\sigma}{dz} = \frac{\beta_{0\sigma}}{\rho_\sigma^2}, \tag{P3.16}$$

with $\beta_{o\sigma} \equiv \beta_\sigma(0)$. Equation (P3.15) is an Ermakov-Pinney equation with solutions given by [Pinney, 1950]:

$$\rho_\sigma(z) = [(\beta_{o\sigma}\, u_\sigma(z))^2 + v_\sigma^2(z)]^{1/2}, \tag{P3.17}$$

$$\rho_\sigma(0) = 1, \quad \rho'_\sigma(0) = 0, \tag{P3.18}$$

and where u_σ and v_σ are linearly independent functions that satisfy equation (P3.5) and have the following initial conditions and Wronskian

$$u_\sigma(0) = v'_\sigma(0) = 0, \tag{P3.19}$$

$$u'_\sigma(0) = v_\sigma(0) = 1, \tag{P3.20}$$

$$W_\sigma = u'_\sigma v_\sigma - v'_\sigma u_\sigma = 1. \tag{P3.21}$$

The quantum complex electric field $\hat{q}_c$ and the absorption operator $\hat{a}$ are related by $\beta_\sigma(z)^{1/2}$, as shown by equations (P3.9,P3.10). Therefore, by means of the use of the solution (P3.14) and equation (P3.16), the following solution to equation (P3.13) is obtained:

$$\hat{a}_\sigma(z) = \sqrt{\frac{\beta_\sigma(z)}{\theta'_\sigma(z)}}\, e^{i\theta_\sigma}\, \hat{a}_\sigma(0). \tag{P3.22}$$

With this solution we can rewrite equation (P3.12) in the following way:

$$\hat{\mathbf{E}}_t(x,y,z,t) = \sum_\sigma \sqrt{\frac{\hbar\omega_\sigma}{T_\sigma \theta'_\sigma(z)}}\xi_{t\sigma}(x,y)\, e^{i(\theta_\sigma(z)-\omega t)}\hat{a}_\sigma(0) + \text{h.c.} \tag{P3.23}$$

This equation shows that the real constant of propagation of the mode is $\tilde{\beta}_\sigma = \theta'_\sigma(z)$. Of course the expectation value of this operator for a coherent state recovers the values of the classical electric field.

P3.3. Propagation of quantum light in the optical-field strength space

In this section we will study the spatial propagation along the z-direction in the optical field-strength (OFS) space $\mathcal{E}$ (see appendix A for a brief review). To this end, we calculate the optical propagator in this sort of longitudinally inhomogeneous media by using path integrals. From an optical point of view, this space is highly interesting as it gives us information about the noise and the mean values of the optical field of a quantum light state through the wavefunction $\Psi(\mathcal{E})$. Accordingly, generalized polarization of quantum states can be obtained and analyzed [Barral et al., 2013, Liñares et al., 2011a]. Moreover, the OFS space is the one where homodyne detection is carried out [Vogel, 1990]. On the other hand, from a formal point of view, there are certain quantum states for which recovering the structure of the state after propagation is far complicated in terms of the $\{\hat{a}_\sigma, \hat{a}^\dagger_\sigma\}$ operators, with series of sums and powers sometimes unknown, which are easier to tackle with propagators.

In a recent work, we calculated optical propagators in the OFS space related to linear and nonlinear homogeneous media by means of path integrals [Liñares et al., 2012]. Here we extend this analysis to longitudinally inhomogeneous media. We proceed to define the optical field-strength operator and its canonical conjugate at the initial point of the medium as

$$\hat{\mathcal{E}}_\sigma = \sqrt{\beta_{0\sigma}/2\hbar}\,\hat{q}_\sigma, \quad \hat{\mathcal{P}}_\sigma = \sqrt{2\hbar/\beta_{0\sigma}}\,\hat{p}_\sigma, \tag{P3.24}$$

where $\hat{\mathcal{E}}_\sigma$ fulfills the eigenvalue equation (appendix A) with $\mathcal{E}_\sigma$ and $|\mathcal{E}_\sigma\rangle$ the optical field-strength eigenvalues and eigenstates, respectively. If we know the N-modal quantum state of light $|L\rangle$ at the start of the medium, $\Psi(\boldsymbol{\mathcal{E}}_0; z=0) = \langle \boldsymbol{\mathcal{E}}_0|L\rangle$ in the OFS representation, where $\boldsymbol{\mathcal{E}}_0 = (\mathcal{E}_{01},\ldots,\mathcal{E}_{0N})$ (from now on, bold stands for N-dimensional variables), the wavefunction at some plane $z_f > 0$ can be obtained by the following N-dimensional integral [Feynman and Hibbs, 1965]

$$\Psi(\boldsymbol{\mathcal{E}}_f; z_f) = \frac{(2\hbar)^{N/2}}{b_0^{1/2}} \int_{-\infty}^{+\infty} K(\boldsymbol{\mathcal{E}}_f, \boldsymbol{\mathcal{E}}_0; z_f)\Psi(\boldsymbol{\mathcal{E}}_0)\mathrm{d}\boldsymbol{\mathcal{E}}_0, \tag{P3.25}$$

with $b_0 = \beta_{01} \dots \beta_{0N}$, $\mathcal{E}_f = (\mathcal{E}_{f1}, \dots, \mathcal{E}_{fN})$ and where the integration is performed over all the possible values of $\mathcal{E}_0$. Likewise, the propagator K is given by the path integral

$$K(\mathcal{E}_f, \mathcal{E}_0; z_f) = \frac{(2\hbar)^{N/2}}{b_0^{1/2}} \int_{\mathcal{E}_0}^{\mathcal{E}_f} \mathcal{D}\mathcal{E}(z) e^{-\frac{i}{\hbar} \mathcal{S}(\mathcal{E}_f, \mathcal{E}_0; z_f)}, \tag{P3.26}$$

with $\mathcal{S}$ the action functional. Therefore, the optical propagator K is the sum over all paths $\mathcal{E}(z) = (\mathcal{E}_1(z), \dots, \mathcal{E}_N(z))$ of the quantity $\exp\{(-i/\hbar)\, \mathcal{S}(\mathcal{E}_f, \mathcal{E}_0; z_f)\}$ evaluated on the path connecting the points $\mathcal{E}_0$ and $\mathcal{E}_f$. The action functional is given by $\mathcal{S} = \int_0^{z_f} \mathcal{L}\, dz$, with $\mathcal{L}$ the spatial Lagrangian associated to the problem, that is, the Legendre transformation of the classical Momentum given by equation (P3.7). Rewriting the Momentum in terms of OFS variables $\mathcal{E}$ and $\mathcal{P}$,

$$M = \sum_\sigma \hbar \beta_{0\sigma} \left[\frac{1}{(2\hbar)^2} \mathcal{P}_\sigma^2 + \left(\frac{\beta_\sigma(z)}{\beta_{0\sigma}}\right)^2 \mathcal{E}_\sigma^2\right], \tag{P3.27}$$

where we have kept $\hbar$ because of consistency of units, we obtain the following classical Lagrangian

$$\mathcal{L} = \sum_\sigma \mathcal{P}_\sigma \frac{\partial M}{\partial \mathcal{P}_\sigma} - M = \sum_\sigma \frac{\hbar}{\beta_{0\sigma}} \left[\mathcal{E}_\sigma'^2 - \beta_\sigma^2(z) \mathcal{E}_\sigma^2\right], \tag{P3.28}$$

with $\mathcal{E}_\sigma'$ standing for the generalized velocity. The above Lagrangian is a quadratic one, therefore the exact optical propagator related to longitudinally inhomogeneous waveguides is given by [Liñares, 1989]

$$K(\mathcal{E}_f, \mathcal{E}_0; z_f) = F(z_f)\, e^{-\frac{i}{\hbar} \mathcal{S}(\mathcal{E}_f, \mathcal{E}_0; z_f)}, \tag{P3.29}$$

where $F(z_f)$ is worked out by means of the Van Vleck determinant

$$F(z_f) = \left(\frac{1}{4i\pi\hbar^2}\right)^{N/2} b_0^{1/2} \left(\det \frac{\partial^2 \mathcal{S}}{\partial \mathcal{E}_f\, \partial \mathcal{E}_0}\right)^{1/2}. \tag{P3.30}$$

From (P3.28) it can be easily proved that the general form of the action functional $\mathcal{S}$ in the field-strength space is given by [Liñares, 1989]

$$\mathcal{S}(\mathcal{E}_f, \mathcal{E}_0) = \sum_\sigma \frac{\hbar}{\beta_{0\sigma}} \left[\mathcal{E}_\sigma'(z)\, \mathcal{E}_\sigma(z)\right]\Big|_0^{z_f}. \tag{P3.31}$$

Likewise, the condition for the action $\mathcal{S}$ to assume an extreme value leads to the Euler's equation

$$\mathcal{E}_\sigma'' + \beta_\sigma^2(z) \mathcal{E}_\sigma = 0. \tag{P3.32}$$

This equation is formally analogous to (P3.5), but with a different physical interpretation, as it represents the connection between values of the optical

field-strength of the quantum state at different points of the OFS space, whereas the other one stands for the evolution of the optical mode, which is the spatial support of the quantum state. The general solution of (P3.32) is given by

$$\mathcal{E}_\sigma(z) = \nu_\sigma(z)\mathcal{E}_{0\sigma} + u_\sigma(z)\mathcal{E}'_{0\sigma}, \tag{P3.33}$$

where $\nu_\sigma(z)$ and $u_\sigma(z)$ are N-modal linearly independent functions that satisfy equation (P3.32) and initial conditions (P3.19 - P3.21). Now, by using equation (P3.33) into (P3.31), with initial conditons $\mathcal{E}_\sigma(0) = \mathcal{E}_{0\sigma}$ and $\mathcal{E}_\sigma(z_f) = \mathcal{E}_{f\sigma}$, we obtain the following action functional, or optical propagator phase,

$$\mathcal{S}(\boldsymbol{\mathcal{E}_f}, \boldsymbol{\mathcal{E}_0}) = \sum_\sigma \frac{\hbar}{\beta_{0\sigma} u_\sigma}[u'_\sigma \mathcal{E}^2_{f\sigma} + \nu_\sigma \mathcal{E}^2_{0\sigma} - 2\mathcal{E}_{f\sigma}\mathcal{E}_{0\sigma}], \tag{P3.34}$$

with $\nu_\sigma \equiv \nu_\sigma(z_f)$ and $u_\sigma \equiv u_\sigma(z_f)$. Applying equation (P3.34) into (P3.30), the optical propagator amplitude is obtained. Finally, we can write the propagator (P3.29) as follows

$$K(\boldsymbol{\mathcal{E}_f}, \boldsymbol{\mathcal{E}_0}; z_f) = \left(\frac{i}{2\pi\hbar}\right)^{N/2} \prod_\sigma u_\sigma^{-1/2} \tag{P3.35}$$

$$\exp\{\frac{i}{\beta_{0\sigma} u_\sigma}[u'_\sigma \mathcal{E}^2_{f\sigma} + \nu_\sigma \mathcal{E}^2_{0\sigma} - 2\mathcal{E}_{f\sigma}\mathcal{E}_{0\sigma}]\}. \tag{P3.36}$$

We get a certain generality of the results if we consider the case of a smoothly varying refractive index, in such a way that WKB approximation can be applied to the trajectories equation (P3.32). Indeed, let us consider a slow variation of the gradient parameter over a wavelength, that is, $|h'(z)|/h^2(z) << 1$. Then, the solutions of equation (P3.32) with initial conditions (P3.19-P3.21) are given by [Morse and Feshbach, 1953]

$$u_\sigma(z) = \frac{1}{\sqrt{\beta_{0\sigma}\,\beta_\sigma(z)}}\,\sin\left(\int_0^z \beta_\sigma(\tilde{z})\,d\tilde{z}\right), \tag{P3.37}$$

$$\begin{aligned}\nu_\sigma(z) = \sqrt{\frac{\beta_{0\sigma}}{\beta_\sigma(z)}}\{&\cos\left(\int_0^z \beta_\sigma(\tilde{z})\,d\tilde{z}\right) + \\ &+ \frac{1}{2}\frac{\beta'_{0\sigma}}{\beta^{3/2}_{0\sigma}\sqrt{\beta_\sigma(z)}}\,\sin\left(\int_0^z \beta_\sigma(\tilde{z})\,d\tilde{z}\right)\}.\end{aligned} \tag{P3.38}$$

Therefore, by inserting these WKB solutions into equation (P3.35), the optical propagator for any longitudinally inhomogeneous multimode waveguide is obtained.

Now, in order to gain insight into the quantum light propagation in a longitudinally inhomogeneous waveguide, we study the spatial propagation of a coherent state $|\alpha\rangle$, where $\alpha = |\alpha|e^{i\Phi}$. Firstly, let us consider for

comparison a single-mode longitudinally homogeneous waveguide with (transverse) propagation constant $\beta_t = \beta_o$ at a certain frequency ω. Moreover, let us consider the following representation of the coherent state in the optical field-strength space,

$$\Psi(\mathcal{E}_o;0) = (\frac{2}{\pi})^{1/4} \exp\{-[\mathcal{E}_o - |\alpha| \cos\phi]^2\} e^{-i\delta_o}, \tag{P3.39}$$

with $\delta_o = \sin\phi\,[|\alpha|^2 \cos\phi - 2|\alpha|\mathcal{E}_o]$, and where, for the sake of simplicity, the subindex σ has been withdrawn. Note that the optical noise, or quantum fluctuations of the optical field, equals one for a coherent state in this representation. The propagation of this state in the OFS space is obtained by inserting equations (P3.35) and (P3.39) into equation (P3.25), and by using the functions $u(z) = \text{sen}\beta_o z/\beta_o$ and $v(z) = \cos\beta_o z$, solutions of (P3.32) in the limit of $\beta(z) = \beta_o$. Therefore, after a straightforward calculation it is obtained

$$\begin{aligned}\Psi(\mathcal{E}_f;z_f) = (\frac{2}{\pi})^{1/4} \exp\{-[\mathcal{E}_f - |\alpha| \cos(\phi + \beta_o z)\,]^2\} \\ \exp\{-i(\delta_z - \beta_o z/2),\end{aligned} \tag{P3.40}$$

with $\delta_z = \sin(\phi + \beta_o z)\,[|\alpha|^2 \cos(\phi + \beta_o z) - 2|\alpha|\,\mathcal{E}_f]$. So the quantum state keeps coherent after propagation in the single-mode homogeneous waveguide with transverse propagation constant β_o, as expected.

On the other hand, let us consider that before $z = 0$ we have a longitudinally homogeneous guide, and after $z = 0$ there is a longitudinally inhomogeneous guide characterized by an arbitrary local propagation constant $\beta(z)$ fulfilling $\beta(0) = \beta_o$. Again, by inserting equation (P3.35) for a single-mode guide and equation (P3.39) into (P3.25), and after a long but straightforward calculation, we obtain the following wavefunction at the end of the waveguide

$$\begin{aligned}\Psi(\mathcal{E}_f;z_f) = (\frac{2}{\pi})^{1/4} \rho^{-1/2} \exp\{-[\frac{\mathcal{E}_f}{\rho} - |\alpha| \cos(\phi + \theta)\,]^2\} \\ \exp\{-i(\frac{\rho'}{\beta_0 \rho}\mathcal{E}_f^2 + \delta)\}\, e^{i\theta/2},\end{aligned} \tag{P3.41}$$

with $\delta = \sin(\phi + \theta)\,[|\alpha|^2 \cos(\phi + \theta) - 2|\alpha|\,\mathcal{E}_f/\rho]$, and where the following relationships have been used

$$v(z) = \rho\,\cos\,\theta, \qquad \beta_0\, u(z) = \rho\,\sin\,\theta. \tag{P3.42}$$

In the case of smooth index variation, by using the WKB approximation via equations (P3.37) and (P3.38), we can write these functions in approx-

imated form as

$$\rho(z) \approx \sqrt{\frac{\beta_0}{\beta(z)} + \frac{1}{2}\frac{\beta_0'}{\beta_0\beta(z)}\,\sin(2\int_0^z \beta_\sigma(\tilde{z})\,d\tilde{z})}, \tag{P3.43}$$

$$\theta(z) \approx \arctan\Big\{\frac{\tan\int_0^z \beta_\sigma(\tilde{z})\,d\tilde{z}}{1+\frac{\beta_o'}{\beta_o}\tan\int_0^z \beta_\sigma(\tilde{z})\,d\tilde{z}}\Big\}. \tag{P3.44}$$

Hence, the wavefunction (P3.41) shows squeezing and acquires a global quantum phase $\theta/2$ and a phase delay θ (corresponding to a time delay $t_d = \theta/\omega$), which, in this case, is the modal classical phase. However, as it was stated for single discontinuities, this squeezing can not be measured [Abram, 1987, Glauber and Lewenstein, 1991], and therefore it should be identified as virtual squeezing. Likewise, more consequences related to quantum phases will appear for other quantum states, as we will show below. In our case the inhomogeneous medium can be regarded as a continuous succession of effective (waveguiding medium) discontinuities, so we can interpret that the coherent state has undergone virtual squeezing accumulated under spatial propagation and, in a certain sense, it leaves its effect by producing different phase changes. Besides, it is important to outline that this kind of result is formally analogous to that obtained in [Yeon et al., 1994] for the mechanical time-dependent harmonic oscillator, where the wavefunction is squeezed after temporal evolution with a change in frequency. However, the physical interpretation is quite different. In any case, all these considerations show that t (time) and z-dependent problems are not trivially related in quantum optics as it is usually considered. In the next section we will discuss this result thoroughly.

P3.4. Virtual squeezing of coherent states

In this section we will analyze the result obained above, that is, quantum state squeezing after propagation in a z-dependent medium. As was pointed out by Abram in his seminal paper about the quantization of light in dielectric media [Abram, 1987], a quantum state propagating in a dielectric seems to be squeezed when it is represented in a free-space photons basis, but inside a dielectric there is no experiment that can detect these free space photons. In fact, Abram claims that these are virtual photons. The same problem would appear between two dielectric media. In our case, we have a longitudinally continuous change of the refractive index and therefore we expect a continuous squeezing. In the same spirit, an interesting discussion about quantization in a dielectric was carried out by Glauber and Lewenstein [Glauber and Lewenstein, 1991], stressing the fact that measurement based on photoabsorption processes is always carried out in the basis which diagonalizes the Hamiltonian in every medium, as the correlation product fulfills normal ordering, and hence the photocount

distribution as well. This fact results from the physical property of photo-absorption, that is, the energy of the field decrease when a photon is absorbed. This statement is closely related with Abram's idea. Likewise, in this study is introduced the unitary transformation between the eigenbasis of the dielectric and an expansion based on plane waves standard for free space. This transformation eliminates the virtual squeezing. We will look for an analogous transformation in this section.

Our primary objective is to find a physical argument to withdraw the virtual squeezing due to the virtual photons. We show that the above interpretations come together to indicate that a scale physical transformation is implemented by the medium. In fact, by inspection of equation (P3.41) we observe that noise squeezing disappears if a scale change is made in the variable $\mathcal{E}$. Indeed, let us consider the interface between two dielectric homogeneous media with refractive indices n_1 and n_2 when, for the sake of simplicity and without loss of generality, reflection is neglected. From photon flux conservation we have (see appendix B)

$$\sqrt{n_1}\,\hat{q}_1 = \sqrt{n_2}\,\hat{q}_2, \tag{P3.45}$$

where $\hat{q}_1$ and $\hat{q}_2$ are the optical fields quantized in every medium up to constants. Moreover, since we use a wavefunction in the OFS space, the above relationship is also fulfilled by their eigenvalues, that is, $\sqrt{n_1}q_1 = \sqrt{n_2}q_2$. This scale transformation has to be accomplished at every discontinuity the wavefunction finds during propagation. As we are dealing with optical modes, we will have a continuous longitudinal change of an effective refractive index. Likewise, in a good approximation, the modal reflection can be neglected differentially (that is, between two very close points z_1 and z_2), because of the mentioned continuous change. Therefore we can rewrite the above equations by using effective refractive indices, and σ-mode propagation constants as well, that is

$$\frac{\sqrt{\beta_1}}{2\hbar}\,\hat{q}_{1\sigma} = \frac{\sqrt{\beta_2}}{2\hbar}\,\hat{q}_{2\sigma}, \tag{P3.46}$$

where $\beta = k_o N$ is the modal propagation constant of the propagating mode and N the its effective refractive index. Of course, performing this scale change differentially in the propagator we would eliminate the squeezing at each plane z and none signature of it would be obtained. In short, the squeezing in these media is virtual, not real.

This scale change can be performed once the propagation has been carried out, that is, on the state given by equation (P3.41). If we take into account our definition of the optical field-strength operator (P3.24) and the invariant (P3.16), we can write

$$\frac{\mathcal{E}_f}{\rho} = \sqrt{\frac{\beta_0}{2\hbar\rho^2}}\,\hat{q}\,(z_f) = \sqrt{\frac{\theta'}{2\hbar}}\,q_f \equiv \sqrt{\frac{\tilde{\beta}}{2\hbar}}\,q_f. \tag{P3.47}$$

Let us recall that $\tilde{\beta}$ is the real propagation constant of the optical mode as it was shown in (P3.23). Therefore, at the end of the z-inhomogeneous medium there is an effective (or real) discontinuity at $z = z_f$, such that from this plane the medium has a transverse propagation constant β_e, then equation (P3.46) can be written as

$$\frac{\mathcal{E}_f}{\rho} = \frac{\sqrt{\tilde{\beta}}}{2\hbar}\, q_f = \frac{\sqrt{\beta_e}}{2\hbar}\, q_e \equiv \mathcal{E}_e \tag{P3.48}$$

This is one of the main result of this work. Thus, by taking into account this relationship, that is $\mathcal{E}_f = \rho\, \mathcal{E}_e$, the wavefunction given by equation (P3.41) can be rewritten as

$$\begin{aligned}\Psi(\mathcal{E}_e; z_f) = (\frac{2}{\pi})^{1/4}\, \exp\{-[\mathcal{E}_e - |\alpha|\, \cos(\phi+\theta)\,]^2\} \\ \exp\{-i(\frac{\rho\rho'}{\beta_0}\mathcal{E}_e^2 + \delta_e\}\, e^{i\theta/2},\end{aligned} \tag{P3.49}$$

with $\delta_e = \sin(\phi+\theta)\,[|\alpha|^2 \cos(\phi+\theta) - 2|\alpha|\, \mathcal{E}_e]$. Therefore the quantum fluctuations are again equal to one, that is, there is no squeezing. Note that the prefactor $\rho^{-1/2}$ in equation (P3.41), has also been cancelled because of normalization. However, the wavefunction (P3.49) still presents a quadratic phase term in the field-strength which would produce squeezing under temporal evolution of the state. This phase is an artifact resulting from the use of a propagator which does not rescale the variables at each z. Hence, for the sake of consistency, this phase is not compatible with no squeezing or, in other words, it is not compatible with relationship (P3.46), and consequently has to be eliminated. By means of a gauge transformation $\exp\{i(\frac{\rho'}{\beta_0\rho})\hat{\mathcal{E}}_e^2\}$ on the wavefunction (P3.49), we obtain

$$\begin{aligned}\Psi(\mathcal{E}_e; z_f) = (\frac{2}{\pi})^{1/4}\, \exp\{-[\mathcal{E}_e - |\alpha|\, \cos(\phi+\theta)\,]^2\} \\ \exp\{-i\delta_e\}\, e^{i\theta/2}.\end{aligned} \tag{P3.50}$$

Therefore we can say that the state has undergone virtual squeezing, as it recovers the coherent shape. Moreover, the quantum state given by equation (P3.50) is the one we would measure by means of photodetectors placed just at the end of the medium, that is, a coherent one with an OFS mean value shifted by an amount θ, and also a global z-dependent phase whose effect could be observed in quantum interference experiments. This example clearly reflects how time-dependent Hamiltonians and z-dependent Momentum operators present different behaviours, which underlines the importance of a quantum theory of light propagation.

On the other hand, equation (P3.50) enables us to justify, in a heuristic way, the optical propagator in a longitudinally inhomogeneous medium.

That is, the above state (P3.50), analogous to (P3.40), is obtained if we rewrite the optical propagator given by equation (P3.35) for a single-mode guide, as follows

$$K(\mathcal{E}_f, \mathcal{E}_0; z_f) = (\frac{i}{2\pi\hbar})^{1/2} (\sin\theta)^{-1/2}$$
$$\exp\{\frac{i}{\sin\theta}[\cos\theta(\mathcal{E}_f^2 + \mathcal{E}_0^2) - 2\mathcal{E}_f\mathcal{E}_0]\}. \tag{P3.51}$$

This is another important result. Indeed, this optical propagator can also be obtained formally by propagating Fock states from $z = 0$. Let us recall that in the optical field-strength space the number states are represented by Hermite-Gaussian functions in the following way

$$\Psi_n(\mathcal{E}_0; 0) = (\frac{2}{\pi})^{1/4} \frac{1}{(2^m m!)^{1/2}} \exp\{-\mathcal{E}_0^2\} H_n(\sqrt{2}\mathcal{E}_0). \tag{P3.52}$$

By means of the single-mode optical propagator given by equation (P3.35), the propagation of these states are worked out. Next, the virtual squeezing is cancelled as it is showed above for coherent states. Finally, by using Mehler's formula, the expression for the optical propagator given by equation (P3.51) is obtained.

In addition, it is worth underlining that after these derivations and results, we can state that the naive variable change given in (P3.24), $\mathcal{E} = \sqrt{\beta_o/2\hbar}\, q$, has a clear physical value. It is the transformation cancelling squeezing between different homogeneous media and in general in longitudinally graded index media, consequence of the scale physical transformation obtained in Appendix B.

P3.5. Quantum Gouy's phase and Infeld-Plebanski transformation

In this section we will analyze in detail the effect left by virtual squeezing on quantum states of light. We choose a single-mode squeezed state in order to make clear these effect, in particular, the acquisition of quantum Gouy's phases. We use this denomination as formally analog phases arise in the classical domain [Boyd, 1980], but here we will show how fully quantum phases are obtained in longitudinally inhomogeneous waveguides. Likewise, we will show how the scale change and phase cancellation introduced in the above section can be formulated in terms of unitary Infeld-Plebanski transformations [Infeld and Plebanski, 1955].

Quantum Gouy's phase

In the case of a squeezed state of light propagating in a z-inhomogeneous medium more interesting results are obtained. Let us consider, for instance,

the one generated in a parametric amplifier [Barral et al., 2013, Liñares et al., 2012], whose quantum noise at $z = 0$ is $\Delta\mathcal{E}_o^2 \neq 1$, given by

$$\Psi(\mathcal{E}_o; 0) = (\frac{2}{\pi\Delta\mathcal{E}_o^2})^{1/4} \exp\{-\frac{1}{\Delta\mathcal{E}_o^2}[\mathcal{E}_0 - |\alpha|\cos\phi]^2\} e^{-i\delta_o}, \tag{P3.53}$$

with $\delta_o = \sin\phi\,[|\alpha|^2\cos\phi - 2|\alpha|\mathcal{E}_o]$. Once more, by inserting equations (P3.35) and (P3.53) into (P3.25), after a long but straightforward calculation and by carrying out both the scale change and the quadratic phase cancellation, we obtain the following normalized wave function at the end of the waveguide

$$\begin{aligned}\Psi(\mathcal{E}_e; z_f) = (\frac{2}{\pi})^{1/4}(\frac{\rho}{\Delta\mathcal{E}_o\rho_s})^{1/2}\, e^{i\theta_s/2} e^{-i\delta_s} \\ \exp\{-\frac{1}{\Delta\mathcal{E}_o^2\,(\rho_s/\rho)^2}[\mathcal{E}_e - |\alpha|\,\cos(\phi+\theta)\,]^2\},\end{aligned} \tag{P3.54}$$

where

$$\frac{\rho_s}{\rho} = [\cos^2\theta + \mathrm{sen}^2\theta\,/\Delta\mathcal{E}_o^4]^{1/2}, \tag{P3.55}$$

$$\theta_s = \arctan(\tan\theta/\Delta\mathcal{E}_o^2). \tag{P3.56}$$

We should stress that the same result is obtained by using the optical propagator (P3.51). Note that no new squeezing appears. However, like in the coherent case, the oscillation period has changed due to the function $\theta(z)$ (phase delay) as expected, and therefore the squeezing oscillation, the distance where quantum noise value is repeated, has changed as well. Likewise, equation (P3.56) indicates that the quantum phase θ_s obtained in (P3.54) is different from the modal phase θ. This phase is analog to Gouy's phase in classical optics [Boyd, 1980], so it can be called quantum Gouy's phase. This phase has not any classical counterpart because it depends on the characteristics of the quantum light state, in this case on the optical noise parameter $\Delta\mathcal{E}_o^2$.

Infeld-Plebanski transformation

Let us consider again equation (P3.41). Firstly, as it was shown above, cancellation of the optical noise squeezing is obtained because a scale physical transformation is implemented by the medium, due to photon flux conservation. From a formal point of view, this scale transformation can be represented by the squeeze operator, that is

$$\hat{S}(\xi) = \exp\{\frac{\xi}{2}(\hat{a}^2 - \hat{a}^{\dagger 2}\} = \exp\{i\frac{\xi}{2}(\hat{\mathcal{E}}_f\hat{\mathcal{P}}_f + \hat{\mathcal{P}}_f\hat{\mathcal{E}}_f\}, \tag{P3.57}$$

where in our case $\xi = \ln \rho$. Likewise, for the sake of physical consistency, a conjugated quadratic phase is introduced by the inhomogeneous medium, that is the following unitary transformation

$$\hat{P}(\rho) = \exp\{i(\frac{\rho'}{\beta_0 \rho})\hat{\mathcal{E}}_f^2\}. \tag{P3.58}$$

Therefore, the total operator is given by the expression

$$\hat{\mathcal{T}}_\rho = \hat{S}(\ln \rho)\hat{P}(\rho). \tag{P3.59}$$

But this transformation is just the unitary Infeld-Plebanski transformation [Infeld and Plebanski, 1955], which is used in sequeezing optical processes as a way to simplify calculations [Fernández Guasti and Moya-Cessa, 2003]. However, in this case, it is a real transformation implemented by the longitudinally inhomogeneous medium. Therefore, by employing directly this transformation over state given by equation (P3.41), equation (P3.50) is obtained. In short, by applying equations (P3.25) and (P3.35) to any input quantum state expressed in the optical field-strength space, and performing the unitary transformation (P3.59) to the corresponding result, a real expression for spatial propagation in longitudinally inhomogeneous media is obtained.

P3.6. Propagation of Bessel-Gauss quantum light states

Finally, in order to illustrate the behaviour of higher-dimension quantum states, in this section we will study the effects an specific longitudinally inhomogeneity causes on two-mode quantum states such as Barut-Girardello quantum states [Barut and Girardello, 1971].

Let us choose a two-mode waveguide whose refractive index is given by the following parametrized local propagation constant

$$\beta^2(z) = \beta_{t0}^2 + k_0^2 \Delta n^2 h_\pm^2(z) = k_0^2 \Delta n^2 \frac{\Gamma_0^2}{\gamma_\pm^r(z)}, \tag{P3.60}$$

where β_{t0} is the transverse single-mode propagation constant, $\gamma_\pm(z) = 1 \pm \frac{z}{L}$ and Γ_0, L and r are free parameters. These parameters define a family of axial graded index enabling us to get the best fit to the longitudinal inhomogeneity if needed.

By substituing (P3.60) in equation (P3.32) we obtain the following solutions [Gómez-Reino et al., 1986]

$$\begin{aligned} u_\pm(z) = \frac{\gamma_\pm^{1/2}(z)}{W_0^\pm} \\ \{Y_{1/(2-r)}(\frac{\beta_0 L}{1-\frac{r}{2}})\, J_{1/(2-r)}[\frac{\beta_0 L}{1-\frac{r}{2}}\gamma_\pm^{1-r/2}(z)] \\ -J_{1/(2-r)}(\frac{\beta_0 L}{1-\frac{r}{2}})\, Y_{1/(2-r)}[\frac{\beta_0 L}{1-\frac{r}{2}}\gamma_\pm^{1-r/2}(z)]\}, \end{aligned} \tag{P3.61}$$

$$
\begin{aligned}
\nu_{\pm}(z) &= \frac{\gamma_{\pm}^{1/2}(z)}{W_0^{\pm}} \\
\Big\{ &- Y_{1/(2-r)}\Big(\frac{\beta_0 L}{1-\frac{r}{2}}\Big)\, J_{1/(2-r)}\Big[\frac{\beta_0 L}{1-\frac{r}{2}}\,\gamma_{\pm}^{1-r/2}(z)\Big] \\
&+ J_{1/(2-r)}\Big(\frac{\beta_0 L}{1-\frac{r}{2}}\Big)\, Y_{1/(2-r)}\Big[\frac{\beta_0 L}{1-\frac{r}{2}}\,\gamma_{\pm}^{1-r/2}(z)\Big]\Big\},
\end{aligned}
\tag{P3.62}
$$

where $\beta_0 = \pm\, k_0 \Delta n\, \Gamma_0$ fulfilling $\beta_0 > 0\,(\beta_0 < 0)$ if $1 - r/2 > 0\,(1 - r/2 < 0)$, $J_{1/(2-r)}$ and $Y_{1/(2-r)}$ are the $1/(2-r)$-order Bessel functions of the first and second kind, respectively, and $W_0^{\pm}$ is the Wronskian of $\gamma_{\pm}^{1/2}(z)\, J_{1/(2-r)}$ and $\gamma_{\pm}^{1/2}(z)\, Y_{1/(2-r)}$ evaluated at $z = 0$, and it is given by

$$
W_0^{\pm} = \begin{cases} \pm\frac{2}{L\pi} & \text{for } 1/(2-r) \text{ integer,} \\ \mp\frac{2\,\sin(\frac{\pi}{2-r})}{L\,\pi} & \text{for } 1/(2-r) \text{ not an integer.} \end{cases}
\tag{P3.63}
$$

We can check a particular case of this family of axial graded index in a single-mode waveguide. We choose $r = 4$ and the negative sign. In this case the general solutions (P3.61) and (P3.62) become a combination of trigonometrical functions given by

$$
u(z) = \frac{\gamma}{\beta_0}\,\sin\Big(\frac{\beta_0 z}{\gamma}\Big),
\tag{P3.64}
$$

$$
v(z) = \gamma\,\Big[\cos\Big(\frac{\beta_0 z}{\gamma}\Big) + \frac{1}{\beta_0 L}\,\sin\Big(\frac{\beta_0 z}{\gamma}\Big)\Big],
\tag{P3.65}
$$

with $\gamma \equiv \gamma_-(z)$. Therefore waveguides with this axial graded index have the following $\rho(z)$ and $\theta(z)$ functions

$$
\rho = \gamma^{1/2}\Big[1 + \frac{1}{\beta_0 L}\,\sin(2\beta_0 z/\gamma) + \frac{1}{(\beta_0 L)^2}\,\sin^2(\beta_0 z/\gamma)\Big]^{1/2},
\tag{P3.66}
$$

$$
\theta = \arctan\Big(\frac{\sin(\beta_0 z/\gamma)}{\cos(\beta_0 z/\gamma) + \frac{1}{\beta_0 L}\,\sin(\beta_0 z/\gamma)}\Big).
\tag{P3.67}
$$

On the other hand, as an example of a non-usual quantum state propagating in this medium, we choose the Barut-Girardello quantum states [Barut and Girardello, 1971]. These states are associated to the $SU(1,1)$ group and are also called coherent because they are eigenstates of the lowering operator $\hat{K}_-$ of this algebra in the following way

$$
\hat{K}_-|\alpha,\, m\rangle = \alpha^2|\alpha,\, m\rangle,
\tag{P3.68}
$$

with α a complex number. In terms of two-mode circular optical field-strength variables $\mathcal{E}_o = [\mathcal{E}_1^2 + \mathcal{E}_2^2]^{1/2}$ and $\varphi = \arctan(\mathcal{E}_2/\mathcal{E}_1)$, these states are given by [Hacyan, 2008]

$$
\Psi_{\alpha,m}(\mathcal{E}_o, \varphi; t) = \frac{C_m}{\Delta r}\, J_{|m|}\Big(\frac{2\sqrt{2}\,\alpha\,\mathcal{E}_o}{\Delta\mathcal{E}_o}\Big)\, e^{-\frac{\mathcal{E}_o^2}{\Delta\mathcal{E}_o^2}}\, e^{i\,(m\varphi+\phi)},
\tag{P3.69}
$$

with $C_m = [\pi I_{|m|}(2\alpha^2)\, e^{-2\alpha^2}/2]^{1/2}$ and where m can be referred as an abstract angular momentum quantum number in the OFS space, J_m and I_m the Bessel and modified Bessel functions of order m, respectively, and $\Delta\mathcal{E}_o^2$ the quantum "radial" optical noise, with value 1 in the case of a coherent state, or different from 1 after passing by a nonlinear medium carrying out equal squeezing in both modes, as two nonlinear twin waveguides performing as degenerate parametric amplifiers. Because of the shape of (P3.69) in the OFS space, we call them Bessel-Gauss quantum states.

If this quantum state of light is propagated in a two-mode waveguide (for instance, the fundamental modes quasi-TE and quasi-TM) with the axial graded index presented above with solutions (P3.66, P3.67) in both modes, that is, two degenerated modes ($\beta_1 = \beta_2$), the propagator (P3.35) can be written as

$$K(\mathcal{E}_f, \Phi_f, \mathcal{E}_0, \Phi_0; z_f) = \frac{i}{2\pi\hbar\, u_f}\, e^{\frac{i}{\beta_0 u_f}[u'_f\, \mathcal{E}_f^2 + \nu_f\, \mathcal{E}_o^2 - 2\,\mathcal{E}_o\, r_f\, cos(\Phi_f - \Phi_0)]}, \tag{P3.70}$$

which is analogous to the Collins diffraction integral for ABCD media. Therefore, by substituting equations (P3.69) and (P3.70) into equation (P3.25), and performing the unitary transformation (P3.59), the following relationship is obtained

$$\Psi_{\alpha,m}(\mathcal{E}_e, \varphi_f; z_f, t) = C_m \frac{\rho}{\rho_{sq}} J_{|m|}(2\sqrt{2}\,\alpha \frac{\rho}{\rho_{sq}}\,\mathcal{E}_e\, e^{i\theta}) \; e^{-(\frac{\rho}{\rho_s}\frac{\mathcal{E}_e}{\Delta\mathcal{E}_o})^2}\, e^{i(m\varphi_f + \Phi)}\, e^{-(\frac{1}{\rho_s^2})(\frac{\sqrt{2}\alpha\beta_0 u}{\Delta\mathcal{E}_o})^2}\, e^{i\theta_s}\, e^{i\theta_\alpha}, \tag{P3.71}$$

where

$$\frac{\rho_s}{\rho} = [\cos^2\theta + \mathrm{sen}^2\theta\,/\Delta\mathcal{E}_o^4]^{1/2}, \tag{P3.72}$$

$$\theta_s = \arctan(\tan\theta/\Delta\mathcal{E}_o^2), \tag{P3.73}$$

$$\theta_\alpha = (\frac{2\alpha^2\beta_0\, u}{\Delta\mathcal{E}_o^2})(u' + u\rho'_s/\rho_s). \tag{P3.74}$$

Note that for $\Delta\mathcal{E}_o^2 \neq 1$ we have squeezing. Again, the Gouy's quantum phase θ_s is different from the classical one θ. This is depicted in Figure 1 for the medium above introduced with $r = 4$, minus sign, $\Gamma_0 = 1.515/\Delta n$, $L = 3.5$ and arbitrary units of length. There we can see how different input squeezings lead to different amounts of Guoy's phase for the same propagation length. Likewise, in this case we have new quantum phases, θ_α, which are related as well with quantum state parameters, in particular, with the optical noise $\Delta\mathcal{E}_o^2$ and the eigenvalue α^2. In the limit of a coherent state ($\Delta\mathcal{E}_o^2 = 1$) and a longitudinally homogeneous waveguide, this phase takes the value $\theta_\alpha = (\alpha\beta_o)^2 \sin(2\beta_o)$. Obviously the z-dependent medium

has modified this phase. It is important to outline that this effect could be meaningful in the case of quantum states of light being used in photonic circuits where phase shifters are based on these effects. As these devices are usually calibrated clasically, they would work differently from expected, turning out in an error inherent to the system. So this effect would have to be taken into account in the design. Finally, it is important to remark that even in the case of an input coherent SU(1,1) state with $\Delta\mathcal{E}_o^2 = 1$, the result of Gouy's phase would not be obvious in other quantum representations, showing the power of this approach in dealing with some kinds of quantum states.

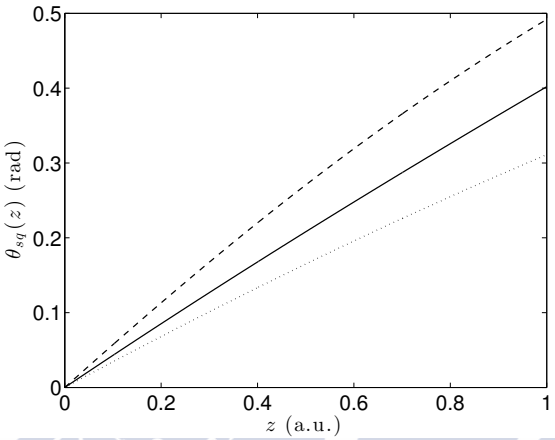

Figure P3.1: Evolution of the quantum Guoy's phase θ_s in longitudinally inhomogeneous medium for a coherent (solid line) and squeezed states of light with $\Delta\mathcal{E}_o^2 = 5/4$ (dotted line) and $\Delta\mathcal{E}_o^2 = 3/4$ (dashed line).

P3.7. Summary

In this work we have studied the propagation of quantum states of light in separable longitudinally inhomogeneous media, in particular, in single-mode and two-mode waveguides. The study is based on the Momentum operator and the optical propagator in the optical field-strength space $\mathcal{E}$. The optical propagator has been obtained by means of the path integral formalism and, in particular, WKB trajectories for the propagator have been given in order to give generality to the results. Next, we have shown that a virtual squeezing appears in these media and have justified its cancellation by using a scale physical transformation provided by photon flux conservation. This contains the classical limit corresponding to the continuity of the product between the optical field and the square root of the refractive index. Furthermore, we have discussed how the quadratic phases related to virtual squeezing have to be cancelled by a conjugate transformation due to

physical consistency. The product of these transformations is just the unitary Infeld-Pleblanski one, so we have concluded these media implement this transformation, cancelling the virtual squeezing. Likewise, we have demonstrated that this virtual squeezing leaves its effect on the quantum light state by generation of quantum Gouy's phases and that the shape of these phases depends on the input quantum state. Finally, we have illustrated these results by analyzing two-mode squeezed states in a power-law parametric family of longitudinally inhomogeneous waveguiding media.

P3.8. Appendix A

Taking into account the following quantum-optical units $T\|\xi_\sigma\|^2/\hbar\omega = 1$, we define the following rescaled operators, so-called canonical optical field-strength and momentum operators for each mode σ of the field [Liñares et al., 2012]

$$\hat{\mathcal{E}}_\sigma = \sqrt{\frac{\beta_\sigma}{2\hbar}}\,\hat{q}_\sigma, \quad \hat{\mathcal{P}}_\sigma \equiv -i\hbar\frac{\partial}{\partial \mathcal{E}_\sigma} = \sqrt{\frac{2\hbar}{\beta_\sigma}}\,\hat{p}_\sigma, \tag{P3.75}$$

which fulfill the following commutation relation

$$[\hat{\mathcal{E}}_\sigma, \hat{\mathcal{P}}_{\sigma'}] = i\hbar\delta_{\sigma,\sigma'}. \tag{P3.76}$$

The OFS operator fulfills the following eigenvalue equation [Welsch et al., 1999]

$$\hat{\mathcal{E}}_\sigma|\mathcal{E}_\sigma\rangle = \mathcal{E}_\sigma|\mathcal{E}_\sigma\rangle, \tag{P3.77}$$

with $\mathcal{E}_\sigma$ and $|\mathcal{E}_\sigma\rangle$ the optical field-strength eigenvalues and eigenstates, respectively. Hence, an electric field in such a state has a well defined amplitude. The space formed by these eigenstates can be used to represent any quantum state by means of the following orthogonality and closure relations

$$\langle\mathcal{E}_\sigma|\mathcal{E}'_{\sigma'}\rangle = \delta(\mathcal{E}-\mathcal{E}')\,\delta_{\sigma,\sigma'}, \tag{P3.78}$$

$$\int |\mathcal{E}_1,\ldots,\mathcal{E}_N\rangle\,\langle\mathcal{E}_1,\ldots,\mathcal{E}_N|\,d\mathcal{E}_1\ldots d\mathcal{E}_N = \hat{1}. \tag{P3.79}$$

Likewise, it is important to outline that both OFS canonical operators are equivalent to the field quadratures for $\hbar = 1/2$. Following this prescription, we can define the rotated OFS operator for the mode σ

$$\hat{\mathcal{E}}_\theta = \hat{\mathcal{E}}\cos\theta + \hat{\mathcal{P}}\sin\theta, \tag{P3.80}$$

with $0 \leqslant \theta < \pi$ and where $\hat{\mathcal{E}}_0 \equiv \hat{\mathcal{E}}$ and $\hat{\mathcal{E}}_{\pi/2} \equiv \hat{\mathcal{P}}$ are the field quadratures. This operator fulfills as well the relations (P3.77) and (P3.78) for a given

θ. In terms of the above-mentioned quantum-optical units, this operator is equivalent to the quantum field operator (P3.12) for $\theta = \omega t + \delta(z)$, with $\delta(z)$ the phase gained after propagation. This relation is very important as the difference photocurrent obtained in homodyne measurements is proportional to rotated OFS values [Barral and Liñares, 2015]. Furthermore, the probability distribution in the N-dimensional optical field-strength space, is given by

$$P(\mathcal{E}) = Tr\{\hat{\rho}\ |\mathcal{E}_1, \ldots, \mathcal{E}_N\rangle\langle\mathcal{E}_1, \ldots, \mathcal{E}_N|\}. \tag{P3.81}$$

where $\hat{\rho}$ is the density operator which defines the quantum state and *Tr* stands for the trace operation.

The main advanges of this distribution are two [Welsch et al., 1999]: it is a well-behaved probability distribution for the field strength $\mathcal{E}$ and it can be directly measured by homodyne detection. Other distributions like the generalized quasi-probability distributions are not distributions of measured quantities, but they can be obtained from a set of OFS distributions. Likewise, the density matrices can be as well obtained as two-fold Fourier transforms of OFS distributions. Moreover, the propagation of the wavefunctions defined in this space is easily tacked by means of optical propagators (P3.25, P3.26).

P3.9. Appendix B

Photon flux conservation, or equally photon number conservation, at a discontinuity between two media with indices n_1 and n_2, is equivalent to an unitary transformation between the operators absorption $\hat{a}$ at both sides of it:

$$\begin{pmatrix} \hat{a}_i \\ \hat{a}_f \end{pmatrix} = \begin{pmatrix} T^{1/2} & -R^{1/2} \\ R^{1/2} & T^{1/2} \end{pmatrix} \begin{pmatrix} \hat{a}_t \\ \hat{a}_r \end{pmatrix}, \tag{P3.82}$$

where i, t and r stands for input, transmitted and reflected, respectively, and $T + R = 1$. In this transformation we have introduced a fictitious mode f in order to preserve commutation relations [Gerry and Knight, 2005]. Inverting this equation we have for the transmitted mode:

$$\hat{a}_t = T^{1/2}\hat{a}_i + R^{1/2}\hat{a}_f. \tag{P3.83}$$

From equations (P3.9-P3.10) for an homogeneous medium, we have $\hat{q}_j = \sqrt{\hbar/2\beta_j}(\hat{a}_j + \hat{a}_j^\dagger)$, with $\beta_j = k_0 n_j$ where $j = t, i, f$. Therefore we can write:

$$\sqrt{n_t}\,\hat{q}_t = T^{1/2}\sqrt{n_i}\,\hat{q}_i + R^{1/2}\sqrt{n_t}\,\hat{q}_f. \tag{P3.84}$$

If the refractive index in the interface varies gradually between n_i and n_t, reflections can be neglected such that $T = 1$, obtaining:

$$\sqrt{n_t}\,\hat{q}_t = \sqrt{n_i}\,\hat{q}_i. \tag{P3.85}$$

Note that this relationship is the classical one for optical fields at a discontinuity when q is taken as the classical optical field.

P4. QUANTUM LIGHT PROPAGATION IN LONGITUDINALLY INHOMOGENEOUS MEDIA AS A SPATIAL LEWIS-ERMAKOV PHYSICAL INVARIANCE

Submitted to OPTICS COMMUNICATIONS

BY DAVID BARRAL & JESÚS LIÑARES

UNIVERSIDADE DE SANTIAGO DE COMPOSTELA

Abstract: *We study the propagation of quantum states of light in separable longitudinally inhomogeneous media. By means of the usual quantization approach this kind of media would lead to the unphysical result of quantum noise squeezing. This problem is solved by means of generalized canonical transformations in a comoving frame. Under these transformations the generator of propagation is a physical Lewis-Ermakov invariant in space which is quantized and, accordingly, a propagator consistent with experiments is obtained. Finally, we show that the net effect produced by propagation in these media is a quantum Gouy's phase with application in quantum interferometry.*

P4.1. Introduction

In the last years great attention has been drawn to the time dependent quantum harmonic oscillator. This problem has been thoroughly studied both from mechanical [Fernández Guasti and Moya-Cessa, 2003, Yeon et al., 1994] and electromagnetic [Choi, 2004, Pedrosa and Rosas, 2009] points of view, showing squeezing effects. The approach most used in the tackle of this sort of problems is the use of quantum mechanical invariant operators, in particular the Lewis-Ermakov invariant [Lewis, 1967].

In the field of guided propagation of light, the analogous problem is the study of longitudinally inhomogeneous (*LI*) media. An invariant approach was extensively used in [Krivoshlykov and Sauter, 1992] and more recently in [Moya-Cessa et al., 2009] in the study of graded index media but, in both cases, they studied classical problems by means of a quantum-theoretical approach. Quantum propagation problems have been dealt with in homogeneous media, as shown in [Luks and Perinová, 2002] and references therein. These studies provided the background of the quantum theory of light propagation showing that the operator which describes correctly the quantum spatial propagation along an arbitrary direction z is the Momentum operator $\hat{\mathcal{M}}$, since the Hamiltonian approach fails for problems like dispersive media, counterpropagation and *LI* media as well [Liñares et al., 2008]. A first approximation to *LI* media were carried out by Abram [Abram, 1987] and Glauber and Lewenstein [Glauber and Lewenstein, 1991], where single optical discontinuities between homogeneous media were analyzed. In these studies they showed the different physical behaviour the fields experience from the analogous mathematical problem of the time dependent quantum harmonic oscillator, proving that the field quadrature noise does not exhibit real squeezing, in agreement with experiments.

As far as we know, there is not any work dealing with quantum states of light propagating in *LI* media in such a way that field quadratures do not exhibit real squeezing. So, our purpose is to give a phenomenological approach to this problem in waveguides. To this end, we will start obtaining the classical solutions which help us to find a reference frame which continuously performs a physical variable change in *LI* media and eliminates the virtual squeezing, leading us to a proper propagation generator, a quantum Lewis-Ermakov type Momentum operator $\hat{\mathcal{M}}$. From this operator we will obtain Fock states in the optical-field strength (OFS) representation $\mathcal{E}$ and derive the propagator, proving the lack of squeezing in this representation and the arising of a quantum Gouy's phase. Furthermore, we will present the particular case of propagation of a gaussian quantum state in a cosine-type *LI* medium, where will be shown that the net effect of this kind of media on quantum states is the generation of a quantum Guoy's phase dependent on features of both the media and the input quantum state.

P4.2. Classical analysis of propagation in longitudinally inhomogeneous media

Our aim is to study the propagation of waveguided modes of quantum light in dispersion-free and non-magnetic media with separable inhomogeneous refractive index in an arbitrary direction of propagation z, given by [Sodha and Ghatak, 1977]:

$$n^2(x,y,z) = n_0^2\, f^2(x,y) + \Delta n^2\, h^2(z), \tag{P4.1}$$

where the longitudinal $h(z)$ and transversal $f(x,y)$ parts of the index are completely independent and n_0 and Δn are constants. We focus on the separable index problem as it does not show coupling and therefore radiation modes (losses).

From Maxwell equations, it is easy to show that the electric field $\mathbf{E}(x,y,z,t)$ obeys the vectorial wave equation [Marcuse, 1974]:

$$\nabla^2 \mathbf{E}_t + \nabla_t(\mathbf{E}\,\nabla(\ln n^2)\,) = \frac{n^2}{c^2}\frac{\partial^2 \mathbf{E}_t}{\partial t^2}, \tag{P4.2}$$

with $\mathbf{E} = (E_x, E_y, E_z) \equiv (\mathbf{E}_t, E_z)$. Let us consider monochromatic guided 1D vector modes with frequency ω_σ represented by vector field solutions with the following factorable complex amplitudes:

$$\mathbf{E}_t(x,y,z,t) = \sum_\sigma q_{\sigma c}(z)\,\xi_{t\sigma}(x,y)\,e^{-i\omega_\sigma t}, \tag{P4.3}$$

where we have used σ for simplicity standing for the modal numbers ν, μ in each transverse direction, z-dependent complex coefficients $q_{\sigma c}(z)$ fulfilling $\sum_\sigma |q_{\sigma c}(z)|^2 = 1$, and electric normalized transverse complex amplitudes $\xi_{t\sigma}(x,y)$ corresponding to quasi-TE (or quasi-TM) modes fulfilling a *quasi*-complete orthonormalization condition [Liñares et al., 2008], which belong to the homogeneous part of the refractive index and satisfy:

$$\begin{aligned}\nabla_t^2\,\xi_{t\sigma} + k_0^2 n_0^2 f^2(x,y)\,\xi_{t\sigma} + \\ \nabla_t(\xi_{t\sigma}\,\nabla_t(\ln n_0^2 f^2(x,y))) = \beta_{t\sigma}^2\,\xi_{t\sigma},\end{aligned} \tag{P4.4}$$

with β_t the transverse propagation constant. Solutions of this equation give us the invariant transverse modal structure of the field. Applying equations (P4.1), (P4.3) and (P4.4) into (P4.2), we obtain:

$$\frac{d^2 q_\sigma}{dz^2} + \beta_\sigma^2(z)\,q_\sigma = 0, \tag{P4.5}$$

where $q_\sigma = (q_{\sigma c} + q_{\sigma c}^*)/2$ stands for the real electric field coefficients, $\beta_\sigma^2(z) = \beta_{t\sigma}^2 + k_0^2 \Delta n^2 h^2(z)$ is the local propagation constant of the σ-mode and where we have used the approximation $E_z \ll E_x, E_y$. It is important

to outline that $E_z = 0$ in the case of TE modes, that is, equation (P4.5) is exact for such modes. This propagation equation clearly suggests a local spatial harmonic oscillator and therefore it can be directly derived from spatial-type Hamilton equations where the Hamilonian is substituted by the Momentum, since it is the generator of spatial translations [Abram, 1987, Liñares et al., 2012], given by:

$$\mathcal{M}_\sigma = \frac{1}{2}[p_\sigma^2 + \beta_\sigma^2(z)\, q_\sigma^2], \tag{P4.6}$$

with $p_\sigma = q'_\sigma$ and prime stands for z-derivative. This result is analogous to that obtained in [Pedrosa and Rosas, 2009] where time-dependent linear media was studied. The classical Momentum (P4.6) is equivalent to the Hamiltonian of a time-dependent harmonic oscillator, with $\beta(z)$ playing the role of $\omega(t)$ [Lewis, 1967]. Likewise, the solution of equation (P4.5) is easily obtained via the use of the complex electric field $q_{\sigma c}$ in the following way:

$$q_{\sigma c}(z) = \rho_\sigma\, e^{i\theta_\sigma} q_{\sigma c}(0), \tag{P4.7}$$

where ρ_σ and θ_σ are real functions obtained by solving:

$$\frac{d^2\rho_\sigma}{dz^2} + \beta_\sigma^2(z)\rho_\sigma = \frac{\beta_{0\sigma}}{\rho_\sigma^3}, \tag{P4.8}$$

$$\frac{d\theta_\sigma}{dz} = \frac{\beta_{0\sigma}}{\rho_\sigma^2}, \tag{P4.9}$$

with $\beta_{o\sigma} \equiv \beta_\sigma(0)$. Equation (P4.8) is an Ermakov-Pinney equation with solutions given by [Pinney, 1950]:

$$\rho_\sigma(z) = [(\beta_{o\sigma}\, u_\sigma(z))^2 + v_\sigma^2(z)]^{1/2}, \tag{P4.10}$$

$$\rho_\sigma(0) = 1, \quad \rho'_\sigma(0) = 0, \tag{P4.11}$$

and where u_σ and v_σ are linearly independent functions that satisfy equation (P4.5) and have the following initial conditions and Wronskian:

$$u_\sigma(0) = v'_\sigma(0) = 0, \tag{P4.12}$$

$$u'_\sigma(0) = v_\sigma(0) = 1, \tag{P4.13}$$

$$W_\sigma = u'_\sigma v_\sigma - v'_\sigma u_\sigma = 1. \tag{P4.14}$$

So, the classical wave amplitude changes continously during propagation by a factor ρ_σ, whereas the modal propagation constant is given by $\tilde{\beta}_\sigma \equiv \theta'_\sigma$ via equation (P4.9) where θ_σ represents the total phase accumulated in the propagation.

P4.3. Quantization in longitudinally inhomogeneous media

The next step is to quantize the classical Momentum (P4.6). But before carrying out this step, some considerations have to be taken into account. Direct quantization of the classsical fields q_σ and p_σ would lead to a quantized z-dependent Momentum analogous to the Hamiltonian for a time-dependent harmonic oscillator and, therefore, following the usual steps, we would have propagation equations leading to quadrature noise squeezing [Choi, 2004, Fernández Guasti and Moya-Cessa, 2003, Pedrosa and Rosas, 2009, Yeon et al., 1994]. But in the sudy of propagation in *LI* dielectric media, this approach does not provide consistent results. As was pointed out by Abram in his seminal paper about quantization of light in dielectric media [Abram, 1987], when quantum states propagating in a dielectric are represented in the basis of free-space photons, they seem to be squeezed, but inside a dielectric there is no experiment that can detect free-space photons. This happens because if we wish to detect photons inside the medium the fields would experiment an effective refractive index equivalent to the squeezing parameter and, therefore, a scale change is necessary. In the same spirit an interesting discussion about quantization in a dielectric was carried out by Glauber and Lewestein in [Glauber and Lewenstein, 1991]. In this study is stressed that the measurement of quantum states of light is based on photoabsorption processes carried out in the basis which diagonalizes the Hamiltonian in every medium. This is so because the photocount distribution is given by a normal ordered correlation product in the local basis, result of the physical property of the photoabsorption process that the energy of the field decreases when a photon is absorbed. But in any other basis this is not true, because of the mixing of absorption and emission operators, and therefore of frequencies, lacking the normal ordering in the correlation product. Thereby the state in these bases can not be measured and the photons are so-called virtual and, accordingly, the squeezing is virtual as well. This statement is closely related with Abram's idea and has to be applied to *LI* media as it is the continuous limit of single discontinuities.

Hence, we look for some transformation which takes the classical Momentum (P4.6) to be a constant of motion suitable to be quantized and simultaneously get rid of the virtual squeezing in a continuous way. Since carrying out the usual approach [Choi, 2004, Fernández Guasti and Moya-Cessa, 2003, Pedrosa and Rosas, 2009, Yeon et al., 1994] squeezing proportional to the function $\rho(z)$ would appear, following the idea of a scale change in the discontinuity [Abram, 1987, Glauber and Lewenstein, 1991] we propose the following generalized canonical transformations from a generating function $G_2(q, \tilde{P}) = \tilde{P}q/\rho$ and z transformation [Chetouani et al.,

1989]:

$$\tilde{Q}_\sigma = \frac{q_\sigma}{\rho_\sigma}, \quad \tilde{P}_\sigma = \rho_\sigma p_\sigma, \quad s_\sigma = (\int_0^z \rho_\sigma^2(z)\, dz)^{-1}; \tag{P4.15}$$

and the next gauge transformations related to the new s-frame:

$$Q_\sigma = \tilde{Q}_\sigma, \qquad P_\sigma = \tilde{P}_\sigma - \frac{\dot{\rho}_\sigma}{\rho_\sigma}\tilde{Q}_\sigma, \tag{P4.16}$$

with the dot standing for an s-derivative. Applying these relations into (P4.6), we directly obtain the following Momentum:

$$\mathcal{M}_\sigma(Q, P, s) = \frac{1}{2}[P_\sigma^2(s) + \beta_{0\sigma}^2\, Q_\sigma^2(s)], \tag{P4.17}$$

where we have used the auxiliar equation (P4.8). It is remarkable that these new phase space and longitudinal coordinates (Q, P, s) are analogous to the comoving coordinates and the conformal (or arc-parameter) time used in cosmology and, likewise, the canonical momentum transformation (P4.16) is related to the Hubble's law [Misner et al., 1973]. After these transformations, the continuous change in the value of the harmonic potential appears as constant in the new comoving frame of reference [Takagi, 1990]. So, in this frame, there are not scale changes differentially and the medium seems to be homogeneous. The generalized canonical transformations eliminate the squeezing at each plane z and none signature of it is obtained. These insights lead us to consider the comoving frame as the physical one and therefore the proper one for quantization. Furthermore, interestingly, if we rewrite this Momentum in the original phase space, we obtain:

$$\mathcal{M}_\sigma(q, p, z) = \frac{1}{2}[(\rho_\sigma\, p_\sigma - q_\sigma\, \rho_\sigma')^2 + \beta_{0\sigma}^2(q_\sigma/\rho_\sigma)^2]. \tag{P4.18}$$

This is the space-analog of an Ermakov-Lewis invariant [Lewis, 1967]. So, it can be said that the Momentum (P4.17) is a spatial Ermakov-Lewis invariant in a comoving frame and that this invariant is the generator of spatial propagation in this kind of media.

Now, following the principle of quantization of quantum mechanics $(Q_\sigma, P_\sigma) \to (\hat{Q}_\sigma, \hat{P}_\sigma)$, where $[\hat{Q}_\sigma, \hat{P}_{\sigma'}] = i\hbar\delta_{\sigma,\sigma'}$, we obtain the Momentum operator:

$$\hat{\mathcal{M}}_\sigma = \frac{1}{2}[\hat{P}_\sigma^2(s) + \beta_{0\sigma}^2\, \hat{Q}_\sigma^2(s)]. \tag{P4.19}$$

In order to obtain the eigenvalues and eigenfunctions of this operator, we define the following annihilation and creation operators:

$$\hat{A}_\sigma(s) = \frac{1}{\sqrt{2\hbar\beta_{0\sigma}}}[\beta_{0\sigma}\hat{Q}_\sigma + i\hat{P}_\sigma], \tag{P4.20}$$

$$\hat{A}_\sigma^\dagger(s) = \frac{1}{\sqrt{2\hbar\beta_{0\sigma}}}[\beta_{0\sigma}\hat{Q}_\sigma - i\hat{P}_\sigma]. \tag{P4.21}$$

Therefore, equation (P4.19) in terms of (P4.21) can be rewritten as:

$$\hat{\mathcal{M}}_\sigma = \hbar\beta_{0\sigma}[\hat{A}_\sigma^\dagger \hat{A}_\sigma + 1/2]. \tag{P4.22}$$

The eigenstates of this Momentum are the same as those of the Number operator $\hat{N}_\sigma = \hat{A}_\sigma^\dagger \hat{A}_\sigma$, which fulfills the next eigenvalue equation:

$$\hat{N}_\sigma |N_\sigma\rangle = N_\sigma |N_\sigma\rangle, \tag{P4.23}$$

where N_σ and $|N_\sigma\rangle$ are eigenvalues and eigenstates for the Number operator, respectively. In terms of quantum-optical units [Loudon, 1982], we can redefine the quantum comoving scaled position $\hat{Q}_\sigma$ as the OFS operator $\hat{\mathcal{E}}_\sigma$, whose eigenstates are those measured in homodyne experiments [Schleich, 2001, Vogel, 1990] and central to generalized quantum polarization [Barral et al., 2013, Liñares et al., 2011a], that is $\hat{\mathcal{E}}_\sigma = \sqrt{\beta_{0\sigma}/2\hbar}\,\hat{Q}_\sigma$. The eigenstates $|N_\sigma\rangle$ in the optical field-strength $\mathcal{E}$ basis are given in terms of Hermite-Gauss functions as:

$$\Psi_N(\mathcal{E}_\sigma, 0) = \frac{2^{1/4}}{\sqrt{2^N \pi^{1/2}\, N!}} H_N(\sqrt{2}\mathcal{E}_\sigma)\, e^{-\mathcal{E}_\sigma^2}, \tag{P4.24}$$

and their quantum propagation is given by a spatial Schrödinger equation:

$$\hat{\mathcal{M}}_\sigma \Psi_N \equiv \hbar\beta_{0\sigma}\,[-\frac{1}{4}\frac{\partial^2}{\partial \mathcal{E}_\sigma{}^2} + \mathcal{E}_\sigma^2]\,\Psi_N = \hbar\beta_{0\sigma}\,\Psi_N. \tag{P4.25}$$

The solution of this equation yields the following propagated eigenstates $|N_\sigma\rangle$:

$$\Psi_N(\mathcal{E}_\sigma; s) = \frac{2^{1/4}\, e^{i(N+1/2)\theta_\sigma}}{\sqrt{2^N \pi^{1/2}\, N!}} H_N(\sqrt{2}\mathcal{E}_\sigma)\, e^{-\mathcal{E}_\sigma^2}, \tag{P4.26}$$

with $\theta_\sigma = \beta_{0\sigma} s_\sigma$ the total accumulated phase, in the same way as a quantum state propagating in a homogeneous medium, but in this case in a comoving frame, which is the physical one for this kind of problems as shown above. Because of the similarity of this phase with the classical Gouy's phase [Boyd, 1980], we call it spatial quantum Gouy's phase.

P4.4. Propagation of quantum light in longitudinally inhomogeneous media

Now, in order to gain insight into the behaviour of the longitudinally inhomogeneous waveguide, we study the spatial propagation of gaussian states, like the coherent and squeezed quantum states of light, in the OFS representation. From the wavefunction (P4.26) and Mehler's formula [Yeon et al., 1994], we easily obtain the propagator of the system for every mode [Liñares et al., 2012]:

$$K(\mathcal{E}, \mathcal{E}_0; z, 0) = (\frac{i}{\pi})^{N/2} \prod_\sigma (\sin\theta_\sigma)^{-1/2}$$

$$e^{-\frac{i}{\sin\theta_\sigma}[\cos\theta_\sigma\,(\mathcal{E}_\sigma^2+\mathcal{E}_{0\sigma}^2)-2\mathcal{E}_\sigma\mathcal{E}_{0\sigma}]}, \tag{P4.27}$$

and the wavefunction of any pure state at the end of the medium can be worked out by means of:

$$\Psi(\mathcal{E};z)=\int K(\mathcal{E},\mathcal{E}_0;z,0)\,\Psi(\mathcal{E}_0;0)\,d\mathcal{E}_0, \tag{P4.28}$$

where $\mathcal{E}_0$ and $\mathcal{E}$ stand for the N-mode field-strength at the beginning and any point of the z-dependent medium, respectively.

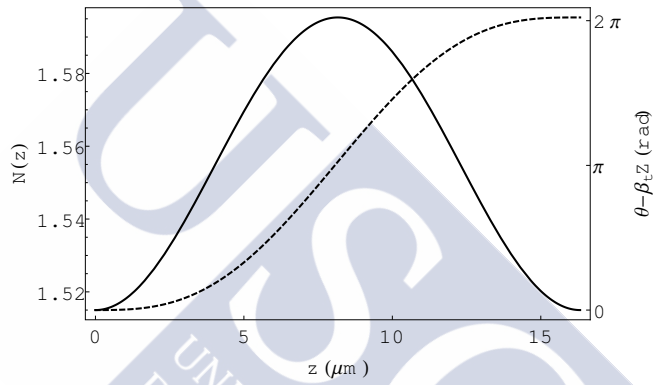

Figure P4.1: Cosine-type effective refractive index $N(z) \equiv \beta(z)/k_0$ (solid line, left) and total accumulated classical phase θ (dash line, right) versus propagation distance z, for parameters $N_t \equiv \beta_t/k_0 = 1.515$, $\Delta n = 0.5$ and $\Lambda = k_0/50\ nm^{-1}$ for a wavelength $\lambda = 653$ nm.

A single-mode gaussian state $|\alpha\rangle$, where $\alpha = |\alpha|e^{i\phi}$, in the OFS space is given by [Liñares et al., 2012]:

$$\Psi(\mathcal{E}_0;0)=\left(\frac{2}{\pi\Delta\mathcal{E}_0^2}\right)^{1/4}\exp\left\{\frac{-[\mathcal{E}_0-|\alpha|\,\cos\phi]^2}{\Delta\mathcal{E}_0^2}\right\}e^{-i\delta_0}, \tag{P4.29}$$

where $\delta_0 = \sin\phi\,[|\alpha|^2\cos\phi - 2|\alpha|\mathcal{E}_0]$, $\phi = -\omega t$ is the phase associated to the temporal evolution of the state at every plane z and $\Delta\mathcal{E}_0^2$ is the quantum noise or squeezing factor, with a value of one for a coherent state or different from one for squeezed states. Inserting equations (P4.27) and (P4.29) in (P4.28), after a long but straightforward calculation, we obtain the wavefunction at any point z of the waveguide:

$$\begin{aligned}\Psi(\mathcal{E};z)=&\left(\frac{2}{\pi\Delta\mathcal{E}^2}\right)^{1/4}e^{i\Theta/2}e^{-i\delta}\\&\exp\left\{\frac{-1}{\Delta\mathcal{E}^2}[\mathcal{E}-|\alpha|\,\cos(\phi+\theta)\,]^2\right\},\end{aligned} \tag{P4.30}$$

where we have denoted $\theta_\sigma \equiv \theta$ and defined $\delta = \sin(\phi + \theta)\,[|\alpha|^2 \cos(\phi + \theta) - 2|\alpha|\mathcal{E}]$ and:

$$\Delta\mathcal{E} = [\frac{\sin^2\theta}{\Delta\mathcal{E}_0^2} + \cos^2\theta\,\Delta\mathcal{E}_0^2]^{1/2}, \tag{P4.31}$$

$$\Theta = \arctan[\frac{\tan\theta}{\Delta\mathcal{E}_0^2}]. \tag{P4.32}$$

Therefore, a coherent state keeps its quantum noise constant through propagation, $\Delta\mathcal{E}^2 = \Delta\mathcal{E}_0^2 = 1$, and gets a Gouy's phase equal to the classical accumulated phase given by (P4.9), $\Theta = \theta$, as expected, unlike what we would obtain via the usual approach. On the other hand, an input squeezed state is both amplitude and phase modulated by the inhomogeneous medium, leading to different squeezing oscillations from those corresponding to an homogeneous medium, and with a squeezing factor given by (P4.31). It is important to outline that the phase acquired by a squeezed state (P4.32) is not predicted by the classical theory.

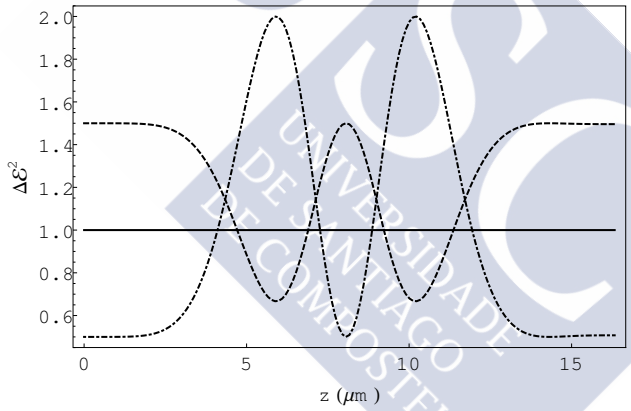

Figure P4.2: Evolution of the quantum noise $\Delta\mathcal{E}^2$ in a cosine-type longitudinally inhomogeneous medium for coherent (solid line) and squeezed (dash and dash-dot lines) states of light.

Next, we show a specific example of the effects this kind of medium produce over a single-mode gaussian quantum state like the above introduced. We present a longitudinally inhomogeneous cosine-type medium with $h(z) = \cos(\Lambda z)$ and length $L = 2\pi/\Lambda$, as that depicted in Figure 1. The solution of equation (P4.8) is given in terms of linearly independent Mathieu functions $u(z)$ and $v(z)$ [Casperson, 1985]. Applying these solutions into equations (P4.9) and (P4.10), we can obtain numerically the value of θ and, therefore, the squeezing factor (P4.31) and the Gouy's phase (P4.32), which characterize the output quantum state after propagation in this medium. In Figures 2 and 3 we show the behaviour of the Gouy's

phase Θ and the quantum noise $\Delta\mathcal{E}^2$, respectively, for three different input quantum states: the solid line stands for the propagation of a coherent state where $\Delta\mathcal{E}_0^2 = 1$ and the dash and dash-dot lines for squeezed states with $\Delta\mathcal{E}_0^2 = 3/2$ and $\Delta\mathcal{E}_0^2 = 1/2$, respectively. As can be checked in Figure 2, the planes where maximum or minimum squeezing of the quantum noise are produced depend on the accumulated phase θ, being different from those corresponding to an homogeneous medium, and the value of the input quantum noise $\Delta\mathcal{E}_0^2$. Likewise, as was outlined above, the classical equations do not predict the behaviour of states far from the classical, since squeezed and coherent states get different amounts of Guoy's phase Θ, as is sketched in Figure 3. The classical phase θ is recovered at the planes of maximum and minimum squeezing. Finally, we stress the interest this phase may have in quantum interferometry, since with an appropriate *LI* medium in one arm of an interferometer, quantum interference can be adjusted controlling the strength of the quantum noise in a squeezed input state via equation (P4.32).

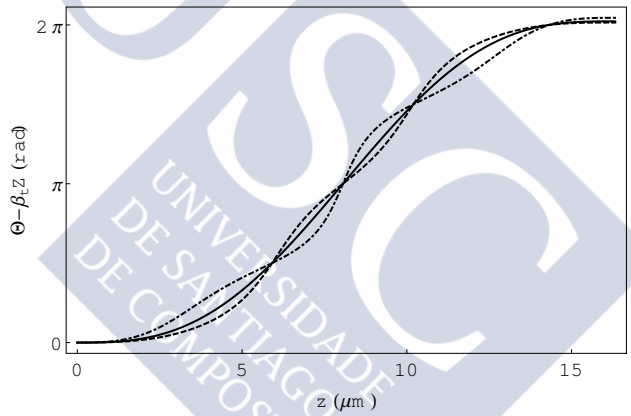

Figure P4.3: Evolution of the quantum Gouy's phase Θ in a cosine-type longitudinally inhomogeneous medium for coherent (solid line) and squeezed (dash and dash-dot lines) states of light.

P4.5. Summary

We have studied the propagation of quantum states of light in separable longitudinally inhomogeneous media. We have proposed canonical transformations in a comoving frame and derived the generator of propagation, the classical Momentum, realizing that it is a spatial Lewis-Ermakov invariant. We have quantized it and obtained the propagator in the OFS representation which is physically consistent. Furthermore, we have presented the propagation of a gaussian quantum state of light in a cosine-type refractive index medium and shown the net effect produced by this family

of media: a quantum Gouy's phase dependent on the input quantum state with application in quantum interferometry.

Chapter 3 bibliography

I. Abram. Quantum theory of light propagation: Linear medium. *Physical Review A*, 35(11):4661–4672, 1987.

D. Barral and J. Liñares. Detection of two-mode spatial quantum states of light by electro-optic integrated directional couplers. *Journal of the Optical Society of America B*, 32(6):1165, 2015.

D. Barral, J. Liñares, and M.C. Nistal. Optical field-strength generalized polarization of non-stationary quantum states in waveguiding photonic devices. *Journal of Modern Optics*, 60(12):941, 2013.

A.O. Barut and L. Girardello. New "coherent" states associated with non-compact groups. *Communications in Mathematical Physics*, 21:41, 1971.

R.W. Boyd. Intuitive explanation of the phase anomaly of focused light beams. *Journal of the Optical Society of America B*, 70(7):877, 1980.

W.K. Burns and A.F. Milton. Waveguide transitions and junctions. In T. Tamir, editor, *Guided-wave optoelectronics*. Springer-Verlag, Berlin, 1994.

K.E. Cahill and R.J. Glauber. Density operators and quasiprobability distributions. *Physical Review*, 177:1882, 1969.

L.W. Casperson. Beam propagation in periodic quadratic-index waveguides. *Applied Optics*, 24(24):4395, 1985.

L. Chetouani, L. Guechi, and Hamman T.F. Generalized canonical transformations and path integrals. *Physical Review A*, 40(3):1157, 1989.

J.-R. Choi. Coherent and squeezed states for light in homogeneous conducting linear media by an invariant operator method. *International Journal of Theoretical Physics*, 43(10):2113, 2004.

R. Cordero-Soto and S. K. Suslov. The degenerate parametric oscillator and ince's equation. *Journal of Physics A: Mathematical and Theoretical*, 44(1): 015101, 2011.

A. Einstein, B. Podolsky, and N. Rosen. Can quantum-mechanical description of physical reality be considered complete? *Physical Review*, 47(10): 777, 1935.

M. Fernández Guasti and H. Moya-Cessa. Solution of the schrödinger equation for time-dependent 1d harmonic oscillators using the orthogonal functions invariant. *Journal of Physics A: Mathematical and Theoretical*, 36:2069, 2003.

R.P. Feynman and A.R. Hibbs. *Quantum Mechanics and Path Integrals*. McGraw-Hill, 1965.

R.P. Feynman and F.L. Vernon. The theory of a general quantum system interacting with a linear dissipative system. *Annals of Physics*, 24:118, 1963.

Christopher C. Gerry and Peter L. Knight. *Introductory Quantum Optics*. Cambridge University Press, 2005.

R.J. Glauber and M. Lewenstein. Quantum optics of dielectric media. *Physical Review A*, 43(1):467, 1991.

C. Gómez-Reino and J. Liñares. Optical path integrals in gradient-index media. *Journal of the Optical Society of America A*, 4:1337, 1987.

C. Gómez-Reino, J. Liñares, and E. Larrea. Imaging and transforming transmission through tapered gradient-index rods: analytical solutions. *Journal of the Optical Society of America A*, 3(10):1604, 1986.

S. Hacyan. Su(1,1) coherent states as bessel-gauss states. *Revista Mexicana de Física*, 54(6):451, 2008.

H. Haken. *Light*. North-Holland, Amsterdam, 1981.

M. Hillery and L.D. Modlinow. Quantization of electrodynamics in nonlinear dielectric media. *Physical Review A*, 30(4):1860–1865, 1984.

L. Infeld and J. Plebanski. On a certain class of unitary transformations. *Acta Physica Polonica*, 14:41, 1955.

G.-L. Ingold. Path integrals and their application to dissipative quantum systems. In A. Buchleitner and K. Hornberger, editors, *Coherent Evolution in Noisy Environments*, volume 611 of *Lecture Notes in Physics*, pages 1–53. Springer-Verlag, Berlin, 2002.

J.D. Jackson. *Classical Electrodynamics*. John Wiley and sons, 1975.

J. Jansky, A. Sibilia, M. Bertolotti, and Y. Yushin. Non-classical light in a linear coupler. *Journal of Modern Optics*, 35:1757, 1988.

M. Khalaj-Amirhosseini. Analysis of longitudinally inhomogeneous waveguides using taylor series expansion. *Journal of Electromagnetic Waves and Applications*, 20:1299, 2006.

T. Kiss, J. Janszky, and P. Adam. Time evolution of harmonic oscillators with time-dependent parameters: a step-function approximation. *Physical Review A*, 49(6):4935, 1994.

H. Kogelnik. Theory of dielectric waveguides. In T. Tamir, editor, *Guided-wave optoelectronics*, chapter 2. Springer-Verlag, Berlin, 1988.

N. Korolkova and J. Perina. Kerr nonlinear coupler with varying linear coupling coefficient. *Journal of Modern Optics*, 44:1525, 1997.

S.G. Krivoshlykov and E.G. Sauter. Transformation of paraxial beams in arbitrary multimode parabolic-index fiber tapers by using a quantum-theoretical approach. *Applied Optics*, 31(12):2017, 1992.

H. Kühn, D.-G. Welsch, and W. Vogel. Determination of density matrices from field distributions and quasiprobabilities. *Journal of Modern Optics*, 41:1607, 1994.

H.R. Lewis. Classical and quantum systems with time-dependent harmonic-oscillator-type hamiltonians. *Physical Review Letters*, 18(13): 510, 1967.

J. Liñares. Maxwell paraxial wave optics in inhomogeneous media by path integral formalism. *Physics Letters A*, 141:207, 1989.

J. Liñares. Optical propagators in vector and spinor theories by path integral formalism. In H.A. Cerdeira, editor, *Lectures on Path Integration: Trieste 1991*, page 378, 1991.

J. Liñares and M.C. Nistal. Single local mode propagation through ion-exchanged waveguide elements with quasi-abrupt transitions. *Japanesse Journal of Applied Physics*, 35:L1596, 1996.

J. Liñares and M.C. Nistal. Quantization of coupled modes propagation in integrated optical waveguides. *Journal of Modern Optics*, 50(5):781–790, 2003.

J. Liñares and M.C. Nistal. Spin operator for quantum light in integrated photonic waveguides. *Journal of Modern Optics*, 56:1244, 2009.

J. Liñares, M.C. Nistal, and D. Barral. Quantization of coupled 1d vector modes in integrated photonic waveguides. *New Journal of Physics*, 10: 063023, 2008.

J. Liñares, D. Barral, M.C. Nistal, and V. Moreno. Optical field-strength generalized polarization of multimode single photon states in integrated directional couplers. *Journal of Modern Optics*, 58(8):711, 2011a.

J. Liñares, M.C. Nistal, D. Barral, V. Moreno, C. Montero, and X. Prieto. Quantum integrated optics: theory and applications. *Optica Pura y Aplicada*, 44:241, 2011b.

J. Liñares, D. Barral, and M.C. Nistal. Spatial propagation of quantum light in nonlinear waveguiding devices: theory and applications. *Journal of Nonlinear Optical Physics and Materials*, 21(3):1250032, 2012.

R. Loudon and P. L. Knight. Squeezed light. *Journal of Modern Optics*, 34 (6/7), 1987.

Rodney Loudon. *The Quantum Theory of Light*. Clarendon Press, Oxford, 1982.

A. Luks and V. Perinová. Canonical quantum description of light propagation in dielectric media. In E. Wolf, editor, *Progress in optics*, volume 43, page 295. North-Holland, 2002.

A.I. Lvovsky. *Squeezed light*, volume 1 of *Photonics: Scientific Foundations, Technology and Applications*, chapter 5. John Wiley and sons, 2015.

A.I. Lvovsky and M.G. Raymer. Continuous-variable optical quantum state tomography. *Review of Modern Physics*, 81:299, 2008.

L. Mandel and E. Wolf. *Optical Coherence and Quantum Optics*. Cambridge University Press, 1995.

D. Marcuse. *Theory of dielectric optical waveguides*. Academic Press Inc, London, 1974.

C.W. Misner, K.S. Thorne, and J.A. Wheeler. *Gravitation*. W.H. Freeman and Co., San Francisco, 1973.

P.M. Morse and H. Feshbach. *Methods of Theoretical Physics*. McGraw-Hill, New York, 1953.

H. Moya-Cessa, M. Fernández Guasti, V.M. Arrizon, and S. Chávez-Cerdá. Optical realization of quantum-mechanical invariants. *Optics Letters*, 34 (9):1459, 2009.

B.M. Nielsen. Generation of a schrodinger kitten state of light. Master's thesis, QUANTOP - The Niels Bohr Institute, University of Copenhagen, 2006.

Jeremy L. O'Brien, A. Furusawa, and J. Vukovic. Photonic quantum technologies. *Nature Photonics*, 3:687, 2009.

I.A. Pedrosa and A. Rosas. Electromagnetic field quantization in time-dependent linear media. *Physical Review Letters*, 103:010402, 2009.

J. Perina. Quantum-statistical properties of a nonlinear asymmetric directional coupler. *Journal of Modern Optics*, 42(7):1517–1522, 1995.

J. Perina and J. Perina Jr. Quantum statistics of a nonlinear asymmetric coupler with strong pumping. *Quantum Semiclassical Optics*, 7:541–552, 1995a.

J. Perina and J. Perina Jr. Photon statistics of a contradirectional nonlinear coupler. *Quantum Semiclassical Optics*, 7:849, 1995b.

J. Perina Jr and J. Perina. Quantum statistics of nonlinear optical couplers. In E. Wolf, editor, *Progress in optics*, volume 41, pages 361–419. Elsevier Science B.V., 2000.

V. Perinová, A. Luks, and J. Krepelka. Linear coupling, loss and gain of counterpropagating beams. *Journal of Physics B: Atomic, Molecular and Optical Physics*, 39:2267, 2006.

E. Pinney. The nonlinear equation $y'' + p(x)y + cy^{-3} = 0$. *Proceedings of the American Mathematical Society*, 1(5):681, 1950.

A. Politi, J.C.F. Matthews, M.G. Thompson, and J.L. O'Brien. Integrated quantum photonics. *IEEE Journal of Selected Topics in Quantum Electronics*, 15:1673, 2009.

S.G. Rajeev. A canonical formulation of dissipative mechanics using complex-valued hamiltonians. *Annals of Physics*, 322:1541, 2007.

W.P. Schleich. *Quantum optics in phase space*. Wiley-VCH, Berlin, 2001.

M.S. Sodha and A.K. Ghatak. *Inhomogeneous optical waveguides*. Plenum Press, New York, 1977.

T. Suhara. Generation of quantum-entangled twin photons by waveguide nonlinear-optic devices. *Laser & Photonics Reviews*, 3(4):370, 2009.

Massood Tabib-Azar. *Integrated Optics, Microstructures, and Sensors*. Kluwer Academic Publishers, 1995.

S. Takagi. Equivalence of a harmonic oscillator with a free particle. *Progress of Theoretical Physics*, 84(6):1019, 1990.

M. Toren and Y. Ben-Aryeh. The problem of propagation in quantum optics, with applications to amplification, coupling of em modes and distributed feedback lasers. *Quantum Optics*, 6:425–444, 1994.

A.A. Tovar and L.W. Casperson. Beam propagation in parabolically tapered graded-index waveguides. *Applied Optics*, 33:7733, 1994.

W. Vogel. Field-strength probability distributions and higher-order squeezing. *Physical Review A*, 42:5754, 1990.

W. Vogel and H. Risken. Determination of quasiprobability distributions in terms of probability distributions for the rotated quadrature phase. *Physical Review A*, 40(5):2847, 1989.

W. Vogel and D.-G. Welsch. *Lectures on Quantum Optics*. Akademie Verlag, Berlin, 1994.

D. F. Walls and G. J. Milburn. *Quantum Optics*. Springer Verlag, Berlin, 1994.

D.-G. Welsch, W. Vogel, and T. Opatrny. Homodyne detection and quantum state reconstruction. In E. Wolf, editor, *Progress in Optics*, volume XXXIX, page 63. Elsevier, 1999.

K.H. Yeon, H.J. Kim, Ch.I. Um, T.F. George, and L.N. Pandey. Wave function in the invariant representation and squeezed-state function of the time-dependent harmonic oscillator. *Physical Review A*, 50(2):1035, 1994.

L.H. Yu and C. Sun. Evolution of the wave function in a dissipative system. *Physical Review A*, 49:592, 1994.

USC
UNIVERSIDADE
DE SANTIAGO
DE COMPOSTELA

CHAPTER

FOUR

CHARACTERIZATION OF QUANTUM STATES IN THE OPTICAL FIELD-STRENGTH SPACE: GENERALIZED POLARIZATION

Since we have performed an analysis of the propagation in waveguides in the previous chapters, we use the present one to introduce a novel approach to characterize quantum states, the quantum generalized polarization. This theory is based on considering the polarization as the confinement of probability distributions in particular regions of the OFS space in analogy with the classical polarization. We will show a polarization degree as a measurement of this confinement, for both vectorial and spatial modes, and we will apply it to different quantum states in various dimensions. To this end, in section 1 we will carry out an introduction to the classical concept of polarization, while in section 2 we will review its quantum version and the different approaches to a polarization degree appearing in the scientific literature. In section 3 we will present the theory of the generalized polarization in the OFS space and propose a quantum polarization degree. Finally, we will show the published research papers where the reader can be find the details of this theory and its application to multimode single-photon (§ P5) and to non-stationary (§ P6) quantum states.

4.1. Classical polarization: polarization ellipse, Stokes parameters and polarization degree

The polarization of light is a well-known phenomena broadly used in different applications for ages. In 1852 G.G. Stokes introduced a systematic approach to the polarization of light which allows to clasify it as a function of operational parameters easily measured [Stokes, 1852]. For a monochromatic plane wave with frequency ω, the complex EM field can be written

as:

$$\mathbf{E} = \{a_1 e^{i\delta_1}\boldsymbol{e}_x + a_2 e^{i\delta_2}\boldsymbol{e}_y\}e^{-i\omega t}, \tag{4.1.1}$$

where a_1, a_2, δ_1 and δ_2 are real numbers and $\boldsymbol{e}_x$, $\boldsymbol{e}_y$ orthogonal unitary vectors. This electric field, $\mathbf{E} \equiv (E_x, E_y)$, describes an ellipse in general, refering this light as *elliptically polarized* [Born and Wolf, 1959]:

$$(\frac{E_x}{a_1})^2 + (\frac{E_y}{a_2})^2 - 2(\frac{E_x}{a_1})(\frac{E_y}{a_2})\cos\delta = \sin^2\delta, \tag{4.1.2}$$

with $\delta = \delta_2 - \delta_1$. This ellipse degenerates to a straight line when $\delta = m\pi$, with m any integer, referred as *linearly polarized* light; and to a circunference when $a_1 = a_2$ and $\delta = m\pi/2$, so we will have *circularlly polarized* light. Besides, the sign of δ gives us information about the two possible senses the electric field vector can spin around the direction of propagation, *right-handed* for $\delta > 0$ and *left-handed* for $\delta < 0$.

This ellipse can be characterized in terms of four parameters introduced by Stokes as follows:

$$s_0 = a_1^2 + a_2^2, \tag{4.1.3}$$
$$s_1 = a_1^2 - a_2^2, \tag{4.1.4}$$
$$s_2 = 2a_1 a_2 \cos\delta, \tag{4.1.5}$$
$$s_3 = 2a_1 a_2 \sin\delta, \tag{4.1.6}$$

where only three of them are independent due to the following identity:

$$s_0^2 = s_1^2 + s_2^2 + s_3^2 \equiv |\mathbf{s}|^2, \tag{4.1.7}$$

with $\mathbf{s} = (s_1, s_2, s_3)$ the so-called *Stokes vector*.

The main significance of these quantities is that they are easily measured by means of polarization filters and phase shifters. In this way the parameter s_0 is proportional to the intensity of the wave, s_1 and s_2 represent its ellipticity, this is if the polarization ellipse is closer either to a line or a circle, and s_3 the sense of spin of the electric field vector. Likewise, it is common to represent the Stokes parameters as points $\mathbf{s}/s_0$ over the surface of a sphere with unit radius, the Poincaré sphere [Born and Wolf, 1959]. Every point at this surface is completely defined by two angles: the polar θ and azimuthal ϕ angles, defined by:

$$\theta = \arccos(s_1/s_0), \qquad \phi = \arg(s_2 - is_3). \tag{4.1.8}$$

It is important to outline that this approach is also correct for fluctuant or stochastic (*quasi*-monochromatic) waves, taking into account the EM wave as the sum of two independent waves, one fully polarized and the other

completely unpolarized. In this case the polarization degree can be defined as follows:

$$\mathcal{G}_c = \frac{\sqrt{s_1^2 + s_2^2 + s_3^2}}{s_0}, \tag{4.1.9}$$

where the Stokes parameters in this relation refer to averages. This polarization degree is normalized to the unity, such that if there is not depolarization component, we have $\mathcal{G}_c = 1$ and the light is said to be completely polarized. Whereas for the reverse case, if there is not polarization component at all, we have $\mathcal{G}_c = 0$ and the light is so-called natural.

4.2. Quantum polarization: Stokes operators and polarization degrees

The approach of Stokes parameters is extended directly to quantum optics by means of the Stokes operators, being their expectation values for coherent states the classical parameters (4.1.3-4.1.6). Quantizing the classical amplitudes, the Stokes operators are written as [Collet, 1970]:

$$\hat{s}_0 \equiv \hat{N} = \hat{a}_1^2 + \hat{a}_2^2, \tag{4.2.10}$$

$$\hat{s}_1 = \hat{a}_1^2 - \hat{a}_2^2, \tag{4.2.11}$$

$$\hat{s}_2 = 2\hat{a}_1\hat{a}_2\cos\delta, \tag{4.2.12}$$

$$\hat{s}_3 = 2\hat{a}_1\hat{a}_2\sin\delta, \tag{4.2.13}$$

where $\hat{N}$ is the operator which represents the total number of photons. These operators fulfill the CR corresponding to an angular momentum, so-called Lie-algebra SU(2) [Greiner and Müller, 1994], given by:

$$[\hat{s}_1, \hat{s}_2] = 2i\hat{s}_3 \text{ (and cyclic permutations)}, \qquad [\hat{\mathbf{s}}, \hat{s}_0] = \mathbf{0}, \tag{4.2.14}$$

and where $\hat{\mathbf{s}}$ is the vector of Stokes operators. The quantization of this problem exchanges the classical relation (4.1.7) by the quantum relation $\hat{\mathbf{s}}^2 = \hat{s}_0$, which together with the inequality $|\langle\hat{\mathbf{s}}\rangle| \leqslant \langle\hat{s}_0\rangle$, leads to the following uncertainty relation [Luis and Sánchez-Soto, 2000]:

$$(\Delta\hat{\mathbf{s}})^2 \geqslant 2\langle\hat{s}_0\rangle, \tag{4.2.15}$$

where $(\Delta X)^2 = \langle X^2\rangle - \langle X\rangle^2$. Therefore, the quantum fluctuations have a lower limit. These relations point out that there is no quantum state with definite values of the three Stokes parameters $\hat{\mathbf{s}}$ simultaneously, unless the vacuum. Hence, the electric field vector of a monochromatic wave never follows a definite ellipse due to the quantum fluctuations [Pollet et al., 1995].

Following the classical definition of polarization degree, it has been proposed the next *quantum* polarization degree (*semiclassical*) [Tanás and Kielich, 1990]:

$$\mathcal{G}_{sc} = \frac{\sqrt{\langle \hat{s}_1^2 \rangle + \langle \hat{s}_2^2 \rangle + \langle \hat{s}_3^2 \rangle}}{\langle \hat{s}_0 \rangle}. \tag{4.2.16}$$

This parameter, in the same way as the classical case, represents the distance of our state to a fully unpolarized state. In this case, the unpolarized light is defined as that with null expectation values of the Stokes parameters: $\langle \hat{\mathbf{s}} \rangle = \mathbf{0}$. For instance, from this definition the two-mode thermal states are fully unpolarized ($\mathcal{G}_{sc} = 0$) and any two-mode coherent state is fully polarized ($\mathcal{G}_{sc} = 1$).

However, this definition shows some problems. The Stokes parameters are proportional to the second order correlations of the field amplitudes, so they do not take into account higher order correlations, which are important, for instance, in multi-photon or squeezed polarization quantum states. Due to this feature, the semiclassical polarization degree does not distinguish between quantum states with very different polarization properties. The broadly accepted definition of two-mode unpolarized quantum light considers a quantum state as unpolarized if it is invariant to any combination of rotations with respect to the propagation direction and to phase shiftings or, equally, to $SU(2)$ transformations [Agarwal, 1971, Lehner et al., 1996, Prakash and Chandra, 1971, Söderholm et al., 2001]. In the case of twin photon states generated via *spontaneous parametric down conversion* (SPDC), we have $\langle \hat{\mathbf{s}} \rangle = \mathbf{0}$, so they would be fully unpolarized according to (4.2.16). But, on the other hand, these states present high values of quantum visibility in the concidence basis under geometrical rotations, so they are not unpolarized in accordance with the quantum definition above introduced [Usachev et al., 2001]. It is said that these states show *hidden polarization* [Klyshko, 1992]: they are unpolarized states in the classical sense (second order) but fully polarized to higher orders. Likewise, this definition does not show the loss of fully polarization of quantum states. For instance, any two-mode coherent state $|\alpha, \beta\rangle$ has a maximum semiclassical polarization degree, $\mathcal{G}_{sc} = 1$, so it would be fully polarized. However, this value is the same for every two-mode coherent state arbitrarily close to the two-mode vacuum:

$$\lim_{\alpha \to 0} \mathcal{G}_{sc}(|\alpha, 0\rangle) = 1. \tag{4.2.17}$$

Another semiclassical definition similar to (4.2.16), where the normalization factor $\langle \hat{s}_0 \rangle$ is changed by $(\sum_{j=1}^{3} \langle \hat{s}_j^2 \rangle)^{1/2}$, does not present this last problem and includes second order information [Alodjants and Arakelian, 1999]. However, this definition has an issue: it does not take into account the fluctuations in the phase space. An alternative definition was proposed in [Klimov et al., 2010] solving this problem.

Due to the reasons above exposed, different polarization degrees of purely quantum character have been proposed in the last years. Most of them take as starting point the definition of an unpolarized state, that is invariant under SU(2) transformations [Agarwal, 1971, Lehner et al., 1996, Prakash and Chandra, 1971, Söderholm et al., 2001], and defining the polarization degree as the distance between the quantum state to be measured and a fully unpolarized one. The density operator related to a unpolarized state may be written in the following general way:

$$\hat{\sigma} = \oplus_{N=0}^{\infty} \lambda_N \hat{\mathbb{1}}_N [1], \tag{4.2.18}$$

with the next normalization condition $\sum_{N=0}^{\infty}(N+1)\lambda_N = 1$ and where $\hat{\mathbb{1}}_N$ is the identity operator in the subspace with exactly N photons and where λ_N are real and nonnegative coefficients. It is important to outline that following this definition the only fully unpolarized pure state is the two-mode vacuum. In the recent literature different polarization degrees have been introduced, each with its advantages and issues, because of the difficulty of characterize the polarization of a quantum state of light with only one number. There are some reviews about this matter [Bjork et al., 2010, Luis, 2007]. We present the main features of the more relevant proposals below:

4.2.1. Distance to an unpolarized distribution

This polarization degree [Luis, 2002] is defined as the distance between the polarization distribution of a quantum state $Q(\Omega)$, which is the Husimi-Kano function in the representation of SU(2)-coherent states, where $\Omega \equiv (\theta, \phi)$ and θ and ϕ are the polar and azimuthal angles, respectively, on the Poincaré sphere (4.1.8); and the uniform polarization distribution related to unpolarized light $Q_u(\Omega) = 1/4\pi$, written as:

$$D_Q = 4\pi \int d\Omega \, [\, Q(\Omega) - \frac{1}{4\pi} \,]^2. \tag{4.2.19}$$

Renormalizating this parameter to fulfill $0 \leqslant \mathcal{G}_Q \leqslant 1$, we have:

$$\mathcal{G}_Q = \frac{D_Q}{1 + D_Q} = 1 - \frac{1}{4\pi \int d\Omega \, Q^2(\Omega)}, \tag{4.2.20}$$

where this last integral is a measure of the effective area of the Poincaré sphere occupied by $Q(\Omega)$. The advantages of this definition are its invariance under SU(2) transformations, that the only states with $\mathcal{G}_Q = 0$ are those fully unpolarized, it is independent of the intensity fluctuations, $\mathcal{G}_Q$ depends on all the moments of the Stokes operators and that this is a measure of confinement.

[1] The symbol $\oplus$ stands for direct sum of vectorial spaces.

Likewise, recently, a multipole expansion of Q has been accomplished showing the consecutive moments of the Stokes parameters and the emergence of the *hidden polarization* in twin photon sates ought to the lack of dipole contribution [Sánchez-Soto et al., 2013].

4.2.2. Entropy of polarization

A similar approach to the above proposal is that related with the entropy of polarization [Luis, 2007], translated to the quantum domain from the classical study of propagation in nonlinear media [Picozzi, 2004], where the polarization degree $\mathcal{G}_E$ is given by:

$$\mathcal{G}_E = 1 - \frac{e^{W_E}}{4\pi}, \qquad W_E = -\int d\Omega\, Q(\Omega) \log Q(\Omega). \tag{4.2.21}$$

Likewise, other measures closely related with this one has been introduced in the classical domain [Réfrégier and Goudail, 2006].

4.2.3. Generalized visibility

A polarization degree related with the definition of fully unpolarized state (4.2.18), is the following for a pure state $|\psi\rangle$ [Björk et al., 2002]:

$$\mathcal{G}_V = \sqrt{1 - \min_U (|\langle\psi|\hat{U}|\psi\rangle|^2)}, \tag{4.2.22}$$

where $\hat{U}$ is an arbitrary $SU(2)$ transformation. This is a measure of the overlap between the wavefunction $|\psi\rangle$ and all its rotations in the Poincaré sphere, giving an idea of the sensitivity of the state to $SU(2)$ transformations, which is directly related with the definition of unpolarized states above shown (4.2.18). States invariant to these rotations will be fully unpolarized, with $\mathcal{G}_V = 0$, while states suitable to be rotated to the orthogonal one will be fully polarized, and therefore $\mathcal{G}_V = 1$.

4.2.4. Measures based on distance

Another series of proposals of characterization of the quantum polarization is based on distances. In general they are given by [Klimov et al., 2005]:

$$\mathcal{G}(\hat{\rho}) \propto \inf_{\sigma \in \mathcal{U}} D(\hat{\rho}, \hat{\sigma}), \tag{4.2.23}$$

where $\hat{\rho}$ and $\hat{\sigma}$ are the density matrices of the state to be measured and of a state belonging to the set of unpolarized states $\mathcal{U}$, respectively, and where D stands for any measure of distance between both matrices. So the polarization degree will be proportional to the distance between the

quantum state to be measured and the unpolarized state which minimizes this distance.

One choice for this measure is the Hilbert-Schmidt distance, given by:

$$D_{HS}(\hat{\rho}, \hat{\sigma}) = Tr[(\hat{\rho} - \hat{\sigma})^2], \tag{4.2.24}$$

which leads to the following polarization degree:

$$\mathcal{G}_{HS}(\hat{\rho}) = Tr(\hat{\rho}^2) - \sum_{N=0}^{\infty} \frac{p_N^2}{N+1}. \tag{4.2.25}$$

This Hilbert-Schmidt polarization degree is characterized by two features of the quantum state: on one hand its purity, given by $Tr(\hat{\rho}^2)$, and on the other hand its distribution of the total number of photons p_N.

Another candidate to polarization degree is the fidelity:

$$F(\hat{\rho}, \hat{\sigma}) = [Tr(\hat{\sigma}^{1/2}\hat{\rho}\hat{\sigma}^{1/2})^{1/2}]^2. \tag{4.2.26}$$

This is not a distance, but a measure of the overlap between two quantum states: maximum when $\hat{\rho} = \hat{\sigma}$ and zero if the states are orthogonal. However, by means of the Bures metric it can be transformed into a distance leading to the Bures polarization degree:

$$\mathcal{G}_B(\hat{\rho}) = 1 - \sup_{\sigma \epsilon U} \sqrt{F(\hat{\rho}, \hat{\sigma})}. \tag{4.2.27}$$

In this case the polarization degree will be conversely proportional to the overlap between the quantum state to be characterized $\hat{\rho}$ and the unpolarized state $\hat{\rho}$, where the latter is chosen such that maximizes the overlap.

Other similar measures of this kind have been proposed like the trace distance or the Chernoff distance [Bjork et al., 2010].

4.3. Generalized polarization in the OFS representation and polarization degree

As was commented in the previous chapter, the OFS space $\mathcal{E}$ is a natural representation in continuous-variable experiments in quantum optics, and analogous to that used in classical optics. The probability distributions in this space are positive and normalized, while its detection is carried out by means of well-known homodyne detection schemes in one or various modes, as we will show in the next chapter. Because of this, we will study the quantum polarization in this space, which will be called generalized polarization, and which is defined as the confinement degree of the probability distributions of quantum states in certain regions of the OFS space. This definition includes both vectorial and spatial modes where, in the case

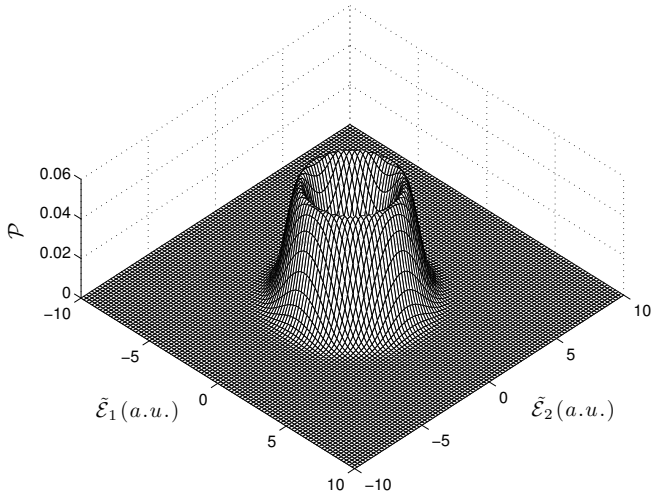

Figure 4.3.1: OFS probability distribution for a two-mode coherent state $|\alpha\, i\alpha\rangle$ with $|\alpha| = 4$.

of two-mode vectorial modes, it agrees with the common quantum polarization above shown. On the other hand, in the case of spatial modes, like the propagation modes in integrated devices, the definition can be extended to N dimensions, where N is the number of propagating modes.

To see how intuitive this concept is, we will analyze a two-mode coherent state $|L\rangle = |\alpha_1\alpha_2\rangle$ in the OFS space $\mathcal{E}$. The complex amplitude of this state is given by (3.2.45):

$$\Psi(\mathcal{E}_1, \mathcal{E}_2) = \langle \mathcal{E}_1\mathcal{E}_2|\alpha_1\alpha_2\rangle = \sqrt{\frac{2}{\pi}}\, e^{-\{(\mathcal{E}_1 - |\alpha_1|\cos\varphi_1)^2 + (\mathcal{E}_2 - |\alpha_2|\cos\varphi_2)^2\}} e^{i\phi}, \tag{4.3.28}$$

where $\varphi_i = \omega t + \delta_i$ with $i = 1, 2$, and ϕ a global phase withtout observable consequences. Likewise, the expected values of the OFS operators $\hat{\mathcal{E}}_i$ will be given by:

$$\langle \hat{\boldsymbol{\mathcal{E}}} \rangle \equiv \langle \hat{\mathcal{E}}_1 \rangle \mathbf{u}_1 + \langle \hat{\mathcal{E}}_2 \rangle \mathbf{u}_2 = |\alpha_1| \cos\varphi_1\, \mathbf{u}_1 + |\alpha_2| \cos\varphi_2\, \mathbf{u}_2, \tag{4.3.29}$$

relation which defines the elliptic path the maximum value of the probability distribution $P = |\Psi(\mathcal{E}_1, \mathcal{E}_2)|^2$ follows. This expression resembles the elliptic polarization of a classical wave[2]. However, the optical field shows fluctuations. From (4.3.28) is easy to show that the fluctuation is gaussian and the variance is constant and equal in both modes, with a value $\Delta\mathcal{E}^2 = 1$. Therefore, the elliptical path shows a quantum uncertainty, that is, there are

[2]Note that this equation is the same as the real part of (4.1.1) if the modes 1 and 2 are vectorial x and y modes.

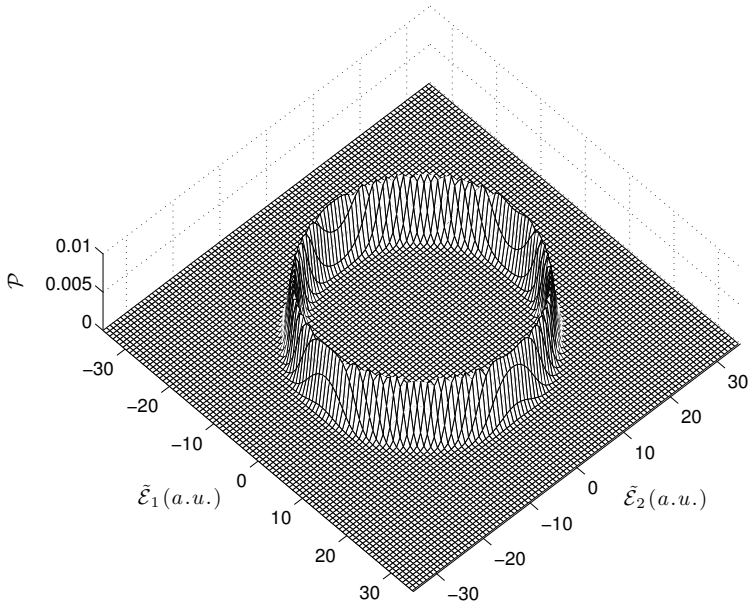

Figure 4.3.2: OFS probability distribution for a two-mode coherent state $|\alpha\, i\alpha\rangle$ with $|\alpha| = 20$.

not well defined trajectories due to the Heisenberg uncertainty principle. As is shown in Figure 4.3.1, for low photonic excitation this uncertainty is important. In the case of a coherent state, these fluctuations can be neglected for high photon number $\bar{n}_i = |\alpha_i|^2 \gg 1$, since the relative quantum uncertainties $\Delta\mathcal{E}_i^2 = 1/|\alpha_i^2|$ are very low, and the classical behaviour naturally appears as shown in Figure 4.3.2. Likewise, for both states sketched in Figures 4.3.1-4.3.2, where $|\alpha_1| = |\alpha_2|$ and $\delta_2 - \delta_1 = \pi/2$, the probability distribution is highly confined, or polarized, along a circular path in the OFS space $\mathcal{E}_1\mathcal{E}_2$. So we will say it shows circular-type generalized polarization. In the same way, we will find quantum states with elliptical and linear-type generalized polarization.

As introduced in the previous section, the polarization degree gives us a measure of how different a quantum state is from a fully unpolarized state. We equally use this idea to define a generalized polarization degree which characterizes N-dimensional quantum states of light. We start taking the N-mode vacuum as a fully unpolarized state, as is generally acepted [Agarwal, 1971, Lehner et al., 1996, Prakash and Chandra, 1971, Söderholm et al., 2001]. We consider this assumption as reasonable since this distribution in the OFS space $\mathcal{E}_1, \ldots, \mathcal{E}_N$ is isotropic and gaussian, so there is no priviledged confinement (polarization) in any Hilbert subspace.

Likewise, it is well known that a symmetric chaotic N-mode quantum state $|\kappa_1,\ldots,\kappa_N\rangle = |\kappa,\ldots,\kappa\rangle$ shows a gaussian isotropic distribution in this space as well, so this state can also be considered as unpolarized. Both sates are related, as the multimode vacuum may be considered as a limit case of the multimode chaotic state when $\kappa \propto \bar{n} \to 0$, with $\bar{n}$ the average photon number. Bearing this in mind, we propose the following N-mode unpolarized pure state with a gaussian probability distribution symmetric between modes $|g\rangle$:

$$P_{|g\rangle}(\mathcal{E}_1,\ldots,\mathcal{E}_N) = \left(\frac{2}{g\,\pi}\right)^{N/2} e^{-\frac{2}{g}\,(\mathcal{E}_1^2+\mathcal{E}_2^2+\cdots+\mathcal{E}_N^2)}, \tag{4.3.30}$$

where g is a free parameter which is calculated such that (4.3.30) reaches the highest overlap with the state to be measured $|L\rangle$, taking a value $g = g_b$. Our approach is closely related to the concept of distance to an unpolarized distribution or states invariant under $SU(2)$ shown in the previous section § 4.2. Following these definitions, we propose the next generalized polarization degree in the OFS space for a N-dimensional quantum state:

$$\mathcal{G}^{(N)}_{|L\rangle} = \frac{1}{2}\int\{\mathbb{P}_{|L\rangle} - \mathbb{P}_{|g_b\rangle}\}^2\,d\mathcal{E}_1\ldots d\mathcal{E}_N, \tag{4.3.31}$$

where, for the sake of normalization, we have introduced the factor $1/2$ and the following normalized distributions:

$$\mathbb{P}_{|L\rangle} = \frac{P_{|L\rangle}(\mathcal{E}_1,\ldots,\mathcal{E}_N)}{\{\int P^2_{|L\rangle}\,d\mathcal{E}_1\ldots d\mathcal{E}_N\}^{1/2}}, \tag{4.3.32}$$

$$\mathbb{P}_{|g_b\rangle} = \frac{P_{|g_b\rangle}(\mathcal{E}_1,\ldots,\mathcal{E}_N)}{\{\int P^2_{|g_b\rangle}\,d\mathcal{E}_1\ldots d\mathcal{E}_N\}^{1/2}}. \tag{4.3.33}$$

This is a Hilbert-Schmidt distance under condition of maximal overlap between the unpolarized state and the state to be characterized. From equation (4.3.31) the following compact expression is obtained for the generalized polarization degree of $|L\rangle$:

$$\mathcal{G}^{(N)}_{|L\rangle} = 1 - \int \mathbb{P}_{|L\rangle}(\mathcal{E}_1,\ldots,\mathcal{E}_N)\,\mathbb{P}_{|g_b\rangle}(\mathcal{E}_1,\ldots,\mathcal{E}_N)\,d\mathcal{E}_1\ldots d\mathcal{E}_N \equiv 1 - \mathcal{D}^{(N)}(g_b) \tag{4.3.34}$$

where g_b defines the best gaussian, or the excitation photon manifold of the unpolarized state, and the maximum value of the function $\mathcal{D}^{(N)}(g)$ as well, which represents the lack of polarization of a quantum state in a N-dimensional space and is given by the overlap integral in (4.3.34). Additionally, we stress that an uniform distribution could be also taken as the unpolarized distribution, but it would not be physically consistent, since the probability for OFS values close to infinite would not be zero.

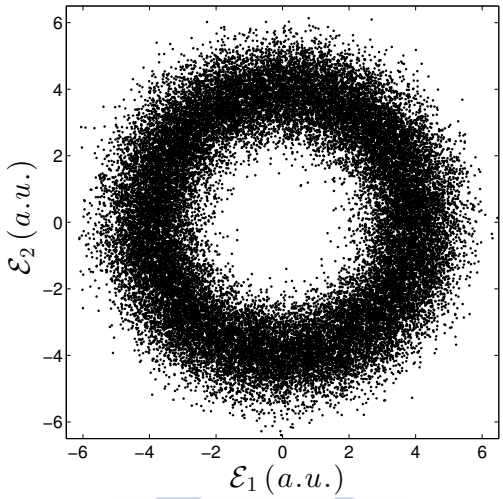

Figure 4.3.3: Simulation of the OFS probability distribution measured by homodyne detection for a two-mode coherent state $|\alpha\, i\alpha\rangle$ with $|\alpha| = 4$.

Likewise, it is important to outline that the choice of the dimension will depend on the specific problem to dealt with. If a quantum state is defined in a Hilbert M-dimension subspace, with $M < N$, or it shows symmetries such that under unitary transformations take it to a subspace of that dimension, an M-dimensional degree $\mathcal{G}^{(M)}$ should be used.

On the other hand, if time-dependent probability distributions are taken into account, we should use accumulated or cycle-average probability distributions:

$$P_{|L\rangle}(\mathcal{E}_1,\ldots,\mathcal{E}_N) = \frac{1}{T}\int_0^T P_{|L\rangle}(\mathcal{E}_1,\ldots,\mathcal{E}_N;t)\,dt. \tag{4.3.35}$$

with T the period of time where the values of field are taken. In fact, the classical polarization is represented by ellipses which can be regarded as the values reached by the optical field after a period T. In the case of coherent quantum states a similar result is obtained. Figure 4.3.3 shows a Monte Carlo simulation of two-mode homodyne detection after a complete cycle of oscillation T for a coherent state with circular-type generalized polarization.

As it will be shown in sections § P5 and § P6, this approach presents consistent results. For instance, for the multimode vacuum we have $\mathcal{G}_{|0,\ldots,0\rangle} = 0$ and, in the same way, quantum states close to the vacuum, that is states with low mean number of photons, show small figures for the polarization degree. Likewise, quantum states with the same excitation photon number in each mode (symmetric) $|\kappa,\ldots,\kappa\rangle$, get $\mathcal{G}_{|\kappa,\ldots,\kappa\rangle} = 0$ as well, while states

far from symmetric $|\kappa,\ldots,0\rangle$, quickly reach the maximum value of polarization $\mathcal{G}_{|\kappa,\ldots,0\rangle} \to 1$ for high excitation numbers $\kappa \propto \bar{n} >>$.

For the sake of clarity, we present here a detailed example to show how to calculate the generalized polarization degree of a quantum state. For example a single photon $|1\,0\rangle$ after propagation in a reconfigurable directional coupler defined by the following unitary matrix:

$$U_{\sigma,\delta} = \begin{pmatrix} \cos\sigma & \sin\sigma\, e^{i\delta} \\ -\sin\sigma & \cos\sigma\, e^{i\delta} \end{pmatrix}, \tag{4.3.36}$$

produces a path-encoded single-photon entangled state, or qubit, $|L\rangle$, which in the OFS space is written as:

$$\Psi_{|L\rangle}(\mathcal{E}_1,\mathcal{E}_2) = \cos\sigma\,\Psi_{|1\rangle}(\mathcal{E}_1)\,\Psi_{|0\rangle}(\mathcal{E}_2) + \sin\sigma\, e^{i\delta}\,\Psi_{|0\rangle}(\mathcal{E}_1)\,\Psi_{|1\rangle}(\mathcal{E}_2) \tag{4.3.37}$$

where $\Psi_{|n\rangle}(\mathcal{E})$ were defined in (3.2.44). The probability of measuring a joint OFS value $(\mathcal{E}_1,\mathcal{E}_2)$ for this quantum state is given as follows:

$$P(\mathcal{E}_1,\mathcal{E}_2) = \frac{2}{\pi}\{\cos^2\sigma\,\mathcal{E}_1^2 + \sin^2\sigma\,\mathcal{E}_2^2 + \sin 2\sigma\,\cos\delta\;\mathcal{E}_1\mathcal{E}_2\}\,e^{-2(\mathcal{E}_1^2+\mathcal{E}_2^2)}. \tag{4.3.38}$$

This probability distribution can be rewritten in a new reference system $\tilde{\mathcal{E}}_1\,\tilde{\mathcal{E}}_2$ obtained under a rotation $\alpha = \arctan(\tan\sigma\cos\delta)$ with respect to the original reference system $\mathcal{E}_1\mathcal{E}_2$, in such a way that a diagonal form for the Gaussian amplitude is obtained. In this new reference frame, equation (4.3.38) can be written as follows:

$$P(\tilde{\mathcal{E}}_1,\tilde{\mathcal{E}}_2) = \frac{2}{\pi}\{\cos^2\tilde{\sigma}\,\tilde{\mathcal{E}}_1^2 + \sin^2\tilde{\sigma}\,\tilde{\mathcal{E}}_2^2\}\,e^{-2(\tilde{\mathcal{E}}_1^2+\tilde{\mathcal{E}}_2^2)}. \tag{4.3.39}$$

where $\sin 2\tilde{\sigma} = \sin 2\sigma\,\sin\delta$ [Born and Wolf, 1959]. Since the polarization degree is independent on the reference system chosen, by inserting the probability distribution (4.3.39) into equation (4.3.34), and performing the calculations above mentioned, we obtain the following result:

$$\mathcal{G}^{(2)}_{|L\rangle} = 1 - \frac{3}{8}\,\frac{\sqrt{6}}{\sqrt{\cos^4\tilde{\sigma} + \sin^4\tilde{\sigma} + \frac{1}{2}}}. \tag{4.3.40}$$

Note that for $\tilde{\sigma} = 0$, or linear-type generalized polarization, we obtain $\mathcal{G} = 1/4$. Likewise the minimum polarization degree for these qubits is obtained for $\tilde{\sigma} = \pi/4$ or circular-type generalized polarization, with $\mathcal{G} = 1 - (3/4)(\sqrt{3/2})$. Other cases take values in between these two presenting the so-called elliptical-type generalized polarization. The result is physically expected. The qubit generalized polarization is quite low because the maximum values of the probability distribution in the $\tilde{\mathcal{E}}_1\tilde{\mathcal{E}}_2$-space are found for low OFS values and therefore comparable to the quantum fluctuations

of vacuum which is, by definition, an unpolarized state. Likewise, it is interesting to underline that the polarization degree increases with the lack of symmetry in analogy with the classical concept.

oOo

In the following sections we present the published research works on generalized quantum polarization where we go in depth with the concepts above introduced and their application to IPDs. Specifically, in § P5 we will focus our attention on *multimode single photon states* (MSP), with interest on *discrete-variable quantum computation* (DVQC). We will start introducing the concept of generalized polarization by comparing the common polarization modes and the propagation modes of integrated optics. We will present the properties of generalized polarization in the OFS space and show their application in a 3×3 DC. Next we will introduce the quantum generalized polarization degree for N-dimensional quantum states and apply it to MSP states. Finally we study the case of quantum superpositions of MSP states with vacuum. On the other hand, in § P6 we center our attention on non-stationary quantum states of light, with interest on *continuous-variable quantum computation* (CVQC). We will begin reviewing the concept of generalized polarization and the quantum generalized polarization degree, adapting it to the characterization of non-stationary states. Right after, we analyze coherent states and the specific example of propagation in a multimode DC. Next we study squeezed states generated in *degenerate* and *non-degenerate parametric amplifiers* and compare its generalized polarization degree with that correponding to *quasi*-classical states. Finally we analyze two-mode Schrödinger's cat states, where entanglement appears as interference in the OFS space.

USC
UNIVERSIDADE
DE SANTIAGO
DE COMPOSTELA

P5. OPTICAL FIELD-STRENGTH GENERALIZED POLARIZATION OF MULTIMODE SINGLE PHOTON STATES IN INTEGRATED DIRECTIONAL COUPLERS

JOURNAL OF MODERN OPTICS
VOL. 58 NO. 8 PAGES 711-725
doi: 10.1080/09500340.2011.568709

PUBLISHED 10 MAY 2011

BY JESÚS LIÑARES, DAVID BARRAL, MARÍA C. NISTAL & VICENTE MORENO

UNIVERSIDADE DE SANTIAGO DE COMPOSTELA

Abstract: *A quantum analysis of the generalized polarization properties of multimode single photon states is presented. It is based on the optical field-strength probability distributions in such a way that generalized polarization is understood as a significant confinement of the probability distribution along certain regions of the multidimensional optical field-strength space. The analysis is addressed to multimode integrated waveguiding devices, such as* $\mathrm{N} \times \mathrm{N}$ *integrated directional couplers, whose modes fulfil a spatial modal orthogonality relationship. For that purpose a definition of the quantum generalized polarization degree in a* N*-dimensional space, based on the concept of distance to a unpolarized* N*-dimensional Gaussian distribution, is proposed. The generalized polarization degree of pure and mixture multimode single photon states and also of some multiphoton states such as coherent and chaotic ones, is evaluated and analyzed.*

P5.1. Introduction

Multimode Single Photon (MSP) states are being of a great interest in many topics of quantum optics such as quantum cryptography, quantum teleportation, quantum computation and so on. Accordingly, large efforts are being made in order to get single-photon sources of a high quality [Grangier, 2002, Grangier et al., 2004], that is, with a reduced contribution of the multimode vacuum state. The study of these MSP states from different points of view will contribute to get a better knowledge of their practical and theoretical properties. Thus in this work we will center our attention on the quantum generalized polarization properties displayed by these MSP states, where generalized polarization will be understood, in a broad sense, as the confinement degree of the optical field-strength $\mathcal{E}$ probability distribution of a MSP state on determined regions of the multimode optical field-strength space. It must be stressed that in the case of single-photon states excited in two polarization (or vectorial) modes the generalized polarization results would correspond to the quantum standard polarization. We also underline that one of the main advantages of using the mentioned distributions is that they are a well-behaved probability distributions and can be measured by the homodyne detection techniques [Bachor, 1998, Vogel, 1990] which can be extended to the multimode case [D'Ariano et al., 1999, Raymer and Funk, 1999].

First of all, and for sake of expositional clarity, we will introduce the concept of generalized polarization from a classical point of view. For that purpose, and for sake of expositional convenience, we will center our attention on the bimode case, that is, let us consider that two normalized modes $\{\boldsymbol{e}_m, \boldsymbol{e}_n\}$ are propagating, for example, along an arbitrary z-direction. A general classical state at a plane z, in complex notation, will be given by the following expression: $\boldsymbol{e}(x,y) = \{a_m e^{-i\omega t}\, \boldsymbol{e}_m(x,y) + a_n e^{-i\omega t}\, \boldsymbol{e}_n(x,y)\}$, where a_m, a_n are complex numbers. For standard polarization the optical modes can be two orthogonal plane waves, called *polarization modes*, whose optical fields are, for instance, oscillating along horizontal and vertical directions and denoted for example as: m=h, n=v. Besides, it is usual to represent the classical field by a Jones vector [Born and Wolf, 1959], that is, $(a_h e^{-i\omega t}, a_v e^{-i\omega t})^{\mathsf{T}}$ (super-index T indicates transposed) whose real part determines, except a constant, the values of the optical field amplitudes on the abstract space $\mathcal{E}_h\mathcal{E}_v$. As it is well-known, the geometrical region where the values of the optical field are found, that is, its polarization, is in general an elliptical curve on the $\mathcal{E}_h\mathcal{E}_v$ space, and therefore the state is said to have an elliptical polarization.

On the other hand let us consider the classical field $\boldsymbol{e}(x,y)$ in an integrated bimode directional coupler formed, for instance, by two identical monomode guides separated a certain distance along x-direction and with normalized modes $\boldsymbol{e}_1(x,y), \boldsymbol{e}_2(x,y)$. Such a field can be also represented

by the same above expressions, that is, a general classical state at a plane z of a bimode coupler will be given by the complex expression: $\boldsymbol{e}(x,y) = \{a_1 e^{-i\omega t}\,\boldsymbol{e}_1(x,y) + a_2 e^{-i\omega t}\,\boldsymbol{e}_2(x,y)\}$, where a_1, a_2 are also complex numbers and therefore the Jones vector representation $(a_1 e^{-i\omega t}, a_2 e^{-i\omega t})^{\top}$ can be used. However in this case the modes are orthogonal from a spatial point of view [Kogelnik, 1988, Liñares and Nistal, 2003] and therefore hereafter we will call them *generalized polarization modes*. Once more we obtain elliptical curves on an abstract plane $\mathcal{E}_1\mathcal{E}_2$ and therefore the field shows a "polarization" on the mentioned space, but in order to distinguish it from the standard polarization we will say that the field has, in general, an elliptical generalized polarization. Obviously generalized polarization, unlike standard polarization, can be extended to N dimensions. For example, if NxN integrated directional couplers (that is, with N monomode guides) are considered then we will have the general classical states $\boldsymbol{e}(x,y) = \sum a_m\, e^{-i\omega t}\,\boldsymbol{e}_m(x,y)$, where the generalized polarization curves would be obtained starting from a generalized Jones vector $(a_1 e^{-i\omega t}, ..., a_N e^{-i\omega t})^{\top}$ on a N-dimensional space $\mathcal{E}_1 ... \mathcal{E}_N$.

Now we can already consider the quantum case and first of all it must be underlined that even for quasi-classical states like coherent states with a high photonic excitation the above classical concept of generalized polarization (or standard polarization) fails because of quantum noise, that is, the mean value of the optical field operator of any coherent state does not follow (or shows) a definite curve (trajectory) of generalized polarization (or polarization) like an ellipse, circle or straight line on a bimode optical field-strength plane, or like hyper-curves on a multimode optical field-strength space. Obviously it happens by similar reasons to those ones that establish that quantum particles can not follow definite trajectories, that is, there are quantum fluctuations which deviate the optical field-strength values from the mentioned trajectories or curves. Likewise, for quantum states very apart from the quasi-classical ones, such as the number states, the above statement is still clearer since the mean value of the optical field operator is zero, and the deviations of the optical field-strength values from any possible curve (or trajectory) are still larger [Vogel, 1990]. Regarding to the above statements it is also convenient to remember that one of the main conceptual difficulties related to quantum standard optical polarization comes from the extension to the quantum domain of the Stokes parameters formalism, i.e., the quantum Stokes parameters [Mandel and Wolf, 1995] would be the mean values of the corresponding Stokes operators, but although they constitute a natural tool appraising some of the quantum polarization properties it is well-known that when they are used to calculate the degree of polarization based on its semiclassical definition then several conceptual misinterpretations and inconsistencies about the optical polarization of quantum states arise. These confusions and inconsisten-

cies have been solved and/or avoided by developing different approaches in standard polarization [Abouraddy et al., 2002, Alodjants and Arakelian, 1999, Klyshko, 1992]. We must stress that similar limitations and problems would arise if we consider two orthogonal spatial modes (two *generalized polarization modes*), such as those ones of a 2x2 directional coupler. Likewise, we can also consider an arbitrary number N of orthogonal spatial modes, such as those ones of *N*x*N* directional couplers, and similar limitations and problems would also arise with the generalized polarization of their multimode quantum states.

In the light of the above considerations, one of the main aims of this work will be to avoid such kind of limitations and problems by studying the quantum generalized polarization by mean of the probability distributions of multimode states on the optical field-strength space. Under this approach both standard polarization and generalized polarization can be studied and analyzed in an unified way. Recently it has been presented for standard quantum polarization (two-mode case) [Liñares et al., 2010], and in this work we will extend such an approach to quantum generalized polarization multimode states. In our opinion this approach offers both for theoretical analysis and even quantum technological purposes a more visual and practical formalism to deal with generalized polarization properties of quantum states, in particular of those states with a great technological potential such as for example MSP states, squeezed states, entangled states and so on. Obviously the semiclassical limit of this formalism recovers the concept of classical generalized polarization as well-defined trajectories on a multimode optical field-strength space. At this point it is convenient to highlight the increasing in the use of optical devices acting on quantum states excited in spatial modes, such as two and three-mode directional couplers [Liñares et al., 2008a,b, Perina, 1995, Perina and Perina Jr, 2000], six-mode logic gates [Kwiat, 2008, Politi et al., 2008] and so on, in order to achieve optical-quantum transformations for different kind of applications. In this work we will preferentially consider the probability distributions of MSP states, that is, $|S\rangle = c_o|0...0\rangle + \sum_{i=1} c_i|0...0\,1_i\,0...0\rangle$. These states are in turn considered as major states in a short term for the future of the quantum optics technology, particularly input states with $c_o \approx 0$, that is, input MSP states without multimode vacuum state which would be obtained by single-photon sources. Obviously under optical transformations the appearance of the multimode vacuum state is an unavoidable result and even necessary to describe devices like an optical linear projector (or linear generalized polarizer) which can be implemented, for example, when all the modes of a directional coupler unless one are cut off. Likewise an optical attenuator, a non perfect single photon source or any other multi-photon source where the average number of photons is strongly reduced gives rise to the vacuum state. In short, the analysis of MSP states entangled with the multimode vacuum state is also necessary.

The primary aim of this work is to provide a formalism based on the distribution of probability on a N-dimensional multimode optical field-strength space, that is, $\mathcal{P}(\mathcal{E}_1,...,\mathcal{E}_N)$, in order to analyze the generalized polarization properties of MPS states. The plan of the work is as follows: in section 2 we present an analysis of the probability distributions of pure and mixture MPS states on the multidimensional space $\mathcal{E}_1...\mathcal{E}_N$ in such a way that their generalized polarization characteristics are shown; we will show that pure MSP states can be more easily represented on a new rotated two-dimensional optical field-strength space $\tilde{\mathcal{E}}_1\tilde{\mathcal{E}}_2$, however mixture MSP states must be, in general, represented in a N-dimensional space. In section 3, a simple definition of a N-dimensional quantum generalized polarization degree is introduced in order to calculate the generalized polarization degree of pure and mixture MSP states; this definition is also valid for any quantum state and therefore applications to coherent and chaotic states are also shown. In section 4 we briefly analyze the probability distributions of pure and mixture $MSP_\emptyset$ states, that is, superposition of MSP states with the multimode vacuum state. In section 5 a summary is presented.

P5.2. Generalized polarization properties of MSP states

MSP states can be obtained by starting from a single photon state source and next to perform a general linear transformation of the state by some optical device. Thus many MSP states can be obtained by using *N*x*N* directional couplers such as for example integrated and/or fibre optical coupler devices, which display very interesting dynamical and topological properties [Liñares and Nistal, 1992] and in turn have shown a great potentiality and feasibility for optical quantum computing [Kwiat, 2008, Politi et al., 2008]. It is also known that these devices variously implement linear and non linear quantum optical transformations by means of light spatial propagation inside them, therefore the proper operator describing the optical quantum propagation is the Momentum operator $\hat{M}$ [Liñares et al., 2008a, Luks and Perinová, 2002, Perinová et al., 2006]. This operator for linear devices operating with N coupled modes with coupling strengths (or coupling coefficients) χ_{ij}, where $i,j = 1,...,N$ and with propagation constants β_i is given by [Liñares et al., 2008a]:

$$\hat{M} = \hbar \sum_{i=1}^{N} \tilde{\beta}_i \, \hat{a}_i^\dagger \hat{a}_i + \sum_{i\neq j}^{N} \hbar \chi_{ij} \, (\hat{a}_i^\dagger \hat{a}_j + c.h.), \tag{P5.1}$$

where $\tilde{\beta}_i$ is the sum of the propagation constant β_i with the self-coupling coefficients χ_{ii}. The quantum light spatial propagation of a single photon state, as for example $|0...0\,1_j\,0...0\rangle \equiv |1_j\rangle$, through the above devices, will be governed by the solutions $\hat{a}_i(z)$ of the Heisenberg's equations for the operator $\hat{M}$, and therefore MSP states will be obtained, that is, $|S\rangle = \sum c_i|1_i\rangle$.

Likewise, if the device performs a non unitary transformation, such as a linear projection, which can be implemented, for example, by cutting off all the modes unless the j-mode, then the following MSP state entangled with the multimode vacuum is obtained: $|S_\emptyset\rangle = c_o|0\rangle + c_j|1_j\rangle$. Obviously these states are also obtained by reducing drastically the main photon number, as for example in the case of a single photon multimode coherent state, that is: $|\alpha\rangle \approx \mathcal{C}(|0\rangle + \sum_{i=1}^{N} \alpha_i|1_i\rangle)$, where $\mathcal{C}$ is a normalization constant, or also in the case of a single photon chaotic state, which can be obtained from the above state by performing the formal change $\alpha_i \rightarrow \bar{n}_i\, e^{i\gamma_i}$, with γ_i a random phase and $\bar{n}_i$ the mean photon number.

Generalized polarization on the $\mathcal{E}_1...\mathcal{E}_N$ space

On the other hand, the well known adimensional optical (electric) field-strength $\hat{\mathcal{E}}_i$ operators with eigenstates (optical field states) $|\mathcal{E}_i\rangle$ are defined as follows:

$$\hat{\mathcal{E}}_i\,|\mathcal{E}_i\rangle = \frac{1}{2}(\hat{a}_i + \hat{a}_i^\dagger)\,|\mathcal{E}_i\rangle = \mathcal{E}_i\,|\mathcal{E}_i\rangle, \tag{P5.2}$$

therefore, as is customary in the quantum theory, we can use the N - dimensional eigenstates $|\mathcal{E}_1...\mathcal{E}_N\rangle$ of the optical field-strength operators $\hat{\mathcal{E}}_i$ in order to represent the MSP states, and therefore the probability distribution $\mathcal{P}$ of the optical field-strength on the abstract multimode space $\mathcal{E}_1...\mathcal{E}_N$. By taking into account the shape of these probability distributions we will be able to determine how much the quantum state is polarized, that is, how large is the confinement of its probability distribution on the multidimensional optical field-strength space.

In order to show how intuitive and useful is to analyze quantum generalized polarization on the $\mathcal{E}_1...\mathcal{E}_N$ space we present the analytical results for a semiclassical state, that is, a coherent state with a high mean photon number. Let us write an arbitrary multimode quantum light state $|L\rangle = |L_1...L_N\rangle \equiv |L_1\rangle...|L_N\rangle$ in the representation of the eigenstates $|\mathcal{E}_1...\mathcal{E}_N\rangle$ of the field-strength operators $\hat{\mathcal{E}}_i$, that is:

$$|L_1...L_N\rangle = \iint \langle\mathcal{E}_1|L_1\rangle...\langle\mathcal{E}_N|L_N\rangle|\mathcal{E}_1\rangle...|\mathcal{E}_N\rangle\, d\mathcal{E}_1...d\mathcal{E}_N. \tag{P5.3}$$

Next we consider the normalised wave function, or complex amplitude of the probability distribution on the space $\mathcal{E}_1...\mathcal{E}_N$ of the following multimode coherent state: $|L_1...L_N\rangle = |\alpha_1...\alpha_N\rangle$, with $\alpha_i = |\alpha_i|e^{i\epsilon_i}$. By taking into account the complex amplitude of a monomode coherent state of a quantum harmonic oscillator [Orszag, 2008] we can easily write the following multimodal complex amplitude:

$$\mathcal{A}(\mathcal{E}_1,...,\mathcal{E}_N) = \langle\mathcal{E}_1|L_1\rangle...\langle\mathcal{E}_N|L_N\rangle = {}_{(1/\pi^{N/4})}\, e^{-\frac{1}{2}\{\sum_{i=1}^{N}(\mathcal{E}_i - |\alpha_i|cos\varphi_i)^2\}} e^{i\phi}, \tag{P5.4}$$

where $\varphi_i = \varphi + \epsilon_i$ and ϕ is a global phase which will not affect the future considerations. Moreover, if we consider that photons are excited with energy $\hbar\omega$ in all spatial modes then we can write $\varphi = \omega t$. After a straightforward calculation, we obtain the following result for the expected values of $\hat{\mathcal{E}}_i$, which for sake of expositional convenience are written in a vector form on the abstract space $\mathcal{E}_1 ... \mathcal{E}_N$, that is, by taking the unitary vectors $\mathbf{u}_i$ along $\mathcal{E}_i$-directions we obtain:

$$\langle \hat{\boldsymbol{\mathcal{E}}} \rangle \equiv \sum_{i=1}^{N} \langle \hat{\mathcal{E}}_i \rangle \mathbf{u}_i = \sum_{i=1}^{N} |\alpha_i| \cos\varphi_i \, \mathbf{u}_i, \tag{P5.5}$$

which, in general, defines a hyperelliptical trajectory for the maximum value of the probability distribution $\mathcal{P} = |\mathcal{A}(\mathcal{E}_1, ..., \mathcal{E}_N)|^2$ with a quantum Gaussian fluctuation $\Delta = 2^{1/2}$, such as it is easily checked from equation

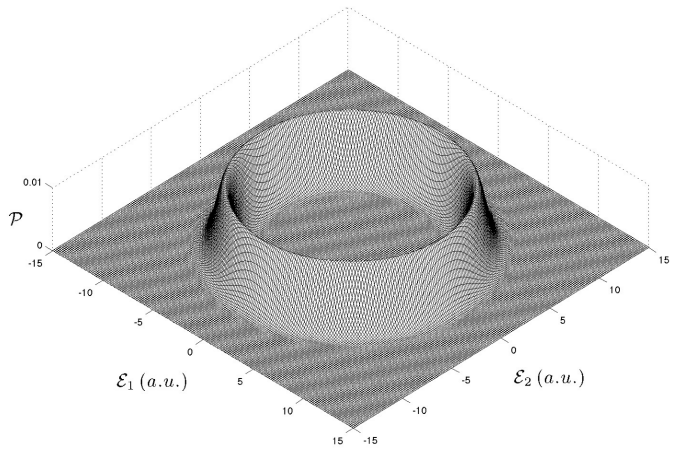

Figure P5.1: Probability distribution of a two-mode circular coherent state with $\bar{n}_1 = \bar{n}_2 = 81$.

(P5.4). In fact for the case N=2 the above expression remind us of the elliptical polarization of a classical wave but with quantum fluctuations. This hyperelliptical trajectory presents a quantum uncertainty which can be neglected as long as the coherent state has a high mean number of photons, that is, the relative uncertainties $\Delta_i = 2^{1/2}/|\alpha_i|$ are more and more negligible and accordingly the classical wave behaviour would be achieved in the limit $|\alpha_i| \gg 1$. As an illustrative example and for sake of simplicity it is shown in Figure P5.1 the probability distribution $\mathcal{P}(\mathcal{E}_1, \mathcal{E}_2)$ for any time (that is, the probability is integrated along the time) of a two-mode circular coherent state for $|\alpha_1| = |\alpha_2| = 9$. This two-mode coherent state $|9 \;\; 9\, e^{\pm i\pi/2}\rangle$ can be obtained by a synchronic ($\beta_1 = \beta_2$) linear directional

coupler 2x2, with coupling coefficient $\chi_{12} = \chi_{21} = \kappa$, after a propagation distance $L = \pi/2\kappa$ [Jansky et al., 1988, Kogelnik, 1988, Liñares et al., 2008b]. Note the circular annular shape of the distribution probability, that is, the high localization (generalized polarization) of the optical field-strength along a circular curve although with a certain dispersion.

Probability distributions of pure MSP states

Pure and mixture MSP states can be represented in a compact way by the density operator $\hat{\rho}$, however for sake of expositional convenience we start by considering pure MSP states $|S\rangle$ together with their $\mathcal{E}_1...\mathcal{E}_N$-representation by using the complex amplitude probability $\mathcal{A}_{|S\rangle} = \langle \mathcal{E}_1...\mathcal{E}_N|S\rangle$, which is given, except by a global phase, by the following expression:

$$\mathcal{A}_{|S\rangle}(\mathcal{E}_1,...,\mathcal{E}_N) = \sum_{i=1}^{N} c_i \langle \mathcal{E}_1...\mathcal{E}_N|1_i\rangle, \tag{P5.6}$$

where $c_i = |c_i|e^{i\epsilon_i}$. Now, by using the notation $\mathcal{A}_{|1_i\rangle} = \langle \mathcal{E}_1...\mathcal{E}_N|1_i\rangle$, the following probability distribution $\mathcal{P}_{|S\rangle} = |\langle \mathcal{E}_1...\mathcal{E}_N|S\rangle|^2$ is obtained:

$$\mathcal{P}(\mathcal{E}_1,...,\mathcal{E}_N) = \sum_{i=1}^{N} |c_i|^2 \mathcal{A}^2_{|1_i\rangle} + 2\sum_{i<j}^{N} |c_i||c_j| cos\epsilon_{ij}\, \mathcal{A}_{|1_i\rangle}\, \mathcal{A}_{|1_j\rangle}, \tag{P5.7}$$

with $\epsilon_{ij} = \epsilon_i - \epsilon_j$. It is also interesting, for future considerations, to write the corresponding density operator $\hat{\rho}^{\,o}$ of a pure MSP state, that is,

$$\hat{\rho}^{\,o} = \sum_{i,j=1}^{N} \rho^o_{ij}\, |1_i\rangle\langle 1_j| = \sum_{i,j=1}^{N} |c_i||c_j|\{\delta_{ij} + e^{\epsilon_{ij}}(1-\delta_{ij})\}|1_i\rangle\langle 1_j|, \tag{P5.8}$$

where δ_{ij} is the Kronecker delta function. Note that for pure MSP states the amplitude and phases of the values ρ^o_{ij} are related among them in a specific way (unlike mixture states), that is,

$$\frac{\rho^o_{ij}}{\rho^o_{jk}} = \frac{\rho^o_{im}}{\rho^o_{mk}}, \quad \epsilon_{ij} + \epsilon_{jk} = \epsilon_{ik}. \tag{P5.9}$$

Next, by taking into account the explicit amplitudes $\mathcal{A}_{|1_i\rangle}$, that is, the well-known first-order Hermite-Gaussian functions on a N-dimensional space: $\mathcal{A}_{|1_i\rangle} = (\sqrt{2}\mathcal{E}_i/\pi^{N/4})\, e^{-\frac{1}{2}(\mathcal{E}_1^2+...+\mathcal{E}_i^2+...+\mathcal{E}_N^2)}$, then equation (P5.7) acquires the very simple form:

$$\mathcal{P}(\mathcal{E}_1,...,\mathcal{E}_N) = \frac{2}{\pi^{N/2}}\{\sum_{i=1}^{N} |c_i|^2\mathcal{E}_i^2 + 2\sum_{i<j}^{N} |c_i||c_j| cos\epsilon_{ij}\, \mathcal{E}_i\mathcal{E}_j\} e^{-(\mathcal{E}_1^2+...+\mathcal{E}_N^2)}. \tag{P5.10}$$

Obviously the same result is obtained from equation (P5.8) by using $\mathcal{P}(\mathcal{E}_1,...\mathcal{E}_N) = \langle \mathcal{E}_1...\mathcal{E}_N|\hat{\rho}|\mathcal{E}_1...\mathcal{E}_N\rangle$. Likewise note that the Gaussian amplitude is a quadratic form on a multidimensional space $\mathcal{E}_1...\mathcal{E}_N$, to which, such as it was made above, we associate a basis of unitary vectors $\{\mathbf{u}_1,...,\mathbf{u}_N\}$. It will allow us to characterize the polarization of MSP states in a very analogous way to the classical one. Such a characterization can be enormously simplified by using a reference system, that is, a new basis $\{\tilde{\mathbf{u}}_1,...,\tilde{\mathbf{u}}_N\}$, where the quadratic form (P5.10) is diagonal, and where moreover only a bidimensional space will be needed. We will show by using a heuristic argument that only a bidimensional space is required to represent MSP states, that is, let us consider the following two-mode state with a diagonal Gaussian amplitude form in a two-dimensional subspace $\tilde{\mathcal{E}}_1\tilde{\mathcal{E}}_2$,

$$\mathcal{A}_{|S\rangle}(\tilde{\mathcal{E}}_1,...,\tilde{\mathcal{E}}_N) = \frac{\sqrt{2}}{\pi^{N/4}}\{\tilde{C}_1\,\tilde{\mathcal{E}}_1 \pm i\tilde{C}_2\,\tilde{\mathcal{E}}_2\}\,e^{-\frac{1}{2}(\tilde{\mathcal{E}}_1^2+...+\tilde{\mathcal{E}}_N^2)}, \qquad \text{(P5.11)}$$

where $\tilde{C}_i \geqslant 0$, $i = 1,2$. Now we can perform a variables transformation which leaves invariant the quadratic form $(\tilde{\mathcal{E}}_1^2+...+\tilde{\mathcal{E}}_N^2)$ in equation (P5.11), that is, if we choose an arbitrary orthogonal transformation $\tilde{\mathcal{E}}_i = \sum_j a_{ij}\mathcal{E}_j$, $i = 1,2; j = 1,..,N$ and we take into account that the group of orthogonal transformations is continuous, we can claim that any MSP state can be obtained, that is,

$$\mathcal{A}_{|S\rangle}(\mathcal{E}_1,...,\mathcal{E}_N) = \frac{\sqrt{2}}{\pi^{N/4}}\sum_{j=1}^{N}(\tilde{C}_1 a_{1j} \pm i\tilde{C}_2 a_{2j})\mathcal{E}_j\,e^{-\frac{1}{2}(\mathcal{E}_1^2+...+\mathcal{E}_N^2)}, \qquad \text{(P5.12)}$$

where the new general complex coefficients are: $c_j = \tilde{C}_1 a_{1j} \pm i\tilde{C}_2 a_{2j} \equiv |c_j|e^{i\epsilon_j}$. The major consequence is that the MSP states are equivalent to two-mode single photon states on a subspace $\tilde{\mathcal{E}}_1\tilde{\mathcal{E}}_2$, and therefore the problem involves to find the subspace $\tilde{\mathcal{E}}_1\tilde{\mathcal{E}}_2$, that is, to solve the inverse problem. In a more rigorous way, we see that the matrix c_{ij} associated to the quadratic form (P5.10) is a symmetric matrix, therefore by taking into account the subadditivity property of the rank of a symmetric matrix together with the relationships given by equation (P5.9) it is easy to prove that $rank(c_{ij}) = 2$ and consequently the number of eigenvalues different to zero are only two. Their particular values must be obtained by the diagonalization of equation (P5.10) and, as a result of the above arguments, we will have only two real (orthogonal transformation) eigenvectors of interest, that is, $\{\tilde{\mathbf{u}}_1, \tilde{\mathbf{u}}_2\}$. Next we will present a suitable method for our purpose of obtaining the diagonal form of the above real and symmetric matrix, which is based on the calculation of the diagonal minors of the matrices c_{ij}. We will apply it to the case of three-mode single photon states, although the results can be easily extended to an arbitrary dimension N.

Three-mode single photon states (TSP)

Let us consider a three-mode single photon state (TSP states), then the general probability distribution on the space $\mathcal{E}_1\mathcal{E}_2\mathcal{E}_3$, with a basis of unitary vectors $\{\mathbf{u}_1, \mathbf{u}_2, \mathbf{u}_3\}$, is given by the expression:

$$\mathcal{P}(\mathcal{E}_1, \mathcal{E}_2, \mathcal{E}_3) = \frac{2}{\pi^{3/2}}\{\sum_{i=1}^{3} |c_i|^2 \mathcal{E}_i^2 + 2\sum_{i<j}^{3} |c_i||c_j| cos\epsilon_{ij}\, \mathcal{E}_i\mathcal{E}_j\} e^{-(\mathcal{E}_1^2+\mathcal{E}_2^2+\mathcal{E}_3^2)}. \tag{P5.13}$$

We diagonalize the matrix c_{ij} associated to the above probability distribution, that is, we will look for the two-dimensional space $\tilde{\mathcal{E}}_1\tilde{\mathcal{E}}_2$ where the mentioned distribution is given by the diagonal expression:

$$\mathcal{P}(\tilde{\mathcal{E}}_1, \tilde{\mathcal{E}}_2, \tilde{\mathcal{E}}_3) = \frac{2}{\pi^{3/2}}\{\tilde{C}_1^2\tilde{\mathcal{E}}_1^2 + \tilde{C}_2^2\tilde{\mathcal{E}}_2^2\}\, e^{-(\tilde{\mathcal{E}}_1^2+\tilde{\mathcal{E}}_2^2+\tilde{\mathcal{E}}_3^2)}. \tag{P5.14}$$

The first aim will be obtain the eigenvalues $\lambda_i = \tilde{C}_i^2 = \tilde{P}_i \neq 0$ and their eigenvectors that let us to determine the new basis of unitary vectors $\{\tilde{\mathbf{u}}_1, \tilde{\mathbf{u}}_2\}$ of the new space $\tilde{\mathcal{E}}_1\tilde{\mathcal{E}}_2$. By using the well-known general diagonalization method based on the diagonal minors o a matrix c_{ij}, that is, the characteristic polynomial is given by the expression:

$$p(\lambda) = det(c_{ij} - \lambda I) = \sum_{k=0}^{N} p_k \lambda^k = \sum_{k=0}^{N} (-1)^k \sum_{i=1}^{N} m_i^{(N-k)} \lambda^k, \tag{P5.15}$$

where $m_i^{(N-k)}$ are the diagonal minors of order $(N-k)$ of the matrix c_{ij}. Note that in the cases $k = 0, N{-}1, N$ we obtain the simple relationships:

$$p_0 = det(c_{ij}),\ p_{N-1} = (-1)^{N-1}\sum_{i=1}^{N} |c_i|^2 = (-1)^{N-1},\ p_N = (-1)^N. \tag{P5.16}$$

Now let us consider the characteristic polynomial of a TSP state, that is, from equation (P5.13) we obtain

$$det\,(c_{ij} - \lambda I) = \begin{vmatrix} |c_1|^2 - \lambda & |c_1||c_2|\cos\epsilon_{12} & |c_1||c_3|\cos\epsilon_{13} \\ |c_1||c_2|\cos\epsilon_{12} & |c_2|^2 - \lambda & |c_2||c_3|\cos\epsilon_{23} \\ |c_1||c_3|\cos\epsilon_{13} & |c_2||c_3|\cos\epsilon_{23} & |c_3|^2 - \lambda \end{vmatrix} = 0, \tag{P5.17}$$

According to the diagonal minors method the coefficients of the characteristic polynomial, after a straightforward calculation, are given by the

following expressions:

$$p_3 = (-1)^3 = -1, \tag{P5.18}$$

$$p_2 = (-1)^2(|c_1|^2 + |c_2|^2 + |c_3|^2) = 1, \tag{P5.19}$$

$$p_1 = (-1)\sum_{i<j}^{3} |c_i|^2|c_j|^2 sin^2\,\epsilon_{ij}, \tag{P5.20}$$

$$p_0 = det(c_{ij}) = 0. \tag{P5.21}$$

If we insert these values into equation (P5.15) for the characteristic polynomial then the following algebraic equation together with its roots λ_i $(i = 1, 2, 3)$ are obtained:

$$p(\lambda) = -\lambda^3 + \lambda^2 - (\sum_{i<j}^{3} |c_i|^2|c_j|^2 sin^2\,\epsilon_{ij})\lambda = 0, \tag{P5.22}$$

$$\lambda_{1,2} = \frac{1 \pm (1 - 4\,\sum_{i<j}^{3} |c_i|^2|c_j|^2 sin^2\,\epsilon_{ij})^{1/2}}{2} \qquad \lambda_3 = 0. \tag{P5.23}$$

Note, such as it was proven, that only two eigenvalues are different to zero, and therefore we only need to calculate two eigenvectors $\tilde{\mathbf{u}}_i = a_{ij}\mathbf{u}_j$, $i = 1, 2; j = 1, 2, 3$, and in this case the third one can be simply obtained as $\tilde{\mathbf{u}}_3 = \tilde{\mathbf{u}}_1 \wedge \tilde{\mathbf{u}}_2$. After a standard and straightforward calculation, the following relationships between the eigenvectors components are obtained for each eigenvalue λ_i:

$$A_{i1} = |c_1||c_2|[\lambda_i \cos\epsilon_{12} + |c_3|^2(\cos\epsilon_{13}\cos\epsilon_{23} - \cos\epsilon_{12})], \tag{P5.24}$$

$$A_{i2} = \lambda_i^2 - (|c_1|^2 + |c_3|^2)\,\lambda_i + |c_1|^2|c_3|^2\,\sin^2\epsilon_{13}, \tag{P5.25}$$

$$A_{i3} = |c_3||c_2|[\lambda_i \cos\epsilon_{23} + |c_1|^2(\cos\epsilon_{13}\cos\epsilon_{12} - \cos\epsilon_{23})], \tag{P5.26}$$

therefore the normalized eigenvectors will be given by the following expressions:

$$\tilde{\mathbf{u}}_i = \frac{1}{[\sum_{j=1}^{3}(A_{ij})^2]^{1/2}}(A_{i1}, A_{i2}, A_{i3})^T \equiv (a_{i1}, a_{i2}, a_{i3})^T, \tag{P5.27}$$

which in turn defines an orthogonal transformation a_{ij} between the coordinates in the new basis of eigenvectors $\tilde{\mathbf{u}}_i$ and in the old basis $\mathbf{u}_j$, that is, $\tilde{\mathcal{E}}_i = a_{ij}\mathcal{E}_j$. Now, the eigenvectors $\tilde{\mathbf{u}}_i$, $i = 1, 2$, define, in general, the new monophoton eigenstates $|\tilde{1}_i\rangle$, $i = 1, 2$, on the $\tilde{\mathcal{E}}_1\tilde{\mathcal{E}}_2$ space, that is:

$$|\tilde{1}_i\rangle = \sum_{j=1}^{N} a_{ij}|0...0\,1_j\,0...0\rangle, \quad i = 1, 2. \tag{P5.28}$$

Note that we could have expressed the above equations as a function of $Re(c_i c_j^\star)=|c_i||c_j|cos\epsilon_{ij}$ and $Im(c_i c_j^\star)=|c_i||c_j|sin\epsilon_{ij}$. By taking into account

these changes it is easy to show that if the coefficientes c_i are real then from equation (P5.23) we obtain that only one eigenvalue λ_1 is different from zero; we must stress that the rest of the eigenvectors can be constructed by any method of orthogonalization because their eigenvalues are equal to zero.

Generalized polarization in *3x3* directional couplers

We will present the generalized polarization properties of a *3x3* linear directional coupler in order to make clear the general procedure for analyzing MSP states. The Momentum operator and Heisenberg's equations corresponding to a *3x3* linear directional coupler are given by equation (P5.1) with $i, j = 1, 2, 3$. For sake of simplicity we will consider the particular case of three identical guides (synchronous directional coupler), that is: $\tilde{\beta}_1 = \tilde{\beta}_2 = \tilde{\beta}_3 \equiv \beta_0$, with only coupling between neighbour (consecutive) guides, that is, $\kappa_{ij} = \kappa_{ij}^{\star} = \kappa$ only if $i = j \pm 1$, and $\kappa_{ij} = 0$ if $i \neq j \pm 1$. From equation (P5.1) and after a simple calculation, the following Heisenberg's equations are obtained:

$$-i\partial_z \hat{a}_1 = \tilde{\beta}_0 \hat{a}_1 + \kappa \hat{a}_2, \tag{P5.29}$$

$$-i\partial_z \hat{a}_2 = \tilde{\beta}_0 \hat{a}_2 + \kappa \hat{a}_1 + \kappa \hat{a}_3, \tag{P5.30}$$

$$-i\partial_z \hat{a}_3 = \tilde{\beta}_0 \hat{a}_3 + \kappa \hat{a}_2. \tag{P5.31}$$

The solutions of these equations can be obtained in a similar way to the classical case. We are interested on the conjugated forms, i.e., emission (creation) operators $\hat{a}^{\dagger}$, in order to determine the quantum states at the output of the *3x3* coupler. The solutions are given by the following expressions [Liñares et al., 2008b]:

$$\hat{a}_1^{\dagger} e^{i\beta_0 z} = \frac{1}{2}[1 + \cos\phi]\, \hat{a}_{01}^{\dagger} - \frac{i}{\sqrt{2}} \sin\phi\, \hat{a}_{02}^{\dagger} - \frac{1}{2}[1 - \cos\phi]\, \hat{a}_{03}^{\dagger}, \tag{P5.32}$$

$$\hat{a}_2^{\dagger} e^{i\beta_0 z} = -\frac{i}{\sqrt{2}} \sin\phi\, \hat{a}_{01}^{\dagger} + \cos\phi\, \hat{a}_{02}^{\dagger} - \frac{i}{\sqrt{2}} \sin\phi\, \hat{a}_{03}^{\dagger}, \tag{P5.33}$$

$$\hat{a}_3^{\dagger} e^{i\beta_0 z} = -\frac{1}{2}[1 - \cos\phi]\, \hat{a}_{01}^{\dagger} - \frac{i}{\sqrt{2}} \sin\phi\, \hat{a}_{02}^{\dagger} + \frac{1}{2}[1 + \cos\phi]\, \hat{a}_{03}^{\dagger}, \tag{P5.34}$$

where $\phi \equiv \phi(z) = \sqrt{2}\kappa z$. Next, we present some illustrative examples. We start by describing the output states when in the mode 1 (guide 1) an input quantum monophoton number state is excited: $|L_e\rangle = |100\rangle$. This state is propagated along the coupler device, and by taking into account equations (P5.32-P5.34), the following output state $|L_o\rangle$ is obtained:

$$|L_o\rangle = \{\frac{1}{2}[1+\cos\phi]\,|100\rangle + \frac{i}{\sqrt{2}} \sin\phi\,|010\rangle - \frac{1}{2}[1-\cos\phi]\,|001\rangle\} e^{i\beta_0 z}. \tag{P5.35}$$

Let us consider the $\mathcal{E}_1...\mathcal{E}_3$-representation of our state $|L_o\rangle$, that is, the associated probability distribution $\mathcal{P}_{|L_o\rangle} = |\langle\mathcal{E}_1...\mathcal{E}_3|L_o\rangle|^2$ will be:

$$\mathcal{P}_{|L_o\rangle} = \frac{2}{\pi^{3/2}}\{\cos^4\frac{\phi}{2}\,\mathcal{E}_1^2 + \frac{\sin^2\phi}{2}\,\mathcal{E}_2^2 + \sin^4\frac{\phi}{2}\,\mathcal{E}_3^2 - \frac{\sin^2\phi}{2}\,\mathcal{E}_1\,\mathcal{E}_3\}\,e^{-\sum_{i=1}^{3}\mathcal{E}_i^2}. \tag{P5.36}$$

The orthogonal transformation a_{ij} can be obtained by using the general expressions (P5.23-P5.27) for TSP, although in this case it can be also obtained in a straightforward way by inspection of equation (P5.35), that is,

$$a_{ij} \equiv \frac{1}{[2(1+\cos^2\phi)]^{1/2}}\begin{pmatrix}(1+\cos\phi) & 0 & (1-\cos\phi)\\ 0 & [2(1+\cos^2\phi)]^{1/2} & 0\\ (\cos\phi-1) & 0 & (1+\cos\phi)\end{pmatrix}, \tag{P5.37}$$

where the relevant eigenvectors $\{\tilde{\mathbf{u}}_1, \tilde{\mathbf{u}}_2\}$, with eigenvalues $\lambda_{1,2} = (1\pm\cos^2\phi)/2$, are given by the following expressions:

$$\tilde{\mathbf{u}}_1 = \frac{1}{[2(1+\cos^2\phi)]^{1/2}}\{(1+\cos\phi)\mathbf{u}_1 + (1-\cos\phi)\mathbf{u}_3\}; \quad \tilde{\mathbf{u}}_2 = \mathbf{u}_2. \tag{P5.38}$$

The probability distribution $\mathcal{P}(\tilde{\mathcal{E}}_1, \tilde{\mathcal{E}}_2, \tilde{\mathcal{E}}_3)$ in the new space is obtained by using the change $\tilde{\mathcal{E}}_i = a_{ij}\mathcal{E}_j$, that is:

$$\mathcal{P}(\tilde{\mathcal{E}}_1, \tilde{\mathcal{E}}_2, \tilde{\mathcal{E}}_3) = \frac{2}{\pi^{3/2}}\{\frac{(1+\cos^2\phi)}{2}\tilde{\mathcal{E}}_1^2 + \frac{(1-\cos^2\phi)}{2}\tilde{\mathcal{E}}_2^2\}\,e^{-(\tilde{\mathcal{E}}_1^2+\tilde{\mathcal{E}}_2^2+\tilde{\mathcal{E}}_3^2)}. \tag{P5.39}$$

Now, in order to present the generalized polarization properties of TSP states generated by *3x3* couplers we give an useful reinterpretation of the distribution probability in the subspace $\tilde{\mathcal{E}}_1\tilde{\mathcal{E}}_2$, that is, let us make the following change of variables: $\tilde{\mathcal{E}}_1 = \tilde{\xi}\cos\tilde{\theta}$, $\tilde{\mathcal{E}}_2 = \tilde{\xi}\sin\tilde{\theta}$, then equation (P5.39) can be rewritten as:

$$\mathcal{P}(\tilde{\xi}, \tilde{\theta}, \tilde{\mathcal{E}}_3) = \{\tilde{a}^2\cos^2\tilde{\theta} + \tilde{b}^2\sin^2\tilde{\theta}\}\,\tilde{\xi}^2 e^{-(\tilde{\xi}^2+\tilde{\mathcal{E}}_3^2)}, \tag{P5.40}$$

where $\tilde{a}^2=(1/\pi^{3/2})(1+\cos^2\phi)$ and $\tilde{b}^2=(1/\pi^{3/2})(1-\cos^2\phi)$. Note that the marginal $\tilde{\theta}$-probability of a TSP is analogous to the classical θ-intensity of a classical wave detected by a linear polarizer, that is, it exhibits the same polar dependence that the intensity of an elliptical ($\tilde{a}^2\neq\tilde{b}^2$), a circular ($\tilde{a}^2=\tilde{b}^2$) and a linear ($\tilde{a}^2\neq\tilde{b}^2=0$) classical state (corresponding to polar dependence of particular cases of the so-called cyclic-harmonic curves). We must also stress that a marginal $\tilde{\theta}$-probability, by either fixing a point $\tilde{\xi}$ or integrating over $\tilde{\xi}$, can be measured by using bimodal homodyne detection [Raymer and Funk, 1999].

Now we will show some probability distributions of TSP states. We start by showing in Figure P5.2 the first and illustrative case: $\phi = \pi/2$.

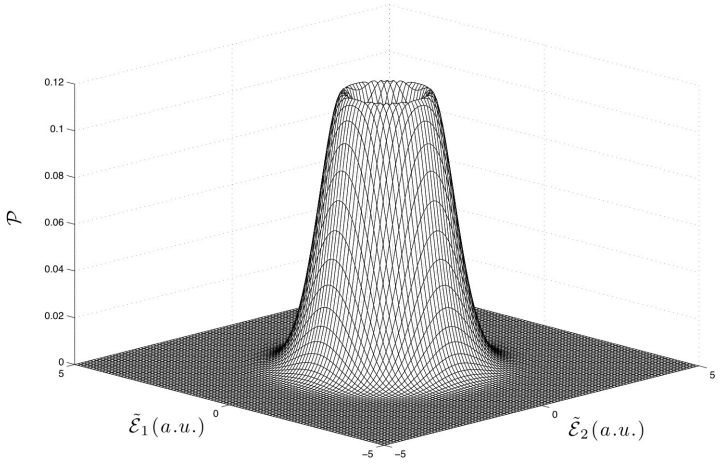

Figure P5.2: Probability of a circular-type TSP state, i.e. $\phi = \pi/2$, $\tilde{\delta} = \pm\pi/2$.

It resembles a circular generalized polarization because of the high confinement of the probability distribution around a circular curve, but with a quantum uncertainty much larger that in a coherent state. It can be called a circular-type TSP state. A second case with $\phi = \pi/4$ is shown in Figure P5.3 which resembles elliptical generalized polarization because the main maxima of probability are located along the axis $\tilde{\mathcal{E}}_1$ and the secondary maxima are located along the orthogonal axis $\tilde{\mathcal{E}}_2$ in an analogous way to the major and minor axis of intensity in classical elliptical polarization. It can be called an elliptical-type TSP state. The third case is for $\phi = 0$ and is shown in Figure P5.4. It resembles a linear generalized polarization because the main maxima of probability are located on a straight line, in this case along the direction $\tilde{\mathcal{E}}_1$. It can be called a linear-type TSP state. Therefore a 3x3 directional coupler transforms an input TSP linear-type state into different generalized polarization states.

On the other hand let us consider the input state $|L_i\rangle = 2^{-1/2}(|100\rangle + |010\rangle)$. This state can be generated, for instance, by using a Y-junction [Kogelnik, 1988] connected to the synchronous 3x3 coupler. Now by using the notation $c \equiv \cos\phi$ and $s \equiv \sin\phi$ the output state is given by the expression:

$$|L_o\rangle = \{(\frac{1}{2}[1+c]+\frac{i}{\sqrt{2}}s)\,|100\rangle+(c+\frac{i}{\sqrt{2}}s)\,|010\rangle-(\frac{1}{2}[1-c]-\frac{i}{\sqrt{2}}s)\,|001\rangle\}\frac{e^{i\beta_0 z}}{\sqrt{2}}, \tag{P5.41}$$

and therefore in this case the coefficients $c_j = |c_j|e^{i\epsilon_j}$ with $j = 1,2,3$ are

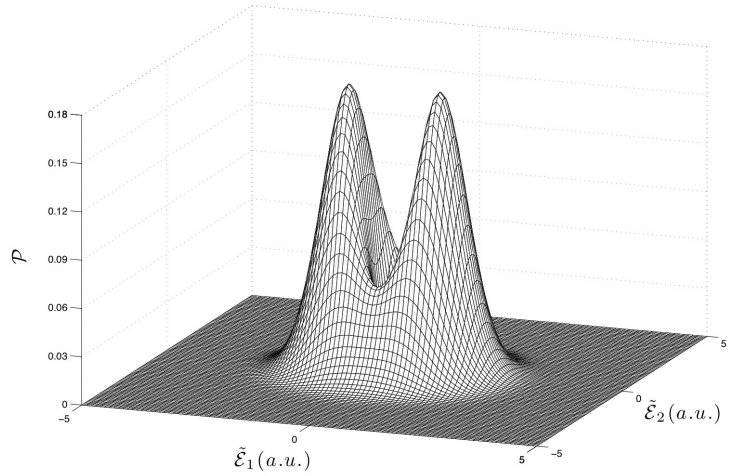

Figure P5.3: Probability of a elliptical-type TSP state, i.e. $\phi = \pi/4$, $\tilde{\delta} = \pm\pi/2$.

given by the following expressions:

$$|c_1|e^{i\epsilon_1} = \frac{1}{\sqrt{2}}[\frac{1}{2}(1+c) + \frac{i}{\sqrt{2}}s] = \frac{1}{2\sqrt{2}}[(1+c)(3-c)]^{1/2}\ e^{i\,atan\{\sqrt{2}\,s/(c+1)\}}, \tag{P5.42}$$

$$|c_2|e^{i\epsilon_2} = \frac{1}{\sqrt{2}}(c + \frac{i}{\sqrt{2}}s) = \frac{1}{2}(1+c^2)^{1/2}\ e^{i\,atan\{s/c\sqrt{2}\}}, \tag{P5.43}$$

$$|c_3|e^{i\epsilon_3} = \frac{1}{\sqrt{2}}[\frac{1}{2}(-1+c) + \frac{i}{\sqrt{2}}s] = \frac{1}{2\sqrt{2}}[(1-c)(3+c)]^{1/2}\ e^{i\,atan\{\sqrt{2}\,s/(c-1)\}}. \tag{P5.44}$$

By taking into account the above equations we can calculate the eigenvalues from equation (P5.23). In Figure P5.5 we plot the eigenvalues $\lambda_{1,2}$ and it is seen that a circular-type TSP state is never reached, and linear-type TSP states are obtained at $\phi = p\pi$ with p an integer. Obviously these results can be extended to any pure MSP state and therefore after diagonalization the generalized polarization state can be easily identified by a vector $(\lambda_1, \lambda_2, 0...0) \equiv (\tilde{P}_1, \tilde{P}_2, ...)$, that is, a linear-type MSP state if $\lambda_1 \neq \lambda_2 = 0$, a circular-type MSP state if $\lambda_1 = \lambda_2$ and an elliptical-type MSP state if $\lambda_1 \neq \lambda_2 \neq 0$. Now the remaining question is to evaluate the generalized polarization degree because, such as it will be shown, it will depend on the values of λ_i. However before pursuing this further we will complete our study of MSP states by analyzing the generalized polarization structure of mixture MSP states.

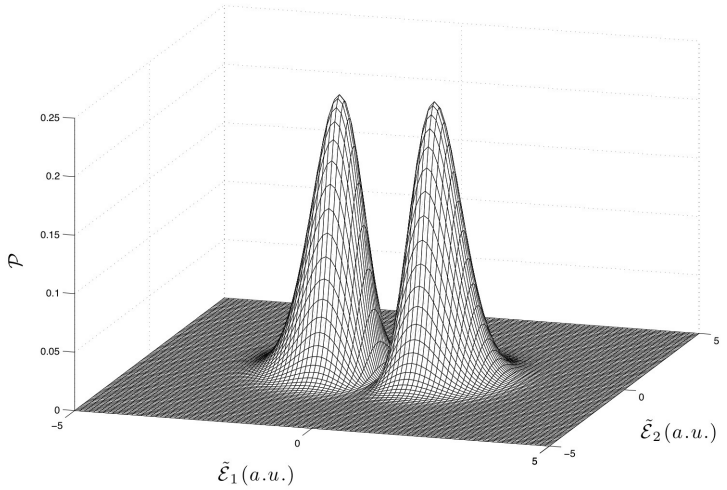

Figure P5.4: Probability of a linear-type TSP state, i.e. $\phi = 2\pi$.

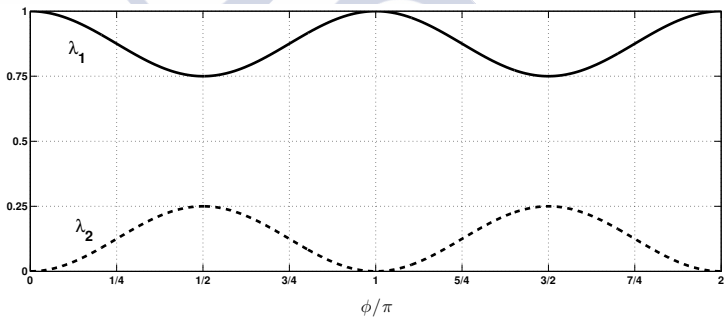

Figure P5.5: Variation of the eigenvalues *vs* $\phi/\pi = \sqrt{2}\kappa z/\pi$.

Probability distributions of Mixture MSP states

As it is well-known the more general MSP state can be represented by the density operator, thus, by denoting $|0...0\,1_i\,0...0\rangle \equiv |1_i\rangle$, a general mixture state MSP will have the following density operator:

$$\hat{\rho} = \sum_{i,j=1}^{N} \rho_{ij}\,|1_i\rangle\langle 1_j| = \sum_{i,j=1}^{N} |\rho_{ij}|\{\delta_{ij} + e^{\gamma_{ij}}(1-\delta_{ij})\}|1_i\rangle\langle 1_j|, \qquad \text{(P5.45)}$$

where, as usual, $\rho_{ii} = |\rho_{ii}|$, $\rho_{ij} = |\rho_{ij}|e^{i\gamma_{ij}} = \rho^*_{ji}$. The probability distribution $\mathcal{P}(\mathcal{E}_1, ...\mathcal{E}_N)$ of a mixture MSP state will be given by the expression:

$$\mathcal{P}(\mathcal{E}_1, ..., \mathcal{E}_N) = \frac{2}{\pi^{N/2}}\{\sum_{i=1}^{N} \rho_{ii}\mathcal{E}_i^2 + 2\sum_{i<j}^{N} |\rho_{ij}|\cos\gamma_{ij}\ \mathcal{E}_i\mathcal{E}_j\}e^{-(\mathcal{E}_1^2+...+\mathcal{E}_N^2)}. \qquad \text{(P5.46)}$$

Once more the Gaussian amplitude is a quadratic form on the multidimensional space $\mathcal{E}_1 ... \mathcal{E}_N$ and, as for pure states we can associate to the above probability distribution (P5.46) a symmetric matrix, however now the values $|\rho_{ij}|$ and γ_{ij} are independent, that is, they do not fulfil relationships analogous to those ones given in equation (P5.9), namely, $|\rho_{ij}|/|\rho_{jk}| \neq |\rho_{im}|/|\rho_{mk}|$ and $\gamma_{ij} + \gamma_{jk} \neq \gamma_{ik}$. Therefore, we will not be able to find under an orthogonal transformation a new reference system $\tilde{\mathcal{E}}_1 \tilde{\mathcal{E}}_2$ where the probability distribution takes a bidimensional form (except in the obvious case $N = 2$). From a different and very interesting perspective a mixture MSP state can be regarded as a state whose quantum complex amplitude is an incoherent superposition [Liñares et al., 2010] of states $|1_i\rangle$, that is, with an amplitude given by equation (P5.12) but whose coefficientes c_i present, in general, an amplitude and a phase varying on the time in a non predetermined way, and accordingly the matrix density coefficients are obtained as a result of an averaging process. Obviously under these circumstances there is not a reference system where the complex amplitude can be given just as in equation (P5.11). In a more rigorous way, the $rank$ of the matrix m_{ij} associated to the probability distribution (P5.46) is in general different to two, however we can still make an orthogonal diagonalization of such a symmetric matrix in which case the distribution probability will present the following diagonal form

$$\mathcal{P}(\tilde{\mathcal{E}}_1, ..., \tilde{\mathcal{E}}_N) = \frac{2}{\pi^{N/2}} \sum_{i=1}^{N} \tilde{P}_i \, \tilde{\mathcal{E}}_i^2 \, e^{-(\tilde{\mathcal{E}}_1^2 + ... + \tilde{\mathcal{E}}_N^2)}, \tag{P5.47}$$

where $\tilde{P}_i$ is the probability of finding the photon in the $\tilde{\mathbf{u}}_i$-mode. The generalized polarization structure can be characterized by the vector $(\lambda_1, \lambda_2, ..., \lambda_N) = (\tilde{P}_1, \tilde{P}_2, ..., \tilde{P}_N)$. Overall it will represent a hyperelliptical generalized polarization, that is, we can define a hypercircular-type MSP state if $\tilde{P}_1 = \tilde{P}_2 = ... = \tilde{P}_N = 1/\sqrt{N}$, otherwise we will have a hyperelliptical-type MSP state. The linear-type MSP mixture state is precluded because in such a case we would have a pure MSP state, that is, $\tilde{P}_1 = 1, \tilde{P}_j = 0, j > 1$. From a geometrical point of view a hypercircular-type MSP state would correspond to a probability distribution quite localized (pseudo-polarized) on a hypersphere, and a hyperelliptical-type MSP state would correspond, as in the case $N = 2$, to a probability distribution presenting primary and secondary maxima along the different principal directions $\tilde{\mathcal{E}}_i$ and proportional to $\tilde{P}_i$. We must stress that from a practical point of view the mixture MSP states will have a different behaviour when optical devices act on them, that is, on the phase and amplitude of the MSP states. Now, once more, we meet the question to evaluate the generalized polarization degree which, such as it will be shown, will depend on the values of $\tilde{P}_i$ of the pure or mixture states.

P5.3. N-dimensional quantum generalized polarization degree

In this section we tackle the question about the quantum generalized polarization degree for N-mode states. We will propose a simple definition of the mentioned generalized polarization degree in order to characterize the generalized polarization of MSP states on the $\mathcal{E}_1...\mathcal{E}_N$ space. This definition was recently applied to the case of standard polarization (two-mode space) [Liñares et al., 2010] and in this work is generalized to a multimode space for MSP states although it can be easily used for other quantum states such as it will be shown below. A very general and detailed analysis on this important issue, but for standard polarization, can be found in different specialized references [Abouraddy et al., 2002, Alodjants and Arakelian, 1999, Klimov et al., 2005, Luis, 2007, Sánchez-Soto et al., 2006]. We start from the very reasonable assumption that the two-mode vacuum state is not polarized such as it is proved in the general theory [Luis, 2002, 2003] and accordingly the N-mode vacuum state will be not polarized either; in fact, its isotropic Gaussian probability distribution on the $\mathcal{E}_1...\mathcal{E}_N$-space suggests that such a state is not polarized at all. On the other hand, it is well-known that a symmetric multimode chaotic quantum state $|\kappa_1...\kappa_N\rangle = |\kappa...\kappa\rangle$ also presents a Gaussian distribution on the $\mathcal{E}_1...\mathcal{E}_N$ space, therefore this multimode state can be also regarded as not polarized. Note that the multimode vacuum state can be seen as a particular case of a symmetric chaotic state in the limit $\bar{n} = 0$. In short, by taking into account the above considerations, we will show that the complementary value of the overlapping between the probability distribution of a quantum state, and in particular a MSP state, and their best Gaussian probability distribution on the $\mathcal{E}_1...\mathcal{E}_N$ space, allow us to calculate how much the quantum state is polarized. Indeed, let consider the N-dimensional Gaussian distribution

$$\mathcal{P}_{|g\rangle}(\mathcal{E}_1...\mathcal{E}_N) = (1/g\pi)^{N/2}\, e^{-\left\{\frac{\mathcal{E}_1^2+\mathcal{E}_2^2+\mathcal{E}_3^2+...+\mathcal{E}_N^2}{g}\right\}}, \tag{P5.48}$$

where the best value of the parameter g must be determined by maximazing the overlapping with the probability distribution of the quantum state $|L\rangle$ to be analyzed. This procedure is highly similar to that one used to analyze coupling efficiency by modal overlapping in integrated optics [Liñares et al., 1991] but moreover it is closely related to the more rigorous concept of distance measure to an unpolarized distribution [Luis, 2007] or to quantum states that are invariant with respect to any SU(2) polarization transformation [Klimov et al., 2005]. Accordingly, by following closely the definition for the quantum polarization degree given by Luis [Luis, 2002] or alternatively by Klimov *et.al* [Klimov et al., 2005] we propose the following definition of the quantum generalized polarization degree of a multimode quantum state $|L\rangle$ in a N-dimensional optical field-strength space [Liñares

et al., 2010]:

$$\mathcal{G}_{|L\rangle}^{(N)} = \frac{1}{2}\int \{\mathbb{P}_{|L\rangle} - \mathbb{P}_{|g_b\rangle}\}^2 \, d\mathcal{E}_1 ... d\mathcal{E}_N, \tag{P5.49}$$

where for sake of normalization we have introduced both the factor $1/2$ and the normalized functions:

$$\mathbb{P}_{|L\rangle} = \frac{\mathcal{P}_{|L\rangle}(\mathcal{E}_1 ... \mathcal{E}_N)}{\{\int \mathcal{P}_{|L\rangle}^2 \, d\mathcal{E}_1 ... d\mathcal{E}_N\}^{1/2}}, \tag{P5.50}$$

$$\mathbb{P}_{|g_b\rangle} = \frac{\mathcal{P}_{|g_b\rangle}}{\{\int \mathcal{P}_{|g_b\rangle}^2 \, d\mathcal{E}_1 ... d\mathcal{E}_N\}^{1/2}}. \tag{P5.51}$$

From equation (P5.49) it is straightforward to derive the following expression for the quantum generalized polarization degree:

$$\mathcal{G}_{|L\rangle}^{(N)} = 1 - \int \mathbb{P}_{|L\rangle}(\mathcal{E}_1 ... \mathcal{E}_N) \, \mathbb{P}_{|g_b\rangle}(\mathcal{E}_1 ... \mathcal{E}_N) \, d\mathcal{E}_1 ... d\mathcal{E}_N \equiv 1 - \mathcal{D}^{(N)}(g_b) \tag{P5.52}$$

where g_b defines the best Gaussian, that is, the maximum value of function $\mathcal{D}^{(N)}(g)$ (depolarization function in a N-dimensional space) which represents nothing but an overlapping integral. We must stress that the choice of the dimension N will depend on the particular problem in which we are interested, that is, if the states of our quantum problem are all found in a M-dimensional space ($M < N$), or even they can be transformed into quantum states within a M-dimensional space then we can simply use the quantum generalized polarization degree $\mathcal{G}_{|L\rangle}^{(M)}$. We must also stress that although an uniform distribution would represent the ideal non-polarized quantum state it would not be physically consistent on the $\mathcal{E}_1 ... \mathcal{E}_N$ space because of the probability in the infinite can not be different from zero. On the other hand we see that consistent results are clearly obtained with the definition given in equation (P5.52), thus, $\mathcal{G}_{|0...0\rangle} = 0$, and therefore any quantum state very close to the multimode vacuum state, such as for example coherent and chaotic states with a very low mean photon number, will have very low quantum generalized polarization degree. Likewise multimode chaotic states with the same average photon number in all modes, that is, $|\kappa ... \kappa\rangle$ (symmetric states) will have $\mathcal{G}_{|\kappa ... \kappa\rangle} = 0$, and the chaotic state $|\kappa ... 0\rangle$ will reach a maximum value of polarization $\mathcal{G}_{|\kappa ... 0\rangle} \approx 1$ for a high mean photon number. Next we will present some illustrative examples of calculation of the quantum generalized polarization degree in order to check the consistency of the definition of $\mathcal{G}_{|L\rangle}^{(N)}$.

Examples of $\mathcal{G}^{(N)}_{|L\rangle}$

Let us consider the probability distribution on the $\mathcal{E}_1...\mathcal{E}_N$ space of the chaotic state $|\kappa\,...0\rangle$ with a mean photon number $\kappa = \bar{n}$:

$$\mathcal{P}_{|\kappa\,...0\rangle} = \frac{1}{\pi^{N/2}\sqrt{1+2\bar{n}}} e^{-\{\frac{\mathcal{E}_1^2}{1+2\bar{n}}+\mathcal{E}_2{}^2+\mathcal{E}_3^2+...+\mathcal{E}_N^2\}}. \tag{P5.53}$$

The best Gaussian distribution, that is, the best value g_b can be obtained by calculating the maximum value of function $\mathcal{D}^{(N)}(g)$ for the chaotic state, therefore, by inserting equations (P5.53) and (P5.48) into equation (P5.52), performing the integrations and finally by taking the derivative with respect to g the minimum (maximum) value of function $\mathcal{P}^{(N)}(g)$ ($\mathcal{D}^{(N)}(g)$), after a long but straightforward calculation, is reached for:

$$g_b = \sqrt{\bar{n}^2(1-\frac{2}{N})^2+(1+2\bar{n})} + \bar{n}\,(\frac{2}{N}-1), \tag{P5.54}$$

and the quantum generalized polarization degree is given by the following expression:

$$\mathcal{G}^{(N)}_{|\kappa 0...0\rangle} = 1 - \frac{1}{(1+2\bar{n})^{1/4}}\sqrt{\frac{2^N(1+2\bar{n})\,g_b^{N/2}}{(g_b+1+2\bar{n})(1+g_b)^{N-1}}}\,. \tag{P5.55}$$

This result shows that in the limit of a large number of photons, that is, $\bar{n} \gg$ the quantum generalized polarization degree $\mathcal{G}^{(N)} \to 1$, that is, there will be a high localization of the probability distribution along the $\mathcal{E}_1$-direction of the $\mathcal{E}_1...\mathcal{E}_N$ space which resembles a linear-type generalized polarization. A similar result would be found for the quantum generalized polarization degree of any monomode state $|L\,0...0\rangle$ with $\bar{n} \gg$. On the other hand, in the limit $\bar{n} = 0$ (the N-mode vacuum) $g_b = 1$ and then $\mathcal{G}^{(N)} = 0$ as it was expected. Likewise if $N = 2$ it is obtained:

$$\mathcal{G}^{(2)}_{|\kappa 0\rangle} = 1 - \frac{2(1+2\bar{n})^{1/4}}{1+(1+2\bar{n})^{1/2}}, \tag{P5.56}$$

such as it was recently obtained [Liñares et al., 2010]. Moreover in the limit $N \gg 1$ it is easy to check that the quantum generalized polarization degree is given by:

$$\mathcal{G}^{(N\gg)}_{|\kappa 0\rangle} \approx 1 - \frac{(1+2\bar{n})^{1/4}}{(1+\bar{n})^{1/2}}. \tag{P5.57}$$

Obviously if $\bar{n} \to \infty$ then $\mathcal{G}^{(N\gg)}_{|\kappa 0\rangle} \to 1$ as it was expected, that is, there is a high localization of the probability distribution along the $\mathcal{E}_1$-direction of the $\mathcal{E}_1...\mathcal{E}_N$ space. It is very interesting to check that $\mathcal{G}^{(2)}_{|\kappa 0\rangle} < \mathcal{G}^{(N\gg 1)}_{|\kappa 0\rangle}$, which may appears paradoxical, however it is consistent with the fact that

the more large is the space dimension more localized (polarized) must be considered the monomode state in one dimension of the multidimensional space where such a state is defined. Anyway it is very convenient that the comparison between generalized polarization degrees be made in the same subspace. Finally, and from a formal point of view, we could even consider a squeezed vacuum state in the first mode, that is: $|\xi,..0\rangle$, with ξ the squeezed parameter, and thus from equation (P5.53) a squeezing would correspond formally, and only formally, to $(1+2\bar{n}) \to 0$ and therefore we would take "$\bar{n} \to -1/2$". Accordingly, after a simple calculation, we obtain from (P5.54) and (P5.55) and $\forall N$ the result: $\mathcal{G}^{(N)}_{|\xi 0\rangle} \to 1$, which is consistent with the theoretical limit of a high squeezing corresponding in turn to a high localization around $\mathcal{E}_1$-direction.

As another explicit and interesting example we will show that the quasi-classical states will also present a maximum generalized polarization, in particular let us consider two-mode coherent states $|\alpha\,\beta\rangle$ with a high mean photon number ($|\alpha|,|\beta| \gg 1$). Since we are concerned only with two-mode states we can use simply the generalized polarization degree $\mathcal{G}^{(2)}$ (formally it could be also a standard polarization degree). Moreover we will restrict our attention on a circular coherent state $|\alpha\ i\alpha\rangle$, although the analysis can be easily extended to an arbitrary bimode coherent state. Let us consider the probability distribution on the $\mathcal{E}_1\mathcal{E}_2$ subspace of a circular coherent state whose amplitude is given by equation (P5.4), and therefore we obtain:

$$\mathcal{P}_{|\alpha\ i\alpha\rangle} = \tfrac{1}{\pi^{N/2}}\, e^{-\{(\mathcal{E}_1-|\alpha|cos\varphi)^2+(\mathcal{E}_2-|\alpha|sin\varphi)^2+\mathcal{E}_3^2+...+\mathcal{E}_N^2\}}. \qquad \text{(P5.58)}$$

By following the same steps than in the case of a chaotic state, we obtain, for $N = 2$ and after a long but straightforward calculation, the following expression for the quantum generalized polarization degree:

$$\mathcal{G}^{(2)}_{|\alpha\ i\alpha\rangle} = 1 - \frac{2(|\alpha|^2+\sqrt{1+|\alpha|^4})\, e^{-\frac{|\alpha|^2}{1+|\alpha|^2+\sqrt{1+|\alpha|^4}}}}{(1+|\alpha|^2+\sqrt{1+|\alpha|^4})\sqrt{|\alpha|^2+\sqrt{1+|\alpha|^4}}}. \qquad \text{(P5.59)}$$

Note that the larger is the mean photon number ($|\alpha| \gg$) closer to the unity is the quantum generalized polarization degree, that is, $\mathcal{G}^{(2)}_{|\alpha\ i\alpha\rangle} \to (1-\sqrt{2}\,e^{-1/2}/|\alpha|) \to 1$ because the probability distribution will be highly localized (polarized) on an annular region of a large radius (semiclassical limit). Likewise, for $|\alpha| = 0$ it is obtained from equation (P5.59) the value $\mathcal{G}_{|00\rangle} = 0$, such as it was expected.

Quantum generalized polarization degree of MSP states

By taking into account the results given above we can calculate the value of the quantum generalized polarization degree of MSP states. As

any MSP state can be transformed into a two-mode photon state on a $\tilde{\mathcal{E}}_1\tilde{\mathcal{E}}_2$ subspace then we will use $\mathcal{G}^{(2)}$, therefore by inserting equation (P5.39) into equation (P5.52) for $N = 2$, after a long but straightforward calculation, we obtain the following general result:

$$\mathcal{G}^{(2)}_{|S_\sigma\rangle} = 1 - \frac{3}{4}\frac{\sqrt{3}}{\sqrt{(1+\cos^4\phi)+1}}. \tag{P5.60}$$

Note that for $\phi = 0$, that is the state $|S_{\phi=0}\rangle$, we obtain $\mathcal{G}$ =1−3/4=1/4, therefore the linear-type MSP states are polarized a 25% according to our generalized polarization degree definition. Likewise the minimum generalized polarization degree for MSP states is obtained for $\phi = \pi/2$, that is, circular-type MSP states with $\mathcal{G}$=1−(3/4)($\sqrt{3/2}$); the rest of cases (elliptical-type MSP states) take values in between these two ones. The result is physically expected, that is, the monophoton generalized polarization is quite low, because the maximum values of the probability distribution on $\tilde{\mathcal{E}}_1\tilde{\mathcal{E}}_2$ subspace are found for low values of the optical field-strength and therefore comparable to the quantum fluctuations values of the optical field-strength itself. Likewise, a circular coherent state $|\alpha\ i\alpha\rangle$ is analogous to the state $|S_{\phi=\pi/2}\rangle$ because in both cases we have an annular shape of the probability distribution but in the first case the maximum values of the probability distribution on $\tilde{\mathcal{E}}_1\tilde{\mathcal{E}}_2$ subspace are found for very high values of the optical field-strength and therefore the quantum fluctuation are negligible and consequently the state will present a high value of the generalized polarization degree. Obviously all these results are also valid for polarization modes [Liñares et al., 2010], that is, for standard polarization.

Now we evaluate the quantum generalized polarization degree of mixture MSP states. Thus, by inserting equation (P5.47) into equation (P5.52) and after a long but very straightforward calculation it is obtained $g_b = 1+4/N$ and therefore the quantum generalized polarization degree is given by the following expression:

$$\mathcal{G}^{(N)}_{|S_M\rangle} = 1 - \frac{(1+\frac{1}{N/4})^{1+N/4}}{(1+\frac{1}{N/2})^{1+N/2}\sqrt{2\sum_{i=1}^{N}\tilde{P}_i^2+1}}. \tag{P5.61}$$

Note that in the particular case of $N = 2$ and $P_1 = 1$ (pure state) it is obtained $\mathcal{G}^{(2)} = 1/4$ such as it was expected for a linear-type generalized polarization. Likewise the quantum generalized polarization degree for $N \gg 1$ becomes:

$$\mathcal{G}^{(N\gg)}_{|S_M\rangle} \approx 1 - \frac{1}{\sqrt{2\sum_{i=1}^{N}\tilde{P}_i^2+1}}. \tag{P5.62}$$

It is interesting to highlight that in this case $g_b \approx 1$, that is, the best Gaussian distribution corresponds to the multimode vacuum state. Obviously

this is a general result and therefore could be used for all kind of states, however it requires to understand the generalized polarization degree as depending on the dimension of the state, which, in general, is far less intuitive. Finally by considering that $\tilde{P}_i = 1/N, \forall i$, then $\mathcal{G}^{(N)} = 0$, which shows that a probability distribution so widespread (non localized) throughout the $\tilde{\mathcal{E}}_1 ... \tilde{\mathcal{E}}_N$ space is equivalent to have a quantum generalized polarization degree equal to zero.

P5.4. Polarization of $MSP_\emptyset$ states

As we have already indicated it is possible to obtain, by non conservative optical transformations, states formed by the quantum superposition of the N-mode vacuum state $|0...0\rangle$ and a pure (or mixture) MSP state, that is, a state $|S_\emptyset\rangle$. For example, a drastic reduction of the photonics excitation of a coherent state, chaotic state, and so on, by means of a photonics attenuator give rise to this kind of states. Likewise a simple generalized linear polarizer, implemented by allowing, after a distance z, that only a guide of a directional coupler propagates light, would also produce this kind of states. For instance, if we only allow the light propagation in the first guide of a 3x3 directional coupler we obtain, by taking into account equation (P5.35), the following $MSP_\emptyset$ state:

$$|L_\emptyset\rangle = \{\sqrt{1 - \cos^4\frac{\phi}{2}}\,|000\rangle + \cos^2\frac{\phi}{2}\,|100\rangle\}e^{i\beta_0 z}. \tag{P5.63}$$

If we use this state as an input state of another 3x3 directional coupler then under propagation we will obtain states whose diagonal probability amplitude, on the $\tilde{\mathcal{E}}_1\tilde{\mathcal{E}}_2\tilde{\mathcal{E}}_3$ space, will have the form:

$$\mathcal{A}_{|S_\emptyset\rangle} = \sin\alpha\langle\tilde{\mathcal{E}}_1\,\tilde{\mathcal{E}}_2,\tilde{\mathcal{E}}_3|000\rangle + \cos\alpha(\tilde{C}_1\,\langle\tilde{\mathcal{E}}_1\,\tilde{\mathcal{E}}_2,\tilde{\mathcal{E}}_3|\tilde{1}_1\rangle \pm i\,\tilde{C}_2\,\langle\tilde{\mathcal{E}}_1\,\tilde{\mathcal{E}}_2,\tilde{\mathcal{E}}_3|\tilde{1}_2\rangle), \tag{P5.64}$$

where $\cos\alpha = \cos^2\frac{\phi}{2}$. The probability distribution can be now calculated, however unlike states analyzed so far, the state (P5.64) is not stationary, that is, the temporal propagation of states $|00\rangle$ and $|\tilde{1}_1\rangle$ (or $|\tilde{1}_2\rangle$), at a plane z of detection, will present a quickly oscillating relative temporal phase $e^{-i\omega t}$. Accordingly we choose a temporal averaging of the probability distribution in order to evaluate the generalized polarization degree. We must stress that it could be measured by a heterodyne detection technique which removes the condition of modes with equal frequency required in homodyne detection. Therefore by standard temporal averaging it is obtained:

$$\langle\mathcal{P}(\tilde{\mathcal{E}}_1,\tilde{\mathcal{E}}_2)\rangle_t = \frac{1}{\pi^{3/2}}\{\sin^2\alpha + 2\cos^2\alpha\,(\tilde{C}_1^2\,\tilde{\mathcal{E}}_1^2 + \tilde{C}_2^2\,\tilde{\mathcal{E}}_2^2)\}e^{-(\tilde{\mathcal{E}}_1^2+\tilde{\mathcal{E}}_2^2+\tilde{\mathcal{E}}_3^2)}, \tag{P5.65}$$

with $\sin^2\alpha$ the contribution of the non polarized quantum light. We should use the definition proposed in this work for the generalized polarization

degree, however by taking advantage that these states are the superposition of the unpolarized state $|000\rangle$, with probability $\sin^2\alpha$ and a polarized (partially) state $|S\rangle$, with probability $\cos^2\alpha$, then, for sake of simplicity and in order to give explicit results and without detriment of using equation (P5.52), we will present an alternative quantum polarization degree $\tilde{\mathcal{G}}^{(N)}$. To this end we assume that the generalized polarization degree is reduced by the depolarization introduced by the three-mode vacuum state in an amount $\sin^2\alpha$, and therefore the generalized polarization degree for a $MSP_\emptyset$ state can be written as follows:

$$\tilde{\mathcal{G}}^{(N)}_{|S_\emptyset\rangle} = 1 - \cos^2\alpha \int \mathbb{P}_{|S\rangle}\, \mathbb{P}_{|g\rangle}\, d\tilde{\mathcal{E}}_1 ... d\tilde{\mathcal{E}}_N - \sin^2\alpha = \cos^2\alpha\, \mathcal{G}^{(N)}_{|S\rangle}, \quad \text{(P5.66)}$$

and therefore for the particular case $N = 2$, that is, the sates given by equation (P5.65), we will have the expression:

$$\mathcal{G}^{(2)}_{|S_\emptyset\rangle} = \cos^2\alpha\Big\{1 - \frac{3}{4}\frac{\sqrt{3}}{\sqrt{2\tilde{C}_1^4 + 2\tilde{C}_2^4 + 1}}\Big\}. \quad \text{(P5.67)}$$

In short, under this approach the polarization quantum degree of a $MSP_\emptyset$ is equal to the product between the generalized polarization degree $\mathcal{G}_\emptyset = \cos^2\alpha$ due to the presence at the quantum superposition of a non polarized state (vacuum state) and what can be called the intrinsic quantum generalized polarization degree of the MSP state. Moreover with this definition we can use all the above results about MSP states, however if we are interested in the comparison with other states different to the MSP ones then the general definition (P5.52) must be used.

P5.5. Summary

In this work the generalized polarization structure of pure and mixture multimodal single photon states has been studied through their probability distributions in the optical field-strength space $\mathcal{E}_1 ... \mathcal{E}_N$. The main advantages of using the mentioned probability distributions is that they are a well-behaved distributions and can be measured by homodyne or heterodyne techniques. Along this work the generalized polarization has been understood as a significative confinement of the optical field values on determined regions of a multimodal optical field-strength space, and accordingly a generalized polarization degree $\mathcal{G}^{(N)}$ for a N-mode state has been proposed. It has been shown that MSP states show, in general, a hyperelliptical-type generalized polarization, that is, the main and secondary maxima of their distribution probabilities are found along principal directions $\tilde{\mathcal{E}}_1 ... \tilde{\mathcal{E}}_N$. Likewise, it has been shown that the proposed generalized polarization degree describes correctly the generalized polarization of well-known states such as monomode chaotic state, coherent circular state, and

so on. Accordingly, the generalized polarization degree of pure and mixture MSP states have been calculated and analysed and the limit case $N = 2$ can be also used to study standard polarization.

USC
UNIVERSIDADE
DE SANTIAGO
DE COMPOSTELA

P6. OPTICAL FIELD-STRENGTH GENERALIZED POLARIZATION OF NON-STATIONARY QUANTUM STATES IN WAVEGUIDING PHOTONIC DEVICES

JOURNAL OF MODERN OPTICS
VOL. 60 NO. 12 PAGES 941-955
doi:10.1080/09500340.2013.824125

PUBLISHED 28 AUGUST 2013

BY DAVID BARRAL, JESÚS LIÑARES & MARÍA C. NISTAL

UNIVERSIDADE DE SANTIAGO DE COMPOSTELA

Abstract: *A quantum analysis of the generalized polarization properties of multimode non-stationary states based on their optical field-strength probability distributions is presented. The quantum generalized polarization is understood as a significant confinement of the probability distribution along certain regions of a multidimensional optical field-strength space. The analysis is addressed to quantum states generated in multimode linear and nonlinear waveguiding (integrated) photonic devices, such as multimode waveguiding directional couplers and waveguiding parametric amplifiers, whose modes fulfill a spatial modal orthogonality. In particular, the generalized polarization degree of coherent, squeezed and Schrödinger's cat states is analyzed.*

P6.1. Introduction

In this paper we present an analysis of the quantum generalized polarization of a set of non-stationary quantum states of light. This analysis is based on the study of the probability distribution of these states in a N-dimensional optical field-strength space, which allows us to characterize quantum states by using a quantum generalized polarization degree. Both the concept of generalized polarization and quantum generalized polarization degree in the optical-field strength space was recently introduced [Liñares and Nistal, 2012, Liñares et al., 2011a]. The analysis was performed for stationary quantum states of light but in this work we extend it to the non-stationary ones. For that purpose we present a slightly different definition of the quantum generalized polarization degree because of the non-stationary character of the quantum light states analyzed. Quantum generalized polarization is related to the confinement of the probability distributions along certain regions of a multidimensional optical field-strength space. These probability distributions can be obtained by making measurements of the optical field by using well-known homodyne and heterodyne detection schemes of quantum light states. The quantum generalized polarization degree gives us a quantitative value about the mentioned confinement. Polarization concepts are very useful to perform significant tasks in quantum optics such as to characterize and classify multimode states, and in particular quantum states in waveguiding photonic devices as directional couplers [Liñares and Nistal, 2003, Liñares et al., 2008a]. Obviously, the standard quantum polarization can be included as a particular case. Moreover, quantum states in directional couplers are crucial to experimentally demonstrate both fundamental properties and application of quantum light such as Hang-Ou-Mandel effect in a two-mode directional coupler [Politi et al., 2008], quantum computation, in particular quantum optical gates and in general quantum optical circuits [Liñares et al., 2011b, Politi et al., 2009, Thompson et al., 2011], quantum metrology and quantum communications.

On the other hand, it is well known that the quantum Momentum operator describes in a fully proper way the spatial propagation of quantum states of light in coupled-mode waveguiding photonic devices [Liñares et al., 2008a]. Starting from this quantum operator we can use different techniques to calculate the propagation of quantum states in photonic devices. In particular, by using the spatial propagation of the quantum absorption ($\hat{a}$) and emission ($\hat{a}^{\dagger}$) operators, the quantum spatial optical propagator in the optical field-strength space can be obtained [Liñares et al., 2012] and accordingly the spatial propagation of the optical field-strength probability distribution can be calculated. Once the spatial propagation has taken place, that is, the light has reached the end of the waveguiding photonic device, we have a particular multimode quantum state which evolves

freely in time and whose quantum polarization we want to study. We will analyze the generalized polarization degree of non-stationary states such as multimode coherent states, and in particular those ones obtained from a 3x3 integrated directional coupler; likewise, we will study squeezed states generated by nonlinear directional couplers [Liñares et al., 2012], and finally Schrödinger's cat states which can be obtained from waveguides by post selection [Ourjoumtsev et al., 2009]. We must stress that these states will not contain a very large mean photon number because only in such a case quantum polarization is highly relevant, as it will be explicitly shown later. In fact, in the limit of a high mean photon number the states mentioned above become fully polarized.

The paper is organized as follows. In section 2 we present, by taking into account the Momentum operator, the formalism of the quantum generalized polarization in the optical field-strength multimode space for its application to quantum states in waveguiding devices. In section 3 we study the quantum polarization of multimode coherent states, analyzing in detail the case of a 3x3 directional coupler. In section 4 we focus on multimode squeezed states obtained by several waveguiding (spatially) degenerate parametric amplifiers; likewise a two-mode squeezed state obtained by a waveguiding non-degenerate parametric amplifier is studied, although the results can be extended to multimode squeezed states of this kind. In section 5 we present the analysis of multimode Schrödinger's cat states although for sake of simplicity only a two-mode Schrödinger's cat states is analyzed in detail. In section 6 a summary is presented.

P6.2. N-dimensional quantum generalized polarization degree

Let us consider a waveguiding photonic device with linear and nonlinear guides coupled. If this device has N coupled modes then we will have quantum states which can be represented on a N-dimensional optical field-strength space. Indeed, let us consider the well-known optical (electric) field-strength $\hat{\mathcal{E}}_i$ operators with eigenstates (optical field states) $|\mathcal{E}_i\rangle$, defined as follows:

$$\hat{\mathcal{E}}_i\,|\mathcal{E}_i\rangle = (\hat{\mathcal{E}}_i^{(+)} + \hat{\mathcal{E}}_i^{(-)})|\mathcal{E}_i\rangle = \frac{1}{2}(\hat{a}_i + \hat{a}_i^{\dagger})\,|\mathcal{E}_i\rangle = \mathcal{E}_i\,|\mathcal{E}_i\rangle. \tag{P6.1}$$

We use the N-dimensional eigenstates $|\mathcal{E}_1...\mathcal{E}_N\rangle$ of the optical field-strength operators $\hat{\mathcal{E}}_i$ in order to represent the quantum states of light by the probability distribution $\mathcal{P}(\mathcal{E}_1,...,\mathcal{E}_N)$ in the abstract multimodal optical field-strength space $\mathcal{E}_1...\mathcal{E}_N$. As shown further on, the shape of these probability distributions is directly related to the polarization of the quantum state analyzed, that is, to the confinement properties of its probability distribution in the optical field-strength space. Let us consider a multimode quantum light state $|L\rangle$ written as a superposition of the eigenstates $|\mathcal{E}_1...\mathcal{E}_N\rangle$ of the

optical field-strength operators $\hat{\mathcal{E}}_i$, that is:

$$|L\rangle = \iint \langle \mathcal{E}_1 ... \mathcal{E}_N | L \rangle |\mathcal{E}_1\rangle ... |\mathcal{E}_N\rangle \, d\mathcal{E}_1 ... d\mathcal{E}_N. \tag{P6.2}$$

Therefore the probability distribution on the N-dimensional optical field-strength space $\mathcal{E}_1 ... \mathcal{E}_N$ is given by:

$$\mathcal{P}(\mathcal{E}_1, ..., \mathcal{E}_N) = |\langle \mathcal{E}_1 ... \mathcal{E}_N | L \rangle|^2 \equiv |\mathcal{A}(\mathcal{E}_1, ..., \mathcal{E}_N)|^2. \tag{P6.3}$$

Accordingly, if we know the complex probability amplitude $\mathcal{A}(\mathcal{E}_1, ..., \mathcal{E}_N)$ of the state, then a quantum polarization analysis can be made. For that purpose we start from the Momentum operator which allows us to obtain the spatial propagation, for instance along z-direction, in a waveguiding photonic device with linear and nonlinear guides coupling N modes, that is:

$$\begin{aligned} \hat{M} = \; & \sum_{i=1}^{N} \hbar \, \mathrm{sgn}(i) \tilde{\beta}_i \, \hat{a}_i^\dagger \hat{a}_i + \sum_{i<j} \{\hbar \, \kappa_{i,j} \; \hat{a}_i \hat{a}_j^\dagger + \mathrm{h.c.}\} + \hat{M}_{NL}, \\ & \hat{M}_{NL} = \tfrac{1}{p+1} \iiint_0^T \hat{\mathbf{P}}_{NL}^{(p)} \, \hat{\mathbf{e}} \; dx dy dt, \end{aligned} \tag{P6.4}$$

where $\tilde{\beta}_i = \beta_i + \kappa_{ii}$, β_i is the propagation constant of the i-mode, κ_{ii} is the self-coupling coefficients, κ_{ij}, $i \neq j$, the cross-coupling coefficients, $\mathbf{P}_{NL}^{(p)}$ the nonlinear polarization, with p its order, and $\hat{\mathbf{e}}$ is the normalized modal optical field operator [Liñares et al., 2008a]. The Momentum operator governs the spatial transformations produced in waveguiding linear and nonlinear devices. In this way, N-dimensional coherent states can be obtained by using *NxN* directional couplers, likewise, N-dimensional squeezing states can be also achieved by coupled nonlinear guides implementing parametric amplifiers, and so on. From the operator Momentum we can work out the z-spatial Heisenberg's propagation equations for the operators $\hat{a}_i(z)$ and $\hat{a}_i^\dagger(z)$ and accordingly, by following the steps indicated in reference [Liñares et al., 2012], the quantum optical propagator is obtained. Starting from the optical propagator and an initial quantum sate we can calculate the probability complex amplitude $\mathcal{A}(\mathcal{E}_1, ..., \mathcal{E}_N; z)$ at any plane z and consequently the probability distribution $\mathcal{P}(\mathcal{E}_1, ..., \mathcal{E}_N; z)$. In Appendix A an explicit example of a spatially non-degenerate parametric amplifier in an integrated guide is presented. Indeed, by starting from the Momentum operator of the spatially non-degenerate parametric amplifier in an optical waveguide the corresponding spatial optical quantum propagator is obtained and an explicit calculation of the probability distribution at the output plane z of the guide is made. We must stress that this parametric amplifier can not be dealt with a Hamiltonian formulation, as it is well-known in the theory about light propagation [Liñares et al., 2008a]. In particular, a two-mode coherent state has been propagated in a two-mode photonic guide and the probability complex amplitude distribution

of a squeezed state at an arbitrary plane z has been obtained. Obviously at that plane (detection plane) the usual temporal evolution of the quantum state happens.

Next, we introduce a definition for the quantum generalized polarization degree based on the probability distribution on the $\mathcal{E}_1, ..., \mathcal{E}_N$ space. A general and detailed analysis on this issue for standard polarization can be found in different specialized references [Klimov et al., 2005, Luis, 2002, 2003, Sánchez-Soto et al., 2006]. In this work we recover the definition recently applied to both the case of standard polarization (two - mode space) [Liñares et al., 2010] and generalized polarization (multimode space) [Liñares et al., 2011a] which are valid for single photon states and other quantum stationary states. However, in this work we consider non - stationary states and accordingly we need to introduce the concept of temporaly accumulated probability which is more suitable for such states. First of all we recall that our polarization degree definition is based on the well-known fact that the symmetric multimode chaotic quantum state $|\kappa_1...\kappa_N\rangle = |\kappa...\kappa\rangle$, and therefore in the limit $\bar{n} = 0$ the N-mode vacuum state [Luis, 2003], is not polarized at all, where $\kappa_i = \bar{n}$ is the mean value of photons in the mode i. For instance, a symmetric two-mode chaotic state $|\kappa\kappa\rangle$ is represented by a bidimensional Gaussian probability distribution in the optical-field strength space $\mathcal{E}_1\mathcal{E}_2$ with a quantum noise of the optical field-strength (root mean-square deviation) equal to $\sqrt{\kappa + 1/2}$. Taking into account the above considerations, it has been shown for stationary quantum states that the complementary value of the overlapping between the probability distribution of a quantum state and the best Gaussian probability distribution on the $\mathcal{E}_1, ..., \mathcal{E}_N$ space (non-polarized state), allows us to calculate how much a quantum state of light $|L\rangle$ is polarized. Indeed, let us consider the following probability distribution of a Gaussian state $|g\rangle$ in the N-dimensional optical field-strength space:

$$\mathcal{P}_{|g\rangle}(\mathcal{E}_1...\mathcal{E}_N) = \frac{1}{g^{1/2}\pi^{N/2}} \exp\Big\{-\frac{\sum_{i=1}^{N}\mathcal{E}_i^2}{g}\Big\}, \tag{P6.5}$$

where g is a free parameter in order to maximize the overlapping with the probability distribution of the quantum state $|L\rangle$. We must stress that this procedure is closely related to the more rigorous concept of distance measure to an unpolarized distribution [Luis, 2003] or to quantum states that are invariant under any SU(2) polarization transformation [Klimov et al., 2005]. Accordingly, by following closely the definition of the quantum polarization degree by Luis [Luis, 2002] or alternatively by Sánchez-Soto et al. [Sánchez-Soto et al., 2006] (which also includes mixture quantum states), the following expression for the quantum generalized polarization degree of a multimode quantum state $|L\rangle$ in a N-dimensional optical field-strength

space can be used [Liñares et al., 2011a]:

$$\mathcal{G}^{(N)} = \frac{1}{2}\int (\mathbb{P}_{|L\rangle} - \mathbb{P}_{|g\rangle})^2 \, d\mathcal{E}_1 ... d\mathcal{E}_N, \tag{P6.6}$$

where normalized probabilities are used in order to make sure that $\mathcal{G}^{(N)} \in [0,1]$, that is,

$$\mathbb{P}_{|L\rangle} = \frac{\mathcal{P}_{|L\rangle}(\mathcal{E}_1 ... \mathcal{E}_N)}{\{\int \mathcal{P}^2_{|L\rangle} \, d\mathcal{E}_1 ... d\mathcal{E}_N\}^{1/2}}, \;\; \mathbb{P}_{|g_b\rangle} = \frac{\mathcal{P}_{|g_b\rangle}}{\{\int \mathcal{P}^2_{|g_b\rangle} \, d\mathcal{E}_1 ... d\mathcal{E}_N\}^{1/2}}. \tag{P6.7}$$

Expression (P6.6) can be rewritten, after a straightforward calculation, in a more suggestive form, that is,

$$\mathcal{G}^{(N)} = 1 - \mathcal{D}^{(N)}(g_b), \tag{P6.8}$$

$$\mathcal{D}^{(N)}(g_b) = \int \mathbb{P}_{|L\rangle}(\mathcal{E}_1 ... \mathcal{E}_N) \, \mathbb{P}_{|g_b\rangle}(\mathcal{E}_1 ... \mathcal{E}_N) \, d\mathcal{E}_1 ... d\mathcal{E}_N, \tag{P6.9}$$

where g_b defines the parameter value of the best Gaussian, that is, the maximum value of function $\mathcal{D}^{(N)}(g)$, which is the same as a depolarization function in a N-dimensional space. It must be stressed that the choice of the dimension N will depend on the particular problem which we are dealing with. For instance, if the quantum states live in a M-dimensional subspace ($M < N$) or present such symmetries that a transformation take them to that subspace, then the quantum generalized polarization degree $\mathcal{G}^{(M)}$ must be used [Liñares et al., 2011a, 2012].

The above definition is also appropriate for non-stationary states, that is, for a time-dependent probability distribution: $\mathbb{P}_{|L\rangle}(\mathcal{E}_1 ... \mathcal{E}_N; t)$. However, when this sort of states are used, a probability distribution accumulated along time is more advisable, or in other words, a cycle-average probability distribution, that is,

$$\mathcal{P}_{|L\rangle}(\mathcal{E}_1 ... \mathcal{E}_N) = \frac{1}{T}\int_0^T \mathcal{P}_{|L\rangle}(\mathcal{E}_1 ... \mathcal{E}_N; t) \, dt. \tag{P6.10}$$

In fact, the classical polarization is represented by elliptical curves which can be regarded as the values reached by the optical field after a period T, and accumulated along an ellipse. A similar result is obtained with the coherent quantum states. For instance, a circular coherent state, that is, $|\alpha \, i\alpha\rangle$ evolves on the two-dimensional space $\mathcal{E}_1\mathcal{E}_2$ by following a circular path but with quantum fluctuations. Accordingly, if we use an accumulated probability distribution we will have the probability of the optical-field values averaged on a period. This accumulated probability provides us a graphical image of the polarization of the quantum state, that is, a picture of the confinement degree of the optical-field values in the optical field-strength

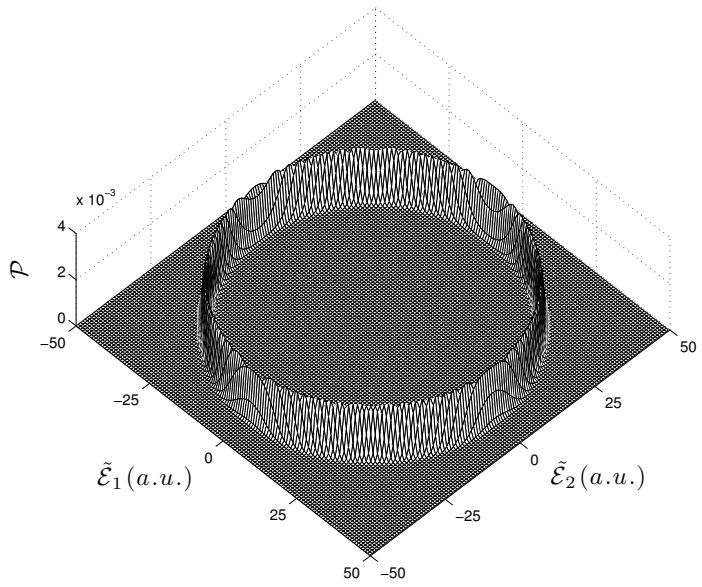

Figure P6.1: Accumulated probability of a circular-type coherent state $|\alpha\, i\alpha\rangle$ with $|\alpha| = 40$.

space. It can be seen for instance in Figure P6.1, where the accumulated probability for a circular coherent state is shown. Finally, we must stress that the Gaussian state (non-polarized state) is stationary by definition and therefore the instantaneous and cycle-average probabilities fit in.

Now a few words must be said concerning to the measurements of the probabilities $P_{|L\rangle}(\mathcal{E}_1 ... \mathcal{E}_N)$. Let us consider the two-mode case: it is well known that the probability function $\mathcal{P}_{|L\rangle}(\mathcal{E}_1\, \mathcal{E}_2; t)$ can be measured by using a two-mode homodyne technique at each time t. However in our case we are interested in the accumulated probability distribution function $\mathcal{P}_{|L\rangle}(\mathcal{E}_1\, \mathcal{E}_2)$ and therefore independent from the measurement time. The main idea is that the polarization properties are related to the set of all values reached by the optical field and their dispersion, in a similar way to the classical case. In other words, the instantaneous polarization could be analyzed but it has no classical counterpart and therefore it does not contain the classical polarization limit. Consequently, a two-mode heterodyne technique would provide the accumulated probability which also means a remarkable simplification of the experimental setup. The most representative example are the coherent states, which in the limit of a high value of the main photon number become classical states, and therefore the accumulated probability describe the values of a classical optical field. In-

deed, as shown in Figure P6.1 the accumulated probability of a circular coherente state becomes a circle with a negligible relative fluctuations for $|\alpha|^2 = 1600 \gg 1$ of the optical field-strenght values, as expected in the classical limit for circular polarization.

P6.3. Generalized polarization of coherent states

In this section we present a general study of the polarization of multimode coherent states. We show that they can always be analyzed in a two - dimensional subspace which notably simplifies the study of the quantum polarization. In particular, and for sake of expositional convenience, the polarization degree of three-mode coherent states generated in a waveguiding directional coupler is analyzed.

Probability distributions

We start by writing the normalized wave function, or complex amplitude of the probability distribution on the space $\mathcal{E}_1 ... \mathcal{E}_N$, of the following multimode coherent (MMC) state: $|L\rangle = |\alpha_1 ... \alpha_N\rangle$, with $\alpha_i = |\alpha_i| e^{i\epsilon_i}$. This state can be obtained, for instance, in a waveguiding directional coupler of length z with N coupled guides (modes) that have equal or different propagation constants β_i and coupling coefficients κ_{ij}, and where we assume that photons are excited with energy $\hbar\omega$ in all these spatial modes; accordingly, α_i are functions of z, β_i and κ_{ij}. We could include several temporal modes ω_i but under linear propagation no new results would be found. If we take into account the complex amplitude of a monomode coherent state of a quantum harmonic oscillator we can write the following multimode complex amplitude for the MMC state at an arbitrary output plane z of the waveguiding coupler:

$$\mathcal{A}_{|L\rangle}(\mathcal{E}_1, ..., \mathcal{E}_N; t) = \langle \mathcal{E}_1 | L_1 \rangle ... \langle \mathcal{E}_N | L_N \rangle = \frac{1}{\pi^{N/4}} e^{-\frac{1}{2}\{\sum_{i=1}^{N} (\mathcal{E}_i - |\alpha_i| cos\varphi_i)^2\}} e^{i\phi}, \tag{P6.11}$$

with $\varphi_i = \omega t + \epsilon_i$ and where $\phi = \sum_{i=1}^{N} \phi_i = (1/2) \sum_{i=1}^{N} sin\varphi_i \, (2|\alpha_i|\mathcal{E}_i - |\alpha_i|^2 cos\varphi_i)$ is a phase which will not affect future derivations.

The optical field-strength representation for quantum states given by (P6.11) is suitable to be transformed by means of a N-dimensional rotation which takes the state to a two dimensional basis, in an analogous way as it is made with classical light [Liñares and Nistal, 2012]. For that purpose we will use a quantum analogue of a classical linear polarizator, that is, if we consider a monochromatic classical field in a complex notation $\mathbf{E}(z = 0, t) = (a\mathbf{u}_1 + b\, e^{i\epsilon}\mathbf{u}_2)\, e^{-i\omega t}$, which represents a plane wave with arbitrary elliptical polarization, and a linear polarizer with its transmission axis along a θ-direction, then the averaged classical intensity $\mathcal{I}(\theta)$ over

a cycle of oscillation emerging from the polarizer[Born and Wolf, 1959] is given by the following expression:

$$\mathcal{I}(\theta) = a^2 \cos^2\theta + b^2 \sin^2\theta + 2ab \sin\theta \cos\theta \cos\epsilon. \tag{P6.12}$$

This quadratic form can be diagonalized obtaining a basis change that takes the classical field to the diagonal elliptical form: $\mathbf{E}(z = 0, t) = (a\mathbf{u}_1 \pm i\, b\mathbf{u}_2)\, e^{-i\omega t}$. Following this idea in the quantum case, we can project an arbitrary MMC state $|L\rangle = |\alpha_1 ... \alpha_N\rangle$ defined in an euclidian N-dimensional space $\mathcal{E}_1 ... \mathcal{E}_N$, with an associate basis of unitary vectors $\{\mathbf{u}_1, ..., \mathbf{u}_N\}$, over a N-dimensional polarizer whose transmission axis is characterized by an arbitrary unitary vector of N components $\mathcal{X}_i$. The quantum action of the polarizer is defined by the quantum emission operator:

$$\hat{a}_p^\dagger = \sum_{i=1}^{N} \mathcal{X}_i\, \hat{a}_i^\dagger. \tag{P6.13}$$

By taking into account this operator, we can calculate the mean value of the intensity operator at the output of the polarizator defined as $\langle \hat{\mathcal{J}} \rangle = \langle \hat{\mathcal{E}}_p^{(-)} \hat{\mathcal{E}}_p^{(+)} \rangle_{|L\rangle}$. Therefore the mean projected quantum intensity can be written as:

$$\langle \hat{\mathcal{J}}(\mathcal{X}_1, ..., \mathcal{X}_N) \rangle = \sum_{i=1}^{N} |\alpha_i|^2 \mathcal{X}_i^2 + 2 \sum_{i<j}^{N} |\alpha_i||\alpha_j| \cos\epsilon_{ij}\, \mathcal{X}_i \mathcal{X}_j, \tag{P6.14}$$

where $\epsilon_{ij} = \epsilon_i - \epsilon_j$. This equation is formally analogous to that one for multimode single photon states [Liñares et al., 2011a], so that we will follow the same argument that was used there, that is, as the α_{ij} matrix associated to the quadratic form (P6.14) is a symmetric one, and by taking into account the subadditivity property of the rank of symmetric matrices, it is easy to prove that $rank(\alpha_{ij}) = 2$ and therefore the mentioned matrix can be diagonalized to a two dimensional form obtaining two real eigenvalues $|\tilde{\alpha}_{1,2}|^2$ different from zero and two real (orthogonal transformation) eigenvectors $\{\tilde{\mathbf{u}}_1, \tilde{\mathbf{u}}_2\}$. In other words, this transformation takes the state to an elliptical two dimensional form, therefore the following two dimensional diagonal form of the probability is obtained:

$$\mathcal{P}(\tilde{\mathcal{E}}_1, \tilde{\mathcal{E}}_2, ..., \tilde{\mathcal{E}}_N) = (1/\pi^{N/2})\, e^{-\{(\tilde{\mathcal{E}}_1 - |\tilde{\alpha}_1| \cos\tilde{\varphi})^2 + (\tilde{\mathcal{E}}_2 - |\tilde{\alpha}_2| \sin\tilde{\varphi})^2 + \tilde{\mathcal{E}}_3^2 + ... + \tilde{\mathcal{E}}_N^2\}}, \tag{P6.15}$$

with $\tilde{\varphi} = \omega t + \epsilon_0$. Both the term ϵ_0 (a common phase in either modes) and the values $|\tilde{\alpha}_i|$ can be obtained by using the fact that the expected values of the coherent states behave like the classical optical field, that is, the transformation between the old and new basis of the states can be expressed as:

$$\langle \hat{\tilde{\mathcal{E}}}_i \rangle = \sum_j a_{ij} \langle \hat{\mathcal{E}}_j \rangle \Leftrightarrow \tilde{\alpha}_i = \sum_j a_{ij} \alpha_j \tag{P6.16}$$

where a_{ij} denotes each element $i, j = 1, 2, ..., N$ of the transformation matrix between the new and old basis. Finally, after splitting in real and imaginary parts, we obtain from Equation (P6.16):

$$\tan \epsilon_0 = \frac{\sum_{j=1}^{N} |\alpha_j| \sin \epsilon_j \, a_{1j}}{\sum_{j=1}^{N} |\alpha_j| \cos \epsilon_j \, a_{1j}} = -\frac{\sum_{j=1}^{N} |\alpha_j| \cos \epsilon_j \, a_{2j}}{\sum_{j=1}^{N} |\alpha_j| \sin \epsilon_j \, a_{2j}}. \tag{P6.17}$$

Next we will present a suitable method to calculate the diagonal form of the real and symmetric α_{ij} matrix associated to the quadratic form (P6.14). For sake of expositional convenience we will analyze the case of a three-mode coherent state, although the analysis can be extended to an arbitrary dimension N.

Three-mode coherent states

Let us consider a three-mode coherent state $|L\rangle = |\alpha_1 \, \alpha_2 \, \alpha_3\rangle$. The general probability distribution in the space $\mathcal{E}_1\mathcal{E}_2\mathcal{E}_3$, with a basis of unitary vectors $\{\mathbf{u}_1, \mathbf{u}_2, \mathbf{u}_3\}$, is given by the expression:

$$\mathcal{P}(\mathcal{E}_1, \mathcal{E}_2, \mathcal{E}_3) = (1/\pi^{3/2}) \, e^{-\{(\mathcal{E}_1 - |\alpha_1| \cos\varphi_1)^2 + (\mathcal{E}_2 - |\alpha_2| \cos\varphi_2)^2 + (\mathcal{E}_3 - |\alpha_3| \cos\varphi_3)^2\}} \tag{P6.18}$$

Our primary aim is to obtain the transformation that diagonalizes the probability (P6.18). For this purpose we use a three-mode polarizator whose emission operator, given by Equation (P6.13), is applied to the state in order to calculate the mean value of the quantum intensity (P6.14), that is,

$$\langle \hat{\mathcal{I}}(\mathcal{X}_1, \mathcal{X}_2, \mathcal{X}_3) \rangle = \sum_{i=1}^{3} |\alpha_i|^2 \mathcal{X}_i^2 + 2 \sum_{i<j}^{3} |\alpha_i||\alpha_j| \cos\epsilon_{ij} \, \mathcal{X}_i \mathcal{X}_j, \tag{P6.19}$$

Next, we must calculate the eigenvalues $\lambda_i = |\tilde{\alpha}_i|^2 \neq 0$ and the eigenvectors of this quadratic form that let us to determine the new basis of unitary vectors $\{\tilde{\mathbf{u}}_1, \tilde{\mathbf{u}}_2\}$ of the new space $\tilde{\mathcal{X}}_1\tilde{\mathcal{X}}_2$. For that we will use a well-known general diagonalization method based on the minors of the diagonal for the α_{ij} matrix, that is, the characteristic polynomial is given by the expression:

$$p(\lambda) = \det(\alpha_{ij} - \lambda I) = \sum_{k=0}^{N} p_k \, \lambda^k = \sum_{k=0}^{N} (-1)^k \sum_{i=1}^{N} m_i^{(N-k)} \, \lambda^k, \tag{P6.20}$$

where $m_i^{(N-k)}$ are the minors of order $(N-k)$ of the diagonal of the α_{ij} matrix. Note that in the cases $k = 0, N-1, N$ we obtain the simple relationships:

$$p_0 = \det(\alpha_{ij}), \; p_{N-1} = (-1)^{N-1} \sum_{i=1}^{N} |\alpha_i|^2, \; p_N = (-1)^N. \tag{P6.21}$$

Let us consider the characteristic polynomial of state, that is, from Equation (P6.14) we obtain:

$$\det(\alpha_{ij} - \lambda I) = \begin{vmatrix} |\alpha_1|^2 - \lambda & |\alpha_1||\alpha_2|\cos\epsilon_{12} & |\alpha_1||\alpha_3|\cos\epsilon_{13} \\ |\alpha_1||\alpha_2|\cos\epsilon_{12} & |\alpha_2|^2 - \lambda & |\alpha_2||\alpha_3|\cos\epsilon_{23} \\ |\alpha_1||\alpha_3|\cos\epsilon_{13} & |\alpha_2||\alpha_3|\cos\epsilon_{23} & |\alpha_3|^2 - \lambda \end{vmatrix} = 0, \tag{P6.22}$$

where $\epsilon_{23} = \epsilon_{12} - \epsilon_{13}$. Therefore, following the indicated above, the coefficients of the characteristic polynomial, after a long but straightforward calculation, are given by the following expressions:

$$p_3 = (-1)^3 = -1, \tag{P6.23}$$

$$p_2 = \sum_{i=1}^{N} |\alpha_i|^2, \tag{P6.24}$$

$$p_1 = (-1)\sum_{i<j}^{3} |\alpha_i|^2|\alpha_j|^2 \sin^2\epsilon_{ij}, \tag{P6.25}$$

$$p_0 = \det(\alpha_{ij}) = 0. \tag{P6.26}$$

If we insert the above values into the Equation (P6.20) defining the characteristic polynomial then the following roots λ_i $(i = 1, 2, 3)$, are obtained:

$$p(\lambda) = -\lambda^3 + (\sum_{i=1}^{N} |\alpha_i|^2)\lambda^2 - (\sum_{i<j}^{3} |\alpha_i|^2|\alpha_j|^2 \sin^2\epsilon_{ij})\lambda = 0, \tag{P6.27}$$

$$\lambda_{1,2} = \frac{\sum_{i=1}^{N} |\alpha_i|^2}{2}\{1 \pm [1 - \frac{4\sum_{i<j}^{3} |\alpha_i|^2|\alpha_j|^2 \sin^2\epsilon_{ij}}{(\sum_{i=1}^{N} |\alpha_i|^2)^2}]^{1/2}\}, \qquad \lambda_3 = 0. \tag{P6.28}$$

Note that, as was justified before, only two of the eigenvalues are different from zero, and therefore we only need to calculate two eigenvectors $\tilde{\mathbf{u}}_i = a_{ij}\mathbf{u}_j$, where $i = 1, 2$ and $j = 1, 2, 3$; and in this case the third one can be simply obtained as $\tilde{\mathbf{u}}_3 = \tilde{\mathbf{u}}_1 \wedge \tilde{\mathbf{u}}_2$. After a long but standard and straightforward calculation, the following relationships between the eigenvectors components are obtained for each eigenvalue λ_i:

$$A_{i1} = |\alpha_1||\alpha_2|[\lambda_i \cos\epsilon_{12} + |\alpha_3|^2(\cos\epsilon_{13}\cos\epsilon_{23} - \cos\epsilon_{12})], \tag{P6.29}$$

$$A_{i2} = \lambda_i^2 - (|\alpha_1|^2 + |\alpha_3|^2)\lambda_i + |\alpha_1|^2|\alpha_3|^2 \sin^2\epsilon_{13}, \tag{P6.30}$$

$$A_{i3} = |\alpha_2||\alpha_3|[\lambda_i \cos\epsilon_{23} + |\alpha_1|^2(\cos\epsilon_{13}\cos\epsilon_{12} - \cos\epsilon_{23})]. \tag{P6.31}$$

Therefore the normalized eigenvectors will be given by the following expression:

$$\tilde{\mathbf{u}}_i = \frac{1}{[\sum_{j=1}^{3}(A_{ij})^2]^{1/2}}(A_{i1}, A_{i2}, A_{i3})^T \equiv (a_{i1}, a_{i2}, a_{i3})^T, \tag{P6.32}$$

which in turn defines an orthogonal transformation a_{ij} between the coordinates in the new basis of eigenvectors $\tilde{\mathbf{u}}_i$ and in the old basis $\mathbf{u}_j$, that is, $\tilde{\mathcal{X}}_i = a_{ij}\mathcal{X}_j$ and accordingly the coordinates $\tilde{\mathcal{E}}_i$ of the new space also fulfil $\tilde{\mathcal{E}}_i = a_{ij}\mathcal{E}_j$.

Finally, we rewrite the probability distribution in the $\tilde{\mathbf{u}}_i$ ($i = 1, 2$) basis. First of all we calculate the common phase ϵ_o of both modes at the initial time $t = 0$ from Equation (P6.17) for $N = 3$. This phase together with the eigenvectors $\tilde{\mathbf{u}}_i$ define the new eigenstates $|\tilde{\alpha}_i\rangle$, in the $\tilde{\mathcal{E}}_1\tilde{\mathcal{E}}_2\tilde{\mathcal{E}}_3$ space, that is:

$$|\tilde{\alpha}_i\rangle = |\sum_{j=1}^{3} a_{ij}\,\alpha_j\,\rangle, \tag{P6.33}$$

where $\tilde{\alpha}_k = -i|\tilde{\alpha}_k|\,e^{i(\tilde{\varphi}+k\pi/2)}$, with $k = 1, 2$ and $\tilde{\varphi} = \omega t + \epsilon_0$. Therefore the distribution probability (P6.18) in this rotated optical field-strength space can be written as:

$$\mathcal{P}(\tilde{\mathcal{E}}_1, \tilde{\mathcal{E}}_2, \tilde{\mathcal{E}}_3) = (1/\pi^{3/2})\, e^{-\{(\tilde{\mathcal{E}}_1 - |\tilde{\alpha}_1| cos\tilde{\varphi})^2 + (\tilde{\mathcal{E}}_2 - |\tilde{\alpha_2}| sin\tilde{\varphi})^2 + \tilde{\mathcal{E}}_3^2\}}. \tag{P6.34}$$

Three-mode coherent states in 3×3 directional couplers

We present the generalized polarization properties in a *3x3* linear directional coupler in order to make clear the general procedure for the analysis of multimode coherent states in waveguiding photonics devices. The Momentum operator and Heisenberg's equations corresponding to a *3x3* linear directional coupler are obtained from Equation (P6.4) with $i, j = 1, 2, 3$ and $\hat{M}_{NL} = 0$. For sake of simplicity we will consider the particular case of three identical guides (synchronous directional coupler), that is: $\tilde{\beta}_1 = \tilde{\beta}_2 = \tilde{\beta}_3 \equiv \beta_0$, with only coupling between neighbour (consecutive) guides, that is, $\kappa_{ij} = \kappa^{\star}_{ij} = \kappa$ only if $i = j \pm 1$, and $\kappa_{ij} = 0$ if $i \neq j \pm 1$. From Equation (P6.4) and after a simple calculation, the following Heisenberg's equations are obtained:

$$-i\partial_z \hat{a}_1 = \tilde{\beta}_0 \hat{a}_1 + \kappa \hat{a}_2, \tag{P6.35}$$

$$-i\partial_z \hat{a}_2 = \tilde{\beta}_0 \hat{a}_2 + \kappa \hat{a}_1 + \kappa \hat{a}_3, \tag{P6.36}$$

$$-i\partial_z \hat{a}_3 = \tilde{\beta}_0 \hat{a}_3 + \kappa \hat{a}_2. \tag{P6.37}$$

The solutions of these equations can be obtained in a similar way as is made in the classical case. We are interested in the conjugated forms, i.e., emission (creation) operators $\hat{a}^{\dagger}$, in order to determine the quantum states at the output of the *3x3* coupler. The solutions are given by the following

expressions [Liñares et al., 2008b]:

$$\hat{a}_1^\dagger e^{-i\beta_0 z} = \frac{1}{2}[1+\cos\phi]\,\hat{a}_{01} + \frac{i}{\sqrt{2}}\sin\phi\,\hat{a}_{02} - \frac{1}{2}[1-\cos\phi]\,\hat{a}_{03}, \quad \text{(P6.38)}$$

$$\hat{a}_2^\dagger e^{-i\beta_0 z} = \frac{i}{\sqrt{2}}\sin\phi\,\hat{a}_{01} + \cos\phi\,\hat{a}_{02} + \frac{i}{\sqrt{2}}\sin\phi\,\hat{a}_{03}, \quad \text{(P6.39)}$$

$$\hat{a}_3^\dagger e^{-i\beta_0 z} = -\frac{1}{2}[1-\cos\phi]\,\hat{a}_{01} + \frac{i}{\sqrt{2}}\sin\phi\,\hat{a}_{02} + \frac{1}{2}[1+\cos\phi]\,\hat{a}_{03}, \quad \text{(P6.40)}$$

where $\phi \equiv \phi(z) = \sqrt{2}\kappa z$. We take advantage of these results to work out, as an example, the output state of this device for the propagation of an input coherent state excited in the first guide: $|L_{in}\rangle = |\alpha_1\,0\,0\rangle$. This state is propagated along the coupler, and by taking into account Equations (P6.38, P6.39, P6.40), the following output state $|L\rangle$ is obtained:

$$|L\rangle = |\,\frac{\alpha_1}{2}\,[1+\cos\phi]\,e^{i\beta_0 z}\rangle\,|\,\frac{\alpha_1}{\sqrt{2}}\,\sin\phi\,e^{i(\beta_0 z+\pi/2)}\rangle\,|\,\frac{\alpha_1}{2}\,[1-\cos\phi]\,e^{i(\beta_0 z+\pi)}\rangle. \quad \text{(P6.41)}$$

Applying a projection of the state over a three-mode quantum polarizer we can obtain the mean value of the quantum intensity by (P6.19):

$$\langle\hat{J}(X_1,X_2,X_3)\rangle = \alpha_1^2\cos^4\frac{\phi}{2}\,X_1^2 + \frac{\alpha_1^2}{2}\sin^2\phi\,X_2^2 + \alpha_1^2\sin^4\frac{\phi}{2}\,X_3^2 - \frac{\alpha_1^2}{2}\sin^2\phi\,X_1\,X_3. \quad \text{(P6.42)}$$

The orthogonal transformation a_{ij} can be obtained by using the general expressions (P6.28, P6.32) for multimode coherent states. However, in this case it can also be obtained in a straightforward way by taking into account Equation (P6.41), that is,

$$a_{ij} \equiv \frac{1}{[2(1+\cos^2\phi)]^{1/2}}\begin{pmatrix}(1+\cos\phi) & 0 & -(1-\cos\phi)\\ 0 & [2(1+\cos^2\phi)]^{1/2} & 0\\ (1-\cos\phi) & 0 & (1+\cos\phi)\end{pmatrix}, \quad \text{(P6.43)}$$

where the relevant eigenvectors $\{\tilde{\mathbf{u}}_1, \tilde{\mathbf{u}}_2\}$, with eigenvalues $\lambda_{1,2} \equiv |\tilde{\alpha}_{1,2}|^2 = \alpha_1^2\,(1 \pm \cos^2\phi)/2$, are given by the following expressions:

$$\tilde{\mathbf{u}}_1 = \frac{1}{[2(1+\cos^2\phi)]^{1/2}}\{(1+\cos\phi)\mathbf{u}_1 + (\cos\phi-1)\mathbf{u}_3\}, \quad \tilde{\mathbf{u}}_2 = \mathbf{u}_2. \quad \text{(P6.44)}$$

Now, by taking into account that $\tilde{\alpha}_i = \sum_j a_{ij}\alpha_j$ and calculating the phase origin by means of (P6.17), that is, $\epsilon_0 = 0$, we can write the probability distribution on the new space as follows:

$$\mathcal{P}(\tilde{\xi}_1,\tilde{\xi}_2,\tilde{\xi}_3,t) = (1/\pi^{3/2})\,e^{-\{(\tilde{\xi}_1-|\tilde{\alpha}_1|\cos\varphi)+(\tilde{\xi}_2-|\tilde{\alpha}_2|\sin\varphi)^2+\tilde{\xi}_3^2\}}. \quad \text{(P6.45)}$$

This probability distribution is time dependent, therefore in order to present the generalized polarization properties of multimode coherent states generated by *3x3* couplers and to make them compatible with the experimental measurements, that is, with the results of a heterodyne detection scheme, we make a temporal averaging, or equivalently we calculate the accumulated probability distribution. The corresponding integrals contain exponential of trigonometric temporal functions that can be solved by writting the exponentials as a product of series of modified Bessel functions of first kind I_r and applying the addition theorem for these functions [Massida, 1983]. For sake of simplicity, we also apply the variable change $\tilde{\mathcal{E}}_1 = \tilde{\xi}\cos\tilde{\theta}$, $\tilde{\mathcal{E}}_2 = \tilde{\xi}\sin\tilde{\theta}$, and after a long but straightforward calculation we obtain the result:

$$\mathcal{P}(\tilde{\xi},\tilde{\theta},\tilde{\mathcal{E}}_3) = \frac{e^{-\{\tilde{\xi}^2+\tilde{\mathcal{E}}_3^2+(|\tilde{\alpha}_1|^2+|\tilde{\alpha}_2|^2)/2\}}}{\pi^{3/2}} \sum_{r=-\infty}^{\infty} I_r\left(\left|\frac{|\tilde{\alpha}_1|^2-|\tilde{\alpha}_2|^2}{2}\right|\right) I_{2r}\left(2\tilde{\xi}\left[|\tilde{\alpha}_1|^2\cos^2\tilde{\theta}+|\tilde{\alpha}_2|^2\sin^2\tilde{\theta}\right]^{1/2}\right)\cos(2r\gamma), \tag{P6.46}$$

where $\tan\gamma = \pm(|\tilde{\alpha}_2|/|\tilde{\alpha}_1|)\tan\tilde{\theta}$. It is important to underline that the argument of the modified Bessel function I_{2r} is a two-dimensional diagonalized function of $|\tilde{\alpha}_i|$, $i = 1,2$, analogous to that obtained starting from a quantum polarizer, that is, we could have started from N-dimensional probability distributions integrated along the time and we would have found that the argument of the modified Bessel function I_{2r} would be analogous to Equation (P6.14). On the other hand, the corresponding diagonalized averaged probability in the optical field-strength space would allow us to use a two-mode heterodyne detection method although we have a multimode state.

Now we show some illustrative cases of probability distributions of three-mode coherent states. For the first case we choose $\phi = \pi/4$ in Equation (P6.41) and accordingly from Equation (P6.46) an elliptical generalized polarization, resembling the classical one, is obtained (see Figure P6.2). Note a high confinement of the probability distribution along an elliptical curve where main and secondary probability maxima are located along the $\tilde{\mathcal{E}}_1$-axis and $\tilde{\mathcal{E}}_2$-axis, respectively. This state can be labelled as an elliptical-type three-mode coherent state. A quantitative value of the polarization will be given when we calculate the polarization degree. In a second case we take $\phi = \pi/2$ in the coherent state (P6.41), then the associated probability distribution takes the form:

$$\mathcal{P}(\tilde{\xi},\tilde{\theta},\tilde{\mathcal{E}}_3) = \frac{e^{-(\tilde{\xi}^2+\tilde{\mathcal{E}}_3^2+|\tilde{\alpha}_1|^2)}}{\pi^{3/2}} I_0(2|\tilde{\alpha}_1|\tilde{\xi}). \tag{P6.47}$$

As we show in Figure P6.1, it resembles a circular classical polarization because of the high confinement of the probability distribution around a

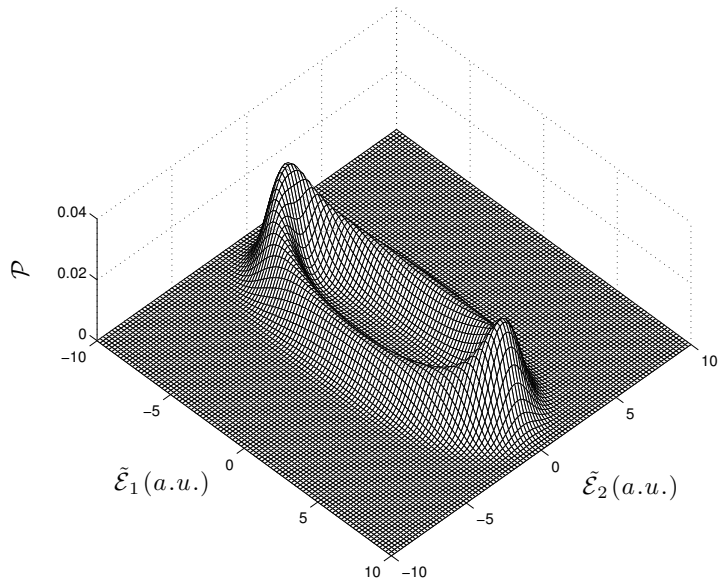

Figure P6.2: Probability of a diagonalized three-mode elliptical-type state with $|\alpha_1| = 10$ and $\phi = \pi/4$.

circular curve; it can be labelled a circular-type three-mode coherent state. When treating with high number of photons, as the case of Figure P6.1, it is interesting to obtain an asymptotic expression, that is, for $|\tilde{\alpha}_1| >> 1$ we obtain:

$$\mathcal{P}(\tilde{\xi}, \tilde{\theta}, \tilde{\mathcal{E}}_3) \simeq \frac{e^{-\{(\tilde{\xi}-|\tilde{\alpha}_1|)^2+\tilde{\mathcal{E}}_3^2\}}}{2\pi^2\sqrt{|\tilde{\alpha}_1|\tilde{\xi}}}, \tag{P6.48}$$

which represents a function localized around a circumference of radius $|\tilde{\alpha}_1|$, and therefore the values of the optical field are also localized.

On the other hand we observe that a reduction of the main number of photons leads to lower confinement of the probability and therefore to lower polarization. In Figure P6.3 we show the probability distribution of a circular-type three-mode coherent state with a low number of photons where this loss of confinement can be appreciated. Likewise, by comparing Figure P6.1 and P6.3 we can also observe how the relative quantum uncertainty diminishes as the number of photons of each mode increases, and how such an uncertainty is increased as this number is reduced.

Finally we study the case $\phi = 0$. In this case the probability distribution takes the form:

$$\mathcal{P}(\tilde{\xi}, \tilde{\theta}, \tilde{\mathcal{E}}_3) = \frac{e^{-\{\tilde{\xi}^2+\tilde{\mathcal{E}}_3^2+(|\tilde{\alpha}_1|^2/2)\}}}{\pi^{3/2}} \sum_{r=-\infty}^{\infty} I_r\left(\frac{|\tilde{\alpha}_1|^2}{2}\right) I_{2r}\left(2|\tilde{\alpha}_1|\,\tilde{\xi}\cos\tilde{\theta}\right), \tag{P6.49}$$

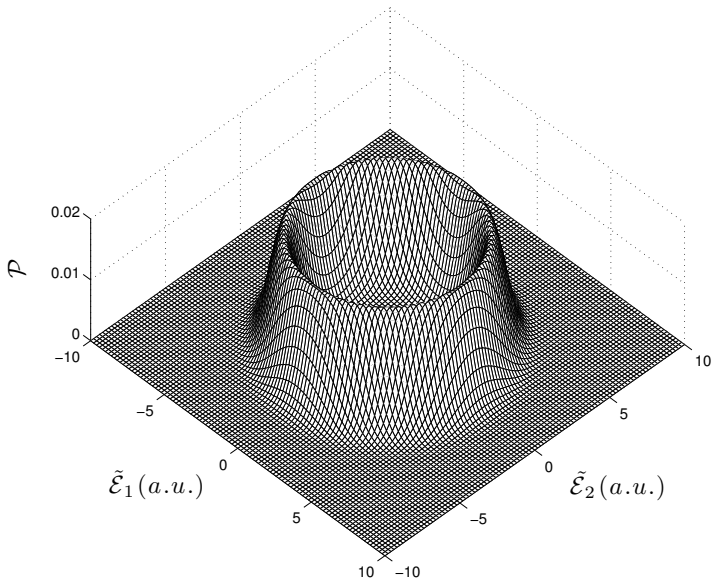

Figure P6.3: Probability of a circular-type state with $|\alpha_1| = 10$ and $\phi = \pi/2$.

which is shown in Figure (P6.4). It resembles a linear classical polarization because the main maxima of probability are on a straight line, in this case along the direction $\tilde{\mathcal{E}}_1$; it can be called a linear-type three-mode state.

In short, starting from a 3x3 directional coupler we can transform an input three-mode linear-type state into different output states with different generalized polarizations. Now we are interested in characterizing the polarization of these states and for that purpose we use the quantum generalized polarization degree in the next section.

Quantum generalized polarization degree of coherent states

Let us consider a N-mode coherent state $|\alpha_1\,\alpha_2\,...\,\alpha_N\rangle$. This quantum state, under transformations like (P6.33), can be rewritten in a two-dimensional subspace as $|\tilde{\alpha}_1\,\tilde{\alpha}_2\rangle$, where $\tilde{\epsilon}_1 - \tilde{\epsilon}_2 = \pi/2$. Therefore we are only concerned with the generalized polarization degree $\mathcal{G}^{(2)}$, which is formally equivalent to a standard polarization degree. Let us consider an elliptical coherent state, that is $|\tilde{\alpha}_1| \neq |\tilde{\alpha}_2| \neq 0$. The probability distribution of this quantum state on the $\tilde{\mathcal{E}}_1\tilde{\mathcal{E}}_2$-subspace can be written as follows:

$$\mathcal{P}_{|\tilde{\alpha}_1\,i\tilde{\alpha}_2\rangle} = (1/\pi^{N/2})\,e^{-\{(\tilde{\mathcal{E}}_1 - |\tilde{\alpha}_1|\cos\tilde{\varphi})^2 + (\tilde{\mathcal{E}}_2 - |\tilde{\alpha}_2|\sin\tilde{\varphi})^2 + \tilde{\mathcal{E}}_3^2 + ... + \tilde{\mathcal{E}}_N^2\}}. \quad \text{(P6.50)}$$

We insert Equation (P6.50) into Equation (P6.10) (temporal averaging), the result is substituted into equation (P6.9), and next by using Equations (P6.7)

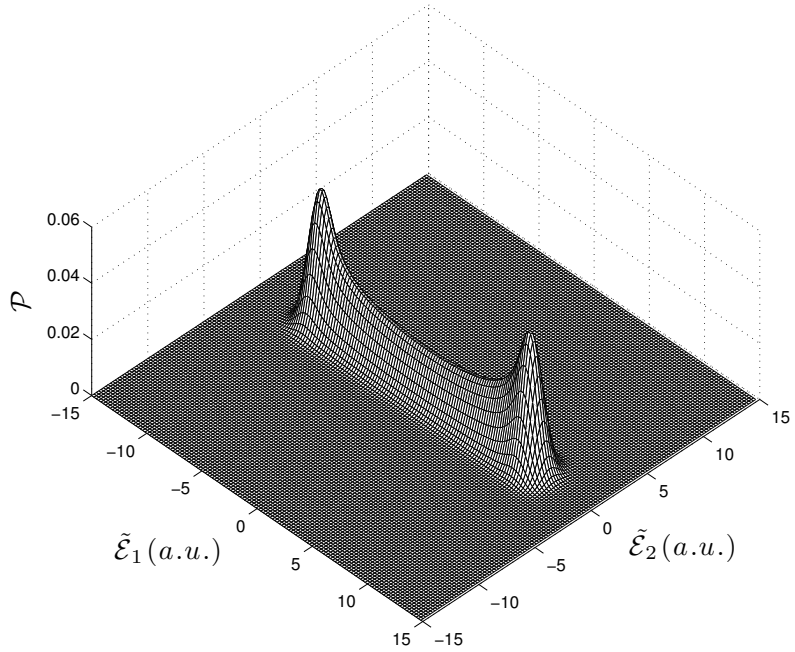

Figure P6.4: Probability of a linear-type three-mode state with $|\alpha_1| = 10$ and $\phi = 0$.

and (P6.8), the following expression for the polarization degree is obtained:

$$\mathcal{G}^{(2)}_{|\tilde{\alpha}_1\, i\tilde{\alpha}_2\rangle}(g_b) = 1 - 2\,\frac{g_b^{1/2}}{1+g_b}\,I_0(\mu)\,e^{-(|\tilde{\alpha}_1|^2+|\tilde{\alpha}_2|^2)/\{2(1+g_b)\}}. \qquad \text{(P6.51)}$$

The polarization degree is calculated by determining the maximum value of function $\mathcal{D}^{(2)}(g)$ for the elliptical coherent state, and therefore the best Gaussian distribution, that is, the best value g_b. After a long but straightforward calculation, the following equation for the parameter g_b is derived:

$$g_b^2 + \frac{1}{I_0(\mu)}\{|\tilde{\alpha}_2|^2[I_1(\mu) - I_0(\mu)] - |\tilde{\alpha}_1|^2[I_1(\mu) + I_0(\mu)]\}\,g_b - 1 = 0, \qquad \text{(P6.52)}$$

where $\mu = (|\tilde{\alpha}_2|^2 - |\tilde{\alpha}_1|^2)/\{2(1+g_b)\}$. This nonlinear algebraic equation can be solved numerically [Yang et al., 2005] and the result is substituted into Equation (P6.51) to calculate the quantum generalized polarization. As an example, in Figure P6.5 we represent the values of $\mathcal{G}^{(2)}_{|L\rangle}$ for a set of coherent states $|L\rangle = |\tilde{\alpha}_1\, i\tilde{\alpha}_2\rangle$ with values of $|\tilde{\alpha}_1|$ from 0 to 10, and $|\tilde{\alpha}_2| = 0, 2, 4, 6, 8$. Each point stands for a quantum state of light with values of the mean

photon number in each mode equal to $|\tilde{\alpha}_1|^2$ and $|\tilde{\alpha}_2|^2$. Note that the larger is the mean photon number in both modes, that is $|\tilde{\alpha}_1|^2 + |\tilde{\alpha}_2|^2$, the closer is the quantum generalized polarization degree to the unity, as expected from the classical limit. For instance, for values of mean photon number around 160, figures of polarization degree close to 0.9 are obtained. Reversely, the shorter the mean photon number is, the closer is the generalized polarization degree to the zero value, as expected because of the proximity to the vacuum state.

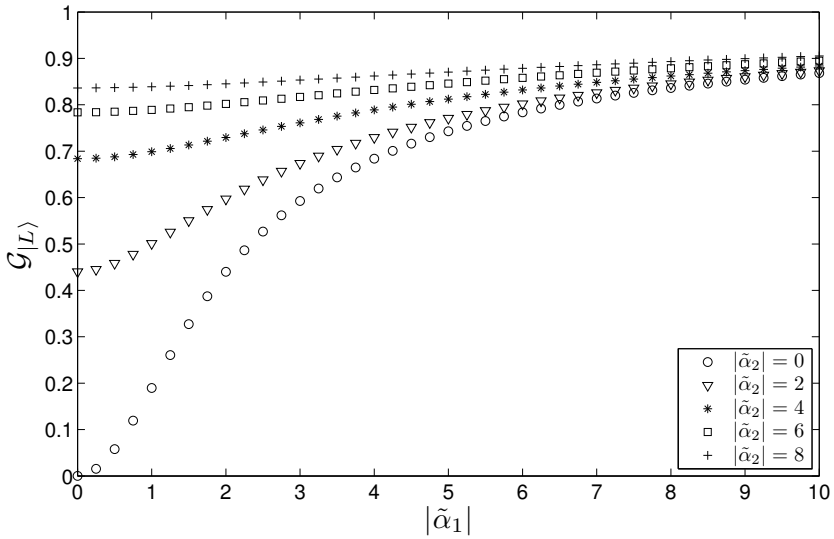

Figure P6.5: Quantum generalized polarization degree $\mathcal{G}^{(2)}_{|L\rangle}$ for multimode coherent states with values of $\tilde{\alpha}_1$ from 0 to 10 and $\tilde{\alpha}_2 = 0, 2, 4, 6, 8$.

P6.4. Generalized polarization of squeezed states

In this section we will deal with squeezed states of light which allows us to obtain more insight about the generalized polarization of quantum states of light. These are minimum uncertainty product states like coherent states, but with the feature of exchanging quantum noise. This exchange can happen between quadratures of the same mode, as in the case of single mode squeezed states, or between quadratures of different modes, as it happens in two-mode correlated squeezed states, etc. [Caves and Schumaker, 1985, Schleich, 2001, Walls and Milburn, 1994]. In any case they overpass the quantum limit of noise. It is well-known that a general multimode squeezed state can be written as $|L\rangle = \prod_{i=1}^{N} \hat{S}_i(\zeta_i)|\alpha_i\rangle$, where $\hat{S}_i(\zeta_i) = exp\{\frac{1}{2}(\zeta_i^* \hat{a}_i^2 - \zeta_i \hat{a}_i^{\dagger 2})\}$ is the single mode squeeze operator and ζ_i is the i-mode squeeze parameter. This kind of states are produced, for instance, in N integrated degenerate parametric amplifiers (DPA) with $\zeta_i = (\kappa_{NL})_i L$, where κ_{NL} is the nonlinear coupling constant of the modes

and L the distance of propagation. In a recent work we presented the characterization of these states in the optical field-strength space [Liñares et al., 2012]. In general, a multimode squeezed state can be represented on the mentioned space as follows:

$$\mathcal{A}_{|L\rangle}(\mathcal{E};t)=\{\prod_{i=1}^{N}[\pi^{1/2}\,\Delta\mathcal{E}_i(t)]^{-1/2}\}\,e^{-\frac{1}{2}\{\sum_{i=1}^{N}\frac{1}{\Delta\mathcal{E}_i^2(t)}(\mathcal{E}_i-|\alpha_i|f_i\cos\varphi_i)^2\}}e^{i\phi}, \tag{P6.53}$$

where $f_i=f(\zeta_i)$ is a real function of both the propagation constant of the guide and the nonlinear coupling, $\Delta\mathcal{E}_i(t)=\Delta\mathcal{E}(\zeta_i,t)$ the time-dependent uncertainty of the i-mode and φ_i and ϕ are phases defined as in (P6.11). This kind of states are more general than the coherent and present different polarization features. By inspection of Equation (P6.53) it is easy to realize that the most noteworthy difference appears in the uncertainties $\Delta\mathcal{E}(\zeta_i,t)$. Overall, this noise will prevent us to apply a change of basis like (P6.32) and therefore simplify the problem as shown in Section 3 for the coherent states. However, it can still be diagonalized in a certain sense. Indeed, let us consider the squeezed state at $t=0$, that is, at the exit of a nonlinear amplifier, then the probability distribution can be written as:

$$\mathcal{P}(\mathcal{E}';0)=\{\prod_{i=1}^{N}[\pi^{1/2}\,\Delta\mathcal{E}_i(0)]^{-1}\}\,e^{-\{\sum_{i=1}^{N}(\mathcal{E}_i'-|\alpha_i'|f_i\cos\epsilon_i)^2\}}, \tag{P6.54}$$

where $\mathcal{E}_i'=\mathcal{E}_i/\Delta\mathcal{E}_i(0)$, and $|\alpha_i|=|\alpha_i'|/\Delta\mathcal{E}_i(0)$. This state is formally a coherent state at $t=0$ but in a scaled space $\mathcal{E}_1'...\mathcal{E}_N'$. Now, we can apply the diagonalization technique shown in the above section and formally we obtain:

$$\mathcal{P}(\tilde{\mathcal{E}}';0)=\mathcal{N}_o\,e^{-\{[\tilde{\mathcal{E}}_1'-|\tilde{\alpha}_1'|\cos(\epsilon_1+\epsilon_o)]^2+[\tilde{\mathcal{E}}_2'-|\tilde{\alpha}_2'|\sin(\epsilon_2+\epsilon_o)]^2+(\tilde{\mathcal{E}}_3')^2+...+(\tilde{\mathcal{E}}_N')^2\}}, \tag{P6.55}$$

where $\mathcal{N}_o=\{\prod_{i=1}^{N}[\pi^{1/2}\,\Delta\mathcal{E}_i(0)]^{-1}\}$. This state is formally a diagonal coherent state in the optical field-strength space $\tilde{\mathcal{E}}_1'...\tilde{\mathcal{E}}_N'$. However when the scaling transformation is undone then a multimode squeezed vacuum is obtained and therefore the N-dimensional polarization degree has to be used.

In order to make clear the quantum polarization degree we will focus on two particular cases, that is, a non-correlated squeezed state, that is one with $\Delta\mathcal{E}_1(0)=\Delta\mathcal{E}_2(0)$, which can be obtained by a DPA, and a correlated state where $\Delta\mathcal{E}_1(0)\neq\Delta\mathcal{E}_2(0)$ and $\Delta\mathcal{E}_1(0)\,\Delta\mathcal{E}_2(0)=1$, which can be obtained by a spatial non-degenerate parametric amplifier (NDPA) [Walls and Milburn, 1994]. In both cases it is assumed $\Delta\mathcal{E}_i(0)=1,\forall i>2$, that is, vacuum states in the modes without nonlinear interaction. In the first case we can again obtain a diagonalized probability distribution, that is,

$$\mathcal{P}(\tilde{\mathcal{E}}_1,\tilde{\mathcal{E}}_2;t)=[\pi\,\Delta\tilde{\mathcal{E}}_1^2]^{-1}\,e^{-\{\frac{(\tilde{\mathcal{E}}_1-|\tilde{\alpha}_1|\cos\omega t)^2}{\Delta\tilde{\mathcal{E}}_1^2}+\frac{(\tilde{\mathcal{E}}_2-|\tilde{\alpha}_2|\sin\omega t)^2}{\Delta\tilde{\mathcal{E}}_1^2}\}}, \tag{P6.56}$$

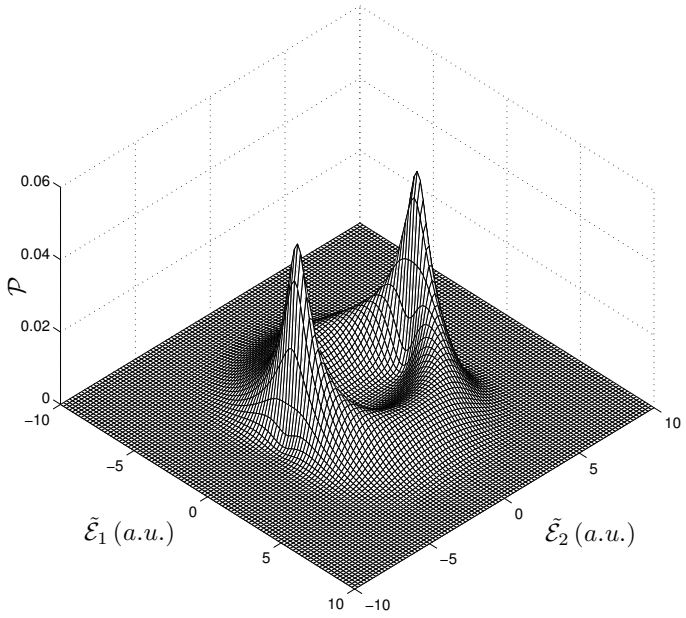

Figure P6.6: Probability of a squeezed state with $|\tilde{\alpha}_1| = |\tilde{\alpha}_2| = 4$ and $\kappa_{NL}L = 1$.

where $[\Delta\tilde{\mathcal{E}}_1(t)]^2 = \Delta\tilde{\mathcal{E}}_1^2(0)\cos^2\omega t + \Delta\tilde{\mathcal{E}}_1^{-2}(0)\sin^2\omega t$. Once more, we are interested in the accumulated probability. As it was made for the coherent case, we have to sum the optical field-strength measurements on every time, which is mathematically equivalent to performing a temporal integration over a period of oscillation (P6.10). However, for squeezed states there are not analytical expressions for the mentioned temporal integration, therefore a numerical integration has to be made. In Figure P6.6 we present the numerical results for the accumulated probability $P(\tilde{\mathcal{E}}_1, \tilde{\mathcal{E}}_2)$ of a non-correlated squeezed state with $|\tilde{\alpha}_1| = |\tilde{\alpha}_2| = 4$, $\Delta\tilde{\mathcal{E}}_1^2(0) = e^{2\kappa_{NL}L}$ and $\kappa_{NL}L = 1$. This probability distribution is confined on a circle, therefore, it can be called a circular-type non-correlated squeezed state. Note that there is a strongly asymmetric noise because the state reaches values of noise lower and higher than that of the quantum vacuum state along its temporal evolution.

On the other hand, we show in Figure P6.7 the generalized polarization degree for these circular-type non-correlated squeezed states, with $|\tilde{\alpha}_1|$ ranging from 0 to 10 and different values of $\kappa_{NL}\,L$ from 0 (that is, a coherent state) to 2. It must be stressed the fact that the non-correlated squeezed vacuum presents a generalized polarization degree higher than zero, which, moreover, rises with the value of $\kappa_{NL}\,L$. This behavior is owing to the loss of overlapping between this state and the Gaussian vacuum as the squeez-

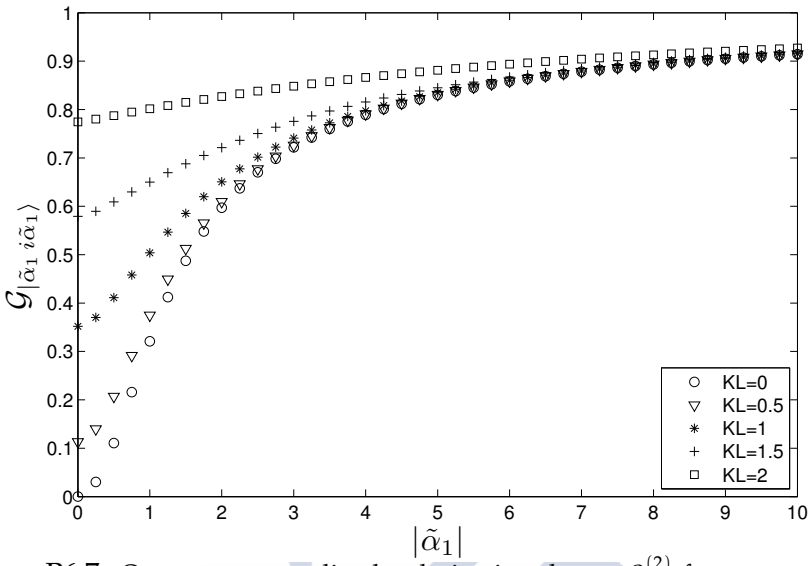

Figure P6.7: Quantum generalized polarization degree $\mathcal{G}^{(2)}_{|L\rangle}$ for squeezed states with $|\tilde{\alpha}_1| = |\tilde{\alpha}_2| = 0, ..., 10$ and different values of $\kappa_{NL}L$.

ing parameter is increased. Likewise, as the number of photons increases, the generalized polarization degree of the squeezed states is also higher than the one of coherent states. Again, due to the lack of symmetry in the quantum noise by squeezing, the non-correlated squeezed states overlap worse with Gaussian (non-polarized) states in comparison with coherent states.

Next, we show the case of a two-mode correlated squeezed state which presents the feature of generating entanglement. This entanglement can be seen as a correlation squeezing in the normal basis of the amplifier, that is, the one rotated $\pi/4$ with respect to the input state basis in the amplifier [Caves and Schumaker, 1985]. In order to make clear the behavior of this kind of devices in the optical field-strength space, we present its derivation in the Appendix A, that is, we calculate the output optical field-strength complex probability amplitude of an input coherent state $|L_{in}\rangle = |\alpha_1\rangle_1 |\alpha_1 e^{i\pi}\rangle_2$ propagating in an integrated nonlinear guide, a spatial NDPA, in such a way that under the considerations presented in the Appendix A the probability distribution of the squeezed state is given by the following expression:

$$\mathcal{P}(\tilde{\mathcal{E}}_1, \tilde{\mathcal{E}}_2; t) = [\pi \Delta\tilde{\mathcal{E}}_1 \Delta\tilde{\mathcal{E}}_2]^{-1}\, e^{-\{\frac{(\tilde{\mathcal{E}}_1 - |\tilde{\alpha}_1|\cos\omega t)^2}{\Delta\tilde{\mathcal{E}}_1^2} + \frac{(\tilde{\mathcal{E}}_2 - |\tilde{\alpha}_2|\sin\omega t)^2}{\Delta\tilde{\mathcal{E}}_2^2}\}}, \qquad \text{(P6.57)}$$

where $|\tilde{\alpha}_i|$ is related to the mean value of the optical field-strength and $[\Delta\tilde{\mathcal{E}}_{1,2}]^2$ are the optical field-strength uncertainties with values:

$$[\Delta\tilde{\mathcal{E}}_{1,2}(t)]^2 = \cosh 2\kappa_{NL}L\,(1 \pm \tanh 2\kappa_{NL}L \cos 2\omega t). \qquad \text{(P6.58)}$$

From the above expression it is easy to see that in this case the noise is shared between the optical field-strength modes of the state, unlike the above case, where the noise was shared between the quadratures of each mode. In the lab, we would obtain data with this probability distribution by using a homodyne detection scheme, but once again we are interested in the accumulated probability which can be measured by heterodyne detection. In Figures P6.8 and P6.9 we present the numerical results for the accumulated probability $P(\tilde{\mathcal{E}}_1, \tilde{\mathcal{E}}_2)$ of correlated squeezed states with $|\tilde{\alpha}_1| = |\tilde{\alpha}_2| = 4$ and $\kappa_{NL}L = 0.8$ and 2, respectively. Both states can be called circular-type correlated squeezed states because under the limit $\kappa_{NL} = 0$ a circular-type coherent state would be obtained. It can be clearly seen from these figures that if the squeezing parameter increases then the probability distribution turns from a "square"-type one into a "cross"-type one.

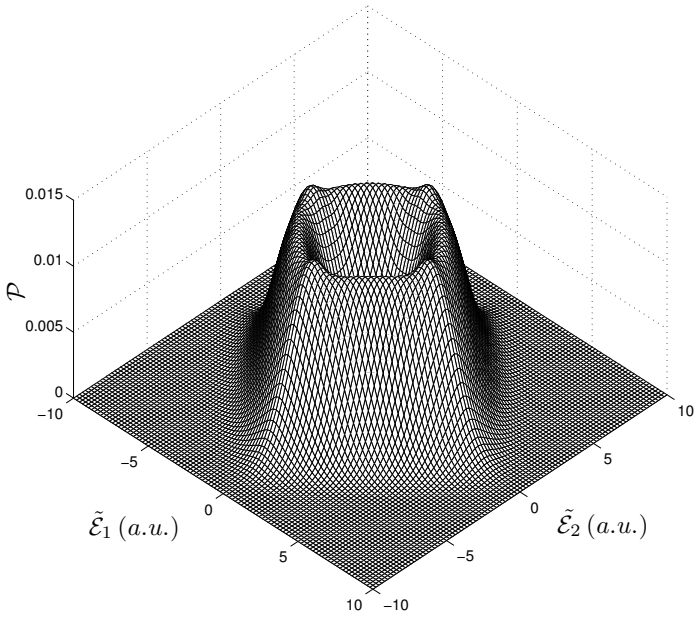

Figure P6.8: Probability of a squeezed state with $|\tilde{\alpha}_1| = |\tilde{\alpha}_2| = 4$ and $\kappa_{NL}L = 0.8$.

Again the calculation of the generalized polarization degree is performed numerically. The results are shown in Figures P6.10 and P6.11. In particular, we present the generalized polarization degree for linear and circular squeezed states, respectively, with $|\tilde{\alpha}_1|$ ranging from 0 to 10 and different values of $\kappa_{NL}\,L$ from 0 to 3. Again the squeezed vacuum presents a generalized polarization degree higher than zero and it increases with the value of $\kappa_{NL}\,L$ as the squeezing factor grows. In this case the probability distribution takes the form of a "cross" in the $\tilde{\mathcal{E}}_1\,\tilde{\mathcal{E}}_2$ space, as it can be seen

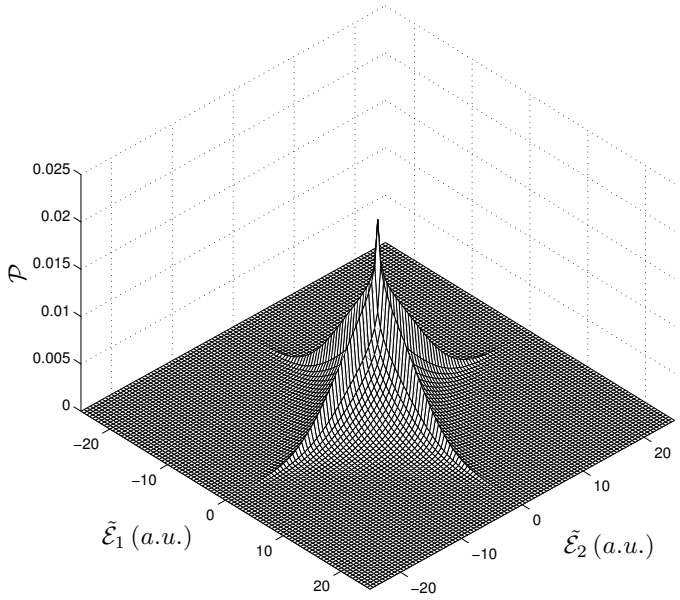

Figure P6.9: Probability of a squeezed state with $|\tilde{\alpha}_1| = |\tilde{\alpha}_2| = 4$ and $\kappa_{NL}L = 2$.

in Figure P6.9. Note that higher (and more confined) values of the optical field-strength are reached and therefore getting further away from a non-polarized state. Likewise, as the number of photons increases, the generalized polarization degree of the squeezed states takes lower figures than that of the coherent states.

P6.5. Generalized polarization of multimode Schrödinger's cat states

The macroscopic quantum superposition states, frequently so-called Schrödinger's cat states, are states without a classic analogue, because their probability presents interference between the components of the superposition [Schleich, 2001]. A short review about the generation of these kind of states can be found in [Lvovsky and Raymer, 2009]. Here we present a study of the generalized polarization of a particular case of these states. Let us consider the following multimode cat state $|L\rangle = \sum_{i=1}^{N} |\alpha_{1i}...\alpha_{Mi}\rangle\, e^{i\delta_i}$, where we take a subspace with M modes excited in separable coherent states such that the following probability amplitude is obtained:

$$\mathcal{A}_{|L\rangle}(\mathcal{E}_1,...,\mathcal{E}_M;t) = \frac{e^{\Phi_i}e^{i\delta_i}}{\pi^{M/4}\mathcal{N}_o}\sum_{i=1}^{N} e^{-\frac{1}{2}[(\mathcal{E}_{1i}-|\alpha_{1i}|\cos\varphi_{1i})^2+...+(\mathcal{E}_{Mi}-|\alpha_{Mi}|\cos\varphi_{Mi})]^2}, \tag{P6.59}$$

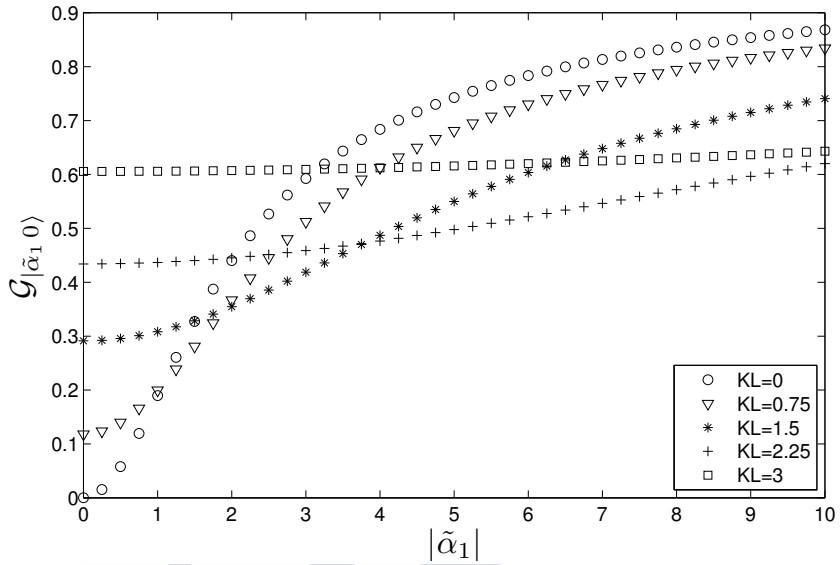

Figure P6.10: Quantum generalized polarization degree $\mathcal{G}^{(2)}_{|L\rangle}$ for squeezed states with $|\tilde{\alpha}_1| \approx 0, ..., 10$, $|\tilde{\alpha}_2| = 0$ and different values of $\kappa_{NL}L$.

where $\mathcal{N}_o$ is a normalization constant and $\Phi_i = (1/2)\sum_{j=1}^{M} \sin\varphi_{ji}(2|\alpha_{ji}|\mathcal{E}_{ji} - |\alpha_{ji}|^2\cos\varphi_{ji}$. For the sake of clarity, we will center our attention in the case of two-mode symmetric cat states, that is:

$$|L\rangle = \frac{1}{N_o}\{|\alpha_{11}\rangle|\alpha_{12}\rangle + e^{i\delta}|\alpha_{21}\rangle|\alpha_{22}\rangle\} \equiv \frac{1}{N_o}\{|\alpha_1\rangle|\alpha_2\rangle + e^{i\delta}|\alpha_2\rangle|\alpha_1\rangle\}, \quad \text{(P6.60)}$$

where δ is a relative phase between the states that compound the cat sate. This kind of states could be created transferring the scheme proposed in [Ourjoumtsev et al., 2009] to integrated waveguiding photonic devices, where single mode cat states produced by recombination of the output modes of a pulsed NDPA are entangled by subtracted photon detection, generating two-mode entangled coherent superpositions. In the optical field-strength space the probability distribution of these states can be expressed as:

$$\mathcal{P}_{|L\rangle}(\mathcal{E}_1, \mathcal{E}_2; t) = N_o^{-2}\{|\mathcal{A}_1|^2 + |\mathcal{A}_2|^2 + 2\cos\Psi\,|\mathcal{A}_1|\,|\mathcal{A}_2|\}, \quad \text{(P6.61)}$$

$$|\mathcal{A}_1(\mathcal{E}_1, \mathcal{E}_2; t)| = (1/\pi^{1/2})\, e^{-\frac{1}{2}(\mathcal{E}_1 - |\alpha_1|\cos\varphi_1)^2}\, e^{-\frac{1}{2}(\mathcal{E}_2 - |\alpha_2|\cos\varphi_2)^2}, \quad \text{(P6.62)}$$

$$|\mathcal{A}_2(\mathcal{E}_1, \mathcal{E}_2; t)| = (1/\pi^{1/2})\, e^{-\frac{1}{2}(\mathcal{E}_1 - |\alpha_2|\cos\varphi_2)^2}\, e^{-\frac{1}{2}(\mathcal{E}_2 - |\alpha_1|\cos\varphi_1)^2}, \quad \text{(P6.63)}$$

where $\Psi = [\delta - (\phi_2 - \phi_1)]$, $N_o^2 = 2\,(1 + \cos\delta\, e^{-\frac{1}{2}(|\alpha_1|^2 + |\alpha_2|^2 - 2|\alpha_1||\alpha_2|\cos\epsilon_{12})})$ is the normalization factor, and $\epsilon_{12} = \epsilon_1 - \epsilon_2$. This probability presents an interference of the probability amplitudes of each of the separable coherent

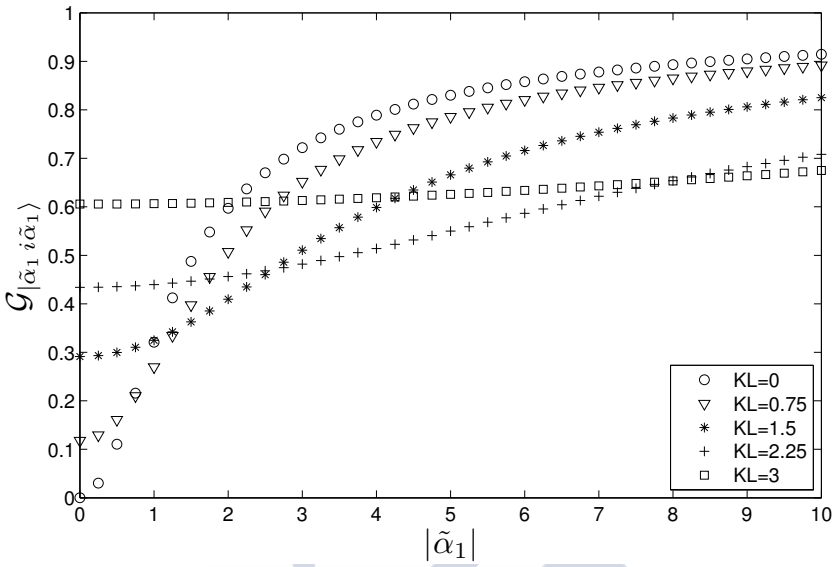

Figure P6.11: Quantum generalized polarization degree $\mathcal{G}^{(2)}_{|L\rangle}$ for squeezed states with $|\tilde{\alpha}_1| = |\tilde{\alpha}_2| \approx 0, ..., 10$ and different values of $\kappa_{NL}L$.

states in the optical field-strength space. As it was outlined above for coherent and squeezed states we are interested in the heterodyne probability which can be worked out again by temporal integration of (P6.61). After a long but straightforward calculation it is obtained:

$$\mathcal{P}_{|L\rangle}(\mathcal{E}_1, \mathcal{E}_2) = \mathcal{C}\Big\{ \sum_{j\neq k=1,2} \sum_{r=-\infty}^{\infty} I_r(\Upsilon_1)\, I_{2r}(\Upsilon_2(j,k)) \cos\left[2\,r\,(\Psi_1 - \Psi_2)\right] + \cos\delta \sum_{s,t=-\infty}^{\infty} I_t(\Upsilon_1)\, I_{s+2t}(\Upsilon_3)\, J_s(\Upsilon_4) \cos\left[2t\,(\Psi_1 - \Psi_2) + s\,(\Psi_1 - \Psi_3 - \pi/2)\right]\Big\}, \tag{P6.64}$$

where the different arguments, characteristic parameters and phases of the equation are defined as follows:

$$\mathcal{C} = \frac{e^{-(\mathcal{E}_1^2+\mathcal{E}_2^2)-(|\alpha_1|^2+|\alpha_2|^2)/2}}{\pi\,\mathcal{N}_o^2}, \tag{P6.65}$$

$$\Upsilon_1 = \frac{1}{2}[\,|\alpha_1|^4 + |\alpha_2|^4 + 2\,|\alpha_1|^2|\alpha_2|^2 \cos 2\,\epsilon_{12}\,]^{1/2}, \tag{P6.66}$$

$$\Upsilon_2(j,k) = 2\,[\,|\alpha_j|^2\,\mathcal{E}_1^2 + |\alpha_k|^2\,\mathcal{E}_2^2 + 2\,|\alpha_j||\alpha_k|\,\mathcal{E}_1\,\mathcal{E}_2 \cos\epsilon_{ij}\,]^{1/2}, \tag{P6.67}$$

$$\Upsilon_3 = 2\,\sigma_+\,(\mathcal{E}_1 + \mathcal{E}_2), \tag{P6.68}$$

$$\Upsilon_4 = \sigma_-\,(\mathcal{E}_1 - \mathcal{E}_2), \tag{P6.69}$$

$$\sigma_{\pm} = [|\alpha_1|^2 + |\alpha_2|^2 \pm 2\,|\alpha_1||\alpha_2|\cos\epsilon_{12}]^{1/2}, \tag{P6.70}$$

$$\tan\Psi_1 = -\frac{|\alpha_1|\sin\epsilon_1 + |\alpha_2|\sin\epsilon_2}{|\alpha_1|\cos\epsilon_1 + |\alpha_2|\cos\epsilon_2}, \tag{P6.71}$$

$$\tan 2\Psi_2 = -\frac{|\alpha_1|^2\sin 2\epsilon_1 + |\alpha_2|^2\sin 2\epsilon_2}{|\alpha_1|^2\cos 2\epsilon_1 + |\alpha_2|^2\cos 2\epsilon_2}, \tag{P6.72}$$

$$\tan\Psi_3 = \frac{|\alpha_2|\sin\epsilon_2 - |\alpha_1|\sin\epsilon_1}{|\alpha_2|\cos\epsilon_2 - |\alpha_1|\cos\epsilon_1}. \tag{P6.73}$$

As expected, the first term of Equation (P6.64) is analogous to Equation (P6.46) for non-diagonalized two-mode coherent states. It describes, in the most general case, two superimposed ellipses with their axis interchanged as it can be seen by inspection of the quadratic form (P6.67). The second term describes interference, specially where the ellipses cross, where the relative phase δ accounts for the sort of interference: destructive or constructive. In Figure P6.12 is shown an example of this distribution for a circular-type cat state with parameters $|\alpha_1| = |\alpha_2| = 3$, $\epsilon_{12} = \pi/2$ and $\delta = 2\pi$. As expected, it is formed by two circular coherent states plus an interference in the crossing areas. It can be called a circular-type Schrödinger's cat state.

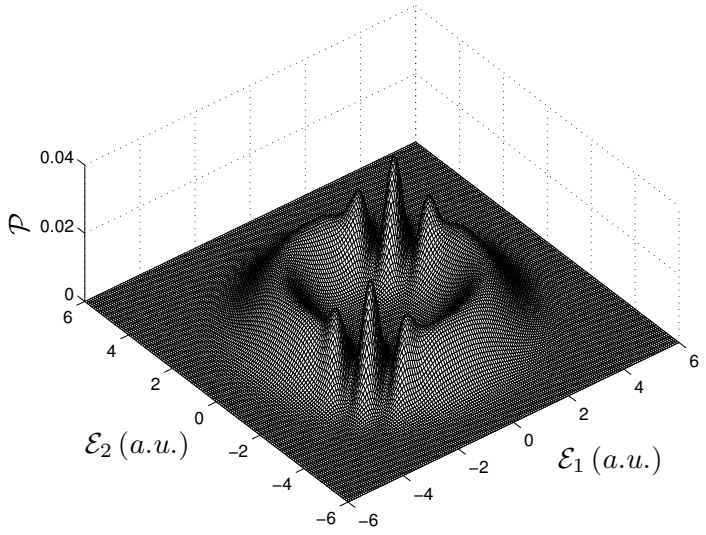

Figure P6.12: Probability of a circular-type Schrödinger's cat state with $|\alpha_1| = |\alpha_2| = 3$, $\epsilon_{12} = \pi/2$ and $\delta = 2\pi$.

Quantum generalized polarization degree of Schrödinger's cat states

In the case of a Schrödinger's cat state as the one presented above in equation (P6.61), the degree of generalized polarization is given, after a

certain calculation, by the expression:

$$\mathcal{G}^{(2)}_{|L\rangle}(g_b) = 1 - \frac{2}{\mathcal{N}_1^2}\frac{g_b^{1/2}}{1+g_b}\, I_0(\mu)\, e^{-\frac{(|\alpha_1|^2+|\alpha_2|^2)}{2(1+g_b)}}\{1+\cos\delta\, e^{-\frac{g_b}{2(1+g_b)}\sigma_-}\}, \quad \text{(P6.74)}$$

where $\mathcal{N}_1^2 = \mathcal{N}_0^2[\frac{T^2}{2\pi\int \mathcal{P}^2_{|L\rangle}\, d\mathcal{E}_1\, d\mathcal{E}_2\, dt}]^{1/2}$, and the parameter g_b is calculated by solving the following equation:

$$\begin{aligned}&\{(1-g_b^2)\, I_0(\mu) - 2\, g_b\, (1+g_b)\, \mu\, I_1(\mu)\}\{1+\cos\delta\, e^{-\frac{g_b}{2(1+g_b)}\sigma_-}\}\\ &+\ g_b\, I_0(\mu)\{|\alpha_1|^2+|\alpha_2|^2+2|\alpha_1||\alpha_2|\cos\epsilon_{12}\cos\delta\, e^{-\frac{g_b}{2(1+g_b)}\sigma_-}\} = 0,\end{aligned} \quad \text{(P6.75)}$$

with $\mu = \Upsilon_1/(1+g_b)$, and Υ_1 and σ_- have been defined in (P6.66, P6.70).

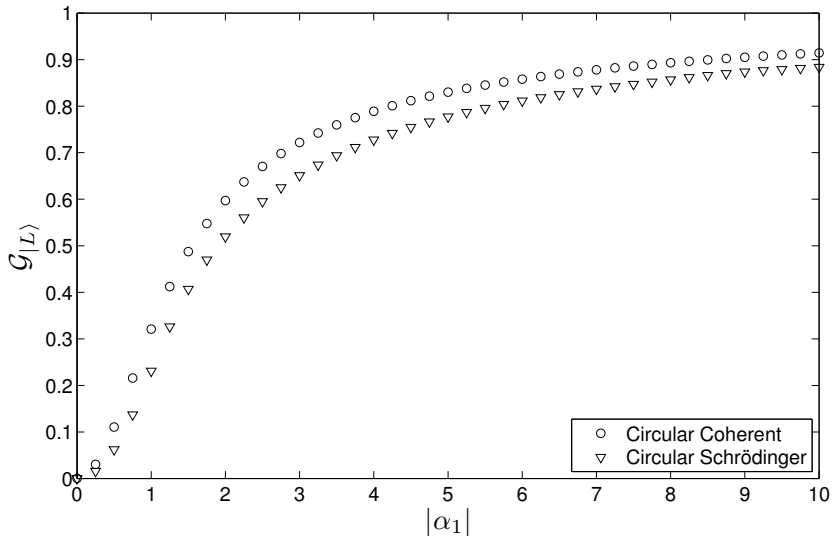

Figure P6.13: Quantum generalized polarization degree $\mathcal{G}^{(2)}_{|L\rangle}$ for circular coherent states and Schrödinger's cat states with $|\alpha_1| = 0, .., 10$, $\delta = 2\pi$ and $\epsilon_{12} = \pi/2$.

In Figure P6.13 we show the values of the generalized polarization degree for circular-type Schrödinger's cat states with different number of photons and compare them with those of circular-type coherent states. If there are a low number of photons then the Schrödinger's cat states present lower values of the generalized polarization degree than the ones corresponding to coherent states because of its higher overlapping with the Gaussian or non-polarized state. On the other hand, the polarization degree of Schrödinger's cat states with high number of photons tends to that one of the coherent states due to the fact that the interference term loses relevance.

P6.6. Summary

A quantum analysis of the generalized polarization properties of multimode non-stationary states based on their optical field-strength probability distributions has been presented. First of all, an appropriate definition of multimode generalized polarization degree has been proposed for non-stationary quantum states. The analysis has been addressed to coherent, squeezed and Schrödinger's cat states propagating in multimode linear and nonlinear integrated waveguiding devices, such as multimode integrated directional couplers and integrated parametric amplifiers. In all cases the quantum polarization properties are relevant under a low mean photon number. In the limit of a high mean photon number the polarization degree tends to the unity. Moreover, in the case of multimode coherent states it has been shown that polarization analysis can be always made on a two-dimensional space which simplifies notably the calculation of the polarization degree. On the other hand, squeezed states present a higher polarization degree than coherent states because the squeezing causes a certain confinement of the optical field-strength values and therefore a certain polarization of the state. In other words, a reduction of the quantum noise in one or several dimensions of the optical field-strength space brings about a polarization of the state, but only when the mean photon number is not high. By contrast, for large values of the mean photon number, squeezing is not an efficient cause of polarization, such as shown in this work. Finally, cat sates analyzed only show specific polarization properties for a low mean photon number, otherwise their polarization properties are very close to the ones of coherent states. In short, the quantum generalized polarization degree, which can be measured by multimode heterodyne detection techniques, provides an interesting characterization of multimode quantum states, specially for low mean photon numbers. This characterization can be of significance and usefulness because directional couplers are successfully being used for quantum computation, quantum metrology and quantum communications.

P6.7. Appendix: the spatially non-degenerate parametric amplifier

The momentum operator for an non-degenerate parametric amplifier pumped with a strong coherent state, can be written as:

$$\hat{M} = \frac{\hbar}{2}\sum_{i=1}^{2}(\hat{a}_i^\dagger \hat{a}_i + \hat{a}_i \hat{a}_i^\dagger) + i\hbar\kappa_{NL}(\hat{a}_1\hat{a}_2\, e^{-i\beta_p z} + h.c.), \qquad \text{(P6.76)}$$

where β_p is the propagation constant of the pump mode and κ_{NL} is a real nonlinear coupling coefficient. Following the procedure proposed in

[Liñares et al., 2012], we calculate the field-strength space quantum propagator associated to (P6.76) for the case of synchronization of phase $\beta_p = \beta_1 + \beta_2$. It can be written as:

$$K(\mathcal{E}_{10}, \mathcal{E}_{20}, \mathcal{E}_{1f}, \mathcal{E}_{2f}; L) = \frac{e^{\{(\frac{i}{2\eta})(\Lambda_1\mathcal{E}_{10}+\Lambda_2\mathcal{E}_{20}-2\Lambda_3\mathcal{E}_{10}\mathcal{E}_{20}+2\Lambda_4\mathcal{E}_{10}+2\Lambda_5\mathcal{E}_{20}+\Lambda_6)\}}}{2\pi i\eta^{1/2}}, \tag{P6.77}$$

with $\eta = \sin\beta_1 L \sin\beta_2 L$ and where:

$$\begin{aligned}
\Lambda_1 &= -(\cosh^2\kappa_{NL}L\cos\beta_1 L\sin\beta_2 L + \sinh^2\kappa_{NL}L\sin\beta_1 L\cos\beta_2 L),\\
\Lambda_2 &= -(\cosh^2\kappa_{NL}L\sin\beta_1 L\cos\beta_2 L + \sinh^2\kappa_{NL}L\cos\beta_1 L\sin\beta_2 L),\\
\Lambda_3 &= \frac{1}{2}\sinh 2\kappa_{NL}L\sin\beta_p L,\\
\Lambda_4 &= \sinh\kappa_{NL}L\sin\beta_1 L\,\mathcal{E}_{2f} + \cosh\kappa_{NL}L\sin\beta_2 L\,\mathcal{E}_{1f},\\
\Lambda_5 &= \sinh\kappa_{NL}L\sin\beta_2 L\,\mathcal{E}_{1f} + \cosh\kappa_{NL}L\sin\beta_1 L\,\mathcal{E}_{2f},\\
\Lambda_6 &= -(\cos\beta_1 L\sin\beta_2 L\,\mathcal{E}_{1f}^2 + \sin\beta_1 L\cos\beta_2 L\,\mathcal{E}_{2f}^2).
\end{aligned} \tag{P6.78}$$

Applying this propagator to a two-mode coherent state $|\alpha_1\,\alpha_2\rangle$, we obtain for a distance of quadrature squeezing $L = 2n\pi/\beta_p$, after a long but straightforward calculation, the following output amplitude probability:

$$\mathcal{A}(\tilde{\mathcal{E}}_1, \tilde{\mathcal{E}}_2) = \pi^{-1/2}\, e^{\frac{1}{4}[(\bar{\alpha}_1^2 - |\bar{\alpha}_1|^2)+(\bar{\alpha}_1^2 - |\bar{\alpha}_1|^2)]}\, e^{-\frac{1}{2}[(e^{-\kappa_{NL}L}\tilde{\mathcal{E}}_1 - \bar{\alpha}_1)^2 + (e^{\kappa_{NL}L}\tilde{\mathcal{E}}_2 - \bar{\alpha}_2)^2]}, \tag{P6.79}$$

where it has been applied the notation $\tilde{\mathcal{E}}_{if} \equiv \tilde{\mathcal{E}}_i$ and the following transformations have been used:

$$\mathcal{E}_1 = \frac{1}{2^{1/2}}(\tilde{\mathcal{E}}_1 - \tilde{\mathcal{E}}_2), \quad \mathcal{E}_2 = \frac{1}{2^{1/2}}(\tilde{\mathcal{E}}_1 + \tilde{\mathcal{E}}_2), \tag{P6.80}$$

$$\bar{\alpha}_1 = \frac{1}{2^{1/2}}[\alpha_1 e^{i\beta_1 L} + \alpha_2 e^{-i\beta_1 L}], \quad \bar{\alpha}_2 = \frac{1}{2^{1/2}}[-\alpha_1 e^{i\beta_1 L} + \alpha_2 e^{-i\beta_1 L}]. \tag{P6.81}$$

This amplitude probability is that at the output of the device. Because of the measurement is done by sampling the data in time we have to obtain the temporal evolution of this state in time. Applying the usual temporal propagator for equal frequency modes $\omega_1 = \omega_2 \equiv \omega$, the following probability amplitude is obtained:

$$\mathcal{A}(\tilde{\mathcal{E}}_1, \tilde{\mathcal{E}}_2) = [\pi\Delta\tilde{\mathcal{E}}_1\Delta\tilde{\mathcal{E}}_2]^{-1/2} e^{-\frac{1}{2}\{\frac{(\tilde{\mathcal{E}}_1 - |\bar{\alpha}_1| f_1(t))^2}{\Delta\tilde{\mathcal{E}}_1^2} + \frac{(\tilde{\mathcal{E}}_2 - |\bar{\alpha}_2| f_2(t))^2}{\Delta\tilde{\mathcal{E}}_2^2}\}} e^{i\phi}, \tag{P6.82}$$

with $\phi(\tilde{\mathcal{E}}_1, \tilde{\mathcal{E}}_2)$ a local phase without interest for polarization and where:

$$f_1(t) = [\cos\bar{\varepsilon}_1\, e^{\kappa_{NL}L}\cos\omega t + \sin\bar{\varepsilon}_1\, e^{-\kappa_{NL}L}\sin\omega t], \tag{P6.83}$$

$$f_2(t) = [\cos\bar{\varepsilon}_2\, e^{-\kappa_{NL}L}\cos\omega t + \sin\bar{\varepsilon}_2\, e^{\kappa_{NL}L}\sin\omega t], \tag{P6.84}$$

$$[\Delta\tilde{\mathcal{E}}_{1,2}(t)]^2 = \cosh 2\kappa_{NL}L\,(1 \pm \tanh 2\kappa_{NL}L\cos 2\omega t), \tag{P6.85}$$

with $\bar{\epsilon}_{1,2}$ the phases of $\bar{\alpha}_{1,2}$. For the particular case of an input state with $|\alpha_1| = |\alpha_2|$ and $\epsilon_2 - \epsilon_1 = \pi$, equation (P6.82) can be rewritten as:

$$\mathcal{A}_{|L\rangle}(\tilde{\mathcal{E}}_1, \tilde{\mathcal{E}}_2; t) = [\pi \Delta\tilde{\mathcal{E}}_1 \Delta\tilde{\mathcal{E}}_2]^{-1/2}\, e^{-\frac{1}{2}\{\frac{(\tilde{\mathcal{E}}_1 - |\tilde{\alpha}_1|\cos\omega t)^2}{\Delta\tilde{\mathcal{E}}_1^2} + \frac{(\tilde{\mathcal{E}}_2 - |\tilde{\alpha}_2|\sin\omega t)^2}{\Delta\tilde{\mathcal{E}}_2^2}\}} e^{i\Phi}, \tag{P6.86}$$

where we have defined $|\tilde{\alpha}_i|$, $i = 1, 2$, as:

$$|\tilde{\alpha}_i| = 2^{1/2}|\alpha_i|\cos(\beta_i L + \epsilon_i) e^{\kappa_{NL} L}. \tag{P6.87}$$

The probability amplitude (P6.86) describes a correlated squeezed state obtained by a non-degenerate parametric amplifier implemented in a waveguiding device.

Chapter 4 bibliography

A.F. Abouraddy, A.V. Sergienko, B.E.A. Saleh, and M.C. Teich. Quantum entanglement and the two-photon stokes parameters. *Optics Communications*, 201:93, 2002.

G.S. Agarwal. On the state of unpolarized radiation. *Lettere Al Nuovo Cimento*, 1(2):53, 1971.

A.P. Alodjants and S.M. Arakelian. Quantum phase measurements and non-classical polarization states of light. *Journal of Modern Optics*, 46(3): 475, 1999.

H.A. Bachor. *A guide to experiments in Quantum Optics*. Wiley-VCH, Weinheim, 1998.

G. Björk, J. Söderholm, A. Trifonov, P. Usachev, L.L. Sánchez-Soto, and A. Klimov. Applications of entangled-state interference. In S.N. Bagayev, editor, *ICONO 2001: Quantum and Atomic Optics, High-Precision Measurements in Optics, and Optical Information Processing*, volume 4750, pages 1–12, 2002.

G. Bjork, J. Söderholm, L.L. Sánchez-Soto, A. Klimov, I. Ghiu, P. Marian, and Marian T.A. Quantum degrees of polarization. *Optics Communications*, 283:4440, 2010.

Max Born and Emil Wolf. *Principles of Optics*. Cambridge University Press, 7th edition, 1959.

C. Caves and B. Schumaker. New formalism for two-photon quantum optics 1. quadrature phases and squeezed states. *Physical Review B*, 31:3068, 1985.

E. Collet. Stokes parameters for quantum systems. *American Journal of Physics*, 38(5):563, 1970.

G.M. D'Ariano, M.F. Sacchi, and P. Kumar. Universal homodyne tomography with a single local oscillator. *Physical Review A*, 61:013806, 1999.

P. Grangier. Quantum physics: Single photons stick together. *Nature*, 419: 577, 2002.

P. Grangier, B. Sanders, and J. Vuckovic. Special issue. focus on single photons on demand. *New Journal of Physics*, 6, 2004.

W. Greiner and B. Müller. *Quantum Mechanics : Symmetries*. Springer, Berlin, 2nd edition, 1994.

J. Jansky, A. Sibilia, M. Bertolotti, and Y. Yushin. Non-classical light in a linear coupler. *Journal of Modern Optics*, 35:1757, 1988.

A. Klimov, L.L. Sánchez-Soto, E.C. Yustas, J. Söderholm, and G. Björk. Distance-based degrees of polarization for a quantum field. *Physical Review A*, 72:033813, 2005.

A. Klimov, G. Björk, J. Söderholm, L.S. Madsen, M. Lassen, U.L. Andersen, J. Heersink, R. Dong, Ch. Marquardt, G. Leuchs, and L.L. Sánchez-Soto. Assesing the polarization of a quantum field from stokes fluctuations. *Physical Review Letters*, 105:153602, 2010.

D.N. Klyshko. Multiphoton interference and polarization effects. *Physics Letters A*, 163:349, 1992.

H. Kogelnik. *Guided-wave optoelectronics*. Springer-Verlag, Berlin, 1988.

P.G. Kwiat. Quantum information: an integrated light circuit. *Nature*, 453: 294, 2008.

J. Lehner, U. Leonhardt, and H. Paul. Unpolarized light: Classical and quantum states. *Physical Review A*, 53(4):2727, 1996.

J. Liñares and M.C. Nistal. Geometric phases in multidirectional electromagnetic coupling theory. *Physics Letters A*, 162:7, 1992.

J. Liñares and M.C. Nistal. Quantization of coupled modes propagation in integrated optical waveguides. *Journal of Modern Optics*, 50(5):781, 2003.

J. Liñares and M.C. Nistal. Multimode polarization degree of mixture optical states in integrated directional couplers. *Journal of Modern Optics*, 59: 61, 2012.

J. Liñares, J.E. Alvarellos, and G.C. Righini. Efficiency of modal coupling between graded-index optical waveguides. *Journal of Modern Optics*, 38: 2177, 1991.

J. Liñares, M.C. Nistal, and D. Barral. Quantization of coupled 1d vector modes in integrated photonic waveguides. *New Journal of Physics*, 10: 063023, 2008a.

J. Liñares, M.C. Nistal, D. Barral, V. Moreno, and C. Montero. Quantization of coupled waveguided modes progression in integrated photonic devices. In Giancarlo C. Righini, Seppo K. Honkanen, Lorenzo Pavesi, and Laurent Vivien, editors, *Proceedings of the SPIE Europe Photonics 2008*, volume 6996 of *Silicon Photonics and Photonic Integrated Circuits*, pages 69961R–69961R–12. S.P.I.E., 2008b.

J. Liñares, M.C. Nistal, D. Barral, and V. Moreno. Optical field-strength generalized polarization of two-mode single photon states. *European Journal of Physics*, 31:991, 2010.

J. Liñares, D. Barral, M.C. Nistal, and V. Moreno. Optical field-strength generalized polarization of multimode single photon states in integrated directional couplers. *Journal of Modern Optics*, 58(8):711, 2011a.

J. Liñares, M.C. Nistal, D. Barral, V. Moreno, C. Montero, and X. Prieto. Quantum integrated optics: theory and applications. *Optica Pura y Aplicada*, 44:241, 2011b.

J. Liñares, D. Barral, and M.C. Nistal. Spatial propagation of quantum light in nonlinear waveguiding devices: theory and applications. *Journal of Nonlinear Optical Physics and Materials*, 21:1250032, 2012.

A. Luis. Degree of polarization in quantum optics. *Physical Review A*, 66: 013806, 2002.

A. Luis. Polarization correlations in quantum optics. *Optics Communications*, 216:165, 2003.

A. Luis. Polarization distributions and degree of polarization for quantum gaussian light fields. *Optics Communications*, 273:173, 2007.

A. Luis and L.L. Sánchez-Soto. Quantum phase difference, phase measurements and stokes operators. In E. Wolf, editor, *Progress in Optics*, volume 41, page 421. Elsevier Science B.V., 2000.

A. Luks and V. Perinová. Quantum description of light propagation in dielectric media. In E. Wolf, editor, *Progress in Optics*, volume 43, chapter 4. Elsevier, Amsterdam, 2002.

A.I. Lvovsky and M.G. Raymer. Continuous-variable optical quantum state tomography. *Review of Modern Physics*, 81:299, 2009.

L. Mandel and E. Wolf. *Optical coherence and quantum optics*. Cambridge University Press, Cambridge, 1995.

V. Massida. Analytical calculation of a class of integrals containing exponential and trigonometric functions. *Mathematics and Computation*, 41: 555, 1983.

M. Orszag. *Quantum Optics*. Springer, Berlin, 2008.

A. Ourjoumtsev, F. Ferreyrol, R. Tualle-Brouri, and P. Grangier. Preparation of non-local superpositions of quasi-classical light states. *Nature Physics*, 5:189, 2009.

J. Perina. Quantum-statistical properties of a nonlinear asymmetric directional coupler. *Journal of Modern Optics*, 42(7):1517, 1995.

J. Perina and J. Perina Jr. Quantum statistics of nonlinear optical couplers. In E. Wolf, editor, *Progress in Optics*, volume 41, chapter 5. Elsevier, Amsterdam, 2000.

V. Perinová, A. Luks, and J. Krepelka. Linear coupling, loss and gain of counterpropagating beams. *Journal of Physics B: Atomic, Molecular and Optical Physics*, 39:2267, 2006.

A. Picozzi. Entropy and degree of polarization for nonlinear optical waves. *Optics Letters*, 29:1653, 2004.

A. Politi, M.J. Cryan, S. Yu, and J.L. O'Brien. Silica-on-silicon waveguide quantum circuits. *Science*, 320:646, 2008.

A. Politi, J.C.F. Matthews, M.G. Thompson, and J.L. O'Brien. Integrated quantum photonics. *IEEE Journal of Selected Topics in Quantum Electronics*, 15:1673, 2009.

J. Pollet, O. Méplan, and C. Cignoux. Elliptic eigenstates for the quantum harmonic oscillator. *Journal of Physics A: Mathematical and General*, 28: 7287, 1995.

H. Prakash and N. Chandra. Density operator of unpolarized radiation. *Physical Review A*, 4(2):796, 1971.

M.G. Raymer and A.C. Funk. Quantum-state tomography of two-mode light using generalized rotations in phase space. *Physical Review A*, 61: 015801, 1999.

P. Réfrégier and F. Goudail. Kullback relative entropy and characterization of partially polarized optical waves. *Journal of the Optical Society of America B*, 23:671, 2006.

L.L. Sánchez-Soto, J. Söderholm, E.C. Yustas, A. Klimov, and G. Björk. Degrees of polarization for a quantum field. *Journal of Physics: Conference Series*, 36:177, 2006.

L.L. Sánchez-Soto, A. Klimov, P. de la Hoz, and G. Leuchs. Quantum versus classical polarization states: when multipoles count. *Journal of Physics B: Atomic, Molecular and Optical Physics*, 46:104011, 2013.

W.P. Schleich. *Quantum optics in phase space*. Wiley-VCH, New York, 2001.

J. Söderholm, G. Björk, and A. Trifonov. Unpolarized light in quantum optics. *Optics and Spectroscopy*, 91(4):532, 2001.

G.G. Stokes. On the composition and resolution of streams of polarized light from different sources. *Transactions of the Cambridge Philosophical Society*, 9:399, 1852.

R. Tanás and S. Kielich. Quantum fluctuations of the stokes parameters of light propagating in a kerr medium. *Journal of Modern Optics*, 37:1935, 1990.

M.G. Thompson, A. Politi, J.C.F. Matthews, and J.L. O'Brien. Integrated waveguide circuits for optical quantum computing. *IET Circuits, Devices and Systems*, 5:94, 2011.

P. Usachev, J. Söderholm, G. Björk, and A. Trifonov. Experimental verification of differences between classical and quantum polarization properties. *Optics Communications*, 193:161, 2001.

W. Vogel. Field-strength probability distributions and higher-order squeezing. *Physical Review A*, 42:5754, 1990.

D. F. Walls and G. J. Milburn. *Quantum Optics*. Springer Verlag, Berlin, 1994.

W.Y. Yang, W. Cao, T.S. Chung, and J. Morris. *Applied numerical methods using Matlab*. Wiley, New York, 2005.

USC
UNIVERSIDADE
DE SANTIAGO
DE COMPOSTELA

CHAPTER

FIVE

DETECTION OF QUANTUM STATES OF LIGHT BASED ON INTEGRATED DIRECTIONAL COUPLERS

FINALLY, following the characterization approach shown in the previous chapter, we present the design and simulation of a measurement system of quantum states of light by means of integrated homodyne detection. This device is based on a directional coupler in an alternating $\Delta\beta$ configuration and two electro-optic phase shifters, which together are able to carry out any $SU(2)$ transformation giving us access to all statistical projections of the state, which allows its total or partial reconstruction, and therefore its characterization. Furthermore, this device can be nested, so its coverage can be extended to N-dimensional states, and it is robust to fabrication imperfections. To present this sketch, in section 1 we will perform an introduction to the homodyne detection approach, while in section 2 we will show different applications of this method in quantum optics. In section 3 we will present a brief introduction to this device and finally, in section P7, we present the published research article where the design and application to generalized polarization and characterization of quantum states via weak values measurement, are detailed.

5.1. Phase-sensitive detection

There are some different techniques to detect quantum states of light. But they can be divided in two big groups: *direct photocount* and *phase-sensitive* (or *coherent*) detection. The first approach gives information about the photon number distribution of the state which falls on the photodetector. In this way, we can characterize the *bunching/antibunching* of photoelectric detections, which tells us about the classical or quantum nature of the state, respectively [Mandel and Wolf, 1995]. However, this approach is not specifically sensitive to squeezing, but only to the antibunching which can also accur for non-squeezed states [Loudon and Knight, 1987]. As we

are interested in a measurement method for generalized polarization and it is related to confinement of the quantum state in the OFS space, and therefore on the quantum optical noise, it is necessary for us to use the second approach: the phase-sensitive detection. This scheme measures the field quadrature distributions of a given quantum state [Lvovsky and Raymer, 2008]. These techniques are usually referred as *homodyne* or *heterodyne detection* depending on the detuning of the analyzed frequencies [Loudon and Knight, 1987]. Here, we are going to focus on the homodyne scheme.

Assuming a single-mode quantum state to be measured given by the operator $\hat{a}_1$, this is mixed in a beam splitter (BS), or in general in a four-port unitary coupler like a directional coupler, with a strong coherent classical field $\hat{a}_2$ of amplitude β. The relation between the output modes $\hat{a}'$ and input modes $\hat{a}$ in the BS, is given by the following unitary SU(2) transformation [Welsch et al., 1999]:

$$\hat{a}'_\nu = \sum_{\nu'=1}^{2} U_{\nu\nu'}\,\hat{a}_{\nu'}, \tag{5.1.1}$$

where the unitarity of the transformation implies the following constraints on the elements of the scattering matrix $U_{\nu\nu'} = |U_{\nu\nu'}|e^{i\phi_{\nu\nu'}}$:

$$|U_{11}|^2 + |U_{12}|^2 = 1, \qquad |U_{11}| = |U_{22}|, \qquad |U_{12}| = |U_{21}|, \tag{5.1.2}$$

$$(\phi_{11} + \phi_{22}) - (\phi_{12} + \phi_{21}) = \pm\pi. \tag{5.1.3}$$

These relations ensure the CR are preserved after propagation. After passing through the BS, the intensity of every output mode (I'_1, I'_2) is measured by photodetectors. In the case of a balanced BS, the unitary scattering matrix can be written as follows:

$$U_{BS} = \begin{pmatrix} 1/\sqrt{2} & i/\sqrt{2} \\ i/\sqrt{2} & 1/\sqrt{2} \end{pmatrix}. \tag{5.1.4}$$

Therefore, the difference of photocurrents measured by the detectors is given by [Gerry and Knight, 2005]:

$$I'_1 - I'_2 \propto \langle \hat{n}'_1 - \hat{n}'_2 \rangle = \langle \hat{a}'^{\dagger}_1 \hat{a}'_1 - \hat{a}'^{\dagger}_2 \hat{a}'_2 \rangle = i\,\langle \hat{a}^{\dagger}_1 \hat{a}_2 - \hat{a}^{\dagger}_2 \hat{a}_1 \rangle. \tag{5.1.5}$$

Taking into account that $\hat{a}_1$ and $\hat{a}_2$ have the same frequency[1] and the input mode $\hat{a}_2$ is excited in a coherent state $|\beta e^{i\chi}\rangle$, so-called *local oscillator* (LO), we can write:

$$I'_1 - I'_2 \propto |\beta|\langle \hat{a}_1 e^{-i\theta} + \hat{a}^{\dagger}_1 e^{i\theta} \rangle = 2|\beta|\langle \hat{\mathcal{E}}_\theta \rangle, \tag{5.1.6}$$

[1] When there is a small detuning $\Delta\omega$ between the two modes, this is called heterodyne detection.

with $\theta = \chi + \pi/2$ and where we have used the definition of OFS operator given in chapter 3. So the photocurrent difference gives a measure of any quadrature of the signal field by only changing the phase of the LO as long as $|\beta|^2$ is large compared with the mean number of signal photons.

This approach can be readily extended to any finite dimension. For N mode detection the unitary transformation SU(2) (5.1.1) is generalized via an unitary SU(N+1) transformation given by:

$$\hat{a}'_\nu = \sum_{\nu'=1}^{N+1} U_{\nu\nu'}\,\hat{a}_{\nu'}, \tag{5.1.7}$$

which mixes the N modes and the LO. Every discrete dimensional unitary matrix can be carried out in a laboratory by means of beam splitters, phase shifters and mirrors as was shown in [Reck et al., 1994]. To clarify this, let us study, for instance, the case of two-mode detection. In this case we would have two stages: the first one would perform all the unitary transformations on the input state in the Hilbert subspace of two dimensions, and the second one would mix one of the outputs with the LO. In this way, equation (5.1.7) would be written as:

$$\begin{pmatrix} \hat{a}'_1 \\ \hat{a}'_2 \\ \hat{a}'_3 \end{pmatrix} = U \begin{pmatrix} \hat{a}_1 \\ \hat{a}_2 \\ \hat{a}_3 \end{pmatrix}, \tag{5.1.8}$$

where $(\hat{a}_1, \hat{a}_2)$ are the modes to be measured, $\hat{a}_3$ is the LO mode excited in the state $|\beta e^{i\chi}\rangle$ and the unitary matrix U is given by:

$$U = U_{BS}\,U_{\Theta,\Phi} = \begin{pmatrix} 1 & 0 & 0 \\ 0 & 1/\sqrt{2} & i/\sqrt{2} \\ 0 & i/\sqrt{2} & 1/\sqrt{2} \end{pmatrix} \begin{pmatrix} \cos\Theta & \sin\Theta\, e^{i\Phi} & 0 \\ -\sin\Theta & \cos\Theta\, e^{i\Phi} & 0 \\ 0 & 0 & 1 \end{pmatrix}, \tag{5.1.9}$$

where U is an unitary matrix with two variable parameters (Θ, Φ). Therefore, the difference of photocurrents $I'_2 - I'_3$ would give us the following combined quadrature [Raymer and Funk, 1999]:

$$\hat{\mathcal{E}}(\Theta, \Phi, \theta) = \cos\Theta\,\hat{\mathcal{E}}_1(\theta) + \sin\Theta\,\hat{\mathcal{E}}_2(\theta - \Phi)^2, \tag{5.1.10}$$

Therefore, measuring repeteadly $\hat{\mathcal{E}}$ for all possible combination of parameters (Θ, Φ, θ), we will have all the statistical projections $P(\mathcal{E}(\Theta, \Phi, \theta))$ of the quantum state we want to characterize. In § 5.3 (and § P7) we will show that the operation of the unitary matrix (5.1.9) can be accomplished by nesting electro-optic directional couplers and phase shifters in an integrated scheme.

[2] We have changed the notation for clarity: $\hat{\mathcal{E}}(\Theta, \Phi, \theta) \equiv \hat{\mathcal{E}}_{\Theta,\Phi,\theta}$.

5.2. Applications in quantum optics

It is well known that in order to measure any quantum state of finite Hilbert dimension, a set of linear transformations must be applied to generate a tomographically complete set of observables, known as *quorum*, whose statistical properties are measured. This is known as *quantum state tomography* (QST) and it enables us to extract all the information of the quantum state reconstructing the Wigner and other quasi-probability functions as well as the density operator in the quadrature, Fock, computational spaces and so on by means of repeated measurements of OFS distributions for different combinations of the parameters defining the unitary transformation (5.1.7), as was shown above for two-mode quantum states, and reconstruction algorithms like either inverse linear transform techniques or statistical inference [Lvovsky and Raymer, 2008].

The current concept of QST in terms of homodyne measurements, so-called *optical homodyne tomography* (OHT), was established in [Vogel and Risken, 1989], where the relation between quasi-probability distributions and probability distributions of the rotated quadrature was established (see § 3.2). This theory was followed by first experiments determining the quantum state of light fields [Breitenbach et al., 1997, Smithey et al., 1993]. Furthermore, the density matrices can be as well obtained as two-fold Fourier transforms of OFS distributions [Kühn et al., 1994] and, in the case of reconstructing photon number statistics, phase-averaged OFS distributions are enough [Munroe et al., 1995]. Likewise, more accurate reconstruction algorithms have been developed during the last years beyond the inverse Radon transformation: sampling functions, maximum-likelihood reconstruction and maximum-entropy reconstruction [Lvovsky and Raymer, 2008, Welsch et al., 1999]. The technology boom of the present century has lead to the generation and characterization by OHT of a plethora of new quantum states in bulk optics: two-mode squeezed states, one and two photons Fock states, optical qubits, Schrödinger cats and *kittens*, photon added states and so on [Lvovsky and Raymer, 2008]. In the context of integrated optics, this same year has been published the first demonstration of continuous-variable entanglement and measurement on-chip [Masada et al., 2015]. Generation of these states and coherent detection is the basis of *continuous-variable quantum computation* (CVQC) [Braunstein and van Loock, 2005]. Furthermore, in the context of polarization, it has been shown recently the reconstruction of the Stokes fluctuations on the Poincaré sphere for a squeezed vacuum state via OHT [Klimov et al., 2010].

On the other hand, in the usual single-mode homodyne detection, QST is carried out by means of modulation of the LO phase which turns out into a rotation in the phase space [Smithey et al., 1993]. When two modes are involved, three parameters are necessary to obtain the quorum, as was shown in equation (5.1.10). Some techniques have been developed to perform this

experimentally, as the *dual-mode-LO* [Opatrny et al., 1997, Raymer et al., 1996] and the *generalized rotations in phase space* (GRIPS) [Raymer and Funk, 1999], where the set of transformations is applied either to a two-mode LO or to the two-mode signal before mixing in a balanced homodyne detector (BHD), respectively. Multimode QST is also possible via equation (5.1.7), but difficult to carry out with bulk optics due to the lack of scalability.

Another way of quantum state reconstruction is based on weak values [Aharonov et al., 1988, Lundeen et al., 2011], where measurement is carried out by imposing postselection of the quantum state and weak interaction between the measurement apparatus and the state itself, leaving the state of interest largely undisturbed. Recently, a weak values scheme was proposed to reconstruct the quantum state of an optical single-mode field [Fischbach and Freyberger, 2012]. This implementation is based on a weak beam splitter interaction between two single-mode quantum states, the one to be measured and the other, a gaussian state, acting as a meter. Afterwards, homodyne detection is performed at each output and, from OFS momentum readings at one output, OFS expectation values at the other output are postselected. This approach enables reconstructing directly both the amplitude and phase of the quantum state.

5.3. Integrated homodyne detection

As we have introduced in the previous chapter, the properties of N - dimensional quantum states propagating in quantum circuits have been studied in the optical field-strength $\mathcal{E}$. In this space, the quantum wavefunction presents a generalized polarization which can be quantifed by a degree of polarization and measured by homodyne detection techniques as well [Barral et al., 2013, Liñares et al., 2010, 2011]. In this context we introduce an integrated device based on an electro-optic directional coupler which performs SU(2) transformations (5.1.9) based on the GRIPS scheme proposed in [Raymer and Funk, 1999], and allows fully integrated OHT and weak values reconstruction of quantum states excited in two or N spatial modes. Other schemes based on Mach-Zehnder interferometers have been introduced to accomplish unitary transformations [Shadbolt et al., 2012]. However, as will be shown in § P7, the performance of our design is better due to its ability to reduce the significance of fabrication errors of the couplers.

5.3.1. The SU(2) integrated device

The device proposed is sketched in Figure 5.3.1. The initial and final stages of the device are electro-optic phase shifters, while the central part is made up of a DC of length L with two sections of reversed electrodes

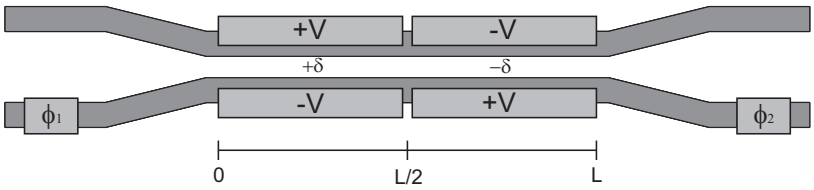

Figure 5.3.1: Sketch of the manipulation system proposed.

over it, an alternating $\Delta\beta$ configuration [Kogelnik and Schmidt, 1976]. The DC is composed of two asynchronous waveguides where optical modes 1 and 2 propagate with propagation constants β_1 and β_2, respectively. $L/2$ are the lengths of the two reversed electrodes, κ is the coupling coefficient of the DC, $\Delta\beta(V) = (\beta_1 - \beta_2) \equiv 2\delta$ is the propagation constant mismatch between the waveguides to be modulated electro-optically by the voltage V [Yariv, 1975] and $\phi_1(V')$, $\phi_2(V'')$ are input and output electro-optic phase shifters controlled by two additional electrodes with voltages V' and V'', respectively. Solving Heisenberg equations of the total system for a pair of reversed input-output phase shifts, where $\phi_1 = -\phi_2$, we obtain the following transformation matrix:

$$U(\Theta, \Phi) = \begin{pmatrix} \cos(\Theta/2) & \sin(\Theta/2)e^{-i\Phi} \\ -\sin(\Theta/2)e^{i\Phi} & \cos(\Theta/2) \end{pmatrix}, \tag{5.3.11}$$

where $\cos(\Theta/2) = u^2 - v^2$, $\sin(\Theta/2) = 2uv$ and $\Phi = \phi_1 - \theta - \pi/2$, and where u, v and θ are the parameters of the $\Delta\beta$ coupler, defined as:

$$u = [\cos^2\beta_r L + \frac{\delta^2}{\beta_r^2}\sin^2\beta_r L]^{1/2}, \quad v = \frac{|\kappa|}{\beta_r}\sin\beta_r L, \quad \theta = \operatorname{atan}(\frac{\delta}{\beta_r}\tan\beta_r L), \tag{5.3.12}$$

with $\beta_r = [\kappa^2 + \delta^2]^{1/2}$. Therefore, the transformation given by equation (5.3.11) is an effective SU(2) unitary up to a global phase without physical significance[3], and a rotation SO(2,R) if $\Phi = n\pi$ is chosen. Then, to get an arbitrary unitary transformation or equally, to select Θ and Φ, firstly δ is set by means of the electrodes voltage V to choose the desired Θ. This assigns θ a value used to adjust the electrode voltages of the phase shifters $\phi_{1,2}$, and obtain the sought value of Φ. Likewise, any N-mode quantum state can be manipulated by means of nesting an array of devices like that depicted in Figure 5.3.1., performing SU(N) transformations (5.1.8). Moreover, this design reduce the significance of fabrication errors of the couplers, which leads to complex values in (5.3.11) unable to be compensated in other configurations [Metcalf et al., 2014, Shadbolt et al., 2012], fact which may be very important in networks made up of a large number of DCs, where the

[3]Basically, we can reach any point on the Poincaré sphere, but performing rotations only in one direction.

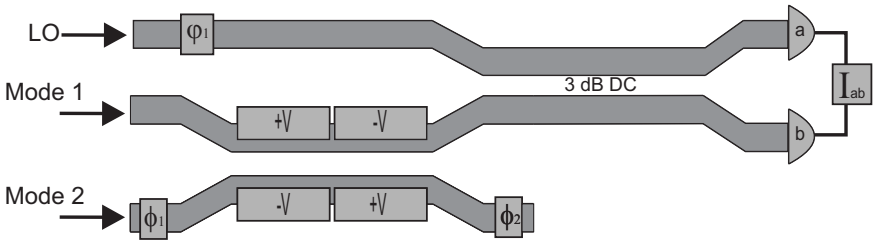

Figure 5.3.2: Sketch of the integrated homodyne detection system proposed.

deviation from the ideal operation can be more pronounced. A more complete review of the operation of the device is shown in § P7.

5.3.2. Application to two-mode homodyne detection

Now, we show the application of the SU(2)-device we are interested in: quantum homodyne detection to measure OFS probability distributions. However, it is important to outline this device can be useful in other areas where manipulation and measurement of quantum states are required as quantum computation, communications, sensing and so on. As outlined above, from the QST is known that in order to measure a quantum state, a set of linear transformations has to be carried out to obtain a *quorum*, whose statistical properties are measured [Raymer and Funk, 1999]. As was introduced above, in the case of two spatial modes as those present in IPDs, GRIPS is suitable to be accomplished. In this way we propose the circuit depicted in Figure 5.3.2. There, we can see how our SU(2) device is placed at one of the arms of an integrated BHD, performing transformations on the two-mode signal before mixing. In our case, in order to get the OFS joint probability distribution, we need to perform rotations in the $\mathcal{E}_1\mathcal{E}_2$-space. Hence, applying the transformation (5.3.11) with $\Phi = n\pi$ on the input state, we obtain the following rotation:

$$\begin{pmatrix} \hat{\mathcal{E}}_3 \\ \hat{\mathcal{E}}_4 \end{pmatrix} = \begin{pmatrix} \cos(\Theta/2) & (-1)^n \sin(\Theta/2) \\ (-1)^{n+1} \sin(\Theta/2) & \cos(\Theta/2) \end{pmatrix} \begin{pmatrix} \hat{\mathcal{E}}_1 \\ \hat{\mathcal{E}}_2 \end{pmatrix}, \tag{5.3.13}$$

equivaltent to the unitary transformation $\hat{U}_R(\Theta) = e^{i\Theta\hat{\sigma}_y/2}$ and where $\hat{\sigma}_y$ is the usual SU(2) Pauli operator equivalent to the Stokes operator $\hat{s}_2$. The output mode 3 is sent to the BHD right after, where is mixed with a strong local oscilator excited in a coherent state $|\alpha\rangle$, with $\alpha = |\alpha|e^{i\psi}$, in the same spatial mode. The output mode 4 can be used for other purposes or, in the case of a N-mode quantum state, it can be the input to the next measurement unit [Raymer and Funk, 1999]. In the BHD, the LO phase ψ performs rotations in the phase space of the output mode 3, $\mathcal{E}_3\mathcal{P}_3$, given by the unitary operator $\hat{U}_{LO}(\psi) = e^{-i\Psi\hat{n}_{LO}}$. From the difference of the a and b

photodetectors readings we can obtain statistical information of the state like the moments of the distribution[Loudon and Knight, 1987]. However, for a complete characterization of the generalized polarization of the state we have to obtain the total probability distribution $P(\mathcal{E}_1, \mathcal{E}_2)$. This can be accomplished performing sampling to buid up a histogram for every rotation angle Θ and LO phase ψ which gives us an approximate probability distribution of obtaining a value of the field-strength $\mathcal{E}_3$:

$$P(\mathcal{E}_3(\Theta, \psi)) = \langle \mathcal{E}_1, \mathcal{E}_2 | \hat{U}^\dagger \, \hat{\rho} \, \hat{U} | \mathcal{E}_1, \mathcal{E}_2 \rangle, \tag{5.3.14}$$

where $\hat{\rho}$ is the density operator which characterizes the input quantum state, $\hat{\rho} = |\Psi\rangle\langle\Psi|$ in the case of a pure state, and $\hat{U} = \hat{U}_{LO}(\psi)\,\hat{U}_R(\Theta)$ the unitary transform performed by the entire detection system.

Likewise, the time-dependence of the quantum state leads to different methods of homodyne measurement. If we are dealing with non-stationary quantum states like, for instance, coherent states, we are interested in the accumulated probability distribution over one temporal cycle $\langle P(\mathcal{E}_1, \mathcal{E}_2)\rangle_t$. This provides us with three methods of sampling this built-up quantum probability distribution:

- *Standard homodyne detection*: the time (phase ψ) is set discretely and measurement in any rotated field-strength $\mathcal{E}_3(\Theta)$ is accomplished, covering all the $\mathcal{E}_1\mathcal{E}_2$-space and a temporal cycle.

- *Phase-random homodyne detection*: we measure at random times (phases ψ) on the discretely-varied OFS value $\mathcal{E}_3(\Theta)$, giving us time-weighted average of the probability $\langle P(\mathcal{E}_3(\Theta)\rangle_t$.

- *Fully-random measurement*: this approach lies in randomize both ψ and Θ, leading to high simplification of the measurement procedure.

The discrete nature of the variation of the two parameters and the same sampling process make this procedure inherentely approximated, such that enough resolution has to be reached to obtain a satisfactory outcome. Likewise, in the case of a stationary state, like a Fock state, the LO phase Ψ is needless, so it could be keep constant while varying Θ.

We show an example of this method in Figure 5.3.3. We have simulated standard homodyne detection of a coherent state with linear-type generalized polarization given by $|L\rangle = |\alpha_1\rangle|\alpha_2\rangle$, with $|\alpha_1| = 5$ and $|\alpha_2| = 0$. This simulation has been carried out creating 10^5 random points by a Monte Carlo method [Martinez and Martinez, 2002]. The outcome obtained performing the experimental procedure explained above would be similar to this. In Figure 5.3.3 (lower Figure) we show the probability distribution reconstructed from the data sampled in Figure 5.3.3 (upper Figure). For more details, see § P7.

Finally , it is important to outline that this scheme is suitable to be generalized to N-mode input states, as the unused output of the directional coupler can be mixed with a third mode and measured by another BHD as well, and so on and so forth up to the N-mode, performing in this way the transformation (5.1.7). Furthermore, this scheme could be used to obtain the Wigner function by means of (5.3.11), repeated measurements of $P(\mathcal{E}_3(\Theta, \psi, \Phi))$ for different combinations of the parameters (Θ, ψ, Φ) and reconstruction algorithms as inverse linear transform techniques or statistical inference [Lvovsky and Raymer, 2008]. Additionally, using phase-averaged distributions, photon number statistics of any input N-mode state can be reconstructed following [Munroe et al., 1995]. Likewise, this device can be also used to get full characterization of the quantum wavefunction via weak measurements. Following this approach simultaneous reconstruction of amplitude and phase of quantum states is accomplished [Fischbach and Freyberger, 2012]. The application of this scheme to two-mode IPDs is sketched in § P7 as well.

oOo

The following section is devoted to present the published research work about on-chip detection based on electro-optic DCs. In this article we review the literature on the manipulation and detection of quantum states with integrated devices and perform a detailed analysis of the design of an IPD based on a EO $\Delta\beta$-DC able to accomplish SU(2) transformations and SU(N) by nesting. Likewise, we compare its operation with that of current designs found in literature, outperforming those. Finally we show two applications of this device: reconstruction of both the optical field-strength quantum probability distribution, via spatial two-mode homodyne detection, and the full optical field-strength wavefunction, by means of a weak values scheme.

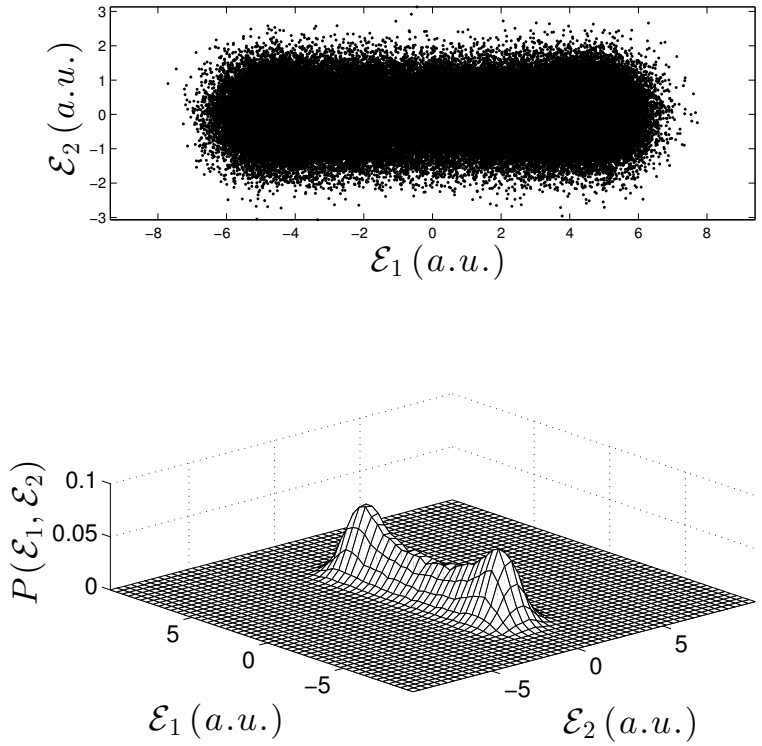

Figure 5.3.3: Simulation of the homodyne measurement and reconstruction of a two-mode coherent state linearly polarized.

P7. DETECTION OF TWO-MODE SPATIAL QUANTUM STATES OF LIGHT BY ELECTRO-OPTIC INTEGRATED DIRECTIONAL COUPLERS

JOURNAL OF THE OPTICAL SOCIETY OF AMERICA B
VOL. 32 NO. 8 PAGES 1165-1173
doi: 101364/JOSAB.32.001165

PUBLISHED 19 MAY 2015

BY DAVID BARRAL[1], MARK G. THOMPSON[2] & JESÚS LIÑARES[1]

[1] UNIVERSIDADE DE SANTIAGO DE COMPOSTELA
[2] UNIVERSITY OF BRISTOL

Abstract: *We study both manipulation and detection of two-mode spatial quantum states of light by means of a reconfigurable integrated device built in an electro-optical material in a Kolgelnik-Schmidt configuration, which provides higher error tolerance to fabrication defects and larger integration density than other current schemes. SU(2) transformations are implemented on guided spatial modes in such a way that reconstruction of both the optical field-strength quantum probability distribution, via spatial two-mode homodyne detection, and the full optical field-strength wavefunction, by means of weak values, are carried out. This approach can easily be extended to spatial N-mode input quantum states. Apart from its usefulness to characterize optical quantum states, it is also emphasized its application to the measurement of the so-called generalized quantum polarization.*

P7.1. Introduction

In the last years great attention has been paid on the capabilities of light spatial modes in quantum mechanics. The technology based on them, integrated photonics, has lead to multiple new approaches on quantum communication, computation and sensing with huge success. These works are based on the processing of encoded quantum states of light in integrated waveguides, like single photons in a discrete space or squeezed light in a continuous-variable space, and measured by single-photon detectors or homodyne detection schemes, respectively [O'Brien et al., 2009].

The two main features for which integrated optics circuits are interesting to quantum information processing (QIP) are the sub-wavelength stability, which enables high-visibility quantum interference, and the great miniaturization they show with respect to bulk optics analogs, providing scalability [Politi et al., 2008]. Likewise, the optical properties of the materials which make up the waveguides, are used for generating quantum states on chip, via their nonlinear features, manipulating them by means of their thermo-optic and electro-optic properties, among others, and even detecting these quantum states.

As QIP technologies grow, quantum circuits become more complex and high-fidelity active control turns into an essential feature. Since the first demonstrations of quantum interference control based on the thermo-optic effect in optical waveguides [Matthews et al., 2009, Smith et al., 2009], this approach has been extensively adopted in Silicon-based (Si) quantum circuits with notable success [Bonneau et al., 2012a, Metcalf et al., 2014, Shadbolt et al., 2012, Silverstone et al., 2014]. Besides, quantum interference has also been shown recently by means of strain-optic based phase controllers in Silica (SiO_2) [Humphreys et al., 2014]. The other main branch, electro-optic based quantum circuits, exhibits very promising attributes as well. Lithium Niobate ($LiNbO_3$) photonic circuits have demonstrated efficient generation of entangled photons and fast control on chip [Jin et al., 2014, Martin et al., 2012], even on both polarization and path degrees of freeedom [Bonneau et al., 2012b], and storage as a quantum memory [Saglamyurek et al., 2011]. Additionally, Gallium Arsenide (GaAs) is another high - performance material capable to generate [Santori et al., 2002], manipulate [Wang et al., 2014] and measure [Sahin et al., 2015] single photons in photonic circuits. These features position electro-optic materials in a pre - eminent place for future quantum photonics technologies, where high integration and fast and precise modulation will be required.

Both the processing and measuring of quantum states, like those carried out in the works presented above, are based on unitary transformations, since they leave all physical predictions of quantum mechanics invariant. When we are dealing with qubits, they are accomplished as rotations in the Bloch sphere like in discete-variable quantum computation

(DVQC) [Nielsen and Chuang, 2010]. Likewise, in the case of looking for full characterization of a quantum state, they appear as rotations in the phase space. This is known as quantum state tomography (QST) and is based on homodyne detection [Lvovsky and Raymer, 2008]. This technique enables us to extract all the information of the quantum state reconstructing the Wigner function and the density operator in the quadrature, Fock, computational spaces and so on [Opatrny et al., 1997, Raymer et al., 1996, Shadbolt et al., 2012, Smithey et al., 1993]. Another way of quantum state reconstruction is based on weak values [Aharonov et al., 1988, Lundeen et al., 2011], where measurement is carried out by imposing postselection of the quantum state and weak interaction between the measurement apparatus and the state itself, leaving the state of interest largely undisturbed. In a similar way, properties of N-dimensional quantum states propagating in quantum circuits have been studied in the optical field-strength $\mathcal{E}$. In this space, the quantum wavefunction presents a generalized polarization which can be quantifed by a degree of polarization and measured by homodyne detection techniques as well [Barral et al., 2013, Liñares et al., 2011, Luis and Sanz, 2013]. Additionally, coherent detection is also carried out in continuous-variable quantum computation (CVQC) [Braunstein and van Loock, 2005].

As manipulation and characterization of quantum states of light in integrated photonics is a very active field of research by all the aforementioned, we introduce a reconfigurable integrated device capable to carry out SU(2) and SO(2,R) operations based on the Kogelnik-Schmidt scheme for electro-optic directional couplers (DC) [Kogelnik and Schmidt, 1976]. The advantages of this proposal are on one hand fast modulation, based on the electro-optic nature of the material, and on the other hand higher error tolerance to fabrication defects and larger integration density than other current schemes due to the design of the device. Its architecture enables carrying out both SU(2) transformations and fabrication defects correction simultaneously, as well as the number of elements is less than in other proposals. All this is a very important fact because as the complexity and number of elements of a photonic circuit network increase, the effect of imperfections in its operation becomes more problematic. Moreover, the integrated nature of our scheme gives access to bigger dimension quantum states by means of nesting. In addition, we propose two original applications: firstly, the measurement and characterization of spatial quantum states of light by means of optical-field strength homodyne detection and secondly, two-dimensional wavefunction reconstruction by means of weak measurements. However, this device can be also applied in QST, DVQC, CVQC or any other task where orthogonal or unitary operations are necessary.

Briefly, the paper is organized as follows. In Section 2 we present the formalism of propagation of quantum states of light in integrated devices

based on the Momentum operator and introduce the optical field-strength representation. In Section 3 we sketch a reconfigurable directional coupler as a device which carries out SU(2) and SO(2,R) transformations in two-mode input quantum states and as a component of a SU(N) / SO(N,R) device, and we compare its performance with that of other current schemes. In Section 4 we focus on possible applications of this device. In the first place we use this device as part of an homodyne detector for optical-field strength measurements of quantum light, and next we apply it to weak measurements of a two-dimensional wavefunction. Finally a summary is presented.

P7.2. Propagation of quantum light in integrated waveguides

It is well-known that the generator of spatial propagation in quantum mechanics is the dynamical Momentum operator $\hat{M}$ [Luks and Perinová, 2002]. In an integrated photonic device composed by N coupled linear single-mode homogeneous waveguides it is given by [Liñares et al., 2008]:

$$\hat{M} = \sum_{\sigma=1}^{N} \hbar\, \tilde{\beta}_\sigma\, \hat{a}_\sigma^\dagger \hat{a}_\sigma + \sum_{\sigma<\sigma'} \{\hbar\, \kappa_{\sigma,\sigma'}\, \hat{a}_\sigma \hat{a}_{\sigma'}^\dagger + \text{h.c.}\}, \tag{P7.1}$$

where $\tilde{\beta}_\sigma = \beta_\sigma + \kappa_{\sigma,\sigma}$, β_σ is the propagation constant of the σ-mode, where σ stands for the modal numbers ν, μ in each transverse direction, $\kappa_{\sigma,\sigma}$ is the self-coupling coefficient, $\kappa_{\sigma,\sigma'}$, where $\sigma \neq \sigma'$, the cross-coupling coefficient, and h.c. stands for hermitian conjugate. $\hat{a}_\sigma$ ($\hat{a}_\sigma^\dagger$) is the usual spatial absorption (emission) operator fulfilling the equal space commutation relation,

$$[\hat{a}_\sigma(z), \hat{a}_{\sigma'}^\dagger(z)] = \delta_{\sigma,\sigma'}, \tag{P7.2}$$

and Heisenberg's equations which describe the propagation of quantum states of light, given by:

$$\frac{d\hat{a}_\sigma}{dz} = \frac{i}{\hbar}[\hat{a}_\sigma, \hat{M}_\sigma]. \tag{P7.3}$$

These operators are central in quantum optics because their eigenstates are the coherent states $|\alpha_\sigma\rangle$. Moreover, from these operators we build the number operator $\hat{n}_\sigma = \hat{a}_\sigma^\dagger \hat{a}_\sigma$, with the Fock states $|n_\sigma\rangle$ as eigenstates, or the optical field-strength operator $\hat{\mathcal{E}}_\sigma = (\hat{a}_\sigma + \hat{a}_\sigma^\dagger)/2$ fulfilling $\hat{\mathcal{E}}_\sigma|\mathcal{E}_\sigma\rangle = \mathcal{E}_\sigma|\mathcal{E}_\sigma\rangle$, with $|\mathcal{E}_\sigma\rangle$ the optical field states, among many others. In particular these operators are very important because any quantum state can be expressed as linear combinations of their eigenstates. Thus, different problems or applications in quantum optics are better suited to different spaces, as the Fock basis for DVQC [Politi et al., 2008] or the optical field-strength basis for the study of quantum polarization [Liñares et al., 2011]. In this work we

will center our attention to this last space since it is the natural one for the problem of homodyne detection, though our approach could work in any of the above-mentioned representations.

Any multimode quantum state of light $|L\rangle$ can be written as a superposition of eigenstates $|\mathcal{E}_1, ..., \mathcal{E}_N\rangle$ of the optical field-strength operators $\hat{\mathcal{E}}_\sigma$,

$$|L\rangle = \int \langle \mathcal{E}_1, ..., \mathcal{E}_N | L\rangle |\mathcal{E}_1, ..., \mathcal{E}_N\rangle \, d\mathcal{E}_1 ... d\mathcal{E}_N, \tag{P7.4}$$

with $\langle \mathcal{E}_1, ..., \mathcal{E}_N | L\rangle \equiv \Psi(\mathcal{E}_1, ..., \mathcal{E}_N) = |\Psi(\mathcal{E}_1, ..., \mathcal{E}_N)| \, e^{i\,\varphi(\mathcal{E}_1,...,\mathcal{E}_N)}$ the complex probability amplitude or wavefunction in the optical field-strength domain. Hence the probability distribution on the N-dimensional optical field-strength space $\boldsymbol{\mathcal{E}} \equiv (\mathcal{E}_1, ..., \mathcal{E}_N)$, is given by:

$$P(\mathcal{E}_1, ..., \mathcal{E}_N) = |\langle \mathcal{E}_1, ..., \mathcal{E}_N | L\rangle|^2 \equiv |\Psi(\mathcal{E}_1, ..., \mathcal{E}_N)|^2. \tag{P7.5}$$

The shape of these probability distributions is directly related to the generalized polarization degree of the quantum state analyzed, that is, to the confinement properties of its probability distribution in the optical field-strength space [Barral et al., 2013, Liñares et al., 2011]. Alternatively, some problems are better suited to be tackled in the conjugate quadrature, the canonical optical momentum $\mathcal{P}$, fulfilling:

$$[\hat{\mathcal{E}}_\sigma(z), \hat{\mathcal{P}}_{\sigma'}(z)] = i\delta_{\sigma,\sigma'}/2. \tag{P7.6}$$

The Fourier transform relates the complex wave function in the optical field-strength and optical momentum domains. Besides, the propagation of these complex probability amplitudes are suitable to be worked out by means of an spatial propagator [Liñares et al., 2012], which simplifies the calculation in some problems.

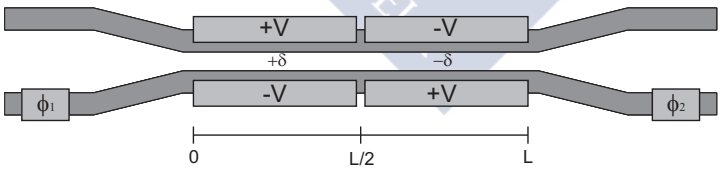

Figure P7.1: Sketch of the device proposed.

P7.3. Reconfigurable directional couplers

As was commented above, high integration density, fidelity and fast control are main goals in future quantum photonic devices. On one hand we have Silicon on insulator technology (SOI), which has exploited the high refractive index contrast and large thermo-optic coefficient of Silicon, demonstrating good performance in QIP [Bonneau et al., 2012a, Metcalf

et al., 2014, Shadbolt et al., 2012, Silverstone et al., 2014]. The main drawback of these devices is a typical length of several hundred micrometers, as they suffer from large power dissipation and therefore thermal crosstalk. Fast modulation can be obtained by means of integrated forward-biased pin-junctions or reverse-biased pn-junctions into the SOI waveguide, but suffer from high energy cost and low phase control efficiency, respectively [Pfeifle et al., 2012]. On the other hand we have the electro-optic-based technology, as $LiNbO_3$ and $GaAs$ photonics. High bandwidths, precise control and integration density can be obtained with this technology. Electro-optic efficiency and bias voltage drift were some of the problems these materials showed in the past, but via engineered solutions they present nowadays an excellent behaviour [Walker and Heaton, 2012, Wooten et al., 2000], and they are making their way in QIP [Bonneau et al., 2012b, Jin et al., 2014, Martin et al., 2012, Saglamyurek et al., 2011, Sahin et al., 2015, Santori et al., 2002, Wang et al., 2014].

The advent of this technology and the need of active control on quantum states for manipulation and measurement, leads us to propose a quantum photonic device which enables reconfigurable SU(2) and SO(2,R) transformations based on a directional coupler with two-section reversed electrodes, that is, an alternating $\Delta\beta$-coupler or Kogelnik-Schmidt scheme [Kogelnik and Schmidt, 1976], together with two electro-optic phase shifters. To our knowledge this is the first report of an electro-optic reconfigurable circuit which performs any unitary operation on spatial modes of quantum light, as previous works dealt only with control of the path photons take [Jin et al., 2014, Martin et al., 2012]. In the case of polarization-encoded quantum light, a reconfigurable unitary device has been previously described [Bonneau et al., 2012b]. We present below the scheme of the device proposed.

The device

It is known that unitarity is a restriction on the allowed operations in quantum mechanics [Nielsen and Chuang, 2010]. Any discrete unitary transformation of a two-mode input state, that is an U(2) transformation, can be accomplished experimentally in bulk optics by means of a beam splitter with variable reflectivity and a phase shifter at one output port or, alternatively, substituting the beam splitter by a Mach-Zehnder interferometer [Reck et al., 1994]. In integrated photonics this last approach has been recently shown using two phase shifters and two passive 3dB DCs [Shadbolt et al., 2012]. Here we adopt the first scheme above introduced by means of an electro-optic DC.

Our device is depicted in Figure 1. The initial and final stages of the device are electro-optic phase shifters, meanwhile the central part is made up of a DC of length L with two sections of reversed electrodes over it [Kogelnik and Schmidt, 1976]. The DC is composed of two asynchronous

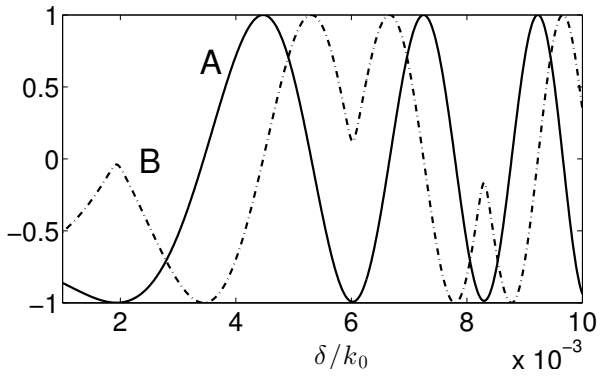

Figure P7.2: Values of A (solid line) and B (dash-dot line) versus δ/k_0 for a directional coupler with parameters $\kappa = 0.1 k_0\, m^{-1}$, $L = 2mm$ and wavelength $\lambda = 650nm$.

waveguides where TE polarized light propagates. Optical modes 1 and 2 propagate in the device with propagation constants β_1 and β_2, respectively. $L/2$ are the lengths of the two reversed electrodes, κ is the coupling coefficient of the DC, $\Delta\beta(V) = (\beta_1 - \beta_2) \equiv 2\delta$ is the propagation constant mismatch between the waveguides to be modulated electro-optically by the voltage V [Yariv, 1975] and $\phi_1(V')$, $\phi_2(V'')$ are input and output electro-optic phase shifts controlled by two additional electrodes with voltages V' and V'', respectively. Solving Heisenberg's equations (P7.3) after applying the Momentum operator which describes this system (P7.1), we obtain the following transformation performed by the device:

$$M(\delta, \phi_1, \phi_2) = \begin{pmatrix} A(\delta) & iB(\delta)\, e^{i(\theta+\phi_2)} \\ iB(\delta)\, e^{-i(\theta-\phi_1)} & A(\delta)\, e^{i(\phi_1+\phi_2)} \end{pmatrix}, \tag{P7.7}$$

where $A = u^2 - v^2$, $B = 2uv$, and the functions u, v and θ:

$$u = [\cos^2\beta_r L + \frac{\delta^2}{\beta_r^2}\sin^2\beta_r L]^{1/2},\ v = \frac{|\kappa|}{\beta_r}\sin\beta_r L, \tag{P7.8}$$

$$\theta = \text{atan}(\frac{\delta}{\beta_r}\tan\beta_r L), \tag{P7.9}$$

with $\beta_r = [\kappa^2 + \delta^2]^{1/2}$ and where $u^2 + v^2 = 1$. In Figure 2 we plot the functions A and B for different values of δ/k_0, with k_0 the propagation constant in vacuum for a given wavelength λ. These functions differ from the cosine and sine at some values, for instance at $\delta/k_0 \approx 6.10^{-3}$ in Figure 2, and their rotation speed increases with δ. To perform the rotation we only need angles between 0 and $\pi/2$, so we can thoroughfully choose a range of values of δ/k_0 where A and B mimic the cosine and sine functions, respectively. The change in the velocity of rotation does not represent a problem in the experimental regime as the values of δ are chosen from discrete equally

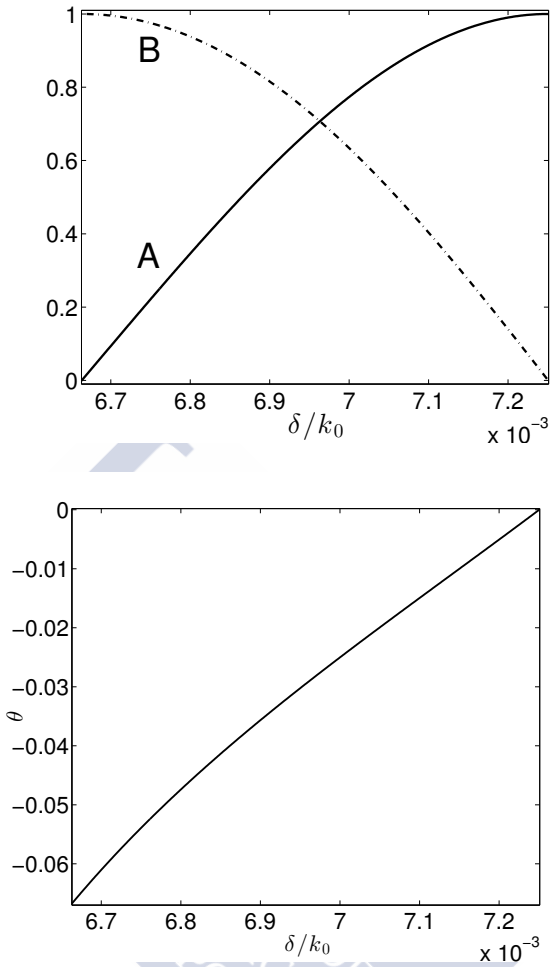

Figure P7.3: Values of A (solid line, upper figure), B (dash-dot line, upper figure) and θ (lower figure) versus δ/k_0 for a directional coupler with parameters $\kappa = 0.1k_0\,m^{-1}$, $L = 2mm$ and wavelength $\lambda = 650nm$.

separated values of A and B preselected by the user. The phase shifters ϕ_1 and ϕ_2 can be adjusted in different ways to accomplish the desired operation. Choosing the next simple way:

$$\phi_1 = \Phi + \theta + \pi/2 = -\phi_2, \tag{P7.10}$$

we obtain the following transformation in equation (P7.7):

$$M(\delta, \Phi) = \begin{pmatrix} A(\delta) & B(\delta)e^{-i\Phi} \\ -B(\delta)e^{i\Phi} & A(\delta) \end{pmatrix}. \tag{P7.11}$$

For the sake of clarity, note that if we take $u = \cos(\Theta(\delta)/4)$ and $v = \sin(\Theta(\delta)/4)$, we can rewrite A and B as:

$$A = \cos(\Theta(\delta)/2), \quad B = \sin(\Theta(\delta)/2). \tag{P7.12}$$

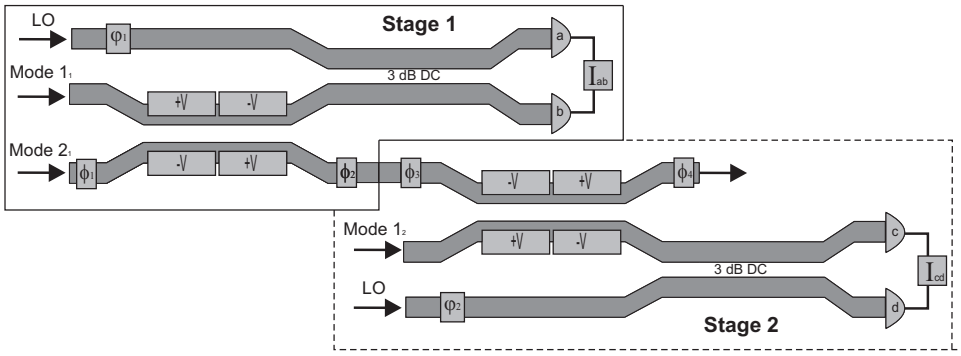

Figure P7.4: Homodyne detection scheme for measurement of generalized polarization of a three-mode input quantum state of light composed by two measurement units, stages 1 and 2. Looking at stage 1 (solid line), 1_1 and 2_1 modes are sent to the Kogelnik-Schmidt coupler where rotations in the field-strength space $\mathcal{E}$ are performed. The upper output mode is then mixed in a BHD with a LO-mode. The lower ouput mode acts as the upper input mode (2_2) of the Kogelnik-Schmidt coupler in the next stage (dashed line), where it is mixed with mode 1_2. The free output of this coupler would act as input in the next stage and so on $N-1$ times for N modes.

Hence, the transformation given by equation (P7.11) is an effective SU(2) unitary up to a global phase without physical significance, and a rotation SO(2,R) if $\Phi = n\pi$ is chosen. Then, to get an arbitrary unitary transformation or equally, to select Θ and Φ, firstly δ is set by means of the electrodes voltage V to choose the desired Θ. This assigns θ a value (P7.9) used in equations (P7.10) to adjust the electrode voltages of the phase shifters $\phi_{1,2}$, and obtain the sought value of Φ. All these adjustments would be controlled continously by a computer. In Figure 3 we show the values of A, B (upper Figure) and θ (lower Figure), respectively, versus δ/k_0 for a bandwith δ completing a rotation.

On the other hand, any N-mode quantum state can be manipulated and measured by means of nesting an array of devices like that depicted in Figure 1. U(N) transformations can be carried out by means of succesive U(2) operations on two-dimensional subspaces leaving an $(N-2)$-dimensional subspace unchanged, with $N > 2$ [Reck et al., 1994]. We can carry out this control on a computational basis, quadrature basis and so on; it does becomes a useful device in quite different quantum optics areas. In the next Section we will apply it to optical quantum measurement, in particular via homodyne and weak values detection.

Performance of the device

Fast modulation and fidelity are significant features of current electro-optic devices. For example, in the case of $LiNbO_3$ used as material support, switching bandwiths of 40 GHz are available in telecommunications commercial modulators as well as 100 GHz modulation has been achieved in the laboratory [Kanno et al., 2010]; likewise, long-term field reliability has been demonstrated [Wooten et al., 2000]. But the main improvement of this design over other current schemes is its ability to reduce the significance of fabrication errors of the couplers, related for instance with the coupling constant κ or the coupling length L, by simply adjusting the electrodes voltage [Kogelnik and Schmidt, 1976]. To demonstrate this, we show what happens in the case of fabrication imperfections in the current integrated SU(2) scheme, that made up of a Mach-Zehnder interferometer (MZI), that is two 3dB passive DCs with an active phase shifter in between, followed by a second active phase shifter [Bonneau et al., 2012a, Jin et al., 2014, Metcalf et al., 2014, Shadbolt et al., 2012, Silverstone et al., 2014]. The scattering matrix of a 3dB DC with fabrication defects is given by:

$$\frac{1}{\sqrt{2}}\begin{pmatrix} 1-\epsilon & i(1+\epsilon) \\ i(1+\epsilon) & 1-\epsilon \end{pmatrix}, \tag{P7.13}$$

with ϵ a parameter standing for the defects and where only first order errors $O(\epsilon)$ have been taken into account. An integrated Mach-Zehnder made up of two 3dB DCs with defects ϵ and ϵ' as in equation (P7.13), respectively, and a phase shifter causing a change η, is given by the next transformation:

$$\begin{pmatrix} \cos(\eta) + i(\epsilon+\epsilon')\sin(\eta) & \sin(\eta) + i(\epsilon'-\epsilon)\cos(\eta) \\ \sin(\eta) - i(\epsilon'-\epsilon)\cos(\eta) & -\cos(\eta) + i(\epsilon+\epsilon')\sin(\eta) \end{pmatrix}, \tag{P7.14}$$

where a global phase has been dismissed. So the scattering matrix of the MZI becomes complex in the case of fabrication errors, which can not be compensated by the output port phase shifter and therefore accurate $SU(2)$ transformations can not be accomplished [Metcalf et al., 2014]. In our case, this is easily solved by adjusting the values of $\delta(V)$, $\phi_1(V')$ and $\phi_2(V'')$, as it can be seen by inspection of equations (P7.8-P7.11). Moreover, the above statement could be refuted by using alternating $\Delta\beta$ couplers in the MZI, but in that case our design saves one DC, improving the integration density. It is important to outline that in complex networks, as more DCs are involved, the higher the probability of fabrication imperfections and, therefore, a larger deviation from their ideal operation. Hence the importance of this scheme in future QIP technologies.

P7.4. Applications to optical quantum detection

In this section we show how our electro-optic SU(2) device can be used to measure the optical field-strength probability distribution of a two-mode quantum state by homodyne detection, that is, $|\Psi(\mathcal{E}_1, \mathcal{E}_2)|^2$, by means of rotations in the optical field-strength space $\mathcal{E}$. Likewise, we extend it to the full reconstruction of the wavefunction, that is getting amplitude and phase of a two-mode quantum state by using weak values detection, that is, $\Psi(\mathcal{E}_1, \mathcal{E}_2)$. For sake of both simplicity and clarity we present the applications with two-mode quantum states although it can be easily extended to N-mode quantum states.

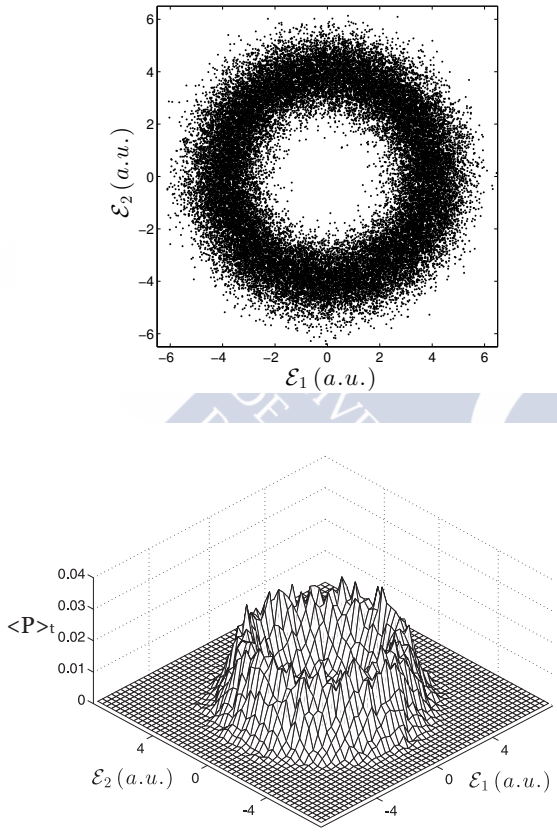

Figure P7.5: Simulation of the measurement of a circularly polarized coherent state (upper figure) and reconstructed probability distribution (lower figure).

Application to quantum homodyne detection

In this subsection we study the application of the electro-optical SU(2) device to measure the optical field strength probability distribution of a

two-mode quantum state. The knowledge of such a distribution is very useful to both obtain the so-called generalized quantum polarization of the state (wich is given by an accumulated probability distribution) and assess its generalized polarization degree [Barral et al., 2013]. The measurement of this feature of any N-mode quantum state of light is accomplished by means of an homodyne scheme, phase-independent in the case of stationary quantum states, or phase-averaged in the case of time-dependent states. From the theory of QST, it is known that in order to measure a quantum state, a set of linear transformations must be applied to generate a tomographically complete set of observables, a quorum, whose statistical properties are measured [Raymer and Funk, 1999]. In the usual single-mode homodyne detection this is carried out by means of modulation of an local oscillator (LO) phase which turns out into a rotation in the phase space [Smithey et al., 1993]. When two modes are involved, three parameters are required to obtain the quorum. Some techniques have been developed to perform this experimentally, as the "Dual-mode-LO" and the generalized rotations in phase space "GRIPS" [Raymer and Funk, 1999], where the set of transformations is applied to a two-mode LO or to the two-mode signal before mixing in a balanced homodyne detector (BHD), respectively. In this paper we apply this last approach to the detection of spatial quantum states of light in the optical field-strength space $\mathcal{E}$. In this case, only one free parameter, or none, will be necessary because of the option of using random measurement, as we will show below. Hence we propose the detection scheme sketched in Figure 4 (solid line): every measurement unit (a stage) is made up by the electro-optic coupler presented in the above Section performing a rotation in the $\mathcal{E}_1\mathcal{E}_2$-space. Mathematically this is equivalent to perform the transformation (P7.11) with $\Phi = n\pi$ on the input state, leading to:

$$\begin{pmatrix} \hat{\mathcal{E}}_3 \\ \hat{\mathcal{E}}_4 \end{pmatrix} = \begin{pmatrix} A(\delta) & (-1)^n B(\delta) \\ (-1)^{n+1} B(\delta) & A(\delta) \end{pmatrix} \begin{pmatrix} \hat{\mathcal{E}}_1 \\ \hat{\mathcal{E}}_2 \end{pmatrix} \tag{P7.15}$$

This transformation in operator form is given by $\hat{U}_R(\chi) = e^{i\chi(\delta)\hat{\sigma}_y}$, where $\chi(\delta) = \text{atan}(B/A) = \Theta/2$ is the effective angle of rotation. The output mode 3 is sent to the integrated BHD right after, where it is mixed with a strong local oscilator excited in a coherent state $|\alpha\rangle$, with $\alpha = |\alpha|e^{i\psi}$, in the same spatial mode (mode 0). The output mode 4 can be used for other purposes or, in the case of a N-mode quantum state, it can be the input to the next measurement unit (stage 2, dashed line, Figure 4)[4] [Raymer and Funk, 1999]. In the BHD the LO phase ψ performs rotations in the phase space of the output mode 3, that is, $\mathcal{E}_3\mathcal{P}_3$. Such a rotation is mathematically

[4]Note not appearing in the original paper: alternatively, three stages composed of two nested devices as that depicted in Figure 1, with one of the three outputs coupled to the input of an integrated BHD, would accomplish the same task.

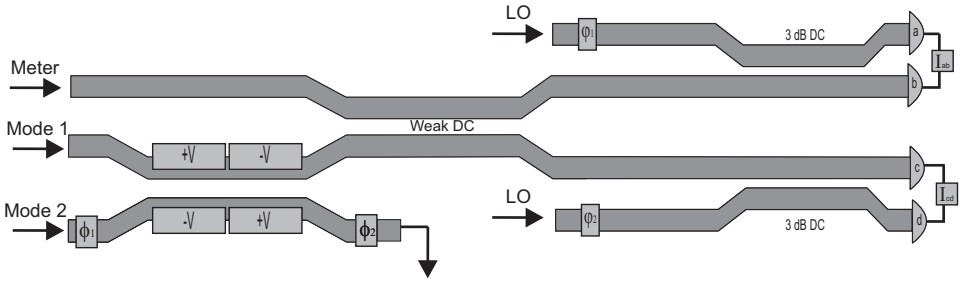

Figure P7.6: Homodyne detection scheme for weak values measurement of a two-mode quantum state of light. Modes 1 and 2 are sent to the Kogelnik-Schmidt coupler where rotations in the field-strength space $\mathcal{E}$ are performed. The upper output mode is weakly coupled in a directional coupler (Weak DC) with a meter mode. The lower ouput mode is sent to a BHD where postselected probabilities are calculated from data and the upper output mode is sent to other BHD where postselected expectation values of the meter conjugate quadrature are calculated.

carried out by the operator $\hat{U}_{LO}(\psi) = e^{-i\psi\hat{n}_0}$. From the difference of the a and b photodetectors readings we can obtain statistical information of the state like the moments of the distribution. The mean value of the field and its variance would be for example [Loudon and Knight, 1987],

$$\langle \hat{J}_{ab}(\chi,\psi)\rangle \propto 2|\alpha|\langle \hat{\mathcal{E}}_3(\chi,\psi)\rangle, \tag{P7.16}$$

$$\langle (\Delta\hat{J}_{ab}(\chi,\psi))^2\rangle \propto 4|\alpha|^2\langle (\Delta\hat{\mathcal{E}}_3(\chi,\psi))^2\rangle, \tag{P7.17}$$

where $\langle \hat{J}_{ab}\rangle$ is the difference of intensities measured by the detectors. However, for a complete characterization of the generalized polarization of the state we have to obtain the total probability distribution $P(\mathcal{E}_1,\mathcal{E}_2)$. This can be accomplished performing sampling to buid up a histogram for every rotation angle χ and LO phase ψ which gives us an approximate probability distribution of obtaining a value of the field-strength $\mathcal{E}_3$:

$$P(\mathcal{E}_3(\chi,\psi)) = \langle \mathcal{E}_1,\mathcal{E}_2|\hat{U}^\dagger\,\hat{\rho}\,\hat{U}|\mathcal{E}_1,\mathcal{E}_2\rangle, \tag{P7.18}$$

where $\hat{\rho}$ is the density operator which characterizes the input quantum state, $\hat{\rho} = |\Psi\rangle\langle\Psi|$ in the case of a pure state, and $\hat{U} = \hat{U}_{LO}(\psi)\,\hat{U}_R(\chi)$ the unitary transform performed by the entire detection system. In the case of non-stationary quantum states, we are interested in the accumulated probability distribution over one temporal cycle $\langle P(\mathcal{E}_1,\mathcal{E}_2)\rangle_t$. This provides us with three methods of sampling this built-up quantum probability distribution: the first one is to control ψ and to vary χ without following any order. We can call this standard homodyne detection, since we set discretely the time (phase) and measure in any field-strength $\mathcal{E}_3$, covering all the $\mathcal{E}_1\mathcal{E}_2$-space and a temporal cycle; the second one is based on setting χ

and uniformly randomize ψ, which it could be called phase-random homodyne detection, given that we measure at random times (phases) on the discretely-varied field-strength $\mathcal{E}_3(\chi)$, giving us time-weighted average of the probability:

$$\langle P(\mathcal{E}_3(\chi)\rangle_t = \frac{1}{2\pi}\int_0^{2\pi} P(\mathcal{E}_3(\chi,\psi))\, d\psi \tag{P7.19}$$

The third one would be to randomize both ψ and χ, leading to high simplification of the measurement procedure. The discrete nature of the variation of the two parameters and the same sampling process make this procedure inherentely approximated, such that enough resolution has to be reached to obtain a satisfactory outcome. Next, for the sake of clarity, we show in Figure 5 (upper Figure) an standard homodyne detection simulation of the quantum polarization of a circularly polarized coherent state given by $|L\rangle = |\alpha\rangle_1|i\alpha\rangle_2$, with $|\alpha| = 4$, where χ has been randomized. This simulation has been carried out creating 10^5 random points by a Monte Carlo method [Martinez and Martinez, 2002]. The outcome obtained performing the experimental procedure explained above would be similar to this. In Figure 5 (lower Figure) we show the probability distribution (P7.19) reconstructed from the data sampled in Figure 5 (upper Figure). Fitting this surface allows us to recover the parameters defining the state, as the photon number in each mode and the quantum noise. In this case we obtain $\langle\hat{\mathcal{E}}_1\rangle = 4.001$, $\langle\hat{\mathcal{E}}_2\rangle = 4.003$, $\langle\Delta\hat{\mathcal{E}}_1\rangle = 1.035$ and $\langle\Delta\hat{\mathcal{E}}_2\rangle = 1.033$, which agree to a great extent with the parameters defining the quantum state $|L\rangle$. These data could be be used as well for working out the generalized polarization degree of the state, as shown in [Barral et al., 2013]. Of course, the procedure above presented can be also carried out with non-gaussian states, as we show in the following section.

It is important to outline that this scheme is able to be generalized to N-mode input states, as the unused output of the directional coupler can be mixed with a third mode and measured by another BHD as well, and so on and so forth up to the N-mode. In Figure 4 is sketched the scheme for the case 3-mode. So we would need one local oscillator mode and one BHD per input mode to be measured. Moreover, this scheme could be used to obtain the Wigner function on chip by using the transformation (P7.11), repeated measurements of $P(\mathcal{E}_3(\chi,\psi,\phi))$ for different combinations of the parameters (χ,ψ,ϕ) and reconstruction algorithms as inverse linear transform techniques or statistical inference [Lvovsky and Raymer, 2008]. Additionally, using the phase-averaged distributions (P7.19), we can reconstruct the photon number statistics of any input N-mode state following [Munroe et al., 1995]. In the next section we show a faster way of obtaining complete information about the quantum state, measuring at the same time amplitude and phase of the input wavefunction.

Application to quantum detection of weak values

Another possible application of this device is the measurement of the wavefunction by means of weak values. Quantum state reconstruction using this approach has become a topic of great interest since its introduction in [Aharonov et al., 1988]. This formalism is founded on the observed outcomes of weak measurements, given by:

$$A_w = \frac{\langle \Psi_j | \hat{A} | \Psi \rangle}{\langle \Psi_j | \Psi \rangle}, \tag{P7.20}$$

where A_w is the complex weak value of the observable given by the quantum operator $\hat{A}$ for a quantum state $|\Psi\rangle$ postselected in $|\Psi_j\rangle$ [Jozsa, 2007]. This value is dependent on two facts: imposing postselection into a given final state and a weak interaction between the mesurement apparatus (the meter) and the quantum system of interest. For a complete and detailed review see [Aharonov and Rohrlich, 2005].

Recently, a weak values scheme was proposed to reconstruct the quantum state of an optical single-mode field [Fischbach and Freyberger, 2012]. This implementation is based on a weak beam splitter interaction between two single-mode quantum states, the one to be measured $|\Psi\rangle$ and the other a gaussian state acting as a meter $|\mu\rangle$. Following this approach the quantum state is reconstructed in the optical field momentum $\mathcal{P}$ basis, where the wavefunction is given by:

$$\Psi(\mathcal{P}) = |\Psi(\mathcal{P})|\, e^{i\,\varphi(\mathcal{P})}. \tag{P7.21}$$

This scheme is also suited to be applied in integrated optics. In this case homodyne detection is carried out on each output guide of a directional coupler with weak coupling parameter $\Gamma_w = \kappa L$, where L is the coupling length (or $\chi_w(\delta)$ if our electro-optic coupler is used for this task), taking postselection probabilities in one guide $P(\mathcal{P}) = |\Psi(\mathcal{P})|^2$ (strong measurement) and postselected expectation values in the conjugate quadrature of the meter $E^{(\mathcal{P})}[\hat{\mathcal{E}}_\mu] = -\Gamma_w\, \partial\varphi(\mathcal{P})/\partial\mathcal{P}$ (weak measurement) in the other guide. From the strong measurement we obtain the amplitude of (P7.21), and from the weak measurement its phase by means of:

$$\varphi(\mathcal{P}) = -\frac{1}{\Gamma_w} \int^{\mathcal{P}} E^{(\mathcal{P}')}[\hat{\mathcal{E}}_\mu]\, d\mathcal{P}'. \tag{P7.22}$$

This section is devoted to extend this weak detection scheme to two-mode (or N-mode) spatial quantum states of light. So, on one hand, since we are interested in measuring spatial quantum states, we have translated this scheme to photonics by the use of a fixed directional coupler, or our reconfigurable device allowing us sharper selection of the strength of the interaction, as weak interaction system. On the other hand, as our aim is

the study of two-mode quantum states, performing rotations in the $\mathcal{P}_1\,\mathcal{P}_2$ plane by means of our device, which, mathematically, consists of substituting $\mathcal{E}$ by $\mathcal{P}$ in equation (P7.15), we can obtain full amplitude and phase information for every rotated angle χ. In Figure 6 we show a sketch of the circuit proposed for this weak measurement-based detector. The principal advantage of this scheme is the quicker acquisition and simpler analysis of data with respect to QST. But unfortunately this approach presents some drawbacks. The main drawback, inherent to the method, is its inability to reconstruct the phase for those values of $\mathcal{P}$ with low probability, as it can be seen in Figures 7 and 8: the lower the probability, the poorer the reconstructed phase. This can be overlooked for the far values of the field, but it is an unavoidable problem when the wavefunction presents gaps [Fischbach and Freyberger, 2012]. A second drawback, dependent in this case on our design, is the inability of reconstruct quantum states which present only angular dependence, not radial, as the postselected expectation value will be zero for every rotation angle χ. In these cases QST has to be chosen. It is important to outline that a hybrid scheme of QST and weak measurement is possible, leaving QST for those states or values of χ not suitable to be measured by the weak scheme.

Figures 7 and 8 show theoretical and simulated reconstructions of the weak measurements carried out over a NOON-type state $|L\rangle = |2\,0\rangle + i|0\,2\rangle$ by means of phase-random homodyne detection. We have used a weak coupling parameter $\Gamma_w = 0.05$ and $N = 10^5$ data points. Figure 7 shows the simulated and theoretical probability for two rotation angles $\chi = 0, \pi/3$ (upper Figure) and the total data sampled in the $\mathcal{P}_1\,\mathcal{P}_2$-space (lower Figure). Likewise, the phase is reconstructed integrating the expectation value of the meter $E^{(\mathcal{P}_3)}[\mathcal{E}_\mu]$, in our case the vaccuum $|\mu = 0\rangle$, over $\mathcal{P}_3$. As it can be seen in the upper Figure 8, where theoretical and reconstructed phases for two rotation angles $\chi = 0, \pi/3$ are shown, they highly agree for values of $|\mathcal{P}_3| < 2.5$ where the probability of the quantum state is high (upper Figure 7), as was discussed above. In the lower Figure 8 we show the reconstructed joint phase of the input quantum state obtained from individual measurements as those depicted on upper Figure 8. Note that as only relative phases are physically meaningful, we have chosen the phase origin at $(\mathcal{P}_1, \mathcal{P}_2) = (0, 0)$ and it acts as the lower bound of integral (P7.22). As can be seen, the phase of $|L\rangle$ varies smoothly unless for $\chi = \pm\pi/4$, where phase jumps appear and the method does not work. To solve this, we have interpolated the data at these planes. Likewise, in lower Figure 8 we have dismissed the reconstructed phases for values of $\mathcal{P}_1$, $\mathcal{P}_2 > 3$, as those values are far from the theoretical.

Hence, this procedure gives us full characterization of the joint quantum wavefunction. It is important to say that the reconstructed wavefunction obtained is the same as that in the field-strength space $\mathcal{E}$ because of the temporal invariance of the quantum state, but in general it can be obtained by a

Fourier Transform. In the case of a non-stationary quantum state, standard homodyne detection would be required for reconstructing the amplitude and phase of the state in every point of a temporal cycle.

P7.5. Summary

In this work we have studied the detection of two-mode spatial quantum states of light with an homodyne on-chip scheme. We have designed a device capable of carry out reconfigurable SU(2) and SO(2,R) transformations on spatial modes by means of a directional coupler built in an electro-optical material, extensible to N-mode input quantum states by nesting, and we have compared its performance with other current schemes. Finally we applied it to the measure of generalized quantum polarization and reconstruction of the wavefunction using weak values.

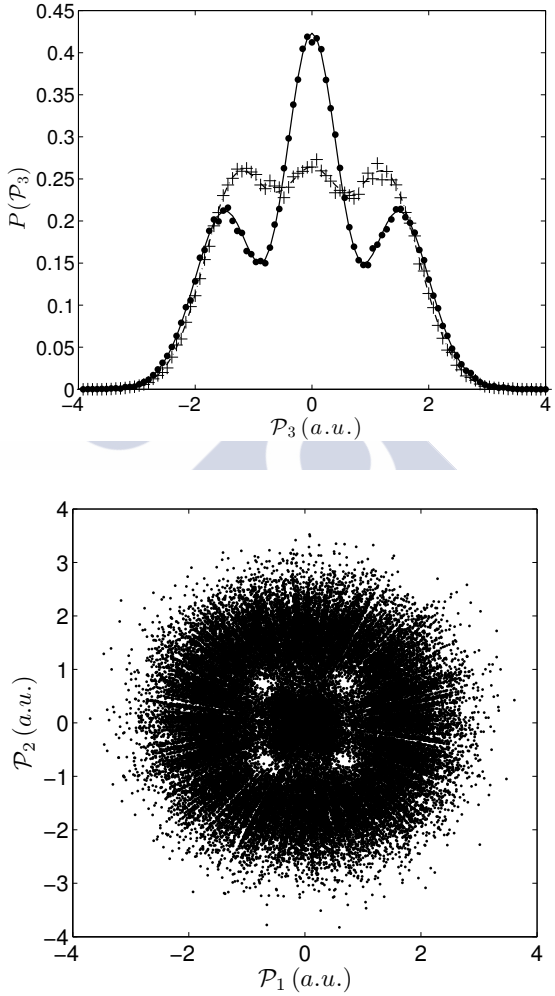

Figure P7.7: Probability corresponding to a NOON-type state with N = 2. Upper Figure: theoretical and simulated probability corresponding to two values of χ: theoretical (solid line) and simulated (dots) probability for $\chi = 0$ and theoretical (dash-dot line) and simulated (crosses) probability for $\chi = \pi/3$. Lower Figure: total data sampled for probability reconstruction.

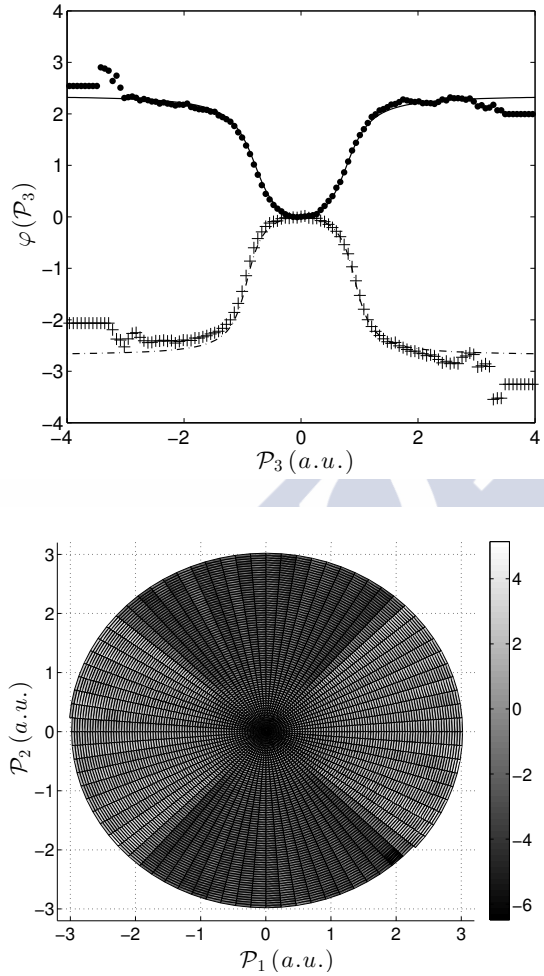

Figure P7.8: Phase corresponding to a NOON-type state with N $= 2$. Upper Figure: theoretical and simulated phase corresponding to two values of χ: theoretical (solid line) and simulated (dots) phase for $\chi = 0$ and theoretical (dash-dot line) and simulated (crosses) phase for $\chi = \pi/3$. Lower Figure: reconstructed joint phase.

Chapter 5 bibliography

Y. Aharonov and D. Rohrlich. *Quantum Paradoxes*. Wiley-VCH, Weinheim, 2005.

Y. Aharonov, D.Z. Albert, and L. Vaidman. How the result of a measurement of a component of the spin of a spin-1/2 particle can turn out to be 100. *Physical Review Letters*, 60:1351, 1988.

D. Barral, J. Liñares, and M.C. Nistal. Optical field-strength generalized polarization of non-stationary quantum states in waveguiding photonic devices. *Journal of Modern Optics*, 60(12):941, 2013.

D. Bonneau, E. Engin, K. Ohira, N. Suzuki, H. Yoshida, N. Iizuka, M. Ezaki, C.M. Natarajan, M.G. Tanner, R.H. Hadfield, S.N. Dorenbos, V. Zwiller, J.L. O'Brien, and M.G. Thompson. Quantum interference and manipulation of entanglement in silicon wire waveguide quantum circuits. *New Journal of Physics*, 14(4):045003, 2012a.

D. Bonneau, M. Lobino, P. Jiang, C.M. Natarajan, Tanner M.G., R.H. Hadfield, S.N. Dorenbos, V. Zwiller, M.G. Thompson, and J.L. O'Brien. Fast path and polarization manipulation of telecom wavelengths single photons in lithium niobate waveguide devices. *Physical Review Letters*, 108:053601, 2012b.

S.L. Braunstein and P. van Loock. Quantum information with continuous variables. *Review of Modern Physics*, 77:513, 2005.

G. Breitenbach, S. Schiller, and J. Mlynek. Measurement of the quantum states of squeezed light. *Nature*, 387:471, 1997.

J. Fischbach and M. Freyberger. Quantum optical reconstruction scheme using weak values. *Physical Review A*, 86:052110, 2012.

C.C. Gerry and P. L. Knight. *Introductory Quantum Optics*. Cambridge University Press, 2005.

P.C. Humphreys, B.J. Metcalf, J.B. Spring, M. Moore, P.S. Salter, M.J. Booth, W.S. Kolthammer, and I.A. Walmsley. Strain-optic active control for quantum integrated photonics. *Optics Express*, 22(18):21719, 2014.

H. Jin, F.M. Liu, P. Xu, J.L. Xia, M.L. Zhong, Y. Yuan, J.W. Zhou, Y.X. Gong, W. Wang, and S.N. Zhu. On-chip generation and manipulation of entangled photons based on reconfigurable lithium-niobate waveguide circuits. *Physical Review Letters*, 113:103601, 2014.

R. Jozsa. Complex weak values in quantum measurement. *Physical Review A*, 76:044103, 2007.

A. Kanno, T. Sakamoto, A. Chiba, T. Kawanishi, K. Higuma, M. Sudou, and J. Ichikawa. 120-gb/s nrz-dqpsk signal generation by a thin-lithium-niobate-substrate modulator. *IEICE Electronics Express*, 7(11):817, 2010.

A. Klimov, G. Björk, J. Söderholm, L.S. Madsen, M. Lassen, U.L. Andersen, J. Heersink, R. Dong, Ch. Marquardt, G. Leuchs, and L.L. Sánchez-Soto. Assesing the polarization of a quantum field from stokes fluctuations. *Physical Review Letters*, 105:153602, 2010.

H. Kogelnik and R.V. Schmidt. Switched directional couplers with alternating $\delta\beta$. *IEEE journal of quantum electronics*, 12(7):396, 1976.

H. Kühn, D.-G. Welsch, and W. Vogel. Determination of density matrices from field distributions and quasiprobabilities. *Journal of Modern Optics*, 41:1607, 1994.

J. Liñares, M.C. Nistal, and D. Barral. Quantization of coupled 1d vector modes in integrated photonic waveguides. *New Journal of Physics*, 10: 063023, 2008.

J. Liñares, M.C. Nistal, D. Barral, and V. Moreno. Optical field-strength generalized polarization of two-mode single photon states. *European Journal of Physics*, 31:991, 2010.

J. Liñares, D. Barral, M.C. Nistal, and V. Moreno. Optical field-strength generalized polarization of multimode single photon states in integrated directional couplers. *Journal of Modern Optics*, 58(8):711, 2011.

J. Liñares, D. Barral, and M.C. Nistal. Spatial propagation of quantum light in nonlinear waveguiding devices: theory and applications. *Journal of Nonlinear Optical Physics and Materials*, 21(3):1250032, 2012.

R. Loudon and P.L. Knight. Squeezed light. *Journal of Modern Optics*, 34 (6-7):709, 1987.

A. Luis and A.S. Sanz. Reconciling quantum trajectories and stationary quantum distributions in single-photon polarization states. *Physical Review A*, 87:063844, 2013.

A. Luks and V. Perinová. Canonical quantum description of light propagation in dielectric media. In E. Wolf, editor, *Progress in optics*, volume 43, page 295. North-Holland, 2002.

J.S. Lundeen, B. Sutherland, P. Aabid, C. Stewart, and C. Bamber. Direct measurement of the quantum wavefunction. *Nature*, 474:188, 2011.

A.I. Lvovsky and M.G. Raymer. Continuous-variable optical quantum state tomography. *Review of Modern Physics*, 81:299, 2008.

L. Mandel and E. Wolf. *Optical Coherence and Quantum Optics*. Cambridge University Press, 1995.

A. Martin, O. Olibart, M.P. De Micheli, D.B. Ostrowsky, and S. Tanzilli. A quantum relay chip based on telecommunication integrated optics technology. *New Journal of Physics*, 14:025002, 2012.

W. Martinez and A. Martinez. *Computational Statistics Handbook with Matlab*. Chapman & Hall/CRC, 2002.

G. Masada, M. Kazunori, A. Politi, T. Hashimoto, J.L. O'Brien, and A. Furusawa. Continuous-variable entanglement on a chip. *Nature Photonics*, 9: 316–319, 2015.

J.C.F. Matthews, A. Politi, A. Stefanov, and J.L. O'Brien. Manipulation of multiphoton entanglement in waveguide quantum circuits. *Nature Photonics*, 3:346, 2009.

B.J. Metcalf, J.B. Spring, P.C. Humphreys, N. Thomas-Peter, M. Barbieri, W.S. Kolthammer, X.-M. Jin, N.K. Langford, D. Kundys, J.C. Gates, B.J. Smith, P.G.R. Smith, and I.A. Walmsley. Quantum teleportation on a photonic chip. *Nature Photonics*, 8(10):770, 2014.

M. Munroe, D. Boggavarapu, M.E. Anderson, and M.G. Raymer. Photon-number statistics from the phase-averaged quadrature-field distribution: theory and ultrafast measurement. *Physical Review A*, 52(2):R924, 1995.

M.A. Nielsen and I.L. Chuang. *Quantum Computation and Quantum Information*. Cambridge University Press, 2010.

J.L. O'Brien, A. Furusawa, and J. Vukovic. Photonic quantum technologies. *Nature Photonics*, 3:687, 2009.

T. Opatrny, D.-G. Welsh, and W. Vogel. Multi-mode density matrices of light via amplitude and phase control. *Optics Communications*, 134:112, 1997.

J. Pfeifle, L. Alloatti, W. Freude, J. Leuthold, and C. Koos. Silicon-organic hybrid phase shifter based on a slot waveguide with a liquid-crystal cladding. *Optics Express*, 20(14):15359, 2012.

Alberto Politi, Martin J. Cryan, John G. Rarity, Siyuan Yu, and Jeremy L. O'Brien. Silica-on-silicon waveguide quantum circuits. *Science*, 2008.

M.G. Raymer and A.C. Funk. Quantum-state tomography of two-mode light using generalized rotations in phase space. *Physical Review A*, 61: 015801, 1999.

M.G. Raymer, D.F. McAlister, and U. Leonhardt. Two-mode quantum-optical state measurement: sampling the joint density matrix. *Physical Review A*, 54(3):2397, 1996.

M. Reck, A. Zeilinger, H.J. Bernstein, and P. Bertani. Experimental realization of any discrete unitary operator. *Physical Review Letters*, 73(1):58, 1994.

E. Saglamyurek, N. Sinclair, J. Jin, J.A. Slater, D. Oblak, F. Bussieres, M. George, R. Ricken, W. Sohler, and W. Tittel. Broadband waveguide quantum memory for entangled photons. *Nature*, 469(7331):512, 2011.

D. Sahin, A. Gaggero, J.-W. Weber, I. Agafonov, M.A. Verheijen, F. Mattioli, J. Beetz, M. Kamp, S. Höfling, M.C.M. van de Sanden, R. Leoni, and A. Fiore. Waveguide nanowire superconducting single-photon detectors fabricated on gaas and the study of their optical properties. *IEEE journal of selected topics in quantum electronics*, 21(2):3800210, 2015.

C. Santori, D. Fattal, J. Vukovic, G.S. Solomon, and Y. Yamamoto. Indistinguishable photons from a single-photon source. *Nature*, 419:594, 2002.

P.J. Shadbolt, Verde M.R., A. Peruzzo, A. Politi, A. Laing, M. Lobino, J.C.F. Matthews, M.G. Thompson, and J.L. O'Brien. Generating, manipulating and measuring entanglement and mixture with a reconfigurable photonic circuit. *Nature Photonics*, 6(1):45, 2012.

J.W. Silverstone, D. Bonneau, K. Ohira, H. Yoshida, N. Iizuka, M. Ezaki, R.H. Hadfield, V. Zwiller, G.D. Marshall, J.G. Rarity, J.L. O'Brien, and M.G. Thompson. On-chip quantum interference between two silicon waveguide sources. *Nature Photonics*, 8(2):104, 2014.

B.J. Smith, D. Kundys, N. Thomas-Peter, P.G.R. Smith, and I.A. Walmsley. Phase-controlled integrated photonic quantum circuits. *Optics Express*, 17(16):13516, 2009.

D.T. Smithey, M. Beck, M.G. Raymer, and A. Faridani. Measurement of the wigner distribution and the density matrix of a light mode using optical homodyne tomography: application to squeezed states and the vacuum. *Physical Review Letters*, 70(9):1244, 1993.

W. Vogel and H. Risken. Determination of quasiprobability distributions in terms of probability distributions for the rotated quadrature phase. *Physical Review A*, 40(5):2847, 1989.

R.G. Walker and J. Heaton. *Broadband Optical Modulators-Science, Technology and Applications*, chapter Gallium arsenide modulator technology. CRC Press, Boca Raton, 2012.

J. Wang, A. Santamato, P. Jiang, D. Bonneau, E. Engin, J.W. Silverstone, M. Lermer, J. Beetz, M. Kamp, S. Höfling, Tanner M.G., C.M. Natarajan, R.H. Hadfield, S.N. Dorenbos, V. Zwiller, J.L. O'Brien, and M.G. Thompson. Gallium arsenide (gaas) quantum photonic waveguide circuits. *Optics Communications*, 327:49, 2014.

D.-G. Welsch, W. Vogel, and T. Opatrny. Homodyne detection and quantum state reconstruction. In E. Wolf, editor, *Progress in Optics*, volume XXXIX, page 63. Elsevier, 1999.

E.L. Wooten, K.M. Kissa, A. Yi-Yan, E.J. Murphy, D.A. Lafaw, P.F. Hallemeier, D. Maack, D.V. Attanasio, D.J. Fritz, G.J. McBrien, and D.E. Bossi. A review of lithium niobate modulators for fiber-optic communications systems. *IEEE journal of selected topics in quantum electronics*, 6(1):69, 2000.

A. Yariv. *Quantum Electronics*. John Wiley & sons, New York, 1975.

CONCLUSIONS & OUTLOOK

Conclusions

In this dissertation we have introduced a quantum theory of propagation of light in integrated photonic devices. The necessity of this theory is justified due to the conceptual and formal inconsistencies the Hamiltonian theory presents when dealing with propagation problems. Taking into account the orthonormalization property and the modal norms, we have carried out a canonical quantization of the flux of Momentum and derived Heisenberg equations. We have applied it to coupling devices with different features of the refractive index: inhomogeneities, nonlinear response and losses; like N $\times$ N linear and nonlinear directional couplers and *spontaneous parametric down conversion* and *spontaneous four wave mixing*-based nonlinear inhomogeneous waveguides.

Likewise, we have introduced the optical field-strength space and the amplitude probability distributions in this representation, and by means of a spatial-type Lagrangian theory we have derived by path integration propagators in this space for different-media based devices. In this way we have solved the propagation for discrete and continuous variables.

Next, we have presented a new method of characterization of quantum states introducing a generalized quantum polarization, based on the confinement in particular regions of the optical field space of the probability distributions of quantum states. Likewise, we have proposed a consistent polarization degree, a figure which measures how different a state is from a full unpolarized one, showing its application to the characterization of various examples of stationary and dynamic quantum states.

Our last objective has been to measure quantum states of light propagating in integrated photonic devices. We have designed a versatile and reliable electro-optic integrated device to accomplish this goal. This device allows carrying out any SU(2) unitary transformation and is able to be nested as well, allowing its extension to SU(N) transformations. Likewise, it outperforms other current schemes based on pasive directional couplers

due to its ability to reduce the effect produced by fabrication errors, a very important fact when complex circuits are involved. We have performed simulations and shown possible applications.

In summary, we have developed tools to design and simulate the performance of photonic devices, as well as proposed a characterization method for quantum states propagating within, with interest in the continuously growing field of integrated quantum photonics.

Outlook

In future works we will extend our OFS theory of the propagation in IPDs to higher order nonlinear interactions by means of perturbative techniques as well as accomplish a wider and more detailed study of losses and its application to nonlinear devices like *SOI* ring resonators. Likewise, we will take advantage of the mathematical tool developed in this thesis to the design of IPDs for specific applications like active devices for performing both generation and manipulation of quantum states with interest in quantum computation and metrology. Besides, a weak-values based integrated homodyne detector will be designed in such a way to avoid some of the limitations found in this dissertation. Furthermore, we will study the relation of Gouy's phases with geometric phases and possible applications to sensing by means of squeezed states of light in interferometers.

APPENDIX

A

HEURISTIC FORMULATION OF QUANTUM DISSIPATION

We start taking into account the losses of the free modes propagating in a waveguide. If we consider dissipation as a perturbation, we can model it in terms of a linear polarization, but where an imaginary electrical permittivity $i\Delta\tilde{\varepsilon}_\nu$ for the ν-mode replaces the real one previously used in § 2.3.2. So we can heuristically introduce the following hermitian polarization operator:

$$\hat{\mathbf{P}}_{Oi} \approx -i\Delta\tilde{\varepsilon}_\nu \left[\hat{\mathbf{e}}_\nu^{(-)}(x,y,t) - \hat{\mathbf{e}}_\nu^{(+)}(x,y,t)\right] \equiv -i\Delta\tilde{\varepsilon}_\nu \hat{\mathbf{e}}_{\nu\_}(x,y,t) \qquad \text{(A.1)}$$

This term can include different types of damping like ohmic or absorption losses, characterized by parameters $\gamma_\nu \propto \Delta\tilde{\varepsilon}_\nu$ [Liñares et al., 2012]. In an analogous way to the procedure carried out in § 2.3 for lossless linear media, we establish that the quantum correction to the Momentum operator for the ν-mode is given by:

$$\hat{M}_{Oi} = \frac{1}{2}\iiint_0^T \hat{\mathbf{P}}_{Oi}\,\hat{\mathbf{e}}_{\nu\_}\,dxdydcdt = -\frac{i}{2}\iiint_0^T \Delta\tilde{\varepsilon}_\nu \hat{\mathbf{e}}_{\nu\_}\hat{\mathbf{e}}_{\nu\_}\,dxdydcdt, \quad \text{(A.2)}$$

where $\hat{\mathbf{e}}_{\nu\_}(x,y,t)$ and not $-\hat{\mathbf{e}}_{\nu\_}(x,y,t)$ has been chosen for sake of physical consistency, that is, the results for the classic limit case are correctly recovered. Likewise, this heuristic derivation could be also applied to a medium with gain, that is, with $-i\Delta\tilde{\varepsilon}_\nu$.

Checking (A.2), we quickly realize that $\hat{M}_{Oi}$ is not hermitian and therefore, the momentum is not conserved. This implies that an amount of the optical momentum is transferred to the medium. Now, by taking into account the expressions for the optical field operators given by equation (2.3.63) we can derive an explicit expression for $\hat{M}_{Oi}$. In order to illustrate it in an explicit form we focus on the particular case of TE modes [Liñares and Nistal, 2003] in a planar guide. Therefore, from equation (A.2), the

following free Momentum corresponding to a lossy or radiation mode is obtained:

$$\hat{M}_{Oi} = i\hbar\frac{\gamma_\nu}{2}\,(\hat{a}_\nu^\dagger\hat{a}_\nu + 1/2). \tag{A.3}$$

This heuristic procedure can be also extended to the calculation of linear and nonlinear modal coupling with losses. So taking a complex electrical permitivity $\Delta\epsilon = \Delta\epsilon_r + i\Delta\epsilon_i$ which couples the optical modes, and following a procedure similar to that developed for the lossless case in § 2.3.2, but by using the new field operator related to losses $\hat{\mathbf{e}}_{\nu\_}(x,y,t)$, and by taking into account all the ν-modes, we obtain the following linear Momentum:

$$\hat{M}_{Li} = -\frac{i}{2}\iiint_0^T \Delta\epsilon_i \sum_\nu \hat{\mathbf{e}}_{\nu\_} \sum_{\nu'} \hat{\mathbf{e}}_{\nu'}\,dxdydcdt. \tag{A.4}$$

After a straightforward calculation, we obtain the following non hermitian Momentum operator describing the losses in a linear modal coupling device:

$$\hat{M}_{Li} = i\hbar\sum_\nu \gamma_{\nu\nu}(\hat{a}_\nu^\dagger\hat{a}_\nu + 1/2) + i\hbar\sum_{\nu<\nu'}\gamma_{\nu\nu'}(\hat{a}_\nu^\dagger\hat{a}_{\nu'} + h.c.), \tag{A.5}$$

where

$$\gamma_{\nu\nu'} = \frac{\omega\iint\Delta\epsilon_i\,(\mathbf{E}_{t\nu}\mathbf{E}^\star_{t\nu'} + \mathbf{E}_{z\nu}\mathbf{E}^\star_{z\nu'})dxdy}{4\,\|\mathbf{E}_\nu\|\,\|\mathbf{E}_{\nu'}\|}. \tag{A.6}$$

In short, losses have included complex coupling coefficients, as expected. In the same way we can assume that nonlinear coupling will be described by complex coefficientes: $\kappa_{NL} + i\gamma_{NL}$. Therefore the Momentum operator will be modified by all these imaginary terms.

Nevertheless, these imaginary terms violate the commutation rules and therefore this approach lacks of quantum consistency [Haken, 1981]. In order to avoid this inconsistency fluctuating operators $\hat{B}$ (quantum noise operators) along the direction z have to be introduced in the Momentum operator in a similar way as the Hamiltonian formulation. These fluctuating operators have well-defined statistical properties in such a way that commutation rules are preserved. The physical origin of these operators is the incoherent properties of the medium with losses, that is the damping mechanism is a statistical process described by stochastic terms modelling the coupling between the light and the medium. Thus, the following heuristic additional term in the Momentum operator should be introduced:

$$\hat{M}_F = \sum_\nu \hbar g_\nu\,(\hat{a}_\nu^\dagger\hat{B} + \hat{a}_\nu\hat{B}^\dagger), \tag{A.7}$$

where g_ν is the coupling strength between the medium and the ν-mode. For the sake of clarity, a single mode in a lossy medium is firstly analyzed.

In this case the Momentum operator in the ν-mode and the corresponding Heisenberg-Langevin equation are:

$$\hat{M}_\nu = \hbar(\beta + i\frac{\gamma_\nu}{2})\,(\hat{a}_\nu^\dagger \hat{a}_\nu + 1/2) + \hbar g_\nu(\hat{a}_\nu^\dagger \hat{B} + \hat{a}_\nu \hat{B}^\dagger), \tag{A.8}$$

$$\frac{\partial \hat{a}_\nu}{\partial z} = (i\beta_\nu - \frac{\gamma_\nu}{2})\hat{a}_\nu + i g_\nu \hat{B}. \tag{A.9}$$

By inspection of equation (A.9) it is easy to realize that if $g_\nu = 0$ then $\hat{a}_\nu(z) = \hat{a}_\nu(0)\; e^{i\beta_\nu z}\, e^{-\frac{\gamma_\nu}{2} z}$, so the classical solution is recovered, but from this solution we also have $[\hat{a}_\nu(z), \hat{a}_\nu^\dagger(z)] = e^{-\gamma_\nu z} \to 0$ for $z \to \infty$ and the quantum nature is lost. However, by considering the fluctuating term we obtain the following formal solution:

$$\hat{a}_\nu(z) = \hat{a}_\nu(0) e^{i\beta_\nu z}\, e^{-\frac{\gamma_\nu}{2} z} + i e^{i\beta_\nu z}\, e^{-\frac{\gamma_\nu}{2} z} \int_0^z e^{-i\beta_\nu z'}\, e^{\frac{\gamma_\nu}{2} z'} g_\nu \hat{B}(z')\mathrm{d}z', \tag{A.10}$$

Now it is the moment to take into account the statistical properties of the noise operators $\hat{B}$ and $\hat{B}^\dagger$. It is assumed that under the z-spatial averaging these operators fulfill [Haken, 1981]:

$$\langle \hat{B}(z) \rangle_z = \langle \hat{B}(z)^\dagger \rangle_z = 0,$$

$$\langle [\hat{B}(z), \hat{B}(z')^\dagger] \rangle_z = \frac{\gamma_\nu}{g_\nu^2} \delta(z - z'), \tag{A.11}$$

From the above properties together with equation (A.10), it is obtained that the spatial propagation of the averaging of operators $\hat{a}_\nu(z)$ and $\hat{a}_\nu(z)^\dagger$ provides the same solution as that one of the complex classical fields, that is:

$$\langle \hat{a}_\nu(z) \rangle_z \approx \hat{a}_\nu(0) e^{i\beta_\nu z}\, e^{-\frac{\gamma_\nu}{2} z}, \tag{A.12}$$

and moreover it can be shown that the commutation rules are preserved in a spatial averaging:

$$\langle [\hat{a}_\nu(z), \hat{a}_\nu(z)^\dagger] \rangle_z = 1. \tag{A.13}$$

So now the quantum nature is recovered and the approach is consistent.

Likewise, the more general Momentum operator for lossy linear and nonlinear waveguiding coupling with will be:

$$\hat{M} = \hat{M}_{OL} + \hat{M}_{Oi} + \hat{M}_{Li} + \hat{M}_F + \hat{M}_{(\kappa_{NL} + i\gamma_{NL})}, \tag{A.14}$$

where $\hat{M}_{OL}$, $\hat{M}_{Oi}$, $\hat{M}_{Li}$ and $\hat{M}_F$ have been defined along this section and § 2.3.2 and $\hat{M}_{(\kappa_{NL} + i\gamma_{NL})}$ is a nonlinear Momentum operator, but in this case the subscript $(\kappa_{NL} + i\gamma_{NL})$ is indicating that each one of the nonlinear coupling coefficients is transformed into a complex number.

Appendix A bibliography

H. Haken. *Light*. North-Holland, Amsterdam, 1981.

J. Liñares and M.C. Nistal. Quantization of coupled modes propagation in integrated optical waveguides. *Journal of Modern Optics*, 50(5):781–790, 2003.

J. Liñares, D. Barral, and M.C. Nistal. Spatial propagation of quantum light in nonlinear waveguiding devices: theory and applications. *Journal of Nonlinear Optical Physics and Materials*, 21(3):1250032, 2012.

RESUMEN

Esta tesis se desarrolla en el marco de la *óptica cuántica integrada*. Este campo de investigación conjuga dos de las áreas de la física más fructíferas del último siglo. Por un lado tenemos la óptica cuántica que abarca desde los pioneros trabajos de Planck y Einstein que introdujeron la cuantización de la energía, la explicación del efecto fotoeléctrico o la emisisión estimulada, pasando por la invención del láser en los años 60, la teoría cuántica de la coherencia y la óptica no-lineal, hasta las más actuales técnicas de enfríamento láser, generación de estados no-clásicos de luz, etc.; y que ha dado lugar a novedosas tecnologías como las comunicaciones, la metrología y la computación cuánticas. Por otro lado tenemos la óptica integrada y las fibras ópticas, que constituyen la base de las actuales comunicaciones ópticas y procesado de información con luz. Los dispositivos integrados se basan en el confinamiento de luz en el orden de la longitud de onda y sus principales fortalezas son la escalabilidad y la estabilidad óptica, a diferencia de sus análogos "*bulk*". Estas características han llevado a la confluencia de ambas áreas mediante el uso de dispositivos integrados en el desarrollo de la óptica cuántica dando lugar en los últimos años a grandes hitos en la investigación en el procesado de información, criptografía y metrología cuántica.

Estos *dispositivos fotónicos integrados* (IPDs, por sus siglas en inglés) tienen en común el uso de modos guiados como base física para el transporte de información cuántica y el uso de acopladores direccionales para la generación de entrelazamiento cuántico, el más notable fenómeno cuántico que aumenta las posibilidades de esta tecnología frente a la clásica. Ahora bien, mientras la teoría clásica funciona bien para dispositivos integrados que funcionan con luz clásica, ésta deja de funcionar cuando son estados cuánticos de luz los que se tienen en cuenta. En ese caso una teoría cuántica de la propagación en IPDs se hace necesaria.

Uno de los objetivo principales de esta tesis es presentar una teoría consistente de la propagación de estados cuánticos de luz codificados en modos guiados en IPDs puesto que la teoría normalmente utilizada, la Hamiltoniana, basada en la cuantización de la energía en un volumen y el uso

de modos espaciales, presenta inconsistencias formales y conceptuales en la propagación en medios dieléctricos. Esto fue demostrado por primera vez a finales de los años 80 por Abram para medios lineales y más tarde Huttner *et al.* lo extendieron para medios no lineales. La teoría estándar de la propagación está basada en la teoría Hamiltoniana y una conexión entre espacio y tiempo mediante un tiempo de interacción efectivo. Sin embargo está aproximación sólo es correcta en el caso de estados estacionarios y no puede ser aplicada de modo riguroso a medios dispersivos, ya que en este caso necesitaríamos una variable temporal para cada frecuencia. Este mismo razonamiento se puede utilizar para demostrar que esta teoría tampoco describe la contrapropagación, ya que necesitaríamos variables temporales negativas. Otro problema aparece a la hora de describir la propagación en una discontinuidad entre el espacio libre y un medio dieléctrico. Aplicando la teoría Hamiltoniana la propagación conduciría a una renormalización de la frecuencia, fenómeno no observado experimentalmente. También tenemos problemas con la teoría Hamiltoniana en el caso de acoplamientos longitudinalmente dependientes, ya que en ella se promedia la energía en el volumen por lo que desaparece esa dependencia longitudinal. En el caso de medios no lineales el mismo problema aparece cuando hay desajuste de fase en las constantes de propagación, ya que equivale a un acoplamiento longitudinalmente dependiente efectivo; o cuando tenemos problemas con mezcla de distintas frecuencias, por lo comentado anteriormente para medios dispersivos. Por todo ello, a principios de los años 90 se desarrolló una teoría de la propagación cuántica que resolvía estos problemas. Esta teoría está basada en la cuantización del flujo de momento electromagnético clásico y el uso de modos temporales, dando lugar a un generador de propagación, el operador Momento. Bajo estas condiciones, la teoría resolvía las inconsistencias que aparecían usando la técnica Hamiltoniana y fue aplicada a distintos problemas en óptica "*bulk*" con éxito.

Por otro lado, la propagación de estados no clásicos en IPDs fue abordada por primera vez a finales de los años 80 por Jansky *et al.* mediante una correspondencia directa entre coeficientes complejos clásicos y operadores, sin una derivación rigurosa. Años después se llevaron a cabo estudios sobre dispositivos integrados lineales y no-lineales, pero en ellos los operadores Momento fueron introducidos o bien de manera heurística o trasladando de manera directa los resultados de ondas planas, pero sin tener en cuenta ni la estructura vectorial ni la propiedad de ortonormalización de los modos guiados. La primera derivación rigurosa de la propagación cuántica en IPDs fue llevada a cabo por Liñares *et al.* a principios de la pasada decada. En ella se tenían en cuenta las componentes longitudinales y la propiedad de ortonormalización de los modos guiados, a diferencia de los estudios previos en medios dieléctricos homogéneos. Usando esta teoría para modos 2D TE (confinados en una dirección del espacio) propagados en estructuras integradas planas, se propusieron campos cuánticos y se obtuvieron

ecuaciones de propagación correctas. En este trabajo se extiende el anterior estudio a modos 1D *quasi*-TE y *quasi*-TM (con confinamiento en dos direcciones del espacio) propagados en estructuras de canal, mediante una cuantización canónica de los campos *ab initio* y obteniendo ecuaciones correctas de evolución espacial en IPDs como acopladores direccionales, redes, uniones, interferómetros, etc.; realizados en medios con distintas características de la permitividad dieléctrica como respuesta no lineal, anisotripía o pérdidas. En particular, este enfoque permite estudiar la contrapropagación y los medios z-dependientes, a diferencia del basado en el Hamiltoniano.

Por ello dedicamos el capítulo 2 a presentar esta teoría. En él, comenzamos introduciendo conceptos clásicos de óptica integrada como los modos guiados y su estructura vectorial, así como sus propiedades de ortonormalización, la teoría de modos acoplados y la óptica no lineal. En siguiente lugar llevamos a cabo una revisión de los trabajos previos en el estudio cuántico de la propagación, donde ilustramos las debilidades y fortalezas de las distintas teorías propuestas e introducimos conceptos necesarios para la cuantización como el flujo de momento clásico y los modos temporales. A continuación presentamos nuestra teoría, que se basa en cuantizar la densidad de flujo de momento electromagnético integrada en una hipersuperficie perpendicular a la propagación mediante el uso de modos temporales y las relaciones de ortonormalidad de los modos en una sección de la estructura guiante. Puesto que el flujo de momento incluye la polarización producida por una perturbación en el medio, anisotropía, no linealidad y pérdidas son aplicadas a esta teoría, obteniendo ecuaciones de propagación libre y de modos acoplados así como los campos cuánticos correspondientes a cada caso. En particular, en el caso de medios no lineales, obtenemos factores que no aparecen cuantizando directamente las ecuaciones clásicas de propagación o mediante una teoría Hamiltoniana. Asimismo, los casos especiales de medios longitudinalmente inhomogéneos con índice de refracción separable y medios con pérdidas, presentan sutilezas que nos llevan a estudiarlas por separado. En el primer caso la cuantización se lleva a cabo identificando un oscilador armónico espacial, mientras que en el segundo mediante acoplamiento a un reservorio. Finalmente, aplicamos la teoría a IPDs acoplados que presentan no-linealidad sin y con pérdidas.

El anterior análisis canónico de la propagación se lleva a cabo en la representación de Heisenberg, interesante en el caso de trabajar con variables discretas como *qubits* codificados en polarización o camino óptico, utilizados en procesado de información cuántica, y cuya medida se realiza mediante detectores de número de fotones. Sin embargo, en problemas de variable continua o donde se estudia el ruido cuántico, como son la polarización cuántica, la tomografía de estados cuánticos o la computación en variable continua, la representación de Schrödinger se adapta mejor. Existen diferentes métodos para resolver la propagación de estados cuánticos en esta representación, como las distintas distribuciones de *quasi-probabilidad*, pero

el más intuitivo físicamente es el de las integrales de camino de Feynman que, en el caso de estudiar el campo electromagnético cuántico, propaga funciones de onda en el espacio de campos ópticos. Este método presenta varias ventajas. Por un lado el uso de integrales de camino en este espacio es matemáticamente análogo al usado en óptica geométrica, y por el otro las distribuciones de probabilidad en el espacio de campos ópticos son funciones *bien comportadas* y se pueden medir directamente mediante métodos homodinos, a diferencia de distribuciones en otras representaciones. Por lo tanto, otro de los objetivos de esta tesis es formular una teoría Lagrangiana de la propagación espacial a partir de la cual obtendremos los propagadores de Feynman de los estados cuánticos de luz en la representación de campos ópticos para distintos IPDs.

En el capítulo 3 planteamos este estudio, donde comenzamos repasando los estados cuánticos que se usan a lo largo del resto del trabajo, centrándonos en sus propiedades de ruido cuántico. En siguiente lugar se presentan las diferentes descripciones que tenemos de los estados cuánticos, que nos dan información puramente cuántica (estados puros) y/o estadística (operador densidad y distribuciones de quasi-probabilidad) del sistema que estudiamos, centrándonos en la representación de estados cuánticos en el espacio de campos ópticos, donde detallamos sus características más importantes y su forma para los estados cuánticos más importantes. A continuación introducimos la teoría de Feynman de integrales de camino en el espacio de campos ópticos mediante una teoría Lagrangiana de tipo espacial, obteniendo propagadores para distintos medios. En primer lugar estudiamos el sencillo caso de un medio lineal y homogéneo donde planteamos varios ejemplos. En segundo lugar abordamos el problema de propagación en medios longitudinalmente inhomogéneos con índice de refracción separable. Este tipo de medios nos lleva a un oscilador armónico con frecuencia espacial dada por una constante de propagación z-dependiente. Como se comentó anteriormente, este tipo de problemas no se puede tratar con una teoría Hamiltoniana. El problema matemático análogo es el de un oscilador armónico con frecuencia temporal dependiente del tiempo. En el caso de usar la teoría de osciladores armónicos de frecuencia variable a nuestro caso, la propagación en este tipo de medios nos llevaría a la conclusión incorrecta de compresión del ruido cuántico del estado cuántico propagado, ya que este fenómeno no se ha observado experimentalmente. Nosotros resolvemos este problema mediante dos métodos: uno aplicando transformaciones unitarias de Infeld-Plebanski al estado cuántico una vez propagado y otro aplicando transformaciones canónicas generalizadas en un sistema de referencia comóvil. Estas transformaciones eliminan la compresión virtual y nos muestran el efecto total producido por el medio, una fase cuántica de Gouy sin contrapartida clásica que se puede usar en problemas de sensorización y procesado de información cuántica. En tercer lugar aplicamos este método al estudio de medios no lineales. En este

caso, un estudio particular debe realizarse para cada problema. Nosotros presentamos su aplicación a un amplificador paramétrico degenerado en el que el acoplamiento no lineal es z-dependiente, problema que de nuevo no podría tratarse con la teoría Hamiltoniana. En cuarto y último lugar presentamos una teoría heurística de la propagación en medios con pérdidas. Además de lo anterior, en las secciones de trabajos de investigación presentamos diferentes aplicaciones de está teoría tanto en IPDs no lineales con y sin pérdidas como para IPDs basados en medios z-dependientes y en los que se propagan estados cuánticos con diferentes características que dan lugar a diferentes fases de Gouy.

Asimismo, una vez analizada la propagación, otro de los objetivos principales de este trabajo es caracterizar de algún modo los estados obtenidos a la salida de los IPDs. Convencionalmente esto se lleva a cabo por medio de distribuciones de quasi-probabilidad o matrices densidad, sin embargo el postprocesado de datos para obtener estas figuras es complicado. Por otro lado, como comentamos anteriormente, en el caso de las distribuciones en el espacio de estados campo, la detección homodina nos ofrece una medida directa de estas distribuciones, así como información del ruido cuántico. De este modo, por analogía con la polarización clásica, acuñamos el término polarización cuántica generalizada como el confinamiento de la distribución de probabilidad del estado cuántico en determinadas regiones del espacio de campos ópticos N-dimensional. Esta definición incluye tanto modos vectoriales como espaciales (en el sentido de ortogonalidad). En el caso de modos vectoriales en dos dimensiones recupera la definición habitual de polarización cuántica, mientras que en el caso de modos espaciales propagándose en IPDs, esta definición se extiende a N dimensiones.

De este modo el capítulo 4 está dedicado a la caracterización de estados cuánticos en el espacio de estados campo o polarización cuántica generalizada. Comenzamos el capítulo introduciendo conceptos clásicos de polarización como los parámetros de Stokes y el grado de polarización. En siguiente lugar pasamos a la polarización cuántica presentando los operadores de Stokes y el problema del grado de polarización semiclásico, ya que debido a que los operadores de Stokes sólo contienen correlaciones de segundo orden, cuando aplicamos esa definición a estados cuánticos con correlaciones de orden superior éste produce resultados inconsistentes. Por este motivo se han propuesto en los últimos años distintos grados de polarización cuánticos que eviten este problema y llevamos a cabo una pequeña revisión de los mismos. Su característica principal es que se basan en la definición de estado cuántico de luz totalmente despolarizado como aquel invariante ante transformaciones SU(2). A continuación, siguiendo las ideas de estos autores, presentamos nuestro formalismo de polarización cuántica generalizada e introducimos el grado de polarización generalizada. Este grado es una medida de cuán diferente es el estado a caracterizar de un estado totalmente despolarizado en el espacio de campos ópticos, que elegi-

mos como un estado gaussiano isótropo en cualquier dimensión, de modo que no hay ningún subespacio con un confinamiento (polarización) privilegiado. Con esta herramienta, caracterizamos estados cuánticos propagados en IPDs en N dimensiones. Finalmente, aplicamos la teoría a distintos estados cuánticos tanto estacionarios como dinámicos que se propagan en IPDs, calculando sus grados de polarización para diferentes parámetros.

Finalmente, como se ha indicado anteriormente, la polarización cuántica generalizada se basa en la medida de estados cuánticos en el espacio de campos ópticos, que se lleva a cabo mediante técnicas sensibles a la fase, como la detección homodina o la heterodina. Estas técnicas se han usado ampliamente durante los últimos años en la tomografía de estados cuánticos en óptica "*bulk*" y este mismo año en óptica integrada. La aproximación habitual monomodo se basa en usar un oscilador local cuya fase actúa como ángulo de rotación en el espacio de fases, barriendo de este modo todo este espacio, lo que permite la reconstrucción del estado. Si tenemos más dimensiones (modos), necesitamos más parámetros. En el caso bimodal una posible técnica es la de *rotaciones generalizadas en el espacio de fases*, donde una serie de transformaciones en dos dimensiones se efectúan sobre el estado antes de mezclar la señal con el oscilador local. La reconstrucción de estados multimodales es posible anidando el esquema bimodal, pero en el caso de óptica "*bulk*" esto se hace engorroso debido a su falta de escalabilidad intrínseca.

Teniendo todo esto en cuenta, nuestro último objetivo es proponer un dispositivo integrado capaz de medir estados cuánticos de luz multimodales en el espacio de campos ópticos, a lo que dedicamos el capítulo 5. Para ello comenzamos con una introducción a la medida homodina en varias dimensiones para, a continuación, revisar las aplicaciones más recientes de esta técnica en óptica cuántica. En siguiente lugar presentamos nuestro diseño: un IPD activo formado por un acoplador direccional electro-óptico en configuración $\Delta\beta$ que lleva a cabo transformaciones unitarias, por lo que permite llevar a cabo tomografía bimodal de estados cuánticos de forma integrada siguiendo el esquema de *rotaciones generalizadas en el espacio de fases*. Este dispositivo permite realizar cualquier transformación unitaria, por lo que puede ser una herramienta útil en cualquier contexto de la óptica cuántica integrada en el que estas transformaciones sean necesarias y, además, debido a su naturaleza integrada, este dispositivo se puede aplicar a estados cuánticos multimodales mediante anidamiento, lo que abre su campo de actuación. Cabe decir que existen otros diseños basados en interferómetros Mach-Zehnder pasivos con moduladores de fase electro- o termo-ópticos que realizan la misma función, pero nuestro dispositivo produce mejores resultados debido a su habilidad de reducir el efecto de los errores producidos en la fabricación de los acopladores direccionales pasivos, efecto que se multiplica cuánto mayor es la complejidad de los circuitos. A continuación, mostramos una simulación de su aplicación a la

medida de estados cuánticos de luz en el espacio de campos ópticos. Finalmente, presentamos el trabajo de investigación donde se recoge el diseño detallado y la simulación de funcionamiento de este dispositivo en dos aplicaciones específicas: polarización generalizada y reconstrucción de la función de onda mediante médida débil.

oOo

USC
UNIVERSIDADE
DE SANTIAGO
DE COMPOSTELA